Commonwealth of Massachusetts
Executive Office of Energy & Environmental Affairs

Department of Environmental Protection
One Winter Street Boston, MA 02108 • 617-292-5500

Charles D. Baker
Governor

Karyn E. Polito
Lieutenant Governor

Kathleen A. Theoharides
Secretary

Martin Suuberg
Commissioner

Technical Support Document

Per- and Polyfluoroalkyl Substances (PFAS): An Updated Subgroup Approach to Groundwater and Drinking Water Values

Prepared for:
Bureau of Waste Site Cleanup

and

Bureau of Water Resources
Drinking Water Program
Massachusetts Department of Environmental Protection

Prepared by:
Office of Research and Standards
Massachusetts Department of Environmental Protection

December 26, 2019

This information is available in alternate format. Contact Michelle Waters-Ekanem, Director of Diversity/Civil Rights at 617-292-5751.
TTY# MassRelay Service 1-800-439-2370
MassDEP Website: www.mass.gov/dep
Printed on Recycled Paper

EXECUTIVE SUMMARY

The Massachusetts Department of Environmental Protection (MassDEP) Office of Research and Standards (ORS) has completed a reassessment of toxicity information for a subgroup of longer-chain per- and polyfluorinated substances (PFAS). Based on this reassessment, MassDEP ORS has revised the toxicity values and associated drinking water values downward for these compounds. These values are the bases of the groundwater standards for water used or potentially used as drinking water under the Massachusetts Contingency Plan (MCP), as well as updated Office of Research and Standards Guidelines (ORSG) for drinking water and proposed Massachusetts Maximum Contaminant Levels (MMCLs), under the Massachusetts Drinking Water Regulation, for these compounds.

In June 2018, MassDEP established an ORSG of 70 parts per trillion (ppt) for drinking water for a subgroup of five closely related PFAS. This subgroup included perfluorooctanoic acid (PFOA), perfluorooctanesulfonic acid (PFOS), perfluorononanoic acid (PFNA), perfluorohexanesulfonic acid (PFHxS) and perfluoroheptanoic acid (PFHpA) (MassDEP 2018a,b). In deriving the 2018 ORSG, MassDEP ORS extended the United States Environmental Protection Agency (USEPA) toxicity values (reference doses or RfDs), Health Advisories (HA) for drinking water and additive toxicity approach for PFOA and PFOS to this subgroup (USEPA 2016a,b,c,d). This was based on the close similarities in chemical structure and similar toxicities for this subgroup of PFAS.

In consideration of recent PFAS assessments by other organizations and states, MassDEP ORS has reassessed the toxicity values and their application to derive groundwater and drinking water standards and guidelines for these compounds. MassDEP ORS also considered whether additional compounds should be added to this subgroup. This reassessment reflects public comments received on the draft Massachusetts Contingency Plan (MCP) PFAS standards issued for public comment on April 19, 2019, as well as technical input from the MassDEP Health Effects Advisory Committee.

In summary, MassDEP ORS's review of current scientific information and assessments by other agencies support the approaches used in the development of the 2018 ORSG for these compounds. Based on its assessment, MassDEP ORS has also concluded that one additional compound, PFDA, should also be included in this subgroup. Additionally, MassDEP ORS concluded that the toxicity value (RfD) for the compounds in this subgroup should be adjusted downward from that used in the 2018 ORSG derivation, to 5×10^{-6} milligrams per kilogram body weight per day (mg/kg-day). The revised MassDEP RfD value results from the application of an additional uncertainty factor (UF) of $10^{1/2}$ to the RfD derivations for PFOA and PFOS. This was done to account for considerable and convincing evidence associating exposures to these compounds with adverse responses in laboratory animals at levels of exposure lower than those

relied upon by USEPA in its 2016 RfD derivations for PFOS and PFOA. The revised MassDEP ORS RfD is applied to the six PFAS in this subgroup. The lower RfD leads to a drinking water value of 20 ppt, which provides a greater degree of health protection than the prior value of 70 ppt, in particular for sensitive groups including pregnant women, nursing mothers and infants.

The PFAS subgroup considered in this reassessment include the closely related longer-chain PFAS that have carbon chain lengths with plus or minus two carbons (C6-C10 compounds) compared to PFOA and PFOS, the most data rich PFAS. There are ten compounds in this subgroup. MassDEP ORS focused its assessment on the seven of these compounds covered in USEPA Method 537.1 for drinking water (USEPA 2018). In addition to PFOA and PFOS, this subgroup includes PFNA, PFHxS and PFHpA, which are included in the current ORSG, as well as PFDA and perfluorohexanoic acid (PFHxA). Three compounds in the targeted subgroup, perfluorodecanesulfonic acid (PFDS), perfluorononanesulfonic acid (PFNS) and perfluoroheptanesulfonic acid (PFHpS), were not addressed in this evaluation because they are not included as USEPA Method 537.1 analytes (USEPA 2018).

In its re-evaluation of these compounds, MassDEP ORS considered key toxicological data and assessments by other state and federal agencies. This information is discussed in the following Technical Support Document. Based on this assessment, MassDEP ORS concluded that the approach previously used in deriving the 2018 MassDEP ORSG continues to be appropriate. MassDEP ORS is thus applying the revised MassDEP ORS RfD for PFOA and PFOS (5×10^{-6} mg/kg-day) to PFNA, PFHxS, PFHpA and PFDA as a group. This conclusion is based on consideration of similarities in chemical structure; overlap in toxicity values derived by various agencies; similarity in toxic responses; prolonged serum half-lives; and evaluation of relative potencies.

USEPA, the federal Agency for Toxic Substances and Disease Registry (ATSDR) and environmental and Public Health agencies in the states of New Hampshire, New Jersey, New York, California, Wisconsin, Minnesota and Michigan, have derived or proposed toxicity values for PFOA, PFOS, PFNA and PFHxS based on available non-cancer toxicity data. Due to differing interpretations of the data and database completeness, these toxicity values vary. Notably, the ranges of toxicity values overlap between states across these compounds and, for each compound, the revised MassDEP RfD falls within the range. Other states, including Vermont and Connecticut, have taken a subgroup approach to PFAS similar to that applied in MassDEP's 2018 ORSG, which considers multiple PFAS to be equipotent. Relative potency evaluations published by other groups and an assessment completed by MassDEP ORS using National Toxicology Program (NTP) data support treating this subgroup of PFAS as being equipotent, since relative potency estimates overlap across various endpoints (NTP 2018; this document). Data was not identified that demonstrates clear quantitative differences in potencies and mode(s) of action between these compounds.

Toxicity values have not been derived by the noted agencies for PFHpA and PFDA. For PFDA, MassDEP ORS's relative potency assessment using the NTP data (presented in Section 3 and Appendix 5 of this Technical Support Document) demonstrates that this compound shares similar toxicity endpoints and potencies with the other compounds in the subgroup (NTP 2018; this document). Applying "read-across," an approach that uses information from other closely related substances that have been more extensively studied to estimate the toxicity of less studied target substances (ECHA 2015), MassDEP ORS has concluded that PFDA should be included in the PFAS subgroup addressed herein.

In the case of PFHpA, no agency has derived a compound specific toxicity value due to a lack of toxicity data. The MassDEP 2018 ORSG, as well as the Connecticut and Vermont drinking water values, consider PFHpA to be equipotent to PFOA based on "read-across." MassDEP ORS continues to conclude that this is an appropriate approach as toxicity data are not available to assign a compound specific or relative potency value for PFHpA or to conclude that it is toxicologically dissimilar to the other compounds in the subgroup.

With respect to the remaining compound in the targeted group, PFHxA, the available data demonstrate that it exhibits a much shorter serum half-life and is substantially less toxic on an applied dose basis than the other compounds. MassDEP ORS has concluded that the data on this compound are sufficient to conclude that it is not appropriate to consider it as being toxicologically equivalent to the other compounds. For other PFAS compounds outside of the C6-C10 longer-chain subgroup, MassDEP ORS concluded that available data indicates that shorter-chain compounds are also likely to be considerably less toxic and were thus not included. This conclusion is consistent with the findings of the National Toxicology Program (NTP 2019a,b), which concluded that "higher doses of short-chain PFAS were needed to have similar effects on liver and thyroid hormone when compared to long-chain PFAS." Compounds with carbon chain lengths greater than 10 were not included as their structural dissimilarity increases the likelihood that they will exhibit different toxicities. At this time there is insufficient toxicity data to address this possibility.

Regarding approaches to addressing risks attributable to exposures to multiple PFAS, MassDEP ORS continues to concur with the USEPA's additivity approach as applied to PFOA and PFOS in deriving the USEPA drinking water HAs for these compounds (USEPA 2016a,b,c,d). Based on their close structural similarities, toxicity and half-lives, MassDEP ORS has also concluded that it is appropriate to extend this additivity approach to the six compounds in the subgroup addressed herein.

Application of the revised RfD in the derivation of drinking water values (revised ORSG and draft MMCLs) and Massachusetts Contingency Plan (MCP) standards for groundwater used as

drinking water, results in a value of 20 ppt (rounded to one significant figure). This value was derived using the same exposure parameters and relative source contribution factor applied by USEPA in deriving the drinking water HAs for PFOA and PFOS, which was previously used by MassDEP ORS to derive the 2018 ORSG (MassDEP 2018a,b) and is applicable to the concentrations of the subgroup of six PFAS individually or summed.

MassDEP ORS also considered the potential carcinogenicity of these compounds. A study of people exposed to PFOA and other PFAS concluded that the data supported a probable link between exposure and cancers of the kidney and testes (Barry et al. 2013). No potency estimates were derived. Animal bioassay data from the NTP (NTP 2019c) reported elevated pancreatic and liver tumor rates following high dose exposures to PFOA. Although NTP has issued summary data tables for this study, a final report has not been issued and, as of June 29, 2019, no agency had established drinking water values based on this data. The cancer data is concerning to MassDEP, because some carcinogens can present a degree of risk at any exposure level. To account for this potential risk, MCL goals (MCLGs) of zero have been established for some chemicals and may ultimately be warranted for certain PFAS. MCLGs are guidance values rather than standards and are levels of a contaminant in drinking water at or below which there is no known or expected risk to health. At this time, however, the level of cancer risk posed by these compounds is unclear. Until the cancer data on these compounds is better understood, MassDEP will move ahead with the drinking water values based on non-cancer effects derived in this assessment. MassDEP ORS will follow and assess research in this area to determine if future revisions to the drinking water values are needed.

TABLE OF CONTENTS

List of Tables

Appendixes

Abbreviations and Acronyms

ATSDR	Agency for Toxic Substances and Disease Registry
AUC	area under the curve
BBMD	Bayesian benchmark dose
BBMDL	Bayesian benchmark dose lower confidence limit
BMDL	benchmark dose lower confidence limit
BMR	benchmark dose response
CDC	Center for Disease Control
GD	gestational day
HA	Health Advisory
HDL	high-density lipoprotein
HED	human equivalent dose
IgM	immunoglobulin M
LDL	low-density lipoprotein
LOAEL	lowest observed adverse effect level
MassDEP	Massachusetts Department of Environmental Protection
MMCL	Massachusetts Maximum Contaminant Level
MMCLG	Massachusetts Maximum Contaminant Level Goal
MDH	Minnesota Department of Health
MISAW	Michigan Science Advisory Workgroup
MOA	mode of action
MRL	minimum risk level
mg/kg-day	milligrams per kilogram body weight per day
mg/L	milligrams per liter
ng/L	nanograms per liter
NHANES	National Health and Nutrition Examination Survey
NTP	National Toxicology Program
NHDES	New Hampshire Department of Environmental Services
NJDWQI	New Jersey Drinking Water Quality Institute
NOAEL	no observed adverse effect level
ORS	Office of Research and Standards
ORSG	Office of Research and Standards Guideline
ppt	part per trillion
PBPK	physiologically based pharmacokinetic model
PFAS	per and polyfluoroalkyl substances
PFDA	perfluorodecanoic acid
PFHpA	perfluoroheptanoic acid
PFHxS	perfluorohexanesulfonic acid
PFNA	perfluorononanoic acid
PFOA	perfluorooctanoic acid
PFOS	perfluorooctanesulfonic acid
PND	post-natal day
POD	point of departure
PPARα	peroxisome proliferator activated receptor alpha
RfD	reference dose

RSC	relative source contribution
SRBC	sheep red blood cell
TWA	time weighted average
UCMR3	Third Unregulated Contaminant Monitoring Rule
UF	uncertainty factor
UF_A	interspecies uncertainty factor
UF_H	intra-individual uncertainty factor
UF_L	LOAEL to NOAEL uncertainty factor
UF_S	subchronic to chronic uncertainty factor
UF_D	incomplete database uncertainty factor
USEPA	United States Environmental Protection Agency
WIDHS	Wisconsin Department of Health Services

1.0 BACKGROUND

The Massachusetts Department of Environmental Protection (MassDEP) issued an Office of Research and Standards Guideline (ORSG) for drinking water for five PFAS compounds on June 8, 2018 (MassDEP 2018a,b). The ORSG focused on the PFAS addressed under the third USEPA Unregulated Contaminant Monitoring Rule (UCMR3). The UCMR3 PFAS compounds included PFOA, PFOS, PFNA, PFHxS, PFHpA and perfluorobutanesulfonic acid (PFBS). Under UCMR3, PFAS were detected in some public drinking water supplies in MA and across the US. In response to these detections, the MassDEP Drinking Water Program requested that the MassDEP Office of Research and Standards (ORS) develop drinking water guidance for the UCMR3 PFAS. The 2018 ORSG was based on the USEPA reference dose (RfD) of 2×10^{-5} milligrams per kilogram body weight per day (mg/kg-day) and drinking water Health Advisory (HA) of 70 nanograms per liter (ng/L, parts per trillion or ppt) for PFOA and PFOS, extended to include PFNA, PFHxS and PFHpA (MassDEP 2018a,b). MassDEP concluded that the data for PFBS, which was also included in UCMR3, did not support its inclusion in the ORSG, as it exhibits a much shorter serum half-life and lower toxicity than the other compounds. The ORSG of 70 ng/L was applied individually and to the sum of the five remaining PFAS. As described in MassDEP (2018b), the available data for PFHxS, PFNA and PFHpA demonstrate that these PFAS compounds are very similar in molecular structure to PFOA and PFOS, have long biological half-lives, and where data exists, elicit similar types of effects at comparable dose ranges as PFOA and PFOS. The 2018 ORSG extended the additivity approach used by the USEPA for PFOA and PFOS to include PFNA, PFHxS and PFHpA. This approach was endorsed by the MassDEP Health Effects Advisory Committee.

Shortly after the ORSG was issued, the Agency for Toxic Substances and Disease Registry (ATSDR 2018a) published a draft Toxicological Profile for Perfluoroalkyls, which included individual Minimum Risk Levels (MRL) for four PFAS including PFOA, PFOS, PFNA and PFHxS. Although USEPA and ATSDR use RfD and MRL values differently, these values are very similar toxicologically. Both RfDs and MRLs are estimates of average daily exposure to a chemical that is likely to be without appreciable risk of adverse non-cancer health effects over a specified exposure duration. MRLs derived by ATSDR are meant to be used as a screening tool. They are derived by dividing a No Observed Adverse Effect Level (NOAEL), a Lowest Observed Adverse Effect Level (LOAEL) or a Benchmark Dose (BMD) by appropriate uncertainty factors to account for extrapolation from an animal study to humans, interindividual variability in sensitivity in the human population, and database limitations among other uncertainties. MRLs are typically in units of mg/kg-day. USEPA RfDs are used in evaluating non-carcinogenic effects resulting from environmental exposures. Like MRLs, the RfD is generally expressed in units of mg/kg-day and is typically derived by dividing a NOAEL, LOAEL or BMD by appropriate uncertainty factors (USEPA 2002a).

The draft ATSDR (2018a) PFOA MRL (3 x 10^{-6} mg/kg-day) is approximately 7-fold lower, and the PFOS draft MRL (2 x 10^{-6} mg/kg-day) is 10-fold lower, than USEPA's RfD of 2 x 10^{-5} mg/kg-day for these compounds. ATSDR (2018a) also published draft MRLs for PFNA (3 x 10^{-6} mg/kg-day) and PFHxS (2 x 10^{-5} mg/kg-day). USEPA has not established any RfD values for these two compounds. Due to data deficiencies, ATSDR (2018a) did not derive draft MRLs for PFHpA or any other PFAS compound.

Other state agencies have also derived toxicity values for PFAS compounds, many of which are lower than USEPA's PFOA/PFOS RfD. These are summarized in Appendix 1, Table 1. Additionally, the European Food Safety Authority (EFSA 2018a) issued an assessment relying on human epidemiological data to derive tolerable weekly intake values of 6 ng/kg body weight (bw) per week for PFOA and 13 ng/kg bw per week for PFOS (equivalent to MRL/RfD values of 1 and 2 x 10^{-6} mg/kg-day, respectively).

The differences between the USEPA RfD and these other toxicity values for PFOA and PFOS, as well as the additional values derived for PFNA and PFHxS, prompted MassDEP to re-evaluate its toxicity and associated drinking water guidance values for these and closely related compounds. As part of MassDEP efforts to address PFAS compounds, MassDEP has reviewed numerous published toxicological assessments and key primary literature publications. These include the USEPA Health Effects Support and Drinking Water Health Advisory (HA) documents for PFOA and PFOS (USEPA 2016a,c,b,d); the ATSDR draft Toxicological Profile for Perfluoroalkyls (ATSDR 2018a); the National Toxicology Program (NTP) Monograph, Immunotoxicity Associated with Exposure to PFOA or PFOS (NTP 2016); the New Jersey Drinking Water Quality Institute (NJDWQI) Maximum Contaminant Level (MCL) recommendation supporting documents for PFNA (NJDWQI 2015), PFOA (NJDWQI 2017) and PFOS (NJDWQI 2018); Minnesota Department of Health (MDH) Risk Limit (HRL)/Health Based Value (HBV) supporting documents for PFOA (MDH 2018a), PFOS (MDH 2018b, 2019a) and PFHxS (MDH 2019b); the New Hampshire Department of Environmental Services (NHDES) Summary Report (NHDES 2019a) and Technical Background Report for the June 2019 Proposed Maximum Contaminant Levels (MCLs) and Ambient Groundwater Quality Standards (AGQSs) for Perfluorooctane sulfonic Acid (PFOS), Perfluorooctanoic Acid (PFOA),Perfluorononanoic Acid (PFNA), and Perfluorohexane sulfonic Acid (PFHxS) (NHDES 2019b); the Michigan Science Advisory Workgroup (MISAW), Health-Based Drinking Water Value Recommendations for PFAS in Michigan (MISAW 2019); the European Food Safety Authority (EFSA 2018a) PFOA and PFOS evaluation and related documents; and the NTP 28-day study (NTP 2018), as well as other sources.

This re-evaluation does not seek to replicate the extensive work already completed and detailed in the noted assessments but rather focuses on key evidence and publications associating

exposures to the longer-chain PFAS of most concern to MassDEP with potential adverse responses in laboratory animals at dose levels below those used in the USEPA RfD calculations.

The remainder of this Technical Support Document summarizes data from key studies, how various organizations have assessed this data and the implications of this information regarding the selection of appropriate toxicity values and drinking water values for PFOA, PFOS and related compounds. Specifically, Section 2 summarizes the basis of the MassDEP revised RfDs for PFOA and PFOS. Data on other selected longer-chain PFAS are summarized in Section 3 and Appendix 2. Section 3 presents data for evaluating toxicological similarity of the PFAS in the longer-chain subgroup and explores relative potency evaluations. Section 4 addresses approaches for addressing co-exposure to one or more PFAS in the longer-chain subgroup. Section 5 presents overall conclusions regarding standards for groundwater used as drinking water, revision of the ORSG for drinking water and considerations regarding drinking water standards (maximum contaminant levels or MCLs) for these PFAS.

2.0 REVISED RFDS FOR PFOA AND PFOS

Since MassDEP's last review of the database for PFOA and PFOS (MassDEP 2018b), a number of states have either revised or derived new RfDs and/or drinking water values for PFOA and PFOS. ATSDR (2018a) also issued draft MRLs for several PFAS. The following sections describe the data and rationale for the choices MassDEP ORS has made in developing its revised RfDs for PFOA and PFOS.

2.1 Summary of USEPA RfDs for PFOA and PFOS

The USEPA (2016a,b) RfDs for PFOA and PFOS (2×10^{-5} mg/kg-day) are based on multiple studies and endpoints. In deriving these values, USEPA extensively reviewed the available human and animal toxicity studies on PFOA and PFOS and selected results from several studies representing various effects and life stages as points of departure (PODs) to derive candidate RfDs for PFOA and PFOS (Tables 1 and 2, respectively) (USEPA 2016 a,b,c,d). USEPA selected the candidate studies and PODs based on their NOAELs/LOAELs, use of control groups, use of two or more doses, and the availability of measured or modeled serum levels. For both PFOA and PFOS, eleven of the twelve candidate RfDs derived by USEPA were within the range of $2 - 5 \times 10^{-5}$ mg/kg-day. These included values derived for several endpoints. The POD and associated RfD selected by USEPA (2016a,b) for both compounds was the lowest and most frequent of the candidate RfD values derived, 2×10^{-5} mg/kg-day[1].

[1] Five of the twelve candidate RfDs were 2×10^{-5} mg/kg-day. The next most frequent value was 4×10^{-5} mg/kg-day which was the calculated value for three of the candidate RfDs.

Table 1. USEPA (2016a) Candidate RfDs Derived from Modeled Animal Average Serum Values of PFOA

Study	Endpoint	Dosing duration (days)	LOAEL (Av serum mg/L) [a]	UFs (total and components)	Candidate RfD (mg/kg-day)
Lau et al. (2006) **CD1 mice** **N not specified**	**Pup ossification (m, f)** **accelerated puberty (m)**	**17** (GD 1–17)	**38.0**	**300** **UF_H = 10** **UF_A = 3** **UF_L = 10**	**2 x 10^{-5} (USEPA RfD)**
DeWitt et al. (2008) C57BL/6N mice N = 8	↓ IgM response to SRBC	15	61.9 [b]	300 UF_H = 10 UF_A = 3 UF_S = 10	2 x 10^{-5}
Palazzolo (1993); Perkins et al. (2004) ChR-CD rat (m) N = 45-55/dose group	↑ Liver weight ↑ Liver necrosis	91	77.4 [c]	30 UF_H = 10 UF_A = 3	1.5 x 10^{-4}
Wolf et al. (2007) CD-1 mice N = 28-48/dose group	↓ Pup body weight	17 (GD 1–17)	77.9	300 UF_H = 10 UF_A = 3 UF_L = 10	4 x 10^{-5}
Wolf et al. (2007) CD-1 mice N = 14	↓ Pup body weight	11 (GD 7–17)	87.9	300 UF_H = 10 UF_A = 3 UF_L = 10	4 x 10^{-5}
Butenhoff et al. (2004) Sprague-Dawley rat N = 30/sex/group	↓ Rat relative body weight/↑ relative kidney weight and ↑ kidney:brain weight ratio in F0 and F1 at sacrifice	84	45.9	300 UF_H = 10 UF_A = 3 UF_L = 10	2 x 10^{-5}

[a] Average serum concentration modeled by USEPA (2016a) using the physiologically based pharmacokinetic model (PBPK) model by Wambaugh et al. (2013) to estimate an area under the curve (AUC).
[b] NOAEL 38.2 milligrams per liter (mg/L) average serum concentration.
[c] NOAEL 31.6 mg/L average serum concentration.
m = male; f = female; N = number of animals; GD = gestational day; IgM = immunoglobulin M; SRBC = sheep red blood cell.

Table 2. USEPA (2016b) Candidate RfDs Derived from Modeled Animal Average Serum Values of PFOS

Study	Endpoint	Dosing duration (days)	NOAEL (Av serum mg/L)[a]	LOAEL (Av serum mg/L)[a]	UFs (total and components)	Candidate RfD (mg/kg-day)
Luebker et al. (2005a) Sprague Dawley rat N = 25	**↓ Pup body weight**	**84**	**6.26**		**30 UF_H = 10 UF_A = 3**	**2×10^{-5} (USEPA RfD)**
Seacat et al. (2003) Sprague-Dawley rat N = 25 m	↑ ALT; ↑ BUN	98	16.5		30 UF_H = 10 UF_A = 3	4×10^{-5}
Lau et al. (2003) Sprague-Dawley rat N not specified	↓Pup survival; ↓ maternal and pup body weight	19 (GD 2-21)	17.6		30 UF_H = 10 UF_A = 3	5×10^{-5}
Butenhoff et al. (2009) Sprague-Dawley rat N =25 f	DNT (↑ motor activity; ↓ habituation)	41	10.4		30 UF_H = 10 UF_A = 3	3×10^{-5}
Luebker et al. (2005b) Sprague- Dawley rat N = 16 f	↓ Maternal body weight, gestation length, and pup survival	63	19.9		30 UF_H = 10 UF_A = 3	5×10^{-5}
Luebker et al. (2005b) Sprague- Dawley rat N = 16 f	↓ Pup body weight	63	none	19.9	100 UF_H = 10 UF_A = 3 UF_L = 3	2×10^{-5}

[a] Average serum concentration modeled by USEPA (2016b) using the PBPK model by Wambaugh et al. (2013) to estimate an AUC.

m = male; f = female; N = number of animals; ALT = alanine transaminase; BUN = blood urea nitrogen; DNT = developmental neurotoxicity

USEPA did not adjust this RfD to account for other studies that reported various adverse effects at lower doses than the PODs selected to derive its candidate RfDs[2].

2.2 Derivation of Revised RfDs for PFOA and PFOS

MassDEP ORS has concluded that it is appropriate to adopt RfD values that are lower than those derived by USEPA (2016a,b) for PFOA and PFOS. The revised MassDEP RfDs reflect the application of an additional uncertainty factor of $10^{1/2}$ (often identified as the rounded value of 3), which results in a RfD of 5×10^{-6} mg/kg-day.[3] This reflects substantial data indicating these compounds cause effects at lower doses than relied upon in the USEPA RfD derivations and provide a greater degree of health protection to sensitive groups. This conclusion is based on the following:

1) RfDs for PFOA and PFOS lower than the USEPA (2016a,b) values are warranted to account for data from multiple studies (summarized in the Tables in this section and further assessed in Appendix 2, reporting effects in laboratory animals at dose levels below those used as POD in the USEPA RfD derivations.
2) The weight of the evidence is compelling regarding potential effects at lower exposure levels. However, various issues relating to study design, execution and data interpretation have raised questions regarding the appropriateness of alternative PODs based on the lower dose effect data from the individual studies. These are discussed in Appendix 2.
3) Thus, although lower PODs can be supported for PFOA and PFOS, MassDEP ORS has taken an alternative approach, which we conclude is preferable, to account for the lower dose effect data. This approach relies on the application of a database uncertainty factor (UF_D) of $10^{1/2}$ in the PFOA and PFOS RfD derivations. Application of an UF_D is an approach that is consistent with well-established protocols used by federal and state agencies and has been used by several states, as well as ATSDR (2018a), for deriving PFAS toxicity values.
4) Although MassDEP is adopting RfDs lower than those issued by USEPA for PFOA and PFOS in 2016, the data underlying the USEPA RfD values provide appropriate starting points for the MassDEP RfD because they were well documented and considered multiple studies and PODs.

[2] Uncertainty factors (UF) for such data issues may be used to account for data gaps or to account for data that indicate more sensitive effects may occur. USEPA states that "The database UF is intended to account for the potential for deriving an under protective RfD/RfC as a result of an incomplete characterization f the chemical's toxicity. In addition to identifying toxicity information that is lacking, review of existing data may also suggest that a lower reference value might result if additional data were available. Consequently, in deciding to apply this factor to account for deficiencies in the available data set and in identifying its magnitude, the assessor should consider both the data lacking and the data available for particular organ systems as well as lifestages" (USEPA 2002a).
[3] Uncertainty factors may be 1, 10, or $10^{1/2}$. Individual UFs are rounded after multiplication, so two factors of $10^{1/2}$ cumulate to 10, but one factor is rounded down to 3 (USEPA 2002a).

The sections below briefly describe the studies observing effects at lower exposure levels (Section 2.3), and the rational for selecting a value of $10^{1/2}$ for the UF_D applied to the USEPA RfDs for PFOA and PFOS (Section 2.4).

2.3 Summary of Effects Observed at Doses Lower than those Relied Upon by USEPA for RfD Derivation

Studies reporting effects at exposure levels below those associated with the PODs selected by USEPA (2016a,b) in its derivation of candidate RfDs for PFOA and PFOS have served as the basis for some recent RfDs developed by other states and the draft ATSDR (2018a) MRLs. The following sections summarize and discuss key aspects of these studies with additional details presented in Appendix 2.

2.3.1 *PFOA*

Several studies have demonstrated various effects at dose levels below that selected as a POD by the USEPA (2016a). These include neurobehavioral, skeletal, and mammary gland development (Table 3) and hepatic toxicity endpoints (Table 4). MassDEP has concluded that these studies, taken together, provide compelling evidence that effects at exposures below the POD selected by USEPA in its RfD derivation for PFOA are likely. However, as discussed below, because of certain questions regarding the appropriate use of the noted data in selecting an alternative POD, MassDEP has instead elected to account for this data through the use of a database uncertainty factor.

2.3.1.1 Developmental Neurobehavioral and Skeletal Effects

The Onishchenko et al. (2011) (neurobehavioral-developmental) and the Koskela et al. (2016) (developmental bone morphology) mouse studies served as the bases of the draft ATSDR PFOA MRL (ATSDR 2018a) (Table 3). The neurobehavioral-developmental effects reported by Onishchenko et al. (2011) were also selected by the Michigan Science Advisory Workgroup (MISAW 2019) as the POD for their PFOA RfD. The modeled serum concentration at the LOAELs for these endpoints equaled approximately 8 mg/L, which is about 5-fold lower than that at the POD in the critical study selected by USEPA (2016a), Lau et al. (2006).

Although the effects reported in the Onishchenko et al. (2011) and Koskela et al. (2016) studies are concerning regarding PFOA toxicity, questions have been raised regarding some aspects of these two publications. Both studies used offspring from the same exposed parental group and serum PFOA concentrations were not directly measured. Relatively small numbers of animals were included. Both studies used a single dose. Although this dose was selected to be within the range of effects seen in previous studies and therefore yields meaningful results, the use of a single dose precludes quantitative evaluation of the dose-response relationship, which introduces uncertainty with respect to use of the data as a POD for deriving a toxicity value. Lastly, the biological significance of the observed skeletal effects is subject to differing interpretations. The

authors (Koskela et al. 2016) classified it as minor as the effects did not appear to lead to any functional deficits while ATSDR (2018a) considered the effects significant and relied on this endpoint and study as basis of its draft MRL derivation.

MassDEP ORS concluded that these developmental effects raise concerns regarding the USEPA PFOA RfD and support a lower value.

2.3.1.2 Developmental Mammary Gland Effects

Macon et al. (2011) and Tucker et al. (2015) evaluated mammary gland development in mice following PFOA exposure (Table 3). To date, MassDEP ORS is unaware of any regulatory agency or organization that has relied on delayed mammary gland development as a POD in developing an RfD, drinking water value or other health-based guideline for PFOA. This can be attributed largely to uncertainty regarding the biological significance of the effects, as they did not lead to any apparent functional impairment based on nursed pups, which exhibited normal growth (White et al. 2011)[4]. Additional concerns relate to data quality and reproducibility attributable to the use of qualitative measures of effect (i.e. mammary histology scores)[5]. Independent replication of this work, with the inclusion of additional quantitative measures of effect, would enhance the strength of this data and should be a research priority.

In light of the fact that mammary gland effects have been reported in multiple studies, MassDEP ORS has concluded that these effects also raise concerns regarding the USEPA PFOA RfD and support a lower value.

2.3.1.3 Developmental and Non-Developmental Hepatic Toxicities

Liver effects are sensitive toxicological endpoints for PFOA and have been observed in response to low doses in studies in mice, rats and non-human primates. Increases in liver weight and liver hypertrophy are two of the most sensitive effects that occur at low PFOA doses in both sexes of tested animals and exhibit clear dose-response relationships. Six studies document PFOA liver effects at doses lower than that used by USEPA in its RfD derivation (2016a) (Table 4). Of the six studies, four are developmental studies. Three of these have reported LOAELs ranging from 0.01 - 0.3 mg/kg-day for liver effects, including hepatic hypertrophy, increased liver weight gain, changes in lipid profiles and periportal inflammation.

Both the USEPA (2016a) and the ATSDR (2018a), based on the "Hall Criteria" (Hall et al. 2012), attributed hepatocellular hypertrophy, increased liver weight, and altered serum lipids observed in rodent studies to peroxisome proliferation and concluded that these effects were not

[4] This is consistent with the effect not being biologically significant but is based on limited data and no overall assessment of the nutritional composition of the milk. Further research regarding potential changes in milk production and quality, as well as effects occurring later in life, are needed.

[5] These concerns are mitigated to some degree by the use of averaged histology slide scores of two pathologists, blind to treatment group and the fact that these PFOA effects were reported in several studies.

Table 3. Developmental Studies with Lower PODs than Used by USEPA (2016a) to Derive Candidate RfDs for PFOA

Study type/Reference	Endpoint	Dosing duration (days)	LOAEL (Av serum mg/L)	Comments
Bone Morphology and Neurotoxicity Effects				
Koskela et al. (2016) C57Bl/6 mice N = 6 f	Altered bone morphology at 17 months of age	21 (GD1-21)	8.29 [a]	Single dose study with small number female mice; serum levels not measured but modeled; skeletal significance of effect unclear as authors classified it as minor. (Used as POD in draft ATSDR (2018a) MRL.)
Onishchenko et al. (2011) C57BL/6 mice N = 6 f	↑ Locomotor activity in adult offspring	21 (GD1-21)	8.29 [a]	Same study as above. Single dose study with small number female mice; serum levels not measured but modeled; significance of effect has been questioned. (Used as POD in draft ATSDR (2018a) MRL.)
Mammary gland				
Macon et al. (2011) CD-1 mice N = 13 f	Impaired development of mammary glands in offspring	17 (GD1-17)	0.285 [b]	Biological significance of the effects have been questioned as they did not lead to any apparent functional impairment based on nursed pups, which exhibited normal growth (White et al. 2011)[c]; response measures based on qualitative mammary histology scores raise concerns regarding data quality and reproducibility[d]. (Not used as POD by any regulatory agency.)
Tucker et al. (2015) CD-1 mice N = 4 -12 f	Developmental delays in the mammary glands on PNDs 35 (26%) and 56 (30%) in CD-1 mice Developmental delays in the mammary glands on PNDs 21 (38%) and 61 (25%) in C57BL/6 mice	17 (GD1-17)	PND 1 serum concentration not reported	Same comments as above.

[a] Average serum concentration modeled by ATSDR (2018a) using PBPK model by Wambaugh et al. (2013) to estimate a time weighted average (TWA). Compare to a serum concentration of 38 mg/L at the USEPA POD.

[b] A Benchmark Dose lower confidence limit (BMDL) of 0.025 mg/L average serum concentration can be estimated.

[c] This is consistent with the effect not being biologically significant but is based on limited data and no overall assessment of the nutritional composition of the milk.

[d] These concerns are mitigated by the use of averaged histology slide scores of two pathologists, blind to treatment group and the fact that these PFOA effects were observed in several studies from the same research group.

m = male; f = female; N = number of animals; DNT = developmental neurotoxicity; GD = gestational day; PND = postnatal day.

Table 4. Hepatic Studies with Lower PODs than Used by USEPA (2016a) to Derive Candidate RfDs for PFOA

Study type/Reference	Endpoint	Dosing duration (days)	LOAEL (Av serum mg/L) [a]	Comments
Developmental Liver Effects				
Quist et al. (2015a,b) CD-1 mice Mouse CD-1 N = 17 – 21 dams/dose 7 -10 f pups (1 per dam)	↑ Severity of hepatocellular hypertrophy at PND 91 and periportal inflammation on PND 21 at ≥0.01 mg/kg-day ↑ Serum total cholesterol, LDL, and HDL levels in high-fat fasted animals on PND 91	17 GD1- 17	Not measured	Only female offspring were investigated; incidence for liver effects not reported; serum levels not measured. It is not known whether these sensitive hepatic effects resulted from *in utero* exposure, lactational exposure, or both.
Filgo et al. (2015) CD-1 mice 129/Sv WT; N = 6-10 f offspring	Increase in severity of centrilobular hepatocyte hypertrophy with significant trend for incidence	17 GD1- 17	12.5 (predicted serum level, ATSDR 2018a)	Only a small number of female offspring were investigated; dose response not clearly exhibited; and serum levels not reported. (Study discussed by ATSDR (2018a) and NJDWQI (2017).)
Macon et al. (2011) CD-1 mice N = 13 f	↑ Relative liver weight on PND 7	17 (GD1-17)	4.98 [b]	Effect diminished after exposure stopped, statistical significance lost by PND14. (Cited by NYDOH in support of PFOA drinking water value).
Non-developmental liver effects				
Loveless et al. (2006) Crl:CD mice N = 10 m	Significant ↑ relative liver weight with hepatocellular hypertrophy	14	13 [b]	The significance of these effects has been questioned on the basis of Hall et al. (2012). However, these effects were considered relevant and significant and were used by NJDWQI (2017) and NHDES (2019b) as a basis for their RfDs.

[a] Average serum concentration modeled by ATSDR (2018a) using PBPK model by Wambaugh et al. (2013) to estimate a TWA.

[b] Measured concentration. N = number of animals tested per group; m = male animals, f = female animals; LDL = low-density lipid protein; HDL = high-density lipid protein.

adverse due to the absence of degenerative lesions or inflammation. In review articles compiled by Bjork et al. (2011) and Hall et al. (2012), the involvement of the peroxisome proliferator activated receptor alpha (PPAR-α) receptor pathway in PFAS liver toxicity was cited as a reason to discount the relevance of certain liver effects observed in response to PFAS in rodents to humans. However, another review article by Guyton et al. (2009) included data that raise questions about whether the hypothesized PPAR-α activation mode of action (MOA) is either necessary or sufficient for rodent liver effects, including hepatocarcinogenesis. Experimental studies that were conducted in standard strains of rats and mice, PPAR-α null mice, and humanized PPAR-α mice provide compelling data that hepatic effects of PFOA are not solely dependent on PPAR-α receptor activation (Abbott et al. 2007; Minata et al. 2010; Nakagawa et al. 2012; Albrecht et al. 2013; Filgo et al. 2015; Tucker et al. 2015). Based on this scientific evidence, the NJDWQI (2017) and the NHDES (2019b) concluded that the noted hepatic effects are well-established effects of PFOA and other PFAS and are relevant to human health risk assessment. Both agencies used PFOA induced liver effects as an endpoint to derive their respective RfDs.

MassDEP ORS has concluded, based on current data, that the various hepatic effects observed in animals are relevant to humans and further support a lower RfD than that developed by the USEPA (2016a) for PFOA.

2.3.2 *PFOS*

Low doses of PFOS have caused immune related effects in several studies (Table 5). Although there is variability in reported effect levels across the various animal immunotoxicity studies, data from several studies noted in Table 5 indicate that immunotoxicity endpoints are more sensitive than those relied upon by USEPA in its RfD derivation for PFOS (USEPA 2016b).

In USEPA's RfD derivation, candidate RfDs were not selected based on these effects nor were they accounted for in the uncertainty factors applied by USEPA. In light of the NTP (2016) conclusion that PFOS should be presumed to be an immune hazard to people based on a high level of evidence from animal studies and a moderate level of evidence from studies in humans, MassDEP ORS believes that it is appropriate to account for immunotoxicity effects in the derivation of an RfD for PFOS.

The relevance of PFOS animal immunotoxicity observations is supported by data from a number of epidemiological studies reviewed by NTP (2016), EFSA (2018a) and NJDWQI (2018). As noted below, concerns over PFOS immunotoxicity have been reflected in the toxicity values derived by a number of organizations, all of which are lower than the USEPA RfD (Table 8). PFOS toxicity values derived by ATSDR (2018a), NJDWQI (2018), MDH (2019a), NHDES (2019b), and MISAW (2019) either relied upon immunotoxicity endpoints as the critical effect

Table 5. Immunotoxicity Studies with Lower PODs than Used by USEPA (2016) to Derive Candidate RfDs for PFOS

Study Type/Reference	Endpoint	Dosing duration (days)	NOAEL (Av serum mg/L)[a]	LOAEL (Av serum mg/L)[a]	Comments
Dong et al. (2009) C57BL/6 mice N = 10 m	Impaired response to SRBC	60	0.674	6.26	NTP rated this study as "probably having high risk of bias" due to uncertainty regarding whether the research personnel were blinded; small dose groups. (Study selected by NJDWQI, MISAW as bases for PFOS RfD derivation.)
Dong et al. (2011) C57BL/6 mice N = 6 m	Impaired response to SRBC	60	2.36	10.75	NTP rated the study as "probably having high risk of bias" due to uncertainty regarding whether the research personnel were blinded; small dose groups. (Study selected by MDH, NHDES as bases for PFOS RfD derivation.)
Peden-Adams et al. (2008) B6C3F1 mice m, f (inbred mice between C57BL/6N and C3H/HeL strains) N = 5	Impaired response to SRBC	28	0.0178	0.0915 m 0.67 f	Corticosteroid levels that may be related to low level effects were not measured; small dose groups; different strain of mice used than the other listed immune studies; some measured immune effects inconsistent with the longer duration studies; NTP rated the study as 'probably having high risk of bias" due to uncertainty regarding whether the research personnel were blinded; LOAEL dose inconsistent with other available studies. (Study not selected by any agency for RfD derivation.)
Gurudge et al. (2009) B6C3F1 mice f; (inbred mice between C57BL/6N and C3H/HeL strains) N = 30 (at 21 days 3/mice per group killed to collect blood and the rest (27 animals/dose group) were challenged with flu virus	↓ Host resistance to influenza virus	21	0.189	0.670	NTP concluded that there is "serious risk of bias with this study" due to concerns about investigator blinding and unexplained attrition in the dose groups; only measured survival rate with no immunological endpoints; and only two dose groups used. (Study not selected by any agency for RfD derivation.)

[a] Average serum concentration modeled by ATSDR (2018a) using PBPK model by Wambaugh et al. (2013) to estimate a TWA.

m = male; f = female; N = number of animals; IgM = immunoglobulin M; SRBC = sheep red blood cell

Note: Immunotoxicity concerns were addressed through application of an UF by ATSDR (2018a). Immunotoxicity PODs were the basis of the PFOS RfDs by MDH, NJDWQI, NHDES, MISAW and NYDOH.

POD or applied an additional UF in their toxicity value derivations to account for, in part, concerns about potentially lower dose immunotoxicity effects.

Based on its review of the data, MassDEP ORS has concluded that the overall evidence regarding immunotoxicity is convincing and sufficient to support a lower RfD for PFOS than previously derived by USEPA (2016b). However, the utility of the available studies for providing an alternative POD is limited by several issues including variable results; uncertainties relating to the execution of some studies, which raise some concerns about potential study bias (as noted in the NTP 2016 review); and small sample sizes (Table 5). Consequently, MassDEP ORS elected not to rely on the immunotoxicity study data to identify an alternative POD. Instead, as discussed below, MassDEP ORS concluded that it is more appropriate to account for this data by including an additional UF for database uncertainty in the PFOS RfD derivation.

2.4 Uncertainty Factors

When deriving an RfD, uncertainty factors (UF) are used to account for a number of areas of uncertainty and variability. These UF are applied in the extrapolation from a study providing a POD to a daily dose that is intended to be without appreciable risk of deleterious effects to the human population, including sensitive subpopulations, during a lifetime of exposure.

Table 6. Uncertainty Factors Used in the Derivation of an Reference Dose (RfD)

Animal to human extrapolation or interspecies (UF_A)	Factor is used to account for uncertainty in extrapolating data from laboratory animals to humans. A factor of 10 is considered to account for both toxicokinetic and toxicodynamic processes. When chemical- and study-specific approaches are used to adjust the animal dose, e.g., toxicokinetic data or body weight scaling, the factor is typically reduced to $10^{1/2}$ to account for the remaining toxicodynamic differences between the species.
Human variation or intraspecies (UF_H)	Factor is used to account for variation in sensitivity among humans.
Subchronic to chronic (UF_S)	Factor is used to adjust the POD from a study of less than chronic duration to account for additional responses that may occur at lower doses following a longer exposure duration.
LOAEL to NOAEL (UF_L)	Factor is used to adjust the dose where an adverse effect was observed to a dose that is below the threshold for the adverse effects, a no effect level.
Database limitations (UF_D)	Factor is used to adjust for the possibility that a more sensitive effect, i.e., one that occurs at a lower dose, may be identified if additional studies were conducted.

The UF and associated sources of uncertainty are briefly described in Table 6. UFs are assigned a value of 1, 10 or the square root of 10 ($10^{1/2}$) (USEPA 2002a). During the calculation of the total or composite uncertainty factor value to apply to a POD, a single partial uncertainty factor is given value of 3 and two partial uncertainty factors are given a value of 10.

When deriving an RfD, a database uncertainty factor (UF_D) is employed when the database for a chemical is judged to have gaps or available data indicate more sensitive effects may exist. It decreases the RfD by a factor of 10 or $10^{1/2}$ to account for the possibility that a lower POD (or more sensitive effect) could have been identified if the database was more complete (USEPA 2002a).

The selection of a particular value for an uncertainty factor depends on the quality of the studies available, the nature and extent of the database, the relevance of the observed effects to humans and scientific judgement (USEPA 2002a). Professional judgement and differing interpretations of the data may lead to selection of alternate values for an uncertainty factor by different groups evaluating the same database.

2.4.1 *Selection of the Database Uncertainty Factor Value*

MassDEP ORS selected a factor of $10^{1/2}$ rather than 10 as the UF_D to account for data uncertainties regarding the lower dose effect data for PFOA and PFOS previously discussed. This decision was based on professional judgement and consideration of the following factors: extent of available data; serum concentrations at key effect and no effect levels; and the magnitude of the composite uncertainty factor. Decisions by various other agencies regarding the need for a UF_D and the reasons provided to support the UF_D used during derivation of their RfDs for PFOA and PFOS are also noted.

2.4.1.1 PFOA

MassDEP ORS compared the PFOA serum concentrations at the PODs selected by other agencies for sensitive endpoints (Table 7) to the equivalent USEPA (2016a) values[6]. This provides insight into the magnitude of the differences, which reflect sensitivity and experimental factors. The serum LOAEL (13 mg/L) for the more sensitive hepatic endpoint selected by NJDWQI (2017) and NHDES (2019b) is approximately 3 times lower than the serum LOAEL at the USEPA (2016b) POD.[7] The serum LOAEL selected by ATSDR (2018a) and MISAW (2019)

[6] Comparing the animal serum levels rather than human equivalent doses (HED) or final RfDs avoids the uncertainty and variability introduced by the selection of differing kinetic parameters such as half-lives, clearance values, and differing uncertainty factors. See Appendix 3 for discussion of HED and serum half-life.

[7] The BMDL of 4.35 mg/L used by NJDWQI (2017) and NHDES (2019b) as the POD is roughly 10-fold lower than the USEPA (2016a) POD (38 mg/L). However, the USEPA POD is based on a LOAEL, which when adjusted by the UF_L (LOAEL to NOAEL adjustment), is approximately equivalent to the BMDL PODs used these states agencies. The 10-fold lower final RfD derived by NJDWQI (2017) vs. the USEPA RfD is attributable to inclusion of an additional UF_D of 10 used to account for potentially more sensitive developmental effects (mammary gland data).

(8.29 mg/L)[8] based on neurodevelopmental and skeletal effects in animals exposed *in utero,* is roughly 5 times lower than the USEPA (2016a) serum LOAEL of 38 mg/L for developmental delays (Table 7). These comparisons indicate that an UF_D of $10^{1/2}$ would more closely account for the differences in sensitivity than a UF_D of 10.

MassDEP ORS also considered the magnitude of the composite UF that would result from application of the two UF_D options. For PFOA, application of an additional UF_D of 10 to the USEPA RfD derivation would lead to a total UF of 3000. This is the maximum recommended composite or total UF per USEPA guidance (USEPA 2002a). Given the nature of the toxicology data available for PFOA, which is fairly extensive compared to that available for many chemicals and includes sensitive endpoints, MassDEP ORS concluded that such a high total UF could overestimate the remaining uncertainty.

MassDEP ORS also considered UF_D values selected by other agencies who took this approach. To account for other potentially more sensitive effects, both NJDWQI (2017) and NHDES (2019b) applied an UF_D to their selected POD, which was based on liver effects. NJDWQI (2017) chose to use a factor of 10 while NHDES (2019b) chose a factor of 3. NHDES concluded that "there is insufficient evidence supporting the application of the more conservative full database uncertainty factor of 10" and "application of an uncertainty factor of 3 is appropriately protective without being overly conservative given the critical health effect selected and the existing database" (NHDES 2019b).

In consideration of these factors and based on professional judgement, MassDEP ORS concluded that a database UF_D value of $10^{1/2}$ is appropriate at this time to account for potentially more sensitive PFOA effects.

2.4.1.2 PFOS

MassDEP ORS compared the PFOS serum concentrations at the PODs selected by other agencies for sensitive endpoints (Table 8) to the equivalent USEPA (2016b) values. ATSDR (2018a), NJ DWQI (2018), MDH (2019a), NHDES (2019b) and MISAW (2019) all have accounted for potentially more sensitive immunological effects in their RfD derivations for this compound (Table 8). NJDWQI (2018), MDH (2019a), NHDES (2019b) and MISAW (2019) selected alternative PODs based on more sensitive immunotoxicity endpoint data. ATSDR (2018a) applied an UF_D of 10 in its draft MRL derivation for PFOS to account for potentially more sensitive immunotoxicity effects.

[8] The POD serum level selected by ATSDR (2018a) is based on a single dose study with relatively small numbers of animals.

Table 7. Human Equivalent Doses (HEDs) and RfDs Derived from the Modeled Animal Average Serum Values of PFOA by Various Agencies

Agency	Study	Dosing duration (days)	LOAEL (Av serum mg/L)	HED (ug/kg-day)	UFs (total and components)	RfD (mg/kg-day)
USEPA (2016a)	Lau et al. (2006) CD-1 mice Decreased pup ossification and accelerated male puberty	17	38 [a]	5.3	300 UF_H = 10 UF_A = 3 UF_L = 10	2 x 10^{-5}
ATSDR (2018a)	Onishchenko et al. (2011) C57BL/6 mice Neurodevelopment; Koskela et al. (2016) Skeletal development	17	8.29 [b]	0.821	300 UF_H = 10 UF_A = 3 UF_L = 10	3 x 10-6
MDH (2018a)	Lau et al. (2006) CD-1 mice Decreased pup ossification and accelerated male puberty	17	38 [a]	5.3	300 UF_H = 10 UF_A = 3 UF_L = 3 mild effect **UF_D = 3 no 2-generation**	2 x 10^{-5} (1.8 x 10^{-5})
NJDWQI (2017)	Loveless et al. (2006) CRL:CDs mice Increased relative liver weight	14	13 [c]	0.61 [d]	300 UF_H = 10 UF_A = 3 **UF_D = 10 developmental mammary**	2 x 10^{-6}
NHDES (2019b)	Loveless et al. (2006) CRL:CDs mice Increased relative liver weight	14	13 [c]	0.61 [d]	100 UF_H = 10 UF_A = 3 **UF_D = 3 developmental mammary**	6 x 10^{-6} (6.1 x 10^{-6})

Agency	Study	Dosing duration (days)	LOAEL (Av serum mg/L)	HED (ug/kg-day)	UFs (total and components)	RfD (mg/kg-day)
MISAW (2019)	Onishchenko et al. (2011) C57BL/6 mice Neurodevelopment; Koskela et al. (2016) Skeletal development	17	8.29 [b]	1.163	300 UF_H = 10 UF_A = 3 UF_L = 3 **UF_D = 3 endocrine effects**	4 x 10^{-6} (3.9 x 10^{-6})
NYDOH (2019)	Macon et al. (2011) CD-1 mice Increased pup relative liver weight on PND 7 male and female pups	17	4.98 [e]	0.15 [d]	100 UF_H = 10 UF_A = 3 **UF_D = 3**	1.5 x 10^{-6}
WIDHS (2019)	Lau et al. (2006) CD-1 mice Decreased pup ossification and accelerated male puberty	17	[f]	0.54 (HED_{50})	300 UF_H = 10 [g] UF_A = 3 UF_L = 10	2 x 10^{-6}
MassDEP ORS	Lau et al. (2006) CD-1 mice Decreased pup ossification and accelerated male puberty	17	38 [a]	5.3	1000 UF_H = 10 UF_A = 3 UF_L = 10 **UF_D = 3 developmental mammary and liver**	5 x 10^{-6} (5.3 x 10^{-6})

[a] Average serum concentration modeled by USEPA (2016a) using Wambaugh et al. (2013) to estimate an AUC.

[b] Average serum concentration modeled by ATSDR (2018a) using Wambaugh et al. (2013) to estimate a TWA.

[c] Measured serum concentration at LOAEL; BMDL of 4.35 mg/L used as POD.

[d] Back calculated from RfD.

[e] Measured serum concentration.

[f] Kinetic model by Kieskamp et al. (2018) based on fetal and child dosimetry used to model the USEPA LOAEL from Lau et al (2006) study.

[g] The UF values for UF_A and UF_H confirmed by personal communication with S Young.

Table 8. Human Equivalent Doses and RfDs Derived from the Modeled Animal Average Serum Values of PFOS by Various Agencies

Agency	Study/Endpoint	Dosing duration (days)	NOAEL (Av serum mg/L)	HED (ug/kg-day)	UFs (total and components)	RfD (mg/kg-day)
USEPA (2016b)	Luebker et al. (2005a) Sprague-Dawley rat Decreased F2 pup body weight	84	6.26 [a]	0.51	30 UF_H = 10 UF_A = 3	2×10^{-5} (1.7×10^{-5})
ATSDR (2018a)	Luebker et al. (2005a) Sprague-Dawley rat Delayed eye opening and decreased F2 pup body weight	84	7.43 [b]	0.51	300 UF_H = 10 UF_A = 3 **UF_D = 10 immune effects**	2×10^{-6}
MDH (2019a)	Dong et al. (2011) C57BL/6N mice Suppressed immune response	60	2.36 [c]	0.31	100 UF_H = 10 UF_A = 3 **UF_D = 3 thyroid effects**	3×10^{-6} (3.1×10^{-6})
NJDWQI (2018)	Dong et al. (2009) C57BL/6N mice Suppressed immune response	60	0.674 [c]	0.054	30 UF_H = 10 UF_A = 3	2×10^{-6} (1.8×10^{-6})
NHDES (2019b)	Dong et al. (2011) C57BL/6N mice Suppressed immune response	60	2.36 [c]	0.31	100 UF_H = 10 UF_A = 3 **UF_D = 3 thyroid effects**	3×10^{-6}
MISAW (2019)	Dong et al. (2009) C57BL/6N mice Suppressed immune response	60	0.674 [c]	0.0866	30 UF_H = 10 UF_A = 3	3×10^{-6} (2.9×10^{-6})
NYDOH (2019)	Same as NJ					
WIDHS (2019)	Same as ATSDR					

Agency	Study/Endpoint	Dosing duration (days)	NOAEL (Av serum mg/L)	HED (ug/kg-day)	UFs (total and components)	RfD (mg/kg-day)
MassDEP ORS	Luebker et al. (2005a) Sprague-Dawley rat Decreased F2 pup body weight	84	6.26 [a]	0.51	100 UF_H = 10 UF_A = 3 **UF_D = 3 immune effects**	5×10^{-6} (5.1×10^{-6})

[a] Average serum concentration modeled by USEPA (2016a) using Wambaugh et al. (2013) to estimate an AUC.

[b] Average serum concentration modeled by ATSDR (2018a) using Wambaugh et al. (2013) to estimate a TWA.

[c] Measured serum concentration

NJDWQI (2018) and MISAW (2019) relied on data from Dong et al. (2009), and MDH (2019a) and NHDES (2019b) on the data from Dong et al. (2011) as PODs[9]. These studies were conducted by the same investigators using the same mouse strain. The latter study included an additional dose between the NOAEL and the LOAEL identified in the Dong et al. (2009) study. Because of the additional dose group, MassDEP ORS concluded that the later study likely provides a better NOAEL estimate.

The measured NOAEL serum concentration of 2.36 mg/L from Dong et al. (2011) can be compared to the measured serum concentration of 4.52 mg/L at the POD NOAEL in the critical study selected by USEPA (2016b) (Luebker et al. 2005a) as the basis of its RfD derivation. These values differ by about a factor of 2 (Table 8)[10]. This suggests that a UF_D of 10 may be unnecessarily conservative and supports the application of an UF_D of 3 to account for potentially more sensitive immune effects.

Based on professional judgement and in consideration of the factors noted above, MassDEP ORS has concluded that a database UF value of $10^{1/2}$ is appropriate at this time to account for potentially more sensitive PFOS effects.

2.5 Carcinogenicity of PFOA and PFOS

As of June 29, 2019, the cut-off date for information considered in this assessment, limited human and animal data were available on the potential carcinogenicity of PFAS. The C8 study of people exposed to PFOA and other PFAS concluded that the data from that population supported a probable link between exposure and cancers of the kidney and testes (Barry et al. 2013). No potency estimates were derived. Animal bioassay data from the NTP (NTP 2019c) reported elevated pancreatic and liver tumor rates following high dose exposures to PFOA. Although NTP has issued summary data tables for this study, a final report has not been published. As of June 29, 2019, no agency had established drinking water values based on carcinogenicity.[11]

[9] MDH (2019a) and NHDES (2019b) applied an UF_D of 3 to their RfD derivations to address concerns about limited data on maternal and developmental thyroid hormone levels and developmental immunotoxicity. MassDEP ORS agrees that additional data are needed to better understand the potential for these effects.

[10] This comparison of serum concentrations is complicated by data from Dong et al. (2012) where the same applied dose used in Dong et al. (2011) resulted in a measured serum concentration of 4.35 mg/L, roughly twice that measured in Dong et al. (2011) and equivalent to the concentration measured in Luebker et al. (2005a). These differences in serum concentrations from the same exposure dose, study design and research group indicate that variability in responses and analytical measurements can be significant and provide a caution regarding interpretation of modest differences in PODs based on reported or modeled results.

[11] In August 2019, the California (CA) Office of Environmental Health Hazard Assessment (OEHHA) issued updated Notification Level Recommendations for PFOA and PFOS (CA OEHHA 2019). The OEHHA document includes an assessment of potential cancer risk for PFOA and PFOS and an associated drinking water notification level of 0.1 ppt at a one in a million excess cancer risk over a lifetime of exposure for PFOA and 0.4 ppt for PFOS. MassDEP has not reviewed this assessment and the corresponding data at this time but notes that these drinking water values are well below the level that can be reliably detected. The CA State Water Boards Division of Drinking Water ultimately did not base its updated drinking water notification levels on these cancer risk values.

The mechanism(s) of action for the reported carcinogenic effects is unclear. These compounds do not appear to be directly genotoxic but may enhance the generation of genotoxic compounds through secondary mechanisms (e.g. peroxisome proliferation). Thus, the observed effects may be due to nonlinear mechanisms of action, so the appropriate extrapolation approach from high to low doses is uncertain.

The cancer data is concerning to MassDEP because some carcinogens can present a degree of risk at any exposure level. To account for this potential risk, MCL goals (MCLGs) of zero have been established for some chemicals and may ultimately be warranted for certain PFAS. At this time, however, the level of cancer risk posed by these compounds is unclear. Until the cancer data on these compounds is better understood, MassDEP ORS has decided to focus on the non-cancer risks of these compounds, in particular those of concern following shorter-term exposures. MassDEP ORS will follow and assess research in this area to determine if future revisions to the drinking water values are needed.

2.6 Conclusions

MassDEP ORS assessed the data demonstrating that adverse effects of concern occur at exposure levels below those relied upon in the derivation of the current USEPA RfD for PFOA and PFOS and found this data, taken as a whole, to be compelling. Various organizations have reached differing conclusions regarding POD selection and questions have been raised regarding data limitations and interpretation relating to some individual study results. MassDEP has noted some of the issues that have been identified regarding key PFOA and PFOS toxicology studies and endpoints, which include: differences in the extent and type of data available for various endpoints; uncertainties with respect to experimental protocols, including number of dose groups, dosing ranges, exposure periods and measures of serum concentrations; and differences in interpretation of the data among toxicologists and regulatory organizations and in the scientific literature regarding the functional significance of some of the lowest dose effects.

MassDEP ORS considered several approaches to account for this data including selection of lower dose PODs; application of an additional UF of 10; and application of an additional UF $10^{1/2}$. Rather than rely on the selection of an alternative POD, MassDEP has decided that it is most appropriate to account for the lower dose effect data by applying an additional UF of $10^{1/2}$ in the RfD derivations for PFOA and PFOS.[12] This approach reflects the range and overlap of observed effects and avoids the uncertainties and limitations associated with specific study PODs. A UF of $10^{1/2}$ was selected based on consideration of the magnitude of the resulting composite UF and because it more closely accounts for the noted differences in potential PODs. Using this approach, the RfD derived for PFOA or PFOS is 5×10^{-6} mg/kg-day, rounded to one

[12] The application of an added UF to account for data indicating lower dose effects has been used by ATSDR, NJDWQI, MDH, NHDES and MISAW in their PFAS toxicity value derivations and is consistent with USEPA guidance.

significant figure[13]. MassDEP notes that this approach does not negate, nor is it inconsistent with, selection of alternative PODs based on differing study and data interpretations.

The revised RfDs account for the animal bioassay data demonstrating lower dose effects; provide a greater degree of health protection to sensitive populations than the USEPA (2016a,b) RfD; and fall within the range of the RfDs developed by USEPA and other agencies using different PODs, endpoints, and animal to human extrapolation parameters, which range from 2×10^{-6} to 2×10^{-5} for PFOA and PFOS.

3.0 BASIS OF RFDS FOR OTHER PFAS IN THE SUBGROUP

The available data for the rest of the PFAS subgroup evaluated here is more limited than that for PFOA and PFOS. To estimate toxicity values (RfDs) for PFNA, PFHxS, PFDA and PFHpA, given the limitations of the data, several options can be considered: use available data to derive individual RfDs; use toxicologically similar chemicals as surrogates; or evaluate whether the available data can provide estimates of relative toxicity. Each option has strengths and limitations. Following our analysis, we elected to continue to use toxicologically similar chemicals as surrogates for less studied members of the PFAS subgroup.

Previously, using a surrogate approach, MassDEP (2018b) and CTDPH (2017) extended the USEPA HA values for PFOA and PFOS (USEPA 2016c,d) to three additional longer-chain PFAS - PFNA, PFHxS and PFHpA - treating all five compounds as being equipotent. The Vermont Department of Health (2018) has also taken this approach but adopted a drinking water value of 20 ppt for these five compounds based on alternative exposure parameters. Since MassDEP's last evaluation of the longer-chain subgroup of PFAS, several states and ATSDR have derived RfDs or draft MRLs for PFNA and PFHxS using new and existing data.

This section:

- Evaluates toxicological similarity and differences across the PFAS.
- Evaluates data pertinent to the potential derivation of relative potency factors (RPFs) across this subgroup of PFAS and investigates whether this approach can support toxicity values for the data poor PFAS in this subgroup.
- Selects toxicity values for PFNA, PFHxS, PFDA and PFHpA.

[13] Alternative ways of addressing the low-dose data, including the addition of a UF of 10, or use of lower PODs based on immune, liver or mammary gland effects could result in RfDs that are lower (more conservative) than those proposed by MassDEP. Rejection of all the lower dose study data would lead to no change to the USEPA RfD.

3.1 Evaluation of Toxicologic Similarity

Toxicity Values Derived by Various Agencies

NJDWQI, MDH, NHDES and MISAW have developed individual RfDs and drinking water values for PFNA and PFHxS. ATSDR (2018a) has also derived draft MRL values for PFNA, and PFHxS. No RfDs have been developed for PFDA and PFHpA. These RfDs and draft MRLs are presented in Table 9. Associated drinking water values and critical elements of their derivation are presented in Appendix 1, Table 1. Summaries of key studies available for PFNA, PFHxS, PFDA and PFHpA and interpretation by various agencies that evaluated them are presented in Appendix 2.

PFNA RfDs were developed by NJDWQI, MDH, NHDES and MISAW using the same animal study (Das et al. 2015) but different endpoints (developmental delays and decreased pup body weight gain; increased maternal liver weight), points of departure (NOAEL, $BMDL_{10}$), uncertainty factors, and parameters for extrapolation to human equivalent dose. The four RfDs for PFNA range from 7.4×10^{-7} to 4.3×10^{-6} mg/kg-day (6-fold). MDH, NHDES and MISAW derived RfDs for PFHxS ranging from 4×10^{-6} to 2×10^{-5} mg/kg-day (5-fold) based on three different animal studies, different endpoints and various parameters for extrapolating to humans.

The RfDs for PFNA and PFHxS, which compared to PFOA and PFOS, have more limited available data to support derivation of candidate RfDs, overlap the range of values derived for PFOA and PFOS, the most well studied of the PFAS (Table 9). The majority of the RfDs derived for PFNA and PFHxS are within 2-fold of the RfD MassDEP ORS derived for PFOA and PFOS, 5×10^{-6} mg/kg-day. These differences are within the range of uncertainty inherent in all RfDs derived by USEPA (2019a) and thus support MassDEP's decision to include these compounds in an equipotent subgroup.

While no RfD has been published for PFDA, MISAW noted that longer-chain PFAS such as PFDA may pose risks of adverse effects and thus should not be ignored when detected. Using a read-across[1] approach based on chemical similarity, they recommended that the drinking water value for PFNA be used as a screening level in the absence of an individual drinking water level for longer chain PFAS like PFDA (MISAW 2019).

Serum Half-Lives

Serum half-life is a metric used to estimate the elimination of a substance from the body and is used in the extrapolation from animal effect level to human equivalent dose when deriving an RfD. For chemicals/substances that are slowly eliminated from the body, such as PFAS, serum half-lives are long. Compounds with long half-lives can accumulate in the body, leading to extended internal exposures at target tissues and in target organs, and are thus of particular concern.

Table 9. RfDs Derived by States for PFOA, PFOS, PFNA, PFHxS, and PFDA

	RfD or MRL (mg/kg-day)[a]					
	PFOA	PFOS	PFNA	PFHxS	PFDA	Range of Values across Compounds
USEPA (2016a,b)	2×10^{-5}	2×10^{-5}	---	---	---	Same
ATSDR (2018a)	0.27×10^{-5}	0.2×10^{-5}	0.3×10^{-5}	2×10^{-5}	---	$0.2 - 2 \times 10^{-5}$
MDH	2×10^{-5} (2018)	0.31×10^{-5} (2019a)	---	0.97×10^{-5} (2019b)	---	$0.31 - 2 \times 10^{-5}$
NJDWQI	0.2×10^{-5} (2017)	0.2×10^{-5} (2018)	0.074×10^{-5} (2015)	---	---	$0.074 – 0.2 \times 10^{-5}$
NHDES (2019b)	0.61×10^{-5}	0.3×10^{-5}	0.43×10^{-5}	0.4×10^{-5}	---	$0.3 – 0.61 \times 10^{-5}$
MISAW (2019)	0.4×10^{-5}	0.3×10^{-5}	0.22×10^{-5}	0.97×10^{-5}	0.22×10^{-5} [b]	$0.22 - 0.97 \times 10^{-5}$
WIDHS (2019)	0.18×10^{-5}	0.2×10^{-5}	---	---	---	---
Range of Values Across Agencies	$0.2 - 2 \times 10^{-5}$	$0.2 - 2 \times 10^{-5}$	$0.074 - 0.43 \times 10^{-5}$	$0.4 - 2 \times 10^{-5}$	NA	$0.074 - 2 \times 10^{-5}$
MassDEP (Section 2)	0.5×10^{-5}	0.5×10^{-5}	0.5×10^{-5}	0.5×10^{-5}	0.5×10^{-5}	not applicable

[a] The range of values reflects: differences in the extent of data available for each compound; uncertainty regarding interpretation of the available data; variability in experimental protocols (e.g. animals tested, dose selection and timing, endpoints evaluated) used to generate the data; and uncertainty and variability in selection of parameters, including serum half-life, used to derive the RfDs .

[b] MISAW (2019) recommended that the PFNA RfD be used as a screening level for longer- chain PFAS that lack individual health-based values.

Human half-life estimates for various PFAS are presented in Appendix 3. In summary, for the three compounds with reasonably robust data, reported central tendency values (geometric or arithmetic means) range from 2.3 - 3.9 years for PFOA; 1.9 - 18 years for PFOS and 5.3 -15.5 years for PFHxS. Within study estimates for PFHxS tend to be somewhat longer than for the PFOS and PFOA. The human data for PFNA, PFDA and PFHpA are limited and inadequate for meaningful comparison. However, animal data demonstrate that PFNA and PFDA also have very long half-lives and suggest that PFHpA's may be shorter.

The available human half-life estimates vary across studies and overlap from compound to compound within and across studies. When available, the data also indicates that great inter-individual variability in serum half-lives exists (Olsen et al. 2007, Nilsson et al. 2010). This is apparent in the ranges of values presented in Appendix 3. This variability may be due to a

combination of factors including actual differences in clearance rates across individuals; differences in ongoing exposures and whether they are explicitly accounted for in the estimate; and the use of different experimental and modeling approaches for estimating the values.

In general, the same relationships in half-lives across the PFAS are also observed in the animal data (Appendix 3).

Taken together the data indicate that these longer-chain compounds exhibit very long half-lives in people, which supports a high level of concern. Estimated half-life central tendency values for PFOA, PFOS and PFHxS overlap. Available data also indicate that half-life estimates for individuals are very variable and extensively overlap. Based on limited data PFHpA may have a shorter half-life compared to PFOS and PFOA. Variability in half-life values and their selection in determining human equivalent doses contribute to the variability in final RfD derivations across the various agencies.

Organ Systems Affected

Epidemiology and animal studies have identified affected endpoints associated with multiple organ systems following exposure to PFOA and PFOS, including liver, immune, development, and thyroid and endocrine systems (ATSDR 2018a, NTP 2016, USEPA 2016a,b)[14]. MassDEP evaluated similarities and differences in organ systems effects for each longer-chain PFAS based on key study endpoints selected as PODs for RfDs or candidate RfDs by USEPA and states. Appendix 4 presents and compares, in tabular format, key effect levels and/or PODs based on serum concentrations, by organ system. This evaluation included studies addressing effects on the liver, development and endocrine-thyroid for PFOS, PFOA, PFNA and PFHxS, and endocrine-thyroid effects for PFDA. The limited information for the toxicity of PFHpA did not permit evaluation of endpoints or target organs. In summary, the serum concentrations associated with the effect levels were within an order of magnitude or less, across the target organ systems for each PFAS considered. Additionally, across PFAS within the same target organ system, the effect levels varied by factors of 3-fold or less.

These results support the relative consistency of responses across the five PFAS in the three target organ systems evaluated.

3.2 Evaluation of Relative Potency Assessments and Exploration of Approaches Using NTP Bioassay Data (NTP 2018)

Comparing the relative toxicity among chemicals can be done quantitatively if similar data are available for each chemical. The relative potency factor (RPF) approach is a general method to quantitatively evaluate differences in potency for a group of chemicals acting through similar

[14] Available studies were limited for evaluating the immune responses for PFOA, PFNA, PFHxS and PFDA. Thus the immune system was not included in this summary.

modes of action or causing similar toxicological effects, using empirically derived scaling factors or RPF (USEPA 2000; ATSDR 2018b; Hertzberg and Mumtaz 2018).

USEPA has used relative potency approaches to evaluate pesticides with the same mode of action (USEPA 2002b) and chemical classes with a large number of structurally related congeners such as polycyclic aromatic hydrocarbons (PAHs) (USEPA 1993) and the receptor mediated biological responses to dioxin-like polychlorinated biphenyls (PCBs) (Van den Berg et al. 2006). RPFs do not generally make fine distinctions in potencies between compounds. Instead RPFs typically vary across compounds by multiples. For example, the USEPA RPFs developed for PAHs (USEPA 1993) are based on potency differences of an order of magnitude (10-fold), while the Toxic Equivalent Factors (TEF), a special case of relative potency factors used when the mechanism of toxicity is well understood, are half an order of magnitude ($10^{1/2}$ or 3-fold) for the data rich dioxin-like PCBs (Van den Berg 2006). The comparative potency databases for PFAS other than PFOA and PFOS are more limited and uncertain than that for PAHs and PCBs. Thus, MassDEP ORS has concluded that substantial differences in potency estimates are needed to firmly establish differences across compounds.

MassDEP evaluated available assessments and data on RPFs for PFAS. Peters and Gonzalez (2011) considered whether TEFs could be developed for perfluoroalkyl compounds. They concluded that mechanistic uncertainties and other data gaps precluded development of this approach for a broad class of perfluoroalkyl compounds. Since that publication, two more recent RPF assessments for PFAS have been completed addressing subsets rather than the broad class of PFAS. One, by Zeilmaker et al. (2018), derived putative RPFs based on data for several liver toxicity endpoints, and the second, by Luz et al. (2019), investigated potential RPFs based on liver, kidney and body weight effects from the NTP (2018) dataset. MassDEP further explored the utility of the NTP dataset for comparative potency evaluation using more robust dose metrics and benchmark dose analysis focusing on two sensitive endpoints, thyroid hormone and liver effects. The former was not addressed in the Lutz et al. (2019) analysis.

The next sections present an overall summary of the two RPF analyses as well as MassDEP's exploration of the NTP data set for RPF derivation, which is presented in detail in Appendix 5.

3.2.1 *Relative Potency Evaluations*

Zeilmaker et al. (2018) developed potential RPFs for several PFAS based on liver toxicity endpoints. This study identified subchronic exposure duration studies for twelve (12) PFAS ranging in carbon chain length from C4 to C18. The group of PFAS considered included PFOA, PFOS, PFNA and PFHxS. The common endpoints identified for these PFAS were measures of liver effects, including increases in absolute and relative liver weight and hepatic hypertrophy. The fitted dose-response function for each liver effect was used to calculate BMDs at 5% increases for absolute and relative liver weight or at 10% extra risk for liver hypertrophy using

external applied dose (mg/kg-day) as the dose metric. RPFs were calculated as the ratio of the BMD for the index chemical PFOA and BMDs for each of the other PFAS. For seven PFAS that did not have data sufficient to derive appropriate BMDs, "read across" values were used. The RPFs for the six PFAS being evaluated by MassDEP are included in Table 10 below. Four of these estimates were based on fitted response data and two on "read across."

Estimates of the RPF for PFOS and PFHxS were 2 and 0.6, respectively, based on relative liver weight. The PFNA RPF for this endpoint was 10 (Zeilmaker et al. 2018). However, there is less confidence associated with the PFNA RPF than the other RPF for several reasons; it was based on a study where PFNA was the main component in a mixture of other PFAS; the confidence intervals of the potency estimates based on different liver toxicity endpoints derived by Zeilmaker et al. (2018) overlapped with other PFAS in the subgroup being evaluated by MassDEP; and it is inconsistent with the toxicity values derived for PFNA, using other data, by NJDWQI, ATSDR, NHDES, and MISAW that varied by a factor of 2 or less from those derived by the same agency for PFOA (see Table 9).

RPF based on read across were reported as a range bounded by the PFAS with 1± carbon. Thus, PFHpA RPF estimates ranged from 0.01, based on read across from PFHxA, to 1, based on read-across from PFOA. PFDA RPF estimates ranged from 4, based on read-across from PFUnDA to 10, based on read-across from PFNA. Where data were available, the range of RPF values over-lapped for one or more of the three liver effects considered in the Zeilmaker et al. (2018) analysis for the longer-chain PFAS that MassDEP is addressing. RPFs for additional endpoints could not be derived due to data limitations. Because these RPF are estimated based on applied dose, the authors suggested that some of the differences in the RPF estimates are likely related to differences in pharmacokinetics for the PFAS (Zeilmaker et al. 2018) suggesting that use of internal or human equivalent doses could yield improved potency comparisons.

Although the noted issues limit confidence in the derived RPFs, the analyses for the compounds with the most extensive data (PFOS, PFOA and PFHxS) fall within a factor of 2 for relative liver weight and the range of read-across values for PFHpA include an RPF of 1. The RPF of 10 for PFNA in the Zeilmaker et al. analysis is highly uncertain due to deficiencies in the underlying data used. Estimated PFDA RPFs range from 4-10, with the higher value being based on read-across from the questionable PFNA value and therefore does not provide reliable evidence of different potencies.

Luz et al. (2019) conducted a relative potency evaluation for the seven PFAS tested in the NTP 28-day bioassays (NTP 2018). Using BMDLs based on applied dose (mg/kg-day) because of poor model fits for the internal dose metric, they calculated RPFs for hepatocellular hypertrophy, liver weight, kidney weight, cholesterol, body weight and reticulocyte count. They derived RPFs

Table 10. RPF Determined Based on Relative Liver Weight in Male Rats using an Applied Dose Metric (mg/kg-day)

Congener	Zeilmaker et al. (2018)	Luz et al. (2019)
PFOA	1	1
PFOS	2	4
PFNA	10 [a]	2
PFHxS	0.6	0.5
PFDA	4 ≤ RPF ≤ 10 [a,b]	2
PFHpA	0.01 ≤ RPF ≤ 1 [b]	-

[a] Based on a study using a PFAS mixture. Other agencies have derived values within a factor of less than 2 vs. PFOA.
[b] estimated from read across.

for five of the six PFAS addressed herein (Table 10). For relative liver weight, the RPF for PFOS was 4, and for the other compounds 2, compared to PFOA. The RPF for PFNA in this assessment was 2. Again, some of the variability in these results may be explained in part by use of an external dose metric and the BMDL, rather than the BMD. These RPF estimates do not demonstrate a magnitude of difference needed to conclude potencies differ significantly across the compounds.

3.2.2 *MassDEP Relative Potency Evaluation Using NTP (2018) Dataset*

Expanding on the assessment of Lutz et al. (2019), MassDEP ORS further explored the potential utility of the data from the 28-day rat bioassays (NTP 2018) to derive RPF for PFOA, PFOS, PFNA, PFHxS and PFDA using internal dose and human equivalent dose metrics with Bayesian benchmark dose evaluation.

The NTP bioassays provide data on seven PFAS, including five of the longer-chain PFAS of interest in this evaluation. For each of these, thyroid and liver effects were observed.

Strengths of this dataset are that:

1) the results include information on a number of endpoints for each compound;
2) all experiments were conducted in the same species and stain;
3) the experimental protocol was consistent; and,
4) the same research group conducted the experiments.

However, this dataset also has a number of limitations, including:

1) the relatively short study duration of 28-days, which introduces uncertainty regarding whether responses would have occurred at lower doses after a longer duration for some of the reported endpoints;
2) the low dose portions of the dose response curves were not well characterized for the thyroid response, where the lowest dose tested for four of the five PFAS (PFOA, PFOS, PFNA, and PFHxS) caused near maximal (53% - 79%) decreases in fT4 compared to

controls (as discussed in Appendix 5) - additional information at lower doses could significantly alter estimates of concentrations associated with a specific response rate, especially for PFHxS, the compound that exhibits the largest difference in Bayesian Benchmark Dose (BBMD) values compared to the others, and for PFOA (see below and the dose response curves in Appendix 5); and,

3) the thyroid hormone bioassay method used by the NTP (2019a,b) for these bioassays could be impacted by presence of PFAS in the serum - NTP has stated that it is assessing this possibility (NTP 2019a,b).

These limitations introduce uncertainty in quantitative relative potency estimates derived from this data set for these compounds, thus limiting inter-compound potency comparisons.

Keeping these uncertainties in mind, MassDEP ORS conducted an explorative RPF assessment using this data. MassDEP ORS identified free thyroxine (fT4) serum concentration and relative liver weight in male rats as the most sensitive endpoints from this data set and selected them for dose-response evaluation and relative potency comparison.

Serum PFAS concentration (mg/L) and human equivalent doses (HED)(mg/kg-day), which account for potential differences in human pharmacokinetics between the PFAS[15], were used as dose metrics for comparing across the five PFAS. The Bayesian Benchmark dose modeling software (BBMD) (Shao and Shapiro 2018) was used for modeling these datasets. The BBMD software allows for modeling of the individual animal serum concentration and endpoint metric (i.e., serum thyroid hormone concentration or liver weight); handles variability in continuous data better than the USEPA BMD software (USEPA 2018; Shao et al. 2013); and can account for uncertainty in the choice of dose-response models (model uncertainty) through weighted model averaging.

Benchmark responses (BMR) for each modeled endpoint were selected as noted below. These considered biological significance (i.e., percent change from control considered adverse) and the magnitude of response observed in the dose response data. For the thyroid, a 20% decrease in serum fT4 was selected because the change from control at the lowest dose tested was greater than 50% for four of the five PFAS evaluated. Although a decrease in thyroid hormone levels from control of 20% is potentially useful for cross-compound potency comparisons, MassDEP notes that decreases of less than 20% may also be biologically significant.[16] A BMR of 5% change from control was selected for relative liver weight.

The upper portion of Table 11 presents the BBMDs estimated for each PFAS evaluated for the two most sensitive endpoints, free thyroxine (fT4) and relative liver weight, in units of serum

[15] See Appendix 5 for additional information on the parameters needed and calculation of a HED.
[16] Note: 50% change from control was also evaluated in order to have the BMR closer to the responses observed in the data (see results in Appendix 5).

PFAS concentration (mg/L) and HED (mg/kg-day). The RPFs, using PFOA as the index chemical, shown in the lower panel of the table, varied between the two endpoints. However, most RPFs were a factor of 2 or less with a maximum difference of 5-fold from PFOA for both animal internal doses and HED, derived as described in Appendix 5. Each compound exhibits a HED RPF of approximately one for either free T4 or relative liver weight. This analysis demonstrates that all these compounds caused similar effects for these endpoints, which occur at similar serum concentrations and HEDs.

Table 11. PFAS Relative Potency to PFOA: Endpoint and Exposure Metric Dependence

End Point	Free T4[a]	Relative Liver Wt	Free T4	Relative Liver Wt
Exposure Metric	**Serum (mg/L)**		**HED (mg/kg-day)[b]**	
BMR[c]	$BBMD_{20}$	$BBMD_{05}$	$BBMD_{20}$	$BBMD_{05}$
PFOA	18	13	0.0018	0.0013
PFOS	6.7	13	0.0005	0.0009
PFNA	5.6	13	0.0013	0.0021
PFHxS	36	82	0.0023	0.0053
PFDA	13	8	0.0014	0.0006
Relative Potency to PFOA				
PFOA	1	1	1	1
PFOS	3	1	4	1
PFNA	3	1	1	0.6
PFHxS	0.5	0.2	0.8	0.2
PFDA	1	2	2	2

[a] Male rat NTP (2018) data. A 20% decrease in fT4 serum concentration was used for comparative purposes in part because the response rates at the lowest dose tested were too high to use a smaller difference from control. Smaller decrements in thyroid hormones could be biologically significant and would likely lead to somewhat lower RfDs if used as a POD.

[b] Animal serum concentrations extrapolated to human equivalent dose using estimates of human half-life specific to each PFAS to estimate the external dose to humans needed to achieve the equivalent serum concentration as animals (Appendix 5). Uncertainty in half-life estimates is not accounted for.

[c] Model average BBMD values from Appendix 5. The central estimate of the serum concentration (BBMD) associated with the benchmark response (BMR), e.g., 20% decrease from control, rather than the 95% lower confidence interval of the estimated serum concentration (BBMDL), was used as the point of comparison across the PFAS. The BBMD estimate is a more stable estimate of the response as it is less influenced by the variability in the dataset.

3.2.3 *Conclusions for Relative Potency Evaluation*

The relative potency evaluations discussed above reaffirm that the compounds addressed herein exhibit similar toxicities with respect to the endpoints considered. The studies all yield potency estimates that, while not identical, are remarkably similar, despite the noted limitations in the

data. The RPF assessments do not provide evidence of a magnitude of difference sufficient to conclude the potencies of the compounds addressed by MassDEP ORS differ significantly[17].

3.3 Toxicity Values for PFNA, PFHxS, PFDA and PFHpA

Numerous assessments have documented that the toxicological database for PFOA and PFOS is far greater than that for other PFAS compounds. The more limited data for the other longer-chain PFAS considered in this document does, however, provide evidence for similarity in toxicological effects and effect levels for PFOS, PFOA, PFNA, PFHxS and PFDA. Insufficient toxicity data exist for PFHpA to assess similarities in effects.

The range of individual PFAS RfDs[18] derived by different agencies overlap the range of RfDs for each of the other individual PFAS. The similarity of RfDs for these PFAS indicates that the available data are not sufficient to firmly distinguish an individual RfD as being significantly different from another. The majority of the RfDs in Table 9 were within a factor of two (2) of the RfD MassDEP ORS derived for PFOA and PFOS, 5×10^{-6} mg/kg-day.

Our exploration of the RPF approach found that the current database of studies for PFAS yields effect levels that often overlap for one or more endpoints or do not achieve the magnitude of difference needed to demonstrate significantly different potencies.

In light of the above considerations and their close structural similarities, MassDEP has concluded that it is appropriate to continue to use a surrogate approach for the subgroup of other longer-chain PFAS considered in this assessment, and to apply the RfD for PFOA and PFOS as the toxicity value for PFNA, PFHxS, PFDA and PFHpA.

4.0 ADDRESSING EXPOSURES TO MULTIPLE PFAS

4.1 Evidence of PFAS Co-exposures and Approaches for Addressing

PFAS co-occur in some drinking water samples collected in Massachusetts, leading to exposure to a mixture of PFAS from a drinking water source. Co-exposures also occur via other media and exposure pathways. National monitoring has documented co-exposures to PFAS via serum

[17] RPFs cannot be assessed for other toxicologically significant effects within additional organ systems and life stages where effects have been observed, including development and immune, because the overall database for these PFAS is insufficient to evaluate quantitative differences in potency.

[18] Reference doses are intended to estimate a daily exposure to the human population, including susceptible subgroups, that is likely to be without appreciable risk of adverse effects during a lifetime (USEPA 2002a, 2019a). An RfD is understood to be uncertain given the uncertainty in the extrapolation from available animal data to estimated human exposure, with the uncertainty described as "perhaps spanning an order of magnitude" (USEPA 2019a).

concentration monitoring, as demonstrated in the data reported through the National Health and Nutrition Examination Survey (CDC 2019).

The prolonged serum half-lives (see Appendix 3) of the PFAS addressed herein, increase the likelihood of exposure of an internal biologic "target" to more than one PFAS at a time even if the (external) exposures are not concurrent, and also increase the duration of exposure at the "target" if (external) exposures are sequential.

These facts led MassDEP to consider approaches to addressing co-exposures. Two different overall approaches have been used to address PFAS co-exposures. These include treating exposures independently or additively[19]. Treating co-exposures independently assumes that the compounds do not contribute to the same toxicological effects and will underestimate risk if they do. Applying an additive approach is a more health protective approach and is consistent with the methods in use by USEPA and several states for PFAS and for other chemical classes.

With respect to PFAS, USEPA (2016c,d) applied dose addition in the drinking water HAs for PFOS and PFOA. This approach has also been used by most states, which have adopted the USEPA HAs. To date, Vermont, Connecticut, Massachusetts and Minnesota (using a combined hazard index approach) have also applied an additive approach to PFOA and PFOS and have included additional structurally-related longer-chain PFAS.

Additivity is also the basis for approaches that have been used for other groups of chemicals with similar structures, similar toxicologic effects and/or a common mode of action. For example, these include the relative potency (RPF) approaches used for evaluating PAHs (USEPA 1993) and the toxic equivalency factors (TEF) developed for dioxins and certain PCBs (Van den Berg et al. 2006).

The MCLs for the disinfection by products (DBP), trihalomethanes (THM) and haloacetic acids (HAA5), are also based on the arithmetic sum of individually monitored indicators for THM and HAA5 (Fed. Reg 1979, 1998, 2006). The rationale for adding the contribution of each of the indicator chemicals, including those with limited toxicity information, was based on structural similarity of the DBPs, best available information on health effects of other DBP, and co-occurrence of DBP.

In Massachusetts, dose addition is the basis for evaluating the potential noncancer hazard posed by exposure to multiple chemicals at a hazardous waste site regulated pursuant to the Massachusetts Contingency Plan (MCP). Under the MCP, a rebuttable presumption requires hazard quotients of each chemical to be added to derive a total hazard index, which is not to

[19] More than additive or less than additive effects are also possible but have not been addressed by any Agency due to a lack of data and default approaches.

exceed one. This is required unless a strong, data driven case is made that additivity is not appropriate and an alternative is supported (e.g., non-additive or more than additive approach).

In another instance, MassDEP has used surrogate toxicity values to assess the toxicity of a range of total petroleum hydrocarbon (TPH) compounds that have similar structures and therefore are likely to have similar toxicological properties. Similar to PFAS, TPH is a complex and variable group of hundreds of individual compounds, many with limited toxicity data. To evaluate health risks in the absence of adequate data to characterize the specific toxicities of all members of the group, data on surrogate chemicals were used to evaluate the toxicity of structurally similar, analytically defined TPH fractions based on carbon number/molecular weights. In this approach compounds within these groups are treated as having similar and additive toxicities (MassDEP 2004)[20]. For example, for the 5 to 8 carbon petroleum aliphatic TPH fractions, n-hexane was chosen as a proxy for the other aliphatic petroleum compounds in the C5-C8 range. The toxicity values of n-hexane were chosen because its toxicity is relatively well characterized and other compounds in the C5-C8 grouping (n-pentane, n-heptane and n-octane) had less toxicity information.

Additivity has been applied for other toxicologically similar chemicals as well (USEPA 2000; ATSDR 2018b; SChER, SCCS, SCE 2012[21]).

4.2 Dose Additivity for Longer-chain PFAS

The longer-chain PFAS evaluated here are structurally very similar, cause similar effects at endpoints mapping to the multiple target organ systems evaluated and have long half-lives. These attributes support treating this subgroup of longer-chain PFAS as having additive toxicity. This approach is appropriately health protective, is an extension of the approach used by USEPA in the HAs for PFOA and PFOS, and is consistent with the established approaches noted above as applied to other chemical classes sharing structural and toxicological similarity.

[20] The MassDEP (2004) TPH approach informed USEPA's (2009) approach for development of TPH guidance for Superfund sites (PPRTV).

[21] "If no mode of action information is available, the dose/concentration addition method should be preferred over the independent action approach. Prediction of possible interaction requires expert judgement and hence needs to be considered on a case-by case basis." (SChER, SCCS, SCE 2012)

5.0 DRINKING WATER VALUES AND OVERALL CONCLUSIONS

5.1 Exposure Parameters

The key elements in the derivation of drinking water values include the toxicity value (e.g. RfD) for the compound in question; exposure parameters relating to the target population; and a relative source contribution term to account for other non-drinking water exposures. For the MassDEP PFAS drinking water value derivations, other than the applicable toxicity value, all other parameters selected by MassDEP are the same as those used by USEPA in deriving the drinking water Health Advisories for PFOA and PFOS (USEPA 2016c,d). These options are neither the most, nor least, conservative of the alternatives.

The water ingestion rate for a lactating woman was applied, which equals 54 ml per kilogram body weight. This is the USEPA consumers-only estimate of the combined direct and indirect community water ingestion at the 90th percentile for this subpopulation[22]. Basing exposure on a lactating woman is also protective of other groups.

A relative source contribution factor (RSC) of 20% was selected. Again, this is consistent with the RSC applied by USEPA in the Health Advisory derivations for PFOA and PFOS. Although higher RSCs have been derived by other state agencies for these longer-chain compounds based on serum concentrations from the NHANES data for the individual compounds (CDC 2019), MassDEP elected to use a 20% value. MassDEP concluded that this more conservative value is warranted to account for other exposures, including in utero and nursing exposures that recent modeling has indicated are significant, and to account for other non-drinking water exposures to the compounds across the subgroup of PFAS being addressed, as well uncharacterized exposures to related compounds.

5.2 MassDEP Drinking Water Value for the Subgroup of Six Longer-chain PFAS

The MassDEP RfD for the subclass is based on that for PFOA and PFOS. The bases of MassDEP's updated RfDs for these compounds was previously described. In summary, MassDEP relied on the same POD and HED calculations used by USEPA with inclusion of an additional UF to account for data indicating effects at lower dose levels, resulting in a RfD of 5.3 x 10^{-6} (rounded to 5 x 10^{-6} mg/kg/day) for PFOA[23] and of 5.1 x 10^{-6} mg/kg/day (rounded to 5 x

[22] From the USEPA Exposure Factors Handbook, Table 3-81, 2019 update (USEPA 2019c), which is identical to that used by USEPA (2016c,d).

[23] The PFOA RfD is based on a developmental study (Lau et al. 2006), supported by a number of candidate RfDs at the same or similar values. The critical endpoints identified in this study were decreased ossification and accelerated male puberty in offspring. An average serum LOAEL of 38 mg/L was determined using the Wambaugh et al. (2013) pharmacokinetic model (PK). A HED of 0.0053 mg/kg-day was calculated using a clearance value (Cl) of 0.00014 L/kg/day, based on an elimination rate of 8.25 x 10^{-4} (0.693 ÷ t ½), a volume of distribution of 0.017 L/kg (Thompson et al. 2010) and an elimination half-life ($t_{1/2}$) of 839.5 days (Bartell et al. 2010). The HED was then

10^{-6} mg/kg/day) for PFOS.[24] The RfDs rounded to one significant figure are the same (5 x 10^{-6} mg/kg/day) and this value was adopted for the PFAS subgroup addressed by MassDEP.

The derivation of the MassDEP drinking water value based on this RfD is described below:

$$\text{Drinking water value} = \frac{\text{RfD} \times \text{RSC}}{\text{Water consumption rate per kg body weight}}$$

Where:

RfD	= 5 x 10^{-6} mg/kg-day
Water consumption rate for lactating woman	= 0.054 L/kg-day
Relative Source Contribution Factor (RSC)	= 0.2

$$\text{Drinking Water Value} = \frac{5 \times 10^{-6} \text{ mg/kg-day} \times 0.2}{0.054 \text{ L/kg-day}}$$

$$= 0.0000185 \text{ mg/L}$$

$$= 0.00002 \text{ mg/L or 20 ng/L (20 ppt), rounded to one significant figure}$$

When these six compounds occur alone, together, or in any combination, the sum of their concentrations should be compared to 0.00002 mg/L.

These MassDEP drinking water values for the longer-chain subgroup of six PFAS, including PFOA, PFOS, PFNA, PFHxS, PFDA and PFHpA are the basis of the final MCP Method 1 standards for ground water used or potentially used as drinking water. These values also serve as the basis of the proposed MassDEP drinking water standards (Maximum Contaminant Level or MCL) for these compounds. MassDEP is also updating the ORSG or state drinking water guideline based on these values, which will be in effect until a final drinking water standard is adopted.

---

converted to the RfD, by applying a total UF of 1000 (10 for human variability, 3 for animal to human extrapolation, 10 for LOAEL to NOAEL adjustment, and 3 for database deficiency accounting for more sensitive endpoints occurring at doses lower than those seen in the critical study) to derive an RfD of 5.3 x 10^{-6} mg/kg-day (rounded to 5 x 10^{-6} mg/kg-day).

[24] The RfD for PFOS was based on a developmental study (Luebker et al. 2005a). The critical endpoints observed in this study were reduced pup body weight and delayed eye opening in offspring. An average serum NOAEL of 6.26 mg/L was determined using the Wambaugh et al. (2013) PK model. An HED of 0.00051 mg/kg-day was calculated using a Cl value of 8.1 x 10^{-5} L/kg/day based on an elimination rate of 3.52 x 10^{-5} (0.693 ÷ $t_{½}$), a volume of distribution value of 0.23 L/kg (Thompson et al. 2010) and an elimination half-life ($t_{1/2}$) of 1971 days (Olsen et al. 2007). The HED was divided by a total uncertainty factor of 100 (10 for human variability, 3 for animal to human extrapolation and 3 to account for database deficiency accounting for more sensitive endpoints occurring at doses lower than those seen in the critical study) to derive an RfD of 5.1 x 10^{-6} mg/kg-day (rounded to 5 x 10^{-6} mg/kg-day).

These drinking water values for this subgroup of PFAS, are health protective for members of the population considered most sensitive to these compounds, pregnant women, nursing mothers and infants. Protecting the sensitive members of the population provides health protection for all.

5.3 Overall Conclusions

MassDEP ORS completed a targeted review of current scientific information and assessments by other agencies addressing a subgroup of structurally similar PFAS. The PFAS subgroup considered in this reassessment includes ten closely related longer-chain PFAS that have carbon chain lengths with plus or minus two carbons (C6-C10 compounds) compared to PFOA and PFOS, the most data rich PFAS. Three compounds in this size range were not addressed in this evaluation because they are not included as USEPA Method 537.1 analytes (USEPA 2018). One compound PFHxA was not included because sufficient data are available demonstrating it is less toxic than the others on an applied dose basis. The remaining six are included in MassDEP ORS's subgroup approach.

The targeted review supports the approaches used in the development of the 2018 ORSG for PFOA, PFOS, PFNA, PFHxS, and PFHpA. Based on its assessment, MassDEP ORS has concluded that one additional compound, PFDA, should also be included in this subgroup as data demonstrates that this compound shares similar toxicity endpoints and potencies with the other compounds in the subgroup (NTP 2018; this document).

MassDEP ORS additionally concluded that the toxicity value (RfD) for the compounds in this subgroup should be adjusted downward from that used in the 2018 ORSG derivation, to 5×10^{-6} mg/kg-day, to account for considerable and convincing evidence associating exposures to PFOA and PFOS with adverse responses in laboratory animals at lower levels of exposure than the PODs selected by USEPA in its 2016 RfD derivations. The revised MassDEP ORS RfD is applied to the six PFAS in this subgroup based on consideration of similarities in chemical structure; overlap in toxicity values derived by various agencies; similarity in toxic responses; prolonged serum half-lives; and evaluation of relative potencies.

Regarding approaches to addressing risks attributable to exposures to multiple PFAS, MassDEP ORS continues to concur with the USEPA's additivity approach as applied to PFOA and PFOS in deriving the USEPA drinking water HAs for these compounds (USEPA 2016a,b,c,d). Based on their close structural similarities, toxicity and half-lives, MassDEP ORS has concluded that it is appropriate to extend this additivity approach to the six compounds in the subgroup addressed herein.

The lower RfD leads to a drinking water value of 20 ppt, which provides a greater degree of health protection than the prior value of 70 ppt, in particular to sensitive groups including pregnant women, nursing mothers and infants.

6.0 REFERENCES

Abbott BD, Wolf CJ, Schmid JE, Das KP, Zehr RD, Helfant L, Nakayama S, Lindstrom AB, Styrnar MJ, Lau C. 2007. Perfluorooctanoic acid induced developmental toxicity in the mouse is dependent on expression of peroxisome proliferator activated receptor-alpha. Toxicol Sci 98:571–581.

ATSDR (Agency for Toxics Substances and Disease Registry). 2018a. Toxicological Profile for Perfluoroalkyls. Draft for Public Comment. June 2018. Atlanta, GA: U.S. Department of Health and Human Services, Public Health Service.

ATSDR (Agency for Toxics Substances and Disease Registry). 2018b. Framework for Assessing Health Impacts of Multiple Chemicals and Other Stressors. Atlanta, GA: U.S. Department of Health and Human Services, Public Health Service.

Albrecht PP, Torsell NE, Krishnan P, Ehresman DJ, Frame SR, Chang SC, Butenhoff JL, Kennedy GL, Gonzalez FJ, Peters JM. 2013. A species difference in the peroxisome proliferator activated receptor alpha-dependent response to the developmental effects of perfluorooctanoic acid. Toxicol Sci 131:568-582.

Bailey SA, Zidell RH, Perry RW. 2004. Relationships between organ weight and body/brain weight in the rat: what is the best analytical endpoint? Tox Path 32:448-466.

Barry V, Winquist A, Steenland K. 2013. Perfluorooctanoic acid (PFOA) exposures and incident cancers among adults living near a chemical plant. Environ Health Perspect 121(11-12):1313-8.

Bartell S, Calafat A, Lyu C, Kato K, Ryan PB, Steenland K. 2010. Rate of decline in serum PFOA concentrations after granular activated carbon filtration at two public water systems in Ohio and West Virginia. Environ Health Perspect 118:222–228.

Berbel P, Mestre JL, Santamaria A, Palazon, I Franco A, Graells M, González-Torga A, de Escobar GM. 2009. Delayed neurobehavioral development in children born to pregnant women with mild hypothyroxinemia during the first month of gestation: the importance of early iodine supplementation. Thyroid 19:511–519.

Bjork JA, Butenhoff JL, Wallace KB 2011. Multiplicity of nuclear receptors activation by PFOA and PFOS in primary human and rodent hepatocytes. Toxicology 288: 8-17

Brede E, Wilhelm M, Göen T, Müller J, Rauchfuss K, Kraft M, Hölzer J. 2010. Two-year follow-up biomonitoring pilot study of residents' and controls' PFC plasma levels after PFOA reduction in public water system in Arnsberg, Germany. Int J Hyg Environ Health 213(3):217-23

Brewster DW, Birnbaum LS. 1989. The biochemical toxicity of perfluorodecanoic acid in the mouse is different from that of 2,3,7,8-tetrachlorodibenzo-p-dioxin. Toxicol Appl Pharmacol 99:544-554.

Butenhoff JL, Kennedy GL, Frame SR, O'Conner JC, York RG. 2004a. The reproductive toxicology of ammonium perfluorooctanoate (APFO) in the rat. Toxicology 196:95–116.

Butenhoff JL, Kennedy GL, Hinderliter PM, Lieder PH, Jung R, Hansen KJ, Gorman GS, Noker PE, Thomford PJ. 2004b. Pharmacokinetics of perfluorooctanoate in Cynomolgus monkeys. Toxicol Sci 82:394-406.

Butenhoff JL, Chang SC, Ehresman DJ, Raymond GY. 2009. Evaluation of potential reproductive and developmental toxicity of potassium perfluorohexanesulfonate in Sprague Dawley rats. Reprod Toxicol 27:331-341.

Butenhoff JL, Chang SC, Olsen GW, Thomford PJ. 2012. Chronic dietary toxicity and carcinogenicity study with potassium perfluorooctanesulfonate in Sprague Dawley rats. Toxicology 293:1-15.

CDC (Centers for Disease Control and Prevention). 2019. Fourth Report on Human Exposure to Environmental Chemicals, Updated Tables, (January 2019). Atlanta, GA: U.S. Department of Health and Human Services, Centers for Disease Control and Prevention. https://www.cdc.gov/exposurereport/.

Chang S-C, Noker PE, Gorman GS, Gibson SJ, Hart JA, Ehresman DJ, Butenhoff J. 2012. Comparative pharmacokinetics of perfluorooctanesulfonate (PFOS) in rats, mice, and monkeys. Reprod Toxicol 33(4):428-440.

Chang S, Butenhoff JL, Parker GA, Coder PS, Zitzow JD, Krisko RM, Bjork JA, Wallace KB, Seed JG. 2018. Reproductive and developmental toxicity of potassium perfluorohexanesulfonate in CD-1 mice. Reproductive Toxicology 78:150-168.

Chen T, Zhang L, Yue JQ, Lv ZQ, Xia W, Wan Y-J, Li Y-Y, Xu S-Q. 2012. Prenatal PFOS exposure 1 induces oxidative stress and apoptosis in the lung of rat off-spring. Reprod Toxico. 33:538-545.

Connecticut Department of Public Health (CTDPH). 2017. Perfluoroalkyl Substances (PFAS) in Drinking Water: Health Concerns. Environmental & Occupational Health Assessment Program, Connecticut Department of Public Health.

Das KP, Grey BE, Rosen MB, Wood CR, Tatum-Gibbs KR, Zehr RD, Strynar MJ, Lindstrom AB, Lau C. 2015. Developmental toxicity of perfluorononanoic acid in mice. Reprod Toxicol 51:133-144, DOI: 10.1016/j.reprotox.2014.12.012

Dewitt JC, Copeland CB, Strynar MJ, Luebke RW. 2008. Perfluorooctanoic acid-induced immunomodulation in adult C57BL/6J or C57BL/6N female mice. Environ. Health Perspect. 116: 644-650.

DeWitt JC, Williams WC, Creech NJ, Luebke RW. 2015. Suppression of antigen-specific antibody responses in mice exposed to perfluorooctanoic acid: Role of PPARα and T- and B-cell targeting. J Immunotoxicol 13: 38-45.

Dong GH, Zhang YH, Zheng L, Liu W, Jin YH, He QC. 2009. Chronic effects of perfluorooctanesulfonate exposure on immunotoxicity in adult male C57BL/6 mice. Arch Toxicol 83:805-815.

Dong GH, Liu MM, Wang D, Zheng L, Liang ZF, Jin YH. 2011. Sub-chronic effect of perfluorooctanesulfonate (PFOS) on the balance of type 1 and type 2 cytokine in adult C57BL6 mice. Arch Toxicol 85:1235-1244.

Dong GH, Zhang YH, Zheng L, Liang ZF, Jin YH, He QC. 2012. Subchronic effects of perfluorooctanesulfonate exposure on inflammation in adult male C57BL/6 mice. Environ Toxicol 27:285-296.

ECHA (European Chemicals Agency). 2015 Committee for Risk Assessment (RAC). Opinion on an Annex XV dossier proposing restrictions on Perfluorooctanoic acid (PFOA), its salts and PFOA-related substances. ECHA/RAC/RES-O-0000006229-70-02/F. Adopted 8 September 2015

ECHA (European Chemicals Agency). 2017. Read Across Assessment Framework (RAAF). March 2017. ECHA-17-R-01-EN. First published in May 2015, updated March 2017.

EFSA (European Food Safety Authority). 2018a. EFSA Panel on Contaminants in the Food Chain. Scientific opinion on the risk to human health related to the presence of perfluorooctanesulfonic acid and perfluorooctanoic acid in food. EFSA Journal 2018;16(12):5194, 284 pp.

EFSA (European Food Safety Authority). 2018b. Minutes of the expert meeting on perfluooroctane sulfonic acid and perfluorooctanoic acid in food assessment. Article 30 of Regulation 178/2002 EFSA – ECHA – BfR - Danish EPA - RIVM (Agreed on 10 December 2018).

Fang X, Gao G, Xue H, Zhang X, Wang H. 2012. Exposure of perfluorononanoic acid suppresses the hepatic insulin signal pathway and increases serum glucose in rats. Toxicology 294(2-3):109-115.

Fed. Reg. (Federal Register). 1979. Environmental Protection Agency; National Interim Primary Drinking Water Regulations; Control of Trihalomethanes in Drinking Water; Final Rule. 44(231) Fed. Reg. 68624-68707 (November 29, 1979)

Fed. Reg. (Federal Register). 1998. Environmental Protection Agency; National Primary Drinking Water Regulations: Disinfectants and Disinfectant Byproducts; Final Rule. 63(241) Fed. Reg. 69390-69476 (December 16, 1998)

Fed. Reg. (Federal Register). 2006. Environmental Protection Agency; National Primary Drinking Water Regulations: Stage 2 Disinfectants and Disinfectant Byproducts; Final Rule. 71(2) Fed. Reg. 388-493 (January 4, 2006)

Filgo, AJ, Quist EM, Hoenerhoff MJ, Brix AE, Kissling GE, Fenton SE. 2015. Perfluorooctanoic acid (PFOA)-induced liver lesions in two strains of mice following developmental exposures: PPARα is not required. Toxicol Pathol 43:558-68.

Foster PM. 2006. Disruption of reproductive development in male rat offspring following in utero exposure to phthalate esters. Int J Androl 29:140-147.

Frawley RP, Smith M, Cesta MF, Hayes-Bouknight S, Blystone C, Kissling GE, Harris S, Germolec D. 2018. Immunotoxic and hepatotoxic effects of perfluoro-n-decanoic acid (PFDA) on female Harlan Sprague-Dawley rats and $B_6C_3F_1$/N mice when administered by oral gavage for 28 days. J Immunotoxicol 15(1):41-52. doi: 10.1080/1547691X.2018.1445145.

Fu J, Gao Y, Cui L, Wang T, Liang Y, Qu G, Yuan B, Wang Y, Zhang A, Jiang G. 2016. Occurrence, temporal trends, and half-lives of perfluoroalkyl acids (PFAAs) in occupational workers in China. Sci Rep. 6:38039. doi: 10.1038/srep38039.

Goeden HM, Greene CW, Jacobus JA. 2019. A transgenerational toxicokinetic model and its use in derivation of Minnesota PFOA water guidance. J Exp Sci Environ Epi 29:183–195.

Gomis MI[1], Vestergren R[1], Nilsson H[2], Cousins IT[1]. 2016. Contribution of Direct and Indirect Exposure to Human Serum Concentrations of Perfluorooctanoic Acid in an Occupationally Exposed group of Ski Waxers. Environ Sci Technol. 50(13):7037-46.

Gomis M, Vestergren R, MacLeod M, Mueller JF, Cousins IT. 2017. Historical human exposure to perfluoroalkyl acids in the United States and Australia reconstructed from biomonitoring data using population-based pharmacokinetic modeling. Environment Int 108: 92-102.

Gomis MI, Vestergren R, Borg D, Cousins IT. 2018. Comparing the toxic potency in vivo of long-chain perfluoroalkyl acids and fluorinated alternatives. Environ Intl 113:1-9.

Grandjean P, Andersen EW, Budtz-Jorgensen E, Nielsen F, Mølbak K, Weihe P, Heilmann C. 2012. Serum vaccine antibody concentrations in children exposed to perfluorinated compounds. J Amer Med Assoc 307:391–397.

Granum B, Haug LS, Namork E, Stolevik SB. Thomsen C, Aaberge IS, van Loveren H, Løvik M, Nygaard UC. 2013. Pre-natal exposure to perfluoroalkyl substances may be associated with altered vaccine antibody levels and immune-related health outcomes in early childhood. J Immunotoxicol 10(4):373–379.

Guruge KS, Hikono H, Shimada N, Murakami K, Hasegawa J, Yeung LWY, Yamanaka N, Yamashita N. 2009. Effect of perfluorooctane sulfonate (PFOS) on influenza A virus-induced mortality in female B6C3F1 mice. Toxicol Sci 34:687–691.

Guyton KZ, Chiu WA, Bateson TF, Jinot J, Scott CS, Brown RC, Caldwell JC. 2009. A reexamination of the PPAR-α activation mode of action as a basis for assessing human cancer risks of environmental contaminants. Environ Health Perspect. 117:1664-1671.

Hall AP, Elcombe CR, Foster JR, Harada T, Kaufmann W, Knippel A, Küttler K, Malarkey DE, Maronpot RR, Nishikawa A, Nolte T, Schulte A, Strauss V, York MJ. 2012. Liver hypertrophy: A review of adaptive (adverse and non-adverse) changes- conclusions from the 3rd International ESTP Expert Workshop. Toxicol Pathol 40:971-994.

Harada K, Inoue K, Morikawa A, Yoshinaga T, Saito N, Koizumi A. 2005. Renal clearance of perfluorooctane sulfonate and perfluorooctanoate in humans and their species-specific excretion. Environ Res 99:253-261.

Harada, K.H., S. Hashida, T. Kaneko, K. Takenaka, M. Minata, K. Inoue, N. Saito, and A. Koizumi. 2007. Biliary excretion and cerebrospinal fluid partition of perfluorooctanoate and perfluorooctane sulfonate in humans. Environ Tox Pharm 24:134–139.

Hertzberg RC, Mumtaz MM. 2018. Component-Based Risk Assessment Approaches with Additivity and Interactions. In Rider CV, Simmons JE (eds), *Chemical Mixtures and Combined Chemical and Nonchemical Stressors*, pp 369-419. Springer International Publishing AG.

Honma S, Suzuki A, Buchanan DL, Katsu Y, Watanabe H, Iguchi T. 2002. Low dose effect of in utero exposure to bisphenol A and diethylstilbestrol on female mouse reproduction. Repro Toxicol 16 (2):117–22.

Huang MC, Dzierlenga AL, Robinson VG, Waidyanatha S, DeVito MJ, Eifrid MA, Granville CA, Gibbs ST, Blystone CR. 2019. Toxicokinetics of perfluorobutane sulfonate (PFBS), perfluorohexane-1-sulphonic acid (PFHxS), and perfluorooctane sulfonic acid (**PFOS**) in male and female Hsd:Sprague Dawley SD rats after intravenous and gavage administration. Toxicol Rep. 2019 6:645-655.

Johansson N, Fredriksson A, Eriksson P. 2008. Neonatal exposure to perfluorooctane sulfonate (PFOS) and perfluorooctanoic acid (PFOA) causes neurobehavioural defects in adult mice. Neurotoxicol 29:160–169.

Kieskamp KK, Worley RR, McLanahan ED, Verner MA. 2018. Incorporation of fetal and child PFOA dosimetry in the derivation of health-based toxicity values. Environ Int. 2018 111:260-267.

Kennedy GL. 1987. Increase in mouse liver weight following feeding of ammonium perfluorooctanoate and related fluorochemicals. Toxicol Lett 39(2-3):295-300.

Kielsen K, Shamim Z, Ryder LP, Nielsen F, Grandjean P, Budtz-Jørgensen E, Heilmann C. 2016. Antibody response to booster vaccination with tetanus and diphtheria in adults exposed to perfluorinated alkylates. J Immunotoxicol 13:270-3.

Kim SJ, Heo SH, Lee DS, Hwang IG, Lee YB, Cho HY. 2016. Gender differences in pharmacokinetics and tissue distribution of 3 perfluoroalkyl and polyfluoroalkyl substances in rats. Food Chem Toxicol 97:243-255.

Koskela A, Finnilä MA, Korkalainen M, Spulber S, Koponen J, Håkansson H, Tuukkanen J, Viluksela M. 2016. Effects of developmental exposure to perfluorooctanoic acid (PFOA) on long bone morphology and bone cell differentiation. Toxicol Appl Pharmacol 301:14-21.

Lau C, Thibodeaux JR, Hanson RG, Rogers JM, Grey BE, Stanton ME, Butenhoff JL, Stevenson LA. 2003. Exposure to perfluorooctane sulfonate during pregnancy in rat and mouse. II: Postnatal evaluation. Toxicol Sci 74:382-392.

Lau C, Thibodeaux JR, Hanson RG, Narotsky MG, Rogers JM, Lindstrom AB, Strynar MJ. 2006. Effects of perfluorooctanoic acid exposure during pregnancy in the mouse. Toxicol Sci 90:510–518.

Lee I and Viberg H. 2013. A single neonatal exposure to perfluorohexane sulfonate (PFHxS) affects the levels of important neuroproteins in the developing mouse brain. NeuroToxicol 37:190–196.

Li K, Sun J, Yang J, Roberts SM, Zhang X, Cui X, Wei S, Ma LQ. 2017. Molecular Mechanisms of Perfluorooctanoate-Induced Hepatocyte Apoptosis in Mice Using Proteomic Techniques. Environ Sci Technol 51(19):11380-11389.

Li Y, Fletcher T, Mucs D, Scott K, Lindh CH, Tallving P, Jakobsson K. 2018. Half-lives of PFOS, PFHxS and PFOA after end of exposure to contaminated drinking water. Occup Environ Med 75(1):46-51. DOI: 10.1136/oemed-2017-104651.

Lou I, Wambaugh JF, Lau C, Hanson RG, Lindstrom AB, Strynar MJ, Zehr RD, Setzer RW, Barton HA. 2009. Modeling single and repeated dose pharmacokinetics of PFOA in mice. Toxicol Sci 107(2):331-41.

Loveless SE, Finlay C, Everds NE, Frame SR, Gillies PJ, O'Connor JC, Powley CR, Kennedy GL. 2006. Comparative responses of rats and mice exposed to linear/branched, linear, or branched ammonium perfluorooctanoate (APFO). Toxicology 220:203–217.

Loveless SE, Slezak B, Serex T, Lewis J, Mukerji P, O'Connor JC, Donner EM, Frame SR, Korzeniowski SH, Buck RC. 2009. Toxicological evaluation of sodium perfluorohexanoate. Toxicology 264(1-2):32-44.

Luebker DJ, Case MT, York RG, Moore JA, Hansen KJ, Butenhoff JL. 2005a. Two-generation reproduction and cross-foster studies of perfluorooctanesulfonate (PFOS) in rats. Toxicology 215(1-2):126-148.

Luebker DJ, York RG, Hansen KJ, Moore JA, Butenhoff JL. 2005b. Neonatal mortality from *in utero* exposure to perfluorooctanesulfonate (PFOS) in Sprague-Dawley rats: Dose-response, and biochemical and pharmacokinetic parameters. Toxicology 215(1-2):149-169.

Luz A, Anderson J, Goodrum P. 2019. Approaches for assessing perfluoroalkyl acid mixture toxicity. Integral Consulting Inc. aluz@integral.corp.com. Society of Toxicology Poster Presentation.

Macon MB, Villanueva LR, Tatum-Gibbs K, Zehr RD, Strynar MJ, Stanko JP, White SS, Helfant L, Fenton SE. 2011. Prenatal perfluorooctanoic acid exposure in CD-1 mice: low dose developmental effects and internal dosimetry. Toxicol Sci 122:134-45.

MDHHS (Maine Department of Health and Human Services). 2014. Maximum Exposure Guideline for Perfluorooctanoic Acid in Drinking Water. Environmental and Occupational Health Program, Division of Environmental Health, Maine Center for Disease Control & Prevention, Department of Health and Human Services. Augusta, ME.

MassDEP (Massachusetts Department of Environmental Protection). 2004. Updated Petroleum Hydrocarbon Fraction Toxicity Values for the VPH/EPH/APH Methodology. Office of Research and Standards, Massachusetts Department of Environmental Protection, Boston, MA https://www.mass.gov/doc/updated-petroleum-hydrocarbon-fraction-toxicity-values-for-the-vphephaph-methodology/download

MassDEP (Massachusetts Department of Environmental Protection). 2018a. Recommendations Regarding Toxicity and Drinking Water Guidance Values for Perfluorinated Alkyl Substances (PFAS) Included in the Unregulated Chemical Monitoring Rule 3. Massachusetts Department of

Environmental Protection, Boston, MA https://www.mass.gov/doc/massdep-ors-guideline-for-pfas/download

MassDEP (Massachusetts Department of Environmental Protection). 2018b. Final Recommendations for Interim Toxicity and Drinking Water Guidance Values for Perfluorinated Alkyl Substances (PFAS) Included in the Unregulated Chemical Monitoring Rule 3. Office of Research and Standards, Massachusetts Department of Environmental Protection, Boston, MA. June 8, 2018. https://www.mass.gov/files/documents/2018/06/11/pfas-ors-ucmr3-recs_0.pdf

Mertens JJWM, Sved DW, Marit GB, Myers NR, Stetson PL, Murphy SR, Schmit B, Shinohara M, Farr CH. 2010. Subchronic Toxicity of S-111-S-WB in Sprague Dawley Rats. Intl J Toxicol 29(4):358-371. (as cited in Zeilmaker et al. 2018)

MISAW (Michigan Science Advisory Workgroup). 2019. Health Based Drinking Water Value Recommendations for PFAS in Michigan. Report developed for the Michigan PFAS Action Response Team, Lansing, Michigan. June 27, 2019.

Minata M, Harada KH, Kärrman A, Hitomi T, Hirosawa M, Murata M, Gonzalez FJ, Koizumi A. 2010. Role of peroxisome proliferator-activated receptor-alpha in hepatobiliary injury induced by ammoniumperfluorooctanoate in mouse liver. Ind. Health 48: 96-107.

MDH (Minnesota Department of Health). 2017. Toxicological Summary for: Perfluorooctane sulfonate. Health Based Guidance for Water. Health Risk Assessment Unit, Environmental Health Division.

MDH (Minnesota Department of Health). 2018. Health Based Guidance for Water Health Risk Assessment Unit, Environmental Health Division. Toxicological Summary for: Perfluorooctanoate. Adopted as Rule: August 2018. https://www.health.state.mn.us/communities/environment/risk/docs/guidance/gw/pfoa.pdf

MDH (Minnesota Department of Health). 2019a. Toxicological Summary for: Perfluorooctane sulfonate. Health Based Guidance for Water. Health Risk Assessment Unit, Environmental Health Division. https://www.health.state.mn.us/communities/environment/risk/docs/guidance/gw/pfos.pdf

MDH (Minnesota Department of Health). 2019b. Toxicological Summary for; Perfluorohexane sulfonate. Health Based Guidance for Water. Health Risk Assessment Unit, Environmental Health Division. https://www.health.state.mn.us/communities/environment/risk/docs/guidance/gw/pfhxs.pdf

Mogensen UB, Grandjean P, Nielsen F, Weihe P, Budtz-Jørgensen E. 2015. Breastfeeding as an Exposure Pathway for Perfluorinated Alkylates. Environ Sci Technol 49:10466-73.

Morreale de Escobar G, Obregon MJ, and Escobar del Rey F. 2000. Is neuropsychological development related to maternal hypothyroidism or to maternal hypothyroxinemia? J Clin Endocrinol Metab 85:3975–3987.

Nakagawa T, Ramdhan DH, Tanaka N, Naito H, Tamada H, Ito Y, Li Y, Hayashi Y, Yamagishi N, Yanagiba Y, Aoyama T, Gonzalez FJ, Nakajima T. 2011. Modulation of ammonium perfluorooctanoate induced hepatic damage by genetically different PPARα in mice. Arch Toxico. 86: 63-74.

NTP (National Toxicology Program). 2016. US Department of Health and Human Services. Systematic review of immunotoxicity associated with exposure to perfluorooctanoic acid (PFOA) or perfluorooctane sulfonate (PFOS). https://ntp.niehs.nih.gov/ntp/ohat/pfoa_pfos/pfoa_pfosmonograph_508.pdf

NTP (National Toxicology Program). 2018. US Department of Health and Human Services. Data Tables for Perfluorinated Sulfonates and Perfluorinated carboxylates. https://tools.niehs.nih.gov/cebs3/views/?action=main.dataReview&bin_id=3875

NTP (National Toxicology Program). 2019a. Toxicity Studies of Perfluoroalkyl Sulfonates (Perfluorobutane Sulfonic Acid, Perfluorohexane Sulfonate Potassium Salt, and Perfluorooctane Sulfonic Acid) Administered by Gavage to Sprague Dawley (Hsd:Sprague Dawley SD) Rats. (TOX-96). August 2019. US Department of Health and Human Services.

NTP (National Toxicology Program). 2019b. Toxicity Studies of Perfluoroalkyl Carboxylates (Perfluorohexanoic Acid, Perfluorooctanoic Acid, Perfluorononanoic Acid, and Perfluorodecanoic Acid) Administered by Gavage to Sprague Dawley (Hsd:Sprague Dawley SD) Rats. (TOX-96). August 2019. US Department of Health and Human Services.

NTP (National Toxicology Program). 2019c. TR-598: Technical Report Pathology Tables and Curves, Pathology Tables, Survival and Growth Curves from NTP. General Study Information and Long-Term Studies. US Department of Health and Human Services. https://tools.niehs.nih.gov/cebs3/views/?action=main.dataReview&bin_id=3875 https://doi.org/10.22427/NTP-DATA-TR598

Nelson, J. 2016. Personal Communication regarding MDH MN (East Metro) PFC biomonitoring project data based on June 9, 2015 Meeting Agenda and Materials for the Advisory Panel to the Environmental Health Tracking and Biomonitoring Program. (as cited in MDH (2019a) http://www.health.state.mn.us/divs/hpcd/tracking/panel/2015Junematerials.pdf.

Nelson, J. 2018. Personal Communication re: NHANES PFAS 2015-2016 Data Release. (as cited in MDH 2019c)

NHDES (New Hampshire Department of Environmental Services Development). 2019a. Summary report on the New Hampshire Department of Environmental Services Development of Maximum Contaminant Levels and Ambient Groundwater Quality Standards for perfluorooctanesulfonic acid (PFOS), perfluorooctanoic acid (PFOA), perfluorononanoic acid (PFNA), and perfluorohexanesulfonic acid (PFHxS) prepared by New Hampshire Department of Environmental Services. January 4, 2019

NHDES (New Hampshire Department of Environmental Services Development). 2019b. Technical Background Report for the June 2019 Proposed Maximum Contaminant Levels (MCLs) and Ambient Groundwater Quality Standards (AGQSs) for Perfluorooctane sulfonic Acid (PFOS), Perfluorooctanoic Acid (PFOA), Perfluorononanoic Acid (PFNA), and Perfluorohexane sulfonic Acid (PFHxS). June 28, 2019.

NJDWQI (New Jersey Drinking Water Quality Institute). 2015. Health-Based Maximum Contaminant Level Support Document: Perfluorononanoic Acid (PFNA).

NJDWQI (New Jersey Drinking Water Quality Institute). 2017. Health-Based Maximum Contaminant Level Support Document: Perfluorooctanoic Acid (PFOA). February 15, 2017.

NJDWQI (New Jersey Drinking Water Quality Institute). 2018. Health-Based Maximum Contaminant Level Support Document: Perfluorooctane Sulfonate (PFOS). June 5, 2018.

NYDoH (New York State Department of Health). 2019. Proposed Rule Making: Maximum Contaminant Levels (MCLs). Incorporating MCLs for perfluorooctanoic acid (PFOA), perfluorooctanesulfonic acid (PFOS) and 1,4-dioxane. July 24, 2019.

Nilsson H, Kärrman A, Westberg H, Rotander A, van Bavel B, Lindström G. 2010. A time trend study of significantly elevated perfluorocarboxylate levels in humans after using fluorinated ski wax. Environ Sci Technol 44(6):2150-5.

Nilsson H, Kärrman A, Rotander A, van Bavel B, Lindström G, Westberg H. 2013. Professional ski waxers' exposure to PFAS and aerosol concentrations in gas phase and different particle size fractions. Environ Sci Process Impacts. 2013 Apr;15(4):814-22.

Numata J, Kowalczyk J, Adolphs J, Ehlers S, Schafft H, Fuerst P, Müller-Graf C, Lahrssen-Wiederholt M, Greiner M. 2014. Toxicokinetics of seven perfluoroalkyl sulfonic and carboxylic acids in pigs fed a contaminated diet. J Agric Food Chem 62(28):6861-70.

Olsen GW, Burris JM, Ehresman DJ, Froehlich JW, Seacat AM, Butenhoff JL, Zobel LR. 2007. Half-life of serum elimination of perfluorooctanesulfonate, perfluorohexanesulfonate and perfluorooctanoate in retired fluorochemical production workers. Environl Health Perspec 115:1298-1305.

Ohmori K, Kudo N, Katayama K, Kawashima Y. 2003. Comparison of the toxicokinetics between perfluorocarboxylic acids with different carbon chain length. Toxicology. 2003 184(2-3):135-40.

Onishchenko N, Fischer C, Wan Ibrahim WN, Negri S, Spulbur S, Cottica S, Ceccatelli S. 2011. Prenatal exposure to PFOS or PFOA alters motor function in mice in a sex-related manner. Neurotox Res 19:452-461.

Palazzolo M.J. 1993. Thirteen-Week Dietary Toxicity Study With T-5180, Ammonium Perfluorooctanoate (CAS No. 3825-26-1) In Male Rats. Final Report. Laboratory Project Identification HWI 6329-100. Hazleton Wisconsin, Inc. U.S. Environmental Protection Agency Administrative Record 226-0449.

Peden-Adams MM, Keller JM, Eudaly JG, Berger J, Gilkeson GS, Keil DE. 2008. Suppression of humoral immunity in mice following exposure to perfluorooctane sulfonate. Toxicol Sci 104:144-154.

Perkins RG, Butenhoff JL, Kennedy GL, Palazzolo, M.J. 2004. 13-Week dietary toxicity study of ammonium perfluorooctanoate (APFO) in male rats. Drug Chem Toxicol 27:361-378.

Peters JM, Gonzalez FJ. 2011. Why toxic equivalency factors are not suitable for perfluoroalkyl chemicals. Chem Res Toxicol 24(10):1601-1609.

Quist EM, Filgo AJ, Cummings CA, Kissling GE, Hoenerhoff. MJ. 2015a. Hepatic mitochondrial alteration in CD-1 mice associated with prenatal exposures to low doses of perfluorooctanoic acid (PFOA). Toxicol Pathol 43:546-57.

Quist EM, Filgo AJ, Cummings CA, Kissling GE, Hoenerhoff MJ, Fenton SE. 2015b. Supplemental data: Hepatic mitochondrial alteration in CD-1 mice associated with prenatal exposures to low doses of perfluorooctanoic acid (PFOA). Toxicol Pathol 43:546-557

Ramhoj L, Hass U, Boberg J, Scholze M, Christiansen S, Nielsen F, Axelstad M. 2018. Perfluorohexane sulfonate (PFHxS) and a mixture of endocrine disrupters reduce thyroxine levels and cause antiandrogenic effects in rats. Toxicol Sci 163(2):579–591.

Russell MH, Nilsson H, Buck RC. 2013. Elimination kinetics of perfluorohexanoic acid in humans and comparison with mouse, rat and monkey. Chemosphere. 2013 93(10):2419-25.

Russell MH, Himmelstein MW, Buck RC. 2015. Inhalation and oral toxicokinetics of 6:2 FTOH and its metabolites in mammals. Chemosphere. 120:328-35

SCHER, SCCS, SCE (Scientific Committee on Health and Environmental Risks (SCHER), Scientific Committee on Emerging and Newly Identified Health Risks (SCENIHR), Scientific

Committee on Consumer Safety (SCCS)). 2012. Opinion on the Toxicity and Assessment of Chemical Mixtures. European Union. European Commission, DG Health & Consumers, Directorate D: Health Systems and Products, Unit D3 - Risk Assessment, Office: B232 B-1049 Brussels.

Seacat AM, Thomford PJ, Hansen KJ, Olsen GW, Case MT, Butenhoff JL. 2002. Subchronic toxicity studies on perfluorooctanesulfonate potassium salt in cynomolgus monkeys. Toxicol Sci 68:249-264.

Seacat AM, Thomford PJ, Hansen KJ, Clemen LA, Eldridge SR, Elcombe CR, Butenhoff JL. 2003. Sub-chronic dietary toxicity of potassium perfluorooctanesulfonate in rats. Toxicology 183:117–131.

Shao K, Shapiro A. 2018. A Web-Based System for Bayesian Benchmark Dose Estimation. Environ Health Perspec 126(1):017002 https://benchmarkdose.org/

Shao K, Gift JS, Setzer RW. 2013. Is the assumption of normality or log-normality for continuous response data critical for benchmark dose estimation? Toxicol Appl Pharmaco. 272(3):767-79.

Shoemaker J. and Tettenhorst D. 2018. Method 537.1: Determination of Selected Per- and Polyfluorinated Alkyl Substances in Drinking Water by Solid Phase Extraction and Liquid Chromatography/Tandem Mass Spectrometry (LC/MS/MS). U.S. Environmental Protection Agency, Office of Research and Development, National Center for Environmental Assessment, Washington, DC, 2018.

Sobolewski M, Conrad K, Allen J.L, Weston H, Martin K, Lawrence BP, Cory-Slechta DA. 2014. Sex-specific enhanced behavioral toxicity induced by maternal exposure to a mixture of low dose endocrine disrupting chemicals. Neurotoxicol 45:121-130.

Son HY, Kim SH, Shin HI, Bae HI, Yang, JH. 2008. Perfluorooctanoic acid-induced hepatic toxicity following 21-day oral exposure in mice. Arch Toxicol 82:239-246.

Stump DG, Holson JF, Murphy SR, Farr CH, Schmit B, Shinohara M. 2008. An oral two-generation reproductive toxicity study of S-111-S-WB in rats. Reprod Toxicol 25:7-20.

Sundstrom M, Chang SC, Noker PE, Gorman GS, Hart JA, Ehresman DJ, Bergman A, Butenhoff JL. 2012. Comparative pharmacokinetics of perfluorohexanesulfonate (PFHxS) in rats, mice, and monkeys. Reprod Toxicol 33:441–451.

Tatum-Gibbs K, Wambaugh JF, Das KP, Zehr RD, Strynar MJ, Lindstrom AB, Delinsky A, Lau C. 2011. Comparative pharmacokinetics of perfluorononanoic acid in rat and mouse. Toxicology 281(1-3):48-55.

Thompson J, Lorber M, Toms L-ML, Kato K, Calafat AM, Mueller JF. 2010a. Use of simple pharmacokinetic modeling to characterize exposure of Australians to perfluorooctanoic acid and perfluorooctane sulfonic acid. Environment International 36:390-397. (as cited in USEPA 2016a).

Thompson J, Toms LML, Eaglesham G, Hobson P, Mueller JF. 2010b. Comparison of PFOS and PFOA serum concentrations in people undergoing regular venesections and in the broader community. Organohalogen Compounds 72:826–829. (as cited in USEPA 2016b).

Tucker DK, Macon MB, Strynar MJ, Dagnino S, Andersen E, Fenton SE. 2015. The mammary gland is a sensitive pubertal target in CD-1 and C57Bl/6 mice following perinatal perfluorooctanoic acid (PFOA) exposure. Reprod Toxicol 54:26-36.

USEPA (U.S. Environmental Protection Agency). 1993. Provisional Guidance for Quantitative Risk Assessment of Polycyclic Aromatic Hydrocarbons. Environmental Criterial and Assessment Office, Office of Health and Environmental Assessment, U.S. Environmental Protection Agency, Cincinnati, OH 45268. (EPA/600/R-93/089)

USEPA (U.S. Environmental Protection Agency). 2000. Supplementary Guidance for Conducting Health Risk Assessment of Chemical Mixtures. Risk Assessment Forum, U.S. Environmental Protection Agency. Washington, DC 20460. (EPA/630/R-00/002)

USEPA (U.S. Environmental Protection Agency). 2002a. A Review of the Reference Dose and Reference Concentration Processes. Risk Assessment Forum, U.S. Environmental Protection Agency. Washington, DC 20460. (EPA/630/P-02/002F)

USEPA (U.S. Environmental Protection Agency). 2002b. Guidance on Cumulative Risk Assessment of Pesticide Chemicals That Have a Common Mechanism of Toxicity. Office of Pesticide Programs, U.S. Environmental Protection Agency, Washington, D.C. 20460.

USEPA (U.S. Environmental Protection Agency). 2009. Provisional Peer-Reviewed Toxicity Values for Complex Mixtures of Aliphatic and Aromatic Hydrocarbons (CASRN Various). Superfund Health Risk Technical Support Center National Center for Environmental Assessment Office of Research and Development U.S. Environmental Protection Agency Cincinnati, OH 45268. FINAL 9-30-2009

USEPA (U.S. Environmental Protection Agency). 2010. Toxicological Review of cis-1,2-Dichloroethylene and trans-1,2- Dichloroethylene. (EPA/635/R-09/006F). Washington, DC.

USEPA (U.S. Environmental Protection Agency). 2011. Toxicological Review of Trichloroethylene. (EPA/635/R-09/011F). Washington, DC.

USEPA (U.S. Environmental Protection Agency). 2012. Benchmark dose technical guidance. Risk Assessment Forum, U.S. Environmental Protection Agency, Washington, DC. (EPA/100/R-12/001). https://www.epa.gov/risk/benchmark-dose-technical-guidance

USEPA (U.S. Environmental Protection Agency). 2014a. Health Effects Document for Perfluorooctanoic Acid (PFOA). U.S. Environmental Protection Agency, Office of Water: Health and Ecological Criteria Division Washington, DC.

USEPA (U.S. Environmental Protection Agency). 2014b. Health Effects Support Document for Perfluorooctane Sulfonate (PFOS) U.S. Environmental Protection Agency, Office of Water: Health and Ecological Criteria Division Washington, DC. http://www.epa.gov/dwstandardsregulations/drinking-water-contaminant-human-health-effects-information

USEPA (U.S. Environmental Protection Agency). 2016a. Health Effects Support Document for Perfluorooctanoic acid (PFOA) US Environmental Protection Agency, Office of Water: Health and Ecological Criteria Division Washington, DC. http://www.epa.gov/dwstandardsregulations/drinking-water-contaminant-human-health-effects-information

USEPA (U.S. Environmental Protection Agency). 2016b. Health Effects Support Document for Perfluorooctane Sulfonate (PFOS) US Environmental Protection Agency, Office of Water: Health and Ecological Criteria Division Washington, DC. http://www.epa.gov/dwstandardsregulations/drinking-water-contaminant-human-health-effects-information

USEPA (U.S. Environmental Protection Agency). 2016c. Drinking water health advisory for perfluorooctanoic acid (PFOA). U.S. Environmental Protection Agency. https://www.epa.gov/sites/production/files/2016-05/documents/pfoa_health_advisory_final-plain.pdf. March 3, 2017.

USEPA (U.S. Environmental Protection Agency). 2016d. Drinking water health advisory for perfluorooctane sulfonate (PFOS). U.S. Environmental Protection Agency. https://www.epa.gov/sites/production/files/2016-05/documents/pfos_health_advisory_final-plain.pdf. March 3, 2017.

USEPA (U.S. Environmental Protection Agency). 2019a. Integrated Risk Information System Glossary. Office of Research and Development/National Center for Environmental Assessment/Integrated Risk Information System. https://www.epa.gov/iris/basic-information-about-integrated-risk-information-system#guidance

USEPA (U.S. Environmental Protection Agency). 2019b. Benchmark Dose Software (BMDS). Version 3.1. Software and User Guide. (EPA/600/R-18/310). https://www.epa.gov/bmds/benchmark-dose-software-bmds-version-31-download

USEPA (U.S. Environmental Protection Agency). 2019c. Update for Chapter 3 of the Exposure Factors Handbook Ingestion of Water and Other Select Liquids. Feb. 2019. (EPA/600/R-18/259F) https://www.epa.gov/sites/production/files/2019-02/documents/efh_-_chapter_3_update.pdf

Van den Berg M, Birnbaum LS, Denison M, De Vito M, Farland W, Feeley M, Fiedler H, Hakansson H, Hanberg A, Haws L, Rose M, Safe S, Schrenk D, Tohyama C, Tritscher A, Tuomisto J, Tysklind M, Walker N, Peterson RE. 2006. The 2005 World Health Organization reevaluation of human and Mammalian toxic equivalency factors for dioxins and dioxin-like compounds. Tox Sci 93(2):223-241

Vermont Department of Health. 2018. Memorandum from Mark A. Levine MD, Commissioner, State of Vermont Department of Health. July 10, 2018. Drinking Water Health Advisory for Five PFAS (per- and polyfluorinated alkyl substances). https://www.healthvermont.gov/sites/default/files/documents/pdf/ENV_DW_PFAS_HealthAdvisory.pdf

Viberg H, Lee I, Eriksson P. 2013. Adult dose-dependent behavioral and cognitive disturbances after a single neonatal PFHxS dose. Toxicology 304:185−191.

Wambaugh JF, Setzer RW, Pitruzzello AM, Liu J, Reif DM, Kleinstreuer NC, Ching N, Wang Y, Sipes N, Martin M, Das K, DeWitt JC, Strynar M, Judson R, Houck KA, Lau C. 2013. Dosimetric anchoring of *in vivo* and *in vitro* studies for perfluorooctanoate and perfluorooctanesulfonate. Toxicol Sci 136:308–327.

Wang J, Yan S, Zhang W, Zhang H, Dai J. 2015. Integrated proteomic and miRNA transcriptional analysis reveals the hepatotoxicity mechanism of PFNA exposure in mice. J Proteome Res 14:330-341.

WIDHS (Wisconsin Department of Human Services). 2019. Recommended Public Health Groundwater Quality Standards, *Scientific Support Documents for Cycle 10 Substances*. June 2019. Madison, WI.

White SS, Calafat AM, Kuklenyik Z, Villanueva L, Zehr RD, Helfant L, Strynar MJ, Lindstrom AB, Thibodeaux JR, Wood C, Fenton SE. 2007. Gestational PFOA exposure of mice is associated with altered mammary gland development in dams and female offspring. Toxicol Sci 96:133-144.

White SS, Kato K, Jia LT, Basden, BJ, Calafat AM, Hines EP, Stanko JP, Wolf CJ, Abbott BD, Fenton SE. 2009. Effects of perfluorooctanoic acid on mouse mammary gland development and differentiation resulting from cross-foster and restricted gestational exposures. Reprod Toxicol 27:289-298.

White SS, Stanko JP, Kato K, Calafat AM, Hines EP, Fenton SE. 2011. Gestational and chronic low-dose PFOA exposures and mammary gland growth and differentiation in three generations of CD-1 Mice. Environ Health Perspect 119:1070-1076.

Wolf CJ, Fenton SE, Schmid JE, Calafat AM, Kuklenyik Z, Bryant XA, Thibodeaux J, Das KP, White SS, Lau CS, Abbott BD. 2007. Developmental toxicity of perfluorooctanoic acid in the CD-1 mouse after cross-foster and restricted gestational exposure. Toxicol Sci 95:462–473.

Wolf CJ, Zehr RD, Schmid JE, Lau C, Abbott BD. 2010. Developmental effects of perfluorononanoic acid in the mouse are dependent on peroxisome proliferator-activated receptor-alpha. PPAR Res 2010: Article ID 282896, 11 pages. doi: 10.1155/2010/282896.

Wong F, MacLeod M, Mueller JF, Cousins IT. 2014. Enhanced elimination of perfluorooctane sulfonic acid by menstruating women: evidence from population-based pharmacokinetic modeling. Environ Sci Technol 48(15):8807-14.

Worley RR, Moore SM, Tierney BC, Ye X, Calafat AM, Campbell S, Woudneh MB, Fisher J. 2017. Per- and polyfluoroalkyl substances in human serum and urine samples from a residentially exposed community. Environ Int. 2017 106:135-143.

Yang Q, Ito S, Gonzalez FJ. 2007. Hepatocyte-restricted constitutive activation of PPAR alpha induces hepatoproliferation but not hepatocarcinogenesis. Carcinogenesis 28(6):1171-1177.

Yang Q, Xie Y, Alexson SE, Nelson BD, DePierre JW. 2002. Involvement of the peroxisome proliferator-activated receptor alpha in the immunomodulation caused by peroxisome proliferators in mice. Biochem Pharmacol 63:1893-1900.

Zeilmaker MJ, Fragki S, Verbruggen EMJ, Bokkers BGH. 2018. Mixture exposure to PFAS: A Relative Potency Factor approach. RIVM (National Institute for Public Health and the Environment) Report 2018-0070.

Zhang Q, Liu W, Niu Q, Wang Y, Zhao H, Zhang H, Song J, Tsuda S, Saito N. 2016. Effects of perfluorooctane sulfonate and its alternatives on long-term potentiation in the hippocampus CA1 region of adult rats in vivo. Toxicol Res 5:539-546. doi: 10.1039/c5tx00184f.

Zhang Y, Beesoon S, Zhu L, Martin JW. 2013. Biomonitoring of perfluoroalkyl acids in human urine and estimates of biological half-life. Environ Sci Technol 47(18):10619-10627. doi: 10.1021/es401905e.

Appendices for the MassDEP ORS Technical Support Document

Per- and Polyfluoroalkyl Substances (PFAS): An Updated Subgroup Approach to Groundwater and Drinking Water Values

December 26, 2019

Appendixes

APPENDIX 1

Table 1. PFAS Toxicity and Drinking Water Values Derived by Various Groups and Their Bases

Agency	Key Study (effect)	POD Animal Serum (mg/L)	Human T½ Used (days)	Dosimetric Adjustment Factor (L/kg/d)	HED (mg/kg-day)	UF	Candidate RfD or MRL (Serum Concentration at RfD, mg/L)	DW Exposure Parameters and Relative Source Contribution Factor (RSC)	DW Value (ppt, ng/L)
PFOA									
USEPA (2016a)	Lau et al. (2006) (mice; developmental, decreased ossification, accelerated male puberty)	38 LOAEL	839.5	1.4×10^{-4}	0.0053	300 $UF_H = 10$ $UF_A = 3$ $UF_L = 10$	2.0×10^{-5} (38/300 = 0.127)	Water ingestion rate of a lactating woman (0.054 L/kg/d)(60 kg; 3.2 L/day) RSC 20%	70
MassDEP (2019)	Lau et al. (2006) (mice; developmental, decreased ossification, accelerated male puberty)	38 LOAEL	839.5	1.4×10^{-4}	0.0053	1000 1000 $UF_H = 10$ $UF_A = 3$ $UF_L = 10$ **$UF_D = 3$ developmental mammary and liver effects**	5.0×10^{-6} (38/300 = 0.127)	Water ingestion rate of a lactating woman (0.054 L/kg/d)(60 kg; 3.2 L/day) RSC 20%	20
ATSDR (2018a)	Onishchenko et al. (2011) (mice; neurodevelopment) Koskela et al. (2016) (mice; skeletal development)	8.29 LOAEL	1400	9.9×10^{-5}	0.000821	300 $UF_H = 10$ $UF_A = 3$ $UF_L = 10$	2.7×10^{-6} (8.29/300 = 0.028)	ND	ND

Agency	Key Study (effect)	POD Animal Serum (mg/L)	Human T ½ Used (days)	Dosimetric Adjustment Factor (L/kg/d)	HED (mg/kg-day)	UF	Candidate RfD or MRL (Serum Concentration at RfD, mg/L)	DW Exposure Parameters and Relative Source Contribution Factor (RSC)	DW Value (ppt, ng/L)
MDH (2018)	Lau et al. (2006) (mice; developmental, delayed ossification, accelerated preputial separation in male offspring, decreased pup body weight, increased maternal liver weight)	38 LOAEL	840	1.4×10^{-4}	0.0053	300 $UF_H = 10$ $UF_A = 3$ $UF_L = 3$ $UF_D = 3$	2.0×10^{-5} (38/300 = 0.127)	Transgenerational toxicokinetic model developed by MDH for breast fed and bottle fed infants (Goeden et al. 2019) RSC 50%	35
NJDWQI (2017)	Loveless et al. (2006) (mice; increased liver weight)	4.35 BMDL	840	1.6×10^{-4} [a]	0.00069	300 $UF_H = 10$ $UF_A = 3$ **UF_D= 10 (delayed mammary gland development, sensitive effects**	2.0×10^{-6} 4.35/300 = 0.015	70 kg adult 2L/day RSC 20%	14
NHDES (2019b)	Loveless et al. (2006) (mice; increased liver weight)	4.35 BMDL	840	1.4×10^{-4}	0.00061	100 $UF_H = 10$ $UF_A = 3$ **UF_D = 3 for immune data deficiency**	6.1×10^{-6} (4.35/100 = 0.043)	Transgenerational toxicokinetic model developed by MDH for breast fed and bottle fed infants (Goeden et al. 2019) RSC 50%	12

Agency	Key Study (effect)	POD Animal Serum (mg/L)	Human T ½ Used (days)	Dosimetric Adjustment Factor (L/kg/d)	HED (mg/kg-day)	UF	Candidate RfD or MRL (Serum Concentration at RfD, mg/L)	DW Exposure Parameters and Relative Source Contribution Factor (RSC)	DW Value (ppt, ng/L)
MISAW (2019)	Onishchenko et al. (2011) (mice; neurodevelopment, decreased num. inactive periods, altered novelty induced activity) Koskela et al. (2016) (mice; skeletal development, altered bone morphology and bone cell differentiation in femurs and tibia)	8.29 [b] LOAEL	840	1.4×10^{-4}	0.001163	300 $UF_H = 10$ $UF_A = 3$ $UF_L = 3$ $UF_D = 3$ **endocrine effects**	4×10^{-6} (3.9×10^{-6}) (8.29/300 = 0.028)	Based on the RfD, exposure considerations and application of transgenerational model developed by MDH (Goeden et al. 2019) RSC 50%	8
NYDOH (2019)	Macon et al. (2011) (mice; developmental liver)	4.98 LOAEL	---	---	0.00015 [a]	100 $UF_H = 10$ $UF_A = 3$ $UF_D = 3$	1.5×10^{-6} (4.98/100 = 0.049)	Not specified	10

Agency	Key Study (effect)	POD Animal Serum (mg/L)	Human T ½ Used (days)	Dosimetric Adjustment Factor (L/kg/d)	HED (mg/kg-day)	UF	Candidate RfD or MRL (Serum Concentration at RfD, mg/L)	DW Exposure Parameters and Relative Source Contribution Factor (RSC)	DW Value (ppt, ng/L)
WIDHS (2019)	Lau et al. (2006) (mice; developmental, decreased ossification, accelerated male puberty)				0.00054 (HED_{50})	300 UF_H = 10 UF_A = 3 UF_L = 10	2.0×10^{-6}	10 kg young child 1L/day RSC 100%	20
PFOS									
USEPA (2016b)	Luebker et al. (2005a) (rats; reduced pup body weight and delayed eye opening)	6.26 NOAEL	1971	8.1×10^{-5}	0.00051	30 UF_H = 10 UF_A = 3	2.0×10^{-5} (6.26/30 = 0.209)	Water ingestion rate of a lactating woman (0.054 L/kg d)(60 kg; 3.2 L/day) RSC 20%	70
MassDEP (2019)	Luebker et al. (2005a) (rats; reduced pup body weight and delayed eye opening)	6.26 NOAEL	1971	8.1×10^{-5}	0.00051	100 UF_H = 10 UF_A = 3 **UF_D = 3 immune effects**	5.0×10^{-5} (6.26/100 = 0.0626)	Water ingestion rate of a lactating woman (0.054 L/kg d)(60 kg; 3.2 L/day) RSC 20%	20
ATSDR (2018)	Luebker et al. (2005a) (rats; reduced pup weight and delayed eye opening)	7.43 NOAEL	2000	6.93×10^{-5}	0.000515	300 UF_H = 10 UF_A = 3 **UF_D = 10 immune effects**	2.0×10^{-6} (7.43/300 = 0.025)	ND	ND
MDH (2019a)	Dong et al. (2011) (mice; immune suppression, decreased IL-4 and decreased SRBC specific IgM levels)	2.36 NOAEL	1241	1.3×10^{-4}	0.000307	100 UF_H = 10 UF_A = 3 **UF_D = 3 immune and thyroid effects**	3.1×10^{-6} (2.36/100 = 0.024)	Transgenerational toxicokinetic model developed by MDH for breast fed and bottle fed infants (Goeden et al. 2019) RSC 20%	15

Agency	Key Study (effect)	POD Animal Serum (mg/L)	Human T ½ Used (days)	Dosimetric Adjustment Factor (L/kg/d)	HED (mg/kg-day)	UF	Candidate RfD or MRL (Serum Concentration at RfD, mg/L)	DW Exposure Parameters and Relative Source Contribution Factor (RSC)	DW Value (ppt, ng/L)
NJDWQI (2018)	Dong et al. (2009) (mice; immune suppression)	0.674 $BMDL_{10}$	1971	8.2×10^{-5} [a]	0.000055	30 $UF_H = 10$ $UF_A = 3$	2×10^{-6} (0.674/30 = 0.022)	70 kg adult 2L/day RSC 20%	13
NHDES (2019b)	Dong et al. (2011) (mice; immune suppression, decreased IL-4 and decreased SRBC specific IgM levels)	2.36 NOAEL	1241	1.28×10^{-4}	0.0003	100 $UF_H = 10$ $UF_A = 3$ **$UF_D = 3$ thyroid effects in neonatal animals**	3.0×10^{-6} (2.36/100 = 0.024)	Transgenerational toxicokinetic model developed by MDH for breast fed and bottle fed infants (Goeden et al. 2019) RSC 50%	15
MISAW (2019)	Dong et al. (2009) (mice; immune suppression of plaque formation, increased liver mass)	0.674 NOAEL	1241	1.28×10^{-4}	0.0000866	30 $UF_H = 10$ $UF_A = 3$	3×10^{-6} (2.9×10^{-6}) (0.674/30 = 0.022)	Transgenerational toxicokinetic model developed by MDH for breast fed and bottle fed infants (Goeden et al. 2019) RSC 50%	16
NYDOH (2018)	Same as NJDWQI (2018)							Not specified	10
WIDHS(2019)	Same as ATSDR (2018a)							10 kg young child 1L/day RSC 100%	20
PFNA									
ATSDR (2018a)	Das et al. (2015) (mice; developmental delays; decreased body weight gain)	6.80 NOAEL	900	1.54×10^{-4}	0.001	300 $UF_A = 3$ $UF_H = 10$ $UF_D = 3$	3.0×10^{-6} (6.8/300 = 0.023)	ND	ND

Agency	Key Study (effect)	POD Animal Serum (mg/L)	Human T ½ Used (days)	Dosimetric Adjustment Factor (L/kg/d)	HED (mg/kg-day)	UF	Candidate RfD or MRL (Serum Concentration at RfD, mg/L)	DW Exposure Parameters and Relative Source Contribution Factor (RSC)	DW Value (ppt, ng/L)
NJDWQI (2015)	Das et al. (2015) (mice; increased maternal relative liver weight)	4.9 $BMDL_{10}$	--	1.51×10^{-4} [a]	0.00074	1000 $UF_H = 10$ $UF_A = 3$ $UF_L = 10$ $UF_D = 3$	7.4×10^{-7} (4.9/1000 = 0.0049)	70 kg adult 2L/day RSC 50%	13
NHDES (2019b)	Das et al. (2015) (mice; increased maternal relative liver weight)	4.9 $BMDL_{10}$	1570	8.83×10^{-5}	0.00043	100 $UF_H = 10$ $UF_A = 3$ $UF_D = 3$ **lack of multigenerational and immune studies**	4.3×10^{-6} (4.9/100 = 0.049)	Transgenerational toxicokinetic model developed by MDH for breast fed and bottle fed infants (Goeden et al. 2019) RSC 50%	11
MISAW (2019)	Das et al. (2015) (mice; decreased body weight gain, delays in eye opening, preputial separation and vaginal opening)	6.8 NOAEL	1417	9.78×10^{-5}	0.000665	300 $UF_H = 10$ $UF_A = 3$ $UF_D = 10$	2.2×10^{-6} (6.8/300 = 0.023)	Transgenerational toxicokinetic model developed by MDH for breast fed and bottle fed infants (Goeden et al. 2019) RSC 50%	6
PFHxS									
ATSDR (2018a)	Butenhoff et al. (2009) (rats; thyroid follicular cell damage)	73.22 NOAEL	3100	6.42×10^{-5}	0.0047	300 $UF_H = 10$ $UF_A = 3$ $UF_D = 10$ **few immune studies**	2×10^{-5} (73.22/300 = 0.244)	ND	ND

Agency	Key Study (effect)	POD Animal Serum (mg/L)	Human T ½ Used (days)	Dosimetric Adjustment Factor (L/kg/d)	HED (mg/kg-day)	UF	Candidate RfD or MRL (Serum Concentration at RfD, mg/L)	DW Exposure Parameters and Relative Source Contribution Factor (RSC)	DW Value (ppt, ng/L)
MDH (2019b)	NTP (2018) (rats; altered thyroid hormone levels)	32.4 $BMDL_{20}$	1935	9.0×10^{-5}	0.00292	300 $UF_H = 10$ $UF_A = 3$ $UF_D = 10$	9.7×10^{-6} 32.4/300 = 0.108)	Transgenerational toxicokinetic model developed by MDH for breast fed and bottle fed infants (Goeden et al. 2019) RSC 50%	47
NHDES (2019b)	Chang et al. (2018) (mice; change in mean litter size)	13.9 BMDL	1716	8.61×10^{-5}	0.0012	300 $UF_H = 10$ $UF_A = 3$ $UF_S = 3$ $UF_D = 3$ **Lack of multigenerational and immune studies**	4×10^{-6} (13.9/300= 0.046)	Transgenerational toxicokinetic model developed by MDH for breast fed and bottle fed infants (Goeden et al. 2019) RSC 50%	18
MISAW (2019)	NTP (2018) (rats; decreased serum free thyroxine (fT4), decreased total T4, triiodothyronine (T3), changes in cholesterol levels and increased hepatic focal necrosis) (MDH 2019b analysis)	32.4 $BMDL_{20}$	1935	9.0×10^{-5}	0.00292	300 $UF_H = 10$ $UF_A = 3$ $UF_D = 10$	9.7×10^{-6} (32.4/300 = 0.108)	Transgenerational toxicokinetic model developed by MDH for breast fed and bottle fed infants (Goeden et al. 2019) RSC 50%	51

[a] personal communication G. Ginsberg.

APPENDIX 2

Review and Discussion of Key Low Dose PFAS Effect Data

Table of Contents

1. PFOA

1.1 Developmental Toxicity

USEPA based its RfD for PFOA (USEPA 2016a) on developmental toxicity endpoints, including reduced ossification of proximal phalanges and preputial separation in mice in a study conducted by Lau et al. (2006). ATSDR also based its draft minimum risk level on developmental outcomes but relied on effect data, reported at lower doses, from two other publications (ATSDR 2018a). These effects included skeletal alterations (Koskela et al. 2016) and neurobehavioral effects (Onishchenko et al. 2011) in offspring of mice exposed throughout pregnancy.

Brief summaries of the key studies are presented in the following sections.

1.1.1 *Skeletal and Neurobehavioral Effects*

The critical developmental endpoint selected by the USEPA to derive its PFOA RfD included reduced ossification of proximal phalanges in a study conducted by Lau et al. (2006), and
The key developmental endpoints relied upon by used by ATSDR in its PFOA MRL derivation included skeletal alterations (Koskela et al. 2016) and neurobehavioral effects (Onishchenko et al. 2011) in offspring of mice exposed throughout pregnancy (ATSDR 2018a). These studies are briefly summarized below.

Key Studies

Lau et al. 2006. Mouse. Lau et al. (2006) treated timed-pregnant CD-1 mice with 0, 1, 3, 5, 10, 20, or 40 mg/kg PFOA daily by oral gavage on GD1-17. Dams were divided into two groups. In the first group, dams were sacrificed on GD18 and underwent gross maternal and fetal examinations. Maternal blood was collected and analyzed for PFOA serum concentration. PFOA levels in the fetuses were not examined. External gross necropsy and skeletal and visceral examinations were conducted in live fetuses. In the second group of dams, an additional dose of PFOA was administered on GD18. Dams were allowed to give birth on GD19. The results of the study showed dose-dependent and statistically significant ($p < 0.05$) increases in maternal liver weigh. The LOAEL for this effect was 1 mg/kg/day and no NOAEL was identified. Ossification (number of sites) of the forelimb proximal phalanges was significantly decreased at all doses except 5 mg/kg and other skeletal anomalies and reduced fetal survival were observed at higher doses. The prenatal developmental LOAEL in this study was 1 mg/kg based on increased skeletal defects, and the NOAEL was not established.

Koskela et al. 2016. Pregnant C57BL/6 mice were treated orally with a daily dose of 0.3 mg PFOA/kg/day throughout gestation, and the female offspring were studied at the age of 13 or 17 months. Bone morphology and function of the femurs and tibias were analyzed. The effects of PFOA on bone cell differentiation were studied in osteoclasts

from PFOA-treated C57BL/6 mice. PFOA exposed mice showed increased femoral periosteal area as well as decreased mineral density of tibias. Biomechanical properties of these bones were not affected. Bone PFOA concentrations remained elevated even at the age of 17 months.

Onishchenko et al. 2011. Female mice were treated with 0.3 mg/kg-day of PFOS or PFOA throughout pregnancy. The authors applied a battery of behavioral tests to evaluate motor function, circadian, and behavioral activity in the exposed offspring. Exposure to PFOS resulted in decreased locomotion in a novel environment and reduced muscle strength only in male offspring. Prenatal exposure to PFOA was associated with changes in exploratory behavior in male and female offspring, as well as with increased global activity in males in their home cage. The authors concluded that prenatal exposure to PFAS in mice resulted in sex-related alterations in motor function.

1.1.1.1 Skeletal and Neurobehavioral Data Interpretation by Various Agencies for PFOA Toxicity Value Derivation

USEPA. The USEPA (2016a) used the skeletsl endpoint identified in the the Lau et al. (2006) study as a basis to derive its RfD for PFOA. The Wisconsin Department of Health Services (WIDHS 2019) also relied on a model-derived human equivalent dose (HED) that was developed by Kieskamp et al (2019) using the LOAEL identified in the Lau et al. (2006) study to derive its toxicity number (See Appendix1, Table 1).

Regarding neurobehavioral effects, the USEPA discussed the Johansson et al. (2008) and Onishchenko et al. (2011) studies on the neurobehavioral effects of PFOA in animals and concluded that the data suggest a need for additional studies of the effects of PFAS, including PFOA, on the brain. No mention of the Koskela et al. (2016) study on bone morphology and function was made in the USEPA document.

ATSDR. ATSDR (2018a) concluded that these studies provided the lowest LOAELs for PFOA effects and an appropriate basis for MRL derivation[1] The draft ATSDR MRL based on these endpoints is 7-times lower than the USEPA RfD.

NJDWQI. NJDWQI (2017) discussed the Johansson et al. (2008), Onishchenko et al (2011) and Sobolewski et al. (2014) neurobehavioral studies. In its "Summary of Conclusions of Toxicology Studies" section, NJDWQI concluded that the various toxicological effects that were observed in the reviewed studies, including the

[1] Note that ATSDR(2018a) did not rely on the very low LOAELs for delays in mammary gland development (Macon et al. 2011; Tucker et al. 2015) or the liver effects resulting from *in utero* exposures (Quist et al. 2015a,b).

neurobehavioral effects, are relevant to humans. The Koskela et al. (2016) study on bone morphology and function was mentioned but was not extensively discussed or critiqued in the NJDWQI document.

The NJDWQI RfD for PFOA is based on liver toxicity (NJDWQI 2017) and includes an uncertainty factor of 10 to account for potentially more sensitive developmental endpoints, in particular developmental effects on the mammary gland. The NJDWQI RfD is 10-times lower than USEPA's.

1.1.1.2 **Conclusions**

There are a number of limitations with respect to the two key publications relied upon by ATSDR (ATSDR 2018a). Both studies used offspring from the same exposed parental group, and serum PFOA concentrations were not measured, necessitating the use of modeled serum values. Further, both studies used a single dose. Although this dose was selected to be within the range of effects seen in previous studies and therefore yields meaningful results, the use of a single dose precludes quantitative evaluation of the dose-response relationship which introduces uncertainty with respect to use of the data as a POD for quantitative derivation of a toxicity value. Lastly, the the authors considered the skeletal effect as minor and it did not appear to lead to any functional deficits.

Because of the issues noted above MassDEP decided not to rely on these endpoints as a POD but rather views these effects as supportive of the use of an additional UF for database uncertainty in the RfD derivation.

1.1.2 ***Mammary Gland Developmental Effects***

Delayed mammary gland development in mice following PFOA exposure is a sensitive toxicological endpoint with effects observed at doses considerably lower than those associated with other outcomes. These effects are of concern because animal bioassay data for this endpoint are considered to be relevant to people due to the fact that mammary gland developmental processes during embryonic, postnatal, and adult life-stages are well conserved across mammalian species.

Nine publications have addressed effects of PFOA exposure in animals on mammary gland development. These studies have been reviewed extensively by USEPA, NJDWQI and ATSDR. All but one of these publications reported that PFOA exposures caused altered mammary gland development based on either qualitative histological and/or quantitative measures (White et al. 2007, 2009, 2011; Macon et al. 2011; Tucker et al. 2015). Effects were demonstrated to persist in exposed pups for at least 18 months, a considerable fraction of the mouse lifespan (White et al. 2009). However, despite significant PFOA effects on measures of mammary gland development, dam nursing efficacy was not noticeably compromised in the only publication addressing the potential functional significance of these mammary effects (White et al. 2011).

The two key studies identifying low effect levels are briefly summarized below.

Key Studies

Macon et al. (2011). The lowest effect levels for the mammary gland development were reported by Macon et al. (2011) and Tucker et al. (2015). Macon et al. (2011) includes data from two studies. Both used CD-1 mice, and PFOA exposures were via gavage. In one study, mice were exposed to 0, 0.3, 1, or 3 mg/kg-day on gestational day (GDs) 1-17. In the second study they were exposed to 0, 0.01, 0.1 or 1 mg/kg-day on GDs 10-17. In both studies, mammary gland development was assessed from whole-mount mammary gland preparations using qualitative histological development scores. In the late gestational exposure study (GDs 10-17), several quantitative measures of gland development, including terminal end bud counts, were also reported. Three to five offspring were evaluated per dose group, and scoring was completed blind to exposure group. Serum PFOA concentration data were also reported, including data from PND 1, allowing for dose response modeling using PFOA serum concentrations as the dose metric. Mammary gland development assessed on PND 21 exhibited statistically significant dose-dependent reductions in development scores, with a LOAEL of 0.01 mg/kg-day, and with no NOAEL identified. A significant dose-dependent reduction in terminal end bud counts was also reported with a LOAEL of 0.1 mg/kg-day. Using those data, NJDWQI (2017) derived a PFOA BMDL for development score of 24.9 ng/ml, based on serum concentrations at PND 1 and a 10% response rate; and, for terminal end bud count, of 22.9 ng/ml.

Tucker et al. (2015). The two studies addressed in this publication evaluated mammary gland development, among other endpoints, in CD-1 and C57BI/6 strains of mice. For CD-1 mice, 8-22 pups, and for C57BI/6, from 2-10 animals, were evaluated in each dose group. Animals were dosed using gavage with 0, 0.01, 0.1, 0.3 or 1 mg/kg-day over GD 1-17. Mammary gland developmental scores were assessed across dose groups based on histological evaluations, blinded as to dose group. No quantitative measures of mammary gland development were reported. Reduced development scores were observed in both strains with a LOAEL of 0.01 mg/kg-day in CD-1 mice and 0.3 mg/kg-day, in C57BI/6 mice. The Tucker et al. (2015) data were not amenable to BMDL analysis as PND 1 serum concentrations were not reported.

1.1.2.1 Mammary Gland Development Data Interpretation by Various Organizations for PFOA Toxicity Value Derivation

ATSDR. ATSDR (2018a) noted that, relative to studies of other toxicity endpoints, these studies identified very low LOAELs (Macon et al. 2011; Tucker et al. 2015; White et al. 2011). However, ATSDR did not elect to rely on the mammary gland effect data stating that it "did not result in an adverse effect on lactational support at maternal doses as high as 1 mg/kg-day, based on normal growth and survival in F2 pups (White et al. 2011). Given that milk production was adequate to support growth, the biological significance of the delayed development of the mammary gland is uncertain and was not considered a suitable basis for the MRL." Instead, ATSDR relied on neurodevelopmental and skeletal developmental effects as the basis for their MRL.

USEPA. USEPA (2016a) provided a review of the mammary gland developmental studies in mice but also chose not to address this effect in their PFOA RfD derivation. USEPA's reasoning for this decision was that: 1) the mode of action for these effects is not known; 2) the effects occurred only at higher doses in a second strain of mice, based on the higher LOAEL observed in the C57BI/6 strain in Tucker at al. (2015); and, 3) the functional significance of the effect is unclear.

NJDWQI. NJ DQWQI (2017) calculated a BMDL serum concentration of 22.9 ng/ml for terminal end bud count, a quantitative measure of effect, from the Macon et al. (2011) publication. Using this value as a POD and applying a total UF of 30, NJDWQI derived a target human PFOA serum concentration for this endpoint of 0.8 ng/ml and a candidate RfD of 1.1×10^{-7} mg/kg-day. This value is well below the USEPA RfD for PFOA of 2×10^{-5} mg/kg-day.

Although NJDWQI (2017) derived a candidate RfD for PFOA based on mammary gland effects, they did not ultimately rely on this value because of a lack of precedent for use of this endpoint. Instead, NJDWQI accounted for the mammary gland effect data through the inclusion of database UF of 10 applied to an RfD derivation based on liver effects.

MDHHS. The Maine Department of Health and Human Services, Center for Disease Control and Prevention (MDHHS), derived a Maximum Exposure Guideline (MEG) for PFOA in drinking water (MDHHS 2014). The MEG was based on liver toxicity data from multiple studies and species and also included a database uncertainty factor of 10, in part to account for the mammary gland data.

1.1.2.2 **Mammary Gland Developmental Toxicity Conclusions**

To date, MassDEP is unaware of any regulatory agency or organization that has relied on delayed mammary gland development as a POD in developing an RfD, drinking water value or other health based guideline for PFOA. This can be attributed to: 1) uncertainty regarding the biological significance of the effects, as they did not lead to any apparent functional impairment based on nursed F2 pups, which exhibited normal growth in the one study where this was assessed (White et al. 2011)[2]; 2) concerns regarding data quality and reproducibility attributable to the use of response measures based on qualitative mammary histology scores[3]; and, 3) a lack of precedent for using such endpoints as a POD.

However, in light of the consistency of mammary gland effects observed in multiple studies and their biological persistence, some agencies have concluded these effects are a concern and have accounted for this data through the use of a database uncertainty factor in their RfD derivations. MassDEP concurs with this later approach.

1.1.3 ***Developmental Liver Effects***

Liver effects are sensitive toxicological endpoints for PFOA and have been observed in response to low doses in many studies in mice, rats and non-human primates. Increases in liver weight and liver hypertrophy are two of the most sensitive effects that occur at low doses in both sexes of tested animals with clear dose response relationships. These effects may exist with or progress to more severe hepatic effects including hepatocellular inflammation, necrosis, fatty liver, increased serum liver enzymes and hyperplastic nodules. Some of these effects on the liver occur at doses below those relied upon by USEPA to derive its RfD for PFOA (USEPA 2016a).

Six studies documenting PFOA liver effects at LOAELs lower than that used by USEPA to derive an RfD for PFOA were identified. Of the six studies, four are developmental studies and three of these have the lowest reported LOAELs (0.01 - 0.3 mg/kg-day) for liver effects. These LOAELs are lower by factors ranging from 3 to 100 than the LOAEL selected by USEPA to derive the PFOA RfD. The key low dose developmental studies are briefly summarized below.

Key Studies

Quist et al. (2015a,b). In this study, pregnant CD-1 mice were treated orally by gavage with 0, 0.01, 0.1, 0.3, or 1 mg/kg-day PFOA from gestation days (GD) 1 - 17. Pups were weaned on postnatal day 21 (PND 21). The female offspring were retained for further

[2] This is consistent with the effect not being biologically significant but is based on very limited data and no overall assessment of the nutritional composition of the milk. Further research regarding potential changes in milk production and quality is needed.

[3] These concerns are mitigated by the use of averaged histology slide scores of two pathologists, blind to treatment group and the fact that these PFOA effects were observed in several studies.

investigation; male offspring were not evaluated. A subset of female mice were given a high fat diet (60% kcal% fat) challenge and control diet (10% kcal% fat) for 6 weeks starting on PND 35. After 6 weeks, animals in the fat diet group were returned to Purina 5001 diet. Significantly increased relative liver weight was observed on PND 21 in the female offspring of PFOA treated dams at 0.3 mg/kg-day, but this effect was not observed on PND 91. Pathological changes observed on PND 21 in the female offspring included chronic active periportal inflammation at 0.01 mg/kg-day that increased in severity by PND 91 in a dose-dependent fashion. Serum lipids (total cholesterol, low density and high density lipoproteins) were significantly altered, especially in animals fed high fat diet, at doses ≥ 0.01 mg/kg-day. Examination of selected liver sections on PND 91 demonstrated PFOA-induced hepatocellular damage and mitochondrial abnormalities with no evidence of peroxisome proliferation. The authors of this study concluded that peroxisome proliferation is not a component of PFOA-induced hepatic toxicity in animals that are exposed to low doses of PFOA *in utero*, and that the proposed mechanism for the observed hepatic effects relates to mitochondrial disruption.

Filgo et al. (2015). Filgo et al. (2015) treated CD-1 mice with 0, 0.01, 0.1, 0.3, 1 mg/kg-day PFOA from GDs 1 – 17. Similarly, timed 129/Sv mice (WT) and PPARa-KO mice were given 0, 0.1, 0.3, 0.6, or 1 mg PFOA/kg/day from GDs 1 – 17. Female offspring from each treated group were necropsied at 18 months of age followed by pathological examination of liver sections. Significant dose-related trends were observed for hepatocyte hypertrophy and hyperplasia, becoming statistically significant at the highest dose (5 mg/kg-day) tested in the CD-1 mice. Hepatocellular adenomas that are not dose-related were also identified in the PFOA treated CD-1 mice. WT mice appeared to be more sensitive than the CD-1 and KO mice for PFOA-induced non-neoplastic lesions. Significant hepatocyte hypertrophy was observed at ≥ 0.3 mg/kg-day in WT mice and bile duct hyperplasia was observed at ≥ 0.01 mg/kg-day in WT mice. However, no hepatocellular adenomas were observed in the WT strain. In the KO mice, a significant trend for dose-response relationship was observed for bile duct hyperplasia and the effect was significant at 3 mg/kg-day. Hepatocellular adenomas were observed in all treated groups but were not dose-related. The authors concluded that low-dose gestational exposures to PFOA induced latent PPARa-independent liver lesions in all treated strains. Similarly to Quist et al. (2015a,b), Filgo et al. (2015) proposed that the mechanism for the *in utero* induced hepatotoxicity by PFOA treatment could be mitochondrial disruption, which is a response that may not be associated with peroxisome proliferation.

Macon et al. 2011. In a study designed primarily to study the effects of PFOA on mammary gland (discussed previously), Macon et al. (2011) treated pregnant CD-1 mice on GD 1-17 with 0, 0.3, 1, 3 mg/kg-day by gavage and found significantly increased

relative liver weight at ≥ 0.3 mg/kg in males and females pups on PND7. The serum level measured at 0.3 mg/kg-day on PND 7 was 4.98 mg/L.

Abbott et al. 2007. In this study pregnant 129S1/SvlmJ (wild type (WT) and PPARα-null (KO) mice were treated from GDs1-17 with 0, 0.1, 0.3, 0.6, 1, 3, 5, 10, or 20 mg/kg-day of PFOA. At weaning, relative liver weights were significantly increased in WT offspring gestationally exposed to ≥ 0.1 mg/kg and in the KO offspring dosed at 3 mg/kg-day. The LOAEL in offspring for increased relative liver weight in WT mice (0.1 mg/kg-day) was 10-fold lower than the maternal LOAEL (1 mg/kg-day) in the same strain. The LOAEL for this effect in KO mice was the same in pups and dams (3 mg/kg-day). PFOA is known to activate PPARα, a pathway proposed to be the sole mode of action for induction of liver toxicity in rodents. However, the hepatic results observed in KO mice treated with PFOA indicate that modes of action other than PPARα are also involved in the hepatic toxicity of PFOA.

In summary, the developmental studies indicate that *in utero* exposure to PFOA may cause necrotic and inflammatory effects in the liver, which could result in permanent alterations in liver physiology and histology at low doses (0.01 - 0.3 mg/kg-day). These effects were not totally dependent on PPARα activation. The lesions observed in mice exposed prenatally also included hepatic adenomas. This observation warrants further studies in larger groups of animals.

1.1.3.1 Liver Developmental Toxicity Data Interpretation by Various Organizations for PFOA RfD Derivation

ATSDR. Although ATSDR (2018a) noted that exposure to low levels of PFOA causes a range of liver effects in various mammalian species, the lowest dose liver effects were not used as a critical endpoint in its MRL derivation for PFOA. The ATSDR, based on the Hall et al. (2012) paper, attributed hepatocellular hypertrophy and altered serum lipids in rodents to peroxisome proliferation and, in the absence of degenerative lesions, or inflammation, these effects were not considered adverse or relevant to humans. ATSDR noted that the Quist et al. (2015a,b) study reported significant hepatic inflammation in prenatally exposed mice but did not rely on this data to derive its MRL because the study did not provide incidence data.

USEPA. USEPA (2014a) extensively reviewed the human and animal toxicity data on PFOA and derived candidate RfDs based largely on increased liver weight in rodents and primates. However, in its PFOA document (USEPA 2016a), the agency chose other developmental endpoints (reduced ossification of the proximal phalanges of the forelimb and hindlimb and accelerated puberty in male pups) as the basis for its RfD derivation. The USEPA stated that it did not consider the PFOA induced liver weight increases as an appropriate basis for RfD derivation because of a lack of data to demonstrate adversity

(i.e., increased hepatocyte necrosis, inflammation, and steatosis) as determined by the Hall et al. (2012) criteria.

The human relevance of the observed rodent PFAS liver effects have been questioned on the basis of the Hall et al. (2012) paper, as well as on the PPARα mode of action. None-the-less, as discussed elsewhere in this document, several states have concluded that these liver effects should not be discounted and have used them as points of departure in their RfD derivations.

NJDWQI. Unlike USEPA (2016a) and ATSDR (2018a), NJDWQI (2017) and NHDES (2019b) have relied on relative increased liver weight as a POD to derive their respective RfDs for PFOA. The NJDWQI considers changes in hepatic parameters to be a well-established and sensitive effect of PFOA and other PFAS in experimental animals and that the liver effects observed in rodents are relevant to humans.

1.1.3.2 Conclusions

Increased liver weight and hypertrophy are the most frequently observed effects in animals treated with PFAS, including PFOA. More serious hepatic effects have been reported in animals exposed *in utero* to low doses of PFOA. These effects include bile duct hyperplasia at ≥ 0.01 mg/kg-day; periportal inflammation at ≥ 0.01 mg/kg-day; and, alterations in serum lipids, especially in animals fed a high fat diet, at ≥ 0.01 mg/kg-day. Increases in liver weight and hepatic cell hypertrophy are also observed at ≥ 0.3 mg/kg-day in these animals. These effects are all associated with PFOA doses below 1 mg/kg-day, the dose level used as the basis for the USEPA PFOA RfD (USEPA 2016a). Both the subchronic (Quist et al. 2015a,b) and chronic (Filgo et al. 2015) studies conducted in the female offspring of mice that were exposed *in utero* to very low doses of PFOA demonstrated that gestational exposure to PFOA results in persistent effects that can progress over time to more serious liver damage. The authors of these studies proposed that the observed hepatic effects are mediated, at least in part, by mitochondrial disruption that does not involve PPARα activation. The results of the Abbott et al. (2007) study in WT and KO mice also indicate that the hepatic effects observed in *in utero* exposed mice in that study are not totally dependent on PPARα activity. The non-PPARα mode of action that is at least partially responsible for these liver effects is not fully understood. In conclusion, after reviewing the low dose hepatic effects of PFOA in rodents exposed prenatally, and the mode of action proposed by various investigators, MassDEP has concluded that the hepatic data on developmental (and non-developmental, see next section) liver effects is relevant to humans and further support a lower RfD than that developed by the USEPA for PFOA (USEPA 2016a).

1.1.4 *Non-Developmental Liver Effects*

Three short-term studies and one subchronic study that reported low dose liver effects not associated with prenatal exposures are summarized below.

Key Studies

Li et al (2017). This study investigated molecular mechanisms of apoptosis associated with PFOA exposure in a mouse model. Male and female Balb/c mice were administered PFOA in corn oil at 0.05, 0.5 or 2.5 mg/kg-day for 28 days. Serum and liver samples were collected from 10 mice/sex/group. The authors reported decreased body weight, increased absolute liver weight, hepatocellular hypertrophy and apoptosis, lipid accumulation in hepatocyte cytoplasm, changes to mitochondrial morphology and membrane potential, and oxidative DNA damage (increased 8-hydroxydeoxyguanosine formation) in the liver. At the lowest dose tested, 0.05 mg/kg-day) female mice were significantly more sensitive than males to PFOA-induced apoptosis mediated by the mitochondrial dysfunction, including mitochondrial membrane potential changes, increased biomarkers of apoptosis, suppression of the Complex I pathway inducing reactive oxygen species, in the absence of PPAR-alpha activation. At the higher doses PPAR-alpha was activated in females and males.

Son et al. (2008). In this study PFOA was administered at 0, 0.49, 2.64, 17.63, or 47.21 mg/kg-day PFOA in drinking water to 4 week old male ICR mice for 21 days. Relative liver weights were significantly increased in all treated animals and the LOAEL for this effect was 0.49 mg/kg-day. Hepatocyte enlargement with acidophilic cytoplasm and an increase in plasma alanine aminotransferase (ALT) levels were observed at higher doses.

Loveless et al. (2006). This study examined the hepatic effects of three isomeric forms of PFOA (linear isomers, branched isomers, and mixed linear/branched isomers) in male rats and mice. The linear and branched isomers affected the mouse liver at lower doses than the rat liver. In the mouse studies, Crl:CDs (ICRR)BR male mice were treated with 0, 0.3, 1, 3, 10 or 30 mg/kg-day of either linear or branched isomer of PFOA for 14 days. Significantly increased relative liver weights were observed in male mice treated with 0.3 mg/kg-day of the linear or the branched isomer of PFOA. The serum level at this dose was 13 mg/L for the linear isomer and 14 mg/L for the branched isomer. In this study increased relative liver weights did not correlate with hepatic peroxisome proliferation, as indicated by palmitoyl CoA oxidase (PCO) activity, which is a biomarker for peroxisome proliferation. In rats, branched isomers of PFOA were more potent in increasing relative liver weight than linear isomers, but were less potent in increasing PCO activity. These results suggest that the observed hepatic effects may occur via PPAR-alpha independent processes.

Perkins et al. 2004. The authors conducted a 13-week dietary toxicity study in male rats. In this study, male rats were treated with 0, 0.06, 0.64, 1.94, and 6.5 mg/kg-day PFOA for 13 weeks. Rats fed 6.5 mg/kg-day PFOA were allowed to recover for 8 weeks. Sacrifices were conducted after 4, 7, and 13 weeks of feeding and after 8 weeks of recovery. Liver weights (absolute and relative), palmitoyl CoA oxidase (PCoAO) activity (biochemical marker of peroxisome proliferation), and hepatocyte hypertrophy (minimal to mild) were increased at ≥ 0.64 mg/kg-day after 4, 7, and 13 weeks of treatment with PFOA. The authors stated that changes observed in the liver could be the result of peroxisome proliferation and other processes, including increased intracellular metabolism and increased storage of metabolic products. They also noted that the severity of cellular enlargement did not appear to increase with duration and the observed hepatic effects were reversible based on the lack of residual effects in the 8 week recovery group. The lack of increase in severity of effects with duration in adult animals is different than that observed in animals exposed *in utero*. The observed reversibility of hepatic effects after 8 weeks of recovery in rats may not occur in humans where the elimination half-life of PFOA is several years compared to days in rats. Perkins et al. (2004) identified the liver as a target organ for PFOA toxicity and 0.64 mg/kg-day as the LOAEL for liver effects.

1.1.4.1 Liver Toxicity Data Interpretation by Various Organizations for PFOA RfD Derivation

ATSDR. As noted previously, ATSDR, based on the Hall et al. (2012) paper, attributed hepatocellular hypertrophy and altered serum lipids in rodents to peroxisome proliferation and, in the absence of degenerative lesions, or inflammation, did not consider these effects to be adverse or relevant to humans (ATSDR 2018a).

USEPA. The USEPA also stated that it did not consider the PFOA induced liver weight increases as a critical endpoint to serve as a basis for RfD derivation because of a lack of data to demonstrate adversity as determined by the Hall et al. (2012) criteria (USEPA 2016a).

NJDWQI and NHDES. The NJDWQI (2017) and NHDES (2019b) selected the Loveless et al. (2006) study described previously as the critical study and identified relative increased liver weight as the POD to derive their respective RfDs for PFOA. The methods used to derive the RfDs by the two organizations and the resulting toxicity values are summarized in Appendix 1, Table 1. NJDWQI considers changes in hepatic parameters to be a well-established effect of PFOA and other PFAS in experimental animals, and that the liver effects observed in rodents are relevant to humans. NHDES has noted that its toxicity values for the different PFAS were derived from the lowest doses in animal studies that were determined to be relevant to human health.

MDHHS. In its derivation of a Maximum Exposure Guideline (MEG) for PFOA in drinking water, MDHHS (2014), in contrast to ATSDR (2018a), did not discount the low dose liver effect data and based their MEG on changes in liver weight and hepatic cell hypertrophy from multiple studies and species.

1.1.4.2 Conclusions

Increase in liver weight and hypertrophy are frequently reported effects in animals treated with PFOA. As stated previously, some agencies have concluded that these effects are adverse and relevant to human health and have used the hepatic results to derive RfDs. Others, citing the Hall et al. (2012) publication that has reported liver weight changes and hepatocellular hypertrophy in rodents to be non-adverse compensatory responses mediated by PPARα activation have not considered them as bases for RfD derivation. However, several state agencies do not agree with this determination and consider liver effects observed in rodents to be adverse and relevant to humans and have relied on such effects in their RfD derivations. The reviewed data show that the LOAELs for PFOA liver effects in adult animals ranged from 0.3 to 0.64 mg/kg-day, while the developmental LOAELS ranged from 0.01 – 0.3 mg/kg-day (Quist et al. 2015a,b; Filgo et al. 2015). All these values are lower than the developmental LOAEL (1 mg/kg-day) used by the USEPA to derive its RfD for PFOA. The developmental studies that reported LOAELs that are orders of magnitude lower than the USEPA POD have various limitations and were not considered by any agency as PODs for either candidate or final RfD derivation. Overall, the liver effect data both following *in utero* and adult exposures indicate that effects may occur at dose levels below those relied upon by USEPA to derive its RfD, supporting an RfD for PFOA lower than that developed by USEPA.

1.2 **Immunotoxicity**

Immunotoxicity has not been a driver in toxicity value derivations for PFOA as other responses in animal studies have been reported to occur at lower dose levels (NTP 2016). For example, in mice treated with PFOA for 15 days, the lowest LOAEL for reduced antibody responses, the most sensitive endpoint identified, was 1.9 mg/kg-day (DeWitt et al. 2008, 2015). However, based on its review, MassDEP has concluded that experimental differences in the available studies, including the use of different animal strains, immune challenge agents from different batches (i.e. SRBC, which can vary in immunogenicity), test methods, dosing periods, immune challenge periods and immunological endpoints assessed, limit the ability to meaningfully evaluate PFAS immunotoxicity across compounds.

2. PFOS

2.1 **Immunotoxicity**

Concerns about immunotoxicity effects have contributed to the derivation of toxicity values for PFOS lower than USEPA's RfD by a number of agencies including, ATSDR (2018a), NJDWQI (2018), MDH (2017, 2019a), NHDES (2019a,b), and EFSA (2018a).

Immunotoxicity was the focus of an NTP (2016) systematic review of PFOA and PFOS in which NTP concluded that both compounds should be presumed to be immune hazards to people based on a high level of evidence from animal studies and a moderate level of evidence from studies in humans. The NTP (2016) review was published after the PFOS Drinking Water Health Advisory and Health Effects Support Document (USEPA 2016b,d) were issued and thus was not cited in those assessments.

Several epidemiological studies have reported associations between levels of PFAS, including PFOS, PFOA and others in serum and various measures of immune function. These have been extensively reviewed in previous assessments completed by the USEPA (2016b), NTP (2016) and NJDWQI (2018). NTP notes that the effects of PFAS on infectious disease resistance involve reduced ability to respond to infectious disease and increased disease incidence. Evaluation of associations between exposures to PFOS or other individual PFAS and lowered disease resistance or antibody responses are complicated by the fact that exposures can occur to multiple PFAS, which may act as effect modifiers. Granum et al. (2013) reported that maternal PFOS serum levels were associated with decreased antibody levels in response to rubella vaccination. No association was reported between PFOS and the common cold or cases of gastroenteritis in children. Associations with lower antibody responses were stronger with

PFOA, PFNA, and PFHxS than with PFOS[4]. Research studies on children in the Faroe Islands also have reported significant associations between PFAS serum levels and measures of immune function (Morgensen et al. 2015; Kielsen et al. 2016; Grandjean et al. 2012). Other studies have not reported such associations (NTP 2016). Taken together, NTP characterized the human data on PFAS and measures of immune function as providing a moderate level of evidence for an effect (NTP 2016). This is typical of epidemiology study data, which are limited in their power to detect effects, in particular with complex exposure situations involving multiple compounds, relatively small sample sizes, and confounding factors. Due to issues relating to statistical power and inconsistencies in reported associations, no US federal or state agency has relied on the human data to derive toxicity or drinking water values for PFAS compounds. However, EFSA has published an assessment of risks to human health posed by PFOS and PFOA in food (EFSA 2018a)[5], which was based on human epidemiological data. EFSA (2018a) conducted an extensive review of epidemiological and dietary exposure data for these compounds. Based on the human data, including data on immune function, EFSA derived a Tolerable Weekly Intake (TWI) value of 13 ng/kg-week for PFOS (equivalent to an RfD/MRL of 2 ng/kg-day) [6]. EFSA (2018a) also noted a number of effects in animals that occurred at doses below 1 mg PFOS (and PFOA)/kg-day, the point of departure (POD) used by USEPA in its RfD derivations.

Numerous animal bioassay studies have also reported PFOS effects on measures of immune function, some at doses well below those used in the USEPA RfD derivation (NTP 2016). NTP concluded that, "there is high confidence that exposure to PFOS is associated with suppression of the antibody response based on the available animal studies and that the results show consistent suppression of the primary antibody responses (NTP 2016)." Immunotoxicity has been identified as one of the most sensitive endpoints following PFOS exposures in animal bioassays (ATSDR 2018a; NJDWQI 2018). Studies conducted by Dong et al. (2009, 2011), Guruge et al. (2009) and Peden-Adams et al. (2008) identified the lowest administered doses of PFOS that caused immunological effects. Immunotoxicity results in mice treated with PFOS for 60 days (Dong et al. 2009), with a LOAEL of 0.08 mg/kg-day and a NOAEL of 0.008 mg/kg-day, served as the basis of the NJDWQI RfD for PFOS (NJDWQI 2018), and resulted in a value 10-fold lower than USEPA's RfD. The evidence for PFOS immunotoxicity from animal bioassay and epidemiological studies also led MDH and ATSDR to incorporate additional uncertainty factors of 3 and 10, respectively, in their 2017 and 2018 toxicity assessments to account for these

[4] The combined maternal PFOA, PFNA, and PFHxS level was, however, associated with both lower vaccination antibody levels and an increased number of colds. Combined PFOA and PFHxS were also associated with cases of gastroenteritis in children.

[5] EFSA's reliance on the human epidemiological data has been criticized and ongoing consultations on this issue among EU member organizations are underway (EFSA 2018b).

[6] EFSA (2018a) also evaluated dietary exposures to PFOS and PFOA. Although EFSA noted that there is considerable uncertainty in the dietary intake estimates, it concluded that "it is clear that a considerable portion of the (European) population exceeds the established TWIs for PFOS and PFOA".

effects, resulting in RfD values lower than USEPA's (MDH 2017; ATSDR 2018a). More recently, MDH used immunotoxicity data as the basis of their updated RfD (MDH 2019a).

The four key studies relied on by these groups are briefly summarized below.

Key Studies

Dong et al. 2009, 2011. These studies included immune response endpoints and were cited in all PFOS assessments reviewed. Results from the 2009 study were used by the NJDWQI (2018) as the POD in their RfD derivation and MDH (2019a) selected data from the 2011 study as a POD in their most recent PFOS toxicity assessment.

In both studies, the control groups were treated with vehicle only, providing appropriate controls.

The Dong et al. (2009) study involved groups of 10 male C57BL/6 mice exposed for 60 days via gavage to 0, 8.33, 83.3, 416.67, 833.33 or 2083.33 ug PFOS/kg-day, using a vehicle of deionized water with 2% Tween. The authors do not state whether the researchers were blinded as to treatment groups in the experiments. Animal serum PFOS concentrations for each dose group were determined at the end of the 60 day dosing regimen. Serum corticosteroid levels, a measure of stress, which can impact immune responses, were also measured and were not significantly different from controls at the LOAEL. The sheep red blood cell (SRBC)-specific IgM plaque forming cell (PFC) response following SRBC challenge 4 days prior to sacrifice was the most sensitive immune response observed and yielded clear dose response relationships across the dose ranges tested. A LOAEL of 83.3 ug/kg-day (corresponding to a mean measured serum concentration of 7.132 mg/L) and a NOAEL of 8.33 ug/kg-day (corresponding to a mean measured serum concentration of 0.674 mg/L) were identified. SRBC immune challenge assays are considered a well-accepted measure of immune function (NTP 2016) and PFC results have been used by USEPA as a critical endpoint in the derivation of RfD's for trans-1,2-dichloroethylene and trichloroethylene (USEPA 2010, 2011).

The Dong et al. (2011) study used the same mouse strain but used six male animals per dose group. This study included a dose level between the LOAEL and NOAEL identified in the Dong et al. (2009) publication. In this study, serum total immunoglobin levels were determined for each dose group using enzyme-linked immunosorbent assays (ELISA). A LOAEL was identified at an applied dose of 83.3 ug/kg-day, the same as that determined by Dong et al. (2009), corresponding to a serum PFAS concentration of 10.750 mg/L). The NOAEL for this endpoint occurred at the added intermediate dose level of 16.7 ug/kg-day (corresponding to a serum concentration of 2.36 mg/L). Serum corticosteroid levels, a measure of stress that can impact immune responses, were also measured and were not significantly different from controls at the LOAEL.

NTP rated both these studies as "probably having a high risk of bias" due to uncertainty regarding whether the research personnel were blinded to the study group (NTP 2016). Although this designation introduces a degree of uncertainty with respect to interpreting the results of these studies, MassDEP does not consider this a sufficient basis to exclude them from consideration. MassDEP therefore concluded that it is appropriate to consider the results from the Dong et al. (2009, 2011) studies in assessing PFOS immune-toxicity risk. The Dong et al. (2011) study is somewhat limited by the small number of animals per dose group.

Peden-Adams et al. 2008. This study reported NOAEL and LOAEL values for decreased PFC response in B6C3F1 mice treated with PFOS for 28 days. The values are almost two-orders of magnitude lower than those reported in the Dong et al. (2009, 2011) studies. Serum corticosteroid levels were not measured in this study precluding evaluation of potential differences in dose group stress levels. Corticosteroid levels have been suggested as a possible explanation for the very low effect levels observed (NJDWQI 2018). The number of animals per dose group was also low (5 per group) in this study. Furthermore, the mouse strain in this study differs from that used by Dong et al. (2009, 2011) which could also account for response differences.

NTP also rated this study as "probably having a high risk of bias" due to uncertainty regarding whether the research personnel were blinded to the study group (NTP 2016).

Guruge et al. 2009. In this study, the effect of a 21 day pre-exposure of 0, 5, or 25 ug PFOS/kg-day on resistance to influenza A virus infection in female B6C3F1 mice was assessed. Control animals were treated with the carrier solution only. Initial dose groups consisted of 30 animals each. At 21 days, three animals from each group were sacrificed to determine PFOS serum and organ concentrations. Measured mean serum PFOS levels were 0.0021 ($\pm$ 0.0003); 0.189 ($\pm$ 0.014); and 0.670 ($\pm$ 0.047) mg/L for the control, intermediate and highest dose levels, respectively. The remaining animals were challenged with mouse-adapted influenza virus at a dose predetermined in the host lab to result in approximately 40% mortality in the mouse strain being used. Animals were then followed for an additional 20 days. Survival rates at 20 days post viral infection were 46% for the untreated animals, 30% for those treated with the intermediate dose and 17% at the highest dose. Mortality at the highest tested dose was significantly different from controls ($p = 0.035$, logistic regression Wald Test) and there was a statistically significant trend in mortality ($p = 0.014$, Cochran-Armitage trend test). To our knowledge, this is the only experimental animal study that has been published addressing increased susceptibility to viral challenge mortality associated with PFOS exposure.

NTP (2016) concluded that there is "serious concern for risk of bias with this study" due to concerns about investigator blinding and attrition in the animal dose groups due to unexplained changes in animal numbers. MassDEP notes that the loss in animal numbers in the dose groups at viral challenge were modest, ranging from 3-4 animals out of 27, per group.

2.1.1 *Immunotoxicity Data Interpretation by Various Organizations for PFOS Toxicity Value Derivations*

USEPA. The USEPA PFOS and PFOA assessments (USEPA 2016a,b) were completed prior to the publication of the NTP PFOS and PFOA Immunotoxicity report (NTP 2016). USEPA (2016a,b) did, however, consider immunotoxicity as an endpoint in their assessments, noting that "taken together, the lower antibody titers associated with PFOS levels in humans and the consistent suppression of SRBC response in animals indicates a concern for adverse effects on the immune system". USEPA did not, however, rely on immunotoxicity data as a POD for their RfD nor include any uncertainty or modifying factor to account for these data. The USEPA stated that this decision was made because of "lack of human dosing information and lack of low-dose confirmation of effects in animals for the short-duration study". In contrast to USEPA's approach three other agencies ATSDR (2018a), NJDWQI (2018), and MDH (2017), as discussed further below, all concluded that low dose immunotoxicity endpoints present a significant concern and explicitly accounted for this concern in their PFOS toxicity assessments.

ATSDR. In its MRL derivation for PFOS, ATSDR chose to rely on time-weighted average (TWA) serum concentrations as an integrated dose metric in deriving PFOS effect levels (ATSDR 2018a). Although Dong et al. (2009, 2011) provided serum PFOS concentrations determined at the end of the dosing period, TWA estimates for these studies could not be calculated due to a lack of necessary pharmacokinetic model parameter information for the species/strain of the mice used in the study (ATSDR 2018a). Thus, ATSDR did not rely on the immunotoxicity data from the Dong et al. (2009, 2011) studies as a POD. ATSDR did, however, account for "concern that immunotoxicity may be more sensitive for PFOS toxicity than developmental toxicity" by applying an additional modifying factor of 10 in the MRL derivation, which was based on developmental endpoints.

NJDWQI. The NJDWQI (2018) PFOS report provides an extensive assessment of data relevant to PFOS toxicity and includes reviews of the animal and epidemiological data on immunotoxicity. Based on their assessment, NJDWQI selected the serum concentration associated with the SRBC PFC immune response from Dong et al. (2009) as the most sensitive POD for deriving their RfD. A BMDL for this data set could not be calculated,

potentially because of the steepness of the dose response. Therefore, NJDWQI used a NOAEL approach with the serum PFOS concentration data reported in the study at the end of the dosing period in their analysis, noting that because of the relatively long serum half-life for PFOS, the measured serum concentrations at the end of the 60 day dosing period would be higher than the TWA dose metric, if calculable, preferred by ATSDR (2018a). In the NJDWQI assessment, use of the Dong et al. (2009) NOAEL as a POD resulted in an RfD of 1.8 x 10^{-6} mg/kg-day, a value 10-fold lower than the USEPA RfD. Rounded to one significant figure, this is equivalent to the draft ATSDR (2018a) MRL of 2 x 10^{-6} mg/kg-day.

MDH. MDH recently revised its RfD for PFOS and used the Dong et al. (2011) immunotoxicity study to derive a RfD of 3 x 10^{-6} mg/kg-day for PFOS and an associated drinking water level of 15 ppt (MDH 2019a). The previous MDH RfD was 5 x 10^{-6} mg/kg-day, which was used to derive a drinking water level of 27 ppt (MDH 2017). Consistent with USEPA (2016b) and ATSDR (2018a), MDH (2017) had previously relied on Luebker et al. (2005a), as the critical study with a POD based on reduced pup body weight. In that case MDH addressed concerns about possible immunotoxicity by including a database UF of 3.

NHDES. In January 2019, the NHDES (2019a) released a proposed RfD of 8 x 10^{-6} mg/kg-day and an associated drinking water level of 70 ppt for PFOS. Consistent with the USEPA (2016b), the NHDES (2019a) RfD was based on developmental delays observed in the Luebker et al. (2005a) study. On June 28, 2019, the NHDES (2019b) proposed an updated RfD of 3 x 10^{-6} mg/kg-day and a corresponding drinking water value of 15 ppt for PFOS (Appendix 1, Table1). Like MDH, NHDES chose the Dong et al. (2011) immunotoxicity study and followed the MDH risk assessment approach to derive its updated health numbers (Appendix 1, Table 1). The Dong et al. (2011) study identified a higher NOAEL POD (0.0167 mg/kg-day; mean measured serum concentration 2.36 mg/L) than the NOAEL POD (0.0083 mg/kg-day; mean measured serum concentration 0.674 mg/L) determined by Dong et al. (2009), the results of which were used by the NJDWQI (2018). Dong et al (2009) and Dong et al. (2011) both measured immune suppression in the same strain of mice, but Dong et al. (2011) included a dose between the NOAEL and the LOAEL observed in the Dong et al. (2009) investigation and that dose was determined to be the NOAEL for immune suppression and thus selected by NHDES and MDH.

2.1.2 *PFOS Immunotoxicity Conclusions*

In light of the NTP (2016) conclusion that both PFOS and PFOA should be presumed to be immune hazards to people based on a high level of evidence from animal studies and a moderate level of evidence from studies in humans, MassDEP believes it is appropriate to

account for immunotoxicity risk in the derivation of an RfD for PFOS. Although there is variability in reported effect levels across the various animal immune toxicity studies, data from several studies (Guruge et al. 2009; Dong et al. 2009, 2011), indicate that measures of immunotoxicity are more sensitive endpoints than those relied upon by USEPA in its RfD derivation for PFOS. The relevance of PFAS animal immunotoxicity observations is further supported by data from a number of epidemiological studies reviewed by NTP (2016), EFSA (2018a) and NJDWQI (2018). As noted above, concerns over PFOS immunotoxicity have been reflected in the toxicity values derived by a number of organizations, all of which are lower than the USEPA RfD. PFOS toxicity values derived by ATSDR, NJDWQI and MDH either relied upon immunotoxicity endpoints as the critical effect POD or applied an additional UF in their toxicity value derivations to account for immunotoxicity concerns.

Based on review of the data and the above documents, MassDEP has concluded that the evidence regarding immunotoxicity is convincing and sufficient to support a lower RfD for PFOS than previously derived by USEPA.

2.2 **Developmental Toxicity**

An extensive number of studies using mice and rats have demonstrated that exposures to PFOS can cause a variety of developmental effects including developmental delays in a number of developmental stages. These include neurodevelopmental effects on spatial learning and activity, developmental malformations and increased pup mortality (USEPA 2016b; ATSDR 2018a; NJDWQI 2018). USEPA and ATSDR relied on the same developmental toxicity study and endpoint as a POD in their RfD and MRL derivations[7]. The key study is summarized below.

Key Study

Luebker et al. 2005b. Sprague-Dawley rats were administered PFOS by gavage at doses of 0, 0.1, 0.4, 1.6, or 3.2 mg/kg-day for 6 weeks before mating and until sacrifice on GD10 (subgroup) or PND21. Dose groups included 35 animals per sex per dose. F1 rats were administered learning, memory retention, and avoidance memory neurobehavioral tests at 24 days and neuromuscular coordination, swimming ability, learning, and memory tests at 70 days. PFOS was analyzed in liver and blood from parental females; in liver from F1 pups on PND 21; and in liver and serum from parental males after mating and after 42–56 days of dosing. High-dose parental males had significantly reduced terminal body weight. Parental females at 0.4 mg/kg-day and higher had localized areas of partial alopecia. The body weight of high-dose parental females was significantly

[7] The ATSDR (2018a) MRL is lower than the USEPA (2016b) RfD because ATSDR included an additional UF to account for data indicating that immunotoxicity effects may be a more sensitive endpoint.

lower during cohabitation and gestation. PFOS did not affect mating or fertility parameters. Estrous cycling was not affected. High-dose parental females exhibited reduced number of implantations per delivered litter and decreased gestational length. The number of dams with all pups dying on PND 1–4 was also increased at 1.6 and 3.2 mg/kg-day. F1 pups during PNDs 1– 21 showed significantly reduced weight and decreased viability (≥ 1.6 mg/kg-day). Developmental delays were noted at 1.6 mg/kg-day (several) and 0.4 mg/kg-day (eye opening). F2 pup weight was significantly reduced at 0.4 mg/kg-day on PND 7 (13%). The study LOAEL and NOAEL were 0.4 and 0.1 mg/kg-day, respectively.

2.2.1 *Data Interpretation by Various Organizations in PFOS Toxicity Value Derivations*

ATSDR. ATSDR (2018a) derived several draft candidate MRLs for PFOS based on developmental toxicity endpoints (ATSDR 2018a). The MRL selected as the final draft value, 2 $x10^{-6}$ mg/kg-day, was based on delayed eye opening and decreased F2 pup weight in mice as reported by Luebker et al. 2005a. These effects were chosen as the critical endpoints because the effects were associated with the lowest predicted serum PFOS concentration and an experimentally derived NOAEL was also identified in the study. This POD was the same as that selected by USEPA (2016b) and MDH (2019a). The difference between the final draft MRL vs. RfD values is attributable to the added MF of 10 applied by ATSDR (2018a) to account for more sensitive immunotoxicity effects that occurred at lower applied doses but were not amenable to extrapolation of serum AUCs, ATSDR's chosen dose metric, as well as (minor) differences in parameters used to calculate human equivalent doses. ATSDR (2018a) also derived three somewhat lower candidate MRLs, ranging from 4.6 - 7.4 X 10^{-7} mg/kg-day, based on developmental effects observed in other studies. These effects included increased pup mortality and lung histopathology (Chen et al. 2012); decreased pup weight (Luebker et al. 2005b) and delayed eye opening in pups (Lau et al. 2003). The Chen et al. 2012 study was not selected because the LOAEL was at a higher serum PFOS concentration and the NOAEL was at a substantially lower dose than in the Luebker et al. (2005a) study. No NOAELs were identified in the other two studies.

USEPA. USEPA (2016b) relied on the same critical study and endpoint but did not include an uncertainty factor to account for other more sensitive endpoints.

WIDHS. WIDHS (2019) adopted the ATSDR (2018a) oral minimum risk level (MRL) of 2 $x10^{-6}$ mg/kg-day as its acceptable daily intake (ADI) value for PFOS (See Appendix 1, Table 1 for details.

2.2.2 *PFOS Developmental Toxicity Conclusions*

ATSDR (2018a) and USEPA (2016b) and WIDHS based their MRL/RfD derivations on the same study and endpoints. Other studies and developmental endpoints that could support a somewhat lower (2-3 fold) RfD were considered quantitatively less preferable to that chosen due to the lack of experimentally derived NOAELs in two (Lau et al. 2003 and Luebker et al. 2005b) and the higher predicted LOAEL serum concentration in the other (Chen et al. 2012). However, these studies do provide evidence supporting a lower RfD for PFOS.

3. PFNA

The current database on the human and animal toxicity of PFNA is not as extensive as it is for PFOA and PFOS. In the US, the ATSDR (2018a), NJDWQI (2015) and NHDES (2019a,b) have derived toxicity values for PFNA. The toxicity values derived by these groups are based on data from the same animal study.

Some of the human cross-sectional studies reviewed by ATSDR (2018a) and NJDWQI (2015) found significant associations between detected serum levels of PFNA in the general population and increases in serum lipids, particularly total cholesterol and low-density lipoprotein (LDL) cholesterol, and decreased antibody response to vaccines. After reviewing the epidemiological data for PFNA, both ATSDR (2018a) and NJDWQI (2015) noted that many individuals were co-exposed to other PFAS and concluded that quantitative exposure-response assessment based on the human data was not feasible. Instead, the three agencies relied on the same animal study to derive their respective toxicity values.

Key elements of this study are summarized below and other supporting data are briefly discussed.

3.1 **Developmental Toxicity**

Key Study

Das et al. (2015). Timed-pregnant CD-1 mice (19-27 per dose group) were administered 0, 1, 3, 5 or 10 mg/kg-day of PFNA by oral gavage on GD 1-17. The 10 mg/kg-day dose was toxic to the fetus and the effects of PFNA in this dose group were not assessed. Although most of the pups were born alive in the 5 mg/kg-day PFNA group, 80% of those neonates died in the first 10 days of life, indicating that a dose as low as 5 mg/kg-day was lethal to the pups that were exposed *in utero*. Postnatal survival in the 1 and 3 mg/kg-day PFNA groups was not different from that in controls. Increases in absolute and relative liver weights were observed in dams exposed to ≥ 1 mg/kg-day when examined on GD17 and post weaning day 28. Also, relative pup liver weights were increased at doses ≥ 1 mg/kg-day when examined at postnatal day (PND) 1, 10, or 24 in a dose-dependent manner. At PND 42 significant increases in relative liver weights were

seen only at doses ≥ 3 mg/kg-day: at PND 70, no significant effects were observed, which may be attributable to the relatively fast clearance (serum half-life of days) of the compound[8]. Since histopathological evaluation of livers was not performed in this study, it is not clear if the changes in liver weight were accompanied with altered histopathology, precluding evaluation of the significance of the liver effects using the Hall criteria (Hall et al. 2012). Delayed postnatal development (eye opening, preputial separation and vaginal opening) and decreased body weight gain, persisting in males up to PND 287, were observed at ≥ 3 mg/kg-day. Measured serum levels at the end of exposure in the dams treated with 0, 1, 3 or 5 mg/kg-day were 0.013, 12.4, 18.3, or 57.1 mg/L (NJDWQI 2015), respectively. ATSDR (2018a) calculated time weighted average (TWA) serum concentrations based on the measured serum concentrations in dams corresponding to 1, 3 or 5 mg/kg-day dose levels were 6.8, 10.9, or 39.7 mg/L, respectively. The study authors identified changes in absolute and relative liver weights (in dams) and relative liver weights (in pups) as the most sensitive endpoints observed in the study. They also stated that the profile of PFNA developmental toxicity in mice generally resembles that of PFOA and PFOS, with PFNA being the more potent.

Supporting Developmental/Reproductive Studies

Wolf et al. (2010). 129S1/SvlmJ PPAR*α* knockout (KO) and wild-type (WT) mice were treated using gavage with 0.83, 1.1, 1.5, or 2 mg/kg-day PFNA on GDs 1−18. In WT mice, PFNA exposure reduced the number of live pups at birth and survival of offspring at weaning in the 1.1 and 2 mg/kg-day dose groups. Eye opening was delayed (mean delay 2.1 days) and pup weight at weaning was reduced in WT pups at 2 mg/kg-day. None of these parameters were altered in the KO mice. Relative liver weights were increased at 0.83 mg/kg-day in pregnant and non-pregnant WT mice and at 1.1 mg/kg-day in KO mice. Liver weights were also increased at 0.83 and 2 mg/kg-day in WT and KO pups respectively. NJDWQI noted that PFNA levels were measured 23 days after dosing ended and these serum levels are not indicative of the maximum exposure levels which may have caused toxicity (NJDWQI 2015). The study authors concluded that: (1) liver effects can be mediated by PPARα dependent and independent pathways; and (2) that PPAR*α* is an essential mediator of PFNA-induced developmental toxicity in the mouse, and the relevance of PPARα to human developmental effects cannot be dismissed as PPARα and other PPAR isoforms are expressed in many fetal and adult tissues in rodents and humans. The LOAEL in this study is 0.83 mg/kg-day for increased relative liver weight in non-pregnant WT adult mice and in WT pups.

[8] Recovery would likely be different in humans where the half-life of PFNA is years rather than days.

Stump et al. (2008). Stump et al. (2008) conducted a two-generation reproductive study using a PFAS mixture with high content of PFNA. This mixture is known as Surflon S-11 and it is normally composed of: PFNA, 74%; perfluoroundecanoic acid (PFUnDA, C11), 20%; perfluorotridecanoic acid (C13) 5%; PFOA (C8) 0.78%; perfluorodecanoic acid (C10) 0.37%; and perfluorododecanoic acid (C12), 0.1%. F0 male and female and F1 male and female Sprague-Dawley rats were dosed starting at age 6 weeks for at least 70 days prior to mating, throughout mating, gestation, and lactation, and until euthanasia (total dosing period is estimated to be 18 weeks) with 0, 0.025, 0.125, or 0.6 mg/kg-day of Surflon S-11 (0, 0.019, 0.09, or 0.44 mg/kg-day PFNA). Observed effects in Surflon-treated rats included: increased absolute and relative liver weight, and decreased body weight in F0 and F1 male rats at 0.125 mg/kg-day. Similar effects were observed in F0 and F1 females at 0.6 mg/kg-day. In F0 males, hepatocellular hypertrophy and necrosis was observed at 0.025 mg/kg-day, which was lower than the dose that caused an increase in liver weight and hepatocellular hypertrophy. In F0 and F1 female rats hepatocyte hypertrophy was increased at 0.6 mg/kg-day. The lowest LOAEL of 0.025 mg/kg-day Surflon S-11 (0.019 mg/kg-day PFNA) was recorded for hepatocellular hypertrophy and necrosis in this study. Although the PFNA concentration is higher than any of the components of the mixture, the results of this study are not suitable to use for PFNA quantitative toxicity assessment as the presence of the other long-chain PFAS in the mixture could contribute to the observed adverse effects. The study, however, suggests that simultaneous exposure to PFNA and other long chain PFAS induces severe hepatic effects at a very low dose level of 0.025 mg/kg-day.

3.2 Data Interpretation by Various Organizations for PFNA Toxicity Value Derivation

ATSDR. ATSDR (2018a) selected the Das et al. (2015) study as the critical study, and chose delayed postnatal development (eye opening, preputial separation and vaginal opening) and decreased body weight gain in pups as the most appropriate endpoints. The NOAEL identified for all these developmental endpoints was 1 mg/kg-day and was used as a POD. Developmental endpoints were also selected by USEPA (2016 a,b) to derive its RfDs for PFOA and PFOS.

ATSDR (2018a) calculated a TWA serum concentration of 6.8 mg/L associated with the NOAEL based on first order kinetics. This serum concentration was converted to a human equivalent dose (HED) using PFNA specific pharmacokinetic parameters derived from the Zhang et al. (2013) publication. The HED was further adjusted by appropriate uncertainty factors resulting in an oral MRL of 3×10^{-6} mg/kg-day (Appendix 1, Table 1).

NJDWQI (2105). Increases in dam absolute and relative liver weight, also from the Das et al. (2015) study, was selected as the most sensitive endpoint by the NJDWQI (2015). A LOAEL of 1 mg/kg-day was identified for this endpoint**.** Since serum levels were measured at the various administered dose levels, the NJDWQI applied a benchmark dose modeling approach and determined a $BMDL_{10}$ serum level of 4.9 mg/L for a 10% increase in liver weight from the mean liver weight in the pregnant controls. This serum level was used as a POD and then adjusted by a total UF of 1000 to yield a human equivalent serum concentration of (HEC). The HEC was further converted to applied dose assuming a blood serum:drinking water ratio of 200:1. The RfD equivalent for PFNA, determined by the NJDWQI was 7.4×10^{-7} mg/kg-day (Appendix 1, Table1).

NHDES. Similarly to ATSDR (2018a) and NJDWQI (2015), NHDES (2019b) relied on the Das et al. (2015) developmental study to derive its RfD for PFNA. NHDES (2019b), consistent with NJDWQI (2015), chose increase in dam liver weight as the key endpoint. As previously discussed, the NJDWQI performed a BMD analysis on the dose-response data from this study to estimate the serum concentration associated with a 10% increase in relative liver weight. The serum concentration of PFNA for the lower 95% confidence limit (the $BMDL_{10}$) from the best fit model was 4.9 mg/L. This same serum value was used by the NHDES as a point of departure (POD) in its RfD derivation process. This serum concentration was then converted into a human equivalent dose of 0.00043 mg/kg-day using available PFNA kinetic parameters. This human equivalent dose was further adjusted by a total uncertainty factor of 100 to derive an RfD of 4.3×10^{-6} mg/kg-day. In comparison, the RfD derived by NJDWQI (2015) was 7.4×10^{-7} mg/kg-day. The difference in these RfDs stems from methodological differences and the magnitude of the UFs and kinetic parameters applied by each organization.

3.3 **Conclusions**

Although the data for PFNA is more limited than for PFOS and PFOA, endpoints are similar for all three compounds and include developmental, liver and thyroid effects. ATSDR (2018a), NJDWQI (2015) and NHDES (2019b) selected the Das et al. (2015) study to derive their respective toxicity values for PFNA. The draft ATSDR MRL for PFNA (3×10^{-6} mg/kg-day) was based on developmental effects (Das et al. 2015) and is equivalent to the draft ATSDR (2018a) MRL value derived for PFOA. It is also very close to the draft MRL derived by ATSDR (2018a) for PFOS (2×10^{-6} mg/kg-day). All three draft MRLs were based on developmental effects (ATSDR 2018a).

On the other hand, some data, although limited, suggest that PFNA may exhibit greater potency compared to PFOA and PFOS with respect to certain liver toxicity endpoints. Although NJDWQI (2015) chose the same critical study in their assessment of PFNA

toxicity as ATSDR (2018a), NJDWQI determined that the reported increase in maternal liver weight in that study was the most sensitive endpoint and an appropriate POD. In contrast, citing the Hall criteria (Hall et al. 2012), ATSDR did not consider these effects to be adverse, as the study did not include pathology data allowing hepatocellular degenerative changes or other evidence of biliary or liver cell damage to be assessed. NJDWQI's use of the liver data resulted in a toxicity value about 4 times lower[9] than ATSDRs.

In conclusion, in light of the similar range of toxic effects; similar toxicity value derivations based on developmental and thyroid data; and issues pertaining to differing interpretation of the liver effect data, MassDEP does not find the data to be sufficient to conclude that there is a significant difference in toxicity between PFNA, PFOA, and PFOS.

4. PFHXS

The current database on the human and animal toxicity of PFHxS is not as extensive as it is for PFOA and PFOS. Based on the available data, ATSDR (2018a), MDH (2019b), NHDES (2019b) have published toxicity values for this compound. Each of the three agencies selected their PODs based on different studies and critical effect endpoints. MassDEP has also derived, for comparative purposes, putative RfDs based on the 28-day rat study peer review data published by the NTP (2018). The following section focuses on the key studies relied upon in these derivations.

4.1 Developmental Toxicity and Thyroid Effect Studies for PFHxS

Butenhoff et al. (2009). Scientists from 3M and related companies evaluated the potential reproductive and developmental toxicity of PFHxS. They treated 15 rats per sex with 0, 0.3, 1, 3, or 10 mg/kg-day PFHxS (potassium salt) by gavage for 14 days prior to cohabitation, during cohabitation, and until the day before sacrifice (PND21). The total days of treatment for parental females and males were about 35 and 42, respectively. The authors measured serum levels in dams and pups, evaluated reproductive success, clinical signs of toxicity, body weight, food consumption, estrous cycling, neurobehavioral effects, gross and microscopic anatomy of selected organs, sperm, hematology, clinical pathology, and the concentration of PFHxS in serum and liver. They reported no treatment-related effects in dams or offspring, but included the following biochemical and pathological results for parental males only: (1) thyroid follicular cell damage at 1 mg/kg-day (which was selected by ATSDR (2018a) as the POD in their MRL derivation,

[9] The serum based BMDL based on liver effects derived and used as a POD by the NJDWQI (2015) is only about 30% lower than ATSDR's (ATSDR 2018a) based on developmental effects. The difference in the final toxicity values derives from the use of different UFs.

73.22 mg/L TWA serum concentration); (2) increased prothrombin time at 0.3 and 10 mg/kg-day; (3); decreased hemoglobin levels at ≥ 1 mg/kg-day; (4) increased liver-to-body weight and liver-to-brain weight ratios, centrilobular hepatocellular hypertrophy, and decreased hematocrit at ≥3 mg/kg-day; and (5) decreased triglycerides and increased albumin, urea nitrogen (BUN), alkaline phosphatase (ALP), calcium (Ca2+), and albumin/globulin ratio (A/G) at 10 mg/kg-day.

The authors tabulated the hematology clinical chemistry, organ weight and pathology results of the parental generation only, and included a statement, without presenting the underlying data, that the control values for pup body weights, liver weights, and liver-to-body weight ratios were not statistically different from treated groups. Only control values were presented. Histological examination of pup livers was not conducted. Upon review of the publication, MassDEP noted that fetal viability appeared compromised at all dose levels as total implants and total number of pups delivered (live born and stillborn) were decreased in a dose-dependent fashion for the 0.3, 1.0, and 3.0 mg/kg-day group compared to concurrent controls. Further decreases were not observed at 10 mg/kg-day, which could be due to a saturation-mediated response. Thyroid hormone levels were not assessed and thyroid histopathology was not determined in the pups.

Ramhoj et al. (2018). Dose-response developmental studies were conducted using PFHxS, or PFHxS plus a fixed dose of EDmix, a mixture containing12 environmentally relevant endocrine disrupting chemicals. In the first set of experiments, time-mated Wistar rats were treated throughout pregnancy and lactation with two high doses of PFHxS (25 or 45 mg/kg-day), or two high doses of PFHxS + EDmix (PFHxS 25 or 40 mg/kg-day + 32.11 mg/kg-day EDmix) (n=5–7). Controls received no treatment. In the second set of experiments, pregnant rats were treated with 0, 0.05, 5, or 25 mg/kg-day PFHxS or EDmix-only, and 0.05, 5, or 25 mg/kg-day PFHxS plus EDmix (31.11 mg/kg-day) (n=13–20).

Serum PFHxS levels were measured on PND 22 in the first set of experiments, in which 25 or 45 mg/kg-day PFHxS were given to pregnant rats with or without the EDmix mixtures. The average PFHxS serum concentrations were 139 and 174 mg/L in animals exposed to 25 and 45 mg/kg-day PFHxS, respectively. No serum levels were measured in the low dose groups. In the groups co-exposed to EDmix and PFHxS, the PFHxS levels were slightly increased by 12.7% and 4.9% respectively, suggesting kinetic interaction between PFHxS and EDmix.

PFHxS caused decreased male pup birth weight and slightly increased liver weights at high doses (25 and 45 mg/kg-day) and in combination of these doses with the EDmix. In female pups, relative liver weight was increased at ≥ 5 mg/kg-day PFHxS + EDmix.

Total T4 levels were significantly decreased in both dams and offspring at doses ≥ 5 mg/kg-day PFHxS. Dams were affected by both PFHxS and EDmix, pups were affected only by PFHxS. The significantly lower T4 levels in the dams were seen at 5 mg/kg-day, after only 7 days of exposure, indicating that PFHxS is an effective thyroid hormone disruptor in rats. In the dams, T4 reductions became more marked with time, with further decrease at weaning (PND 22), compared with GD 15. Postnatal T4 decreases in offspring on PND 16/17 were likely due to lactational transfer of PFHxS. The apparent LOAEL in this study is 5 mg/kg-day for changes in thyroid hormone levels (dams and offspring) and for increase in relative liver weight (in offspring). However, the next lower dose of 0.05 mg/kg-day which can be designated as the NOAEL is two orders magnitude lower than the LOAEL of 5 mg/kg-day. This large dose spacing makes it hard to conclude with any confidence that 5 mg/kg day is indeed a LOAEL for changes in relative liver weight and thyroid hormone levels.

While the study supports the other animal data that show PFHxS to be toxic to the thyroid and liver, the dose spacing makes it hard to determine a reliable NOAEL or LOAEL. A recent study conducted in rats by NTP (2018), which will be discussed in the following section, showed that thyroid hormone levels were decreased at doses about 8 times lower than the LOAEL (5 mg/kg-day) identified in this study.

Chang et al. (2018). In this reproductive/developmental toxicity study, scientists from 3M and other affiliates treated CD-1 mice (n= 30/sex/dose group) with 0, 0.3, 1 or 3 mg/kg-day potassium perfluohexanesulfonate (K^+PFHxS) (Chang et al. 2018). F0 males were treated for at least 40 days; F0 females were treated throughout gestation and lactation. F1 pups were directly dosed (at the same maternal dose) with K+PFHxS for 14 days after weaning (36 days altogether). In F0 males, body weight gain was significantly increased at 0.3 and 1 mg/kg-day. In both F0 male and female mice, absolute and relative liver weights were significantly increased at ≥ 1 mg/kg-day. The NOAEL for change in absolute and relative liver weights in both males and females was 0.3 mg/kg-day. Microscopic evaluation of the F0 male and female livers showed centrilobular hepatocellular hypertrophy with the affected hepatocytes exhibiting ground-glass cytoplasmic alterations. The LOAEL in both parental males and females for hepatic hypertrophy was 0.3 mg/kg-day In F1 male pups, anogenital distance was significantly increased at all doses but the increase was not dose dependent. In F1 females, the anogenital distance was decreased but did not reach statistical significance. The mean litter size was significantly decreased at ≥ 1 mg/kg-day. The NOAEL for decrease in mean litter size was 0.3 mg/kg/day. Increases in absolute liver weight, hepatocellular hypertrophy, relative thyroid weight (females only) were observed in F0 males and females at higher doses.

Anogenital distance (AGD) was statistically significantly increased in male rats and non-significantly decreased in female pups on PND 1. There have been extensive studies of AGD effects of chemicals in animals, and these studies usually have shown a shortened AGD in male offspring reflecting decreased *in utero* androgen exposure and conversely a longer distance in females reflecting increased *in utero* androgen exposure (Foster 2006), which is the opposite of what is observed in the Chang et al. study. Others have also reported increases in AGD in both male and female animals exposed to endocrine disruptors like bisphenol A and diethylstilbestrol (Honma et al. 2002). PFHxS's effect on AGD is regarded as an endpoint of concern to MassDEP as changes in AGD in either sex have been linked to altered fertility and sexual organ structure and function.

Other Supporting Studies

Viberg et al. (2013). Male and female mice were administered 0.61, 6.1 or 9.2 mg/kg PFHxS as a single oral dose on PND 10, via a metal gastric tube. The results showed that a single exposure during a vulnerable period of brain development altered adult spontaneous behavior and cognitive function in both male and female mice in a dose-dependent fashion. PFHxS also affected the cholinergic system, manifested as altered nicotine-induced behavior in adult animals. Serum levels of PFHxS were not determined in this study. The LOAEL for decreased habituation observed in 2 month-old mice dosed earlier in life was 0.61 mg/kg, the lowest dose tested. The same patterns of neurotoxic effects were observed at 4 months of age, but the effects were seen at the highest dose.

Lee and Viberg (2013). Male and female mice were treated with 6.1 or 9.2 mg/kg of PFHxS as a single oral dose on postnatal day 10 (PND 10). Control mice received the vehicle only. The animals were sacrificed 24 h after the PFHxS exposure and the cerebral cortex and hippocampus brain regions were isolated and examined. The results of the study indicated that neonatal exposure to PFHxS, during the peak of the brain growth spurt, altered neuroprotein levels which are essential for normal brain development in mice. These proteins are essential for normal brain development and cognitive function. In a different study Zhang et al. (2016) performed a mechanistic study in rats injected with environmentally relevant doses of PFHxS and PFOA and determined that both compounds impaired the synaptic plasticity in the hippocampus CA1 region of the brain. The authors, Zhang et al. (2016), noted that the results of their study provided a potential mechanism for the neurotoxicity induced by PFHxS and PFOS.

4.2 Toxicity Data Interpretation by Various Organizations for PFHxS Toxicity Value Derivation

ATSDR). ATSDR (2018a) relied on the Butenhoff et al. (2009) study as the basis to derive its draft MRL. The selected endpoint was thyroid follicular cell hypertrophy and the NOAEL for this endpoint was 1 mg/kg-day. ATSDR, using the measured serum concentrations and a first-order single compartment model, calculated a time weighted average serum concentration of 73.22 mg/L as an internal dose NOAEL. This serum level was then converted to an HED of 0.0047 mg/kg-day using PFHxS specific kinetic parameters. The HED of 0.0047 mg/kg-day was further adjusted by various uncertainty factors to derive an MRL of 2×10^{-5} mg/kg-day (Appendix 1, Table 1). This MRL value is an order of magnitude higher than the MRL of 2×10^{-6} mg/kg-day that ATSDR derived for PFOS. However, an MRL that is about an order of magnitude lower for PFHxS could be derived based on increased prothrombin time, a more sensitive endpoint observed in the same study (Butenhoff et al. 2009), which occurred at a LOAEL of 0.3 mg/kg-day. ATSDR did not discuss this endpoint in their analysis.

MDH. MDH (2019b) issued revised guidance for PFHxS in April 2019. Previously, MDH had recommended that the PFOS value be used for this compound. The revised MDH (2019b) RfD of 9.7×10^{-6} mg/kg-day was derived from a calculated $BMDL_{20}$ for decreased free T4 from the NTP (2018) study, with a total UF of 300 applied.

NHDES. NHDES (2019b) released revised guidance including a new RfD of 4×10^{-6} mg/kg-day based on toxicity study conducted by Chang et al. (2018) that was reviewed previously. The critical endpoint selected was change in the mean live litter size for adult CD-1 mice and the associated measured serum level BMDL POD was 13.9 mg/L. This serum level was converted to human equivalent dose of 0.0012 mg/kg/day using PFHxS specific kinetic parameters. An RfD of 4×10^{-6} was calculated by applying various uncertainty factors to the HED.

Conclusions

Similar to PFOS and PFOA, animal studies indicate that PFHxS affects the thyroid, liver, hematologic system and developing brain. No immunotoxicity studies were identified in animals, although epidemiological studies suggest that PFHxS could compromise the human immune system.

ATSDR (2018a) derived an MRL of 2×10^{-5} mg/kg-day for PFHxS, which is about an order of magnitude higher than the MRL it derived for PFOA (2.7×10^{-6} mg/kg-day) and for PFOS (2×10^{-6} mg/kg-day). If prothrombin time, a more sensitive endpoint observed in the same study, had been selected as a POD, a RfD about 10-fold lower would result.

MDH (2019b) and NHDES (2019b) derived RfDs of 9.7 x 10^{-6} mg/kg-day and 9.3 x 10^{-6} mg/kg-day, respectively. These RfDs were based on thyroid effect (MDH 2019b) and reduced litter size (NHDES 2019b) data from different studies.

In conclusion, although the data allow for the derivation of PFHxS-specific RfDs MassDEP does not believe that the weight of the evidence is currently sufficient to conclude that its potency differs significantly from that of PFOS and PFOA. As discussed elsewhere in this report available comparative potency data do not provide strong support for a substantial difference in potency between PFHxS and the other longer chain PFAS The relative paucity of toxicity data, gaps regarding developmental and immunotoxicity data, and data that indicates the PFHxS human serum half-life may be significantly longer than for PFOA and PFOS (Appendix 4, Table 1) have lead MassDEP to conclude that it is prudent and appropriate to treat PFHxS as having the same potency as PFOS.

5. PFDA

The available data on PFDA toxicokinetic behavior and toxicity is sparse. Two organizations have applied a "read-across" approach to assess PFDA's potential toxicity relative to other related PFAS and recent data from the NTP 28-day study (NTP 2018) provide quantitative data on PFDA toxicity based on a number of endpoints. As discussed below and in Section 3.2 and Appendix 5, MassDEP has evaluated the comparative potency of this compound to other PFAS with respect to impacts on thyroid hormone levels, one of the most sensitive endpoints from the NTP data tables (NTP 2018). Key information is summarized below.

5.1 PFDA Data Summary

Key Studies

Frawley et al. 2018. Female Harlan Sprague-Dawley rats (4-6 weeks of age) were exposed to 0, 0.125, 0.25, 0.5 mg PFDA/kg by oral gavage daily for 28 days. Female B6C3F1/N mice were exposed once/week to 0.312, 0.625, 1.25, 2.5, or 5.0 mg/kg PFDA orally by gavage once a week for 4 weeks (on days 1, 8, 16, and 22). Animals were evaluated for various immune effects and other systemic effects. Treatment-related hepatocyte necrosis and hepatomegaly were observed in rats treated with 0.5 mg PFDA/kg-d. In mice, hepatomegaly (26–89%) was observed following exposure to 0.625 mg PFDA/kg/week, while splenic atrophy (20%) was observed at 5.0 mg PFDA/kg/week. Phagocytosis by fixed-tissue macrophages was decreased in liver (specific activity, 24–39%) at 0.25 mg PFDA/kg-d in rats. The authors concluded that their data suggest that exposure to PFDA may induce adverse effects in rat liver in a manner consistent with the PFAS class and may also alter the balance of immune cell populations in lymphoid tissues in mice.

Using the relationship (slope of the linear regression) between applied dose and serum concentration from the 28 day NTP 2018 study in same strain of rats (Sprague-Dawley), the estimated serum concentration associated with the NOAEL of 0.125 mg/kg-day is approximately 7 mg/L PFDA serum concentration; the LOAEL of 0.25 mg/kg-day is estimated as 19.5 mg/L. The NOAEL is consistent with the $BBMDL_{05}$ of 8 mg/L for decreased relative liver weight estimated by ORS (Appendix 5) using the NTP study data (NTP 2018).

NTP 2018. The National Toxicology Program (NTP 2018) evaluated PFDA in a 28-day study in male and female rats. In this study male and female male Harlan-Sprague Dawley rats (10 rats per dose group and per sex) were treated with oral doses of PFDA at 0, 0.156, 0.312, 0.625, 1.25, or 2.5 mg/kg-day for 28 days. Plasma concentrations of PFDA and several toxicity parameters were measured at study termination in controls and treated groups. PFDA altered body and organ weights, the histopathology of various organs, as well as clinical chemistry and hematology parameters in both male and female rats. In summary, the NTP (2018) study data indicates that PFDA effects the thyroid, liver, thymus and testes in male rats. The lowest LOAEL, 0.312 mg/kg-day (23 mg/mL measured serum concentration), was from decrease in fT4 levels in male rats.

Zeilmarker et al. **2018.** Zeilmarker et al. (2018) calculated a RPF for PFDA compared to PFOA of $4 \leq RPF \leq 10$. This range was based on a "Read Across" using available data on PFOA, PFNA and perfluoroundecanoic acid (PFUnDA) (Zeilmarker et al. 2018). This estimate suggests that PFDA may exhibit greater toxicity than the other PFAS considered in this report but is based on limited indirect data.

Brewster and Birnbaum 1989. In the only developmental study identified, pregnant micewere treated on GD 6 -15 with doses ranging from 0.03 to 12.8 mg/kg-day. Decreases in fetal weight per litter were observed at $\geq$ 1 mg/kg-day and fetal weight and fetal viability were decreased at the highest dose.

5.2 Toxicity Data Interpretation by Various Organizations for PFDA Toxicity Value Derivation

ATSDR. ATSDR (2018a) briefly reviewed the available studies on this compound. Most were conducted in adult animals that were administered PFDA as a single dose, precluding dose response analysis. The effects observed in these studies were similar to those observed with the other well studied PFAS like PFOA and PFOS and included changes in liver, body, spleen, and thymus weights, altered thyroid hormone levels and altered hepatic lipid parameters.

ATSDR (2018a) concluded that there were insufficient data for the derivation of MRLs for any route or duration of exposure. The ATSDR did not use data from the Brewster and Birnbaum study to derive a draft MRL because maternal serum PFDA levels were not measured. ATSDR also stated that other approaches such as "read across" or equivalency factors were considered. However, ATSDR concluded that there were insufficient data available to allow for comparison of the toxicity and toxicokinetic properties of PFDA with different perfluoroalkyl compounds. The NTP peer review data tables were published after ATSDR released its assessment and thus were not included in the ATSDR document (NTP 2018, ATSDR 2018a).

EU Committee for Risk Assessment (2015). This group relied on data available from the closely related analogs PFNA and PFOA as surrogates to fill data gaps for PFDA in a process termed "Read Across" (ECHA 2015). They concluded it is likely that PFDA would exhibit similar toxicological and kinetic properties to its structural homologs PFOA and PFNA.

5.3 Conclusions

The available studies indicate that PFDA affects the developing fetus, the liver, the blood and immune systems, and the thyroid. These are similar to the effects observed with PFOA, PFOS and PFNA. The limited half-life estimates are also similar to those reported for the other PFAS considered in this report.

To our knowledge no national or state agency has developed a toxicity value for PFDA and none of the reviewed data, except for that from the NTP (2018) study, are amenable to deriving an RfD. Two groups have applied read across approaches to consider PFDA's toxicity. One decided to treat PFDA as exhibiting toxicities similar to those associated with PFOA and PFNA (ECHA 2015). The other determined that PFDA could exhibit greater (4 to 10-fold) liver toxicity compared to PFOA (Zeilmarker et al. 2018).

Data from the NTP study were released after the ATSDR document was issued and were not considered in that assessment. As discussed elsewhere in this report the NTP data support treating PFDA similarly based on thyroid and liver effects.

6. PFHPA

PFHpA is one of the least studied of the longer-chain PFAS considered in this assessment. Based on the limited data available, ATSDR (2018a) noted that evidence from acute, intermediate, and chronic studies in rats, mice, and monkeys indicate that the liver is likely to be a target for PFHpA toxicity. However, ATSDR (2018a) concluded that the data were insufficient to derive an MRL for PFHpA for any duration of exposure.

Based on its structure, MassDEP believes that it is likely that PFHpA will fall between PFHxA and PFOA in potency. Unfortunately, at this time, there are no well-designed toxicity studies to allow for a determination to be made of whether PFHpA is more like PFHxA or PFOA. Until more toxicity data are available, MassDEP has concluded that it is prudent to assume that this compound causes toxic effects similar to its well-studied structural homologs PFOA and PFNA.

7. PFHXA

MassDEP previously concluded that the available data provides considerable evidence indicating the PFHxA is less toxic and is cleared more quickly from the body following exposures (MassDEP 2018).

> *In vivo* data (Chengelis et al. 2009; Loveless et al. 2009) indicate that PFHxA is toxicologically considerably less potent than PFHxS, PFOS, PFOA and PFNA on an applied dose basis. In a subchronic study in rats, the lowest NOAEL identified for liver effects in rats was 50 mg/kg-day. In a reproductive and developmental study, the NOAEL for body weight change in the P1 (parental) and F1 (offspring) generations were reported to be 20 mg/kg-day and 100 mg/kg-day, respectively. In comparison LOAELs for liver effects and other developmental outcomes for PFOS, PFOA and PFNA range from 0.01 - 2 mg/kg-day. Using the available animal liver toxicity data, Zeilmaker et al. (2018) derived a relative potency factor (RPF) of 0.01 for PFHxA compared to PFOA.

APPENDIX 3

Serum Half-Life for PFAS

Serum half-life is a metric used to estimate the elimination rate of a substance from the body (the amount of time for the serum concentration to decrease by one-half). For substances that are slowly eliminated from the body, such as PFAS, serum half-lives are long. Compounds with long half-lives can accumulate in the body, leading to extended internal exposures in target organs and tissues, and are thus of particular concern.

Individual PFAS have species and sex specific pharmacokinetics that have been characterized using serum half-life. Table 3-1 below shows the range of half-life values reported for PFAS in human and animal serum for the PFAS considered in this assessment. Human and animal half-life estimates vary considerably across studies and often overlap from compound to compound within and across studies.

Table 1. Summary of Half-Life Durations for Humans and Animals[a]

	PFOA	PFOS	PFNA	PFHxS	PFDA
Humans (years)	2.3 - 3.9	1.9 - 18	1.7 – 3.2[b]	5.3 - 15.5	4 – 7 [b]
Rodents (days)	0.15 – 21	19 – 62	2.4 – 34	0.7 – 31	40 – 59[b]

[a] Tables with data for each study are in Tables 2 and 3.
[b] Range from a single study.

Multiple studies provide estimates of human and animal half-lives for PFAS. These studies are summarized in Table 3-2 and 3-3, respectively. The human serum half-lives estimated from different occupational and community exposures demonstrate considerable inter-individual variability.

Evaluation of serum half-lives demonstrates similar long serum half-lives for five of the PFAS considered here, including PFOA, PFOS, PFNA, PFHxS and PFDA. This consistent evidence for very long human half-lives for each of these PFAS supports a high level of concern for internal exposures for long periods of time after exposure to these PFAS. The serum half-life data for PFHpA is very limited but suggests it may exhibit a shorter half-life compared to the other longer-chain PFAS evaluated here.

Extrapolation to Human Equivalent Dose (HED)

Because of the differences in half-lives between rodents and humans, serum half-life information is a critical element of deriving HED for PFAS. Human equivalent doses were estimated by adjusting the animal PFAS serum concentration[10] by the human clearance rate estimated for each PFAS, applying the approach used by USEPA (2016a,b) and ATSDR (2018a). The human serum

[10] The serum concentration from a study in animals can be extrapolated to an external dose/exposure concentration (i.e., HED) for humans that would result in a human serum concentration equivalent to the animal serum concentration. Estimates of serum half-life in humans are used for this extrapolation.

half-life (and volume of distribution) selected for estimating clearance contributes to uncertainty and the variability in the RfDs derived by different agencies.

Clearance was calculated based on the elimination half-life ($t_{1/2}$) and volume of distribution (Vd) using the following equation.

$$Cl = Vd \times (\ln 2 / t_{1/2})$$

Where:
Cl = clearance (L/kg bw/day)
Vd -= volume of distribution in the human body (L/kg bw)
ln2 = 0.693
$t_{1/2}$ = half-life in humans (days)

Table 2. Human Half-Lives (Years) for PFAS)

Half-life estimates (years; geometric mean unless otherwise noted) (range if given) (N = number of subjects if given

Study population (ages)	PFOA	PFOS	PFNA	PFHxS	PFDA	PFHpA	PFHxA
Workers							
Olsen et al. 2007 Ages 55-75 (N=26, 44 males, 2 females)	3.5 (95% CI 3.0 – 4.1) AM 3.8 (95% CI 3.1 – 4.4) (1.5 - 9.1) N = 26	4.8 (95% CI 4.0 – 5.8) AM 5.4 (95% CI 3.9 – 6.9) (2.4 – 21.7) N = 26		7.3 (95% CI 5.8 – 9.2) AM 8.5 (95% CI 6.4 – 10.6) (2.2 - 27) N = 26			
Ski Waxers							
Gomis et al. 2016 (using data of Nilsson et al. 2013) Ages 27-51	Median 2.4 (1.8 – 3.1) N = 4 males						
Russell et al. 2015 (using data of Nilsson et al. 2013) Ages 27-51						0.192 (0.0849 – 0.337) N = 8 males	0.0877 (0.0384 – 0.134) N = 8 males (Russell et al 2013)
Community							
Li et al. 2018 Ages 4-83 (male and female) Ages 15-50 (n=20 males)	AM 2.7 (95% CI 2.5 - 2.9) N = 106 AM 2.8 (95% CI 2.4 – 3.4)	AM 3.4 (95% CI 3.1 – 3.7) N = 106 AM 4.6 (95% CI 3.7 – 6.1)		AM 5.3 (95% CI 4.6 – 6.0) N = 106 AM 7.4 (95% CI 6.0 – 9.7)			

Study population (ages)	PFOA	PFOS	PFNA	PFHxS	PFDA	PFHpA	PFHxA
Ages 15-50 (n=30 females)	N = 20 males AM 2.4 (95% CI 2.0 – 3.0) N = 30 females	N = 20 males AM 3.1 (95% CI 2.7 – 3.7) N = 30 females		N = 20 males AM 4.7 (95% CI 3.9 – 5.9) N = 30 females			
Worley et al. 2017 Ages Mean = 62.6 (N=45, 22 males, 23 females)	AM 3.9 N = 45	AM 3.3 N = 45		AM 15.5 N = 45			
Bartell et al. 2010 Ages 38-68 (50% male)	AM 2.3 (95% CI 2.1 - 2.4) (1.5 – 4.6) N = 200 AM 2.1 (95% CI 1.9 - 2.4) N = 102 not consuming homegrown vegetables						
Brede et al. 2010 Ages 7.4-71 (n=65) Ages 27-71 (N=45)	3.3 (1.0 - 14.7) N = 65 adjusted for background exposure, i.e., intrinsic $t_{1/2}$ by Russell et al. (2015) 2.4						

Study population (ages)	PFOA	PFOS	PFNA	PFHxS	PFDA	PFHpA	PFHxA
	(95%CI 2.1 – 2.4) N = 65 2.5 (95%CI 2.4 – 2.7) N = 45 adults only						
General Population							
Zhang et al. 2013 Ages: females <50 and all men and females >50 (Chinese, one-time sample of serum and spot sample of urine)	1.5 (females <50 y) 1.2 (males & females >50y) N = 20, 66	5.8 (females <50 y) 18 (males & females >50y) N = 20, 66	1.7 (females <50 y) 3.2 (males & females >50y) N = 16, 50	7.1 (females <50 y) 25 (males & females >50y) N = 19, 64	4.0 (females <50 y) 7.1 (males & females >50y) N = 19, 60	1.0 (females <50 y) 0.82 ((males & females >50y) N = 12, 31	---
Nelson et al. 2016 (MDH 2019a); Nelson et al. 2018 (MDH 2019b) Ages Mean = 53		6.3 N = 149		8.6 N = 149			
Gomis et al. 2017; MDH 2019a Ages not reported (US)		AM 3.3 (females) AM 3.8 (males) N = not reported					
Wong et al, 2014; 2015 Ages 12-80 (NHANES, USA)		AM 4 (females) Model includes menstrual loss. AM 4.7 (males) N = 2000 (even					

Study population (ages)	PFOA	PFOS	PFNA	PFHxS	PFDA	PFHpA	PFHxA
		gender split					
Data sets excluded due to study quality issues							
Fu et al. 2016 Workers Ages 19-65 Limitations of results: different workers were used for each annual sample collection; worker retention 1-3 years, shorter than study period; volume (tons) of PFOS, PFHxS used at the facility changed most years.		32.6 (clearance based) 1.9 (annual decline based) N = 302 (n=46 with ≥3 samples)		14.7 (clearance based) 3.6 (annual decline based) N = 302 (n=46 with ≥3 samples)			

Table 3. Animal Half-Lives (Days) for PFAS

	Substance						
Species	**PFOA**	**PFOS**	**PFNA**	**PFHxS**	**PFDA**	**PFHpA**	**PFHxA**
Rat	1.6-1.8 (males) 0.15-0.19 (females) (Kim et al. 2016) 5.6 (males) 0.08 (females) (i.v.)(Ohmori et al. 2003)	22 (males) 23 (females) (i.v.)(Huang et al. 2019) (NTP) 19 (males) 21 (females) (gavage x 5 days)(Huang et al. 2019) (NTP) 27.8 (males) 24.8 (females) (Kim et al. 2016) 38 ± 2 (males) 62 ± 2 (females) (2 mg/kg gavage)(Chang et al. 2012)	24 (95% CI 20.2-27.8) (males) 32 (95% CI 3.2-119.1) (females) (3 mg/kg gavage)(Tatum-Gibbs et al. 2011) 30 (males) 2.4 (females) (i.v.)(Ohmori et al. 2003)	13 (males) 0.7 (females) (i.v.)(Huang et al. 2019 (NTP)) 18 (males) 2.3 (females) (gavage x 1 day)(Huang et al. 2019 (NTP)) 20.7–26.9 (males) 0.9–1.7 (females) (Kim et al. 2016) 29.1 (males) 1.64 (females) (Sundström et al. 2012)	40 (males) 59 (females) (i.v.)(Ohmori et al. 2003)	0.7 (males) (inhal 23 days at 6 hr/day)(Russell et al. 2015) 0.64-1 (males) 0.05 - 0.088 (females) (inhal 1 day for 6 hr)(Russell et al. 2015) 0.1 (males) 0.05 (females) (i.v.)(Ohmori et al. 2003)	0.158 (males) (inhal 23 days at 6 hr/day)(Russell et al. 2015) 0.054 (males) 0.0208 (females) (inhal 1 day for 6 hr/day)(Russell et al. 2015) 0.092-0.117 (males) 0.0875-0.113 (females) (oral 25 days)(Chengelis et al 2009)(N=3)
Mouse	21.7 (95% CI 19.5-24.1) (males) 15.6 (95% CI 14.7-16.5) (females) (gavage)(Lou et al. 2009)	42.8 (males) 37.8 (females) (1 mg/kg gavage)(Chang et al. 2012)	34.4 (95% CI 29.1-41.1) (males) 25.7 (95% CI 22.7-29.3) (females) (1 mg/kg gavage)(Tatum-Gibbs et al. 2011)	31 (males) 25 (females) (Sundström et al. 2012)	-		
Pig	236 (feed)(Numata et al. 2014)(N=24, males and	634 (feed)(Numata et al. 2014)(N=24)	-	713 (feed)(Numata et al. 2014)(N=24)	-	74 (feed)(Numata et al. 2014)(N=24)	4.1 (feed)(Numata et al. 2014)(N=24)

	females))						
Monkey	21 ± 12.5 (males) 33 ± 8 (females) (IV)(Butenhoff et al. 2004)	132 ± 7 (males) 110 ± 15 (females) (Chang et al. 2012)	-	141 ± 30 (males) 87 ± 27 (females) (Sundström et al. 2012)	-	-	0.104-0.221 (males) 0.071-0.10 (females) (IV one dose)(Chengelis et al 2009)(N=3)

APPENDIX 4

Table 1. Points of Departure for Endpoints by Target Organ Systems: Serum Concentrations Selected for Candidate RfDs, Final RfDs, and other Recent Critical Endpoints from Published Studies

Chemicals ↓	**Point of departure (NOAEL/LOAEL/BMDL/BBMD mg/L), Dosing duration, Species, Critical effects[1]**		
Endpoints →	**Hepatotoxicity**	**Developmental Effects**	**Endocrine-Thyroid Effects (NTP 2018)**
PFOA	32 (NOAEL), 77 (LOAEL)[2], 91 days, rats 4.5 (BMDL = (NOAEL)[3] 12.4 (LOAEL), 14 days mice, 13 (NOAEL), 39 (LOAEL)[4], 17 days mice	0.8 (NOAEL), 8.29 (LOAEL)[5] 17 days, mice, 6 (NOAEL), 38 (LOAEL)[6], 17 days, rats 13 NOAEL, 39 (LOAEL), 17 days. mice (same as [4]) 5 (LOAEL)[7], 17 days, mice	50 (LOAEL) 28-days *** rat, decreased serum fT4 14 ($BBMDL_{20}$)[8]
	NOAEL range 4.5-32 LOAEL range 12-77	NOAEL range 0.829–13 LOAEL range 8.29-39	
PFOS	17 (NOAEL)[9], 65 (LOAEL) 98 days, rats 38 (NOAEL)[10], 157 (LOAEL) 26 weeks, monkeys (only 2-6 animals/group)	6 (NOAEL), 25 (LOAEL)[11] 84 days, rats 18 (NOAEL)12, 35 (LOAEL) 19 days, rat 10 (NOAEL)[13],35 (LOAEL), 41 days, rat 20 (NOAEL)[14], 38 (L)AEL), 63 days, rat 6 (NOAEL) 19 (LOAEL)[15], 63 days, rat	52 (LOAEL) 28-days *** rat, decreased serum fT4 5 ($BBMDL_{20}$)
	NOAEL range = 17–38 2 limited studies LOAEL range 65-157	NOAEL range rats = 6–20 LOAEL range 25-38	
PFNA	5 ($BMDL_{10}$ = NOAEL)[16] 12 (LOAEL), 17 days, mice (insufficient and limited database)	9 (TWA NOAEL)[17] 12 (LOAEL), 17 days, mice (insufficient and limited database)	57 (LOAEL), 28-days *** rat, decreased serum fT4 5 (($BBMDL_{20}$)
PFHxS	44 (NOAEL)[18] 89 (LOAEL), 43 days, rats (insufficient and limited)	27 (NOAEL)[19] (no serum level reported at the LOAEL), 49 days mice (insufficient and limited database)	67 (LOAEL) 28-days *** rat decreased serum fT4 27 (($BBMDL_{20}$)
PFDA	9 (LOAEL)[20], 28 days, rat 7 ($BBMDL_{05}$ ≡ NOAEL)	No in vivo animal data	43 (LOAEL) 28-days *** rat, decreased serum fT4 11 ($BBMDL_{20}$)

[1] These parameters except PODs for each chemical are presented in the following footnotes and PODS are rounded to one significant figure.
[2] 91 days, rats, increased liver weight and liver necrosis (USEPA 2016), basis for EPA candidate RfD (cRFD)
[3] 14 days, mice, increased relative maternal liver weight (NJDWQI 2017; NHDES 2019b) bases for NJDWQI and NHDES RfDs
[4] 17 days, mice, increased severity of chronic inflammation in liver of offspring aged 18 months (ATSDR 2018a), bases for ATSDR cRFD
[5] 17days, mice, Neuro- and skeletal development (ATSDR 2018a; MISAW 2019) bases for ATSDR and MISAW RFD
[6] 17 days, rats, skeletal anomalies and accelerated puberty (USEPA 2016, MDH 2018,) bases for USEPA and MDH RfDs
[7] 17 days, mice, increase in pup relative liver weight (NYDOH 2019), basis for NYDOH RfD
[8] BBMDL (Bayesian Benchmark Dose lower confidence limit) is assumed to be equivalent to NOAELs
[9] 98 days, rats, increased ALT (USEPA 2016), basis for EPA cRFD
[10] 26 weeks, monkeys, Increased liver weight, decreased serum cholesterol, hepatocellular hypertrophy, mild bile stasis, lipid vacuolation (ATSDR 2018a). Study is very limited by sample size (2-6 per group), bases for ATSDR cRFD
[11] 84 days, rat, decreased pup body weight (6.26 is average serum level by USEPA (2016b) and 7.43 mg/L is TWA by ATSDR (2018a) from the same study) serum levels are the bases for USEPA and ATSDR RfDs respectively)
[12] 19 days, rat, decreased pup survival and pup body weight (USEPA 2016b), bases for EPA cRfD)
[13] 41 days, rat increased motor activity and decreased habituation, bases for USEPA cRfD
[14] 63 days, rat, decreased gestation length and pup survival, bases for USEPA cRfD
[15] 63 days, rat decreased pup body weight., bases for USEPA cRfD
[16] 17 days, increased maternal liver weight, bases for NJWQI (2015) and NHDES (2019b) RfDs
[17] 17 days, mice, developmental delays, bases for ATSDR (2018a) MRL
[18] 42 days, rat Increased liver-to-body weight and liver-to-brain weight ratios, centrilobular hepatocellular hypertrophy in male parental rat (Butenhoff et al., 2009), not selected by any group but study reviewed by ATSDR (2018a), MDH (2019b), NHDES (2019b) and MassDEP
[19] 49 days, mice, change in mean litter size, bases for NHDES (2019b) RfD
[20] 28 days, rat increased relative liver (NTP 2018), study evaluated by MassDEP for comparative purposes
[***] serum levels measured at similar external dose effect levels for all listed PFAS

APPENDIX 5

APPENDIX 5 – TABLE OF CONTENTS

List of Tables

List of Figures

APPENDIX 5 - SUPPLEMENTAL DATA

Bayesian Benchmark Dose Output Plots and Tables

Thyroid free T4 (BBMDR for 20% and 50% change from control)

Relative Liver Weight (BBMDR for 5% change from control)

Comparative Evaluation of Thyroid Hormone and Liver Responses following 28-day Exposure to PFAS in the NTP 2018 Bioassay.

1. INTRODUCTION

The results from the NTP PFAS testing program provide an opportunity to compare effects from exposure to a group of chemicals tested using the same protocol in the same animal species and strain..

The National Toxicology Program (NTP) published Data Tables for Peer Review in July 2018 (NTP 2018) for seven PFAS chemicals, PFOA, PFOS, PFHxS, PFNA, PFDA PFBS and PFHxA. The data tables present the results for all endpoints evaluated in the study after 28-day exposures in male and female Sprague-Dawley rats. Endpoints were evaluated across multiple organ systems. Based on a review of the data tables, thyroid and liver effects were the most sensitive endpoints in the NTP study; male rats were more sensitive than female rats. MassDEP focused the following comparative potency assessment on these endpoints.

Table 1. PFAS evaluated by NTP (2018)

# Carbons	Perfluorinated Sulfonates:	Perfluorinated Carboxylates:
4	PFBS Perfluorobutane sulfonate	---
6	PFHxS Perfluorohexane sulfonate potassium salt	PFHxA Perfluorohexanoic acid
8	PFOS Perfluorooctane sulfonate	PFOA Perfluorooctanoic acid
9	---	PFNA Perfluorononanoic acid
10	---	PFDA Perfluorodecanoic acid

This Office of Research and Standards (ORS) assessment focuses on evaluation of responses associated with thyroid hormone serum concentrations and liver weights collected at the end of the 28-day study period. The results for the subgroup of PFAS, PFOA, PFOS, PFNA, PFHxS and PFDA, of current regulatory interest, were evaluated for comparison of potency based on serum concentration and human equivalent doses.

2. METHODS

NTP Study description

Adolescent male and female Harlan-Sprague Dawley rats were dosed daily by gavage for 28-days (NTP 2018; 2019a,b). For each PFAS there were five treatment groups and a vehicle (deionized water with 2% Tween-80) control group with 10 males and 10 females per group.

The last dose of PFAS was administered the day prior to sacrifice on day 28. Blood was collected from each animal surviving to the end of the study. The time between the final dose of PFAS and collection of serum was unavailable. Serum from each animal was evaluated for PFAS concentration (LOQ 0.025 mg/L) and levels of thyroid stimulating hormone (TSH), total

thyroxine (TT4), free thyroxine (fT4) and triiodothyronine (T3) were determined. thyroid hormones were measured using radioimmunoassay (NTP personal communication). Body weight, liver weight, organ weights were among the endpoints collected at time of sacrifice.

Data and Analysis Summary

Group and individual animal thyroid hormone, body weight, liver weight and PFAS serum level data from NTP studies Tox-96 and Tox-97 were downloaded from the NTP Data Tables for Peer Review webpage (available; https://ntp.niehs.nih.gov/results/path/index.html). Group data (mean, number of animals and standard error) were transcribed from pdf tables and are presented in the Supplemental Tables S-1 and 2 of this report for males and females, respectively. Individual animal data were downloaded as Excel files (data files are available on request). All data underwent internal QA/QC.

Model Fitting and Benchmark Dose Estimation

Selected endpoints were evaluated at the group and individual animal levels compared to the applied exposure dose (mg/kg-day), measured internal PFAS serum concentration (mg/L) and human equivalent dose (HED) (mg/kg-day) for each PFAS.

The Bayesian Benchmark Dose modeling software (BBMD)(Shao and Shapiro 2018) was used for modeling the datasets. The BBMD software allows for modeling of the individual animal serum concentration and endpoint metric, i.e., serum thyroid hormone concentration or liver weight; handles variability in continuous data better than the USEPA BMD software (USEPA 2019; Shao et al. 2013); and can account for uncertainty in the choice of dose-response models (model uncertainty) through weighted model averaging.

Seven dose-response models, exponential 2, exponential 3, exponential 4, exponential 5, Hill, power, Michaelis-Menten, and linear models were fit to individual animal doses and responses. The weighted average of the models (model average) generated from the BBMD software was used for estimating the benchmark dose and confidence intervals. Benchmark response levels (e.g., 5% change from control for liver weight) were selected based on response rates used for the endpoints in previous studies to permit comparison and on the response range observed in the data. The upper and lower 95% confidence intervals were reported for each BMR.

Estimate of the human equivalent dose (HED)

Human equivalent doses were estimated by adjusting the animal PFAS serum concentration by the human clearance rate estimated for each PFAS, applying the approach used by USEPA (2016 a,b) and ATSDR (2018a). Clearance was calculated based on the elimination half-life ($t_{1/2}$) and volume of distribution (Vd) using the following equation:

$$Cl = Vd \times (\ln 2 / t_{1/2})$$

Where:
Cl = clearance (L/kg bw/day)
Vd = volume of distribution in the human body (L/kg bw)
ln2 = 0.693
$t_{1/2}$ = half-life in humans (days)

The parameters for estimating clearance identified by ATSDR (2018a) were used in this analysis, unless noted otherwise (Table 4).

Relative Potency Factor (RPF) Estimate
The relative potency factor was estimated using the following equation:

$$RPF_i = \frac{\text{Index Chemical}}{PFAS_i}$$

PFOA was selected as the index chemical. The relative potency for each endpoint evaluated for the individual PFAS were compared using the same BMR and dose metric. The central estimate of the serum concentration (BBMD) associated with the benchmark response (BMR), i.e., 20% decrease from control for thyroid hormone and 5% for liver weight, was used as the point of comparison across the PFAS. The BBMD estimate is a more stable estimate of the response than the BBMDL as it is less influenced by the variability in the dataset and was thus selected as the point of comparison for the comparative potency assessment.

3. RESULTS

3.1 Thyroid Hormone Responses

Free T4 had the most consistent dose response relationships of the four thyroid hormones for each of the PFAS evaluated in this study; as indicated by trend and pair-wise tests across the four measures of thyroid hormone response (see Supplemental Tables S-1 and S-2, males and females, respectively). Based on this observation, fT4, the biologically active form of this hormone, was selected for further evaluation.

Male rat fT4 concentrations (ng/dL) associated with the internal measure of dose (PFAS serum concentration (mg/L)) after 28 days of exposure, decreased faster as internal dose increased and to a greater extent than female fT4 levels for each of the five PFAS, shown in Figure 1.

The lowest dose tested in male rats resulted in a 50% or greater decrease in free T4 from control levels for PFOA, PFOS, PFNA and PFHxS (Figure 1-A and Table 2). PFDA was the only one of this subgroup to be tested at a lower dose level resulting in less than 10% change from control. PFDA exhibited a decrease of 40% from control at the next highest dose, which yielded a serum

concentration in the range of the lowest dose tested for other compounds. The large decrease in fT4 concentration from the control group at the lowest dose tested and the nearly level concentrations of fT4 as the PFAS serum concentrations increase indicates that additional information at lower doses could significantly alter estimates of concentrations associated with a specific response rate.

As shown in Figure 1, male rats exhibited greater sensitivity to thyroid hormone responses than female rats, and thus the male rat responses are the focus of this comparative analysis.

3.2 **Liver Weight Responses**

Absolute and relative liver weight were sensitive endpoints in the NTP (2018) bioassay of PFAS as indicated by trend and pair-wise tests (Supplemental Tables S-1 and S-2, males and females, respectively). Due to body weight loss in rats exposed to several of the PFAS at the higher doses, the relative liver weight was considered a more reliable estimator of liver weight response. This is consistent with the analysis by Bailey et al. (2004) showing the organ to body weight ratio is predictive for analyzing liver weights.

Relative liver weight increased with increasing internal concentration of PFAS (Figure 2 A and B, males and females respectively). Males were more sensitive than females to the liver weight effects from PFAS exposure, and thus were the focus of this comparative analysis.

3.3 **Benchmark Dose Analysis**

Bayesian benchmark dose modeling (BBMD) was used to provide a consistent point of departure for comparison across the PFAS. Percent change from control was used as the response, rather than 1 standard deviation (SD) from control as is recommended in the USEPA BMD Technical Guidance (2012) for two related reasons, 1) the standard deviation of the control response from one particular experiment defines what is considered different from control, and this could vary from control group to control group; and, 2) in order to compare responses across five different PFAS, a consistent response metric is needed.

Initially, dose response modeling of individual and grouped continuous data was conducted using USEPA BMD software (BMDS) using several versions of the software, 2.7, 3.0, and 3.1 (USEPA 2019). However, BMDS cannot model individual animal serum concentrations; the model structure requires a single estimate of exposure for each dose group. Using a single estimate of the internal dose for each dose group of animals does not account for the variability in the dose response created by interindividual differences in toxicokinetics observed in the study

Figure 1. Free T4 Serum Concentration Percent Change from Control associated with PFAS Serum (mg/L) concentration on day 28 in (A) male and (B) female Harlan Sprague Dawley rats (NTP 2018)

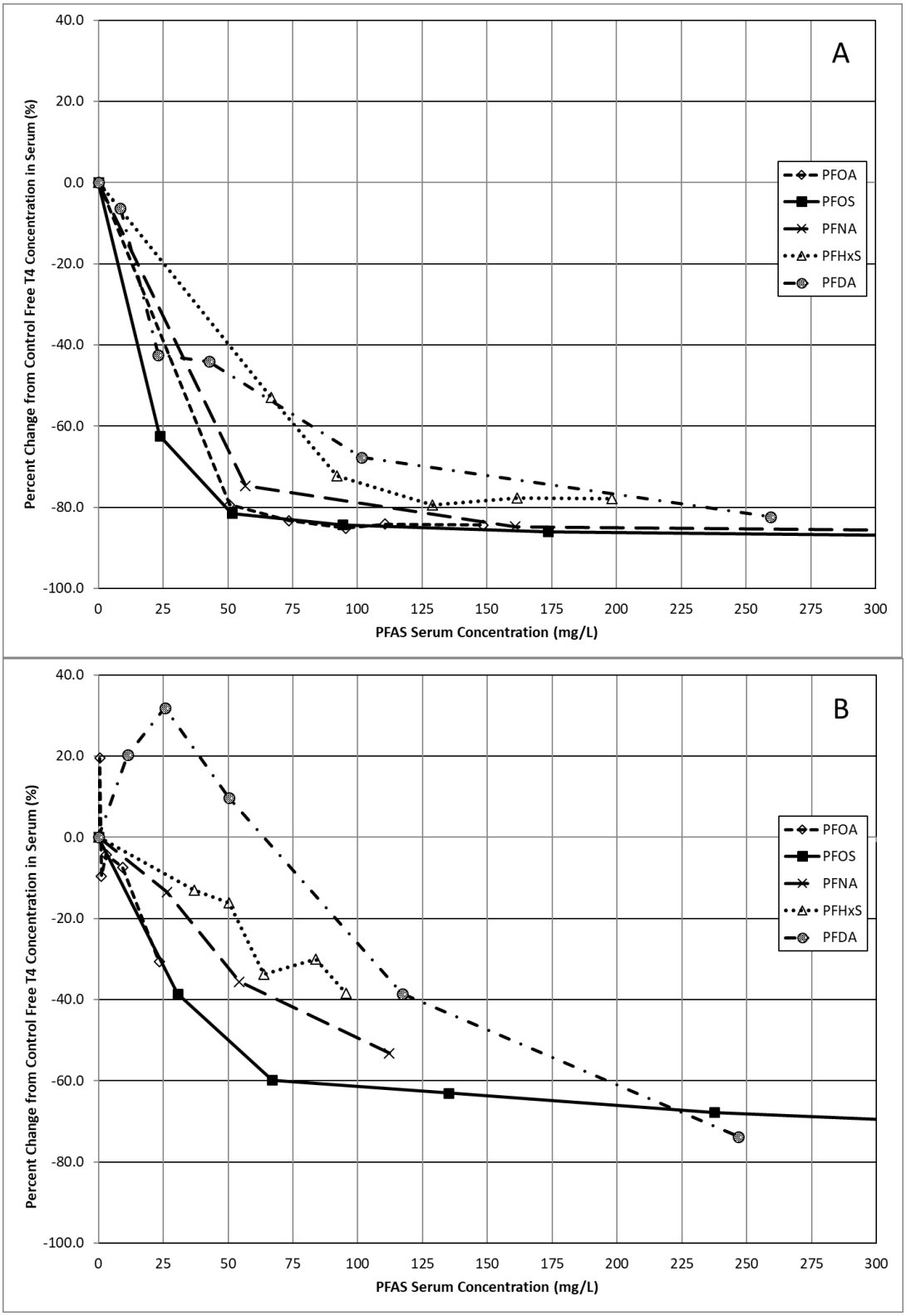

Figure 2. Relative Liver Weight Percent Change from Control associated with PFAS Serum (mg/L) concentration on day 28 in (A) male and (B) female Harlan Sprague Dawley rats (NTP 2018)

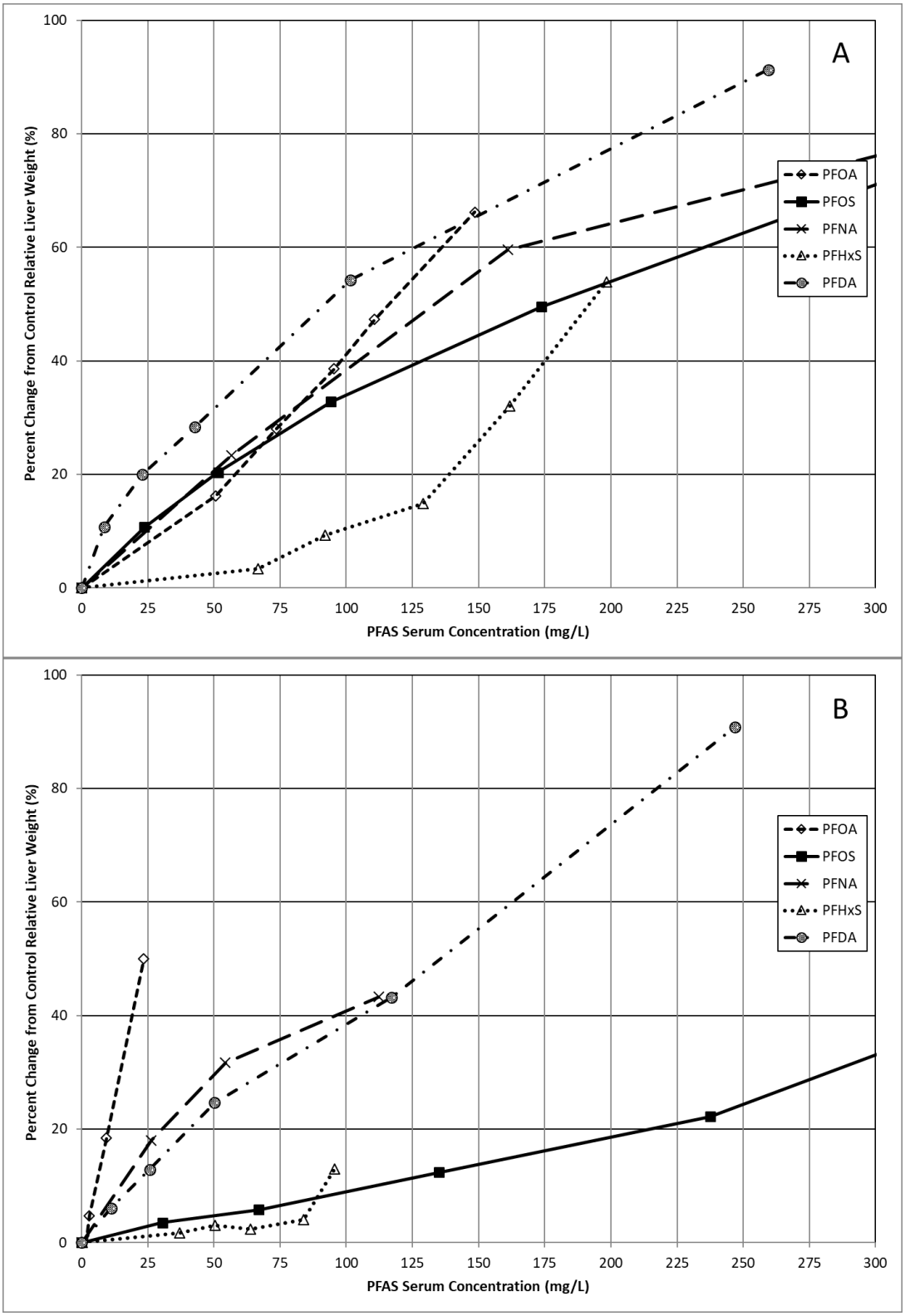

animals.[11] The Bayesian benchmark dose modeling was able to model the individual animal serum concentration and response measure.

3.3.1 *Free thyroxine (fT4) BBMD*

A 20% decrease in fT4 serum concentration was selected for the benchmark response ($BBMR_{20}$). This was selected in part because the response rates at the lowest dose tested were too high to use a smaller difference from control. $BBMR_{50}$ was also included in the relative potency evaluation because it was closer to the observed response rates. MDH relied upon a BMR_{20} in their derivation of an RfD for PFHxS (MDH 2019b). Although MassDEP has used a $BBMR_{20}$ as a basis for these cross-chemical response comparisons, it is important to note that smaller decrements in thyroid hormones could well be biologically significant.

The USEPA BMDS had difficulty modeling the fT4 data. Using a BMR_{20} and the PFAS data sets without the highest dose groups, only the PFHxS and PFOA data sets yielded BMD models with "viable" fits using the BMDS criteria (USEPA 2019 BMD manual for 3.1) (BMDS 3.1 results shown in Supplemental data Table S-3).[12] Visually the dose response curves for the PFAS appeared to fit different models, e.g., Hill and 4 parameter exponential models, equally well yet produced BMD and BMDL estimates that could be more than five-fold different. The weighted model averaging feature of the Bayesian benchmark dose modeling provided a BBMD estimate that incorporated the estimated model uncertainty, instead of needing to select one out of two equally well fitting models to be the BMD estimate used for further analysis.

The $BBMD/L_{20}$ for the thyroid effects were all within the range of the POD used by different agencies for deriving RfDs for the respective PFAS (shown in Appendix 1).

3.3.2 *Relative liver weight BBMD*

The estimated BBMD and BBMDLs for serum concentration associated with a 5% increase in relative liver weight compared to control were consistent with expectations from mean group responses (Table 3). The data sets for relative liver weight were only modeled using the BBMD software.

A limitation in the evaluation of liver effects was related the limited data in the low dose/low response portion of the dose-response curves for PFOA and PFNA liver effects as well as the relatively short duration of the exposures (28-days).

[11] We note that given the other contributors to uncertainty in the process beginning with a dose-response assessment of animal data and extrapolation to humans through to an RfD, the contribution to overall variability from this source is small. However, if an approach can account for it, there is no reason to not include it.

[12] The most frequent reason for model results that met goodness of fit criteria to be labeled "questionable" was an indicator that the constant model assumption was violated when data were modeled assuming a constant variance, and the non-constant model assumption being violated when the same data were modeled assuming non-constant variance.

Table 2. FreeT4 Bayesian Benchmark Dose Estimates for Male Rats

	Lowest Dose Tested (LDT) (mg/kg-day)	LOAEL/ NOAEL	Mean Serum Conc. at LDT (mg/L)	% Decrease from Control	$BBMD_{20}$ (mg/L)	$BBMDL_{20}$ (mg/L)	$BBMDU_{20}$ (mg/L)	$BBMD_{50}$ (mg/L)	$BBMDL_{50}$ (mg/L)	$BBMDU_{50}$ (mg/L)
PFOA	0.625	LOAEL	51	79	19	14	23	28	24	31
PFOS	0.312	LOAEL	24	62	6.7	5.4	7.9	16	14	18
PFNA	0.625	LOAEL	57	75	5.6	4.6	7.0	19	17	21
PFHxS	0.625	LOAEL	67	53	36	27	45	61	53	67
PFDA	0.156	NOAEL	9	6	13	11	16	48	40	59

Table 3. Relative Liver Weight Bayesian Benchmark Dose Estimates for Male Rats

	Lowest Tested Dose (mg/kg-day)	LOAEL/ NOAEL	Mean Serum Conc. at LTD (mg/L)	% Increase from Control	$BBMD_{05}$ (mg/L)	$BBMDL_{05}$ (mg/L)	$BBMDU_{05}$ (mg/L)
PFOA	0.625	LOAEL	51	16	13	12	14
PFOS	0.312	LOAEL	24	11	13	11	15
PFNA	0.625	LOAEL	57	23	13	12	14
PFHxS	0.625	NOAEL	67	3	82	73	92
PFDA	0.156	LOAEL	9	11	7.9	6.8	10

3.4 **Calculation of Human Equivalent Dose (HED)**

Human equivalent dose (HED) is an estimate of the applied dose for humans that will result in an equivalent PFAS serum concentration as observed in the study animals. The assumption underlying the use of an estimated HED is that animal and human responses will be similar when serum concentrations (internal dose) are similar, i.e. similar toxicodynamics.

Because we are ultimately interested in determining an external exposure dose that is "acceptable" and given the evidence that the half-life of PFAS in serum is different in different species (e.g., rats, mice, monkeys, humans) and across PFAS, relative potency of the five PFAS was evaluated in terms of external doses (mg/kg-day) that would be equivalent in humans, the HED.

HED were estimated from the PFAS concentrations in male rat serum using estimates of clearance calculated from the volume of distribution and half-life as described in the methods

section. The values used for the volume of distribution (Vd) and half-life ($t_{1/2}$) for each of the PFAS are shown in Table 4.

Table 4. Parameters for Calculation of Human Clearance Rate

	Volume of Distribution Vd (L/kg)	Human Half-life t1/2 (days)	Clearance Rate humans CL_h (L/kg bw/day)	Agency	Source of Vd	Source of t1/2
PFOA	0.2	1400	9.9E-05	ATSDR 2018a	Butenhoff et al. 2004c; Chang et al. 2012; Harada et al. 2005a	Olsen et al. 2007a
PFOA	0.17	839.5	1.4E-04	EPA 2016 a	Thompson et al. 2010	Bartell et al 2010
PFOA	0.17	840	1.4E-04	MDH 2017	EPA 2016 a	EPA 2016 a
PFOS	0.2	2000	6.9E-05	ATSDR 2018a	Butenhoff et al. 2004c; Chang et al. 2012; Harada et al. 2005a	Olsen et al. 2007a
PFOS	0.23	1971	8.1E-05	EPA 2016 b	Thompson et al. 2010	Olsen et al. 2007a
PFOS	0.23	1241	1.3E-04	MDH 2019	EPA 2016 b	Li et al 2018
PFNA	0.2	900	1.5E-04	ATSDR 2018a	Butenhoff et al. 2004c; Chang et al. 2012; Harada et al. 2005a	Zhang et al. (2013) for young females
PFNA	0.2	1600	8.7E-05	MassDEP, extension of ATSDR 2018a PFNA	Butenhoff et al. 2004c; Chang et al. 2012; Harada et al. 2005a	Zhang et al. (2013) for all men and older women
PFHxS	0.287	3100	6.4E-05	ATSDR 2018a	Sundström et al. 2012 male nonhuman primate	Olsen et al. 2007a
PFHxS	0.25	1935	9.0E-05	MDH 2019	Sundström et al. 2012 mean of males and female nonhuman primates	Li et al. 2018
PFDA	0.2	1600	8.7E-05	MassDEP, extension of ATSDR 2018a PFNA	Butenhoff et al. 2004c; Chang et al. 2012; Harada et al. 2005a	Zhang et al. (2013) for young females
PFDA	0.2	4400	3.2E-05	MassDEP, extension of ATSDR 2018a PFNA	Butenhoff et al. 2004c; Chang et al. 2012; Harada et al. 2005a	Zhang et al. (2013) for all men and older women

For the PFOS and PFOA health advisories, USEPA (2016 a,b) selected half-life values from Olsen et al. (2007) and Bartell et al. (2010), respectively, and volume of distribution values from Thompson et al. (2010a). The parameters chosen by USEPA (2016 a,b) resulted in clearance values that were 20-30% higher than those used by ATSDR (2018a) for PFOA and PFOS. The higher clearance values lead to higher HED values which result in higher (less conservative) point of departures for the RfD compared to those selected by ATSDR (2018a). For this comparative analysis, MassDEP used the ATSDR (2018a) clearance values.

For PFNA, ATSDR used half-life values estimated by Zhang et al. (2013); the only available human information. Zhang et al. (2013) also estimated a half-life for PFDA that was used in this analysis. Zhang et al. (2013) estimated half-life values from serum and urine collected on the same day for two groups, young women (≤ 50 years old) and older women and all men; groups were established after observing differences between younger women and the other study populations. For consistency in this analysis, the same age group used by ATSDR (2018a) for PFNA, younger women (≤ 50 years old), was used for PFDA. Estimates of half-life were shorter for younger women compared to older women and all men, possibly due to loss attributable to childbirth, nursing and menstruation (Zhang et al. 2013). If the longer half-life values from the older women and men were used to estimate the HED, the clearance would be slower and the HED values would be lower leading to lower (more conservative) points of departure for the RfD. Because the half-life values estimated by Zhang et al. (2013) were modeled based on serum and urine collected at a single point in time there is less confidence in the clearance values for PFNA and PFDA than for the other PFAS.

To estimate the potential impact of the parameters selected for calculating clearance of PFAS on the HED, the clearance parameters in Table 4 were used to explore the range of HEDs that could be estimated using the BBMDs for relative liver weight for each PFAS were calculated. Using a combination of the lowest Vd and the highest $t_{1/2}$, the slowest clearance rate that can be calculated from these data was estimated; conversely the fastest clearance rate was estimated using the largest Vd and the shortest $t_{1/2}$, for each PFAS. The HEDs, which differ by roughly 2-fold, are presented in Table 5 along with the HEDs calculated using the clearance parameters selected by ATSDR (2018a). The largest difference in HEDs (3-fold) was for PFDA, where the clearance estimates rely on a single study evaluating two populations that differ by age.

Table 5. Estimation of Human Equivalent Concentration: Impact of Clearance Parameter Selection [a]

		Human Equivalent Concentrations (mg/kg-day)		
	Relative Liver Weight $BBMD_{05}$	**Slowest Clearance** (Lowest Vd and Highest $t_{1/2}$)	**ATSDR (2018a)**	**Fastest Clearance** (Highest Vd and Lowest $t_{1/2}$)
PFOA	13	1.1E-03	1.3E-03	2.1E-03
PFOS	13	8.9E-04	8.9E-04	1.6E-03
PFNA	13	1.2E-03	2.1E-03	2.1E-03
PFHxS	82	4.6E-03	5.3E-03	8.5E-03
PFDA	7.9	2.2E-04	6.0E-04	6.0E-04

[a] Clearance parameters from Table 4.

3.5 **Relative Potency**

The relative potency factor (RPF) approach is a general method to quantitatively evaluate differences in potency for a group of chemicals acting through similar modes of action or causing similar toxicological effects, using empirically derived scaling factors or RPF (USEPA 2000; ATSDR 2018b; Hertzberg and Mumtaz 2018).

RPFs that have been used in risk assessment have not made fine distinctions in potencies between compounds. For example, the USEPA RPFs developed for PAHs (USEPA 1993) are based on potency differences of an order of magnitude (10-fold), while the Toxic Equivalent Factors (TEF), a special case of relative potency factors used when the mechanism of toxicity is well understood, are half an order of magnitude ($10^{1/2}$ or 3-fold) for the data rich dioxin-like PCBs (Van den Berg 2006). The comparative potency databases for PFAS other than PFOA and PFOS are more limited and uncertain than that for PAHs and PCBs. Thus, MassDEP ORS has concluded that substantial differences in potency estimates are needed to firmly establish differences across compounds at this time.

Table 6. PFAS Relative Potency to PFOA: Endpoint and Exposure Metric Dependence

End Point	Free T4[a]	Relative Liver Wt	Free T4	Relative Liver Wt
Exposure Metric	Serum (mg/L)		HED (mg/kg-day)[b]	
BMR[c]	$BBMD_{20}$	$BBMD_{05}$	$BBMD_{20}$	$BBMD_{05}$
PFOA	19	13	0.0018	0.0013
PFOS	6.7	13	0.0005	0.0009
PFNA	5.6	13	0.0013	0.0021
PFHxS	36	82	0.0023	0.0053
PFDA	13	8	0.0014	0.0006
Relative Potency to PFOA				
PFOA	1	1	1	1
PFOS	3	1	4	1
PFNA	2	1	1	0.6
PFHxS	0.5	0.2	0.8	0.2
PFDA	1	2	1	2

[a] Male rat NTP (2018) data.
[b] HED calculated using parameters for the main HED calculations (i.e., ATSDR 2018a and extension).
[c] Model average BBMD values from Tables 2 and 3.

The serum concentration associated with the BBMDs in male rats for fT4 and relative liver weights from Tables 2 and 3 are shown in the top section of Table 6; the HEDs associated with

each concentration are in the top right section. The lower portion of Table 6 shows the potency of PFOS, PFNA, PFHxS and PFDA relative to PFOA.

The RPFs, using PFOA as the index chemical, shown in the lower panel of the table, varied between the two endpoints. However, most RPFs were a factor of 2 or less with a maximum difference of 5-fold from PFOA for both animal internal doses and HED. Each compound exhibits a HED RPF of approximately one for either free T4 or relative liver weight.

This analysis demonstrates that all these compounds caused similar effects for these endpoints, which occur at similar serum concentrations and HEDs. MassDEP has concluded that these differences in relative potency estimates are not sufficient to conclude that they are in fact different.

Supplemental Information for the MassDEP ORS Technical Support Document

Per- and Polyfluoroalkyl Substances (PFAS): An Updated Subgroup Approach to Groundwater and Drinking Water Values

December 26, 2019

SUPPLEMENTAL DATA - APPENDIX 5

Table of Contents

Table S-1. Thyroid Hormone and Liver Weight Results for Male Rats 28-day Exposure via Gavage (NTP 2018)

Dose		Serum (mg/L)			TSH (ng/ml)			T3 (ng/dL)			Total T4 (ug/dL)			Free T4 (ng/dL)			Abs Liver Wt (g)			Rel Liver Wt (mg/g)		
(mg/kg-day)	N	Mean	SE		Mean	SE		Mean	SE		Mean	SE		Mean	SE		Mean	SE		Mean	SE	
PFOA																						
0	10	0.098	0.01	**	21.76	2.66	**	88.55	5.58		2.34	0.242	**	2.137	0.131	**	12.96	0.41		37.34	0.72	
0.625	10	50.69	2.21	**	23.74	2.34		53.52	1.45	**	0.21	0.048	**	0.44	0.042	**	14.94	0.32	**	43.41	0.55	**
1.25	10	73.48	3.21	**	15.50	1.94		56.93	2.48	**	0.17	0.056	**	0.357	0.024	**	15.8	0.29	**	47.8	0.54	**
2.5	10	95.43	4.04	**	15.85	2.43		61.47	3.64	*	0.07	0.05	**	0.318	0.008	**	16.44	0.64	**	51.75	1.09	**
5	10	110.7	3.89	**	12.63	1.20	**	58.98	3.52	**	0.11	0.059	**	0.339	0.015	**	16.7	0.46	**	55.01	0.89	**
10	10	148.6	15.4	**	15.07	2.04	*	85.33	6.72		0.39	0.147	**	0.334	0.018	**	17.22	0.38	**	62.05	2.23	**
PFOS																						
0	10	0		#	20.39	1.40		87.37	5.32	**	3.51	0.30	**	2.534	0.216	**	11.79	0.290		34.92	0.22	
0.312	10	23.73	1.11		14.94	1.74		77.81	5.44		1.33	0.19	**	0.952	0.099	**	13.14	0.280		38.66	0.47	
0.625	10	51.56	3.22		14.79	1.20		60.63	4.64	**	0.53	0.09	**	0.469	0.054	**	14.210	0.32		42.04	0.48	
1.25	10	94.26	3.14		23.33	2.94		57.5	2.67	**	0.26	0.07	**	0.398	0.022	**	15.34	0.370		46.38	0.99	
2.5	10	173.7	9.04		24.19	3.38		55.35	2.75	**	0.22	0.04	**	0.355	0.05	**	17.37	0.360		52.21	0.93	
5	10	318.2	8.87		18.9	2.39		50	0.00	**	0.48	0.70	**	0.328	0.011	**	18.81	0.410		60.8	0.77	
PFNA																						
0	10	0.055	0.01	**	20.33	2.31	**	78.21	4.54	**	2.36	0.27		2.157	0.152	**	11.73	0.23		34.14	0.32	
0.625	9	56.73	1.88	**	13.70	1.27		58.54	2.11		0.21	0.07	**	0.546	0.024	**	13.99	0.33	*	42.12	0.58	**
1.25	10	161.0	4.93	**	10.97	1.22	**	84.93	2.94		0.38	0.07	**	0.328	0.009	**	15.58	0.27	**	54.47	0.59	**
2.5	7[a]	380.0	15.6	**	10.16	3.35	**	111.8	10.16	*	1.49	0.13		0.302	0.001	**	12.33	0.92		63.37	1.86	**
5	2[b]	358.0	54.0	**													12.53	0.03		81.01	2.27	
PFHxS																						
0	10	0.102	0.01	**	17.31	2.39		85.18	5.74	**	4.24	0.23	**	1.737	0.1	**	11.36	0.32		33.77	0.36	
0.625	10	66.76	3.52	**	18.58	1.95		66.21	4.20	*	2.39	0.08	**	0.817	0.067	**	12.1	0.36		34.91	0.43	
1.25	10	92.08	3.35	**	20.78	1.82		58.67	2.87	**	1.7	0.06	**	0.481	0.031	**	12.58	0.25	*	36.91	0.39	**
2.5	10	129.0	5.50	**	21.88	3.13		54.25	2.31	**	1.47	0.07	**	0.357	0.022	**	13.3	0.35	**	38.79	0.62	**
5	10	161.7	2.51	**	19.69	1.75		52.50	1.42	**	1.54	0.09	**	0.386	0.032	**	15.24	0.56	**	44.61	1.16	**
10	10	198.3	5.00	**	24.96	4.31		56.83	3.96	**	1.66	0.05	**	0.385	0.027	**	17.43	0.52	**	51.96	1.24	**
PFDA																						
0	10	0.022	0.004	**	19.79	3.75	*	95.86	4.01	**	4.36	0.32		2.024	0.205	**	11.87	0.51		35.5	0.97	
0.156	10	8.505	0.58	**	16.16	1.88		72.87	2.66		4.27	0.23		1.897	0.216		13.54	0.4	*	39.32	0.53	**
0.312	10	23.03	1.77	**	17.73	2.70		66.14	2.84		3.24	0.18	*	1.165	0.106	**	14.1	0.38	**	42.61	0.56	**
0.625	10	42.72	2.96	**	15.52	2.50		74.74	5.45		3.82	0.09		1.132	0.057	**	14.65	0.35	**	45.56	0.84	**
1.25	10	101.6	4.01	**	11.63	1.18		148.0	9.69		4.59	0.26		0.653	0.053	**	14.4	0.2	**	54.77	0.68	**
2.5	6[a]	259.4	20.2	**	8.97	2.28		180.0	13.7		4.64	0.15		0.357	0.046	**	14.11	0.7	**	67.9	1.19	**

Data source: NTP 2018. Displayed as mean ± standard error (SE)
Statistical significance performed by NTP using Jonchkeere (trend) and Shirley or Dunn (pairwise) tests
Statistical significance for the control group indicates a significant trend
Statistical significance for the treatment group indicates a significant pairwise test compared to vehicle control
* Statisically significant at P<= 0.05
** Statisically significant at P<= 0.01
# Group did not have over 20% of its values above the limit of quantification, statistical analysis was not done for this group
a Missing animals not evaluated for freeT4

Table S-2. Thyroid Hormone and Liver Weight Results for Female Rats 28-day Exposure via Gavage (NTP 2018)

Dose		Serum (mg/L)			TSH (ng/ml)			T3 (ng/dL)			Total T4 (ug/dL)			Free T4 (ng/dL)			Abs Liver Wt (g)			Rel Liver Wt (mg/g)		
(mg/kg-day)	N	Mean	SE		Mean	SE		Mean	SE		Mean	SE		Mean	SE		Mean	SE		Mean	SE	
PFOA																						
0	10	0		#	10.05	0.81	**	109.1	6.72		2.1	0.36	**	1.631	0.179	**	7.77	0.34		34.2	0.98	
6.25	10	0.49	0.07		14.08	1.17	**	115.3	6.41		2.43	0.28		1.949	0.146		8.13	0.19		36.06	0.65	
12.5	10	1.153	0.19		12.99	1.27	*	94.87	5.94		1.56	0.24		1.475	0.106		8.21	0.2		36.44	0.58	
25	10	2.96	0.48		13.97	1.49	*	116.5	6.33		2.03	0.33		1.561	0.195		8.58	0.14	*	39.12	0.54	**
50	10	9.33	1.82		17.81	1.72	**	114.4	5.31		1.56	0.23		1.511	0.126		9.79	0.27	**	44.22	0.88	**
100	9[b]	23.44	3.25		15.83	2.20	**	104.7	4.14		1.11	0.24	*	1.13	0.144	*	12.07	0.4	**	56	1.09	**
PFOS																						
0	10	0.054	0.004	**	12.86	0.73		93.05	5.04	**	2.21	0.24	**	1.74	0.231	**	7.37	0.180		33.56	0.66	
0.312	10	30.53	0.92	**	14.76	0.88		81.4	3.02		1.11	0.12	**	1.069	0.089	**	8.26	0.220	*	36.15	0.54	*
0.625	10	66.97	1.63	**	12.76	0.85		72.52	4.27	**	0.55	0.07	**	0.699	0.034	**	8.200	0.17	*	36.95	0.73	*
1.25	10	135.1	3.88	**	13.25	1.15		69.2	3.63	**	0.33	0.07	**	0.643	0.052	**	8.59	0.260	**	39.25	1.06	**
2.5	10	237.5	5.22	**	14.91	1.95		62.03	1.78	**	0.35	0.09	**	0.561	0.047	**	9.17	0.280	**	42.67	0.87	**
5	9[b]	413.6	8.07	**	15.36	0.73		51.57	1.43	**	0.378	0.05	**	0.479	0.03	**	10.92	0.290	*	53.37	1.48	**
PFNA																						
0	10	0.098	0.01	**	14.64	1.66		93.7	6.03		4.37	0.41	**	1.702	0.199	**	7.67	0.29		33.29	0.7	
1.56	10	26.4	1.09	**	15.52	1.53		84.1	4.15		3.57	0.28		1.473	0.154		9.3	0.3	**	40.3	0.91	**
3.12	10	54.36	2.49	**	14.11	1.13		83.3	2.67		2.81	0.17	*	1.096	0.097	*	9.74	0.22	**	44.95	0.74	**
6.25	10	112.2	9.77	**	14.33	1.08		89.9	6.82		2.61	0.24	**	0.797	0.096	**	10.12	0.28	**	48.92	0.68	**
PFHxS																						
0	10	0.175	0.02	**	12.40	0.89		111.8	7.60		3.990	0.19	**	1.522	0.103	**	7.14	0.2		31.92	0.68	
3.12	10	37.03	1.65	**	15.66	1.07		98.89	4.94		3.530	0.20		1.323	0.097		8.02	0.26	*	34.36	0.88	*
6.25	10	50.41	1.55	**	15.72	1.64		99.05	7.29		3.370	0.17	*	1.275	0.126		8.24	0.3	*	34.8	0.72	**
12.5	10	63.82	3.20	**	17.46	1.94		96.71	6.36		2.970	0.11	**	1.009	0.054	**	7.86	0.25	*	34.58	0.66	**
25	10	83.82	3.74	**	14.02	1.04		96.89	6.04		2.960	0.19	**	1.065	0.093	**	8.07	0.16	**	35.14	0.51	**
50	10	95.51	3.75	**	14.50	1.13		91.51	5.49		2.690	0.15	**	0.938	0.08	**	8.8	0.24	**	38.16	0.75	**
PFDA																						
0	9[a]	0.042	0.02	**	12.10	0.96		100.7	8.81	**	3.867	0.35		1.78	0.218	**	7.63	0.28		33.52	0.75	
0.156	9[a]	11.21	0.44	**	15.44	1.23		107.3	6.41		4.278	0.31		2.14	0.187		8.94	0.36	**	37.66	0.89	**
0.312	10	25.7	1.05	**	15.36	1.21		97.14	4.51		4.200	0.25		2.35	0.164		9.46	0.16	**	40.08	0.56	**
0.625	10	50.29	3.31	**	12.50	0.99		106.0	5.72		3.920	0.37		1.95	0.223		10.06	0.31	**	44.25	0.82	**
1.25	10	117.2	6.50	**	16.28	2.34		124.4	10.3	*	3.530	0.21		1.09	0.078	*	10.09	0.18	**	50.84	0.67	**
2.5	3[a]	246.9	13.3	**	15.42	1.78		210.6	37.7	**	4.386	0.14		0.47	0.019	*	9.85	0.32	**	67.75	0.9	**

Data source: NTP 2018. Displayed as mean ± standard error (SE)
Statistical significance performed by NTP using Jonchkeere (trend) and Shirley or Dunn (pairwise) tests
Statistical significance for the control group indicates a significant trend
Statistical significance for the treatment group indicates a significant pairwise test compared to vehicle control
* Statisically significant at P<= 0.05
** Statisically significant at P<= 0.010
# Group did not have over 20% of its values above the limit of quantification, statistical analysis was not done for this group
a Missing animals not evaluated for freeT4
b Missing animals died before end of study

Table S-3. Benchmark Dose Modeling Results for Male Rat Free T4

	BMD (PFAS mg/L)			BMDL (PFAS mg/L)		
BMR	1SD[a]	20%[b]	20%[c]	1SD[a]	20%[b]	20%[c]
PFOA	1.8	5.2	5.4	0.8	4.5	4.6
PFOS	2.8	5.0	**4.7**	2.1	4.1	**3.9**
PFNA[d]	3.8	7.3	7.3	2.5	4.8	4.8
PFHxS	40.8	**41.6**	**41.3**	30.1	**32.8**	**32.0**
PFDA	13.7	12.8	11.4	8.4	8.6	7.2

[a] Model fits were questionable for all PFAS using 1SD BMR.
[b] Model fits were questionable for all PFAS, except PFHxS using BMR_{20}.
[c] Model fits were questionable for all PFAS, except PFHxS and PFOS using BMR_{20} while excluding the highest dose.
[d] PFNA results were limited to the control and three treated groups. The BMR_{20} results include all dose groups in both cases.
Data source NTP 2018, average PFAS serum concentration (mg/L) for each dose group.
Modeled using BMDS 3.1
Bolded values indicate BMDS outputs considered "viable" by BMDS software. All other values were selected from the model with the lowest AIC of the models passing the goodness of fit test (p>0.1).

PFOA fT4 male 5 ds grps Nov 4, 2019

Report created on Nov 04, 2019 at 09:03 PM.

Pystan model version 2.19.0.0.

Dataset

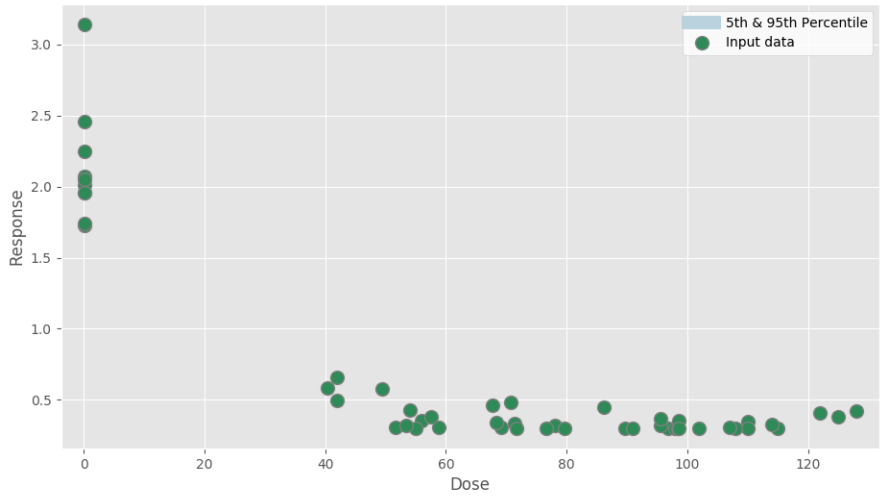

Dose	Response
0.11	2.25
0.08	2.46
0.12	3.14
0.09	1.96
0.12	1.73
0.12	2.01
0.08	2.07
0.1	2.05
0.07	1.96
0.08	1.74
41.9	0.659
51.7	0.307
56.0	0.356
57.6	0.378
49.5	0.578
41.9	0.498
58.9	0.309
54.1	0.428
40.3	0.582
55.0	0.3

71.4	0.336
70.7	0.48
78.1	0.319
67.8	0.459
69.2	0.304
76.6	0.3
53.4	0.319
89.7	0.3
86.2	0.449
71.7	0.3
110.0	0.348
96.9	0.301
97.9	0.3
102.0	0.3
68.4	0.342
95.5	0.322
98.4	0.3
79.6	0.3
110.0	0.3
95.6	0.37
91.0	0.3
115.0	0.3
98.6	0.353
98.6	0.3
108.0	0.3
128.0	0.419
107.0	0.308
122.0	0.406
114.0	0.327
125.0	0.379

BMD results

20% Central tendency: Relative

BMR: None

Adversity value: 0.200

20% Central tendency: Relative

BMD summary tables: 20%

Statistic	Model average	Exponential2	Exponential3	Exponential4	Exponential5	Hill	Power	MichaelisMenten	Linear
Prior model weight	N/A	0.125	0.125	0.125	0.125	0.125	0.125	0.125	0.125
Posterior model weight	N/A	2.47e-18	1.7e-19	0.245	0.354	0.389	7.31e-26	0.012	1.13e-24
BMD (median)	18.424	13.848	14.884	4.574	19.141	27.726	35.097	1.554	32.151
BMDL (5th percentile)	12.585	12.079	12.680	3.794	4.989	18.732	30.763	0.853	29.398
25th percentile	16.324	13.071	13.841	4.278	14.140	24.565	32.936	1.260	30.848
Mean (SD)	18.201 (3.081)	13.950 (1.265)	15.152 (1.886)	4.553 (0.503)	18.496 (7.171)	27.022 (4.494)	36.137 (4.704)	1.562 (0.449)	32.534 (2.447)
75th percentile	20.331	14.707	16.132	4.862	23.187	30.294	38.152	1.849	33.744
95th percentile	22.905	16.175	18.582	5.287	29.629	32.900	45.079	2.315	37.006

BMD estimates

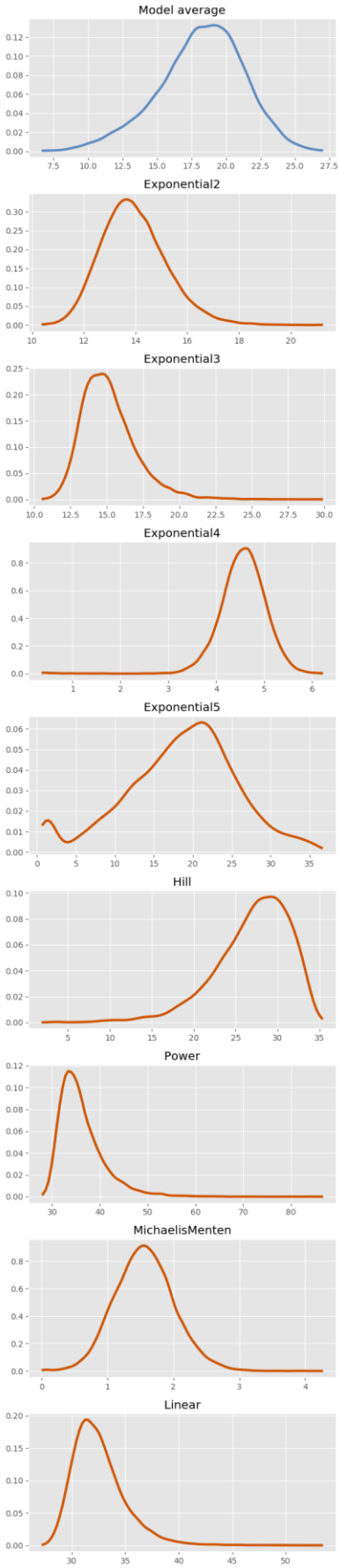
Model average
Exponential2
Exponential3
Exponential4
Exponential5
Hill
Power
MichaelisMenten
Linear

50% Central tendency: Relative

BMR: None

Adversity value: 0.500

50% Central tendency: Relative

BMD summary tables:

Statistic	Model average	Exponential2	Exponential3	Exponential4	Exponential5	Hill	Power	MichaelisMenten	Linear
Prior model weight	N/A	0.125	0.125	0.125	0.125	0.125	0.125	0.125	0.125
Posterior model weight	N/A	2.47e-18	1.7e-19	0.245	0.354	0.389	7.31e-26	0.012	1.13e-24
BMD (median)	27.509	43.016	44.767	15.136	30.440	34.049	83.392	6.853	80.379
BMDL (5th percentile)	19.854	37.522	38.723	12.571	14.990	27.001	75.469	3.848	73.495
25th percentile	25.751	40.601	42.012	14.165	26.330	31.747	79.775	5.613	77.120
Mean (SD)	26.895 (3.007)	43.333 (3.929)	45.216 (4.568)	15.072 (1.663)	28.649 (7.551)	33.345 (3.432)	84.531 (6.963)	6.864 (1.885)	81.334 (6.117)
75th percentile	28.868	45.685	47.840	16.088	33.269	35.723	88.068	8.081	84.360
95th percentile	30.429	50.245	53.338	17.500	36.663	37.414	97.232	9.998	92.514

BMD estimates

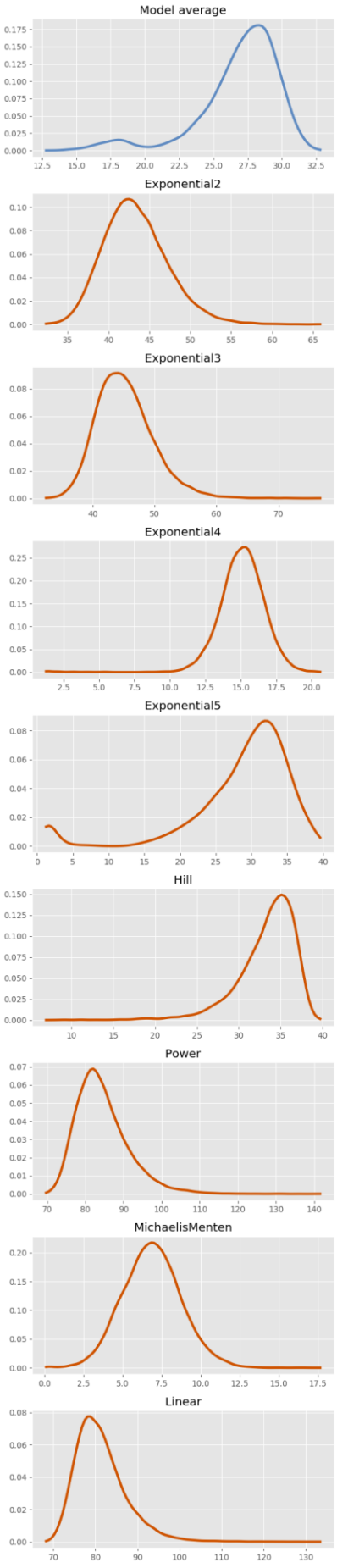
Model average
Exponential2
Exponential3
Exponential4
Exponential5
Hill
Power
MichaelisMenten
Linear

BMD Markov chain Monte Carlo settings

Iterations: 30,000

Number of chains: 1

Warmup fraction: 0.5

Seed: 84,447

Model results

Exponential2

$$f(dose) = a \times e^{b \times dose}$$

Model fit summary

```
Inference for Stan model: exponential2_individual_pkl_be58f7567ba64ec5547642f54ef3b89e.
1 chains, each with iter=30000; warmup=15000; thin=1;
post-warmup draws per chain=15000, total post-warmup draws=15000.

        mean se_mean     sd   2.5%    25%    50%    75%  97.5%  n_eff   Rhat
a       1.48  2.1e-3   0.16   1.19   1.37   1.47   1.59   1.83   6085    1.0
b      -2.06  2.4e-3   0.18  -2.43  -2.19  -2.06  -1.94  -1.71   6039    1.0
sigma    0.4  5.0e-4   0.04   0.33   0.37    0.4   0.43   0.49   7333    1.0
lp__   21.04    0.02   1.26  17.79  20.45  21.34  21.96  22.49   5632    1.0

Samples were drawn using NUTS at Mon Nov  4 20:58:06 2019.
For each parameter, n_eff is a crude measure of effective sample size,
and Rhat is the potential scale reduction factor on split chains (at
convergence, Rhat=1).
```

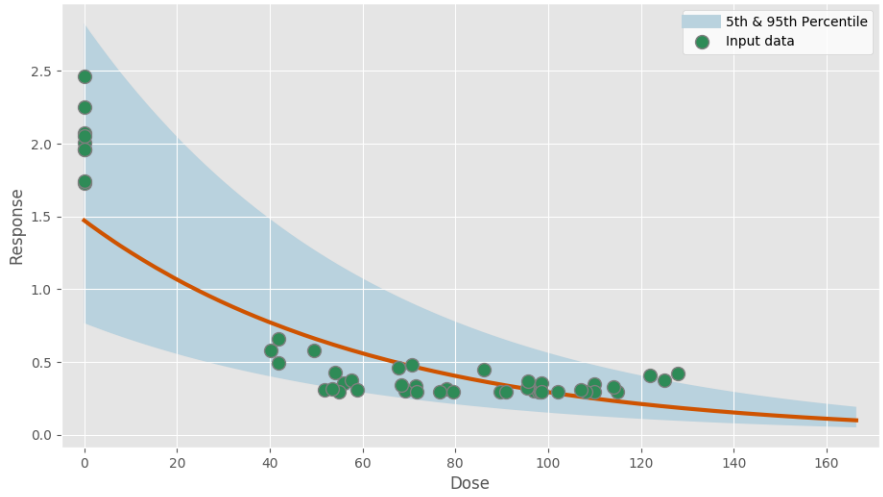

Posterior predictive p-value for model fit: 0.528

Model weight: 0.0%

Correlation matrix

	a	b	sigma
a	-	-0.853	0.036
b	-0.853	-	-0.0173
sigma	0.036	-0.0173	-

Parameter charts

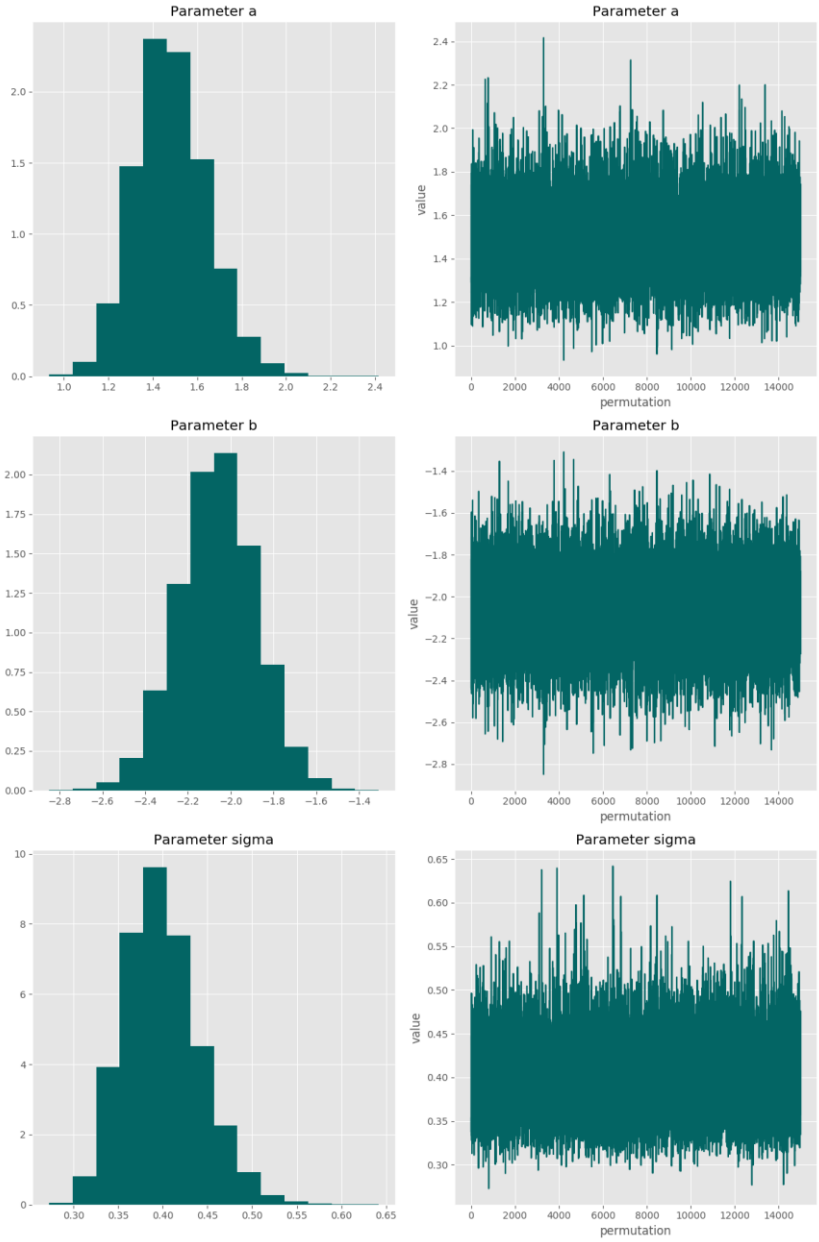

Exponential3

$$f(dose) = a \times e^{b \times dose^{g}}$$

Power parameter lower-bound: 1.000

Model fit summary

```
Inference for Stan model: exponential3_individual_pkl_df53333b36693dd0ad892f92a4fc7532.
1 chains, each with iter=30000; warmup=15000; thin=1;
post-warmup draws per chain=15000, total post-warmup draws=15000.

        mean se_mean     sd   2.5%    25%    50%    75%  97.5%  n_eff   Rhat
a       1.45  2.0e-3   0.17   1.15   1.34   1.45   1.56   1.81   6679    1.0
b      -2.05  2.4e-3   0.19  -2.42  -2.18  -2.06  -1.93  -1.68   6413    1.0
g       1.04  3.4e-4   0.04    1.0   1.01   1.02   1.05   1.14  12185    1.0
sigma   0.41  4.8e-4   0.04   0.33   0.38   0.41   0.44    0.5   8409    1.0
lp__    16.0    0.02   1.49  12.18  15.27  16.35   17.1  17.87   5437    1.0

Samples were drawn using NUTS at Mon Nov  4 20:58:16 2019.
For each parameter, n_eff is a crude measure of effective sample size,
and Rhat is the potential scale reduction factor on split chains (at
convergence, Rhat=1).
```

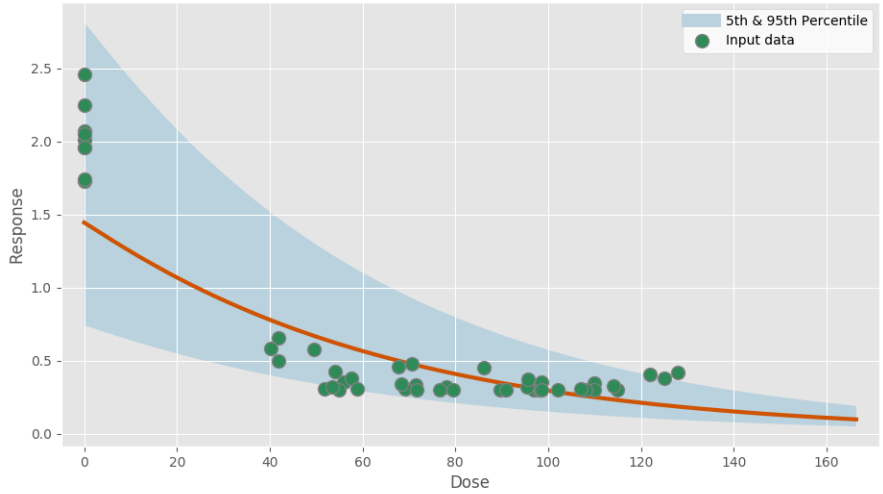

Posterior predictive p-value for model fit: 0.528

Model weight: 0.0%

Correlation matrix

	a	b	g	sigma
a	-	-0.846	-0.175	0.017
b	-0.846	-	0.053	-0.0219
g	-0.175	0.053	-	0.198
sigma	0.017	-0.0219	0.198	-

Parameter charts

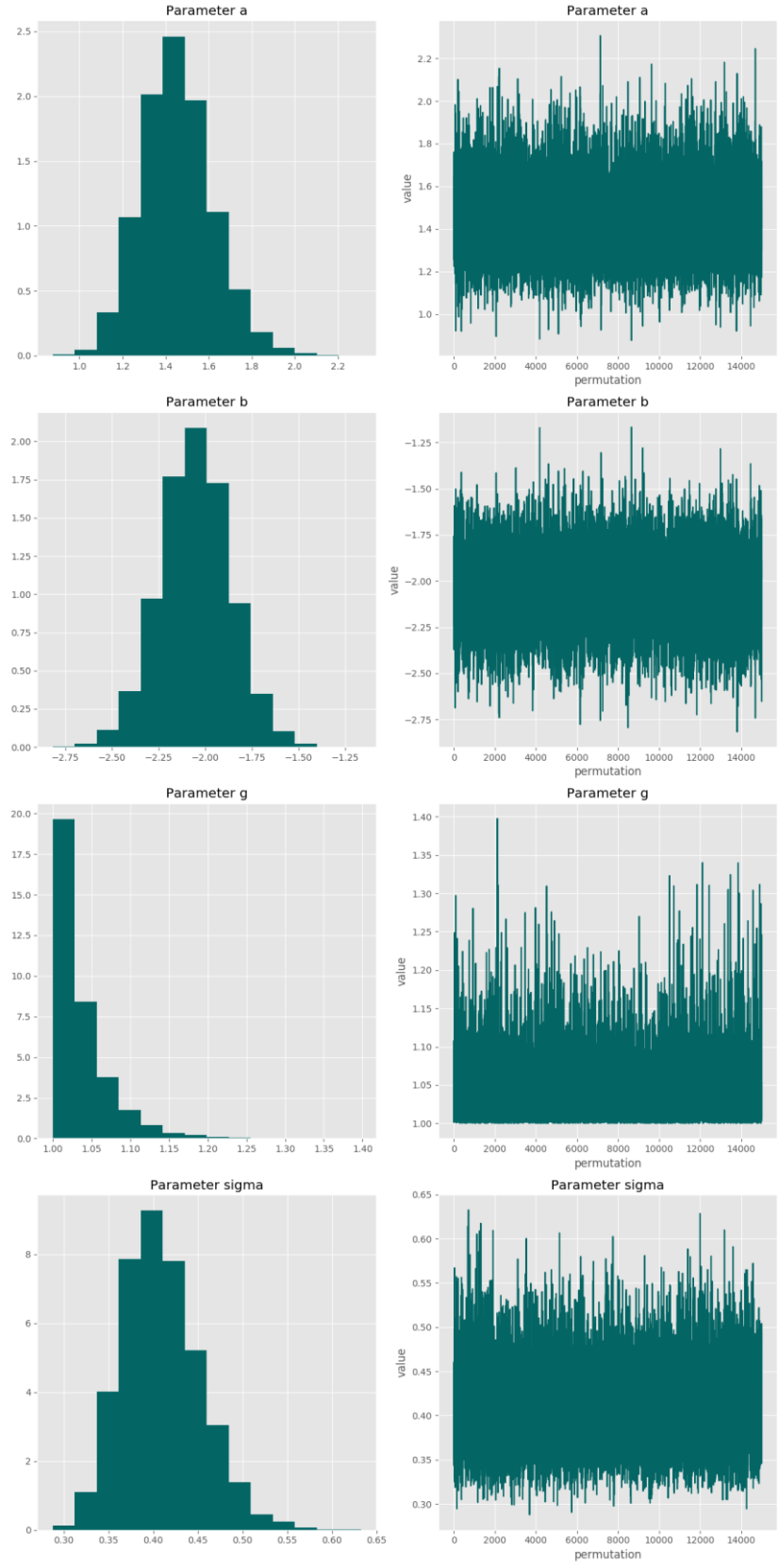

Exponential4

$$f(dose) = a \times [c - (c - 1) \times e^{-b \times dose}]$$

Model fit summary

```
Inference for Stan model: exponential4_individual_pkl_fa67b4bb1853dd3a882bdb66cdb5191d.
1 chains, each with iter=30000; warmup=15000; thin=1;
post-warmup draws per chain=15000, total post-warmup draws=15000.

        mean se_mean     sd   2.5%    25%    50%    75%  97.5%  n_eff   Rhat
a       2.13  1.5e-3   0.12   1.91   2.05   2.13   2.21   2.37   6040    1.0
b       7.79    0.12   3.41   6.32   7.06   7.52   8.05   9.57    791    1.0
c       0.15  1.3e-4   0.01   0.13   0.14   0.15   0.16   0.17   5853    1.0
sigma   0.18  2.5e-4   0.02   0.14   0.16   0.17   0.19   0.22   5970    1.0
lp__   62.01    0.03   1.59  57.97  61.28  62.39  63.14   63.9   2614    1.0

Samples were drawn using NUTS at Mon Nov  4 20:58:26 2019.
For each parameter, n_eff is a crude measure of effective sample size,
and Rhat is the potential scale reduction factor on split chains (at
convergence, Rhat=1).
```

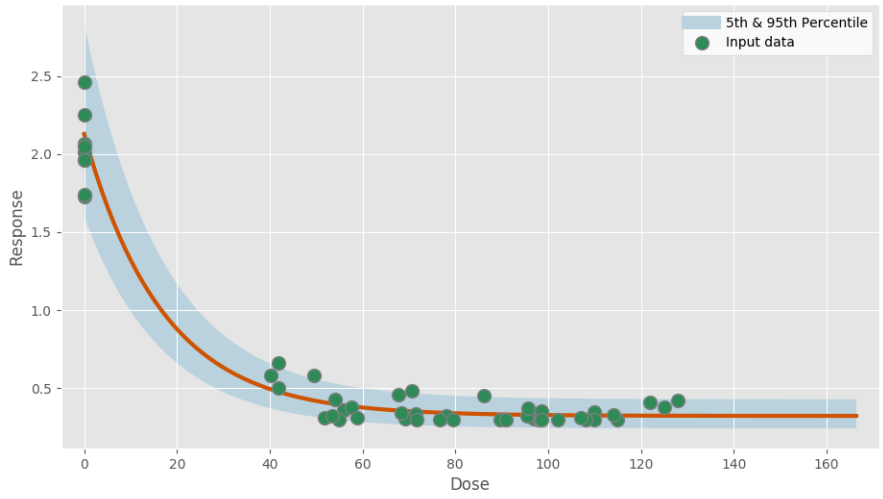

Posterior predictive p-value for model fit: 0.523

Model weight: 24.5%

Correlation matrix

	a	b	c	sigma
a	-	0.075	-0.788	0.009
b	0.075	-	0.116	0.119
c	-0.788	0.116	-	0.038
sigma	0.009	0.119	0.038	-

Parameter charts

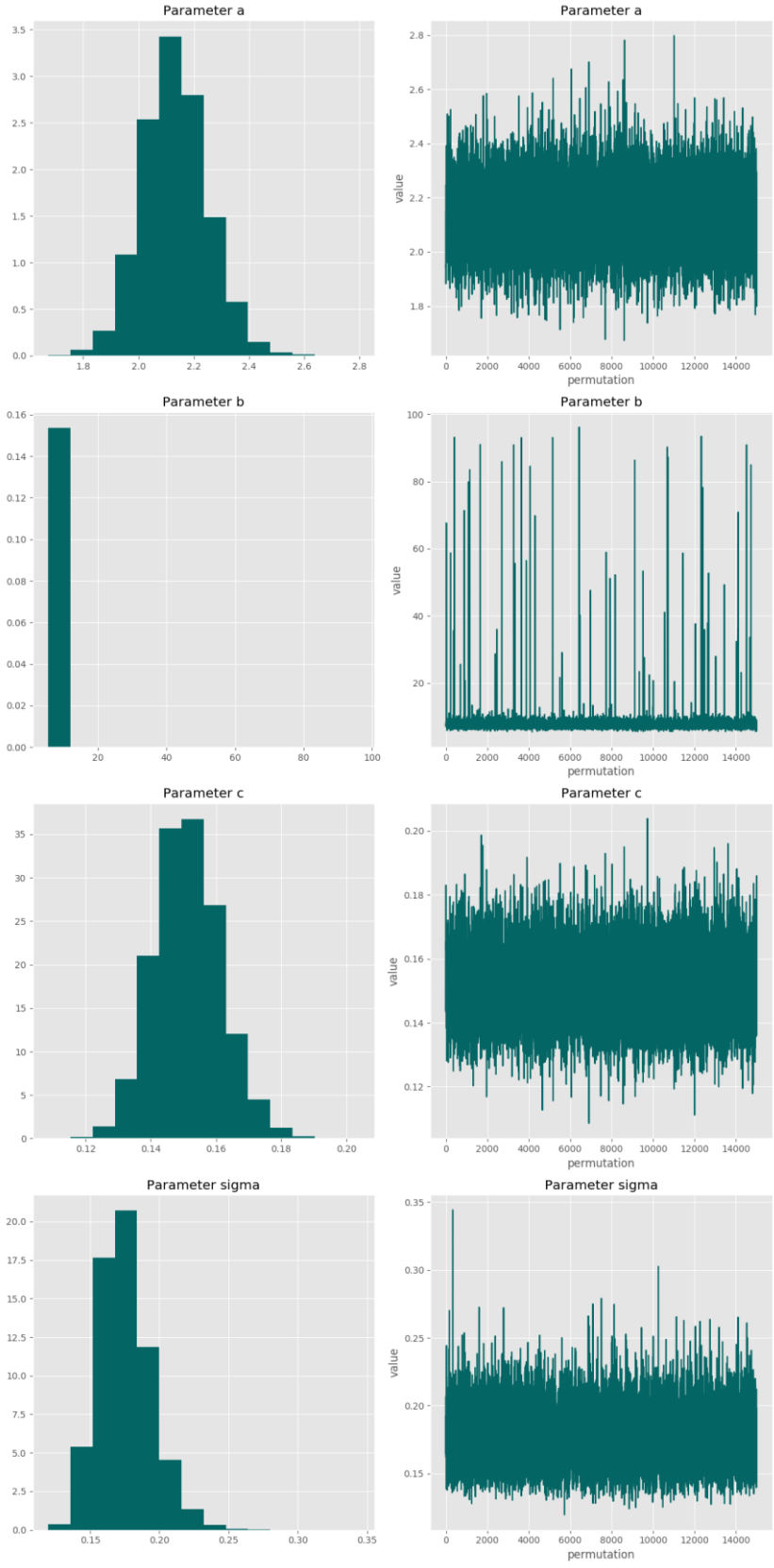

Exponential5

$$f(dose) = a \times [c - (c - 1) \times e^{-(b \times dose)^g}]$$

Power parameter lower-bound: 1.000

Model fit summary

```
Inference for Stan model: exponential5_individual_pkl_0fe35d8b796f8736b80743a2674317fc.
1 chains, each with iter=30000; warmup=15000; thin=1;
post-warmup draws per chain=15000, total post-warmup draws=15000.

        mean se_mean     sd   2.5%    25%    50%    75%  97.5%  n_eff   Rhat
a       2.11  2.1e-3   0.11   1.89   2.03    2.1   2.18   2.34   2822    1.0
b       7.48    3.14  15.56   3.36   3.74   4.04    4.6  78.29     25   1.05
c       0.16  2.2e-4   0.01   0.14   0.15   0.16   0.17   0.18   2168    1.0
g       3.23    0.19   2.09   1.24   2.05    2.7   3.53  10.21    117   1.01
sigma   0.17  2.1e-3   0.02   0.14   0.15   0.17   0.18   0.22    102   1.01
lp__   63.96    0.37   2.55  56.25  63.15   64.6  65.65  66.77     48   1.02

Samples were drawn using NUTS at Mon Nov  4 20:58:42 2019.
For each parameter, n_eff is a crude measure of effective sample size,
and Rhat is the potential scale reduction factor on split chains (at
convergence, Rhat=1).
```

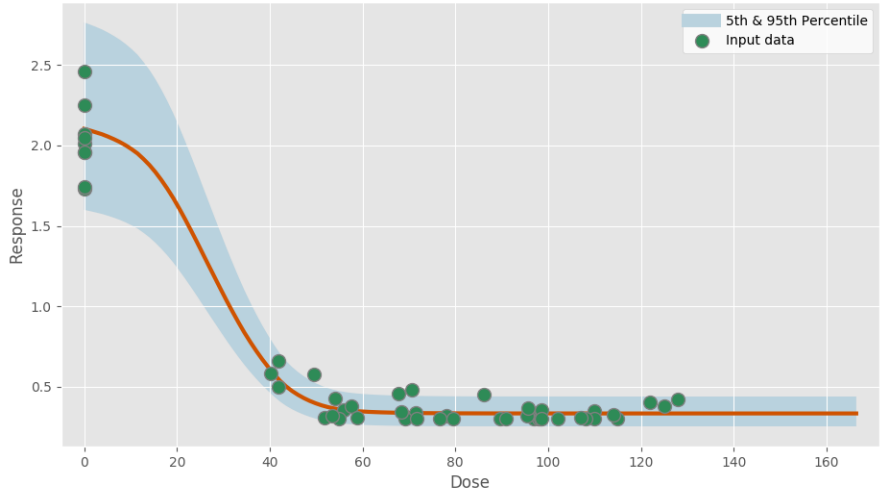

Posterior predictive p-value for model fit: 0.532

Model weight: 35.4%

Correlation matrix

	a	b	c	g	sigma
a	-	0.064	-0.832	0.018	0.039
b	0.064	-	0.135	0.435	0.457
c	-0.832	0.135	-	0.196	0.085
g	0.018	0.435	0.196	-	0.280

sigma	0.039	0.457	0.085	0.280	-

Parameter charts

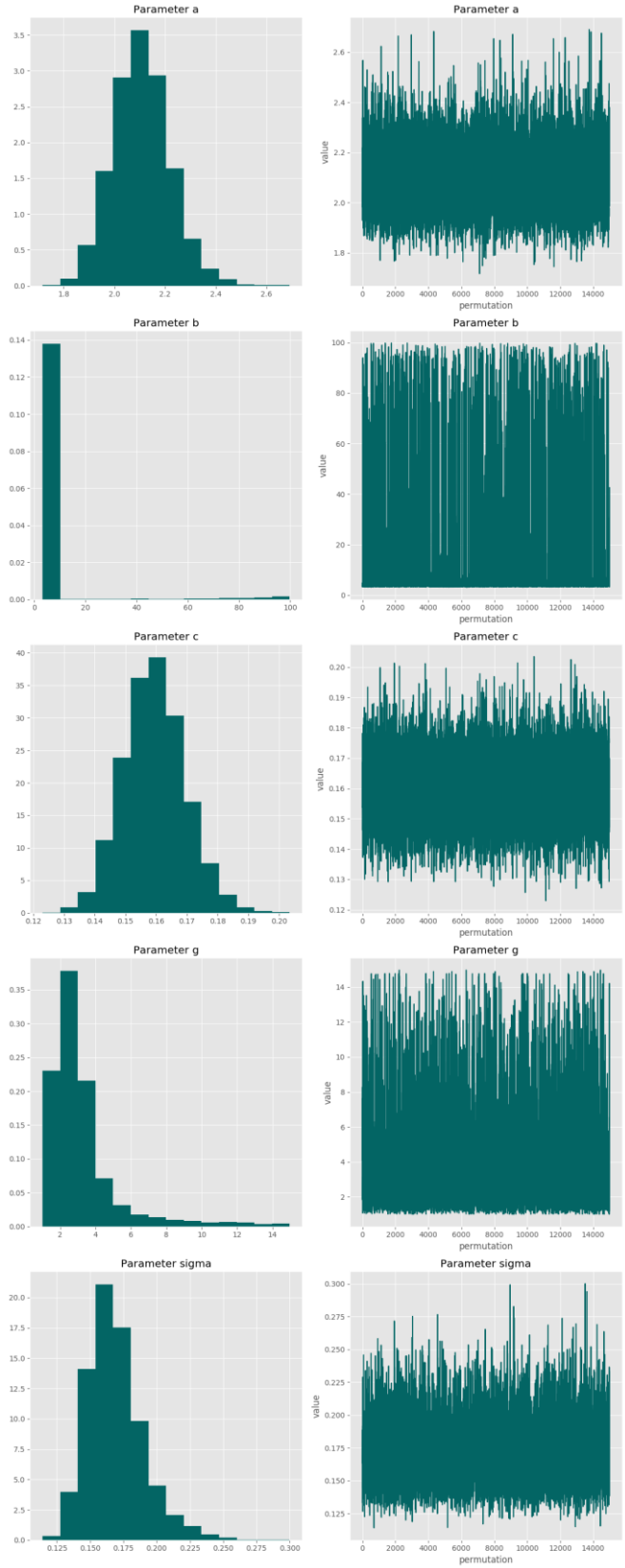

Hill

$$f(dose) = a + \frac{b \times dose^g}{c^g + dose^g}$$

Power parameter lower-bound: 1.000

Model fit summary

```
Inference for Stan model: hill_individual_pkl_f14f62088318f1a4663f986868dc9b40.
1 chains, each with iter=30000; warmup=15000; thin=1;
post-warmup draws per chain=15000, total post-warmup draws=15000.

        mean se_mean     sd   2.5%    25%    50%    75%  97.5%  n_eff   Rhat
a       2.11  1.8e-3   0.11    1.9   2.04   2.11   2.19   2.35   4227    1.0
b      -1.78  1.8e-3   0.11  -2.02  -1.86  -1.78  -1.71  -1.57   4172    1.0
c       0.25  5.9e-4   0.03   0.18   0.23   0.25   0.27   0.29   2415    1.0
g       7.87    0.04   2.61   3.56   5.97   7.54   9.53  13.74   3461    1.0
sigma   0.17  2.4e-4   0.02   0.14   0.15   0.16   0.18   0.21   5631    1.0
lp__   64.87    0.03    1.8   60.3  64.02  65.26  66.15  67.14   2730    1.0

Samples were drawn using NUTS at Mon Nov  4 20:59:24 2019.
For each parameter, n_eff is a crude measure of effective sample size,
and Rhat is the potential scale reduction factor on split chains (at
convergence, Rhat=1).
```

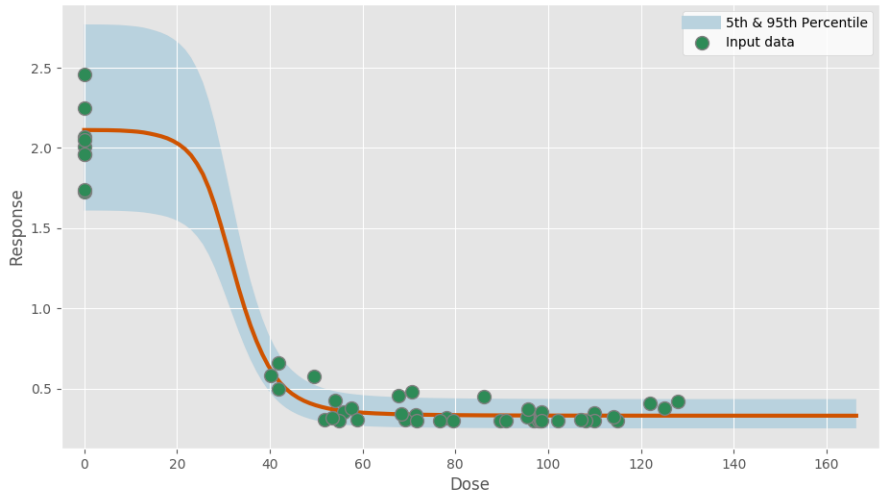

Posterior predictive p-value for model fit: 0.533

Model weight: 38.9%

Correlation matrix

	a	b	c	g	sigma
a	-	-0.995	-0.0974	-0.000691	0.032
b	-0.995	-	0.139	0.050	-0.0322
c	-0.0974	0.139	-	0.846	-0.057
g	-0.000691	0.050	0.846	-	-3.31e-05

sigma	0.032	-0.0322	-0.057	-3.31e-05	-

Parameter charts

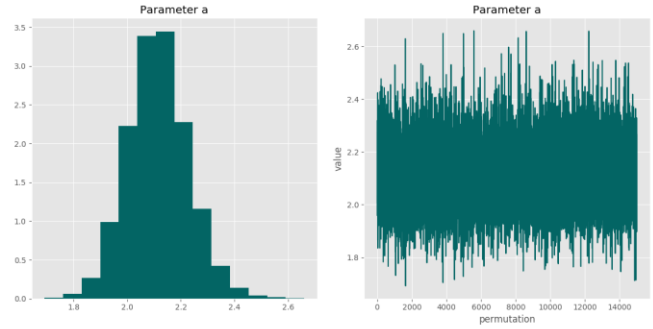

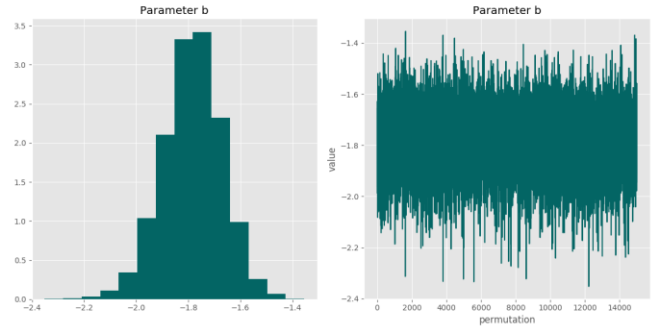

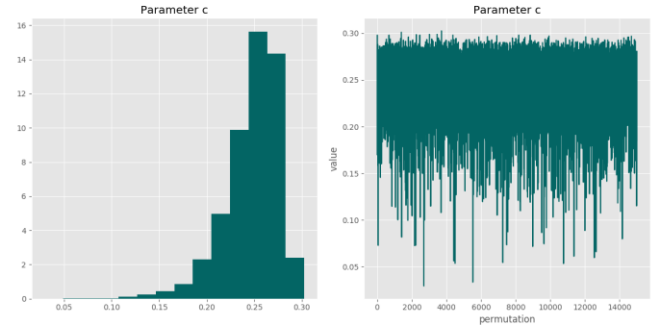

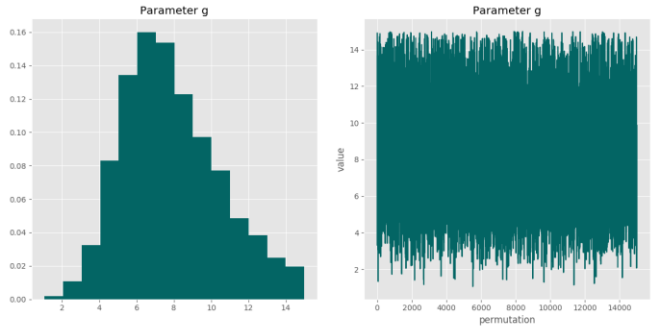

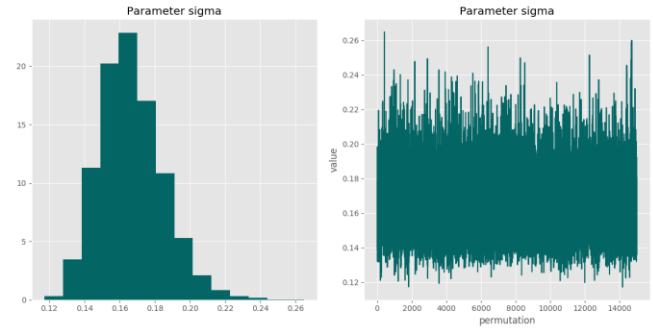

Power

$$f(dose) = a + b \times dose^{g}$$

Power parameter lower-bound: 1.000

Model fit summary

```
Inference for Stan model: power_individual_pkl_8682a4681cf39e692df770d4639a86e2.
1 chains, each with iter=30000; warmup=15000; thin=1;
post-warmup draws per chain=15000, total post-warmup draws=15000.

        mean se_mean     sd   2.5%    25%    50%    75%  97.5%  n_eff   Rhat
a       0.93  1.5e-3    0.1   0.74   0.86   0.93   0.99   1.14   4766    1.0
b      -0.73  1.7e-3   0.12  -0.98  -0.81  -0.73  -0.65   -0.5   4789    1.0
g       1.08  1.0e-3   0.09    1.0   1.02   1.05   1.11   1.33   8232    1.0
sigma   0.55  6.7e-4   0.06   0.44    0.5   0.54   0.58   0.68   8021    1.0
lp__    1.95    0.02   1.49  -1.77    1.2   2.28   3.05   3.81   4934    1.0

Samples were drawn using NUTS at Mon Nov  4 20:59:37 2019.
For each parameter, n_eff is a crude measure of effective sample size,
and Rhat is the potential scale reduction factor on split chains (at
convergence, Rhat=1).
```

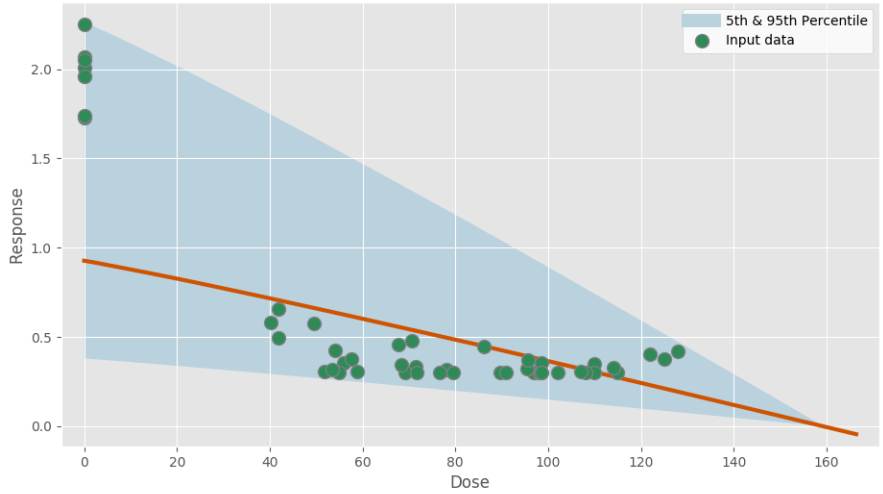

Posterior predictive p-value for model fit: 0.523

Model weight: 0.0%

Correlation matrix

	a	b	g	sigma
a	-	-0.948	-0.261	-0.0501
b	-0.948	-	0.216	0.060
g	-0.261	0.216	-	0.228
sigma	-0.0501	0.060	0.228	-

Parameter charts

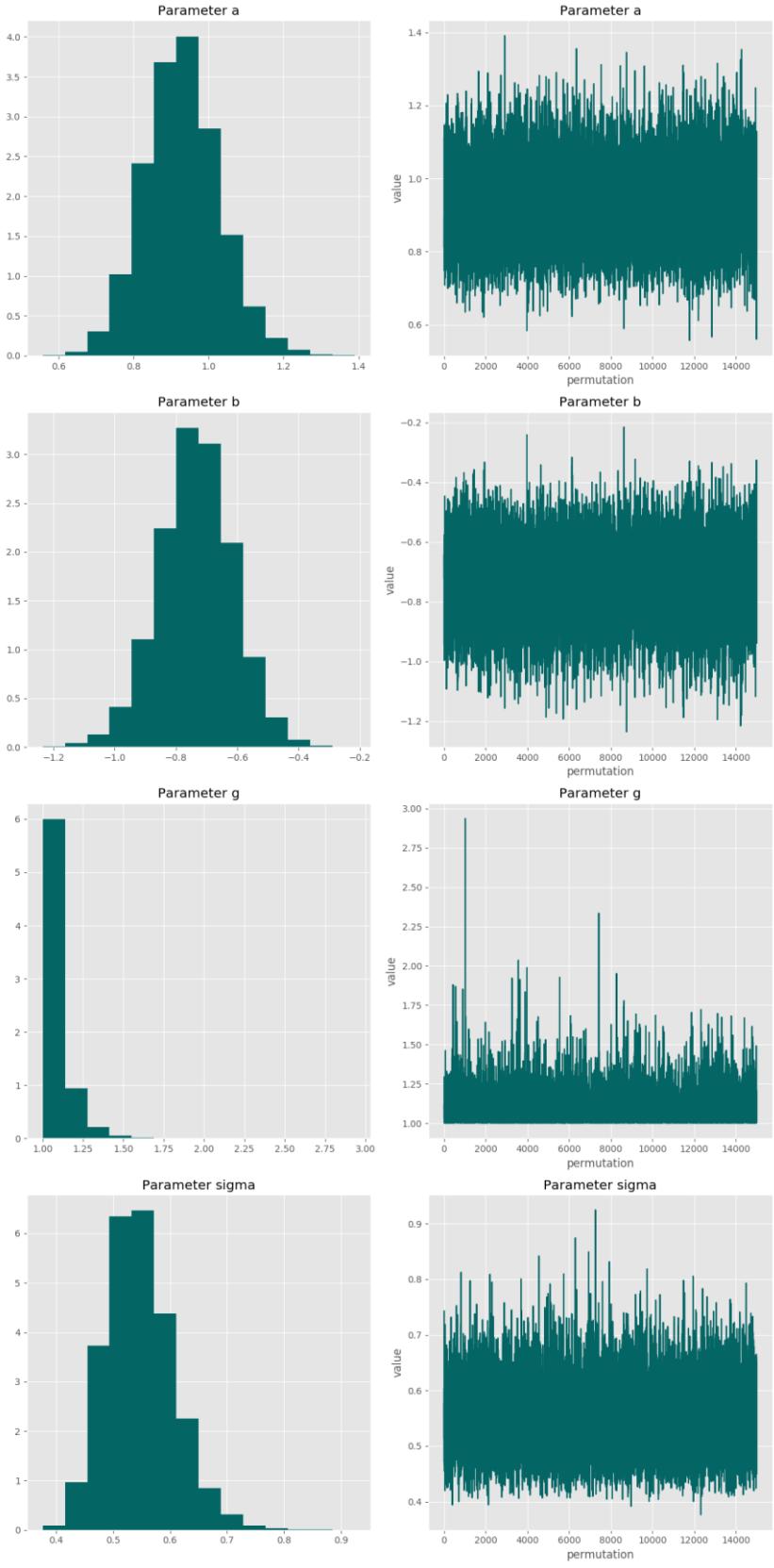

MichaelisMenten

$$f(dose) = a + \frac{b \times dose}{c + dose}$$

Model fit summary

```
Inference for Stan model: michaelismenten_individual_pkl_8a1ee8a1062ea9c00f6bd83f5c89e8d5.
1 chains, each with iter=30000; warmup=15000; thin=1;
post-warmup draws per chain=15000, total post-warmup draws=15000.

        mean se_mean     sd   2.5%    25%    50%    75%  97.5%  n_eff   Rhat
a       2.15  2.1e-3   0.14    1.9   2.06   2.14   2.23   2.43   4395    1.0
b      -1.92  2.0e-3   0.14   -2.2   -2.0  -1.91  -1.83  -1.67   4760    1.0
c       0.04  1.5e-4   0.01   0.02   0.03   0.04   0.05   0.07   7361    1.0
sigma   0.19  2.2e-4   0.02   0.15   0.17   0.19    0.2   0.23   8090    1.0
lp__   55.38    0.03   1.53  51.59  54.65  55.74  56.49  57.24   3651    1.0

Samples were drawn using NUTS at Mon Nov  4 20:59:57 2019.
For each parameter, n_eff is a crude measure of effective sample size,
and Rhat is the potential scale reduction factor on split chains (at
convergence, Rhat=1).
```

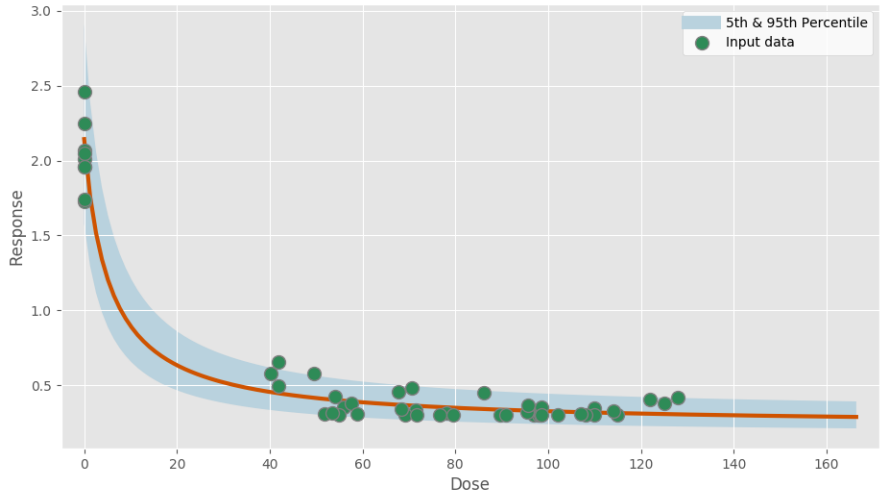

Posterior predictive p-value for model fit: 0.525

Model weight: 1.2%

Correlation matrix

	a	b	c	sigma
a	-	-0.967	-0.357	0.022
b	-0.967	-	0.122	-0.0268
c	-0.357	0.122	-	0.025
sigma	0.022	-0.0268	0.025	-

Parameter charts

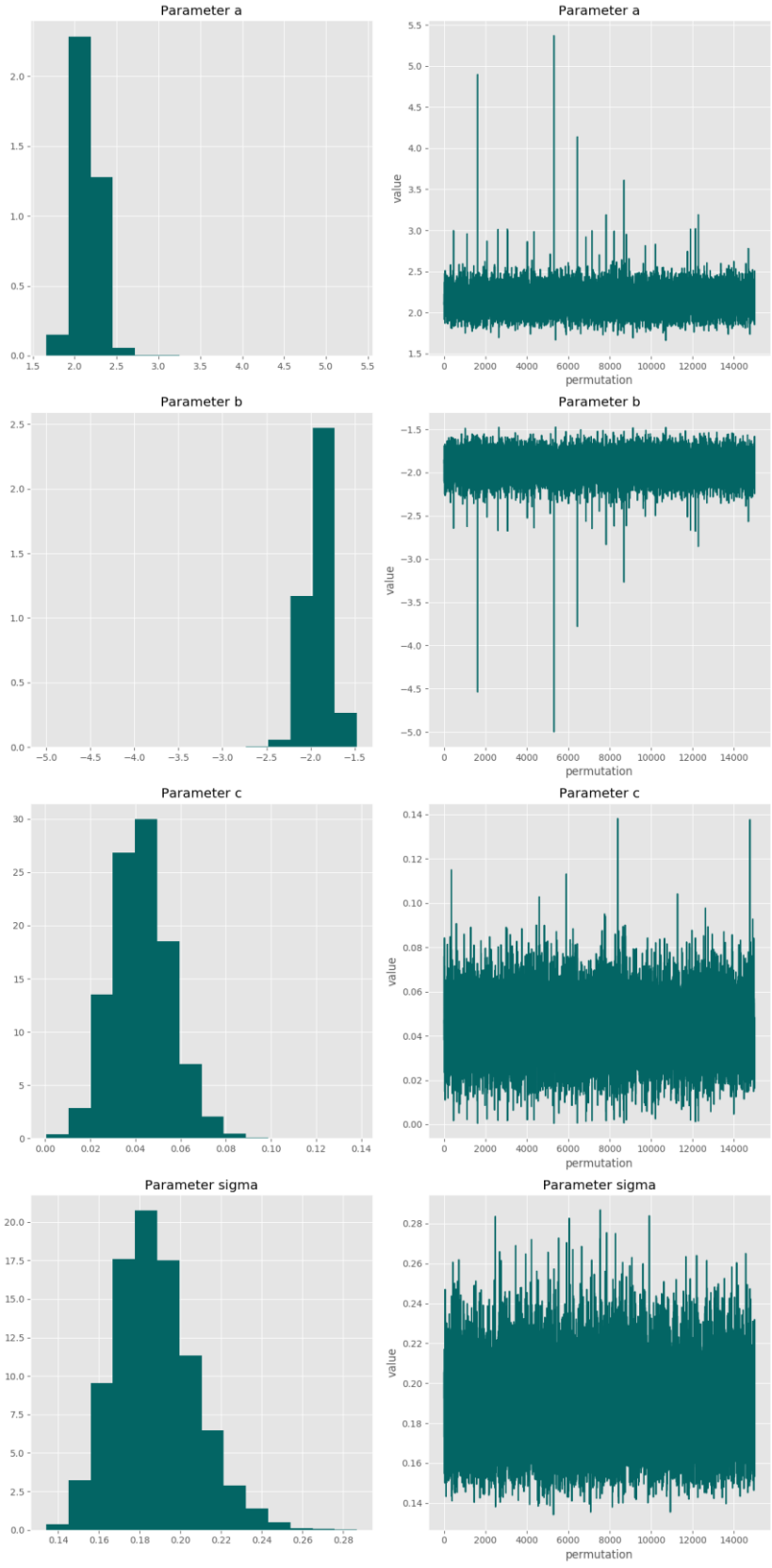

Linear

$$f(dose) = a + b \times dose$$

Model fit summary

```
Inference for Stan model: linear_individual_pkl_6f560bd3666c0b0a5c004ccddf0ad3ca.
1 chains, each with iter=30000; warmup=15000; thin=1;
post-warmup draws per chain=15000, total post-warmup draws=15000.

        mean se_mean     sd   2.5%    25%    50%    75%  97.5%  n_eff   Rhat
a       0.96  1.5e-3    0.1   0.78   0.89   0.95   1.02   1.17   4615    1.0
b      -0.76  1.8e-3   0.12  -1.01  -0.84  -0.76  -0.68  -0.53   4474    1.0
sigma   0.54  6.9e-4   0.06   0.44    0.5   0.53   0.57   0.66   6803    1.0
lp__    6.26    0.02   1.29   2.92   5.66    6.6    7.2   7.73   4856    1.0

Samples were drawn using NUTS at Mon Nov  4 21:00:06 2019.
For each parameter, n_eff is a crude measure of effective sample size,
and Rhat is the potential scale reduction factor on split chains (at
convergence, Rhat=1).
```

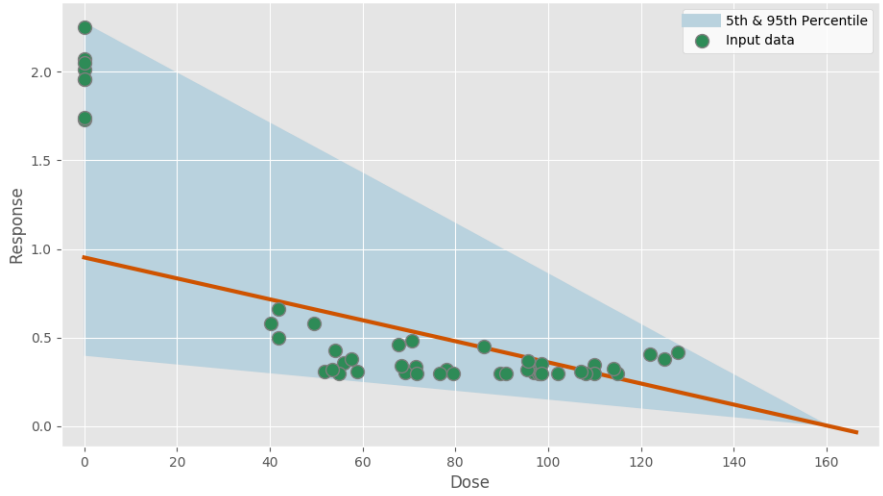

Posterior predictive p-value for model fit: 0.526

Model weight: 0.0%

Correlation matrix

	a	b	sigma
a	-	-0.948	0.029
b	-0.948	-	-0.0141
sigma	0.029	-0.0141	-

Parameter charts

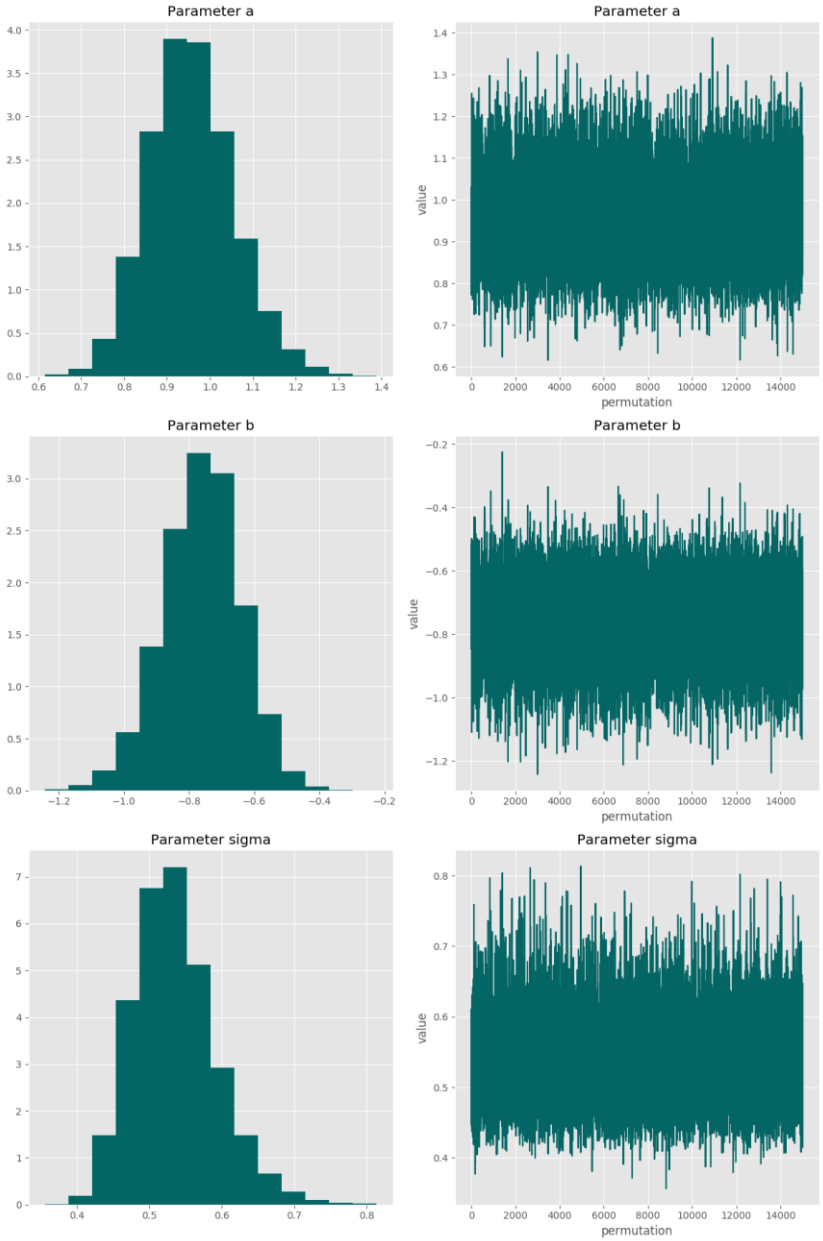

PFOS fT4 male Nov 4 2019

Report created on Nov 04, 2019 at 08:09 PM.

Pystan model version 2.19.0.0.

Dataset

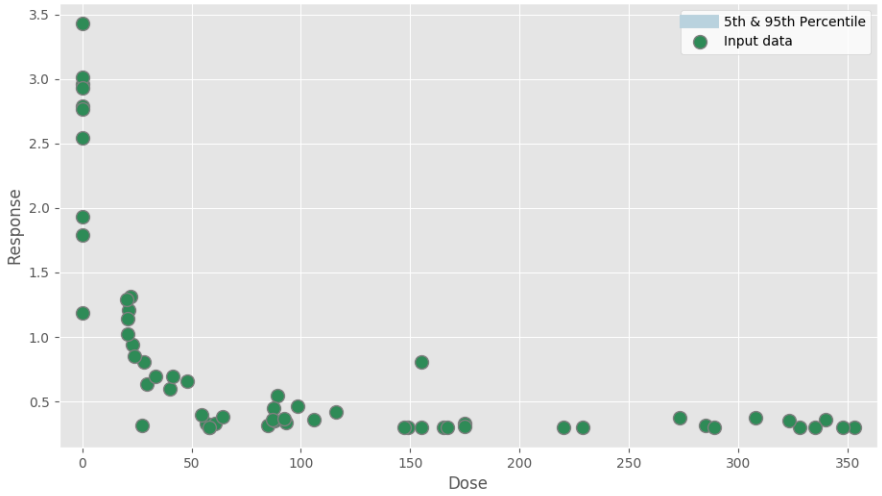

Dose	Response
0.0125	3.43
0.0125	2.54
0.0125	1.79
0.0125	2.79
0.0125	1.93
0.0125	1.19
0.0125	2.77
0.0125	2.96
0.0125	3.01
0.0125	2.93
23.1	0.938
21.1	1.21
20.6	1.02
28.3	0.807
20.8	1.14
22.1	1.31
20.3	1.29
29.7	0.639
23.7	0.852
27.6	0.314
58.3	0.3
56.8	0.329

60.6	0.332
40.3	0.597
57.9	0.3
64.4	0.382
33.5	0.696
54.4	0.397
47.8	0.658
41.6	0.695
93.1	0.339
84.8	0.317
98.7	0.466
89.1	0.545
87.8	0.354
106.0	0.362
116.0	0.419
87.6	0.447
87.0	0.361
92.5	0.37
155.0	0.808
165.0	0.3
149.0	0.3
167.0	0.3
155.0	0.3
147.0	0.3
175.0	0.328
175.0	0.311
229.0	0.3
220.0	0.3
285.0	0.315
289.0	0.3
308.0	0.375
353.0	0.3
273.0	0.377
348.0	0.3
328.0	0.3
323.0	0.349
340.0	0.363
335.0	0.3

20% Central tendency: Relative

BMR: None

Adversity value: 0.200

BMD summary tables:

Statistic	Model average	Exponential2	Exponential3	Exponential4	Exponential5	Hill	Power	Michaelis Menten	Linear
Prior model weight	N/A	0.125	0.125	0.125	0.125	0.125	0.125	0.125	0.125
Posterior model weight	N/A	3.66e-21	2.14e-22	0.600	0.157	0.238	1.02e-24	0.005	1.92e-23
BMD (median)	6.661	47.842	54.648	4.502	7.297	11.477	116.132	2.088	97.791
BMDL (5th percentile)	5.433	38.189	41.370	3.785	4.708	7.225	91.933	1.490	85.067
25th percentile	6.152	43.331	48.233	4.195	5.942	9.768	103.239	1.820	91.656
Mean (SD)	6.665 (0.755)	49.027 (8.493)	57.809 (15.569)	4.532 (0.488)	7.665 (2.285)	11.459 (2.507)	128.383 (41.816)	2.131 (0.440)	100.624 (13.691)
75th percentile	7.162	53.279	63.187	4.833	8.965	13.184	137.138	2.392	106.290
95th percentile	7.919	63.700	84.723	5.386	11.848	15.571	211.418	2.912	125.444

BMD estimates

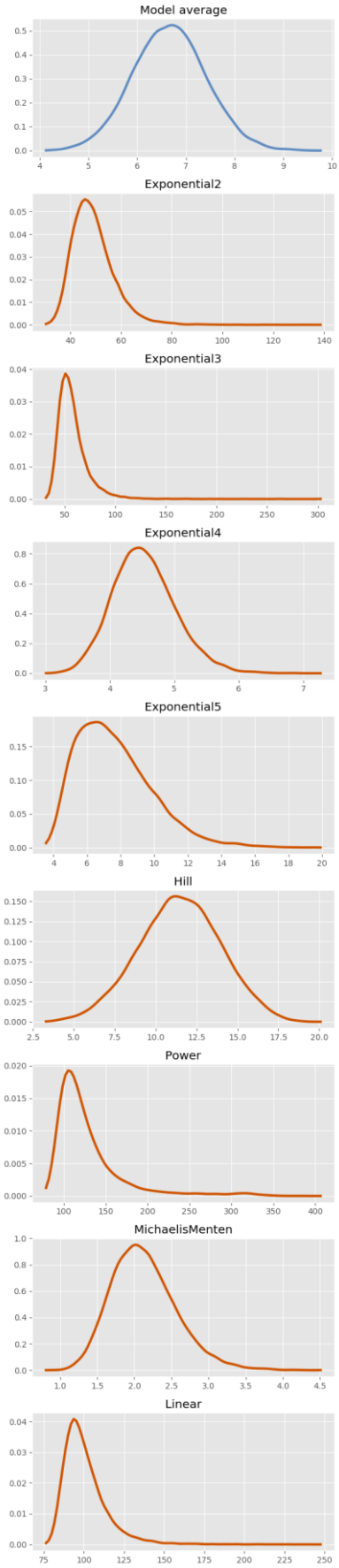
Model average
Exponential2
Exponential3
Exponential4
Exponential5
Hill
Power
MichaelisMenten
Linear

BMD results

Central tendency: Relative

BMR: None

Adversity value: 0.500

BMD summary tables:

Statistic	Model average	Exponential2	Exponential3	Exponential4	Exponential5	Hill	Power	Michaelis Menten	Linear
Prior model weight	N/A	0.125	0.125	0.125	0.125	0.125	0.125	0.125	0.125
Posterior model weight	N/A	3.66e-21	2.14e-22	0.600	0.157	0.238	1.02e-24	0.005	1.92e-23
BMD (median)	16.307	148.610	159.853	14.787	17.899	19.189	262.704	9.145	244.477
BMDL (5th percentile)	14.489	118.627	124.916	12.380	14.181	15.304	222.561	6.503	212.668
25th percentile	15.556	134.600	143.693	13.757	16.280	17.741	242.757	7.964	229.141
Mean (SD)	16.349 (1.178)	152.291 (26.382)	165.140 (31.509)	14.899 (1.653)	17.989 (2.409)	19.049 (2.141)	271.473 (42.410)	9.334 (1.941)	251.559 (34.228)
75th percentile	17.105	165.500	180.227	15.914	19.607	20.505	290.131	10.481	265.724
95th percentile	18.350	197.869	223.080	17.801	22.094	22.289	348.759	12.793	313.610

BMD estimates

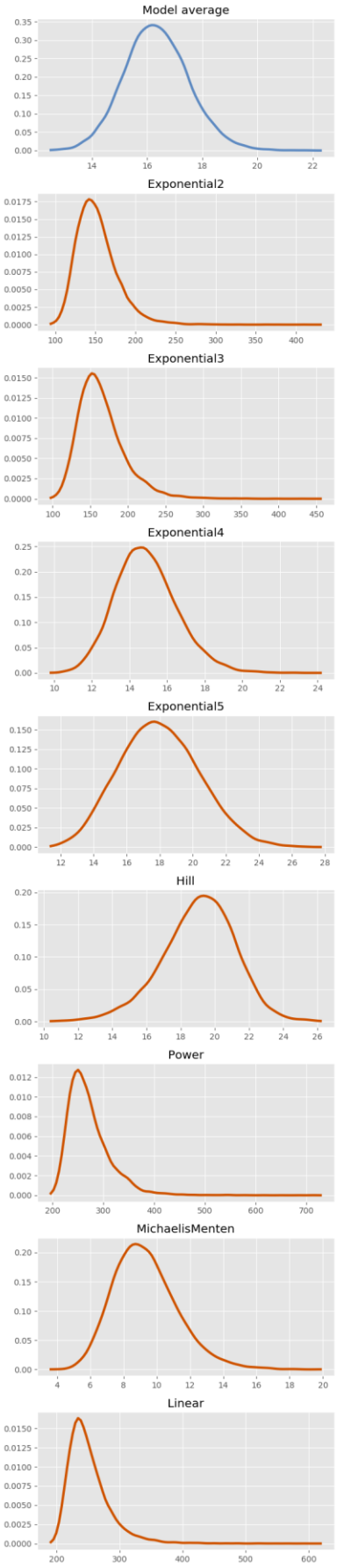
Model average
Exponential2
Exponential3
Exponential4
Exponential5
Hill
Power
MichaelisMenten
Linear

BMD Markov chain Monte Carlo settings

Iterations: 30,000

Number of chains: 1

Warmup fraction: 0.5

Seed: 79,520

Model results

Exponential2

$$f(dose) = a \times e^{b \times dose}$$

Model fit summary

```
Inference for Stan model: exponential2_individual_pkl_be58f7567ba64ec5547642f54ef3b89e.
1 chains, each with iter=30000; warmup=15000; thin=1;
post-warmup draws per chain=15000, total post-warmup draws=15000.

        mean se_mean     sd   2.5%    25%    50%    75%  97.5%  n_eff   Rhat
a        1.0  1.3e-3   0.11   0.79   0.92   0.99   1.07   1.23   7167    1.0
b      -1.65  2.9e-3   0.25  -2.15  -1.82  -1.65  -1.48  -1.15   7570    1.0
sigma   0.61  5.8e-4   0.06   0.51   0.57    0.6   0.64   0.73   9865    1.0
lp__    0.07    0.02   1.27  -3.23  -0.46   0.39   0.98    1.5   6123    1.0

Samples were drawn using NUTS at Mon Nov  4 20:05:15 2019.
For each parameter, n_eff is a crude measure of effective sample size,
and Rhat is the potential scale reduction factor on split chains (at
convergence, Rhat=1).
```

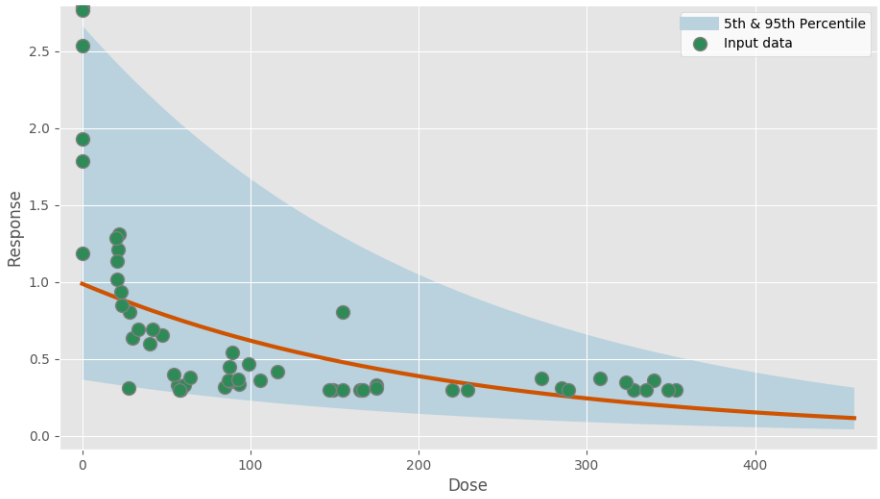

Posterior predictive p-value for model fit: 0.529

Model weight: 0.0%

Correlation matrix

	a	b	sigma
a	-	-0.707	0.029
b	-0.707	-	-0.0113
sigma	0.029	-0.0113	-

Parameter charts

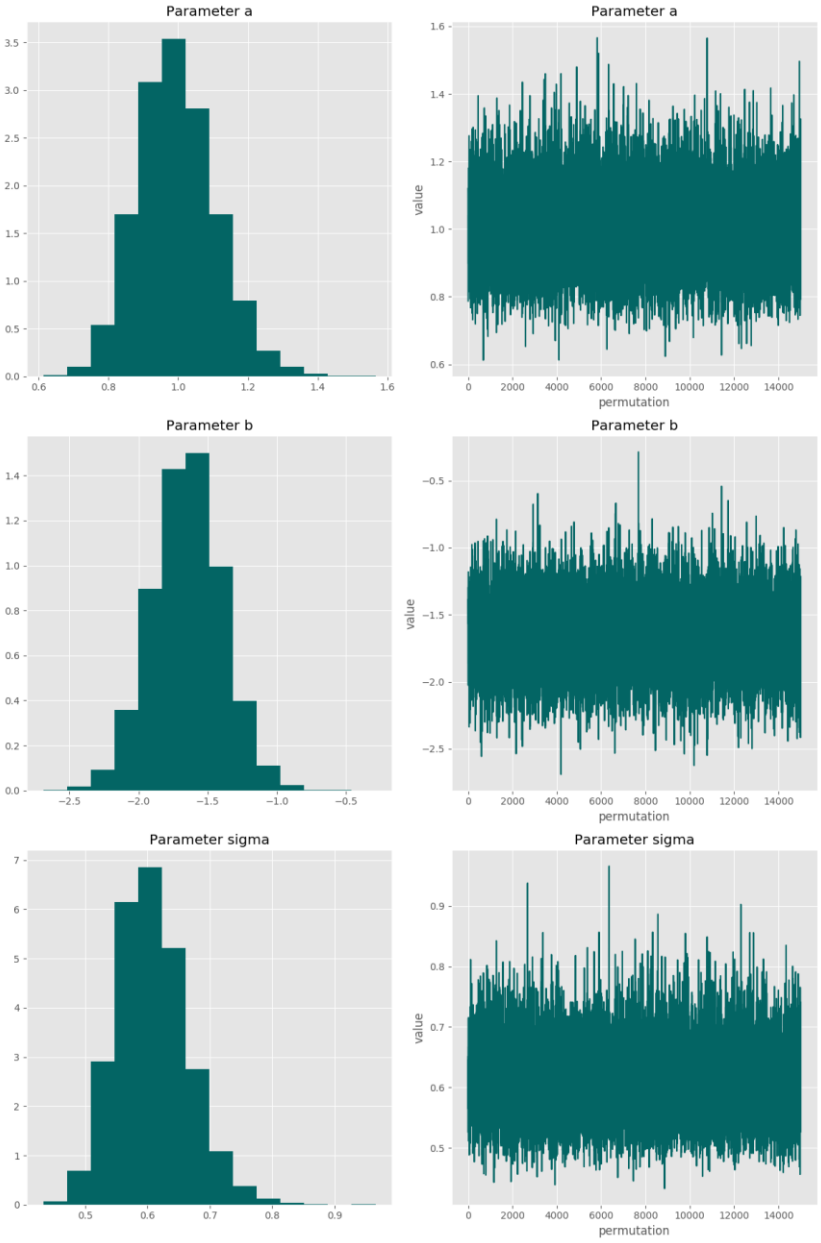

Exponential3

$$f(dose) = a \times e^{b \times dose^g}$$

Power parameter lower-bound: 1.000

Model fit summary

```
Inference for Stan model: exponential3_individual_pkl_df53333b36693dd0ad892f92a4fc7532.
1 chains, each with iter=30000; warmup=15000; thin=1;
post-warmup draws per chain=15000, total post-warmup draws=15000.

        mean se_mean     sd   2.5%    25%    50%    75%  97.5%  n_eff   Rhat
a       0.96  1.4e-3   0.11   0.75   0.89   0.96   1.04    1.2   6879    1.0
b      -1.61  3.1e-3   0.27  -2.13  -1.78  -1.61  -1.43  -1.08   7189    1.0
g       1.08  2.3e-3   0.16    1.0   1.02   1.05   1.09   1.32   4769    1.0
sigma   0.62  6.1e-4   0.06   0.52   0.58   0.61   0.66   0.75   9522    1.0
lp__   -4.42    0.02   1.51  -8.22  -5.16  -4.08  -3.31  -2.53   5256    1.0

Samples were drawn using NUTS at Mon Nov  4 20:05:25 2019.
For each parameter, n_eff is a crude measure of effective sample size,
and Rhat is the potential scale reduction factor on split chains (at
convergence, Rhat=1).
```

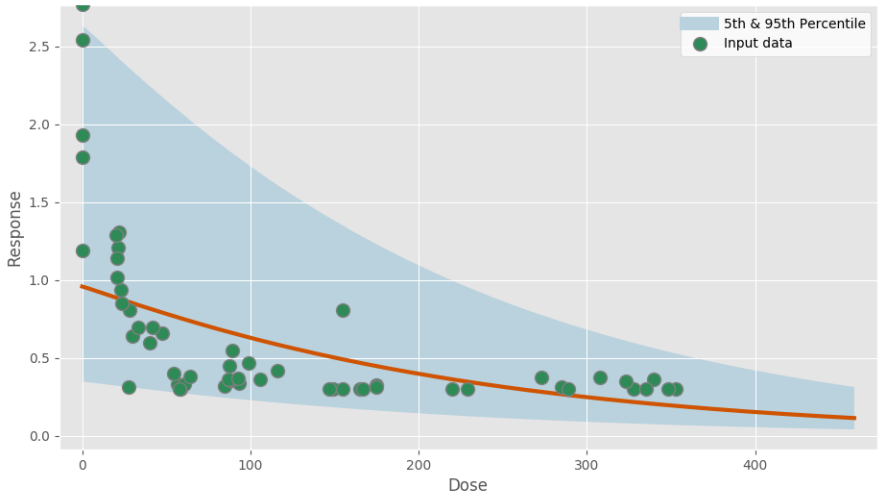

Posterior predictive p-value for model fit: 0.524

Model weight: 0.0%

Correlation matrix

	a	b	g	sigma
a	-	-0.71	-0.217	-0.0186
b	-0.71	-	0.149	0.012
g	-0.217	0.149	-	0.152
sigma	-0.0186	0.012	0.152	-

Parameter charts

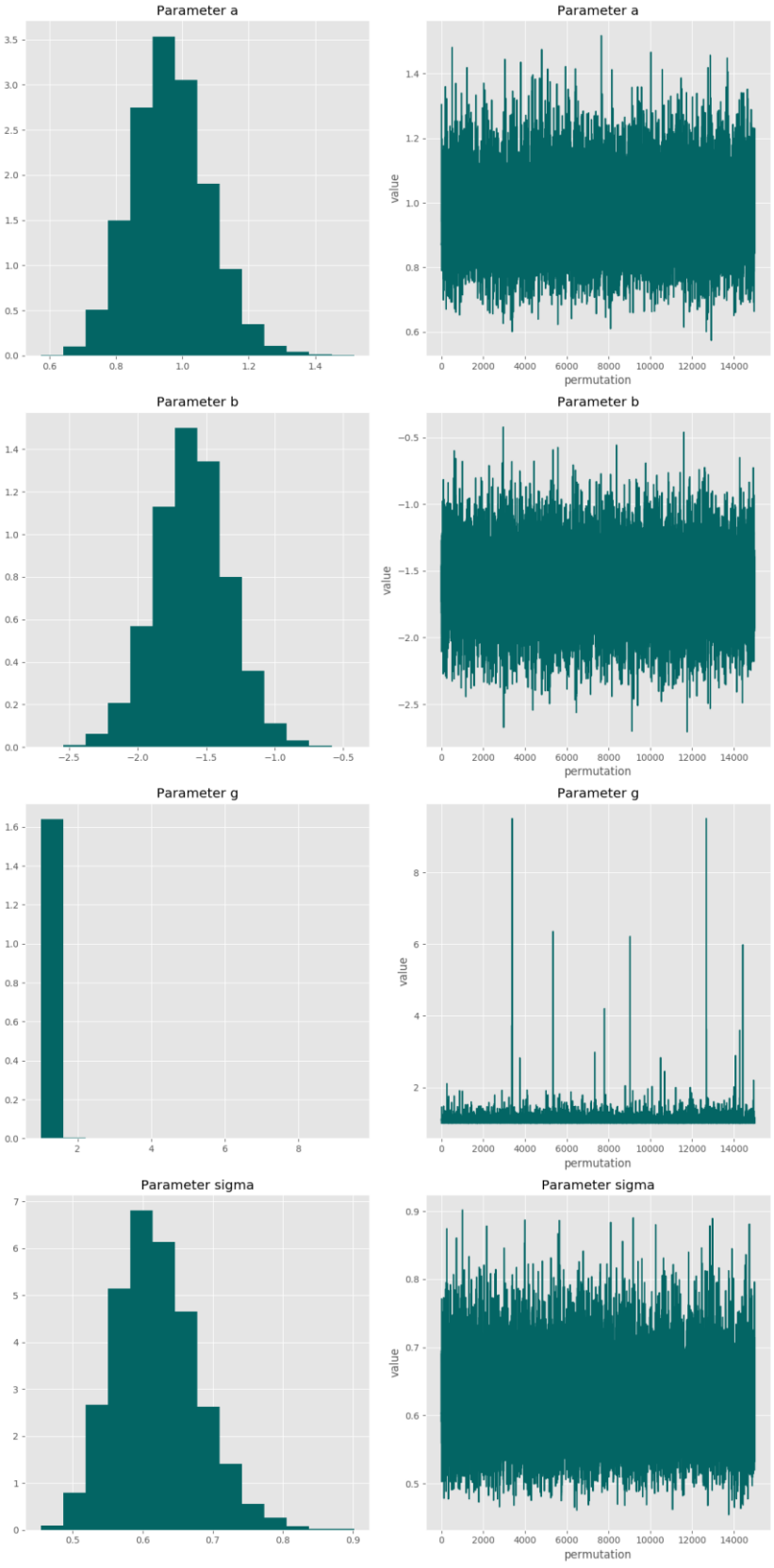

Exponential4

$$f(dose) = a \times [c - (c - 1) \times e^{-b \times dose}]$$

Model fit summary

```
Inference for Stan model: exponential4_individual_pkl_fa67b4bb1853dd3a882bdb66cdb5191d.
1 chains, each with iter=30000; warmup=15000; thin=1;
post-warmup draws per chain=15000, total post-warmup draws=15000.

        mean se_mean     sd   2.5%    25%    50%    75%  97.5%  n_eff   Rhat
a        2.5  2.4e-3   0.21   2.12   2.36   2.49   2.63   2.93   7481    1.0
b      20.77    0.02   2.09  16.92  19.34  20.69   22.1  25.18   9040    1.0
c       0.14  1.5e-4   0.01   0.11   0.13   0.14   0.15   0.17   7930    1.0
sigma   0.27  2.5e-4   0.03   0.22   0.25   0.27   0.28   0.32  10281    1.0
lp__   50.53    0.02   1.48  46.79   49.8  50.86  51.61  52.35   5957    1.0

Samples were drawn using NUTS at Mon Nov  4 20:05:36 2019.
For each parameter, n_eff is a crude measure of effective sample size,
and Rhat is the potential scale reduction factor on split chains (at
convergence, Rhat=1).
```

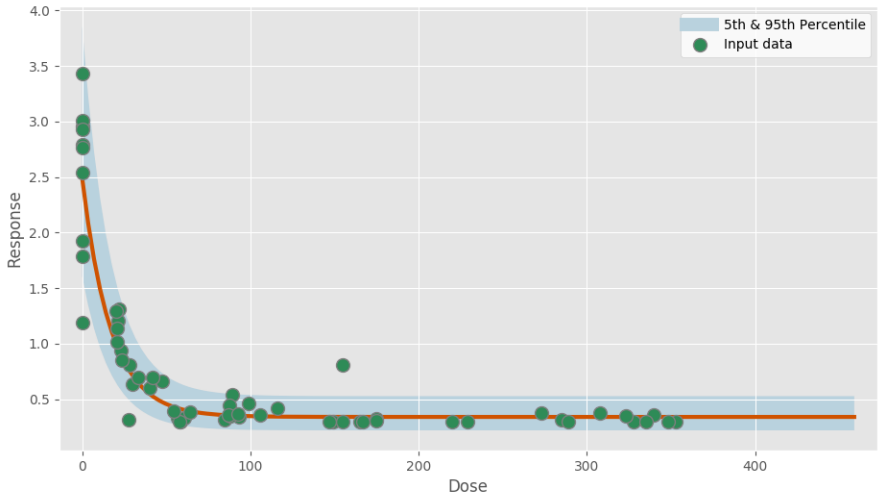

Posterior predictive p-value for model fit: 0.526

Model weight: 60.0%

Correlation matrix

	a	b	c	sigma
a	-	0.551	-0.839	0.020
b	0.551	-	-0.28	0.027
c	-0.839	-0.28	-	0.004
sigma	0.020	0.027	0.004	-

Parameter charts

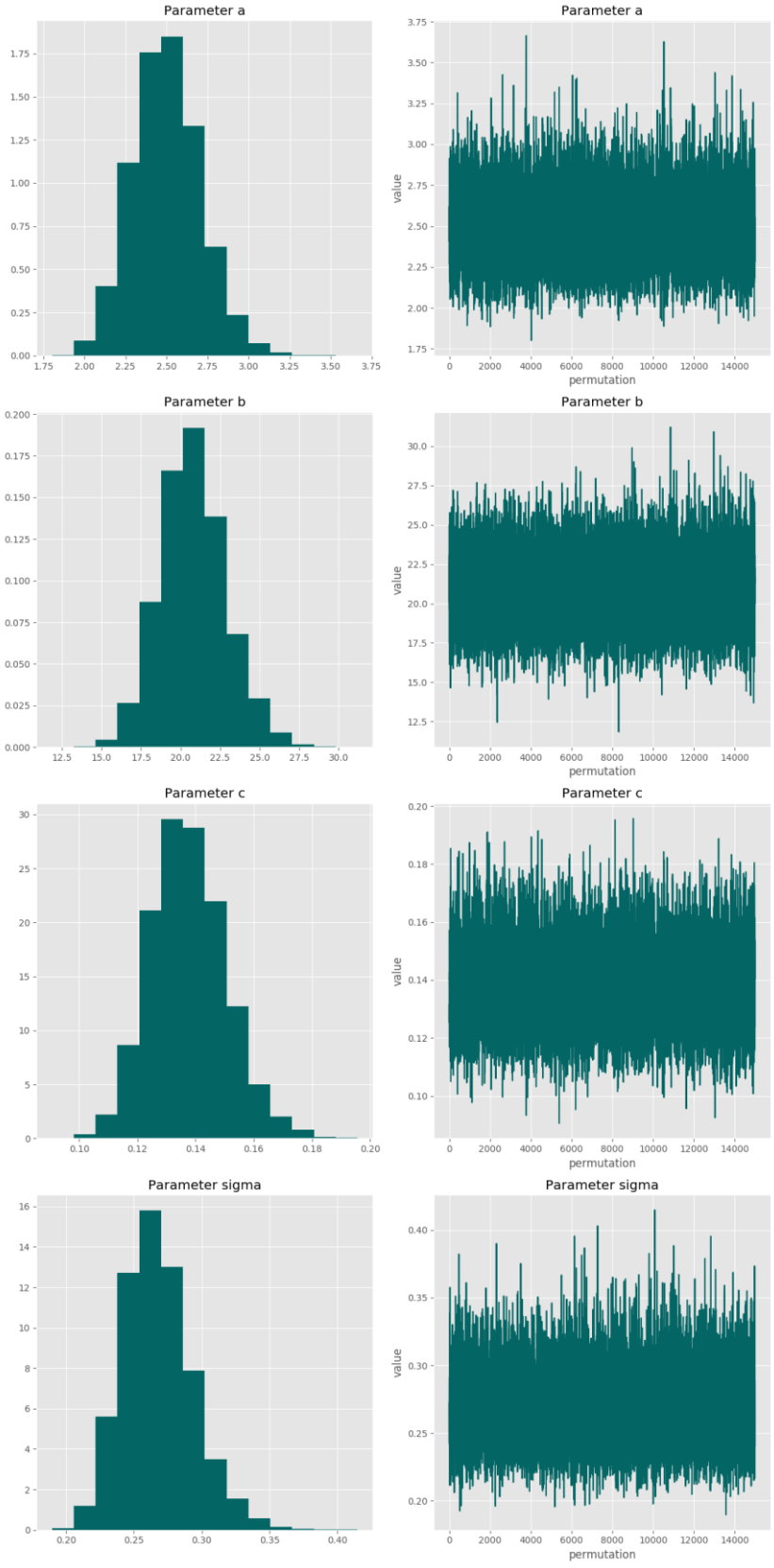

Exponential5

$$f(dose) = a \times [c - (c - 1) \times e^{-(b \times dose)^g}]$$

Power parameter lower-bound: 1.000

Model fit summary

```
Inference for Stan model: exponential5_individual_pkl_0fe35d8b796f8736b80743a2674317fc.
1 chains, each with iter=30000; warmup=15000; thin=1;
post-warmup draws per chain=15000, total post-warmup draws=15000.

        mean se_mean     sd   2.5%    25%    50%    75%  97.5%  n_eff   Rhat
a       2.44  2.5e-3   0.21   2.05    2.3   2.43   2.57   2.87   6694    1.0
b      18.08    0.02   2.06   14.6  16.62  17.91  19.36  22.59   7299    1.0
c       0.14  1.8e-4   0.01   0.12   0.14   0.14   0.15   0.18   6599    1.0
g       1.42  5.1e-3   0.46   1.02   1.17   1.33   1.54   2.42   7903    1.0
sigma   0.27  2.7e-4   0.03   0.22   0.25   0.27   0.28   0.32   9383    1.0
lp__   49.13    0.02   1.78  44.81  48.21  49.48  50.45   51.5   5146    1.0

Samples were drawn using NUTS at Mon Nov  4 20:05:49 2019.
For each parameter, n_eff is a crude measure of effective sample size,
and Rhat is the potential scale reduction factor on split chains (at
convergence, Rhat=1).
```

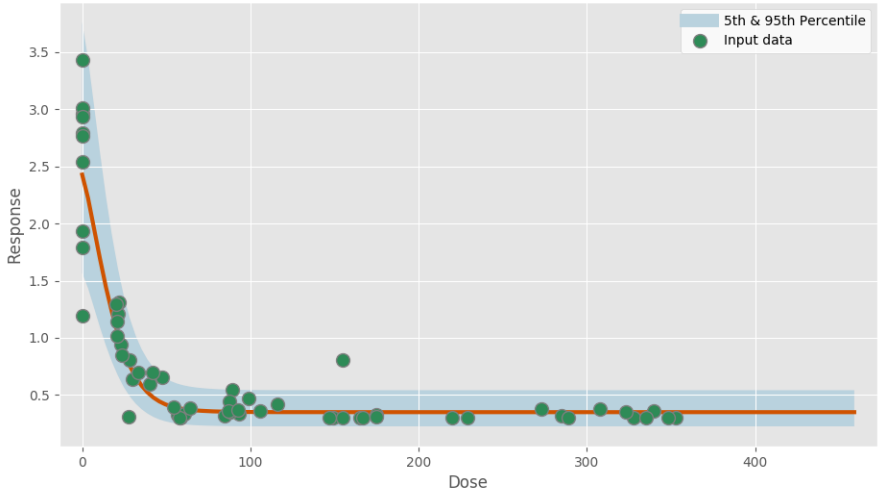

Posterior predictive p-value for model fit: 0.531

Model weight: 15.7%

Correlation matrix

	a	b	c	g	sigma
a	-	0.549	-0.853	-0.157	-0.0113
b	0.549	-	-0.443	-0.437	-0.0529
c	-0.853	-0.443	-	0.301	0.061
g	-0.157	-0.437	0.301	-	0.160

sigma	-0.0113	-0.0529	0.061	0.160	-

Parameter charts

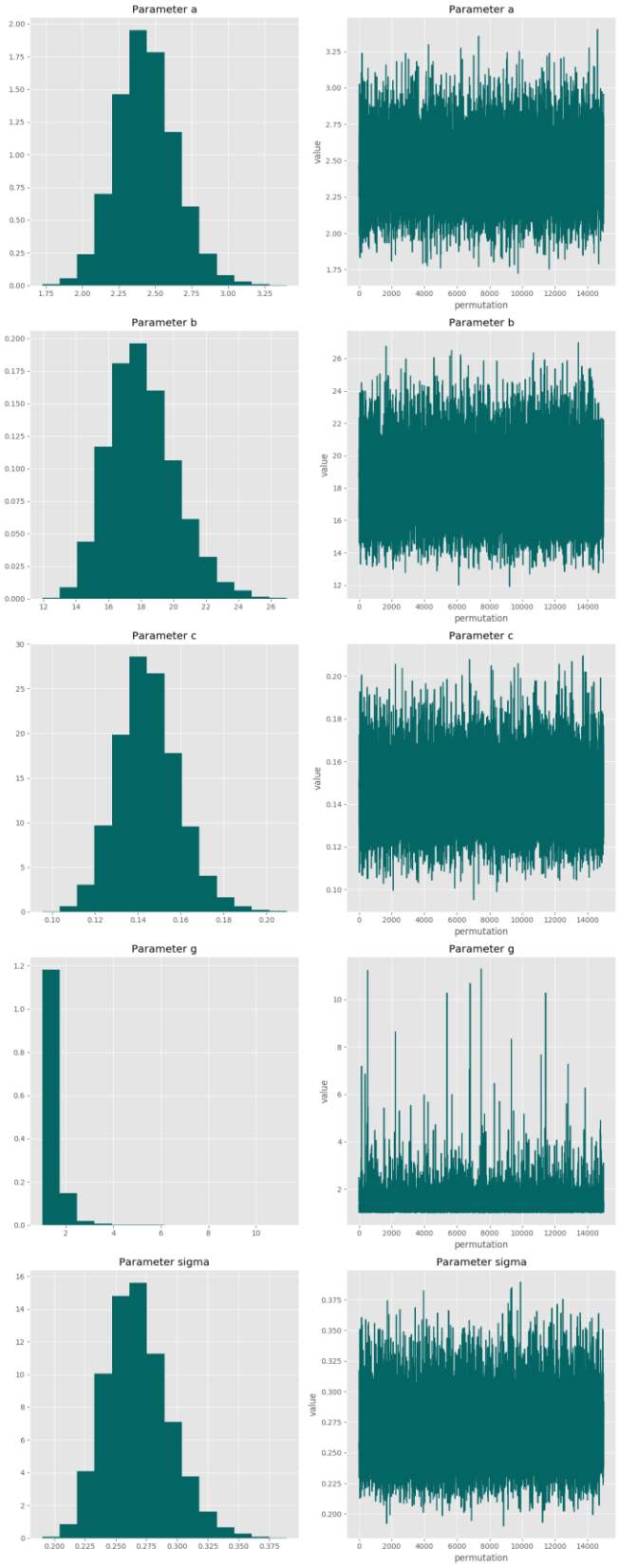

Hill

$$f(dose) = a + \frac{b \times dose^g}{c^g + dose^g}$$

Power parameter lower-bound: 1.000

Model fit summary

```
Inference for Stan model: hill_individual_pkl_f14f62088318f1a4663f986868dc9b40.
1 chains, each with iter=30000; warmup=15000; thin=1;
post-warmup draws per chain=15000, total post-warmup draws=15000.

        mean se_mean     sd   2.5%    25%    50%    75%  97.5%  n_eff   Rhat
a       2.44  2.8e-3    0.2   2.06    2.3   2.43   2.57   2.86   5290    1.0
b       -2.1  2.8e-3    0.2  -2.52  -2.23  -2.09  -1.96  -1.72   5318    1.0
c       0.05  8.1e-5 6.1e-3   0.04   0.04   0.05   0.05   0.06   5642    1.0
g       3.12    0.01   0.93    1.8   2.49   2.96   3.55   5.38   7022    1.0
sigma   0.27  3.0e-4   0.03   0.22   0.25   0.26   0.28   0.32   7684    1.0
lp__   47.65    0.03    1.7   43.5  46.76  48.01  48.91   49.9   4506    1.0

Samples were drawn using NUTS at Mon Nov  4 20:06:47 2019.
For each parameter, n_eff is a crude measure of effective sample size,
and Rhat is the potential scale reduction factor on split chains (at
convergence, Rhat=1).
```

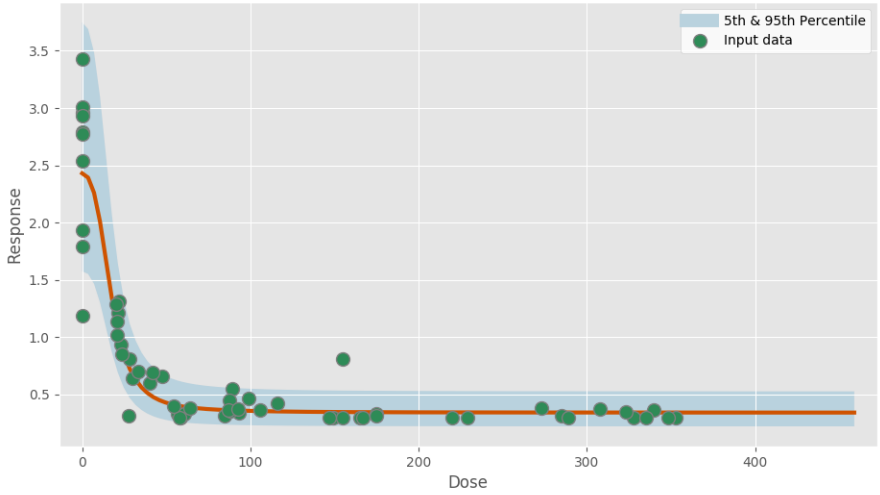

Posterior predictive p-value for model fit: 0.529

Model weight: 23.8%

Correlation matrix

	a	b	c	g	sigma
a	-	-0.995	-0.384	-0.0348	-0.0171
b	-0.995	-	0.416	0.092	0.020
c	-0.384	0.416	-	0.707	0.043
g	-0.0348	0.092	0.707	-	0.094

sigma	-0.0171	0.020	0.043	0.094	-

Parameter charts

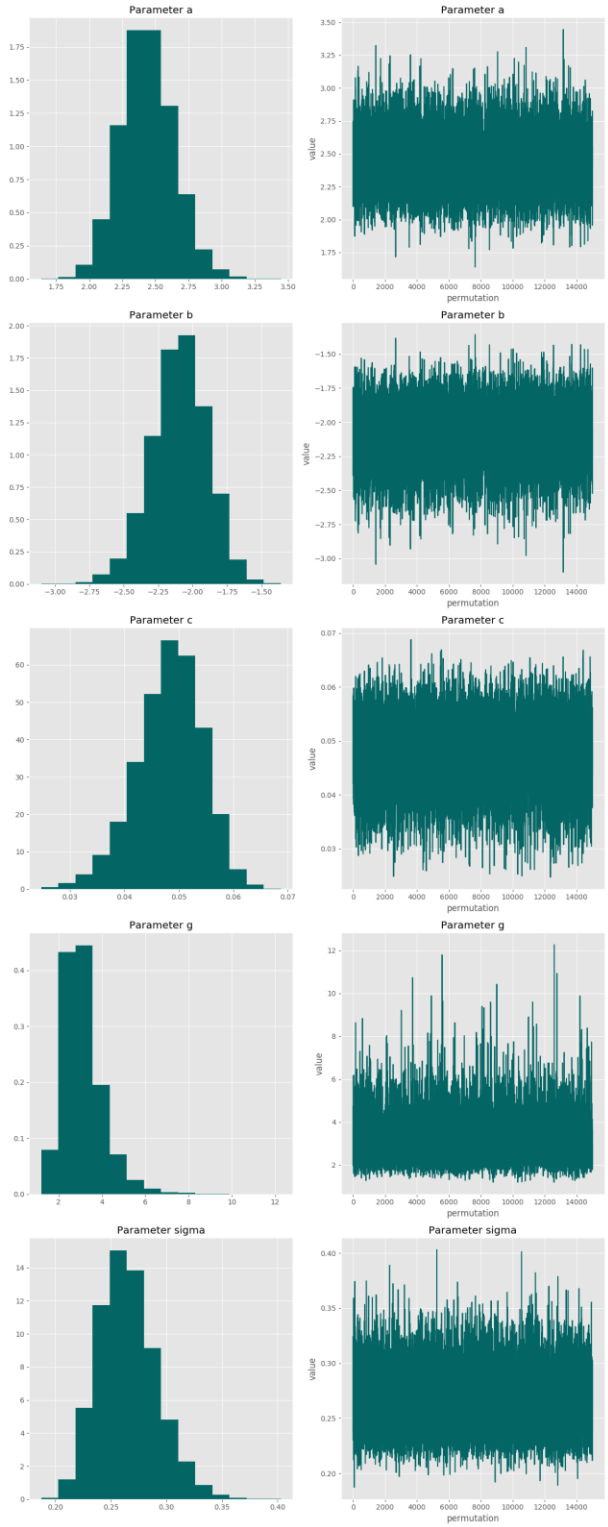

Power

$$f(dose) = a + b \times dose^{g}$$

Power parameter lower-bound: 1.000

Model fit summary

```
Inference for Stan model: power_individual_pkl_8682a4681cf39e692df770d4639a86e2.
1 chains, each with iter=30000; warmup=15000; thin=1;
post-warmup draws per chain=15000, total post-warmup draws=15000.

        mean se_mean     sd   2.5%    25%    50%    75%  97.5%  n_eff   Rhat
a       0.79  1.3e-3   0.09   0.62   0.73   0.78   0.84   0.96   4805    1.0
b      -0.55  1.8e-3   0.12  -0.77  -0.63  -0.55  -0.47   -0.3   4456    1.0
g       1.35    0.02   1.15    1.0   1.04   1.11   1.25   3.44   2253    1.0
sigma   0.68  8.4e-4   0.07   0.56   0.63   0.67   0.72   0.83   6384    1.0
lp__   -9.18    0.02   1.57 -13.01  -10.0  -8.81  -8.02  -7.22   4235    1.0

Samples were drawn using NUTS at Mon Nov  4 20:06:59 2019.
For each parameter, n_eff is a crude measure of effective sample size,
and Rhat is the potential scale reduction factor on split chains (at
convergence, Rhat=1).
```

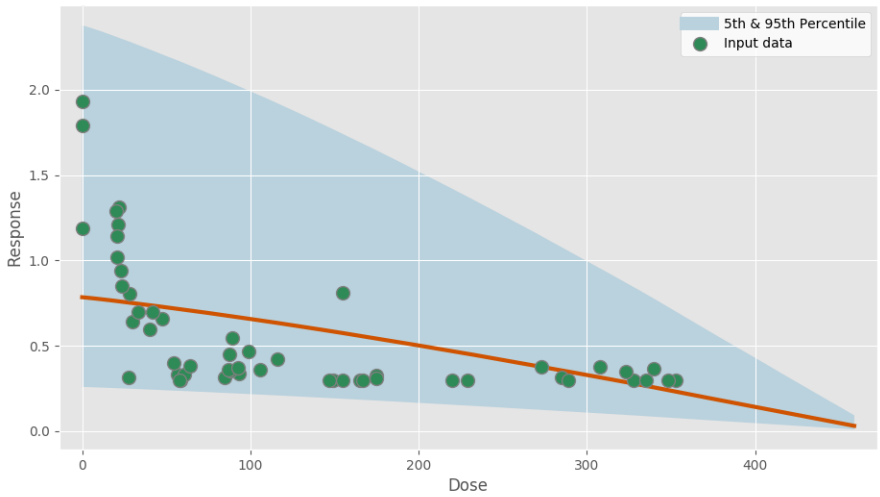

Posterior predictive p-value for model fit: 0.520

Model weight: 0.0%

Correlation matrix

	a	b	g	sigma
a	-	-0.84	-0.288	-0.0904
b	-0.84	-	0.263	0.116
g	-0.288	0.263	-	0.212
sigma	-0.0904	0.116	0.212	-

Parameter charts

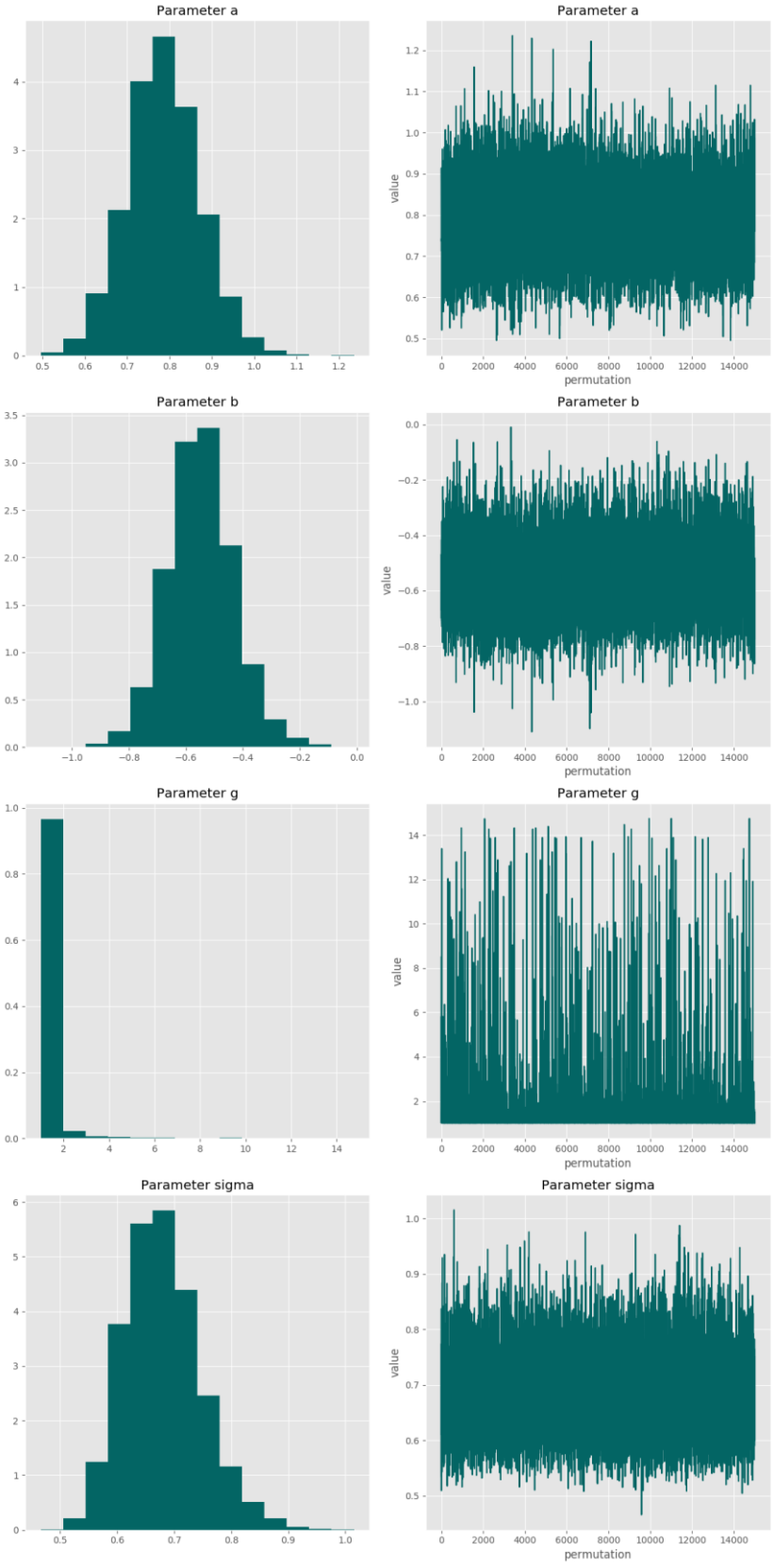

MichaelisMenten

$$f(dose) = a + \frac{b \times dose}{c + dose}$$

Model fit summary

```
Inference for Stan model:
michaelismenten_individual_pkl_8a1ee8a1062ea9c00f6bd83f5c89e8d5.
1 chains, each with iter=30000; warmup=15000; thin=1;
post-warmup draws per chain=15000, total post-warmup draws=15000.

        mean se_mean     sd    2.5%    25%    50%    75%  97.5%  n_eff   Rhat
a       2.48  3.7e-3   0.23    2.05   2.32   2.47   2.63   2.96   3854    1.0
b      -2.23  3.7e-3   0.23   -2.71  -2.38  -2.23  -2.07  -1.81   3940    1.0
c       0.02  6.0e-5 4.4e-3    0.01   0.02   0.02   0.02   0.03   5336    1.0
sigma   0.29  3.3e-4   0.03    0.24   0.27   0.29   0.31   0.36   7384    1.0
lp__   39.95    0.02   1.48   36.18  39.22  40.29  41.04   41.8   5166    1.0

Samples were drawn using NUTS at Mon Nov  4 20:07:23 2019.
For each parameter, n_eff is a crude measure of effective sample size,
and Rhat is the potential scale reduction factor on split chains (at
convergence, Rhat=1).
```

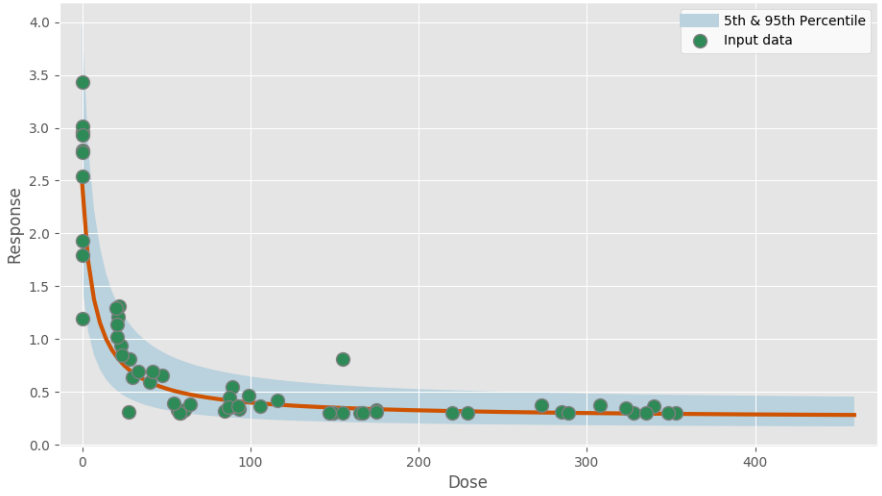

Posterior predictive p-value for model fit: 0.519

Model weight: 0.5%

Correlation matrix

	a	b	c	sigma
a	-	-0.994	-0.611	-0.00306
b	-0.994	-	0.544	0.004
c	-0.611	0.544	-	0.022
sigma	-0.00306	0.004	0.022	-

Parameter charts

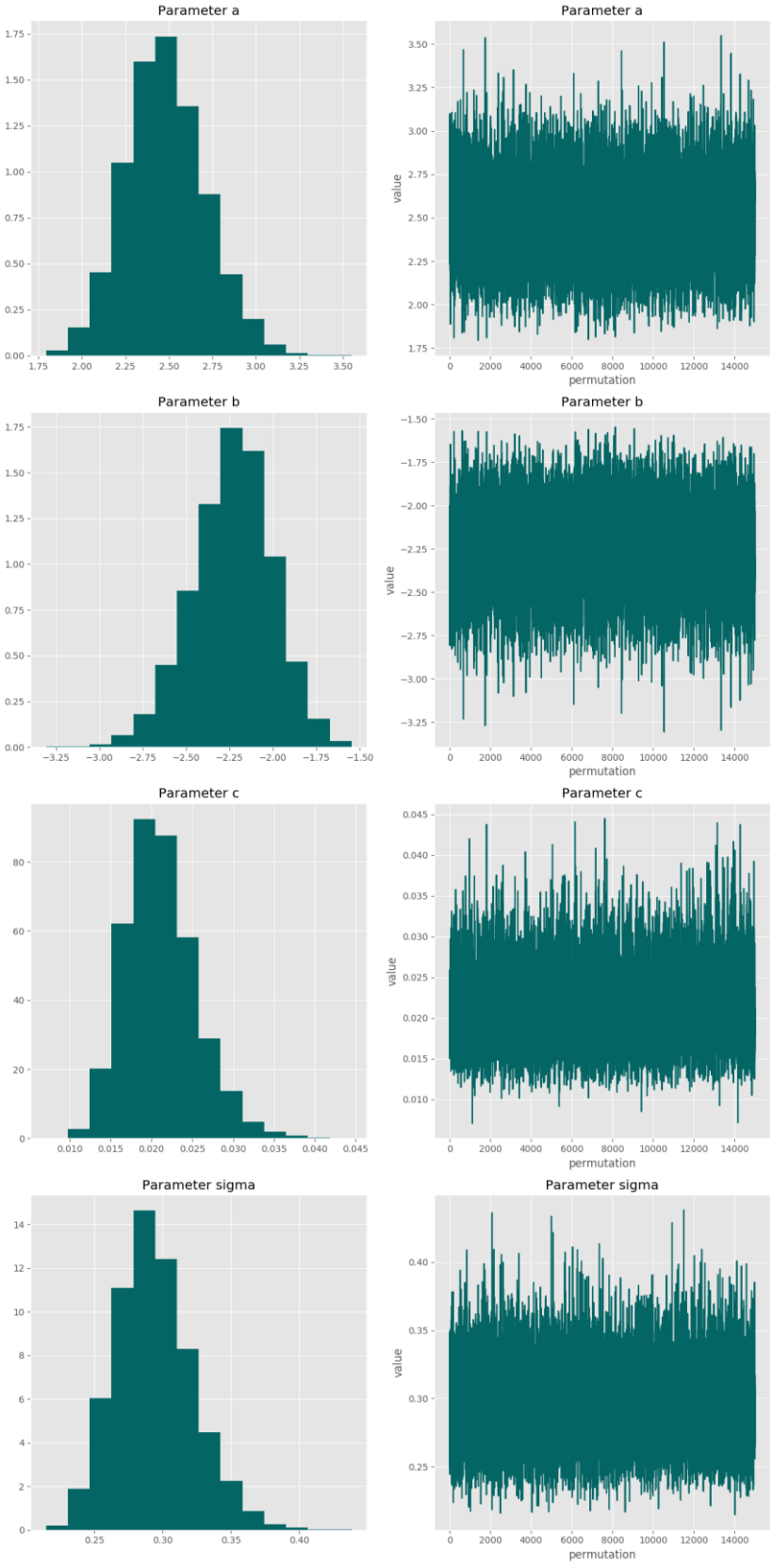

Linear

$$f(dose) = a + b \times dose$$

Model fit summary

```
Inference for Stan model: linear_individual_pkl_6f560bd3666c0b0a5c004ccddf0ad3ca.
1 chains, each with iter=30000; warmup=15000; thin=1;
post-warmup draws per chain=15000, total post-warmup draws=15000.

        mean se_mean     sd   2.5%    25%    50%    75%  97.5%  n_eff   Rhat
a       0.82  1.1e-3   0.08   0.67   0.76   0.81   0.87   0.99   6047    1.0
b      -0.59  1.4e-3   0.11   -0.8  -0.66  -0.59  -0.51  -0.37   5798    1.0
sigma   0.66  7.8e-4   0.06   0.55   0.62   0.66    0.7    0.8   6711    1.0
lp__   -5.29    0.02   1.29  -8.63  -5.86  -4.97  -4.36  -3.83   5013    1.0

Samples were drawn using NUTS at Mon Nov  4 20:07:31 2019.
For each parameter, n_eff is a crude measure of effective sample size,
and Rhat is the potential scale reduction factor on split chains (at
convergence, Rhat=1).
```

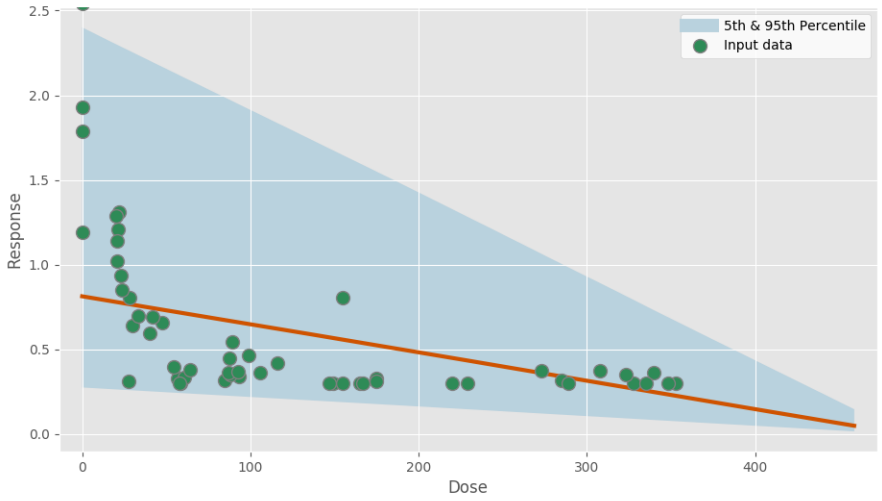

Posterior predictive p-value for model fit: 0.518

Model weight: 0.0%

Correlation matrix

	a	b	sigma
a	-	-0.862	0.017
b	-0.862	-	0.009
sigma	0.017	0.009	-

Parameter charts

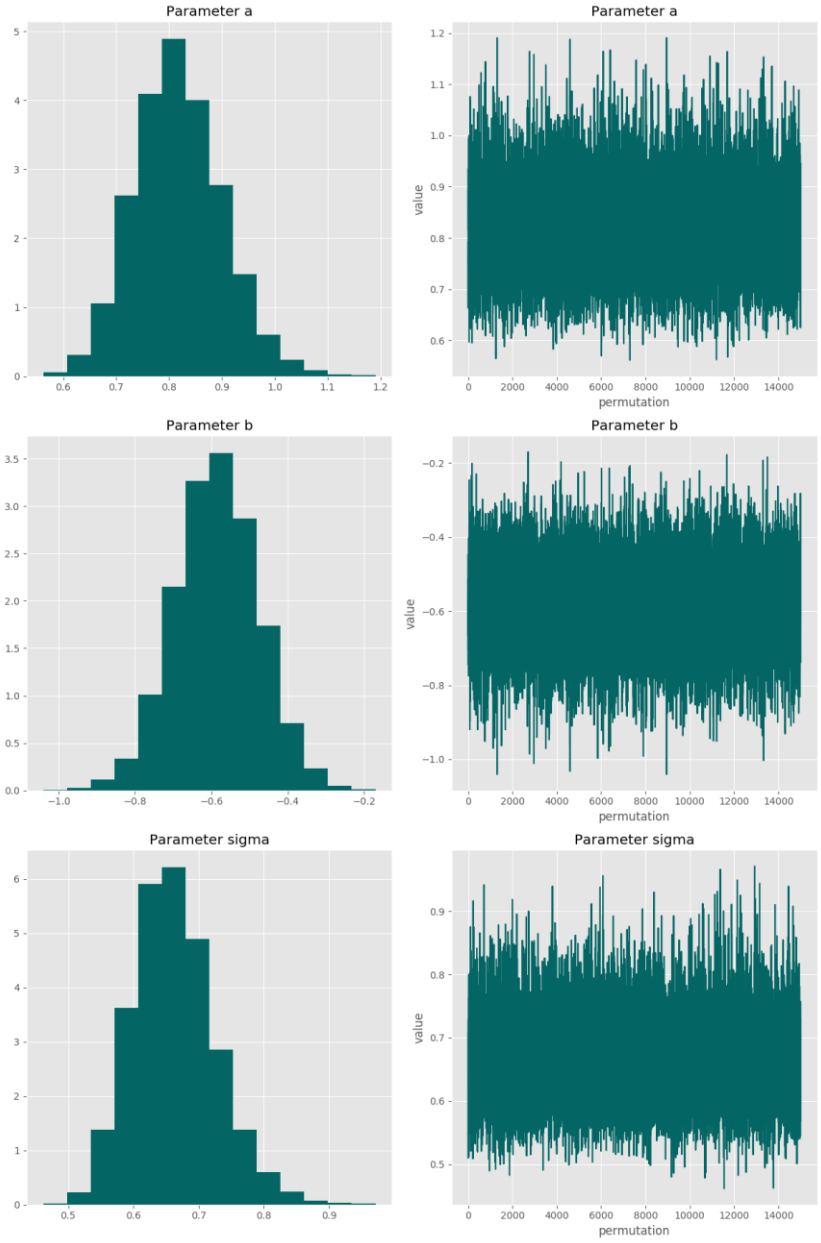

PFNA fT4 male Nov 4 2019

Report created on Nov 04, 2019 at 08:25 PM.

Pystan model version 2.19.0.0.

Dataset

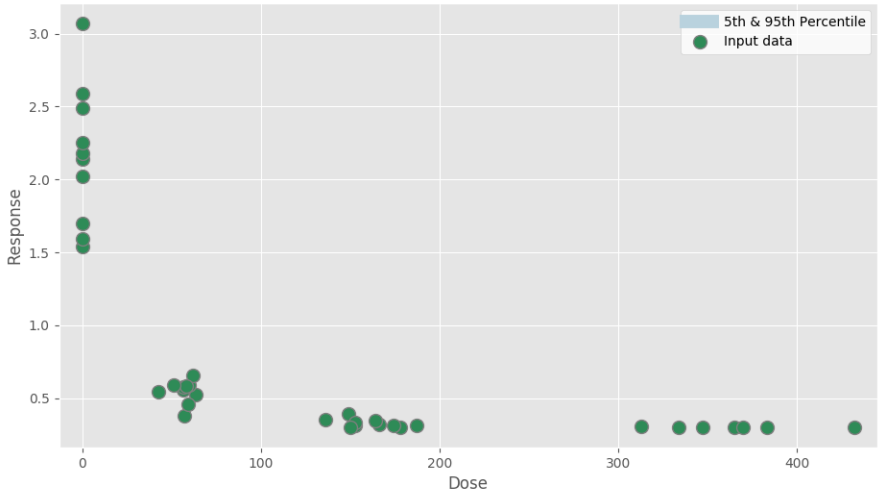

Dose	Response
0.05	2.02
0.03	2.14
0.05	2.59
0.04	3.07
0.04	2.49
0.05	1.54
0.04	2.18
0.05	2.25
0.04	1.7
0.16	1.59
63.4	0.526
57.0	0.382
56.8	0.557
60.0	0.588
59.1	0.457
62.0	0.658
56.8	0.577
58.1	0.583
42.6	0.546
51.5	0.59
153.0	0.311
178.0	0.3

149.0	0.39
136.0	0.354
166.0	0.319
153.0	0.334
174.0	0.312
187.0	0.314
164.0	0.346
150.0	0.3
383.0	0.3
432.0	0.3
313.0	0.309
334.0	0.3
365.0	0.302
347.0	0.3
370.0	0.3

20 % Central tendency: Relative

BMR: None

Adversity value: 0.200

BMD summary tables:

Statistic	Model average	Exponential2	Exponential3	Exponential4	Exponential5	Hill	Power	Michaelis Menten	Linear
Prior model weight	N/A	0.125	0.125	0.125	0.125	0.125	0.125	0.125	0.125
Posterior model weight	N/A	1.86e-20	1.34e-21	0.327	0.041	0.142	3.53e-24	0.491	6e-23
BMD (median)	5.632	47.838	55.802	7.318	9.164	9.428	138.789	2.991	109.721
BMDL (5th percentile)	4.646	38.157	41.626	6.428	7.128	3.743	105.348	2.288	96.184
25th percentile	5.169	43.387	48.812	6.941	8.054	6.441	119.619	2.693	102.860
Mean (SD)	5.701 (0.724)	48.996 (8.201)	59.617 (18.983)	7.340 (0.585)	9.908 (2.641)	10.032 (4.609)	165.459 (98.994)	3.016 (0.475)	114.611 (37.412)
75th percentile	6.157	53.205	65.276	7.703	10.989	12.890	178.129	3.308	119.573
95th percentile	7.027	63.773	89.360	8.331	15.271	18.569	337.493	3.831	144.697

BMD estimates

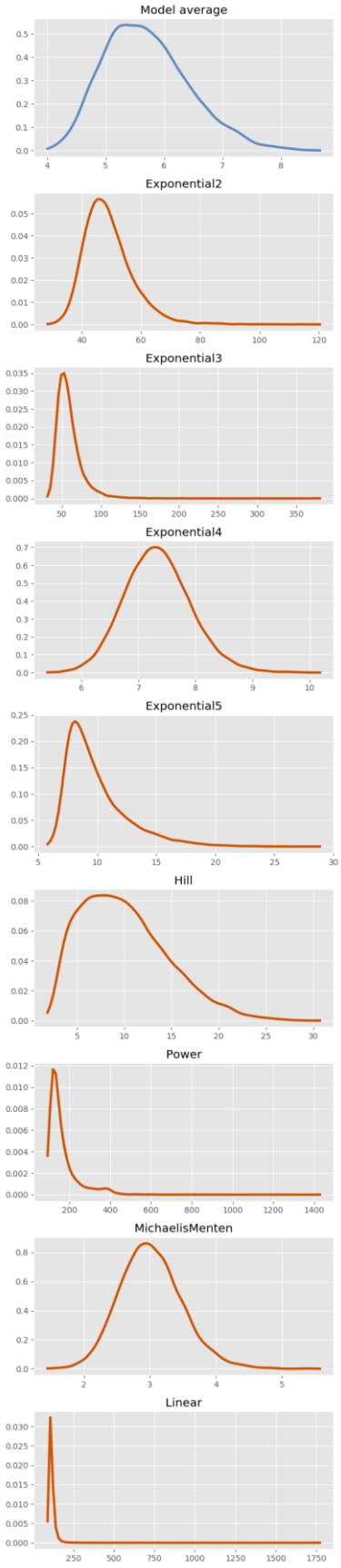
Model average
Exponential2
Exponential3
Exponential4
Exponential5
Hill
Power
MichaelisMenten
Linear

BMD results

50% Central tendency: Relative

BMR: None

Adversity value: 0.500

BMD summary tables:

Statistic	Model average	Exponential2	Exponential3	Exponential4	Exponential5	Hill	Power	Michaelis Menten	Linear
Prior model weight	N/A	0.125	0.125	0.125	0.125	0.125	0.125	0.125	0.125
Posterior model weight	N/A	1.86e-20	1.34e-21	0.327	0.041	0.142	3.53e-24	0.491	6e-23
BMD (median)	18.832	148.597	162.825	24.194	26.791	23.078	304.353	13.235	274.303
BMDL (5th percentile)	16.587	118.527	125.726	21.235	22.708	14.247	253.825	10.196	240.460
25th percentile	17.897	134.771	145.258	22.940	24.927	19.027	277.399	11.946	257.151
Mean (SD)	18.870 (1.426)	152.194 (25.474)	168.364 (34.277)	24.283 (1.965)	27.257 (3.277)	23.142 (5.570)	323.564 (134.570)	13.348 (2.049)	286.528 (93.530)
75th percentile	19.806	165.271	184.174	25.506	29.117	27.003	347.703	14.615	298.933
95th percentile	21.257	198.096	230.331	27.627	33.431	32.575	434.451	16.877	361.743

BMD estimates

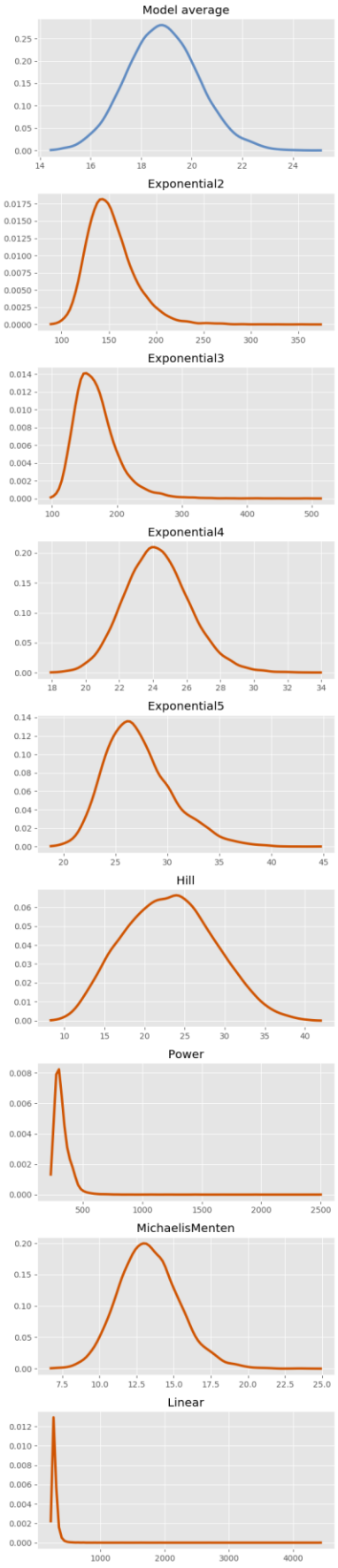
Model average
Exponential2
Exponential3
Exponential4
Exponential5
Hill
Power
MichaelisMenten
Linear

BMD Markov chain Monte Carlo settings

Iterations: 30,000

Number of chains: 1

Warmup fraction: 0.5

Seed: 62,882

Model results

Exponential2

$$f(dose) = a \times e^{b \times dose}$$

Model fit summary

```
Inference for Stan model: exponential2_individual_pkl_be58f7567ba64ec5547642f54ef3b89e.
1 chains, each with iter=30000; warmup=15000; thin=1;
post-warmup draws per chain=15000, total post-warmup draws=15000.

        mean se_mean     sd   2.5%    25%    50%    75%  97.5%  n_eff   Rhat
a       1.13  1.8e-3   0.15   0.87   1.02   1.12   1.22   1.45   6682    1.0
b      -2.02  3.8e-3   0.31  -2.64  -2.22  -2.02  -1.81  -1.42   6680    1.0
sigma   0.56  7.3e-4   0.07   0.45   0.51   0.56   0.61   0.73   9504    1.0
lp__    2.87    0.02   1.28  -0.44   2.29    3.2   3.81   4.33   5453    1.0

Samples were drawn using NUTS at Mon Nov  4 20:17:41 2019.
For each parameter, n_eff is a crude measure of effective sample size,
and Rhat is the potential scale reduction factor on split chains (at
convergence, Rhat=1).
```

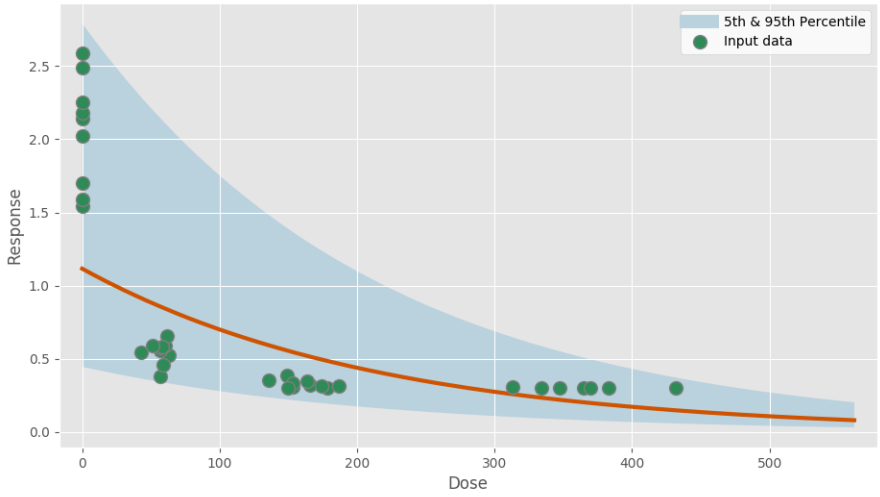

Posterior predictive p-value for model fit: 0.526

Model weight: 0.0%

Correlation matrix

	a	b	sigma
a	-	-0.703	0.089
b	-0.703	-	-0.0474
sigma	0.089	-0.0474	-

Parameter charts

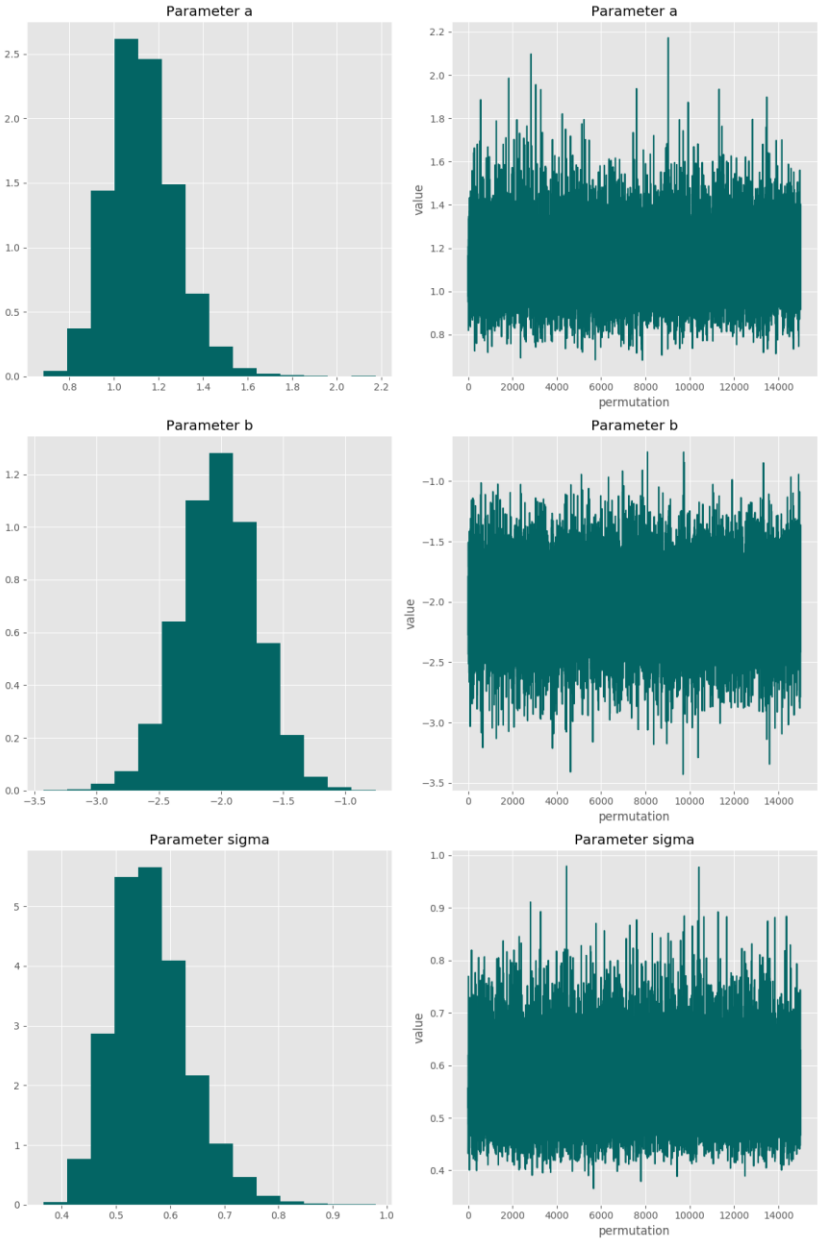

Exponential3

$$f(dose) = a \times e^{b \times dose^{g}}$$

Power parameter lower-bound: 1.000

Model fit summary

```
Inference for Stan model: exponential3_individual_pkl_df53333b36693dd0ad892f92a4fc7532.
1 chains, each with iter=30000; warmup=15000; thin=1;
post-warmup draws per chain=15000, total post-warmup draws=15000.

        mean se_mean     sd   2.5%    25%    50%    75%  97.5%  n_eff   Rhat
a       1.08  1.7e-3   0.15   0.81   0.98   1.07   1.18   1.41   8503    1.0
b      -1.97  3.6e-3   0.33  -2.61  -2.19  -1.97  -1.75  -1.31   8475    1.0
g       1.09  3.8e-3   0.25    1.0   1.02   1.05   1.11   1.36   4365    1.0
sigma   0.58  7.4e-4   0.08   0.46   0.53   0.58   0.63   0.75  10361    1.0
lp__   -1.59    0.02   1.52  -5.36  -2.36  -1.25  -0.47   0.31   5942    1.0

Samples were drawn using NUTS at Mon Nov  4 20:17:49 2019.
For each parameter, n_eff is a crude measure of effective sample size,
and Rhat is the potential scale reduction factor on split chains (at
convergence, Rhat=1).
```

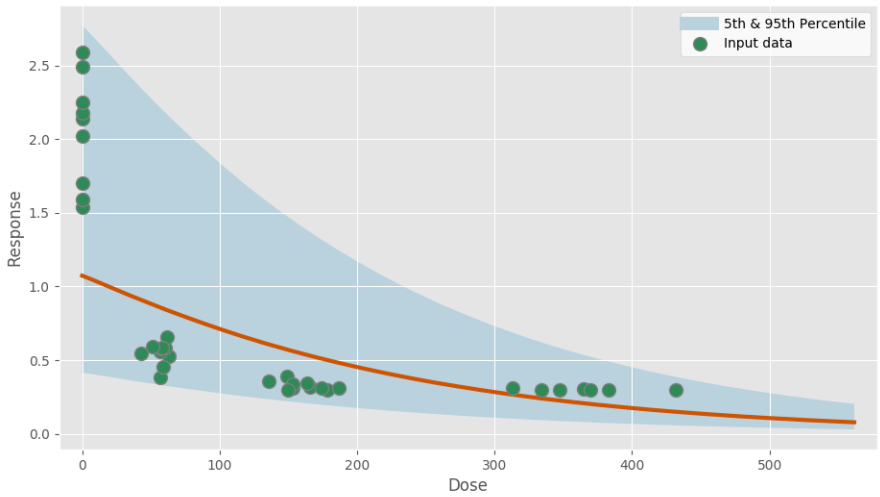

Posterior predictive p-value for model fit: 0.522

Model weight: 0.0%

Correlation matrix

	a	b	g	sigma
a	-	-0.689	-0.197	-0.048
b	-0.689	-	0.127	0.039
g	-0.197	0.127	-	0.188
sigma	-0.048	0.039	0.188	-

Parameter charts

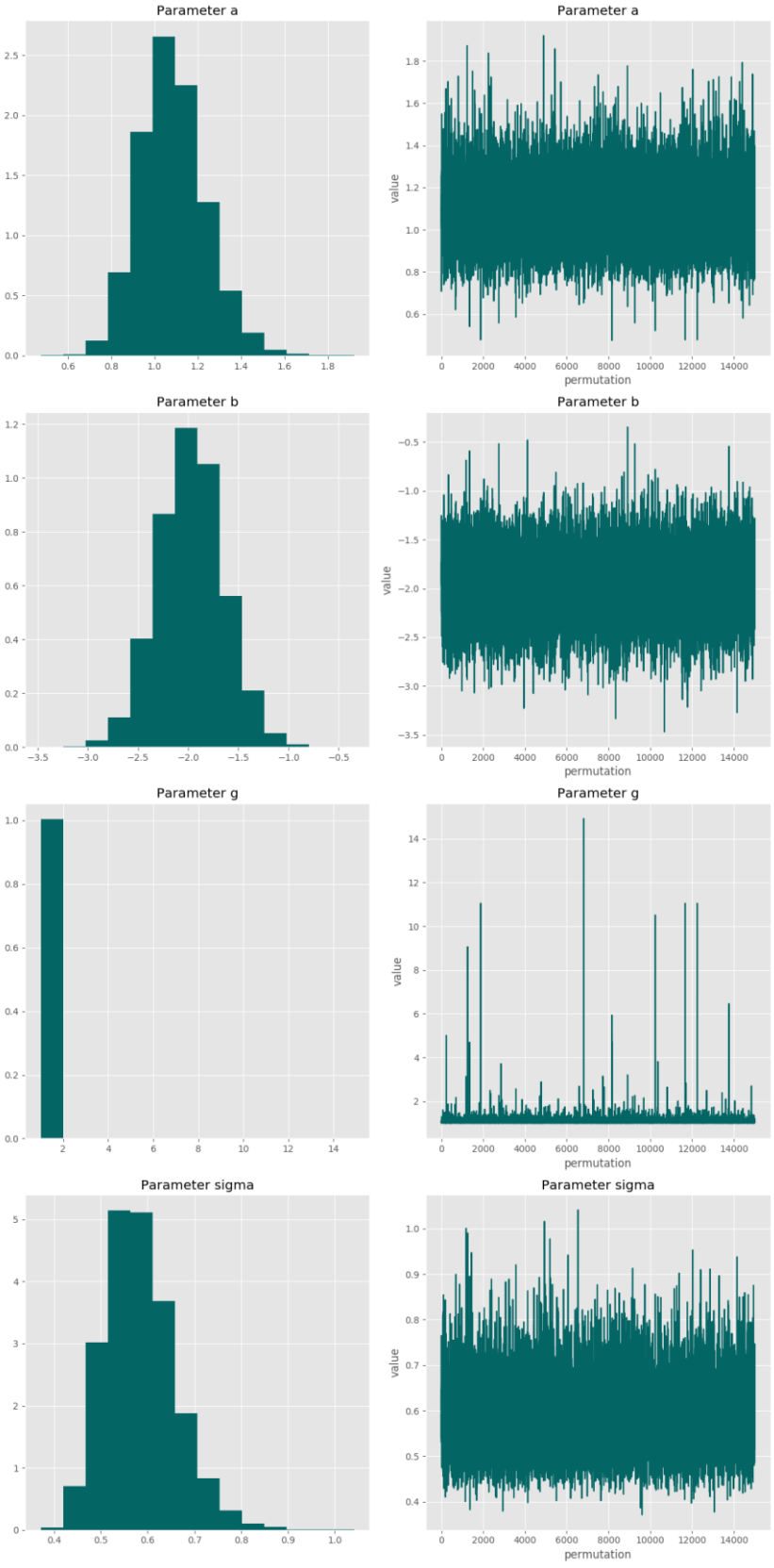

Exponential4

$$f(dose) = a \times [c - (c - 1) \times e^{-b \times dose}]$$

Model fit summary

```
Inference for Stan model: exponential4_individual_pkl_fa67b4bb1853dd3a882bdb66cdb5191d.
1 chains, each with iter=30000; warmup=15000; thin=1;
post-warmup draws per chain=15000, total post-warmup draws=15000.

        mean se_mean     sd   2.5%    25%    50%    75%  97.5%  n_eff   Rhat
a        2.1  1.3e-3   0.11    1.9   2.03    2.1   2.17   2.33   7233    1.0
b      15.89    0.01   1.24  13.58  15.05  15.83  16.68   18.5   9499    1.0
c       0.15  1.1e-4 9.8e-3   0.13   0.14   0.15   0.16   0.17   8186    1.0
sigma   0.16  2.0e-4   0.02   0.13   0.15   0.16   0.17   0.21  10069    1.0
lp__   49.59    0.02    1.5  45.81  48.84  49.93  50.69  51.48   5790    1.0

Samples were drawn using NUTS at Mon Nov  4 20:17:57 2019.
For each parameter, n_eff is a crude measure of effective sample size,
and Rhat is the potential scale reduction factor on split chains (at
convergence, Rhat=1).
```

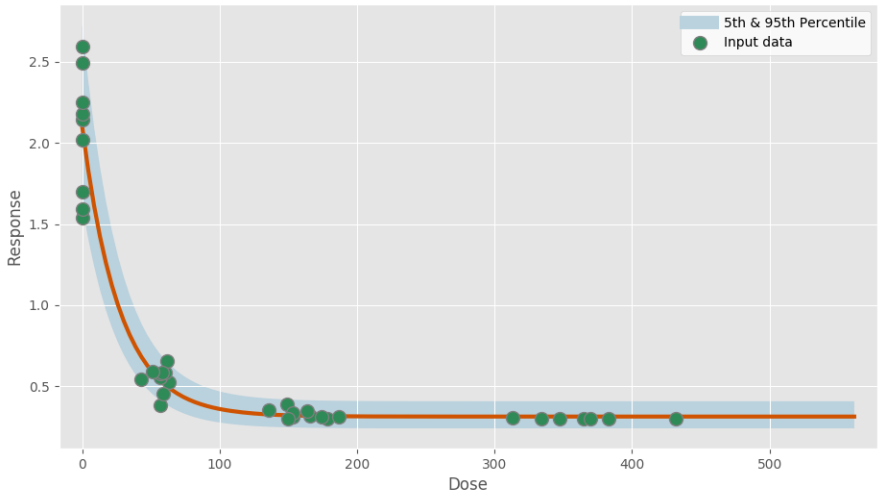

Posterior predictive p-value for model fit: 0.526

Model weight: 32.7%

Correlation matrix

	a	b	c	sigma
a	-	0.403	-0.758	-0.00668
b	0.403	-	-0.0194	0.026
c	-0.758	-0.0194	-	0.034
sigma	-0.00668	0.026	0.034	-

Parameter charts

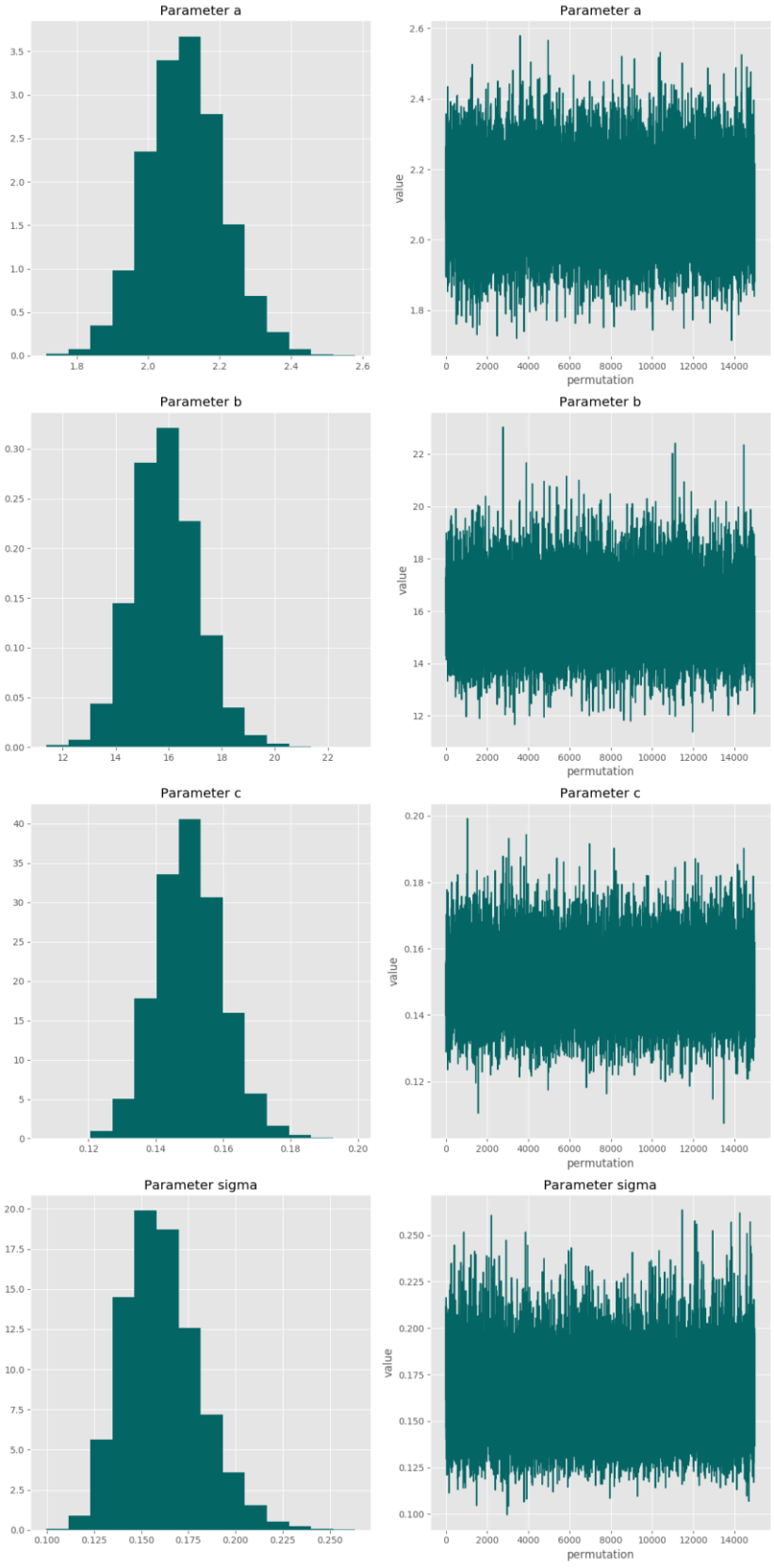

Exponential5

$$f(dose) = a \times [c - (c - 1) \times e^{-(b \times dose)^g}]$$

Power parameter lower-bound: 1.000

Model fit summary

```
Inference for Stan model: exponential5_individual_pkl_0fe35d8b796f8736b80743a2674317fc.
1 chains, each with iter=30000; warmup=15000; thin=1;
post-warmup draws per chain=15000, total post-warmup draws=15000.

        mean se_mean     sd   2.5%    25%    50%    75%  97.5%  n_eff   Rhat
a        2.1  1.3e-3   0.11   1.89   2.02    2.1   2.17   2.33   6946    1.0
b      14.51    0.02   1.49   11.6  13.51  14.53  15.52  17.41   6025    1.0
c       0.15  1.2e-4   0.01   0.13   0.14   0.15   0.16   0.17   7077    1.0
g       1.18  2.6e-3   0.19    1.0   1.05   1.12   1.25   1.69   5384    1.0
sigma   0.17  2.2e-4   0.02   0.13   0.15   0.16   0.18   0.21   9499    1.0
lp__   46.27    0.02   1.69  42.22  45.39  46.62  47.52  48.51   5395    1.0

Samples were drawn using NUTS at Mon Nov  4 20:18:09 2019.
For each parameter, n_eff is a crude measure of effective sample size,
and Rhat is the potential scale reduction factor on split chains (at
convergence, Rhat=1).
```

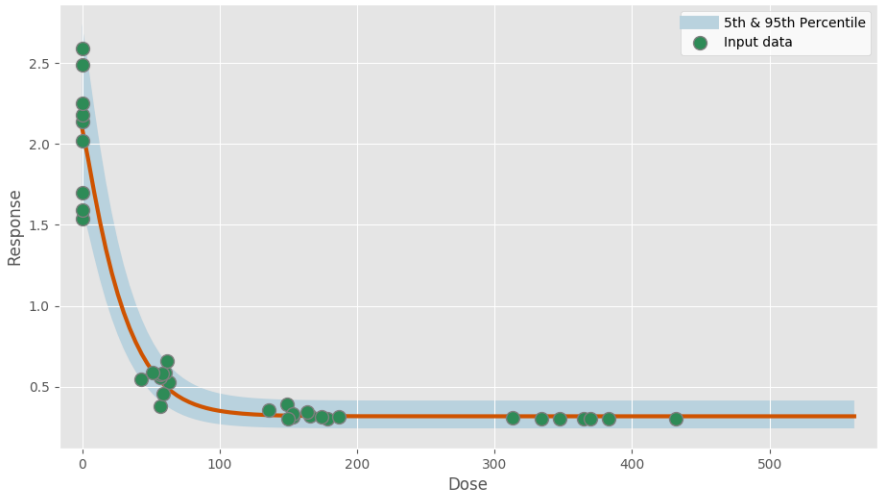

Posterior predictive p-value for model fit: 0.525

Model weight: 4.1%

Correlation matrix

	a	b	c	g	sigma
a	-	0.301	-0.774	-0.0522	0.010
b	0.301	-	-0.128	-0.71	-0.127
c	-0.774	-0.128	-	0.125	0.033
g	-0.0522	-0.71	0.125	-	0.210

sigma	0.010	-0.127	0.033	0.210	-

Parameter charts

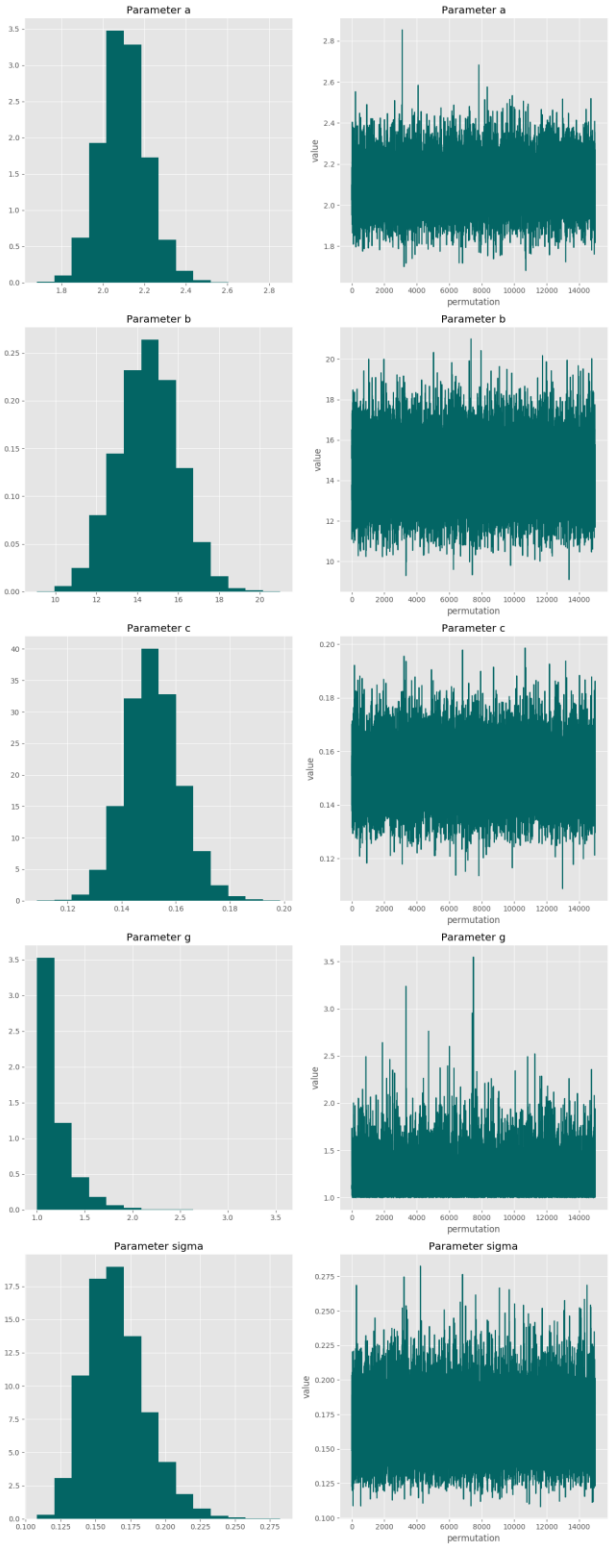

Hill

$$f(dose) = a + \frac{b \times dose^g}{c^g + dose^g}$$

Power parameter lower-bound: 1.000

Model fit summary

```
Inference for Stan model: hill_individual_pkl_f14f62088318f1a4663f986868dc9b40.
1 chains, each with iter=30000; warmup=15000; thin=1;
post-warmup draws per chain=15000, total post-warmup draws=15000.

        mean se_mean     sd   2.5%    25%    50%    75%  97.5%  n_eff   Rhat
a       2.11  1.4e-3   0.11   1.91   2.04   2.11   2.18   2.33   5921    1.0
b      -1.83  1.5e-3   0.11  -2.05   -1.9  -1.83  -1.75  -1.62   5492    1.0
c       0.04  1.8e-4   0.01   0.02   0.04   0.04   0.05   0.07   4504    1.0
g       1.79  7.6e-3   0.54   1.06   1.39    1.7   2.08   3.09   5077    1.0
sigma   0.16  2.4e-4   0.02   0.12   0.14   0.16   0.17   0.21   7839    1.0
lp__   45.63    0.03   1.85  41.04  44.66  45.99   47.0  48.09   3436    1.0

Samples were drawn using NUTS at Mon Nov  4 20:18:39 2019.
For each parameter, n_eff is a crude measure of effective sample size,
and Rhat is the potential scale reduction factor on split chains (at
convergence, Rhat=1).
```

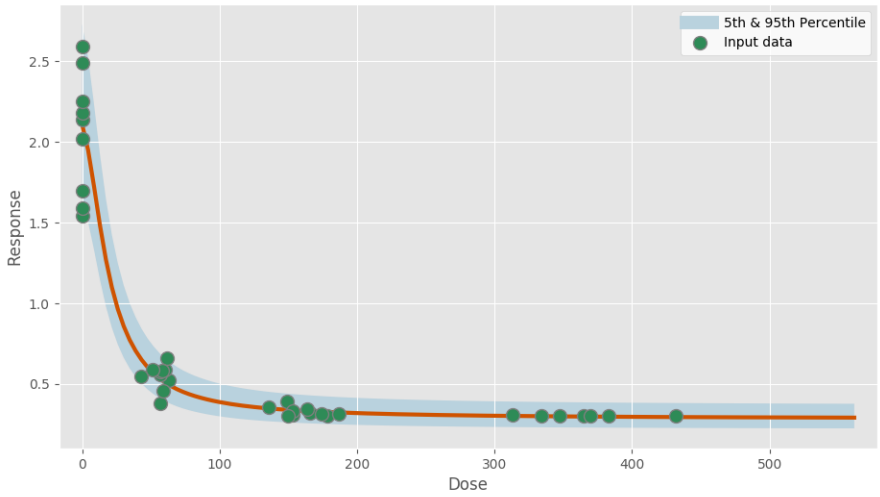

Posterior predictive p-value for model fit: 0.534

Model weight: 14.2%

Correlation matrix

	a	b	c	g	sigma
a	-	-0.974	-0.185	-0.0407	0.018
b	-0.974	-	0.314	0.205	-0.00325
c	-0.185	0.314	-	0.918	0.087
g	-0.0407	0.205	0.918	-	0.118

sigma	0.018	-0.00325	0.087	0.118	-

Parameter charts

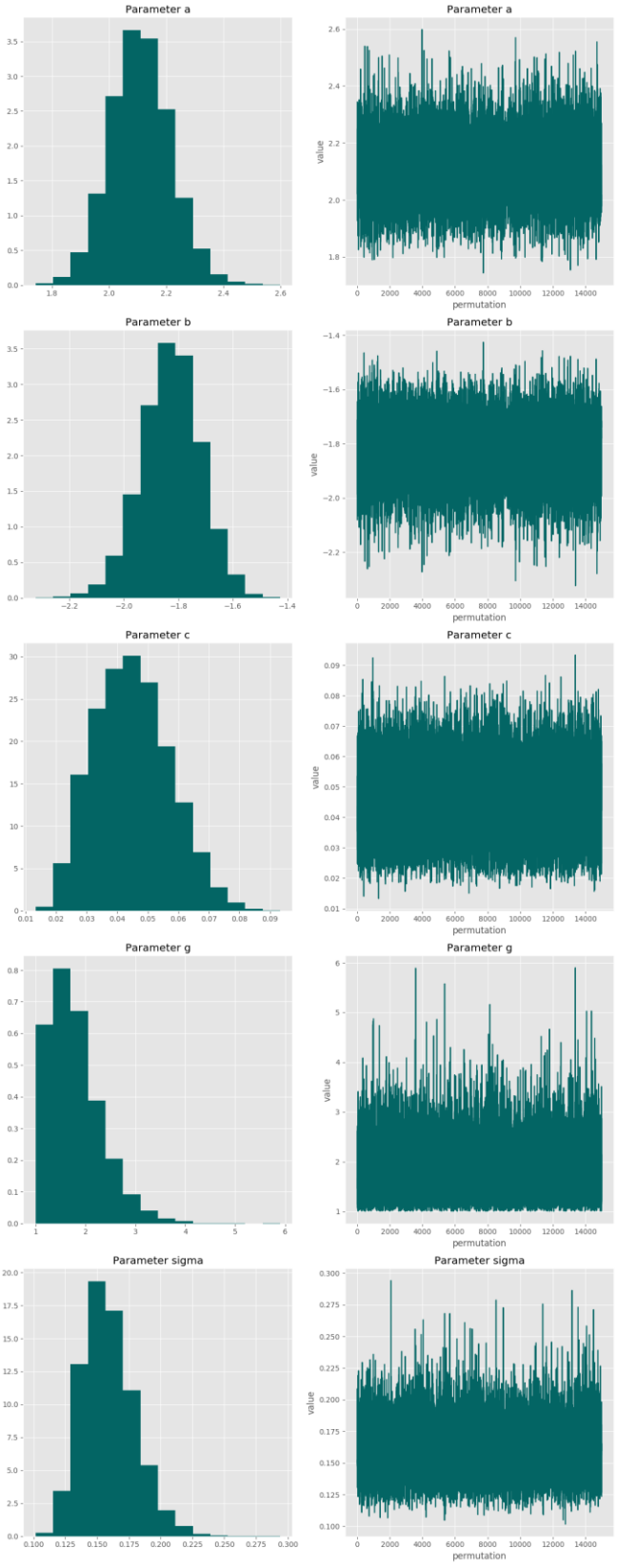

Power

$$f(dose) = a + b \times dose^{g}$$

Power parameter lower-bound: 1.000

Model fit summary

```
Inference for Stan model: power_individual_pkl_8682a4681cf39e692df770d4639a86e2.
1 chains, each with iter=30000; warmup=15000; thin=1;
post-warmup draws per chain=15000, total post-warmup draws=15000.

        mean se_mean     sd   2.5%    25%    50%    75%  97.5%  n_eff   Rhat
a       0.82  1.9e-3   0.12    0.6   0.74   0.82    0.9   1.07   3688   1.01
b      -0.62  3.4e-3   0.16  -0.91  -0.72  -0.63  -0.52  -0.26   2346   1.01
g       1.62    0.05   1.63   1.01   1.06   1.16    1.4   6.71   1270   1.01
sigma   0.69  1.4e-3   0.09   0.54   0.63   0.68   0.75   0.91   4536    1.0
lp__   -6.78    0.03   1.58 -10.53  -7.67  -6.45  -5.58  -4.73   3299    1.0

Samples were drawn using NUTS at Mon Nov  4 20:18:50 2019.
For each parameter, n_eff is a crude measure of effective sample size,
and Rhat is the potential scale reduction factor on split chains (at
convergence, Rhat=1).
```

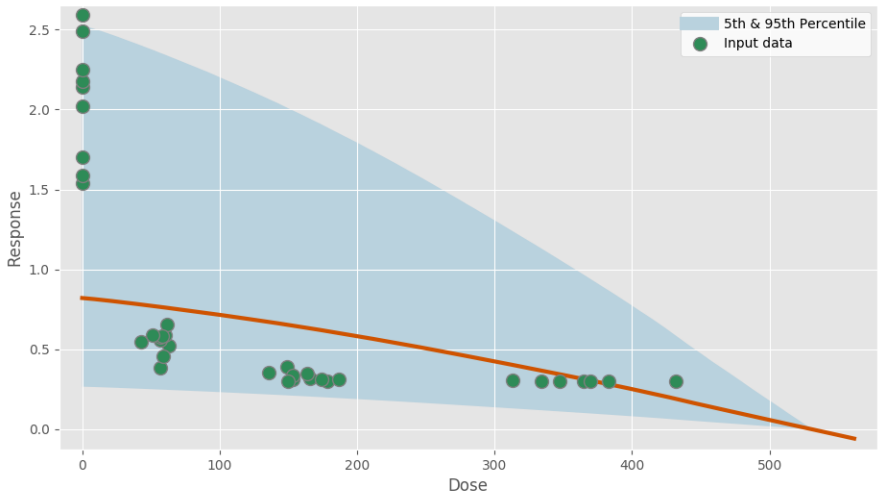

Posterior predictive p-value for model fit: 0.518

Model weight: 0.0%

Correlation matrix

	a	b	g	sigma
a	-	-0.839	-0.322	-0.156
b	-0.839	-	0.373	0.224
g	-0.322	0.373	-	0.310
sigma	-0.156	0.224	0.310	-

Parameter charts

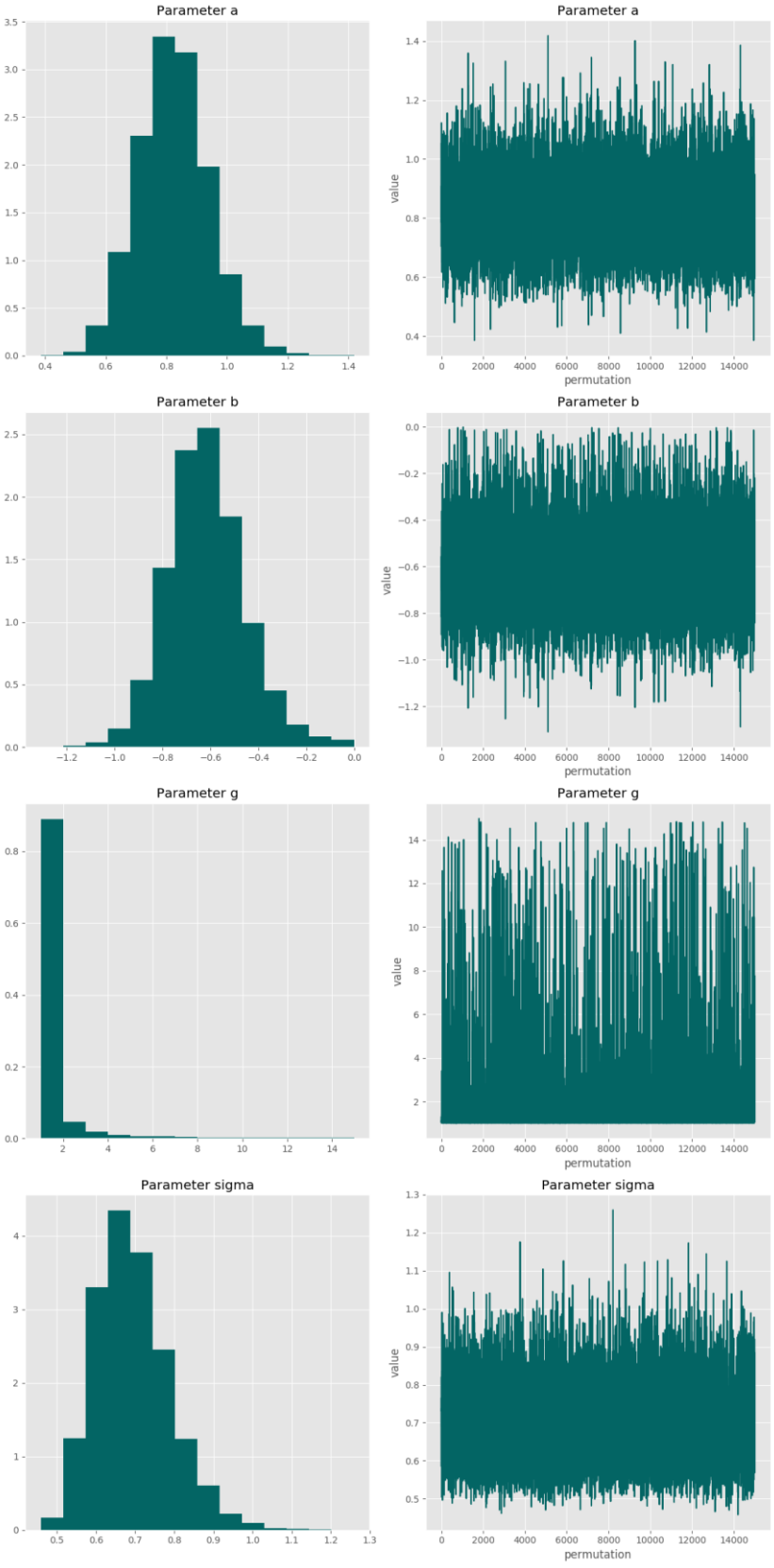

MichaelisMenten

$$f(dose) = a + \frac{b \times dose}{c + dose}$$

Model fit summary

```
Inference for Stan model:
michaelismenten_individual_pkl_8a1ee8a1062ea9c00f6bd83f5c89e8d5.
1 chains, each with iter=30000; warmup=15000; thin=1;
post-warmup draws per chain=15000, total post-warmup draws=15000.

        mean se_mean     sd    2.5%    25%    50%    75%  97.5%  n_eff   Rhat
a       2.12  1.5e-3   0.11    1.92   2.05   2.12   2.19   2.34   5074    1.0
b      -1.89  1.5e-3   0.11   -2.11  -1.96  -1.89  -1.82  -1.69   5368    1.0
c       0.02  4.7e-5 3.9e-3    0.02   0.02   0.02   0.03   0.03   6984    1.0
sigma   0.16  2.3e-4   0.02    0.13   0.14   0.16   0.17    0.2   7710    1.0
lp__   45.59    0.02   1.47   41.91  44.86  45.93  46.68  47.43   5024    1.0

Samples were drawn using NUTS at Mon Nov  4 20:19:03 2019.
For each parameter, n_eff is a crude measure of effective sample size,
and Rhat is the potential scale reduction factor on split chains (at
convergence, Rhat=1).
```

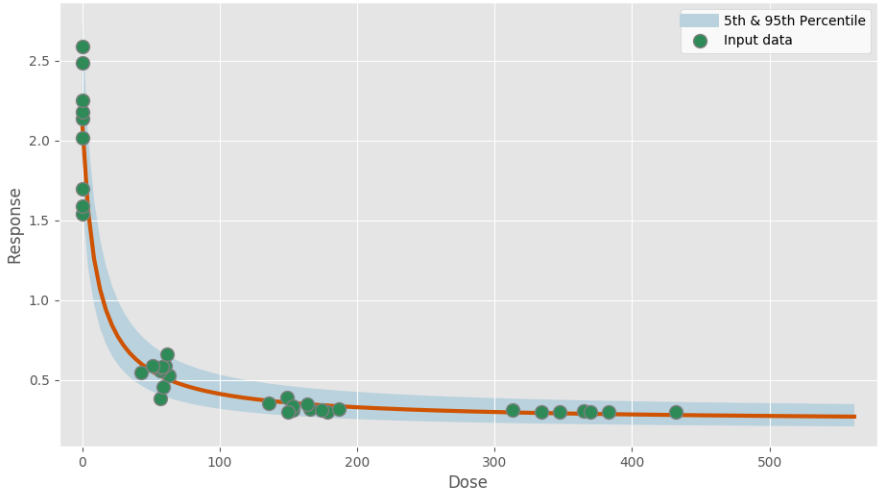

Posterior predictive p-value for model fit: 0.524

Model weight: 49.1%

Correlation matrix

	a	b	c	sigma
a	-	-0.982	-0.434	0.012
b	-0.982	-	0.290	-0.014
c	-0.434	0.290	-	0.031
sigma	0.012	-0.014	0.031	-

Parameter charts

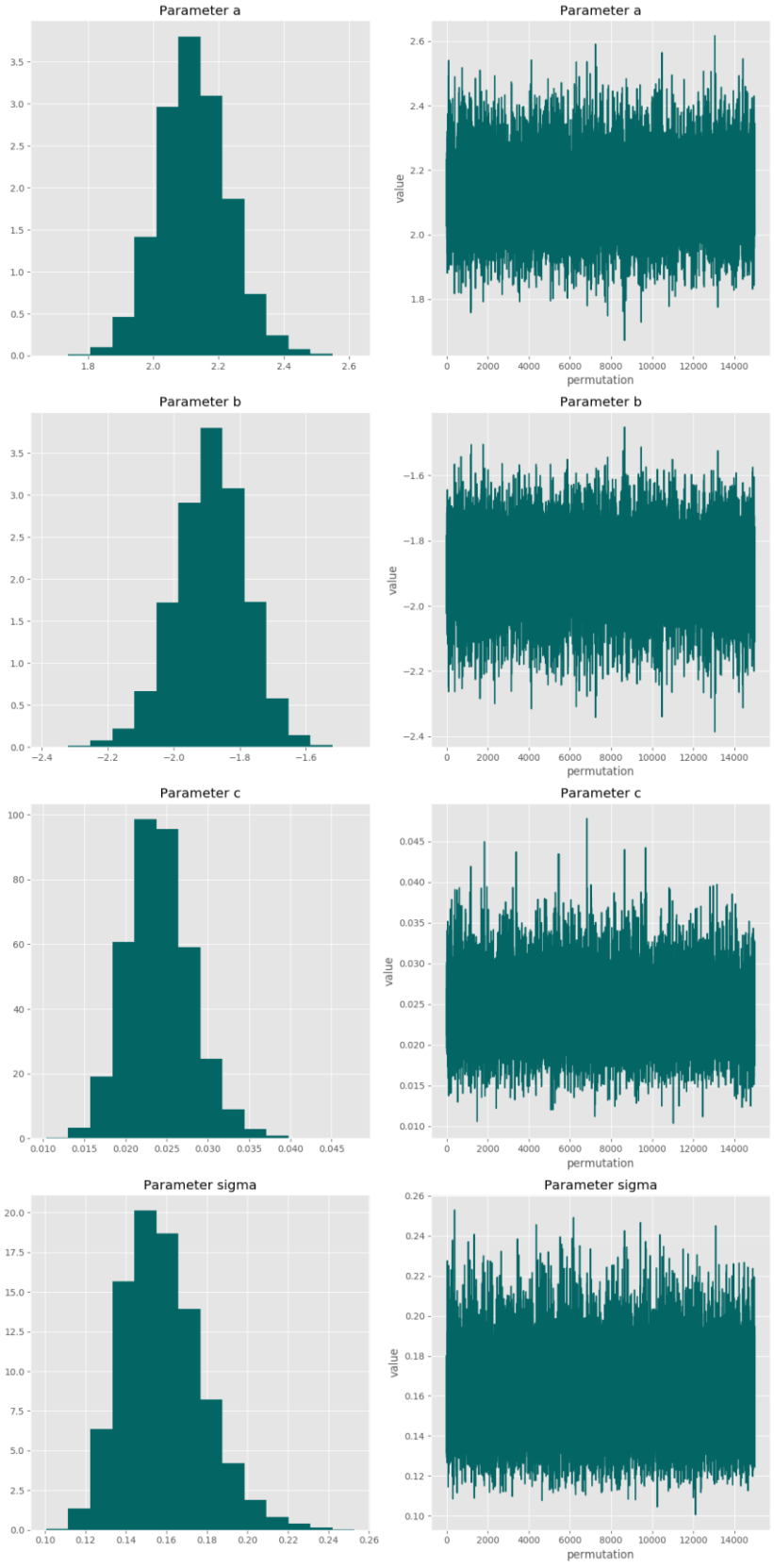

Linear

$$f(dose) = a + b \times dose$$

Model fit summary

```
Inference for Stan model: linear_individual_pkl_6f560bd3666c0b0a5c004ccddf0ad3ca.
1 chains, each with iter=30000; warmup=15000; thin=1;
post-warmup draws per chain=15000, total post-warmup draws=15000.

        mean se_mean     sd   2.5%    25%    50%    75%  97.5%  n_eff   Rhat
a       0.87  1.6e-3   0.11   0.68    0.8   0.87   0.94   1.11   4619    1.0
b      -0.68  2.2e-3   0.14  -0.96  -0.77  -0.68  -0.59   -0.4   4216    1.0
sigma   0.66  1.1e-3   0.08   0.52    0.6   0.65   0.71   0.85   5768    1.0
lp__   -3.01    0.02   1.34  -6.52  -3.63  -2.65  -2.03  -1.51   3967    1.0

Samples were drawn using NUTS at Mon Nov  4 20:19:11 2019.
For each parameter, n_eff is a crude measure of effective sample size,
and Rhat is the potential scale reduction factor on split chains (at
convergence, Rhat=1).
```

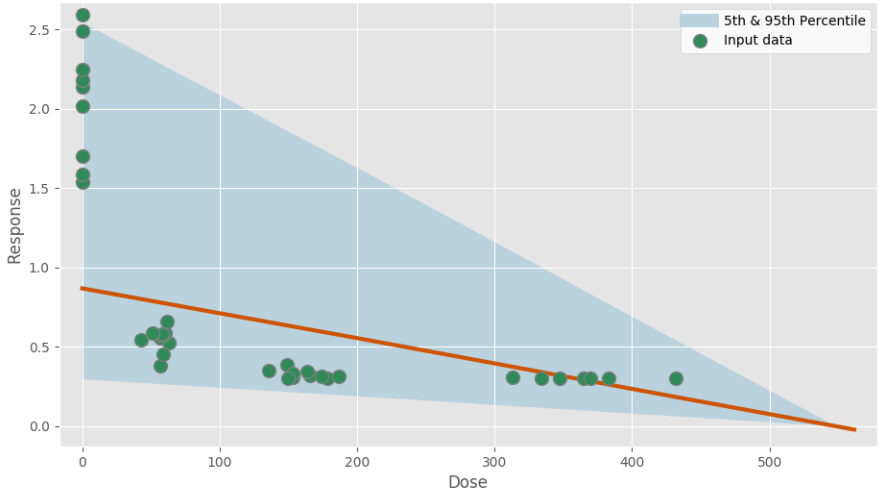

Posterior predictive p-value for model fit: 0.529

Model weight: 0.0%

Correlation matrix

	a	b	sigma
a	-	-0.862	0.027
b	-0.862	-	0.041
sigma	0.027	0.041	-

Parameter charts

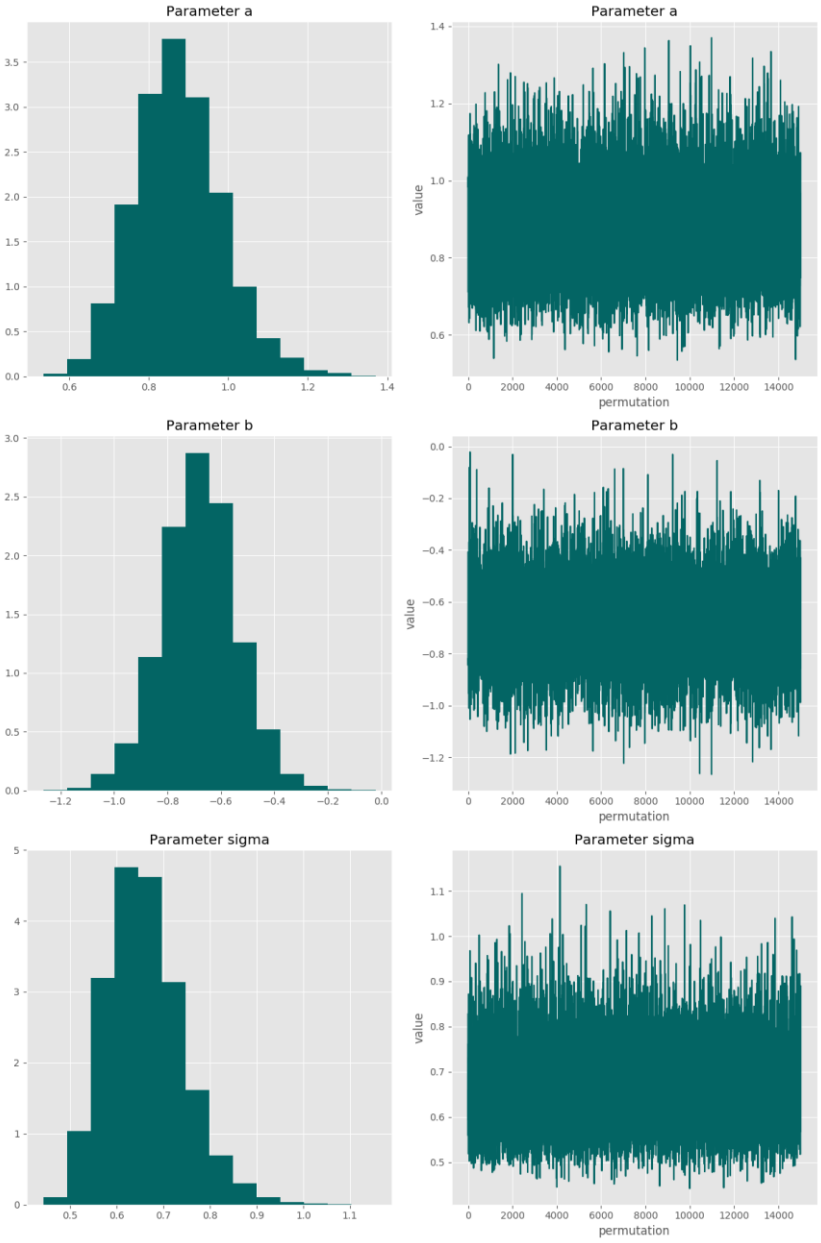

PFHxS fT4 male Nov 4 2019

Report created on Nov 04, 2019 at 08:16 PM.

Pystan model version 2.19.0.0.

Dataset

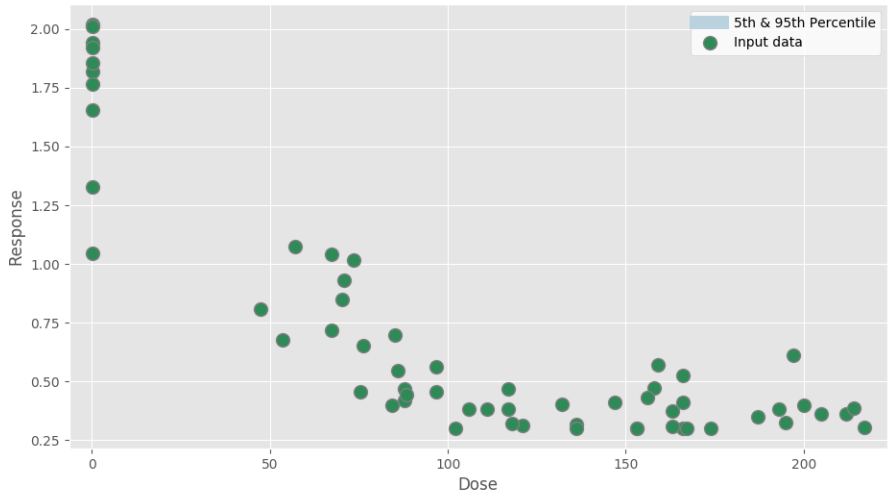

Dose	Response
0.0973	1.0465
0.073	2.02
0.106	1.8203
0.0952	1.942
0.0598	1.3293
0.135	2.0137
0.214	1.8559
0.104	1.6552
0.064	1.7675
0.074	1.9203
57.0	1.0749
47.5	0.8075
53.5	0.6787
70.2	0.8501
67.4	0.7173
84.3	0.3982
76.3	0.6502
70.7	0.9326
73.5	1.0183
67.2	1.0403

75.4	0.4556
85.2	0.6988
111.0	0.3811
96.7	0.5625
87.8	0.4181
87.7	0.4688
88.3	0.4423
96.7	0.4566
86.0	0.5472
106.0	0.3834
136.0	0.3171
121.0	0.311
132.0	0.4039
118.0	0.3207
117.0	0.4666
136.0	0.3
158.0	0.4725
117.0	0.3822
153.0	0.3
102.0	0.3
166.0	0.3
167.0	0.3
156.0	0.4313
163.0	0.31
147.0	0.4111
166.0	0.4096
153.0	0.3
159.0	0.5713
166.0	0.5266
174.0	0.3
200.0	0.3986
205.0	0.3613
217.0	0.303
212.0	0.3615
187.0	0.3498
195.0	0.3255
197.0	0.6092
214.0	0.3878
163.0	0.3731
193.0	0.3801

BMD results

20% Central tendency: Relative

BMR: None

Adversity value: 0.200

BMD summary tables:

Statistic	Model average	Exponential2	Exponential3	Exponential4	Exponential5	Hill	Power	Michaelis Menten	Linear
Prior model weight	N/A	0.125	0.125	0.125	0.125	0.125	0.125	0.125	0.125
Posterior model weight	N/A	9.8e-09	5.87e-10	0.092	0.715	0.189	1.64e-15	0.004	2.87e-14
BMD (median)	36.282	28.544	30.731	12.489	37.733	42.959	62.042	8.784	57.697
BMDL (5th percentile)	26.551	25.053	26.272	10.442	24.731	29.611	55.183	6.113	53.017
25th percentile	32.391	27.010	28.691	11.612	32.484	37.865	58.695	7.618	55.547
Mean (SD)	36.173 (5.717)	28.768 (2.518)	31.259 (3.732)	12.593 (1.426)	37.577 (7.704)	42.875 (7.973)	63.429 (6.931)	8.976 (1.956)	58.211 (3.836)
75th percentile	40.105	30.294	33.223	13.472	42.888	48.107	66.489	10.157	60.266
95th percentile	45.335	33.223	38.095	15.085	49.895	55.812	76.560	12.444	65.150

BMD estimates

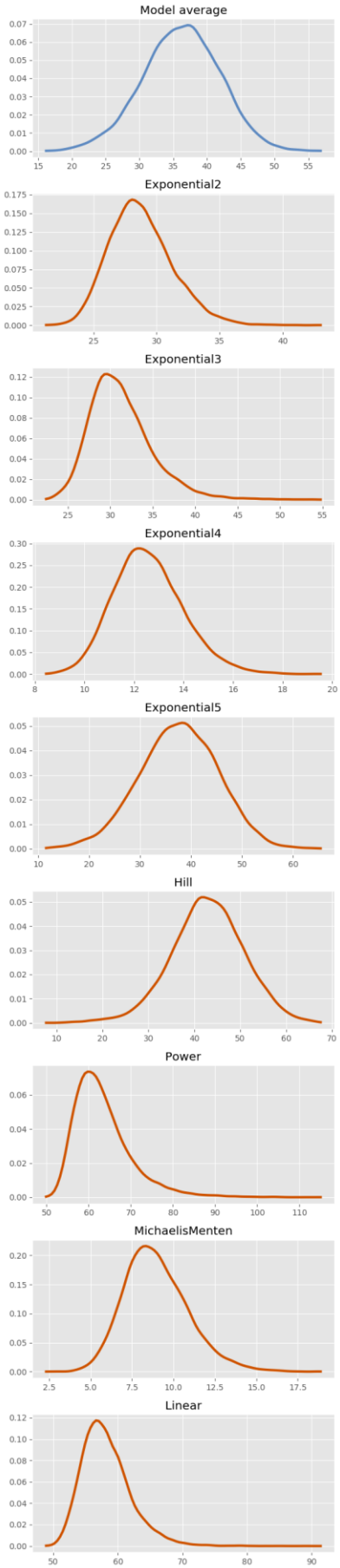
Model average
Exponential2
Exponential3
Exponential4
Exponential5
Hill
Power
MichaelisMenten
Linear

50% Central tendency: Relative

BMR: None

Adversity value: 0.500

BMD summary tables:

Statistic	Model average	Exponential2	Exponential3	Exponential4	Exponential5	Hill	Power	Michaelis Menten	Linear
Prior model weight	N/A	0.125	0.125	0.125	0.125	0.125	0.125	0.125	0.125
Posterior model weight	N/A	9.8e-09	5.87e-10	0.092	0.715	0.189	1.64e-15	0.004	2.87e-14
BMD (median)	60.928	88.665	92.129	42.291	63.042	62.581	148.395	37.052	144.243
BMDL (5th percentile)	53.143	77.823	80.099	35.270	52.579	52.242	135.279	26.696	132.541
25th percentile	57.992	83.902	86.927	39.267	59.116	58.558	142.254	32.573	138.867
Mean (SD)	60.686 (4.334)	89.361 (7.821)	93.023 (8.834)	42.638 (4.901)	62.691 (5.813)	62.338 (5.975)	149.869 (10.604)	37.644 (7.309)	145.528 (9.591)
75th percentile	63.668	94.101	98.263	45.630	66.701	66.447	155.804	42.167	150.664
95th percentile	67.285	103.199	108.737	51.212	71.569	71.647	169.143	50.624	162.876

BMD estimates

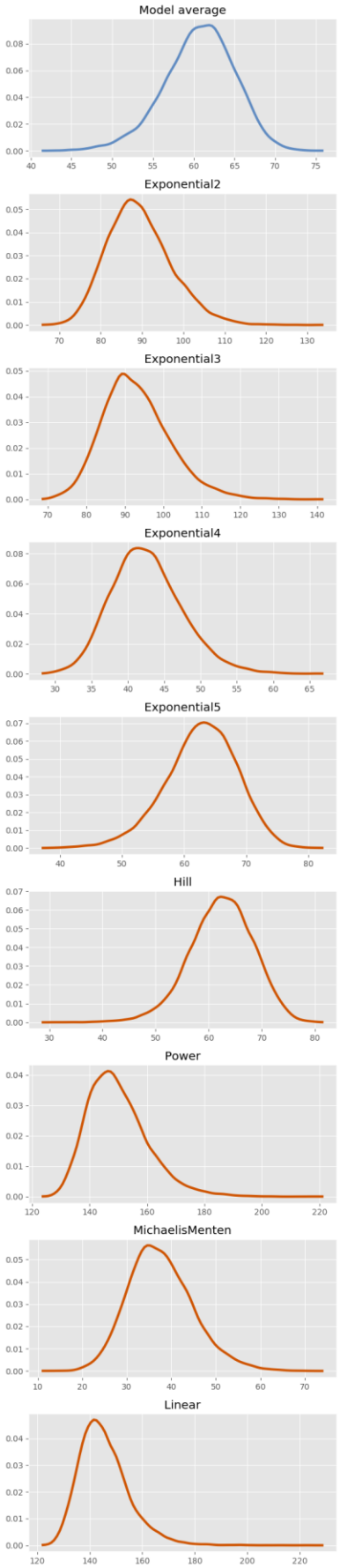
Model average
Exponential2
Exponential3
Exponential4
Exponential5
Hill
Power
MichaelisMenten
Linear

BMD Markov chain Monte Carlo settings

Iterations: 30,000

Number of chains: 1

Warmup fraction: 0.5

Seed: 9,553

Model results

Exponential2

$$f(dose) = a \times e^{b \times dose}$$

Model fit summary

```
Inference for Stan model: exponential2_individual_pkl_be58f7567ba64ec5547642f54ef3b89e.
1 chains, each with iter=30000; warmup=15000; thin=1;
post-warmup draws per chain=15000, total post-warmup draws=15000.

        mean se_mean     sd   2.5%    25%    50%    75%  97.5%  n_eff   Rhat
a       1.32  1.4e-3   0.11   1.11   1.24   1.31   1.39   1.54   5985    1.0
b       -1.7  1.8e-3   0.14  -1.98  -1.79   -1.7   -1.6  -1.41   6187    1.0
sigma   0.34  3.3e-4   0.03   0.28   0.31   0.33   0.36   0.41   9115    1.0
lp__   35.31    0.02   1.25  32.12  34.74  35.63  36.22  36.73   5514    1.0

Samples were drawn using NUTS at Mon Nov  4 20:10:55 2019.
For each parameter, n_eff is a crude measure of effective sample size,
and Rhat is the potential scale reduction factor on split chains (at
convergence, Rhat=1).
```

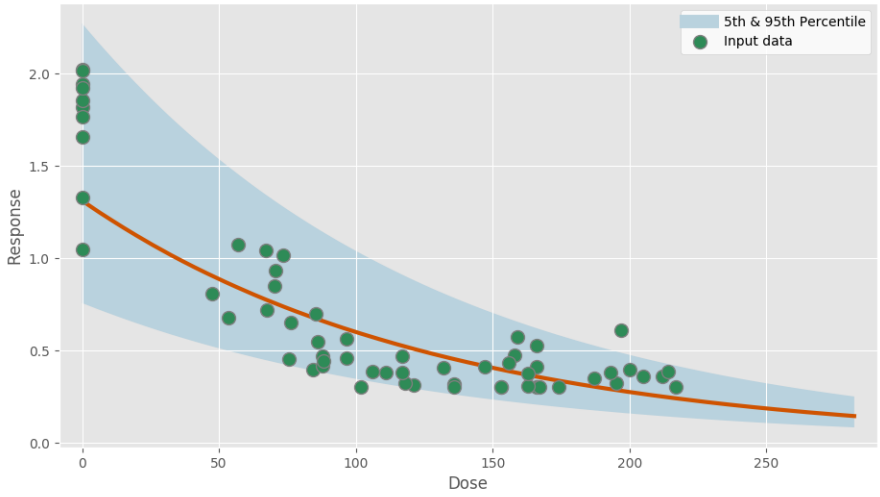

Posterior predictive p-value for model fit: 0.524

Model weight: 0.0%

Correlation matrix

	a	b	sigma
a	-	-0.854	0.027
b	-0.854	-	-0.0155
sigma	0.027	-0.0155	-

Parameter charts

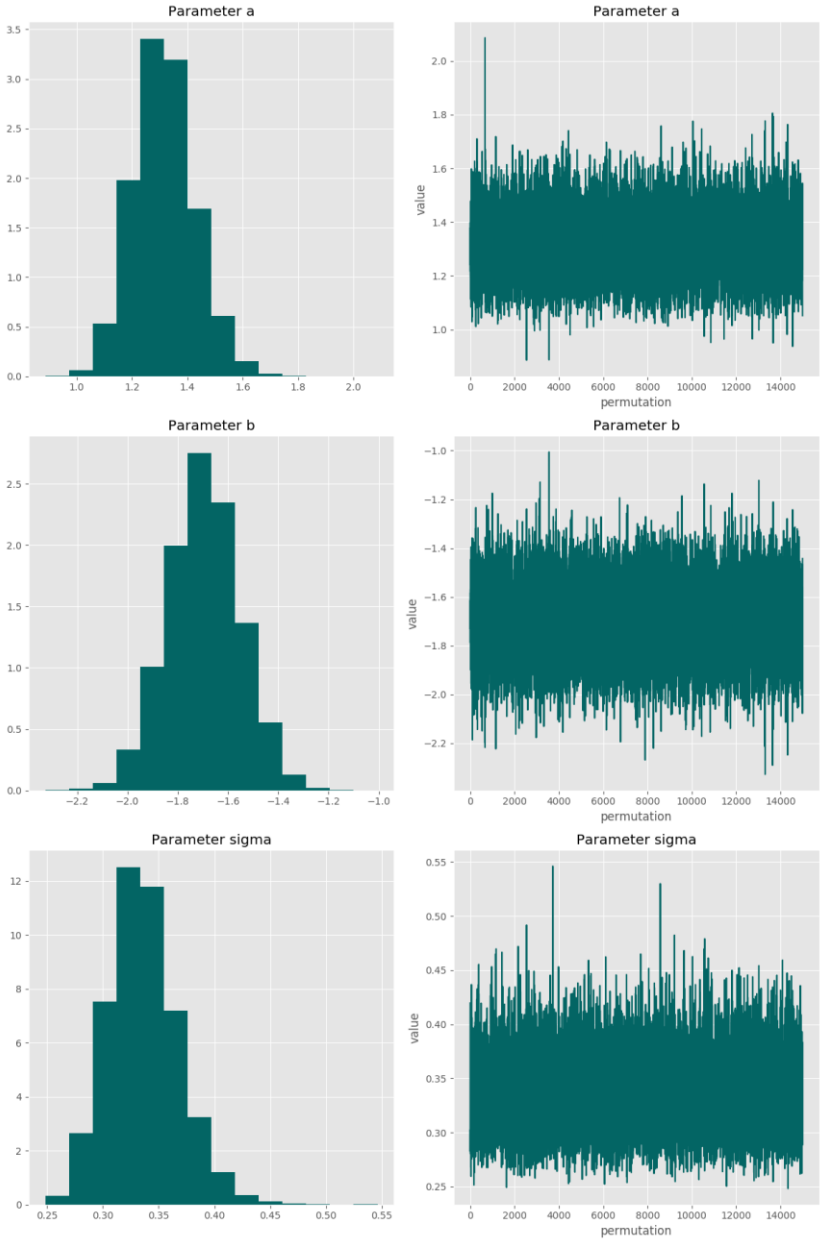

Exponential3

$$f(dose) = a \times e^{b \times dose^g}$$

Power parameter lower-bound: 1.000

Model fit summary

```
Inference for Stan model: exponential3_individual_pkl_df53333b36693dd0ad892f92a4fc7532.
1 chains, each with iter=30000; warmup=15000; thin=1;
post-warmup draws per chain=15000, total post-warmup draws=15000.

        mean se_mean     sd   2.5%    25%    50%    75%  97.5%  n_eff   Rhat
a       1.29  1.3e-3   0.11   1.08   1.21   1.29   1.36   1.52   7141    1.0
b      -1.68  1.7e-3   0.15  -1.97  -1.78  -1.68  -1.58  -1.39   7405    1.0
g       1.04  3.8e-4   0.04    1.0   1.01   1.03   1.05   1.15  10980    1.0
sigma   0.34  3.4e-4   0.03   0.28   0.32   0.34   0.36   0.41   9479    1.0
lp__   30.34    0.02   1.51  26.51  29.59  30.67  31.46  32.25   5336    1.0

Samples were drawn using NUTS at Mon Nov  4 20:11:06 2019.
For each parameter, n_eff is a crude measure of effective sample size,
and Rhat is the potential scale reduction factor on split chains (at
convergence, Rhat=1).
```

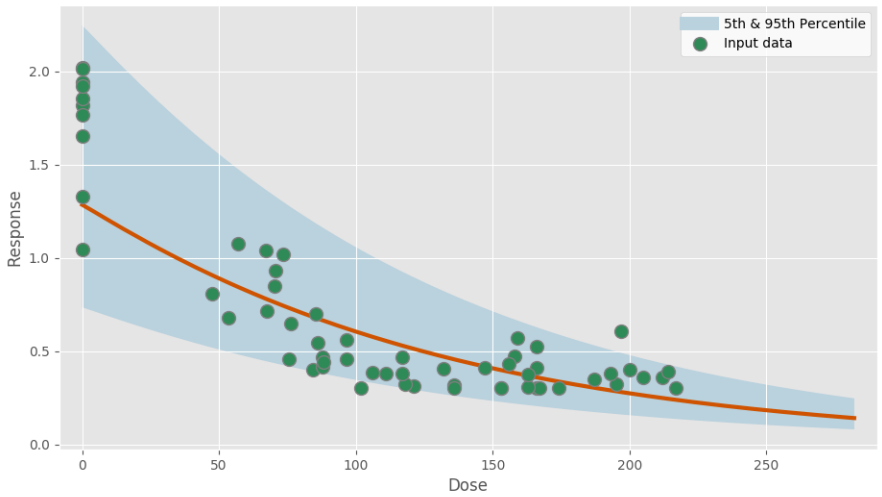

Posterior predictive p-value for model fit: 0.522

Model weight: 0.0%

Correlation matrix

	a	b	g	sigma
a	-	-0.842	-0.22	-0.0383
b	-0.842	-	0.077	0.023
g	-0.22	0.077	-	0.188
sigma	-0.0383	0.023	0.188	-

Parameter charts

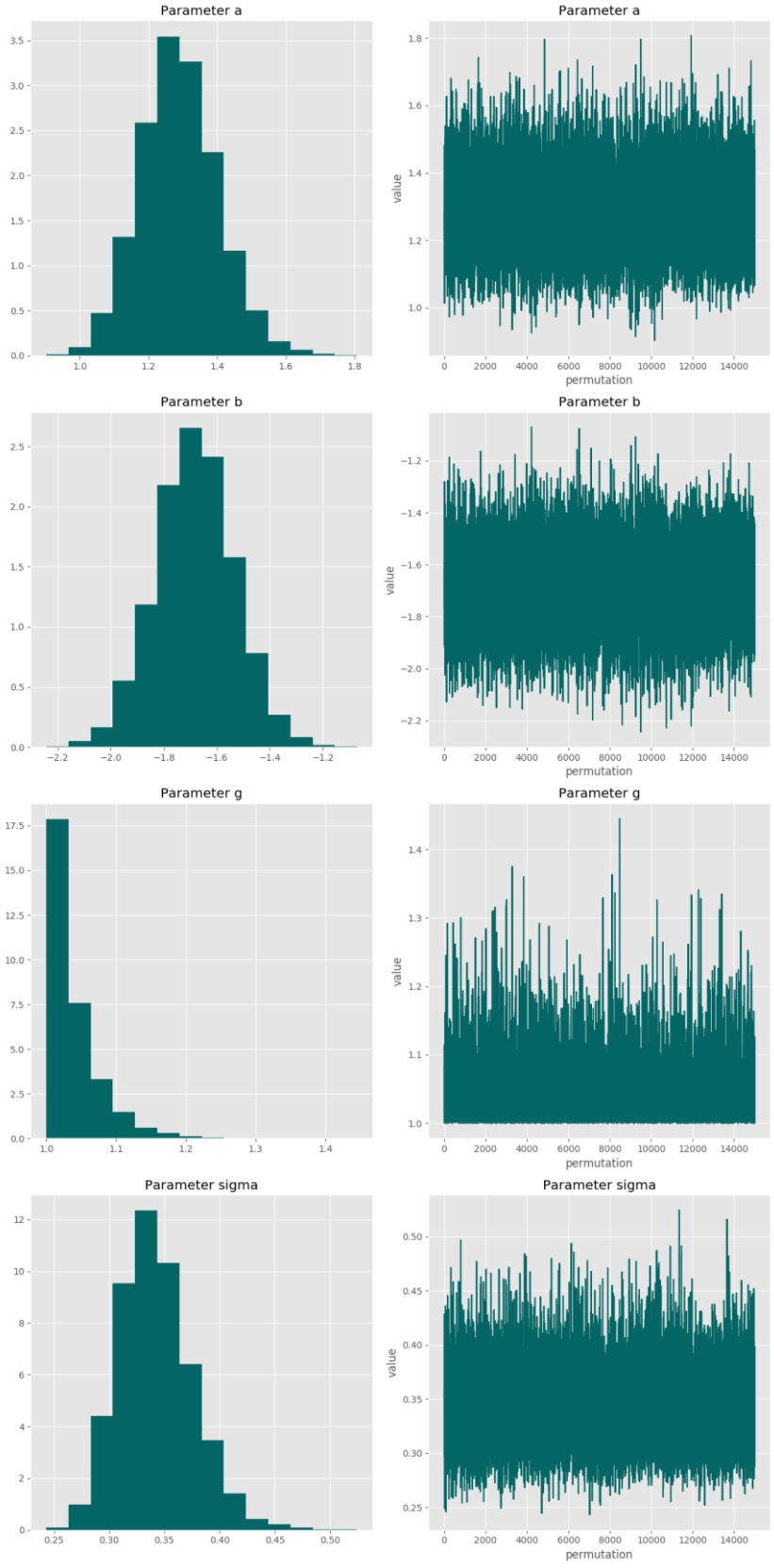

Exponential4

$$f(dose) = a \times [c - (c - 1) \times e^{-b \times dose}]$$

Model fit summary

```
Inference for Stan model: exponential4_individual_pkl_fa67b4bb1853dd3a882bdb66cdb5191d.
1 chains, each with iter=30000; warmup=15000; thin=1;
post-warmup draws per chain=15000, total post-warmup draws=15000.

        mean se_mean     sd   2.5%    25%    50%    75%  97.5%  n_eff   Rhat
a       1.77  1.4e-3   0.14   1.51   1.68   1.77   1.86   2.06   9101    1.0
b       4.94  5.3e-3   0.56    3.9   4.55   4.92    5.3   6.12  11274    1.0
c       0.19  2.0e-4   0.02   0.15   0.18   0.19    0.2   0.23   9492    1.0
sigma   0.25  2.3e-4   0.02   0.21   0.23   0.25   0.26    0.3  11229    1.0
lp__    53.4    0.02   1.51  49.53  52.68  53.75  54.51  55.26   5015    1.0

Samples were drawn using NUTS at Mon Nov  4 20:11:17 2019.
For each parameter, n_eff is a crude measure of effective sample size,
and Rhat is the potential scale reduction factor on split chains (at
convergence, Rhat=1).
```

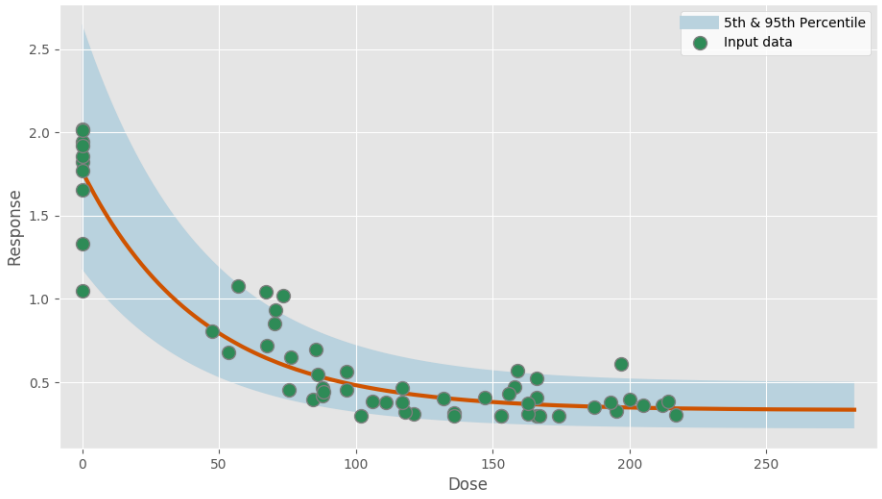

Posterior predictive p-value for model fit: 0.518

Model weight: 9.2%

Correlation matrix

	a	b	c	sigma
a	-	0.499	-0.656	-0.012
b	0.499	-	0.162	0.021
c	-0.656	0.162	-	0.030
sigma	-0.012	0.021	0.030	-

Parameter charts

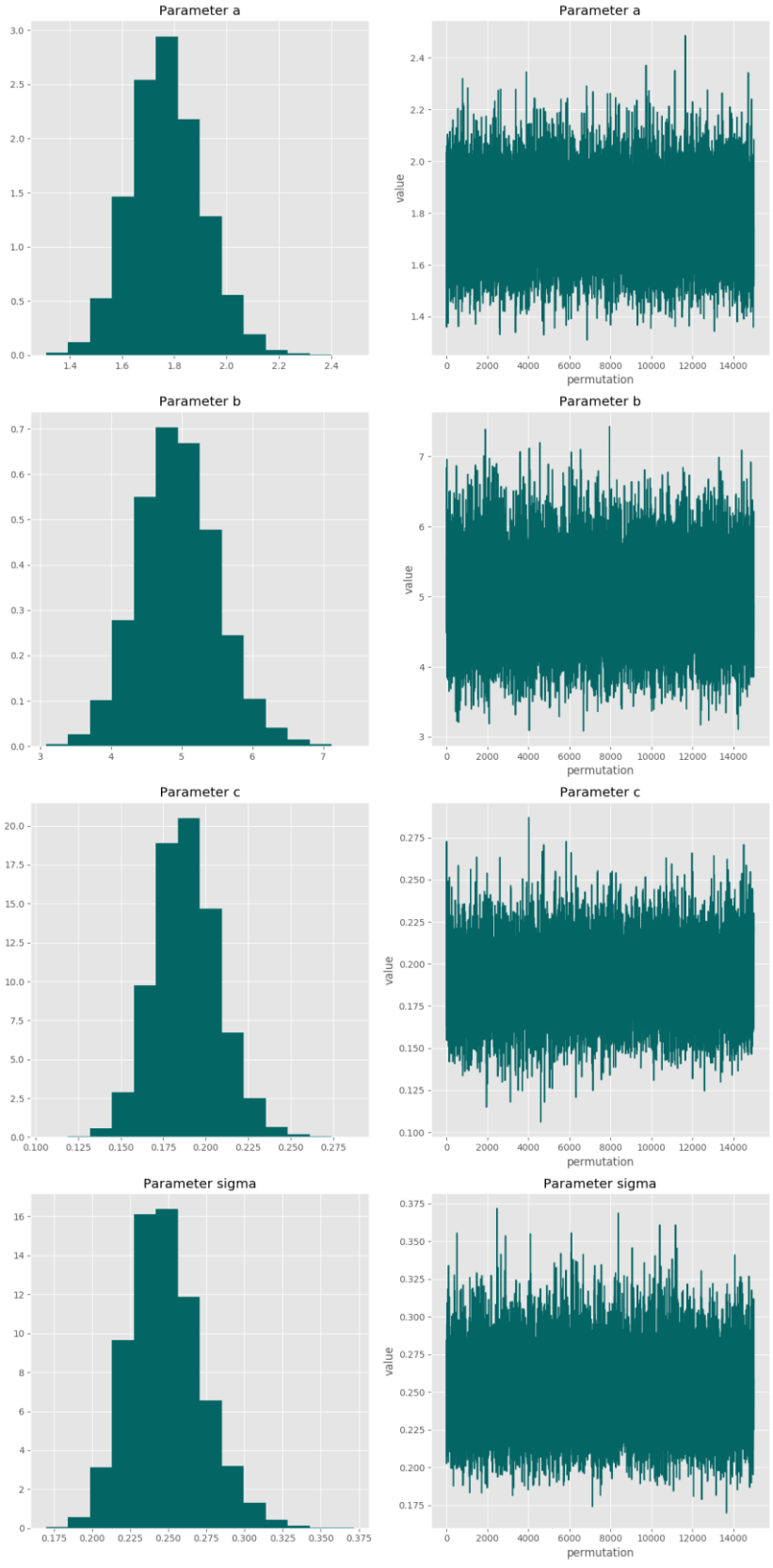

Exponential5

$$f(dose) = a \times [c - (c - 1) \times e^{-(b \times dose)^g}]$$

Power parameter lower-bound: 1.000

Model fit summary

```
Inference for Stan model: exponential5_individual_pkl_0fe35d8b796f8736b80743a2674317fc.
1 chains, each with iter=30000; warmup=15000; thin=1;
post-warmup draws per chain=15000, total post-warmup draws=15000.

        mean se_mean     sd   2.5%    25%    50%    75%  97.5%  n_eff   Rhat
a       1.68  1.7e-3   0.13   1.44   1.59   1.67   1.76   1.94   5962    1.0
b       3.52  4.8e-3   0.32   3.04    3.3   3.48   3.69   4.28   4417    1.0
c       0.22  2.6e-4   0.02   0.18   0.21   0.22   0.23   0.26   5858    1.0
g        2.5  8.6e-3   0.67   1.46   2.04   2.42   2.86   4.04   6021    1.0
sigma   0.23  2.3e-4   0.02   0.19   0.21   0.23   0.24   0.28   9184    1.0
lp__   58.42    0.03   1.78  53.95  57.53  58.81  59.72  60.74   4525    1.0

Samples were drawn using NUTS at Mon Nov  4 20:11:31 2019.
For each parameter, n_eff is a crude measure of effective sample size,
and Rhat is the potential scale reduction factor on split chains (at
convergence, Rhat=1).
```

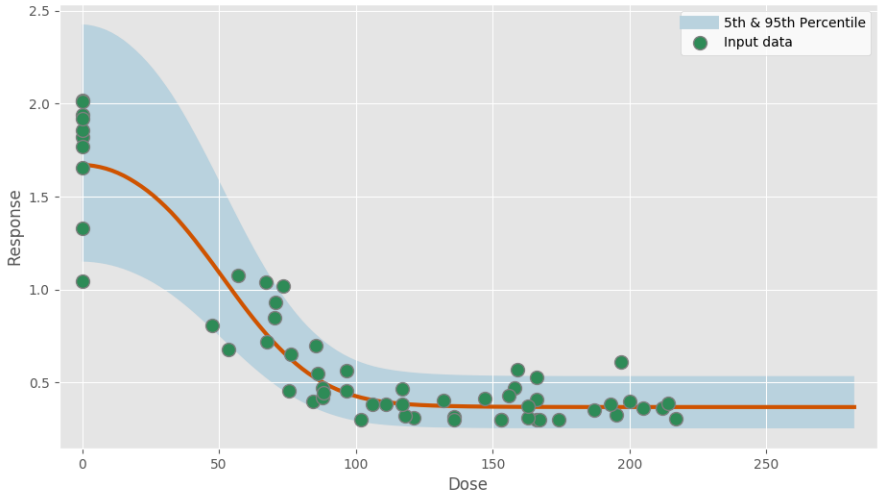

Posterior predictive p-value for model fit: 0.526

Model weight: 71.5%

Correlation matrix

	a	b	c	g	sigma
a	-	0.537	-0.862	-0.371	0.009
b	0.537	-	-0.458	-0.744	0.060
c	-0.862	-0.458	-	0.449	0.006
g	-0.371	-0.744	0.449	-	0.019

sigma	0.009	0.060	0.006	0.019	-

Parameter charts

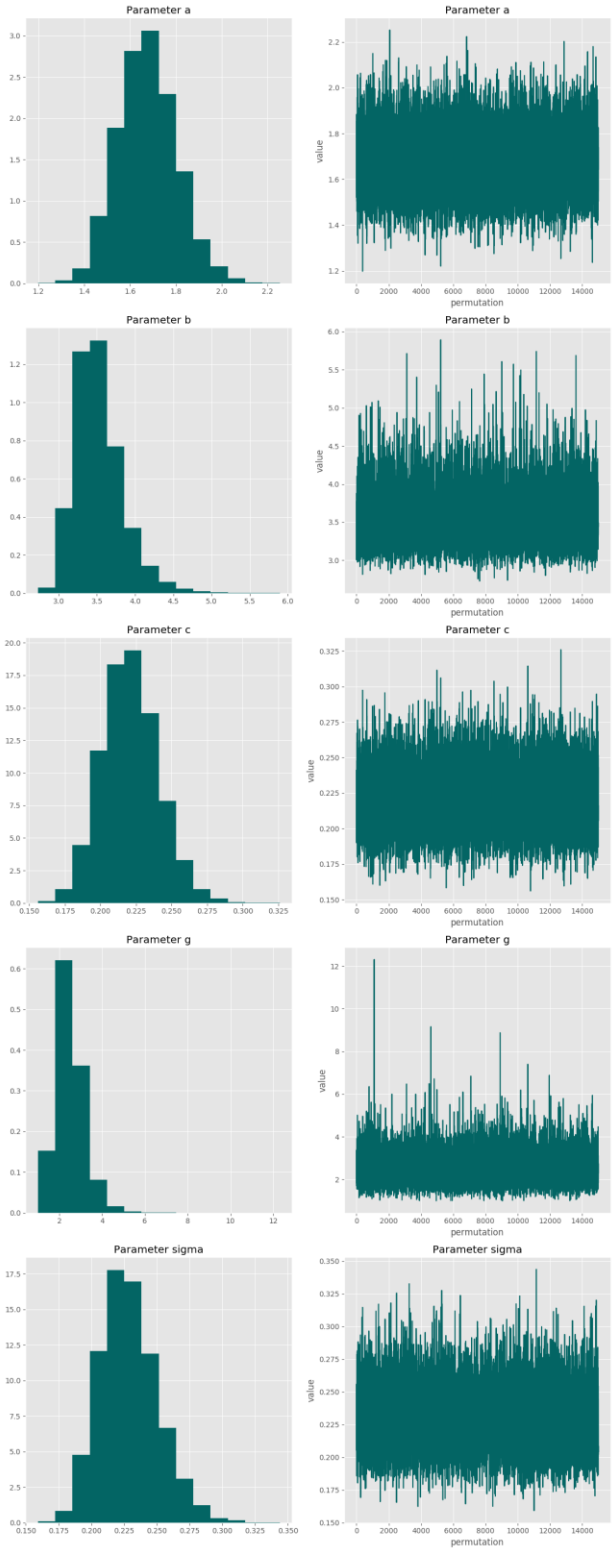

Hill

$$f(dose) = a + \frac{b \times dose^g}{c^g + dose^g}$$

Power parameter lower-bound: 1.000

Model fit summary

```
Inference for Stan model: hill_individual_pkl_f14f62088318f1a4663f986868dc9b40.
1 chains, each with iter=30000; warmup=15000; thin=1;
post-warmup draws per chain=15000, total post-warmup draws=15000.

        mean se_mean     sd   2.5%    25%    50%    75%  97.5%  n_eff   Rhat
a       1.66  1.8e-3   0.13   1.42   1.57   1.66   1.75   1.93   5351    1.0
b      -1.31  1.9e-3   0.14  -1.59   -1.4  -1.31  -1.22  -1.06   5052    1.0
c       0.25  4.1e-4   0.03   0.19   0.23   0.25   0.27   0.31   4856    1.0
g       4.59    0.02   1.46   2.38   3.63   4.38   5.28   8.12   5119    1.0
sigma   0.24  2.8e-4   0.02    0.2   0.22   0.24   0.25   0.29   6889    1.0
lp__   56.04    0.03   1.76  51.61  55.15   56.4  57.33  58.35   4014    1.0

Samples were drawn using NUTS at Mon Nov  4 20:12:12 2019.
For each parameter, n_eff is a crude measure of effective sample size,
and Rhat is the potential scale reduction factor on split chains (at
convergence, Rhat=1).
```

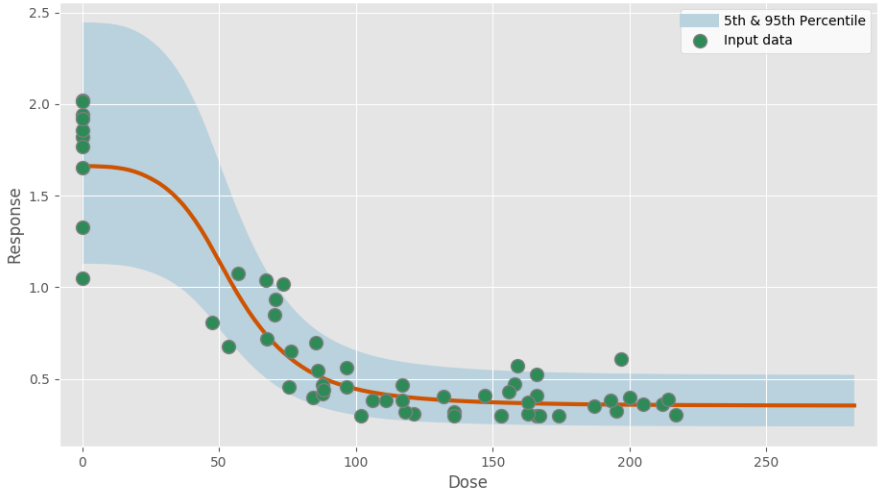

Posterior predictive p-value for model fit: 0.521

Model weight: 18.9%

Correlation matrix

	a	b	c	g	sigma
a	-	-0.983	-0.55	-0.353	-0.0289
b	-0.983	-	0.599	0.442	0.023
c	-0.55	0.599	-	0.819	0.020
g	-0.353	0.442	0.819	-	0.072

sigma	-0.0289	0.023	0.020	0.072	-

Parameter charts

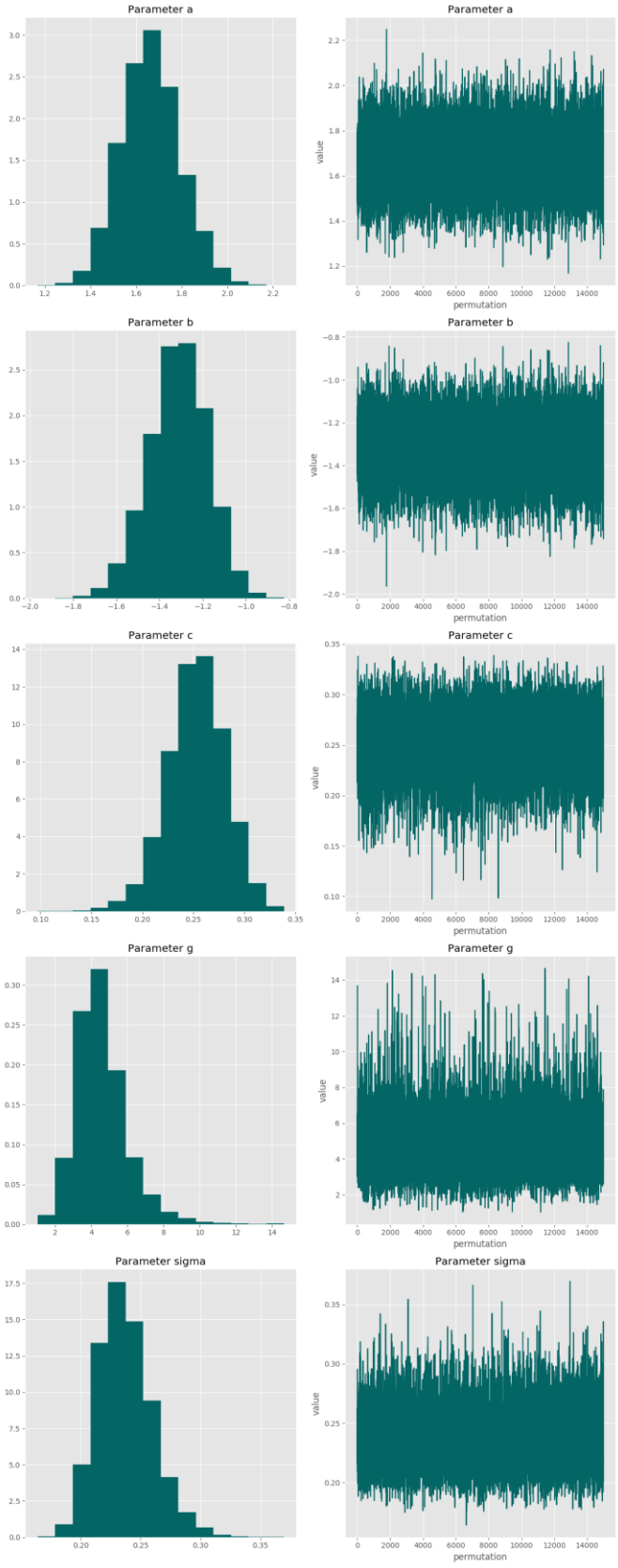

Power

$$f(dose) = a + b \times dose^{g}$$

Power parameter lower-bound: 1.000

Model fit summary

```
Inference for Stan model: power_individual_pkl_8682a4681cf39e692df770d4639a86e2.
1 chains, each with iter=30000; warmup=15000; thin=1;
post-warmup draws per chain=15000, total post-warmup draws=15000.

        mean se_mean     sd   2.5%    25%    50%    75%  97.5%  n_eff   Rhat
a       0.95  9.3e-4   0.08   0.81    0.9   0.95    1.0    1.1   6582    1.0
b      -0.71  1.2e-3   0.09   -0.9  -0.77  -0.71  -0.65  -0.53   6585    1.0
g       1.07  7.7e-4   0.08    1.0   1.02   1.04   1.09   1.27   9478    1.0
sigma   0.42  4.4e-4   0.04   0.35   0.39   0.42   0.45   0.52   9305    1.0
lp__   17.96    0.02   1.49  14.23  17.22  18.29  19.05  19.83   5098    1.0

Samples were drawn using NUTS at Mon Nov  4 20:12:26 2019.
For each parameter, n_eff is a crude measure of effective sample size,
and Rhat is the potential scale reduction factor on split chains (at
convergence, Rhat=1).
```

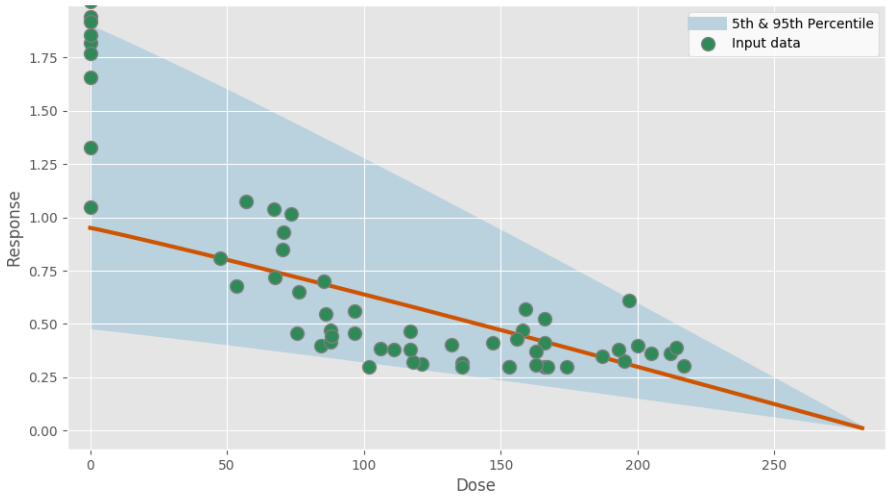

Posterior predictive p-value for model fit: 0.525

Model weight: 0.0%

Correlation matrix

	a	b	g	sigma
a	-	-0.935	-0.294	-0.0421
b	-0.935	-	0.230	0.039
g	-0.294	0.230	-	0.198
sigma	-0.0421	0.039	0.198	-

Parameter charts

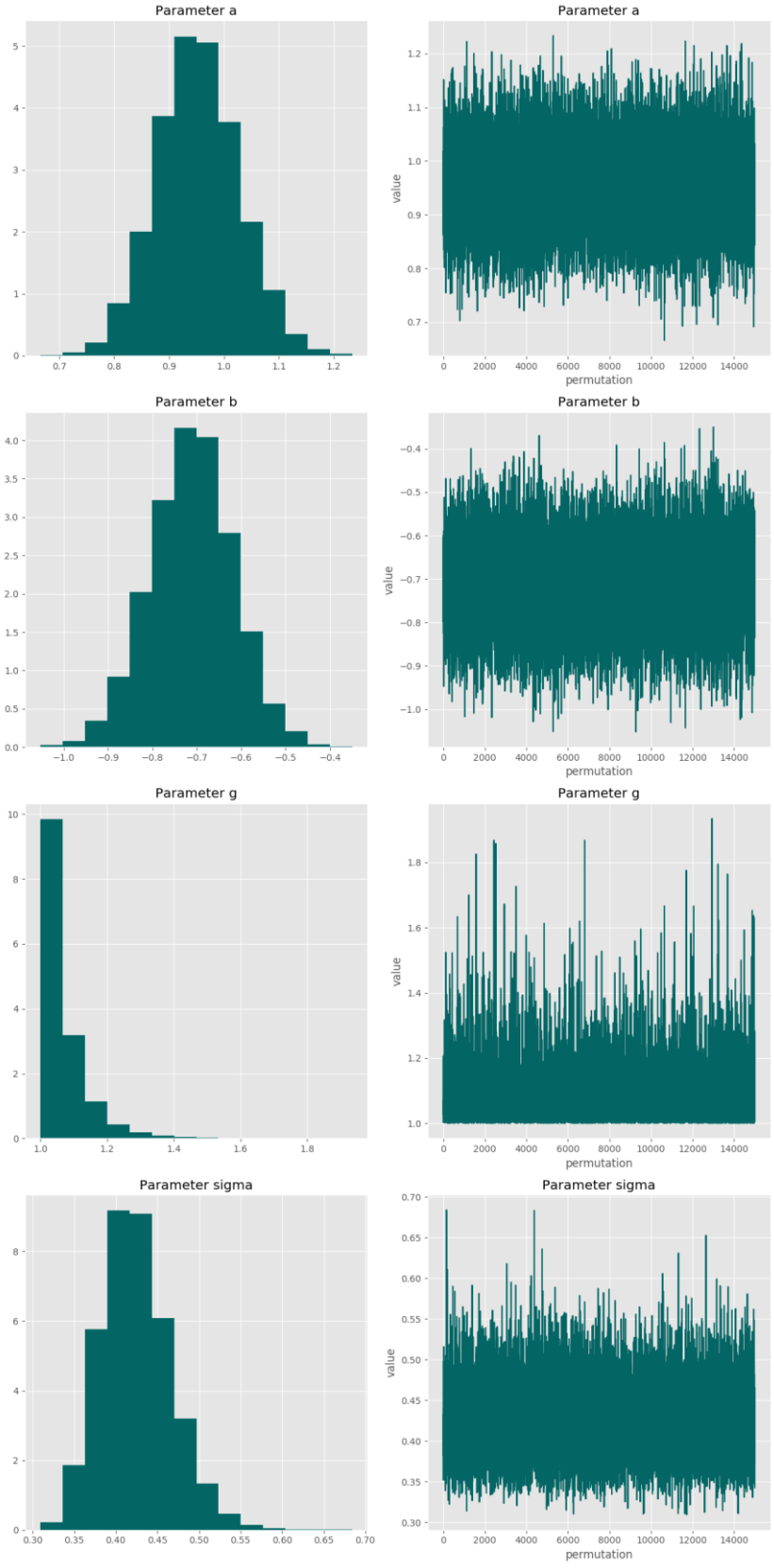

MichaelisMenten

$$f(dose) = a + \frac{b \times dose}{c + dose}$$

Model fit summary

```
Inference for Stan model:
michaelismenten_individual_pkl_8a1ee8a1062ea9c00f6bd83f5c89e8d5.
1 chains, each with iter=30000; warmup=15000; thin=1;
post-warmup draws per chain=15000, total post-warmup draws=15000.

        mean se_mean     sd    2.5%    25%    50%    75%  97.5%  n_eff   Rhat
a       1.73  2.0e-3   0.14    1.46   1.63   1.73   1.82   2.02   4849    1.0
b      -1.63  2.0e-3   0.15   -1.93  -1.72  -1.62  -1.52  -1.35   5400    1.0
c       0.15  4.8e-4   0.04    0.09   0.13   0.15   0.18   0.25   7117    1.0
sigma   0.26  2.9e-4   0.03    0.22   0.25   0.26   0.28   0.32   7663    1.0
lp__    48.2    0.02   1.47   44.45  47.48  48.52  49.28  50.03   5051    1.0

Samples were drawn using NUTS at Mon Nov  4 20:12:43 2019.
For each parameter, n_eff is a crude measure of effective sample size,
and Rhat is the potential scale reduction factor on split chains (at
convergence, Rhat=1).
```

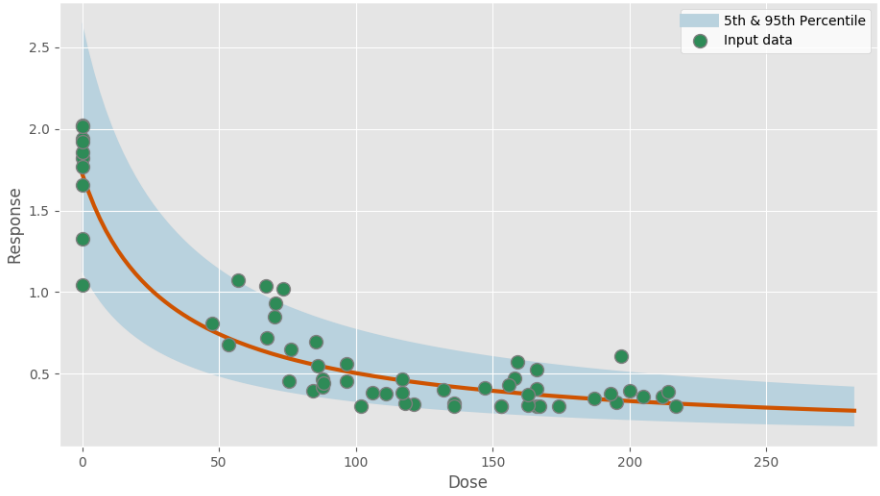

Posterior predictive p-value for model fit: 0.526

Model weight: 0.4%

Correlation matrix

	a	b	c	sigma
a	-	-0.897	-0.559	-0.0176
b	-0.897	-	0.156	0.002
c	-0.559	0.156	-	0.053
sigma	-0.0176	0.002	0.053	-

Parameter charts

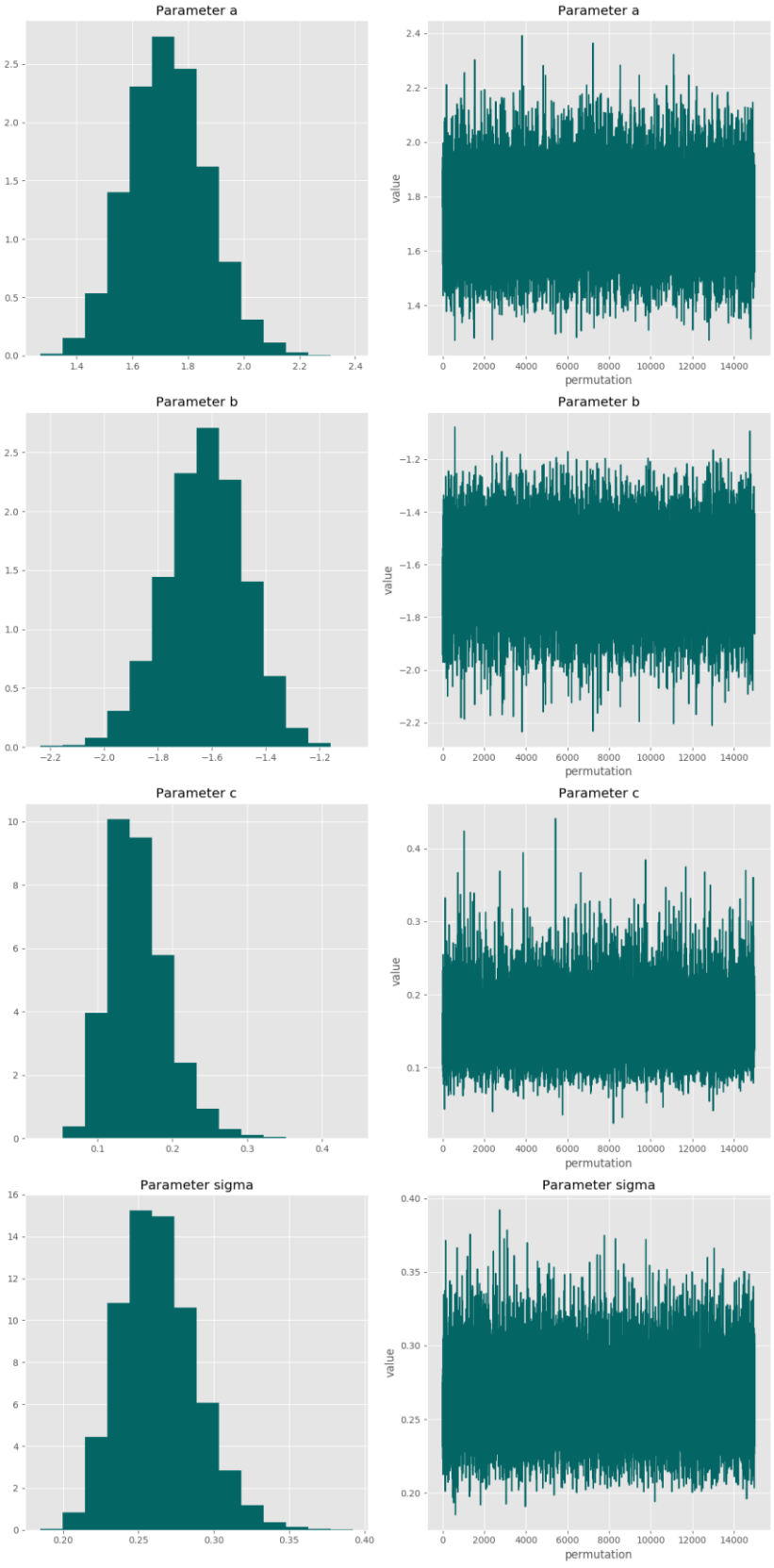

Linear

$$f(dose) = a + b \times dose$$

Model fit summary

```
Inference for Stan model: linear_individual_pkl_6f560bd3666c0b0a5c004ccddf0ad3ca.
1 chains, each with iter=30000; warmup=15000; thin=1;
post-warmup draws per chain=15000, total post-warmup draws=15000.

        mean se_mean     sd   2.5%    25%    50%    75%  97.5%  n_eff   Rhat
a       0.97  9.6e-4   0.07   0.83   0.92   0.97   1.02   1.12   5792    1.0
b      -0.73  1.2e-3   0.09  -0.91  -0.79  -0.73  -0.67  -0.55   5794    1.0
sigma   0.42  4.6e-4   0.04   0.35   0.39   0.41   0.44    0.5   7074    1.0
lp__   22.45    0.02   1.26  19.19  21.88  22.78  23.37  23.87   5122    1.0

Samples were drawn using NUTS at Mon Nov  4 20:12:52 2019.
For each parameter, n_eff is a crude measure of effective sample size,
and Rhat is the potential scale reduction factor on split chains (at
convergence, Rhat=1).
```

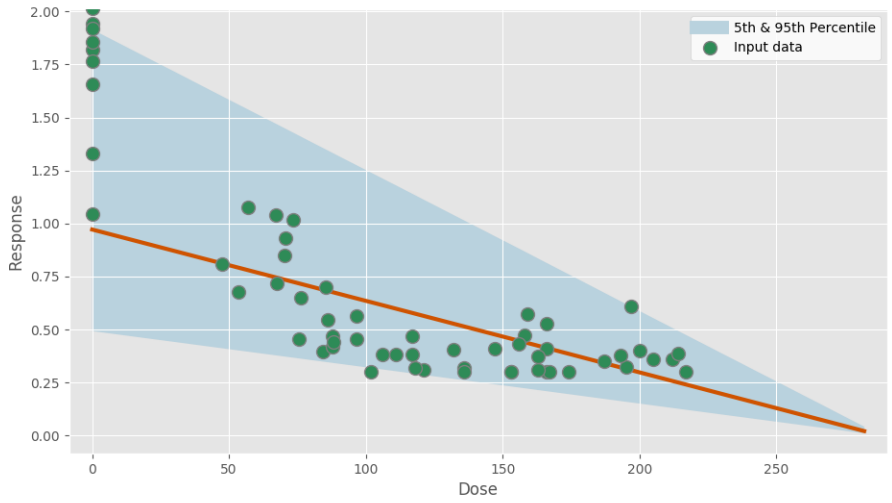

Posterior predictive p-value for model fit: 0.517

Model weight: 0.0%

Correlation matrix

	a	b	sigma
a	-	-0.936	-0.00886
b	-0.936	-	0.020
sigma	-0.00886	0.020	-

Parameter charts

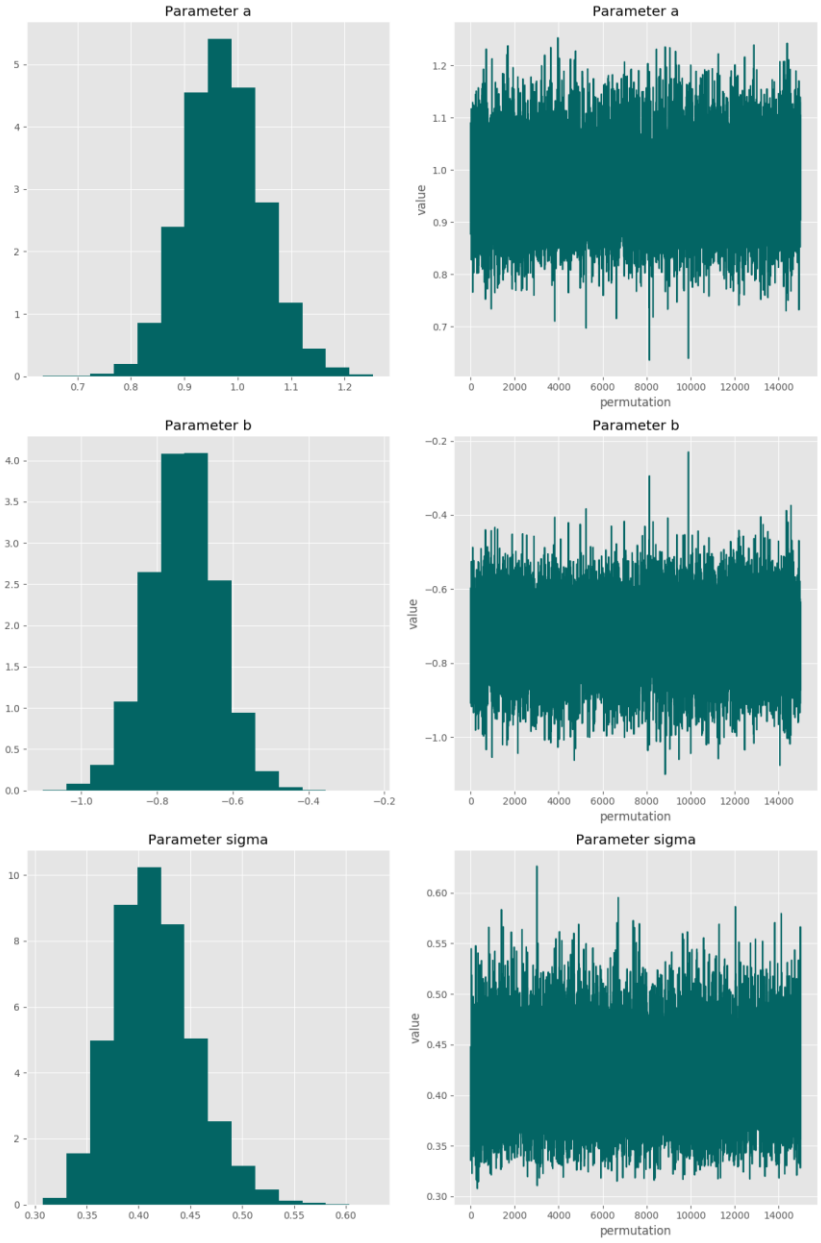

PFDA fT4 male Nov 4 2019

Report created on Nov 04, 2019 at 08:56 PM.

Pystan model version 2.19.0.0.

Dataset

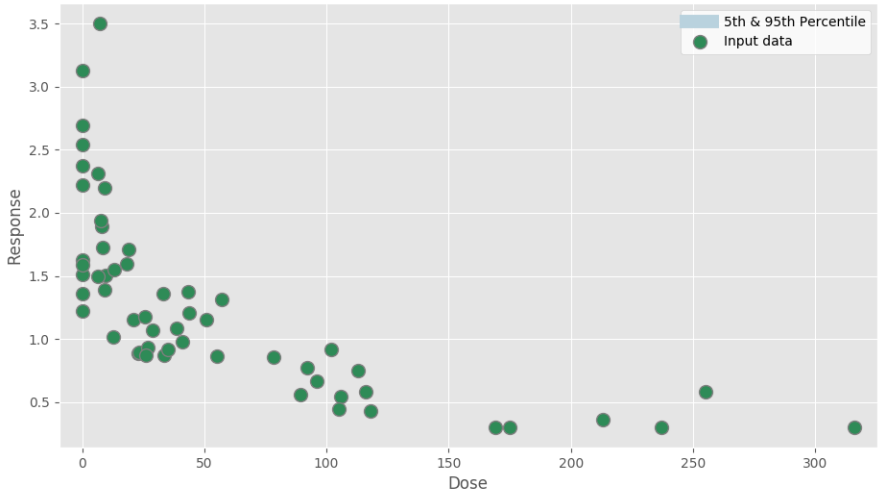

Dose	Response
0.0313	1.3555
0.0125	2.2207
0.0319	3.1272
0.0125	2.689
0.0125	1.5095
0.0289	1.2198
0.0125	2.3722
0.0125	1.6231
0.0477	2.5379
0.0125	1.5865
9.05	2.2001
12.8	1.0187
9.51	1.5017
8.56	1.7231
7.4	3.5003
7.93	1.8946
6.58	2.3145
9.03	1.3886
7.72	1.9347
6.47	1.4953
23.0	0.8897
23.5	0.8957

18.3	1.5969
33.5	0.8703
20.8	1.1548
27.0	0.9326
25.8	1.1781
13.2	1.5511
19.1	1.7088
26.1	0.871
33.1	1.3561
50.9	1.1545
35.3	0.9189
29.0	1.0723
55.0	0.8663
57.3	1.3098
41.0	0.9794
43.9	1.2101
38.5	1.0843
43.2	1.373
113.0	0.753
78.4	0.8533
116.0	0.583
106.0	0.5473
105.0	0.448
95.9	0.6658
118.0	0.432
89.5	0.5555
92.0	0.7741
102.0	0.9198
255.0	0.5798
213.0	0.363
175.0	0.3
169.0	0.3
316.0	0.3001
237.0	0.3

20% Central tendency: Relative

BMR: None

Adversity value: 0.200

BMD summary tables:

Statistic	Model average	Exponential2	Exponential3	Exponential4	Exponential5	Hill	Power	Michaelis Menten	Linear
Prior model weight	N/A	0.125	0.125	0.125	0.125	0.125	0.125	0.125	0.125
Posterior model weight	N/A	0.000172	1.08e-05	0.381	0.044	0.079	1.25e-11	0.496	1.98e-10
BMD (median)	13.285	31.046	33.725	15.309	18.459	14.175	79.957	10.754	73.522
BMDL (5th percentile)	10.894	27.033	28.417	11.730	13.245	8.859	71.294	7.276	68.718
25th percentile	12.264	29.321	31.257	13.786	16.077	11.648	75.602	9.217	71.172
Mean (SD)	13.405 (1.662)	31.294 (2.875)	34.476 (4.649)	15.458 (2.439)	19.303 (4.747)	14.997 (4.894)	82.400 (10.274)	11.046 (2.624)	74.361 (4.564)
75th percentile	14.418	32.957	36.813	16.962	21.571	17.382	86.449	12.552	76.669
95th percentile	16.335	36.395	43.079	19.700	28.094	23.782	101.472	15.772	82.749

BMD estimates

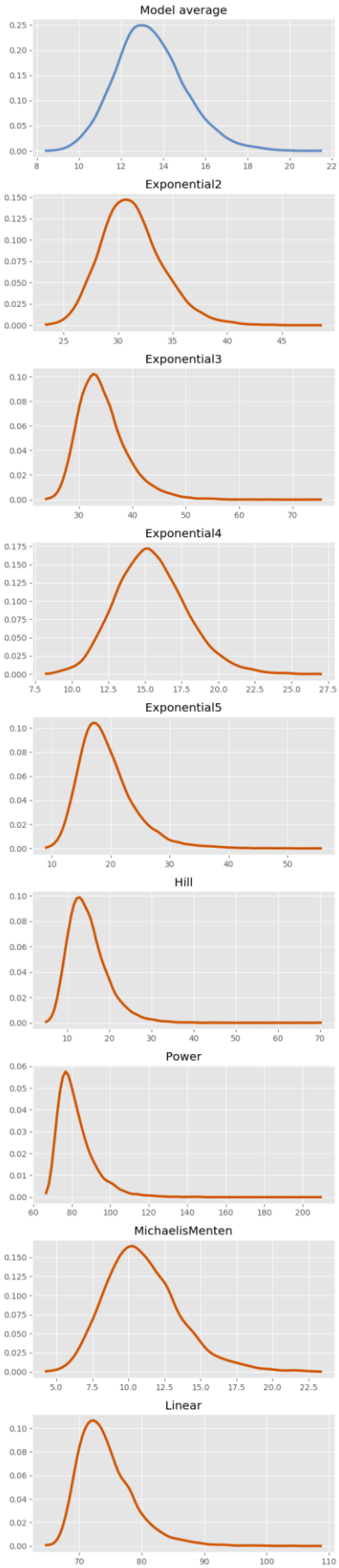
Model average
Exponential2
Exponential3
Exponential4
Exponential5
Hill
Power
MichaelisMenten
Linear

BMD results

50% Central tendency: Relative

BMR: None

Adversity value: 0.500

BMD summary tables:

Statistic	Model average	Exponential2	Exponential3	Exponential4	Exponential5	Hill	Power	Michaelis Menten	Linear
Prior model weight	N/A	0.125	0.125	0.125	0.125	0.125	0.125	0.125	0.125
Posterior model weight	N/A	0.000172	1.08e-05	0.381	0.044	0.079	1.25e-11	0.496	1.98e-10
BMD (median)	48.306	96.437	100.873	51.686	55.961	47.593	190.899	44.414	183.805
BMDL (5th percentile)	39.870	83.972	86.609	39.920	42.539	33.676	175.681	31.290	171.794
25th percentile	44.769	91.079	94.477	46.678	50.334	41.435	183.466	38.721	177.931
Mean (SD)	48.646 (5.659)	97.208 (8.931)	101.969 (10.612)	52.132 (7.967)	56.564 (9.093)	48.483 (10.112)	193.309 (13.799)	45.275 (9.439)	185.903 (11.411)
75th percentile	52.118	102.373	108.394	57.089	62.266	54.379	200.495	50.862	191.673
95th percentile	58.667	113.052	120.841	65.895	72.435	66.623	218.906	62.182	206.871

BMD estimates

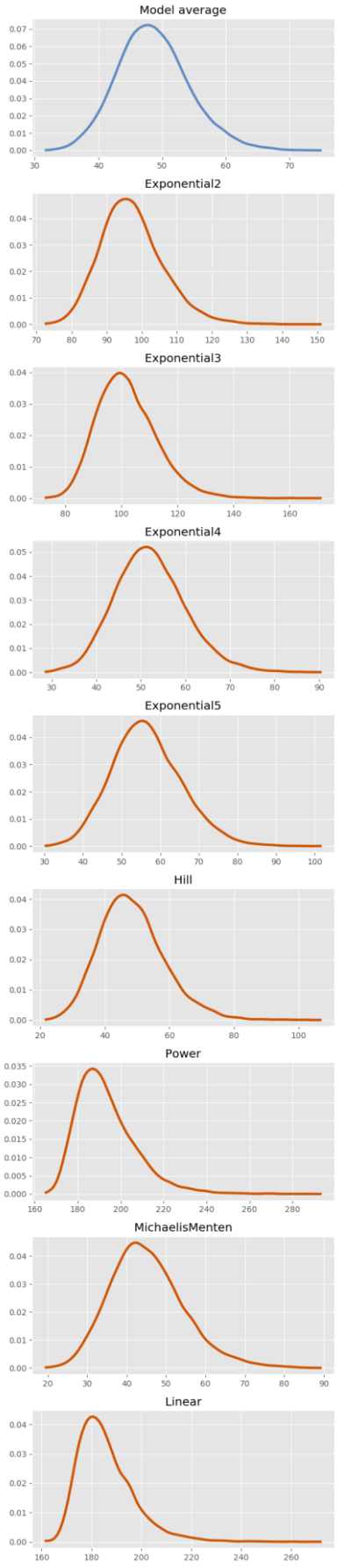
Model average
Exponential2
Exponential3
Exponential4
Exponential5
Hill
Power
MichaelisMenten
Linear

BMD Markov chain Monte Carlo settings

Iterations: 30,000

Number of chains: 1

Warmup fraction: 0.5

Seed: 54,178

Model results

Exponential2

$$f(dose) = a \times e^{b \times dose}$$

Model fit summary

```
Inference for Stan model: exponential2_individual_pkl_be58f7567ba64ec5547642f54ef3b89e.
1 chains, each with iter=30000; warmup=15000; thin=1;
post-warmup draws per chain=15000, total post-warmup draws=15000.

        mean se_mean     sd   2.5%    25%    50%    75%  97.5%  n_eff   Rhat
a       1.61  9.7e-4   0.09   1.43   1.54    1.6   1.67    1.8   9297    1.0
b      -2.27  2.1e-3    0.2  -2.67   -2.4  -2.27  -2.14  -1.87   9072    1.0
sigma   0.34  3.5e-4   0.03   0.28   0.32   0.34   0.36   0.42   9346    1.0
lp__   32.14    0.02   1.25   28.9  31.58  32.47  33.05  33.55   5957    1.0

Samples were drawn using NUTS at Mon Nov  4 20:27:01 2019.
For each parameter, n_eff is a crude measure of effective sample size,
and Rhat is the potential scale reduction factor on split chains (at
convergence, Rhat=1).
```

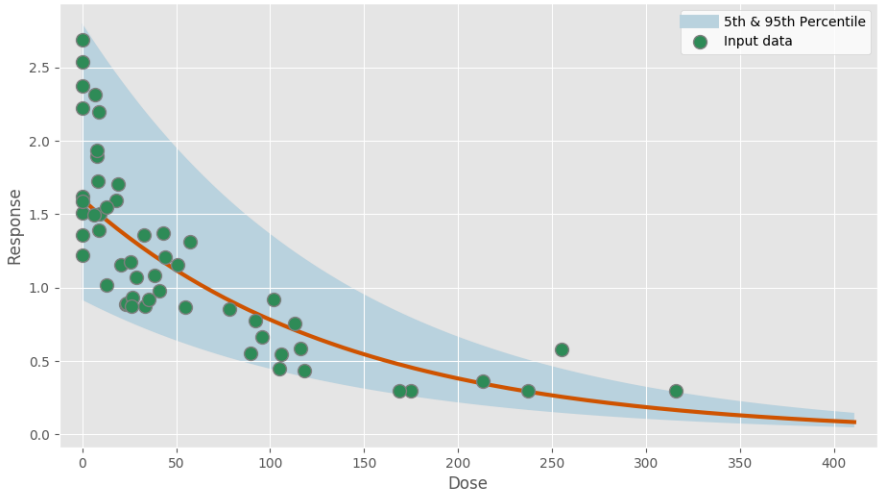

Posterior predictive p-value for model fit: 0.527

Model weight: 0.0%

Correlation matrix

	a	b	sigma
a	-	-0.617	0.035
b	-0.617	-	-0.0242
sigma	0.035	-0.0242	-

Parameter charts

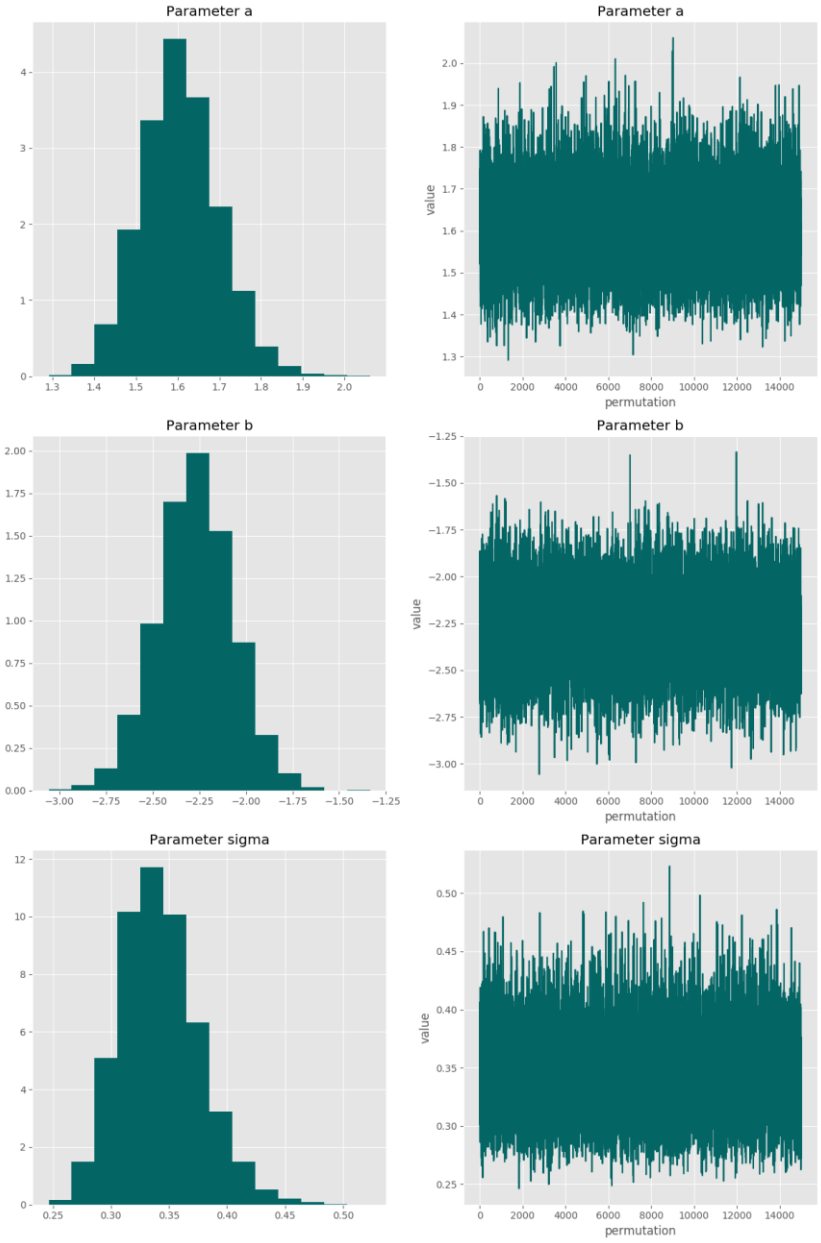

Exponential3

$$f(dose) = a \times e^{b \times dose^{g}}$$

Power parameter lower-bound: 1.000

Model fit summary

```
Inference for Stan model: exponential3_individual_pkl_df53333b36693dd0ad892f92a4fc7532.
1 chains, each with iter=30000; warmup=15000; thin=1;
post-warmup draws per chain=15000, total post-warmup draws=15000.

        mean se_mean     sd   2.5%    25%    50%    75%  97.5%  n_eff   Rhat
a       1.58  1.1e-3    0.1    1.4   1.51   1.58   1.64   1.78   8451    1.0
b      -2.28  2.4e-3   0.22  -2.69  -2.42  -2.27  -2.13  -1.86   8335    1.0
g       1.04  4.2e-4   0.05    1.0   1.01   1.03   1.06   1.17  12669    1.0
sigma   0.35  3.4e-4   0.04   0.29   0.32   0.35   0.37   0.43  10742    1.0
lp__   27.27    0.02   1.53  23.43  26.52  27.62  28.39  29.17   5462    1.0

Samples were drawn using NUTS at Mon Nov  4 20:27:11 2019.
For each parameter, n_eff is a crude measure of effective sample size,
and Rhat is the potential scale reduction factor on split chains (at
convergence, Rhat=1).
```

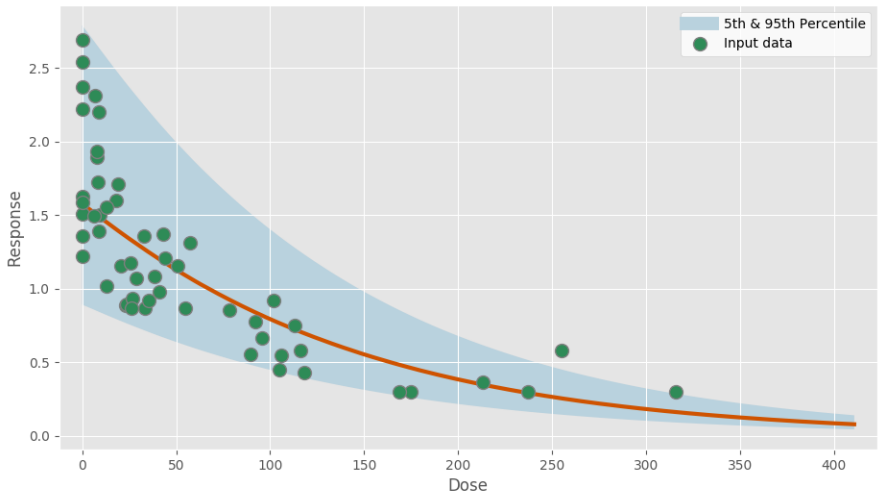

Posterior predictive p-value for model fit: 0.524

Model weight: 0.0%

Correlation matrix

	a	b	g	sigma
a	-	-0.585	-0.251	-0.045
b	-0.585	-	-0.0241	-0.00867
g	-0.251	-0.0241	-	0.200
sigma	-0.045	-0.00867	0.200	-

Parameter charts

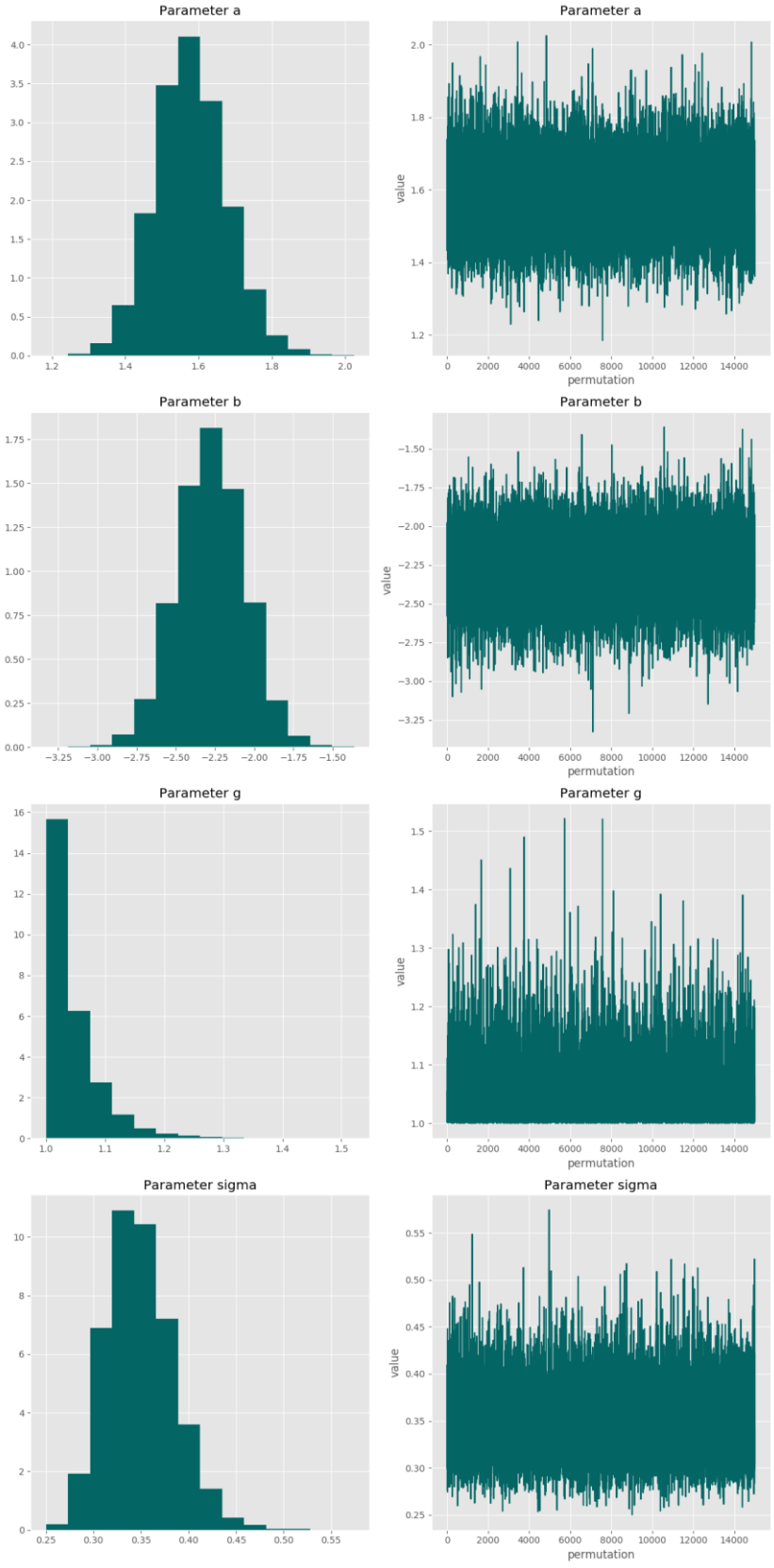

Exponential4

$$f(dose) = a \times [c - (c - 1) \times e^{-b \times dose}]$$

Model fit summary

```
Inference for Stan model: exponential4_individual_pkl_fa67b4bb1853dd3a882bdb66cdb5191d.
1 chains, each with iter=30000; warmup=15000; thin=1;
post-warmup draws per chain=15000, total post-warmup draws=15000.

        mean se_mean     sd   2.5%    25%    50%    75%  97.5%  n_eff   Rhat
a       1.89  1.3e-3   0.12   1.67   1.81   1.89   1.97   2.15   8477    1.0
b        5.9    0.01   1.06   4.12   5.17    5.8   6.51   8.28   7275    1.0
c       0.18  3.0e-4   0.03   0.13   0.16   0.18    0.2   0.24   9411    1.0
sigma   0.29  2.8e-4   0.03   0.24   0.27   0.28    0.3   0.35  10433    1.0
lp__   42.26    0.02    1.5  38.49  41.51  42.61  43.36  44.11   5590    1.0

Samples were drawn using NUTS at Mon Nov  4 20:27:20 2019.
For each parameter, n_eff is a crude measure of effective sample size,
and Rhat is the potential scale reduction factor on split chains (at
convergence, Rhat=1).
```

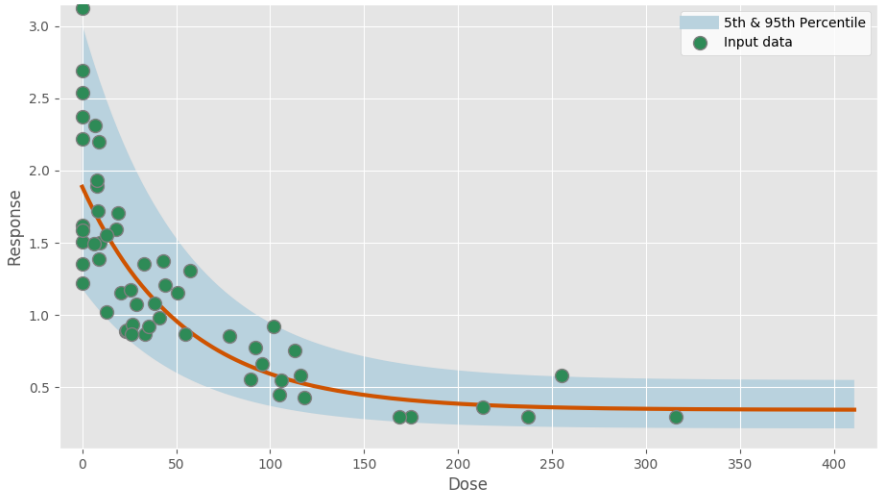

Posterior predictive p-value for model fit: 0.530

Model weight: 38.1%

Correlation matrix

	a	b	c	sigma
a	-	0.604	-0.105	0.040
b	0.604	-	0.522	0.079
c	-0.105	0.522	-	0.047
sigma	0.040	0.079	0.047	-

Parameter charts

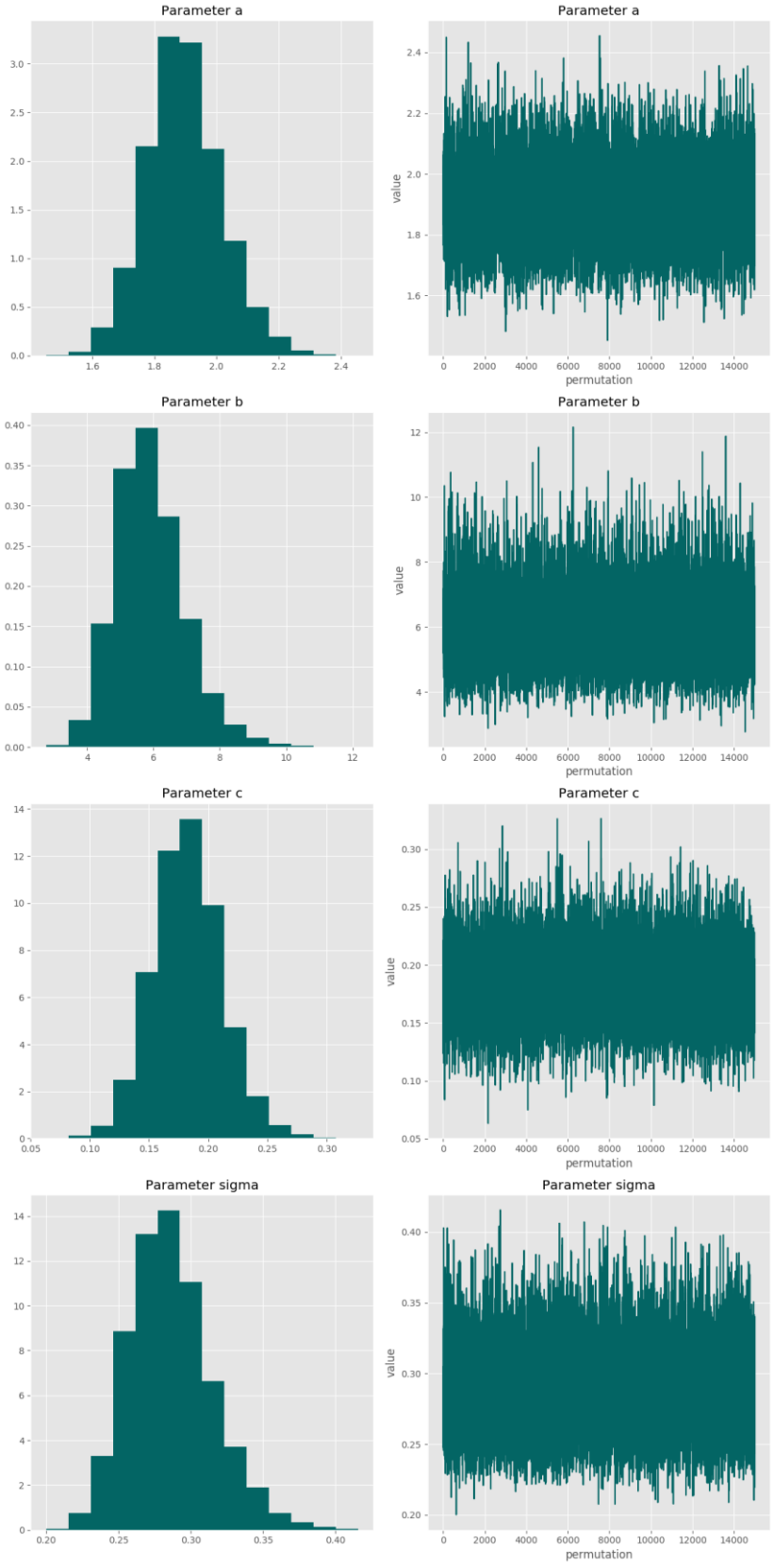

Exponential5

$$f(dose) = a \times [c - (c - 1) \times e^{-(b \times dose)^g}]$$

Power parameter lower-bound: 1.000

Model fit summary

```
Inference for Stan model: exponential5_individual_pkl_0fe35d8b796f8736b80743a2674317fc.
1 chains, each with iter=30000; warmup=15000; thin=1;
post-warmup draws per chain=15000, total post-warmup draws=15000.

        mean se_mean     sd   2.5%    25%    50%    75%  97.5%  n_eff   Rhat
a       1.83  1.3e-3   0.13   1.59   1.75   1.83   1.91   2.09   9377    1.0
b       5.61    0.01    1.0   3.99   4.91   5.49   6.16    7.9   9078    1.0
c        0.2  3.4e-4   0.03   0.14   0.17   0.19   0.22   0.26   9014    1.0
g       1.14  1.5e-3   0.14    1.0   1.04    1.1   1.19   1.52   8847    1.0
sigma   0.29  2.8e-4   0.03   0.24   0.27   0.29   0.31   0.36  10801    1.0
lp__   38.84    0.02   1.73   34.6  37.95   39.2  40.11  41.11   4996    1.0

Samples were drawn using NUTS at Mon Nov  4 20:27:34 2019.
For each parameter, n_eff is a crude measure of effective sample size,
and Rhat is the potential scale reduction factor on split chains (at
convergence, Rhat=1).
```

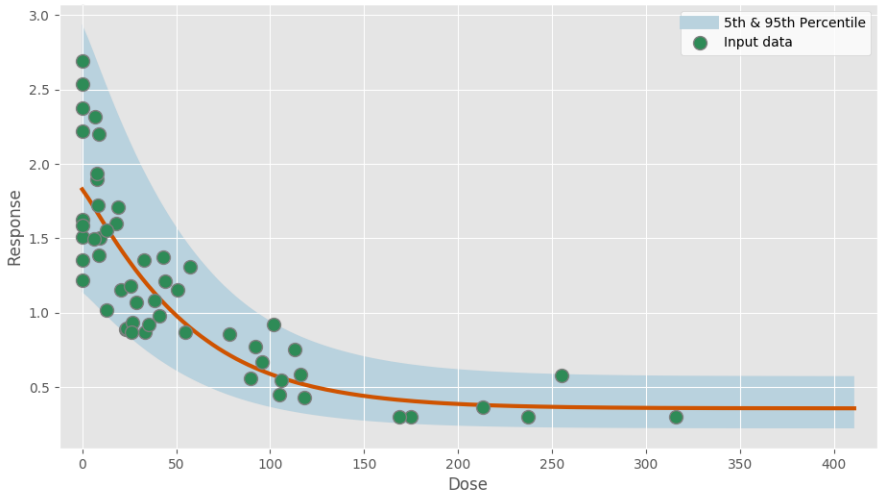

Posterior predictive p-value for model fit: 0.523

Model weight: 4.4%

Correlation matrix

	a	b	c	g	sigma
a	-	0.618	-0.252	-0.404	-0.0382
b	0.618	-	0.371	-0.245	0.026
c	-0.252	0.371	-	0.349	0.088
g	-0.404	-0.245	0.349	-	0.161

sigma	-0.0382	0.026	0.088	0.161	-

Parameter charts

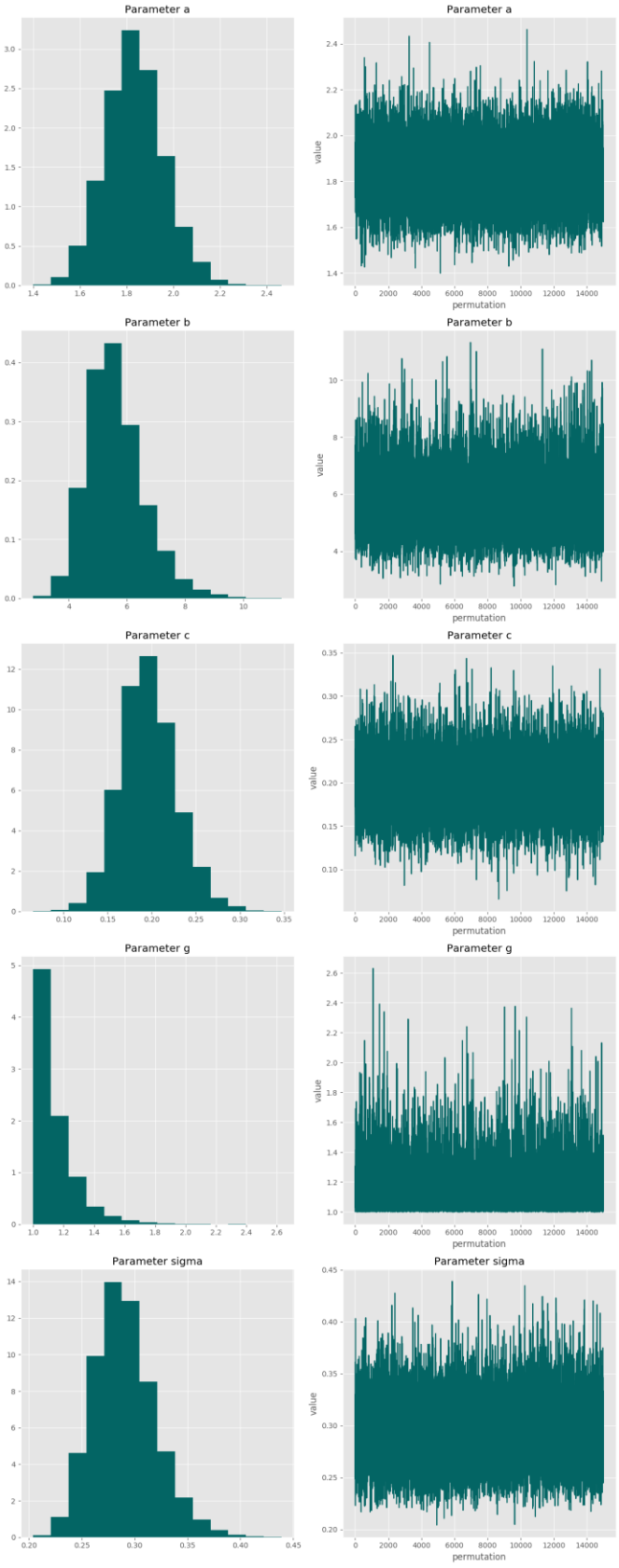

Hill

$$f(dose) = a + \frac{b \times dose^g}{c^g + dose^g}$$

Power parameter lower-bound: 1.000

Model fit summary

```
Inference for Stan model: hill_individual_pkl_f14f62088318f1a4663f986868dc9b40.
1 chains, each with iter=30000; warmup=15000; thin=1;
post-warmup draws per chain=15000, total post-warmup draws=15000.

        mean se_mean     sd   2.5%    25%    50%    75%  97.5%  n_eff   Rhat
a       1.92  2.1e-3   0.15   1.64   1.82   1.91   2.02   2.23   5174    1.0
b      -1.74  2.5e-3   0.18  -2.09  -1.86  -1.74  -1.62  -1.38   5041    1.0
c       0.13  4.2e-4   0.03   0.08   0.11   0.13   0.15   0.21   6737    1.0
g       1.26  4.5e-3   0.27   1.01   1.09    1.2   1.36   1.84   3639    1.0
sigma   0.29  3.2e-4   0.03   0.24   0.27   0.28   0.31   0.35   8534    1.0
lp__    38.2    0.03    1.8  33.78  37.26  38.57  39.53  40.55   3755    1.0

Samples were drawn using NUTS at Mon Nov  4 20:28:03 2019.
For each parameter, n_eff is a crude measure of effective sample size,
and Rhat is the potential scale reduction factor on split chains (at
convergence, Rhat=1).
```

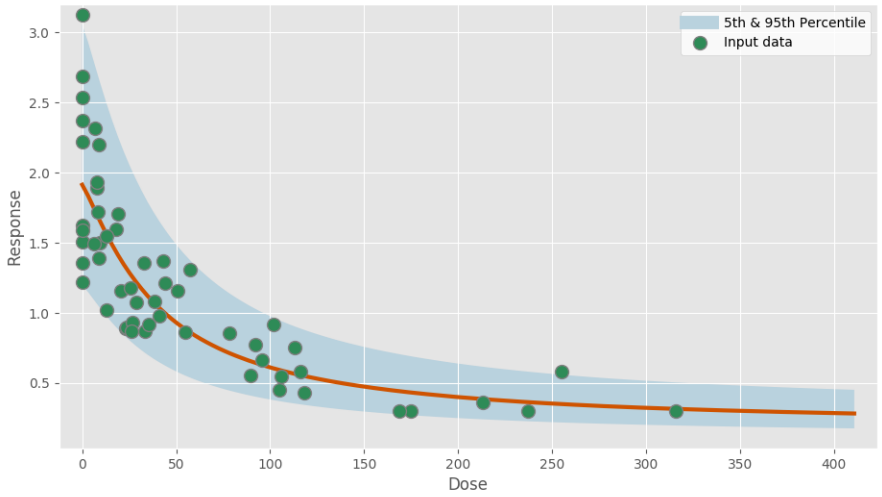

Posterior predictive p-value for model fit: 0.533

Model weight: 7.9%

Correlation matrix

	a	b	c	g	sigma
a	-	-0.808	-0.661	-0.331	-0.0719
b	-0.808	-	0.195	0.597	0.097
c	-0.661	0.195	-	0.069	0.078
g	-0.331	0.597	0.069	-	0.145

sigma	-0.0719	0.097	0.078	0.145	-

Parameter charts

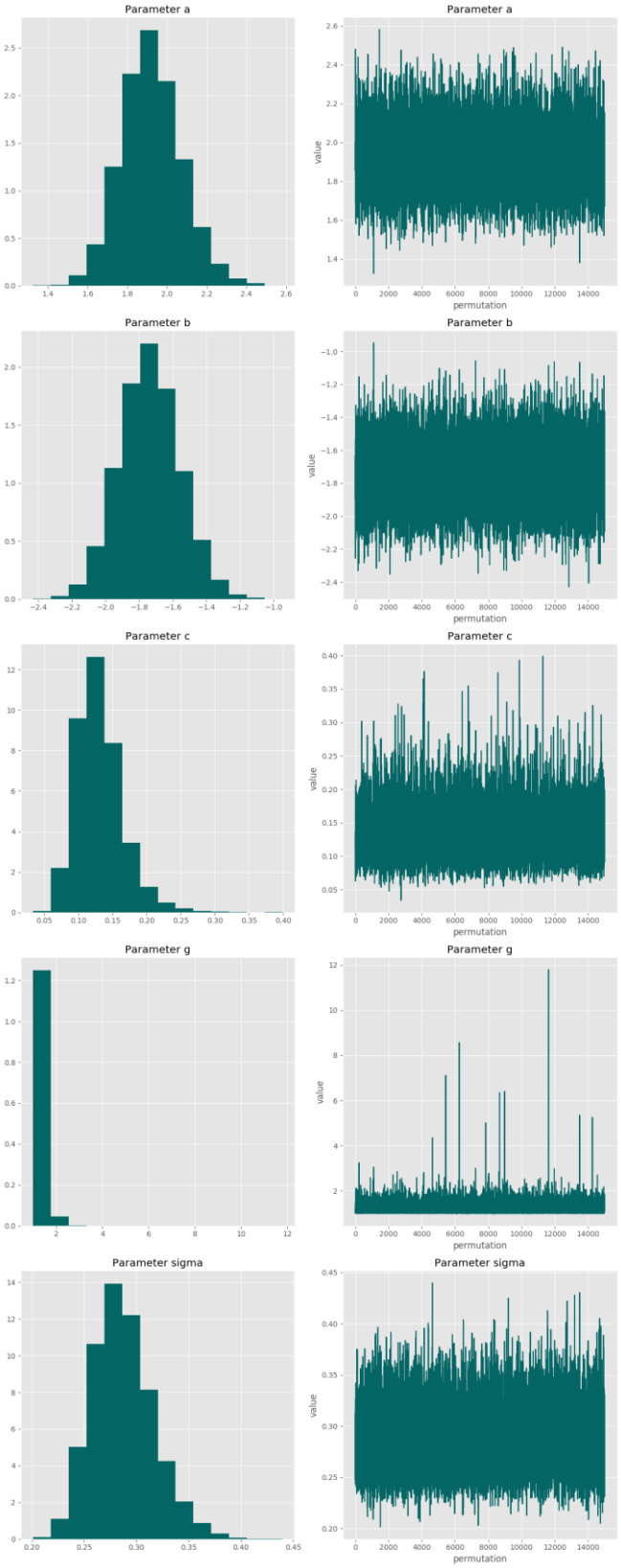

Power

$$f(dose) = a + b \times dose^{g}$$

Power parameter lower-bound: 1.000

Model fit summary

```
Inference for Stan model: power_individual_pkl_8682a4681cf39e692df770d4639a86e2.
1 chains, each with iter=30000; warmup=15000; thin=1;
post-warmup draws per chain=15000, total post-warmup draws=15000.

        mean se_mean     sd   2.5%    25%    50%    75%  97.5%  n_eff   Rhat
a       1.31  1.1e-3   0.08   1.15   1.25   1.31   1.37   1.48   5551    1.0
b      -1.11  1.5e-3   0.11  -1.33  -1.19  -1.12  -1.04  -0.89   5481    1.0
g       1.08  1.0e-3    0.1    1.0   1.02   1.05    1.1   1.31   9553    1.0
sigma   0.45  4.7e-4   0.04   0.37   0.41   0.44   0.47   0.54   8796    1.0
lp__   14.13    0.02    1.5  10.36   13.4  14.47  15.21  15.99   4937    1.0

Samples were drawn using NUTS at Mon Nov  4 20:28:15 2019.
For each parameter, n_eff is a crude measure of effective sample size,
and Rhat is the potential scale reduction factor on split chains (at
convergence, Rhat=1).
```

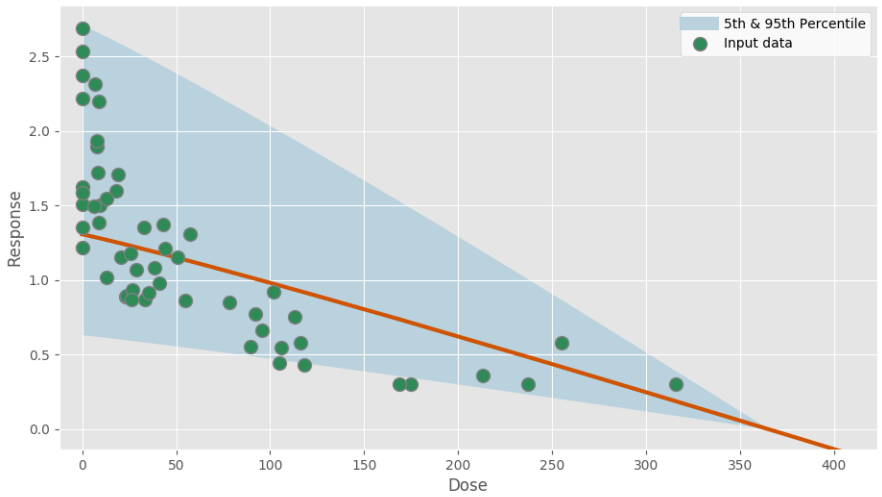

Posterior predictive p-value for model fit: 0.528

Model weight: 0.0%

Correlation matrix

	a	b	g	sigma
a	-	-0.824	-0.219	-0.0166
b	-0.824	-	0.193	0.056
g	-0.219	0.193	-	0.200
sigma	-0.0166	0.056	0.200	-

Parameter charts

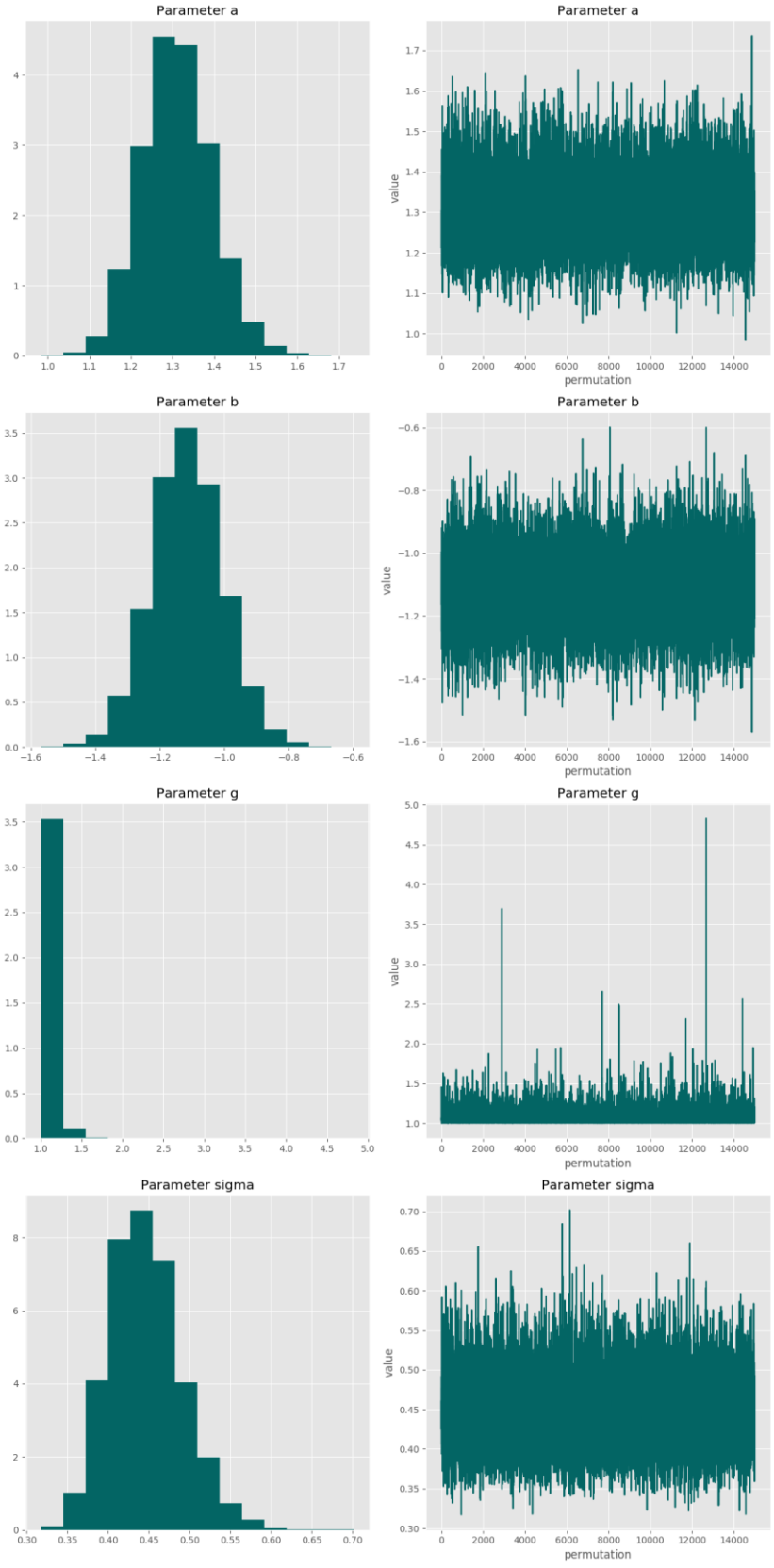

MichaelisMenten

$$f(dose) = a + \frac{b \times dose}{c + dose}$$

Model fit summary

```
Inference for Stan model:
michaelismenten_individual_pkl_8a1ee8a1062ea9c00f6bd83f5c89e8d5.
1 chains, each with iter=30000; warmup=15000; thin=1;
post-warmup draws per chain=15000, total post-warmup draws=15000.

        mean se_mean     sd    2.5%    25%    50%    75%  97.5%  n_eff   Rhat
a       1.99  1.9e-3   0.15    1.72   1.89   1.98   2.08   2.29   6067    1.0
b      -1.92  1.6e-3   0.14   -2.19  -2.01  -1.91  -1.83  -1.65   7247    1.0
c       0.14  4.6e-4   0.04    0.08   0.11   0.13   0.16   0.23   7331    1.0
sigma   0.28  3.1e-4   0.03    0.23   0.26   0.28    0.3   0.35   8131    1.0
lp__   40.62    0.02   1.45   37.02   39.9  40.95  41.69  42.42   5356    1.0

Samples were drawn using NUTS at Mon Nov  4 20:28:27 2019.
For each parameter, n_eff is a crude measure of effective sample size,
and Rhat is the potential scale reduction factor on split chains (at
convergence, Rhat=1).
```

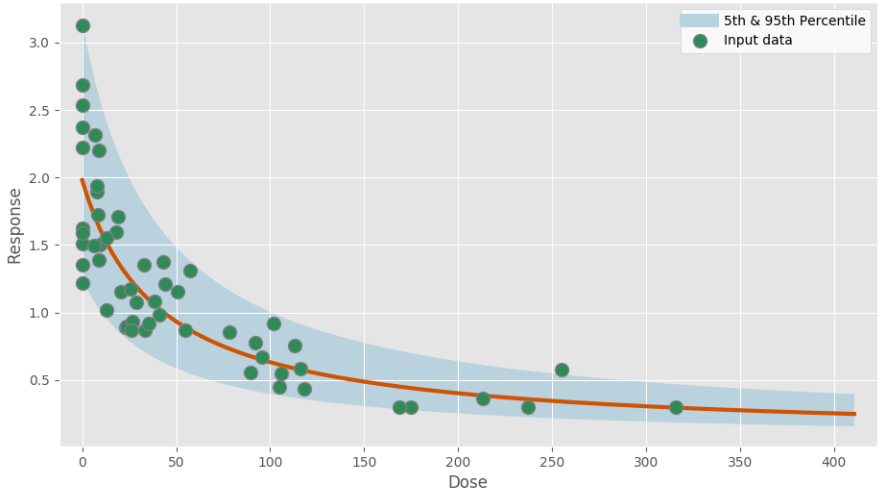

Posterior predictive p-value for model fit: 0.528

Model weight: 49.6%

Correlation matrix

	a	b	c	sigma
a	-	-0.777	-0.712	-0.0238
b	-0.777	-	0.173	0.005
c	-0.712	0.173	-	0.069
sigma	-0.0238	0.005	0.069	-

Parameter charts

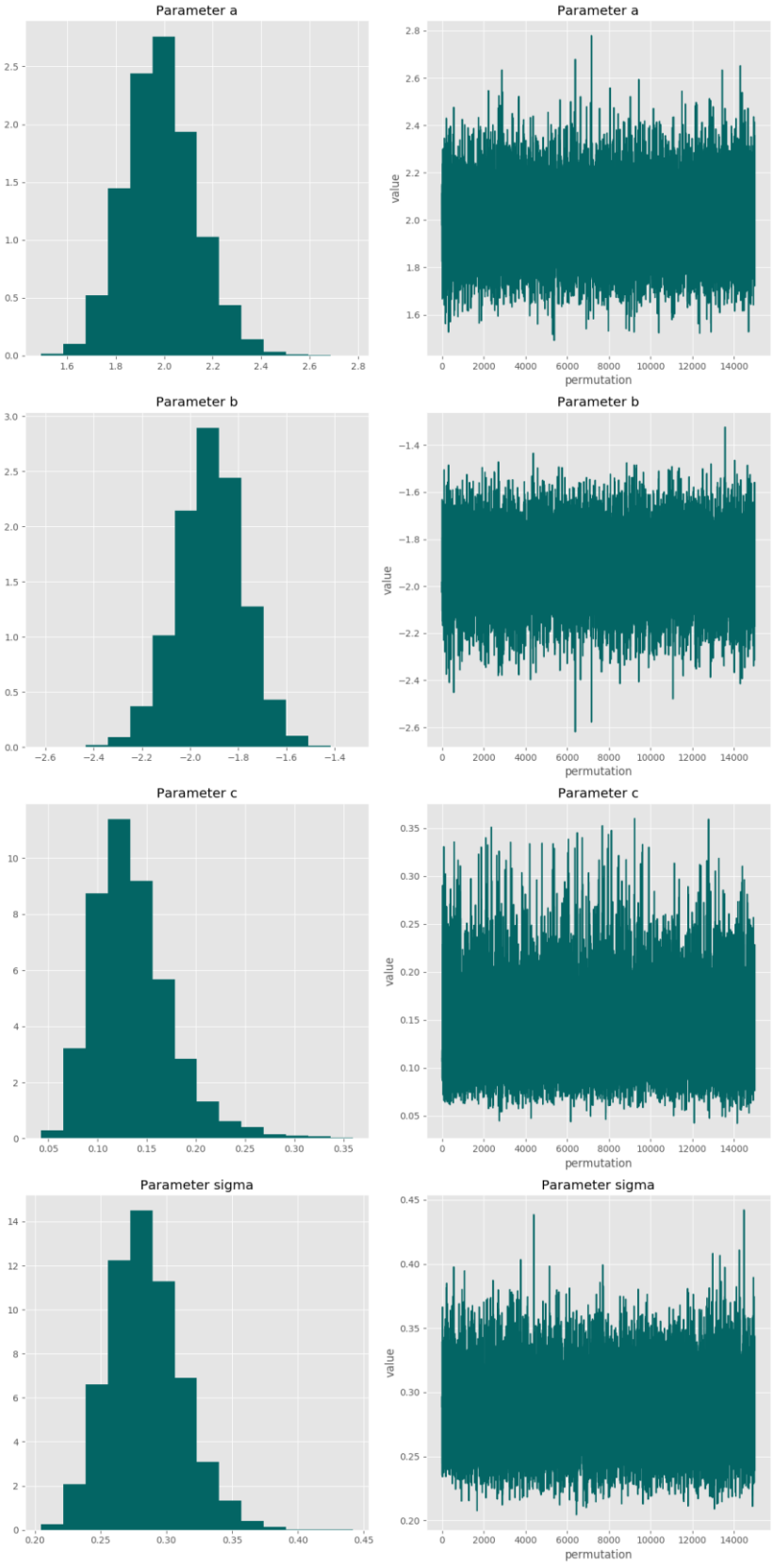

Linear

$$f(dose) = a + b \times dose$$

Model fit summary

```
Inference for Stan model: linear_individual_pkl_6f560bd3666c0b0a5c004ccddf0ad3ca.
1 chains, each with iter=30000; warmup=15000; thin=1;
post-warmup draws per chain=15000, total post-warmup draws=15000.

        mean se_mean     sd   2.5%    25%    50%    75%  97.5%  n_eff   Rhat
a       1.33  1.1e-3   0.08   1.17   1.27   1.33   1.38    1.5   5907    1.0
b      -1.13  1.5e-3   0.11  -1.34  -1.21  -1.14  -1.06  -0.91   5533    1.0
sigma   0.44  4.9e-4   0.04   0.36   0.41   0.43   0.46   0.53   7753    1.0
lp__   18.49    0.02    1.3  15.18  17.93  18.82  19.43  19.94   4258    1.0

Samples were drawn using NUTS at Mon Nov  4 20:28:36 2019.
For each parameter, n_eff is a crude measure of effective sample size,
and Rhat is the potential scale reduction factor on split chains (at
convergence, Rhat=1).
```

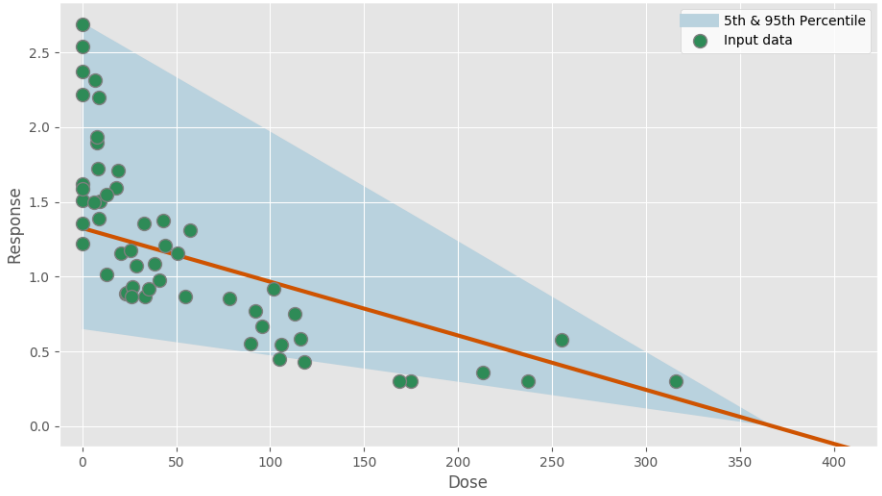

Posterior predictive p-value for model fit: 0.525

Model weight: 0.0%

Correlation matrix

	a	b	sigma
a	-	-0.826	0.013
b	-0.826	-	0.028
sigma	0.013	0.028	-

Parameter charts

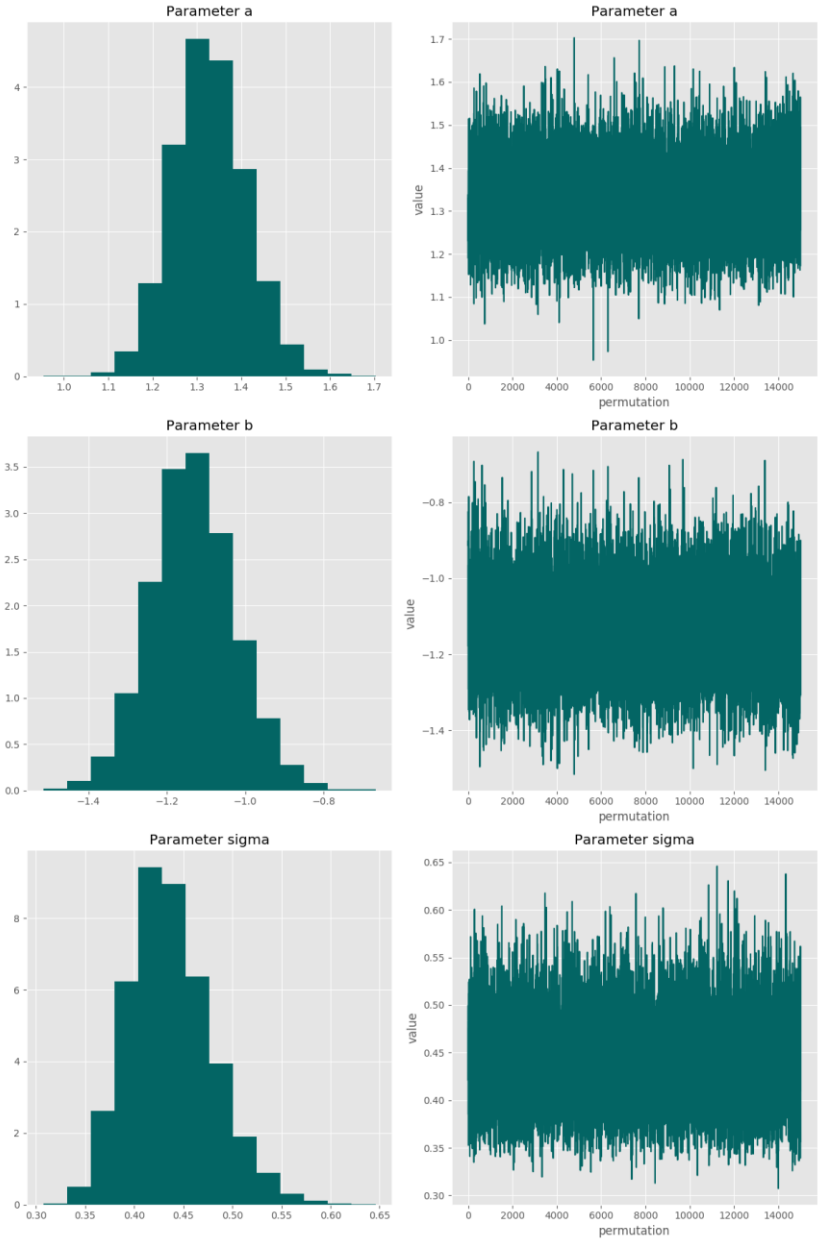

PFOA Rel Lv Wt 5% Jul 29 2019, 11:43 AM

Report created on Jul 31, 2019 at 04:30 PM.

Pystan model version 2.19.0.0.

Dataset

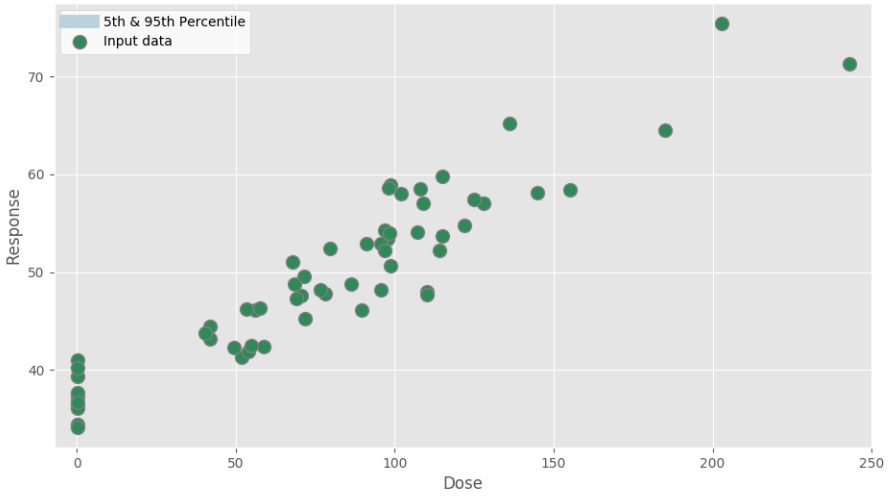

Dose	Response
0.11	34.47543966
0.0772	37.31301939
0.119	36.40167364
0.0904	36.09383833
0.122	34.13642053
0.117	37.70789235
0.0833	40.97507532
0.104	39.37899013
0.0727	36.68327796
0.0807	40.23619885
41.9	43.15484805
51.7	41.26848692
56.0	46.16317865
57.6	46.30325815
49.5	42.24489796
41.9	44.41890166
58.9	42.37612921
54.1	41.91438763
40.3	43.7240971
55.0	42.51162791
71.4	49.56546929
70.7	47.62951334

78.1	47.81445138
67.8	51.02967898
69.2	47.33268671
76.6	48.21802935
53.4	46.20826259
89.7	46.13686534
86.2	48.73873874
71.7	45.28532194
110.0	47.97687861
96.9	54.23675024
97.9	53.40192499
102.0	58.02130898
68.4	48.73737374
95.5	52.86956522
98.4	53.97590361
79.6	52.3796034
110.0	47.68618944
95.6	48.20143885
91.0	52.889766
115.0	53.67887995
98.6	58.86206897
98.6	50.65394132
108.0	58.50362558
128.0	57.03408267
107.0	54.06749556
122.0	54.73751601
114.0	52.24948875
125.0	57.38396624
98.0	58.58617454
155.0	58.37988827
136.0	65.16641452
185.0	64.53971419
203.0	75.41484716
109.0	57.00712589
96.7	52.22490514
145.0	58.08547009
115.0	59.80191257
243.0	71.28540305

BMD Markov chain Monte Carlo settings

Iterations: 30,000

Number of chains: 1

Warmup fraction: 0.5

Seed: 2,969

BMD results

Central tendency: Relative 5%

BMR: None

Adversity value: 0.050

BMD summary tables:

Statistic	Model average	Linear	Power	Hill	Exponential2	Exponential3	Exponential4	Exponential5
Prior model weight	N/A	0.143	0.143	0.143	0.143	0.143	0.143	0.143
Posterior model weight	N/A	**0.642**	**0.122**	0.029	0.085	0.006	0.088	0.029
BMD (median)	12.719	11.684	14.670	16.271	15.365	16.569	11.056	17.557
BMDL (5th percentile)	11.815	10.570	11.741	11.677	14.146	14.772	9.686	12.220
25th percentile	12.337	11.210	13.186	14.109	14.826	15.724	10.505	14.904
Mean (SD)	12.748 (0.600)	11.728 (0.752)	15.050 (2.498)	16.761 (3.683)	15.400 (0.811)	16.858 (1.646)	11.073 (0.871)	18.095 (4.237)
75th percentile	13.137	12.191	16.505	18.888	15.921	17.651	11.620	20.633
95th percentile	13.781	13.036	19.730	23.519	16.808	19.966	12.523	25.928

BMD estimates

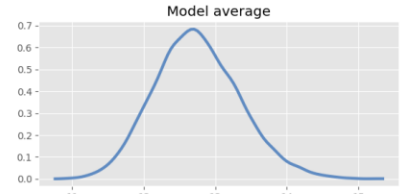

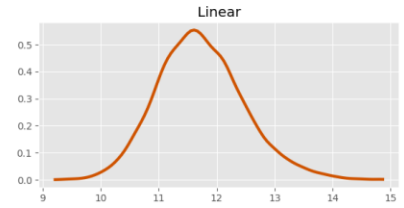

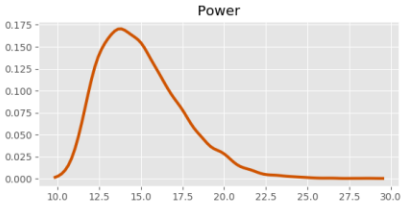

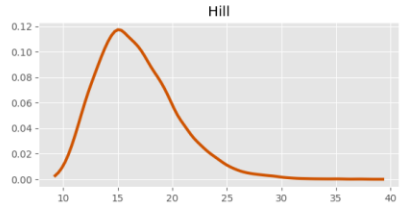

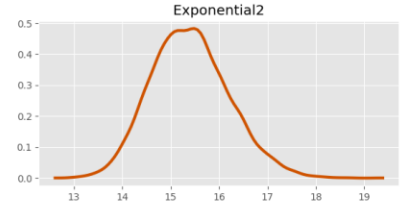

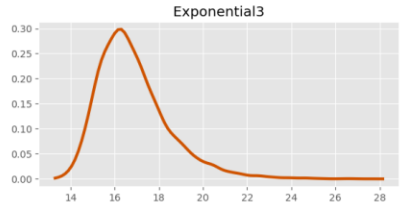

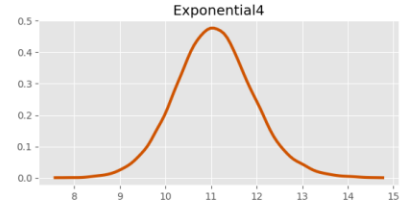

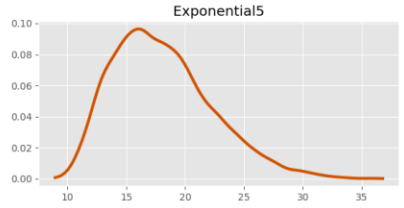

Model results

Linear

$$f(dose) = a + b \times dose$$

Model fit summary

```
Inference for Stan model: linear_individual_pkl_6f560bd3666c0b0a5c004ccddf0ad3ca.
1 chains, each with iter=30000; warmup=15000; thin=1;
post-warmup draws per chain=15000, total post-warmup draws=15000.

        mean se_mean     sd   2.5%    25%    50%    75%  97.5%  n_eff   Rhat
a      36.88  7.9e-3   0.62  35.68  36.46  36.87  37.29  38.13   6249    1.0
b      38.33    0.02    1.9  34.53  37.08  38.34  39.59  42.02   6258    1.0
sigma   0.06  6.3e-5 5.9e-3   0.05   0.06   0.06   0.07   0.08   8840    1.0
lp__  138.13    0.02   1.26 134.85 137.58 138.47 139.04 139.55   6057    1.0

Samples were drawn using NUTS at Mon Jul 29 17:38:26 2019.
For each parameter, n_eff is a crude measure of effective sample size,
and Rhat is the potential scale reduction factor on split chains (at
convergence, Rhat=1).
```

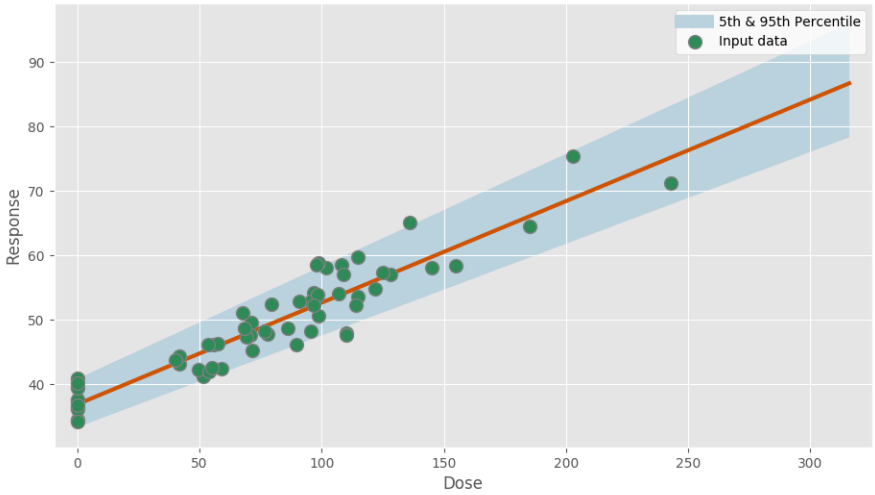

Posterior predictive p-value for model fit: 0.526

Model weight: 64.2%

Correlation matrix

	a	b	sigma
a	-	-0.789	0.013
b	-0.789	-	-0.00219
sigma	0.013	-0.00219	-

Parameter charts

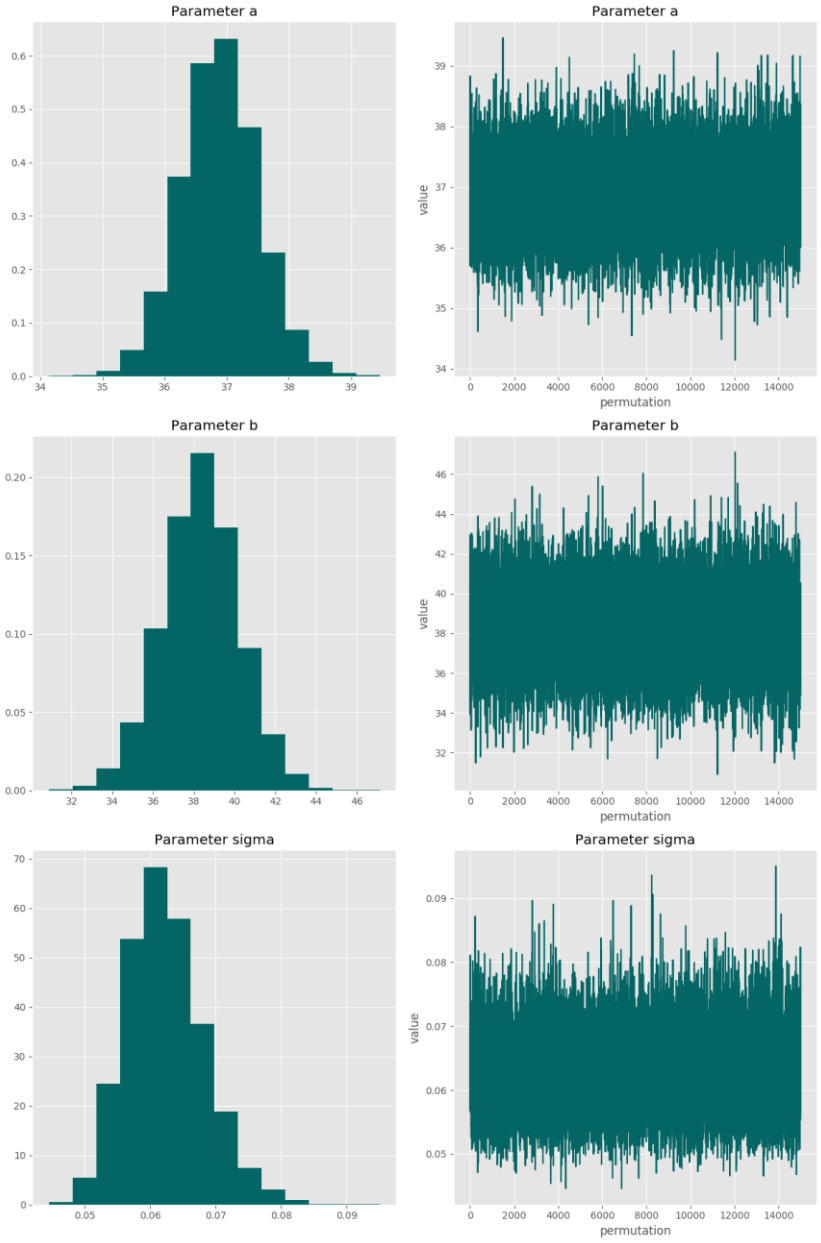

Power

$$f(dose) = a + b \times dose^{g}$$

Power parameter lower-bound: 1.000

Model fit summary

```
Inference for Stan model: power_individual_pkl_8682a4681cf39e692df770d4639a86e2.
1 chains, each with iter=30000; warmup=15000; thin=1;
post-warmup draws per chain=15000, total post-warmup draws=15000.

        mean se_mean     sd   2.5%    25%    50%    75%  97.5%  n_eff   Rhat
a       37.3  7.6e-3   0.69  35.98  36.83  37.29  37.75  38.69   8308    1.0
b       40.5    0.03   2.43  36.03  38.82  40.39  42.04  45.63   7309    1.0
g        1.1  8.6e-4   0.07   1.01   1.05   1.09   1.15   1.26   6661    1.0
sigma   0.06  6.4e-5 5.9e-3   0.05   0.06   0.06   0.07   0.08   8748    1.0
lp__  135.37    0.02    1.5 131.56 134.61 135.71 136.49 137.29   4641    1.0

Samples were drawn using NUTS at Mon Jul 29 17:38:40 2019.
For each parameter, n_eff is a crude measure of effective sample size,
and Rhat is the potential scale reduction factor on split chains (at
convergence, Rhat=1).
```

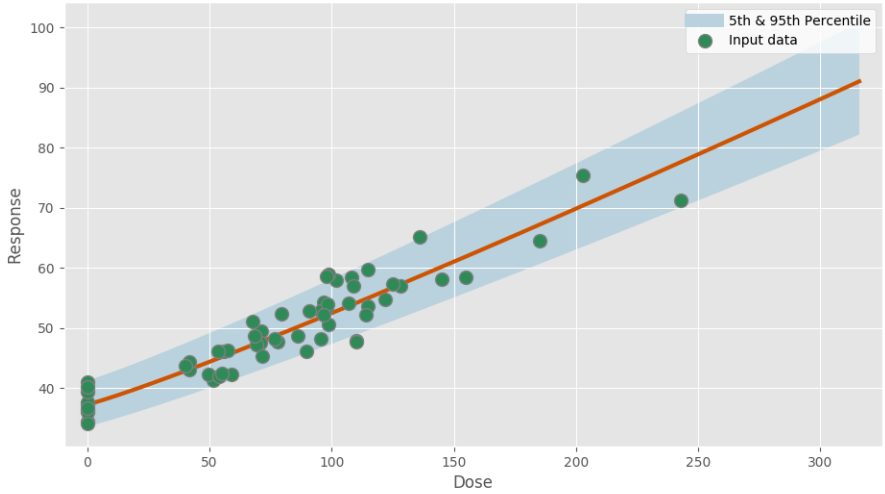

Posterior predictive p-value for model fit: 0.529

Model weight: 12.2%

Correlation matrix

	a	b	g	sigma
a	-	-0.335	0.445	0.043
b	-0.335	-	0.552	0.060
g	0.445	0.552	-	0.106
sigma	0.043	0.060	0.106	-

Parameter charts

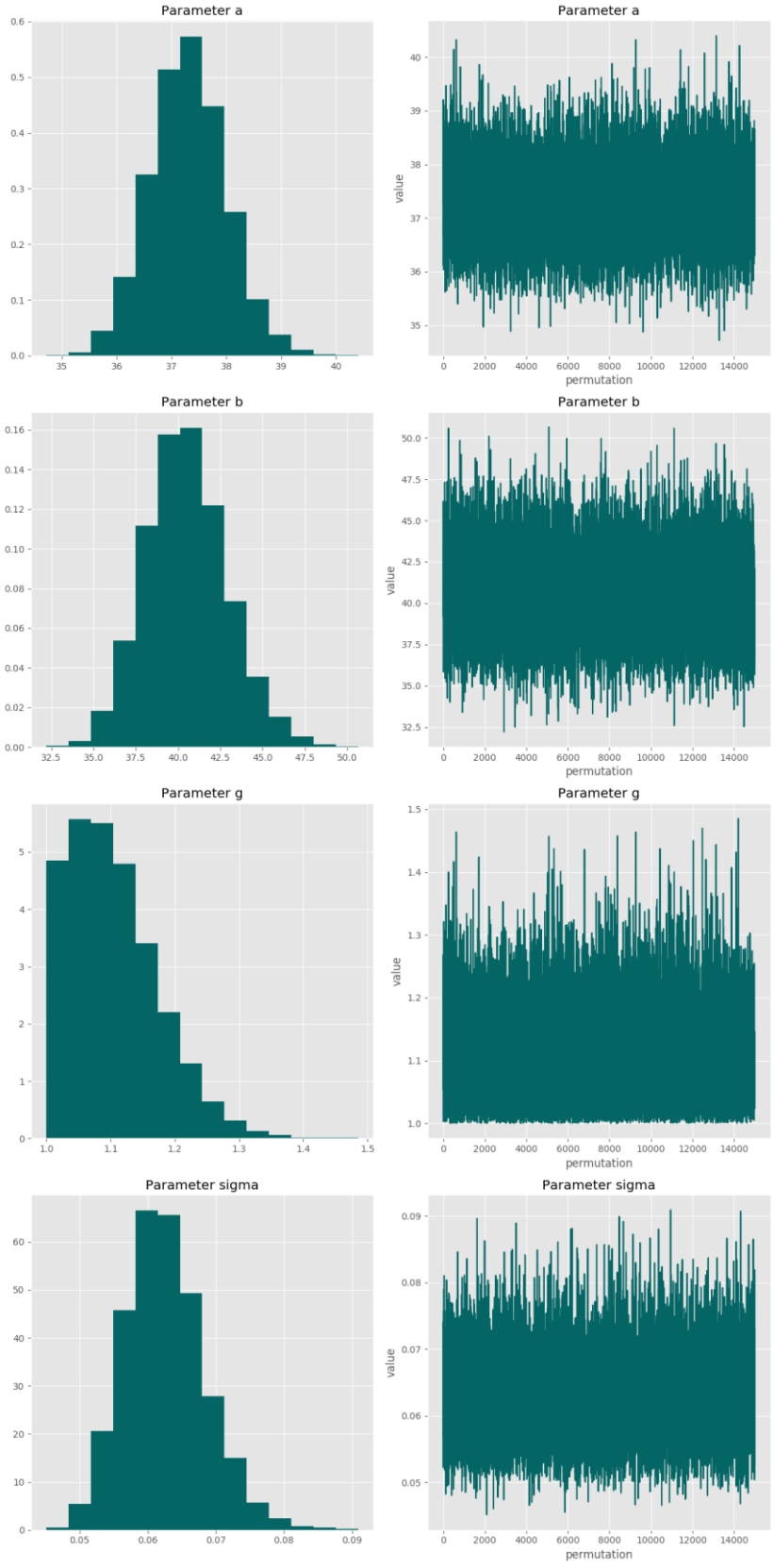

Hill

$$f(dose) = a + \frac{b \times dose^g}{c^g + dose^g}$$

Power parameter lower-bound: 1.000

Model fit summary

```
Inference for Stan model: hill_individual_pkl_f14f62088318f1a4663f986868dc9b40.
1 chains, each with iter=30000; warmup=15000; thin=1;
post-warmup draws per chain=15000, total post-warmup draws=15000.

        mean se_mean     sd   2.5%    25%    50%    75%  97.5%  n_eff   Rhat
a      37.26    0.01   0.71   35.9  36.78  37.24  37.74   38.7   3605    1.0
b     161.16    1.58  55.82  54.27 116.93 166.85 209.19 243.58   1242    1.0
c       2.74    0.04   1.18   0.72    1.8   2.74    3.6   5.05   1070    1.0
g       1.25  3.7e-3   0.16   1.03   1.13   1.22   1.32   1.68   1993    1.0
sigma   0.06  9.5e-5 5.9e-3   0.05   0.06   0.06   0.07   0.07   3826    1.0
lp__  137.68    0.03   1.57 133.78 136.88 138.03 138.85 139.67   2576    1.0

Samples were drawn using NUTS at Mon Jul 29 17:39:36 2019.
For each parameter, n_eff is a crude measure of effective sample size,
and Rhat is the potential scale reduction factor on split chains (at
convergence, Rhat=1).
```

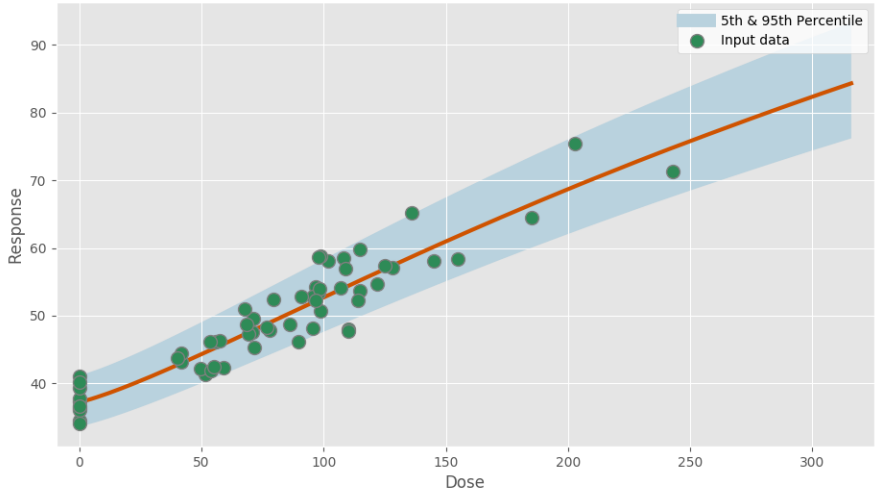

Posterior predictive p-value for model fit: 0.524

Model weight: 2.9%

Correlation matrix

	a	b	c	g	sigma
a	-	-0.0707	-0.103	0.329	0.044
b	-0.0707	-	0.930	-0.653	0.027
c	-0.103	0.930	-	-0.765	0.023
g	0.329	-0.653	-0.765	-	0.000605

sigma	0.044	0.027	0.023	0.000605	-

Parameter charts

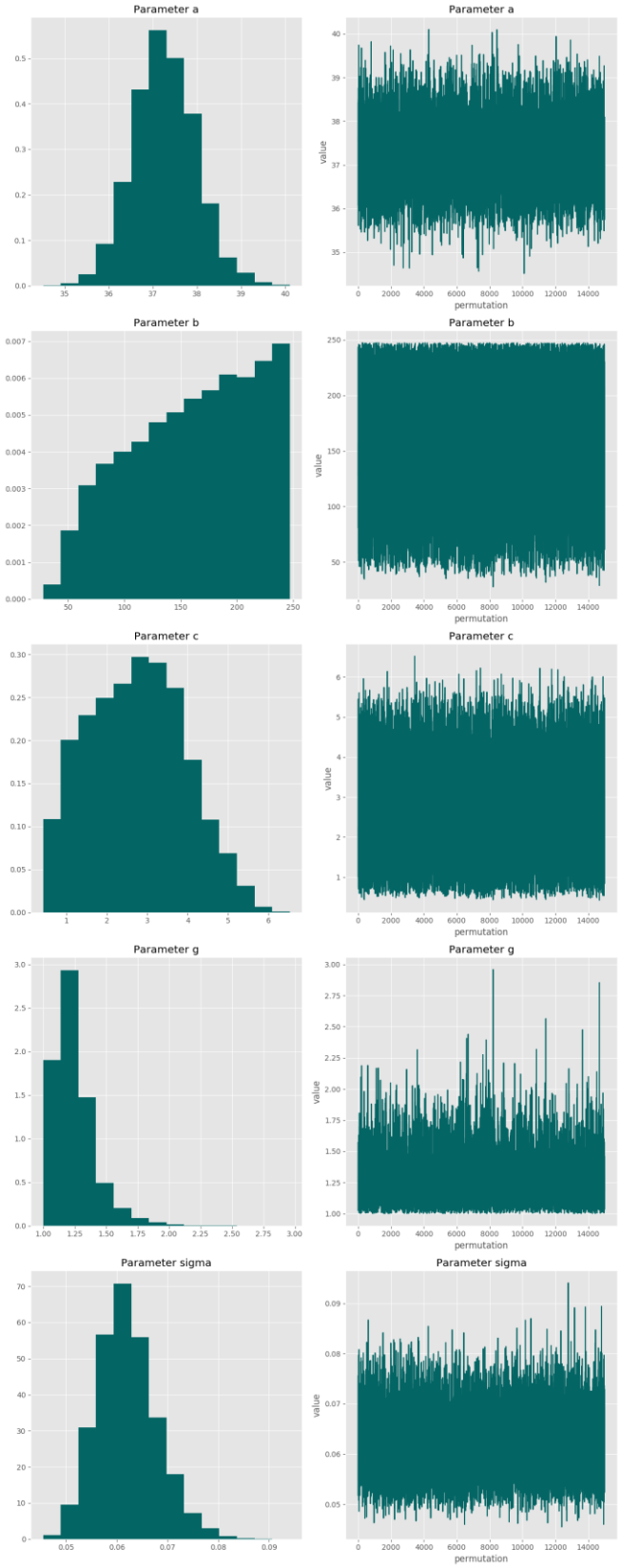

Exponential2

$$f(dose) = a \times e^{b \times dose}$$

Model fit summary

```
Inference for Stan model: exponential2_individual_pkl_be58f7567ba64ec5547642f54ef3b89e.
1 chains, each with iter=30000; warmup=15000; thin=1;
post-warmup draws per chain=15000, total post-warmup draws=15000.

        mean se_mean     sd    2.5%    25%    50%    75%  97.5%  n_eff   Rhat
a      37.88  7.9e-3    0.6   36.72  37.48  37.88  38.28  39.07   5649    1.0
b       0.77  5.3e-4   0.04    0.69   0.74   0.77    0.8   0.85   5908    1.0
sigma   0.06  6.6e-5 6.1e-3    0.05   0.06   0.06   0.07   0.08   8530    1.0
lp__  135.69    0.02   1.24  132.54  135.1 136.01  136.6 137.11   5497    1.0

Samples were drawn using NUTS at Mon Jul 29 17:39:45 2019.
For each parameter, n_eff is a crude measure of effective sample size,
and Rhat is the potential scale reduction factor on split chains (at
convergence, Rhat=1).
```

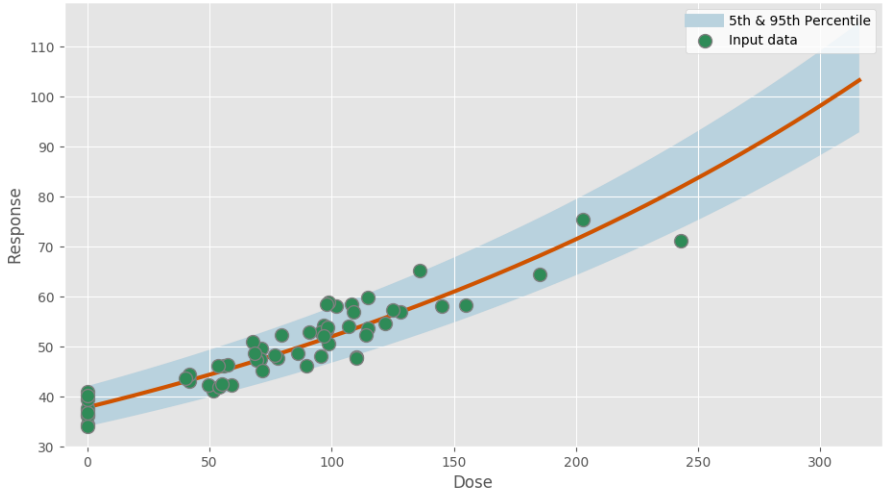

Posterior predictive p-value for model fit: 0.527

Model weight: 8.5%

Correlation matrix

	a	b	sigma
a	-	-0.843	-0.00207
b	-0.843	-	-0.00255
sigma	-0.00207	-0.00255	-

Parameter charts

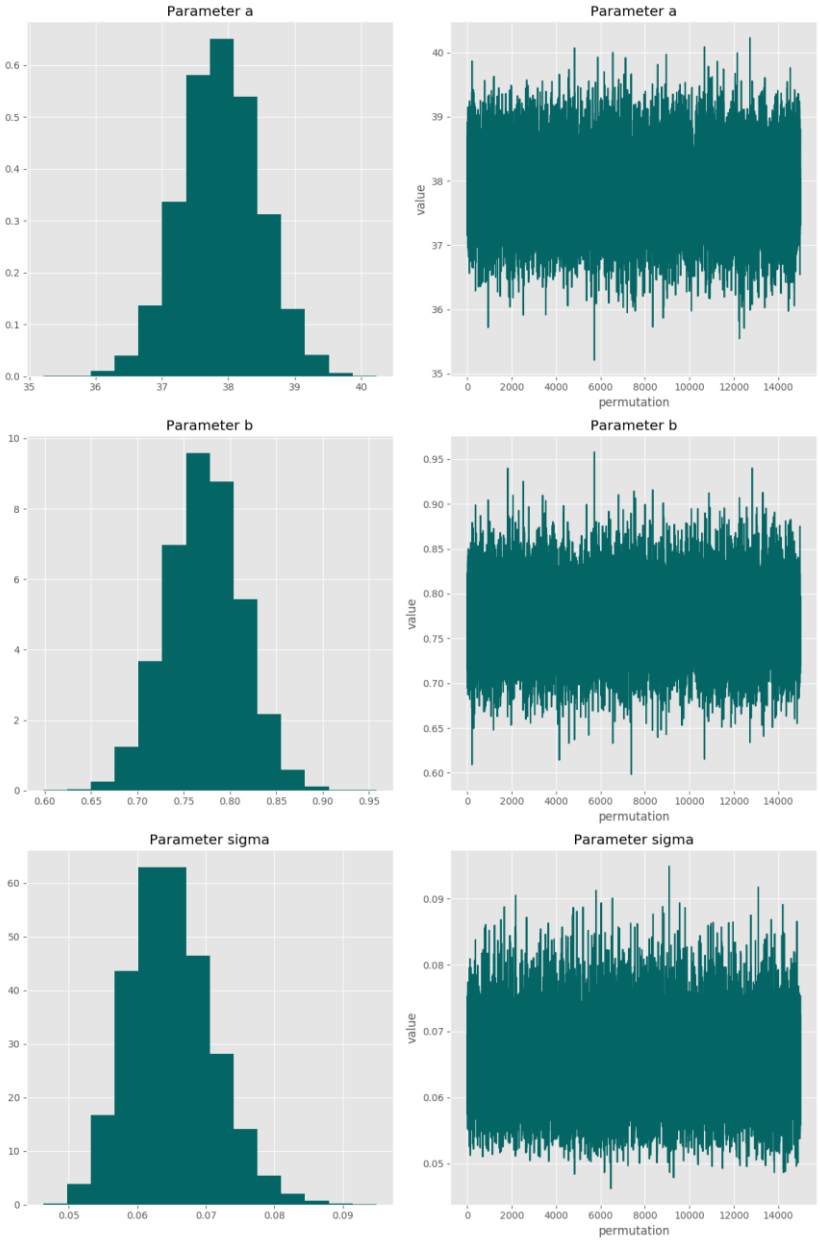

Exponential3

$$f(dose) = a \times e^{b \times dose^{g}}$$

Power parameter lower-bound: 1.000

Model fit summary

```
Inference for Stan model: exponential3_individual_pkl_df53333b36693dd0ad892f92a4fc7532.
1 chains, each with iter=30000; warmup=15000; thin=1;
post-warmup draws per chain=15000, total post-warmup draws=15000.

        mean se_mean     sd   2.5%    25%    50%    75%  97.5%  n_eff   Rhat
a       38.1  7.3e-3   0.62  36.89  37.68  38.08  38.52  39.37   7382    1.0
b       0.78  4.8e-4   0.04    0.7   0.75   0.78   0.81   0.86   7383    1.0
g       1.04  3.6e-4   0.03    1.0   1.01   1.03   1.05   1.13   9492    1.0
sigma   0.07  6.5e-5 6.4e-3   0.05   0.06   0.07   0.07   0.08   9815    1.0
lp__  130.91    0.02   1.49 127.14 130.16 131.25 132.01 132.77   4464    1.0

Samples were drawn using NUTS at Mon Jul 29 17:39:57 2019.
For each parameter, n_eff is a crude measure of effective sample size,
and Rhat is the potential scale reduction factor on split chains (at
convergence, Rhat=1).
```

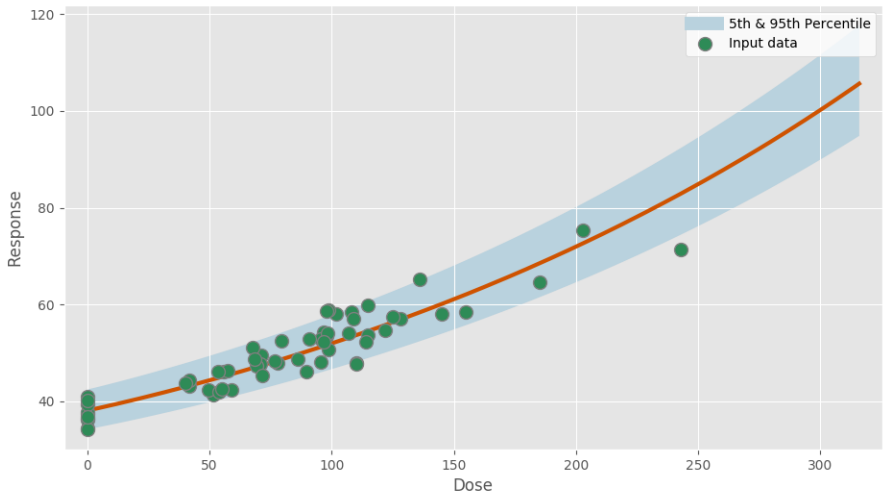

Posterior predictive p-value for model fit: 0.528

Model weight: 0.6%

Correlation matrix

	a	b	g	sigma
a	-	-0.737	0.321	0.059
b	-0.737	-	0.138	0.005
g	0.321	0.138	-	0.158
sigma	0.059	0.005	0.158	-

Parameter charts

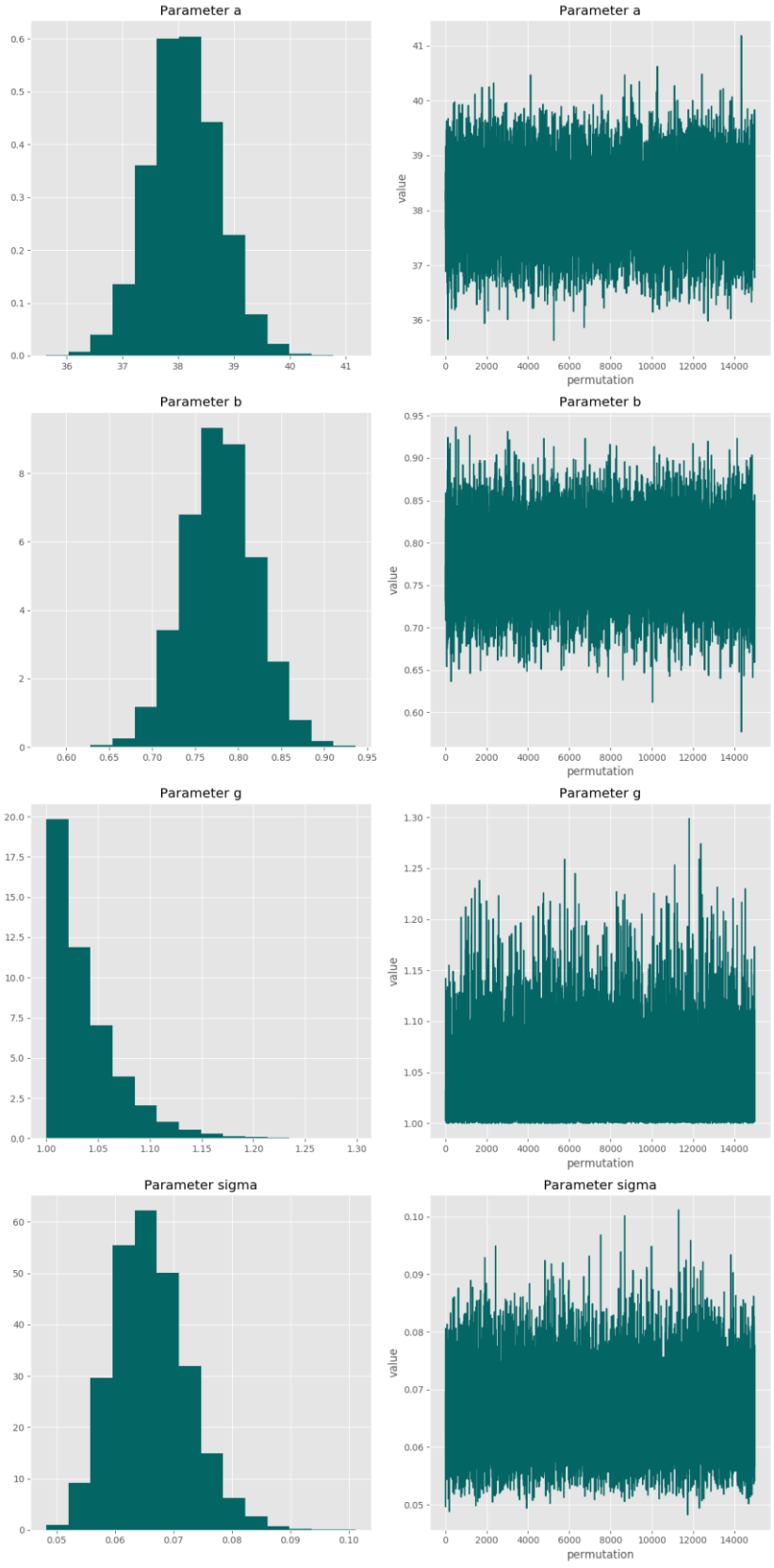

Exponential4

$$f(dose) = a \times [c - (c - 1) \times e^{-b \times dose}]$$

Model fit summary

```
Inference for Stan model: exponential4_individual_pkl_fa67b4bb1853dd3a882bdb66cdb5191d.
1 chains, each with iter=30000; warmup=15000; thin=1;
post-warmup draws per chain=15000, total post-warmup draws=15000.

        mean se_mean     sd    2.5%    25%    50%    75%  97.5%  n_eff   Rhat
a      36.74    0.01   0.66   35.46  36.29  36.73  37.17  38.06   3711    1.0
b       0.22  3.0e-3   0.15    0.08   0.11   0.17   0.27   0.62   2499    1.0
c        8.0    0.08    3.4    2.99   5.12   7.52  10.66  14.56   1656    1.0
sigma   0.06  8.8e-5 6.0e-3    0.05   0.06   0.06   0.07   0.08   4676    1.0
lp__  137.87    0.02   1.35  134.41 137.24  138.2 138.87 139.48   3790    1.0

Samples were drawn using NUTS at Mon Jul 29 17:40:27 2019.
For each parameter, n_eff is a crude measure of effective sample size,
and Rhat is the potential scale reduction factor on split chains (at
convergence, Rhat=1).
```

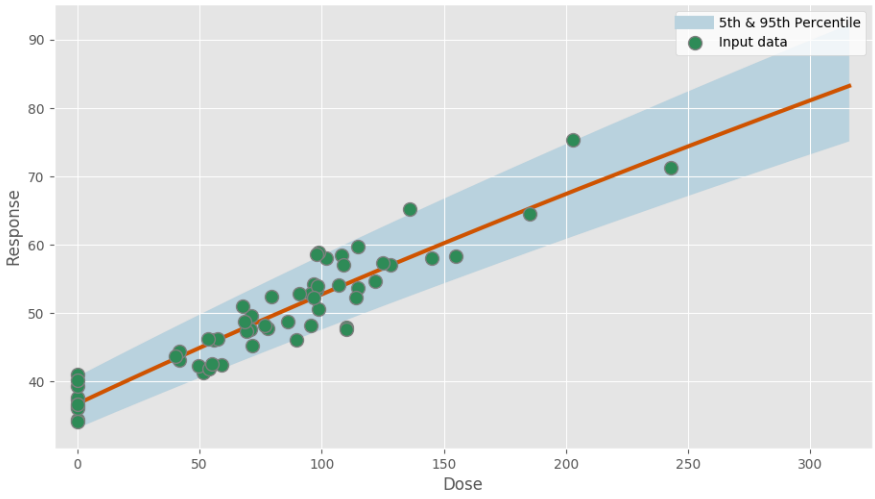

Posterior predictive p-value for model fit: 0.525

Model weight: 8.8%

Correlation matrix

	a	b	c	sigma
a	-	-0.2	0.122	0.004
b	-0.2	-	-0.812	0.096
c	0.122	-0.812	-	-0.0793
sigma	0.004	0.096	-0.0793	-

Parameter charts

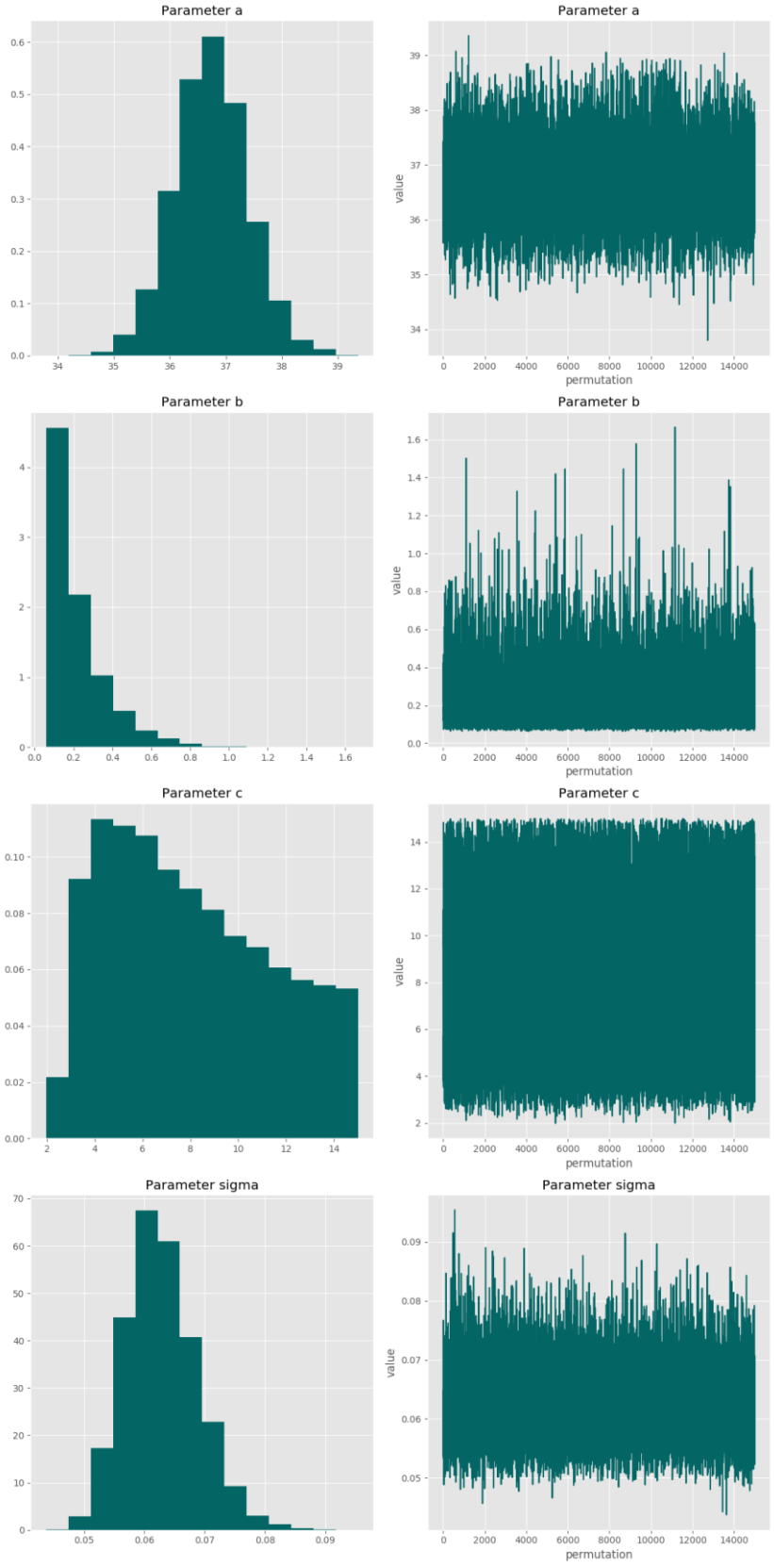

Exponential5

$$f(dose) = a \times [c - (c - 1) \times e^{-(b \times dose)^g}]$$

Power parameter lower-bound: 1.000

Model fit summary

```
Inference for Stan model: exponential5_individual_pkl_0fe35d8b796f8736b80743a2674317fc.
1 chains, each with iter=30000; warmup=15000; thin=1;
post-warmup draws per chain=15000, total post-warmup draws=15000.

        mean se_mean     sd   2.5%    25%    50%    75%  97.5%  n_eff   Rhat
a      37.29    0.01   0.71  35.92  36.81  37.28  37.76  38.72   4943    1.0
b       0.84    0.01   0.54   0.12   0.34   0.77   1.28   1.92   1855    1.0
c       4.32    0.09   3.03   1.87   2.26   2.99    5.2   13.1   1228    1.0
g       1.31  4.3e-3    0.2   1.03   1.15   1.26   1.43    1.8   2305    1.0
sigma   0.06  8.1e-5 6.0e-3   0.05   0.06   0.06   0.07   0.08   5484    1.0
lp__  137.79    0.04   1.83 133.52 136.77 137.99 139.15 140.53   2400    1.0

Samples were drawn using NUTS at Mon Jul 29 17:41:35 2019.
For each parameter, n_eff is a crude measure of effective sample size,
and Rhat is the potential scale reduction factor on split chains (at
convergence, Rhat=1).
```

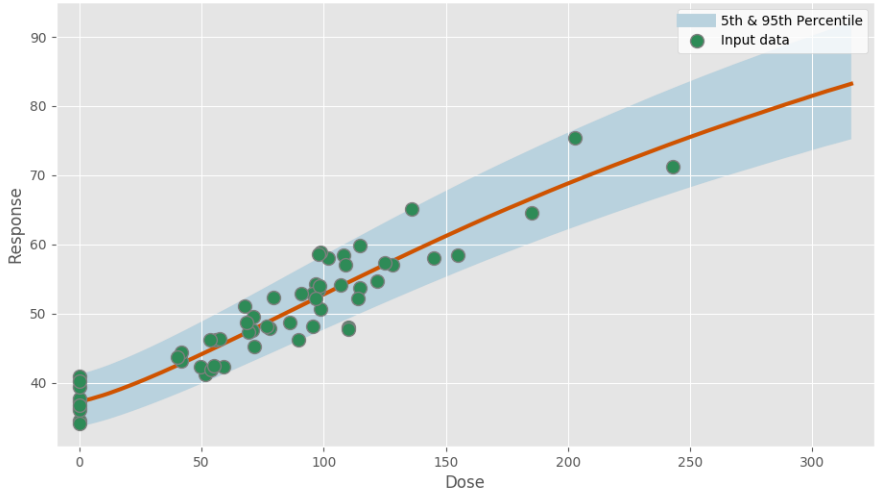

Posterior predictive p-value for model fit: 0.527

Model weight: 2.9%

Correlation matrix

	a	b	c	g	sigma
a	-	0.072	-0.0305	0.318	0.007
b	0.072	-	-0.762	0.857	-0.0147
c	-0.0305	-0.762	-	-0.561	0.050
g	0.318	0.857	-0.561	-	0.012

sigma	0.007	-0.0147	0.050	0.012	-

Parameter charts

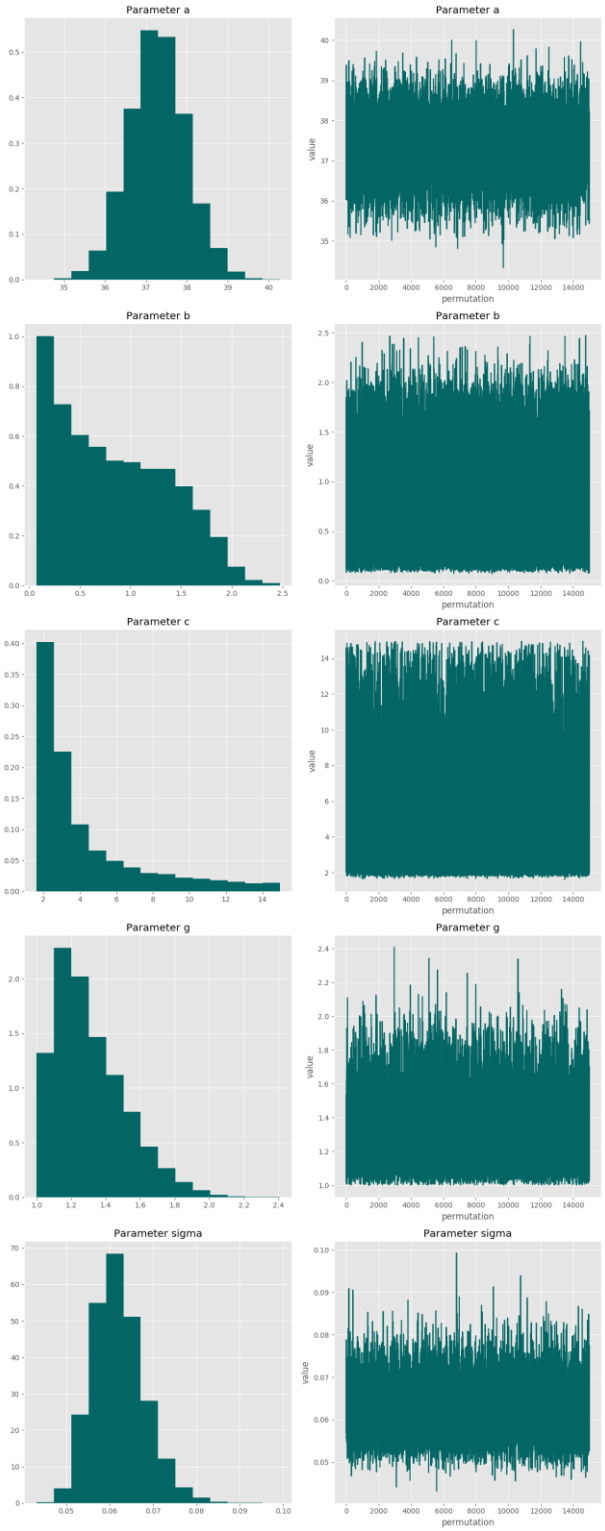

Central tendency: Relative 10%

BMR: None

Adversity value: 0.100

BMD estimates

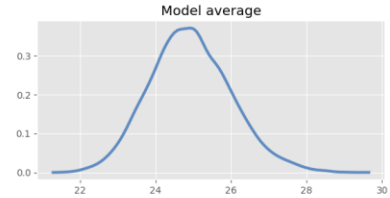

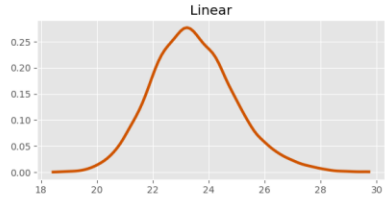

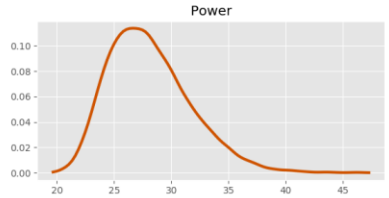

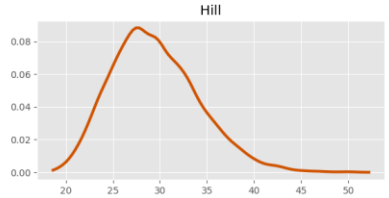

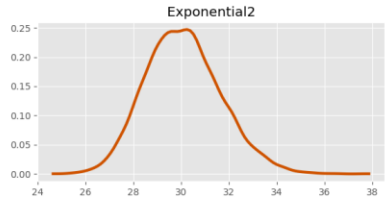

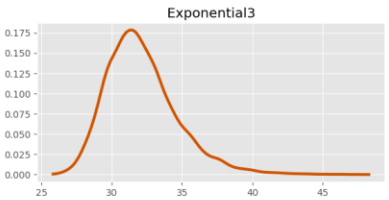

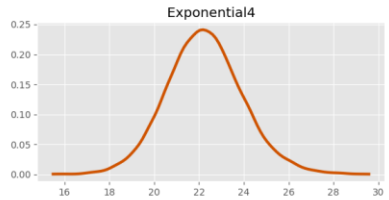

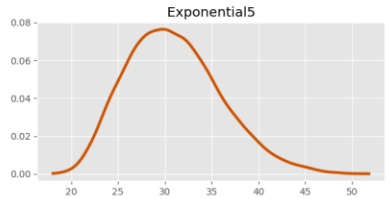

BMD summary tables:

Statistic	Model average	Linear	Power	Hill	Exponential2	Exponential3	Exponential4	Exponential5
Prior model weight	N/A	0.143	0.143	0.143	0.143	0.143	0.143	0.143
Posterior model weight	N/A	0.642	0.122	0.029	0.085	0.006	0.088	0.029
BMD (median)	24.884	23.368	27.663	29.052	30.015	31.791	22.212	30.563
BMDL (5th percentile)	23.207	21.139	23.126	22.674	27.633	28.656	19.528	23.500
25th percentile	24.179	22.420	25.468	26.149	28.963	30.366	21.120	27.253
Mean (SD)	24.925 (1.094)	23.455 (1.505)	28.114 (3.596)	29.482 (4.638)	30.084 (1.585)	32.135 (2.541)	22.252 (1.722)	30.980 (5.047)
75th percentile	25.630	24.382	30.254	32.422	31.102	33.466	23.333	34.226
95th percentile	26.801	26.073	34.670	37.763	32.833	36.784	25.148	39.905

PFOS Rel Liv Wt Jul 30 2019, 05:30 PM

Report created on Jul 31, 2019 at 04:34 PM.

Pystan model version 2.19.0.0.

Dataset

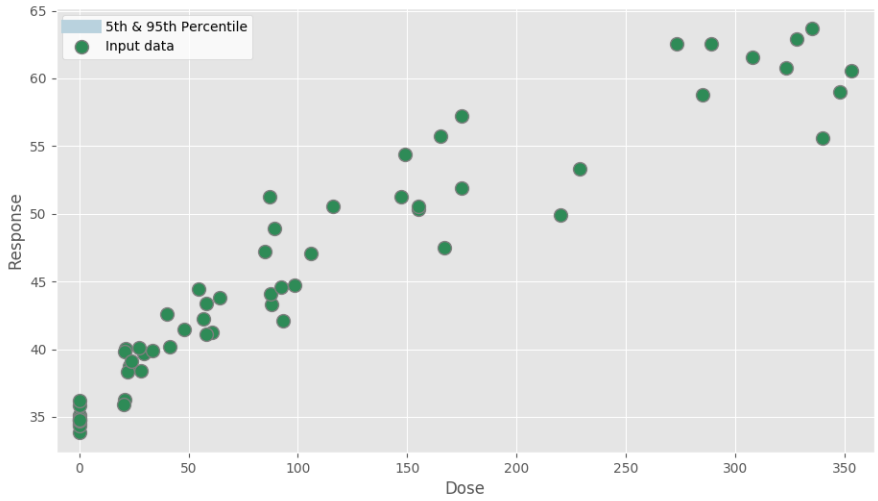

Dose	Response
0.0125	34.47196129
0.0125	33.85982231
0.0125	35.16178737
0.0125	34.34769509
0.0125	34.74719101
0.0125	34.90279465
0.0125	34.81146305
0.0125	35.83655439
0.0125	34.79365079
0.0125	36.23778502
23.1	38.77964141
21.1	40.06060606
20.6	36.2640801
28.3	38.42671194
20.8	39.81028152
22.1	38.36848635
20.3	35.9500446
29.7	39.70288378
23.7	39.11973756
27.6	40.10180995
58.3	43.38790932
56.8	42.25929178
60.6	41.248
40.3	42.58456201

57.9	41.13865932
64.4	43.78801043
33.5	39.91690636
54.4	44.43124443
47.8	41.48424987
41.6	40.17467249
93.1	42.10526316
84.8	47.23391461
98.7	44.72283119
89.1	48.90236857
87.8	43.28644501
106.0	47.07781724
116.0	50.53467767
87.6	44.06041243
87.0	51.23739688
92.5	44.59691252
155.0	50.30138638
165.0	55.75194727
149.0	54.38596491
167.0	47.50154226
155.0	50.5528778
147.0	51.23264381
175.0	57.2238806
175.0	51.88560654
229.0	53.35035099
220.0	49.92508241
285.0	58.77912701
289.0	62.51883097
308.0	61.56505343
353.0	60.54158607
273.0	62.5797783
348.0	58.99833055
328.0	62.92481977
323.0	60.76311606
340.0	55.61497326
335.0	63.68663594

BMD Markov chain Monte Carlo settings

Iterations: 30,000

Number of chains: 1

Warmup fraction: 0.5

Seed: 46,728

BMD results

Central tendency: Relative 5%

BMR: None

Adversity value: 0.050

BMD summary tables:

Statistic	Model average	Linear	Power	Hill	Exponential 2	Exponential 3	Exponential 4	Exponential 5
Prior model weight	N/A	0.143	0.143	0.143	0.143	0.143	0.143	0.143
Posterior model weight	N/A	5.13e-06	3.17e-07	**0.148**	6.34e-10	3.89e-11	**0.730**	**0.122**
BMD (median)	12.754	22.485	23.606	13.630	30.256	31.735	12.253	14.021
BMDL (5th percentile)	11.233	20.521	21.207	10.754	27.858	28.695	10.367	11.258
25th percentile	12.091	21.655	22.542	12.324	29.242	30.407	11.430	12.753
Mean (SD)	12.819 (1.037)	22.538 (1.286)	23.836 (1.893)	13.935 (2.297)	30.337 (1.601)	32.102 (2.544)	12.328 (1.285)	14.404 (2.363)
75th percentile	13.487	23.348	24.874	15.220	31.330	33.379	13.116	15.651
95th percentile	14.617	24.760	27.248	18.166	33.108	36.699	14.562	18.829

BMD estimates

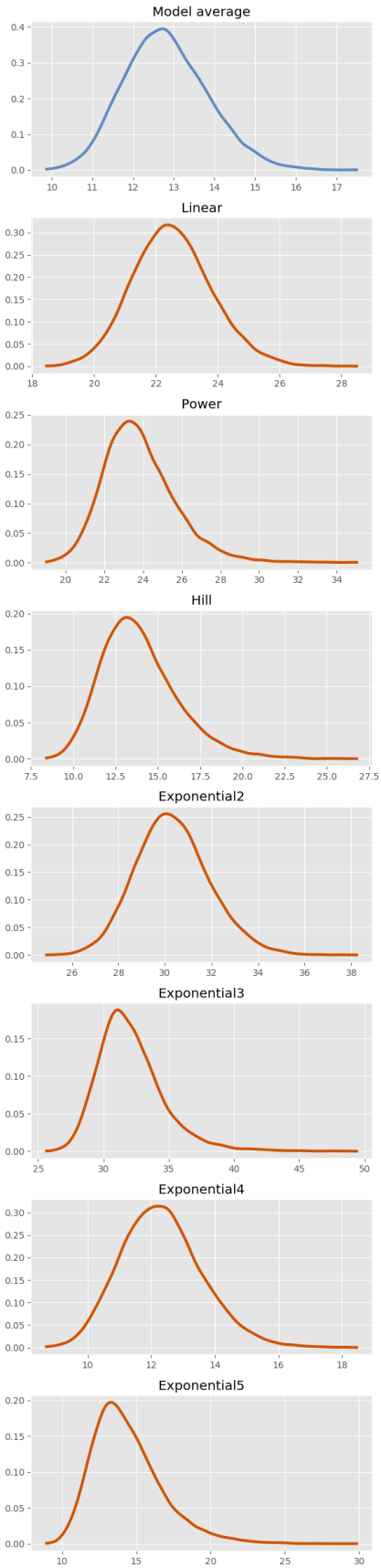

Model results

Linear

$$f(dose) = a + b \times dose$$

Model fit summary

```
Inference for Stan model: linear_individual_pkl_6f560bd3666c0b0a5c004ccddf0ad3ca.
1 chains, each with iter=30000; warmup=15000; thin=1;
post-warmup draws per chain=15000, total post-warmup draws=15000.

        mean se_mean     sd   2.5%    25%    50%    75%  97.5%  n_eff   Rhat
a      36.79  5.3e-3   0.46  35.87  36.48  36.78  37.09   37.7   7680    1.0
b      28.88    0.02   1.38  26.19  27.97  28.87  29.81  31.65   8107    1.0
sigma   0.06  5.8e-5 5.8e-3   0.05   0.06   0.06   0.06   0.07   9785    1.0
lp__  139.34    0.02   1.24  136.1 138.77 139.66 140.24 140.76   6355    1.0

Samples were drawn using NUTS at Tue Jul 30 17:32:31 2019.
For each parameter, n_eff is a crude measure of effective sample size,
and Rhat is the potential scale reduction factor on split chains (at
convergence, Rhat=1).
```

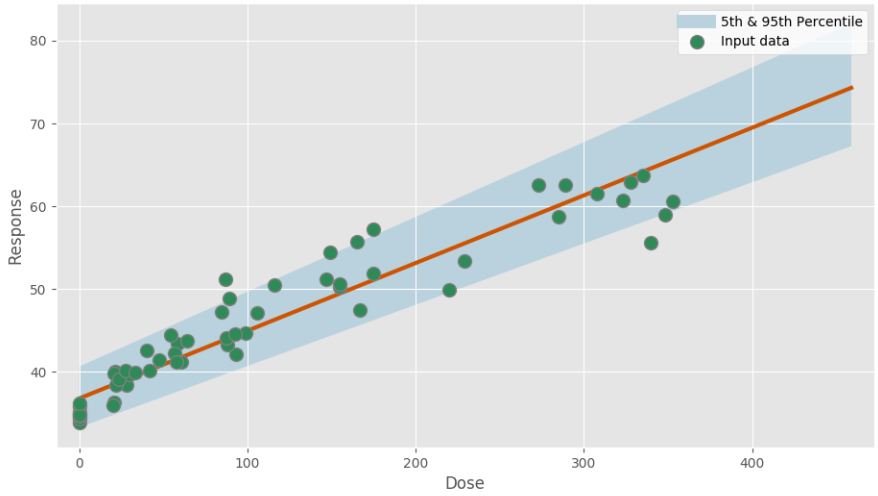

Posterior predictive p-value for model fit: 0.528

Model weight: 0.0%

Correlation matrix

	a	b	sigma
a	-	-0.66	-0.00303
b	-0.66	-	0.006
sigma	-0.00303	0.006	-

Parameter charts

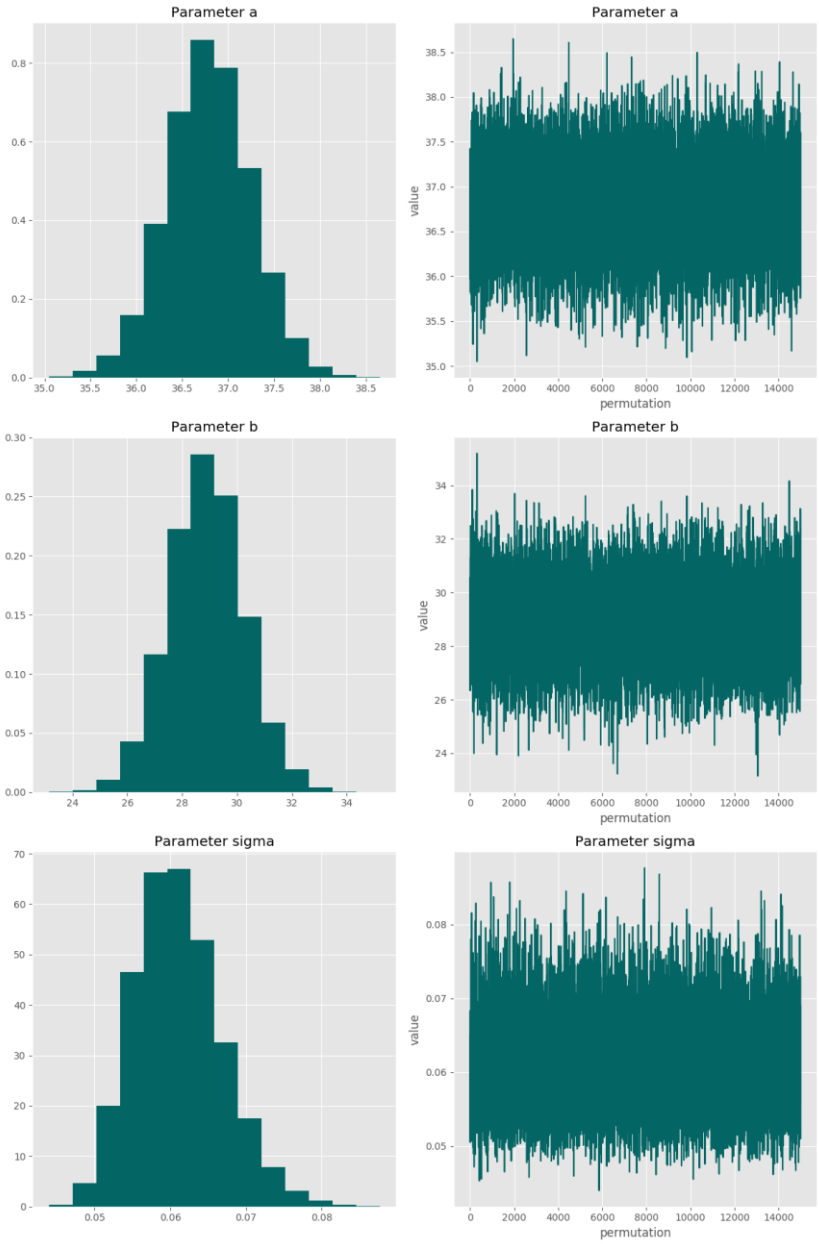

Power

$$f(dose) = a + b \times dose^{g}$$

Power parameter lower-bound: 1.000

Model fit summary

```
Inference for Stan model: power_individual_pkl_8682a4681cf39e692df770d4639a86e2.
1 chains, each with iter=30000; warmup=15000; thin=1;
post-warmup draws per chain=15000, total post-warmup draws=15000.

        mean se_mean     sd   2.5%    25%    50%    75%  97.5%  n_eff   Rhat
a       36.9  5.1e-3   0.48  35.96  36.58   36.9  37.21  37.85   8621    1.0
b      28.89    0.01   1.42  26.13  27.94  28.89  29.82  31.75   8962    1.0
g       1.02  1.8e-4   0.02    1.0   1.01   1.01   1.03   1.07  11806    1.0
sigma   0.06  5.6e-5 6.0e-3   0.05   0.06   0.06   0.07   0.08  11451    1.0
lp__  133.77    0.02   1.47 130.07 133.04 134.11 134.85 135.62   6307    1.0

Samples were drawn using NUTS at Tue Jul 30 17:32:40 2019.
For each parameter, n_eff is a crude measure of effective sample size,
and Rhat is the potential scale reduction factor on split chains (at
convergence, Rhat=1).
```

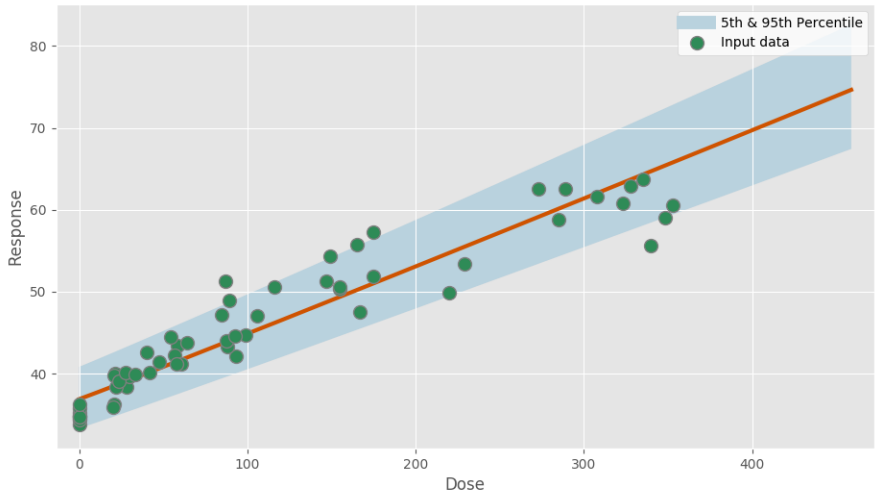

Posterior predictive p-value for model fit: 0.532

Model weight: 0.0%

Correlation matrix

	a	b	g	sigma
a	-	-0.636	0.200	0.034
b	-0.636	-	0.020	0.007
g	0.200	0.020	-	0.188
sigma	0.034	0.007	0.188	-

Parameter charts

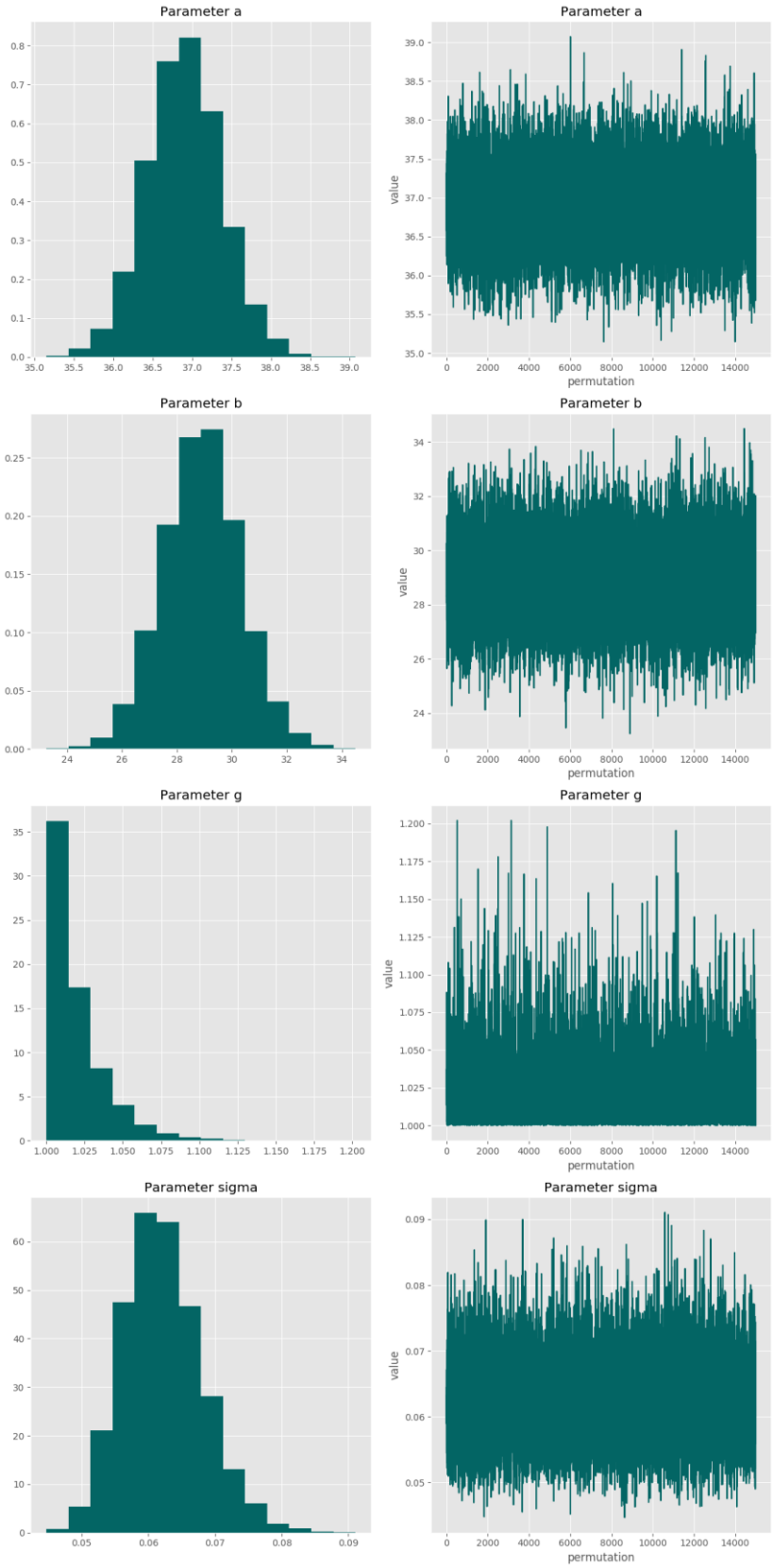

Hill

$$f(dose) = a + \frac{b \times dose^g}{c^g + dose^g}$$

Power parameter lower-bound: 1.000

Model fit summary

```
Inference for Stan model: hill_individual_pkl_f14f62088318f1a4663f986868dc9b40.
1 chains, each with iter=30000; warmup=15000; thin=1;
post-warmup draws per chain=15000, total post-warmup draws=15000.

        mean se_mean     sd   2.5%    25%    50%    75%  97.5%  n_eff   Rhat
a      35.26  5.7e-3   0.49  34.32  34.93  35.26  35.59  36.24   7371    1.0
b      48.11    0.16   9.38  34.22  41.77  46.79  52.76  70.54   3357    1.0
c       0.84  5.1e-3   0.29   0.45   0.64   0.79   0.97   1.56   3218    1.0
g       1.08  1.1e-3   0.08    1.0   1.02   1.06   1.12    1.3   5432    1.0
sigma   0.05  5.1e-5 4.7e-3   0.04   0.04   0.05   0.05   0.06   8599    1.0
lp__  150.14    0.03    1.8 145.67 149.24 150.51 151.46 152.51   3860    1.0

Samples were drawn using NUTS at Tue Jul 30 17:33:15 2019.
For each parameter, n_eff is a crude measure of effective sample size,
and Rhat is the potential scale reduction factor on split chains (at
convergence, Rhat=1).
```

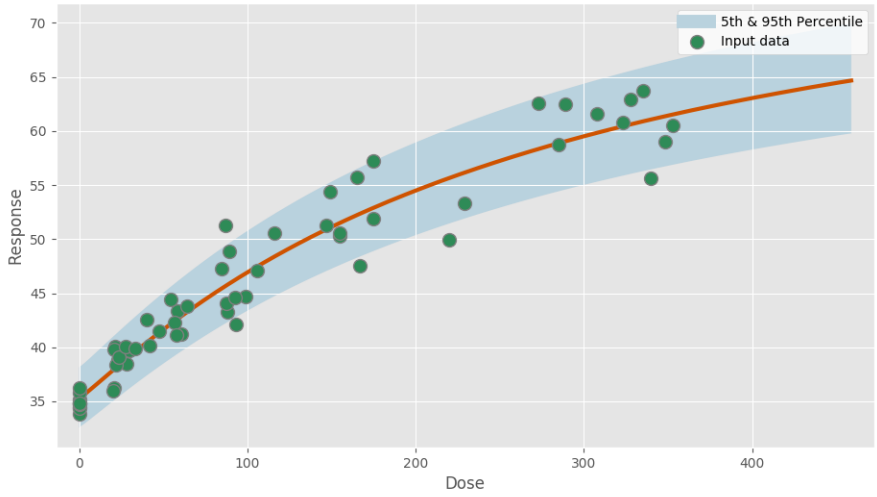

Posterior predictive p-value for model fit: 0.526

Model weight: 14.8%

Correlation matrix

	a	b	c	g	sigma
a	-	0.221	0.338	0.191	0.079
b	0.221	-	0.981	-0.577	0.064
c	0.338	0.981	-	-0.55	0.072
g	0.191	-0.577	-0.55	-	0.075
sigma	0.079	0.064	0.072	0.075	-

Parameter charts

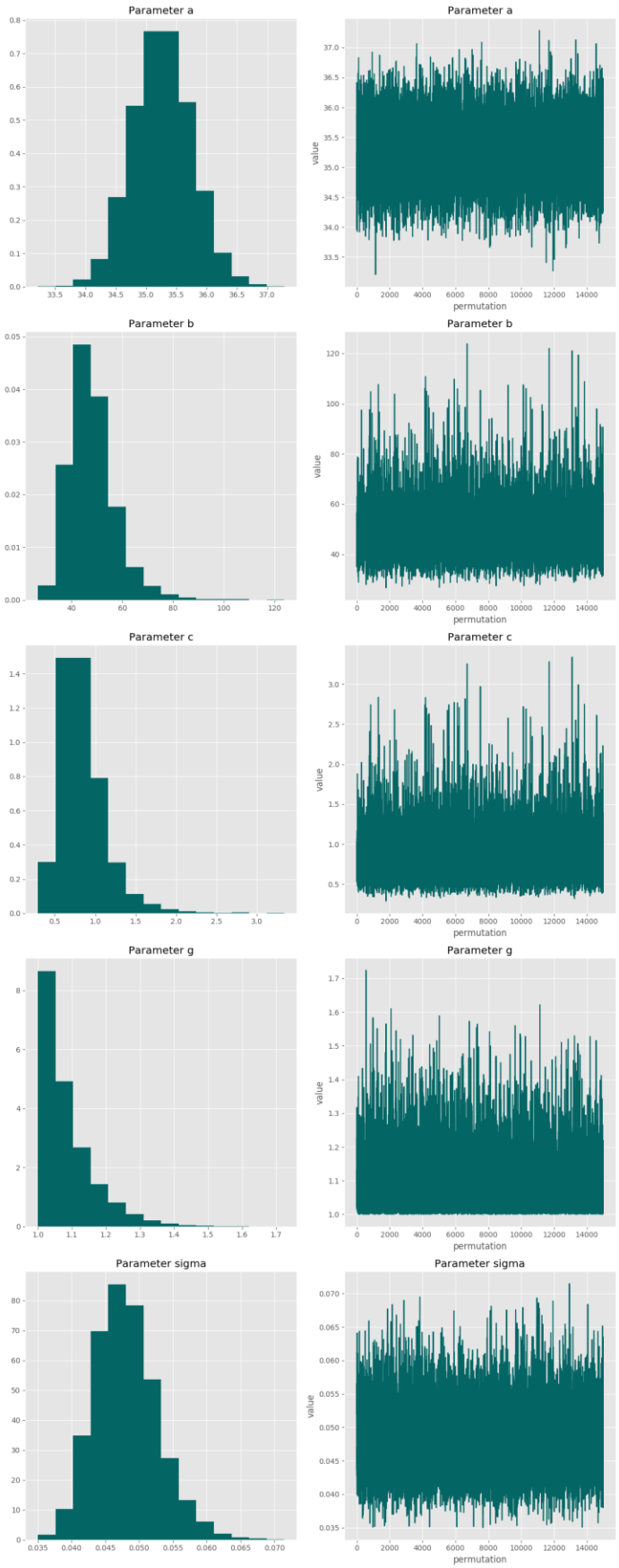

Exponential2

$$f(dose) = a \times e^{b \times dose}$$

Model fit summary

```
Inference for Stan model: exponential2_individual_pkl_be58f7567ba64ec5547642f54ef3b89e.
1 chains, each with iter=30000; warmup=15000; thin=1;
post-warmup draws per chain=15000, total post-warmup draws=15000.

        mean se_mean     sd   2.5%    25%    50%    75%  97.5%  n_eff   Rhat
a      37.67  5.8e-3   0.49  36.71  37.34  37.67  38.01  38.63   7262    1.0
b       0.57  3.5e-4   0.03   0.51   0.55   0.57   0.59   0.63   7078    1.0
sigma   0.07  7.1e-5 6.8e-3   0.06   0.07   0.07   0.08   0.09   9136    1.0
lp__  130.49    0.02   1.27 127.18 129.93 130.82 131.41 131.92   5736    1.0

Samples were drawn using NUTS at Tue Jul 30 17:33:24 2019.
For each parameter, n_eff is a crude measure of effective sample size,
and Rhat is the potential scale reduction factor on split chains (at
convergence, Rhat=1).
```

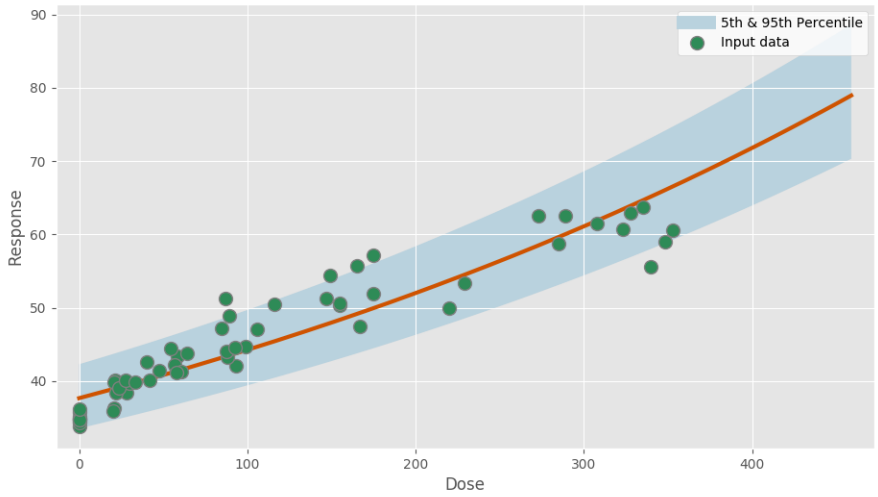

Posterior predictive p-value for model fit: 0.526

Model weight: 0.0%

Correlation matrix

	a	b	sigma
a	-	-0.714	0.001
b	-0.714	-	0.006
sigma	0.001	0.006	-

Parameter charts

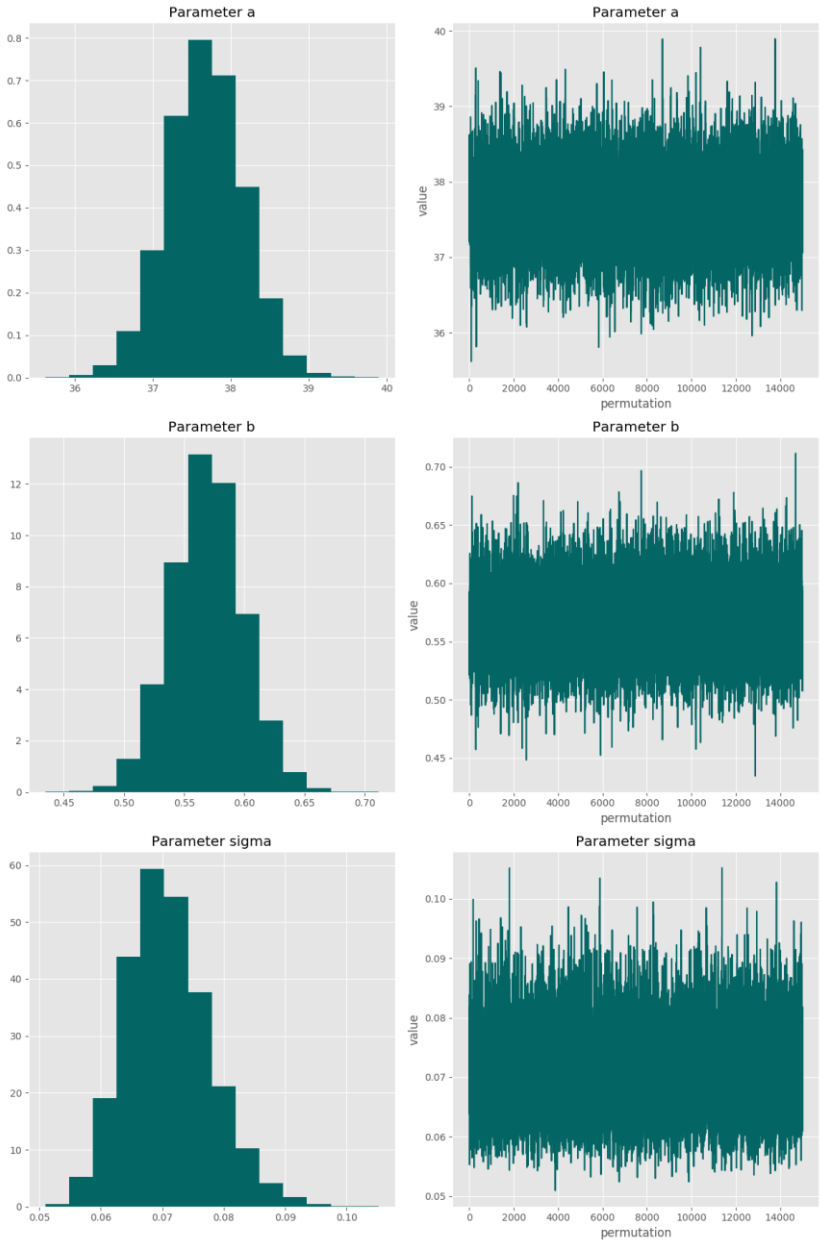

Exponential3

$$f(dose) = a \times e^{b \times dose^{g}}$$

Power parameter lower-bound: 1.000

Model fit summary

```
Inference for Stan model: exponential3_individual_pkl_df53333b36693dd0ad892f92a4fc7532.
1 chains, each with iter=30000; warmup=15000; thin=1;
post-warmup draws per chain=15000, total post-warmup draws=15000.

        mean se_mean     sd   2.5%    25%    50%    75%  97.5%  n_eff   Rhat
a      37.79  5.6e-3   0.51  36.81  37.44  37.79  38.12  38.83   8203    1.0
b       0.57  3.3e-4   0.03   0.51   0.55   0.57   0.59   0.63   8289    1.0
g       1.02  2.2e-4   0.02    1.0   1.01   1.02   1.03   1.09  11990    1.0
sigma   0.07  7.1e-5 7.2e-3   0.06   0.07   0.07   0.08   0.09  10163    1.0
lp__  125.01    0.02    1.5 121.21 124.28 125.35 126.12 126.88   5705    1.0

Samples were drawn using NUTS at Tue Jul 30 17:33:34 2019.
For each parameter, n_eff is a crude measure of effective sample size,
and Rhat is the potential scale reduction factor on split chains (at
convergence, Rhat=1).
```

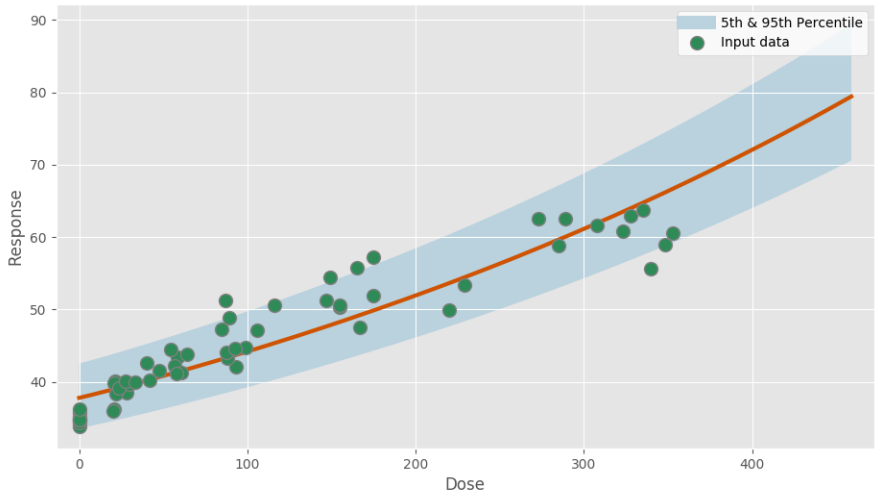

Posterior predictive p-value for model fit: 0.531

Model weight: 0.0%

Correlation matrix

	a	b	g	sigma
a	-	-0.687	0.240	0.043
b	-0.687	-	-0.0768	-0.0158
g	0.240	-0.0768	-	0.170
sigma	0.043	-0.0158	0.170	-

Parameter charts

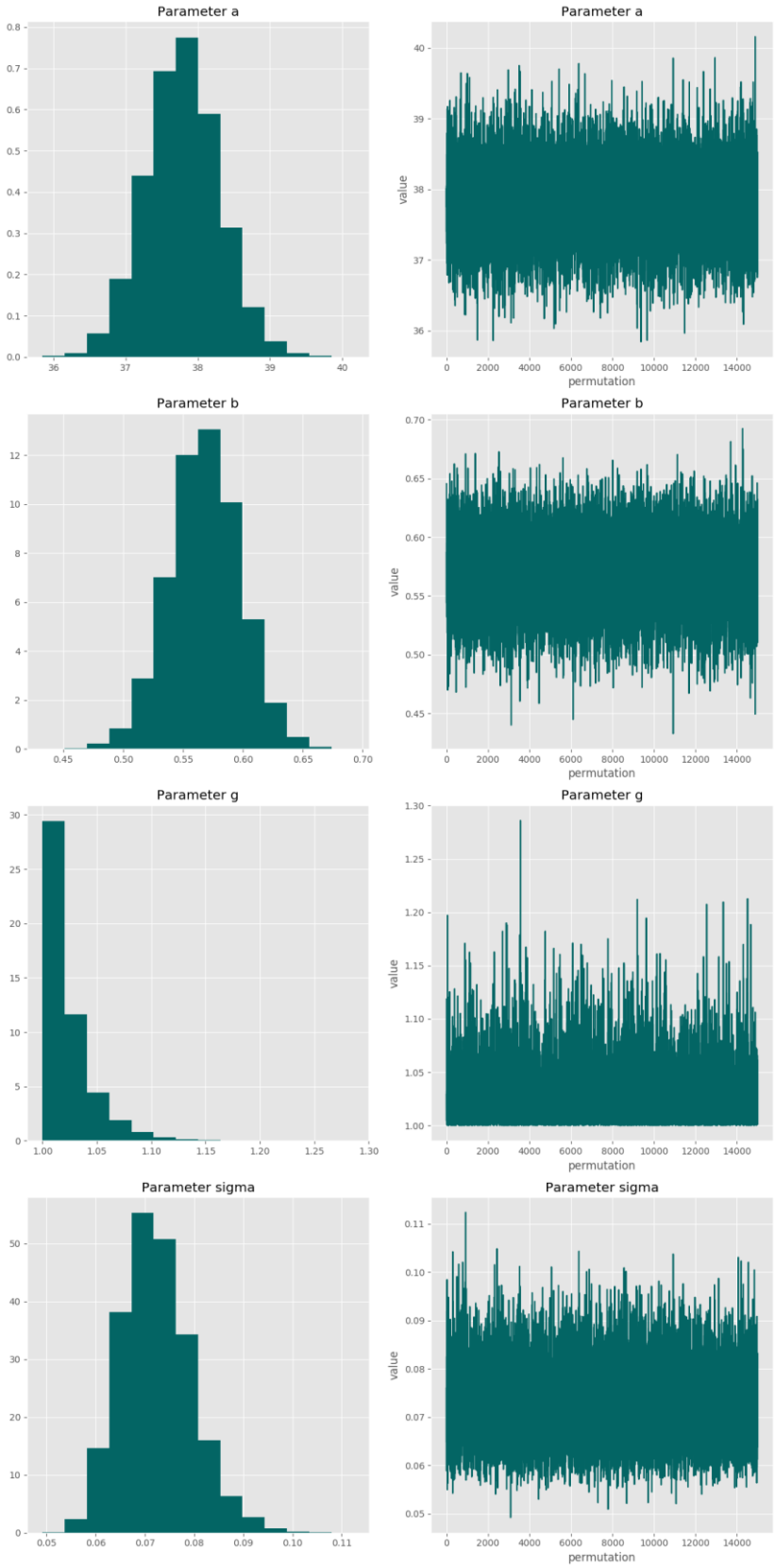

Exponential4

$$f(dose) = a \times [c - (c - 1) \times e^{-b \times dose}]$$

Model fit summary

```
Inference for Stan model: exponential4_individual_pkl_fa67b4bb1853dd3a882bdb66cdb5191d.
1 chains, each with iter=30000; warmup=15000; thin=1;
post-warmup draws per chain=15000, total post-warmup draws=15000.

        mean se_mean     sd   2.5%    25%    50%    75%  97.5%  n_eff   Rhat
a      35.12  5.3e-3   0.46  34.22  34.81  35.12  35.42  36.03   7486    1.0
b       1.58  3.7e-3   0.29   1.02   1.39   1.58   1.78   2.17   6256    1.0
c       1.96  1.4e-3   0.11    1.8   1.88   1.94   2.01   2.21   5542    1.0
sigma   0.05  5.1e-5 4.6e-3   0.04   0.04   0.05   0.05   0.06   8239    1.0
lp__  154.93    0.02   1.48 151.23  154.2 155.28 156.03  156.8   5102    1.0

Samples were drawn using NUTS at Tue Jul 30 17:33:48 2019.
For each parameter, n_eff is a crude measure of effective sample size,
and Rhat is the potential scale reduction factor on split chains (at
convergence, Rhat=1).
```

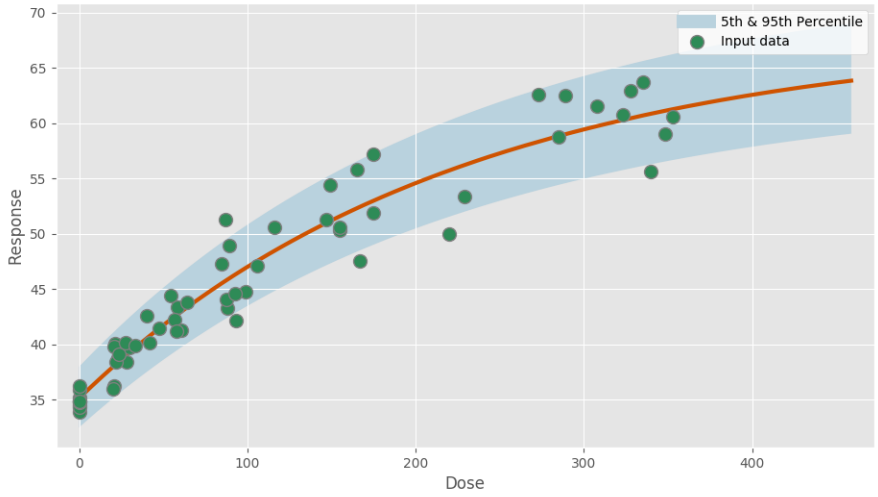

Posterior predictive p-value for model fit: 0.530

Model weight: 73.0%

Correlation matrix

	a	b	c	sigma
a	-	-0.545	0.213	0.027
b	-0.545	-	-0.873	-0.0379
c	0.213	-0.873	-	0.074
sigma	0.027	-0.0379	0.074	-

Parameter charts

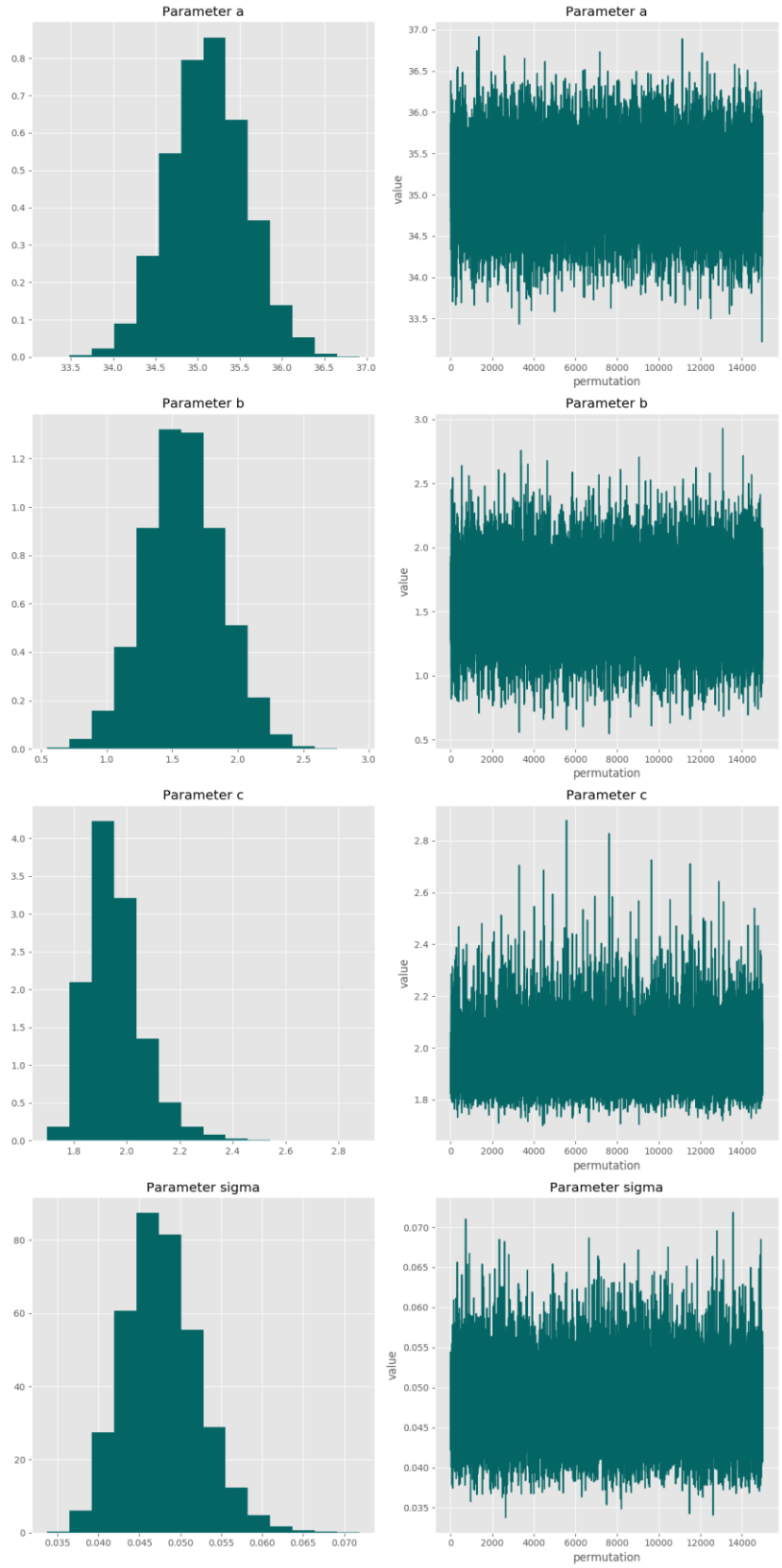

Exponential5

$$f(dose) = a \times [c - (c - 1) \times e^{-(b \times dose)^g}]$$

Power parameter lower-bound: 1.000

Model fit summary

```
Inference for Stan model: exponential5_individual_pkl_0fe35d8b796f8736b80743a2674317fc.
1 chains, each with iter=30000; warmup=15000; thin=1;
post-warmup draws per chain=15000, total post-warmup draws=15000.

        mean se_mean     sd   2.5%    25%    50%    75%  97.5%  n_eff   Rhat
a      35.28  5.3e-3   0.48  34.37  34.95  35.27   35.6  36.26   8227    1.0
b       1.84  4.4e-3   0.34   1.19   1.61   1.84   2.07    2.5   5748    1.0
c       1.87  1.4e-3    0.1   1.71    1.8   1.86   1.92   2.09   4900    1.0
g       1.08  9.1e-4   0.07    1.0   1.03   1.06   1.12   1.27   6376    1.0
sigma   0.05  5.0e-5 4.8e-3   0.04   0.04   0.05   0.05   0.06   9055    1.0
lp__   151.4    0.02   1.72 147.18 150.49 151.75 152.67 153.68   4893    1.0

Samples were drawn using NUTS at Tue Jul 30 17:34:08 2019.
For each parameter, n_eff is a crude measure of effective sample size,
and Rhat is the potential scale reduction factor on split chains (at
convergence, Rhat=1).
```

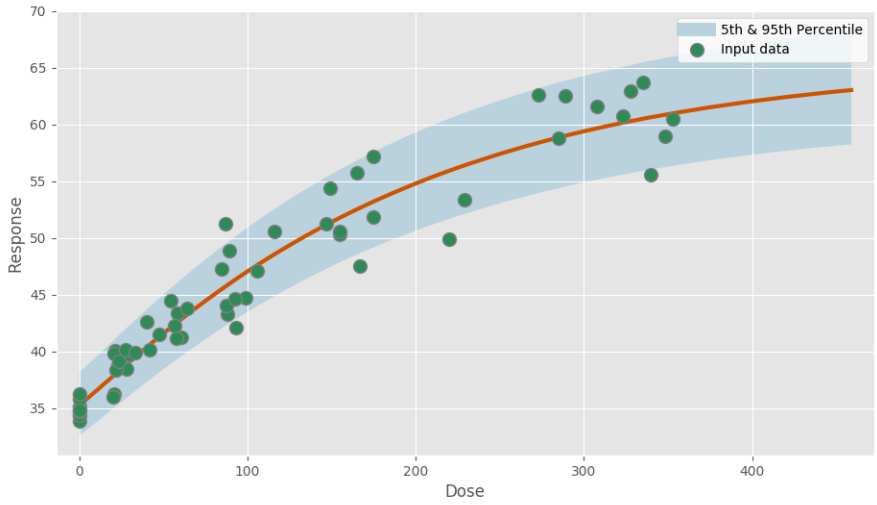

Posterior predictive p-value for model fit: 0.524

Model weight: 12.2%

Correlation matrix

	a	b	c	g	sigma
a	-	-0.263	-0.0747	0.318	0.062
b	-0.263	-	-0.871	0.540	0.061
c	-0.0747	-0.871	-	-0.563	-0.0369
g	0.318	0.540	-0.563	-	0.136
sigma	0.062	0.061	-0.0369	0.136	-

Parameter charts

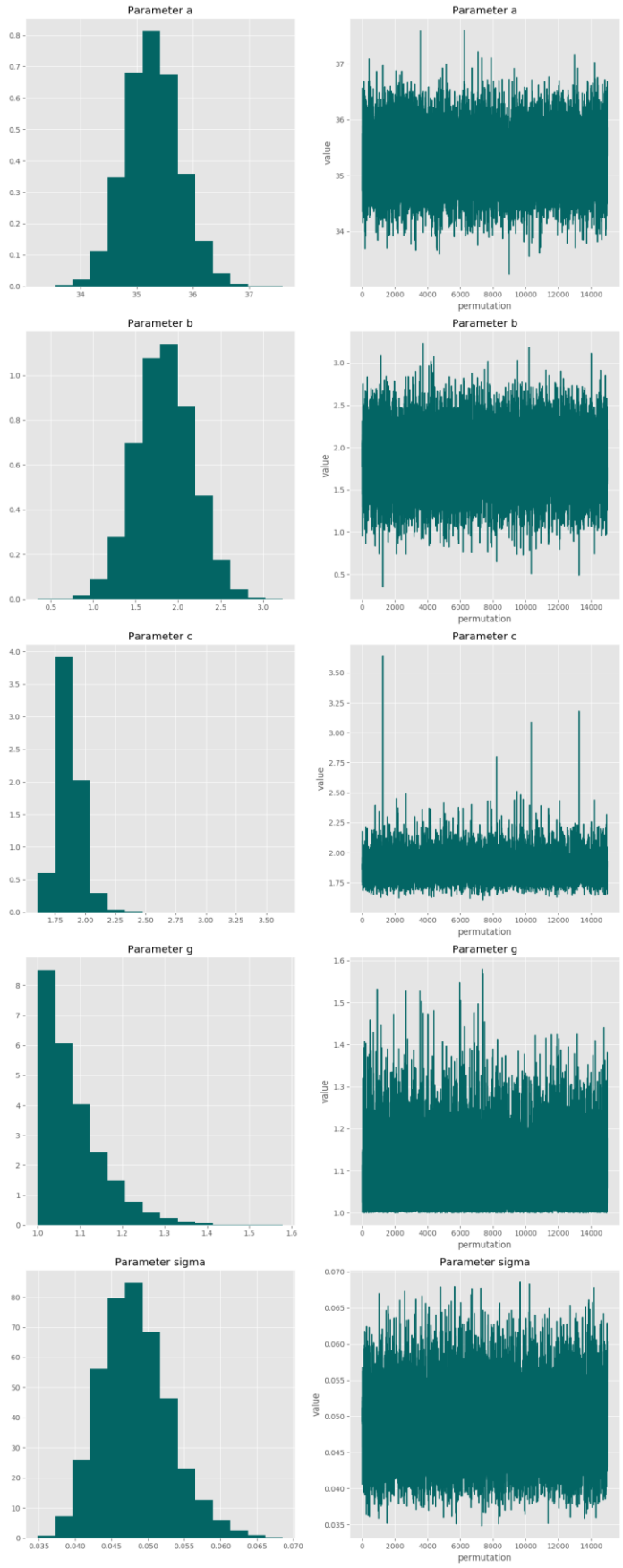

Central tendency: Relative

BMR: None

Adversity value: 0.100

BMD estimates

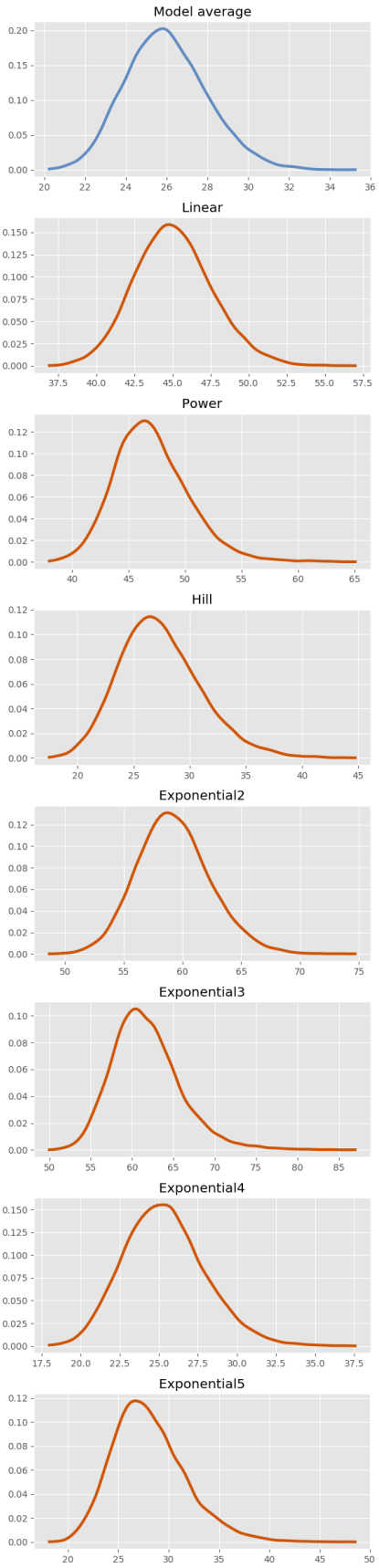

BMD summary tables:

Statistic	Model average	Linear	Power	Hill	Exponential 2	Exponential 3	Exponential 4	Exponential 5
Prior model weight	N/A	0.143	0.143	0.143	0.143	0.143	0.143	0.143
Posterior model weight	N/A	5.13e-06	3.17e-07	0.148	6.34e-10	3.89e-11	0.730	0.122
BMD (median)	25.884	44.969	46.716	27.041	59.103	61.294	25.216	27.648
BMDL (5th percentile)	22.896	41.043	42.176	21.930	54.421	55.782	21.384	22.834
25th percentile	24.579	43.311	44.740	24.816	57.123	58.894	23.552	25.524
Mean (SD)	25.990 (2.016)	45.076 (2.572)	47.025 (3.312)	27.380 (3.674)	59.263 (3.127)	61.762 (4.193)	25.361 (2.593)	28.068 (3.643)
75th percentile	27.274	46.697	48.970	29.598	61.202	64.090	26.967	30.174
95th percentile	29.462	49.520	52.786	33.891	64.675	69.175	29.836	34.734

PFNA Rel Lv Wt 3 ds grp Jul 31 2019, 05:10 PM

Report created on Jul 31, 2019 at 05:14 PM.

Pystan model version 2.19.0.0.

Dataset

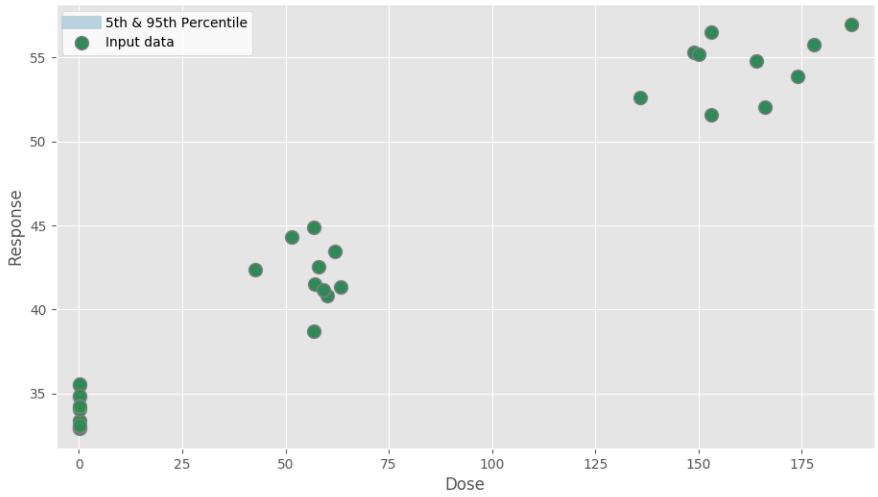

Dose	Response
0.05	34.78393183
0.03	33.39100346
0.05	34.08571429
0.04	35.47158758
0.04	35.52747576
0.05	34.8699095
0.04	32.91740939
0.05	34.23519957
0.04	32.99641343
0.16	33.0726257
63.4	41.35941007
57.0	41.51891253
56.8	38.72849227
60.0	40.79951175
59.1	41.18223383
62.0	43.45137718
56.8	44.91471889
58.1	42.54057428
42.6	42.38275561
51.5	44.32614178
153.0	56.50340577
178.0	55.77195467
149.0	55.31019979

136.0	52.64248705
166.0	52.04359673
153.0	51.5729585
174.0	53.89561271
187.0	56.97318008
164.0	54.78384125
150.0	55.21783181

BMD Markov chain Monte Carlo settings

Iterations: 30,000

Number of chains: 1

Warmup fraction: 0.5

Seed: 89,071

BMD results

Central tendency: Relative 5%

BMR: None

Adversity value: 0.050

BMD summary tables:

Statistic	Model average	Linear	Power	Hill	Exponential 2	Exponential 3	Exponential 4	Exponential 5
Prior model weight	N/A	0.143	0.143	0.143	0.143	0.143	0.143	0.143
Posterior model weight	N/A	**0.500**	0.065	0.070	0.016	0.001	**0.293**	0.055
BMD (median)	13.440	13.680	14.982	13.408	17.385	18.665	11.843	15.008
BMDL (5th percentile)	12.464	12.571	13.213	10.583	16.126	16.784	9.516	10.965
25th percentile	13.034	13.221	14.135	12.021	16.866	17.763	10.847	13.017
Mean (SD)	13.450 (0.612)	13.704 (0.716)	15.347 (1.784)	13.996 (2.806)	17.423 (0.834)	19.075 (1.971)	11.757 (1.315)	15.922 (4.102)
75th percentile	13.853	14.151	16.137	15.407	17.945	19.893	12.726	18.001
95th percentile	14.465	14.937	18.751	19.395	18.833	22.812	13.767	23.826

BMD estimates

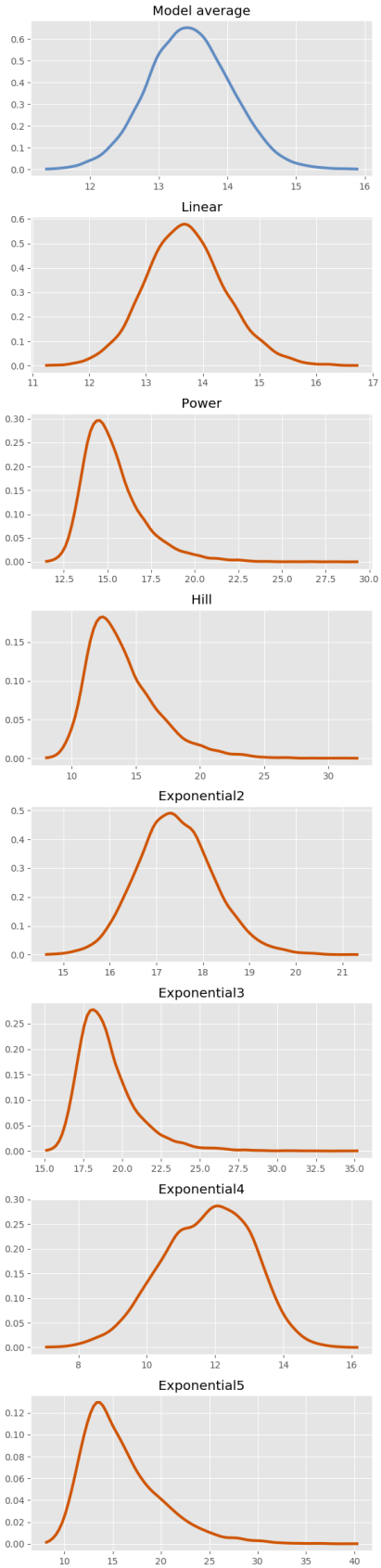

Model results

Linear

$$f(dose) = a + b \times dose$$

Model fit summary

```
Inference for Stan model: linear_individual_pkl_6f560bd3666c0b0a5c004ccddf0ad3ca.
1 chains, each with iter=30000; warmup=15000; thin=1;
post-warmup draws per chain=15000, total post-warmup draws=15000.

        mean se_mean     sd   2.5%    25%    50%    75%  97.5%  n_eff   Rhat
a      34.42  4.6e-3   0.42  33.58  34.15  34.43   34.7  35.26   8310    1.0
b      23.54    0.01   1.02  21.54  22.86  23.53  24.21   25.6   7312    1.0
sigma   0.04  6.7e-5 6.1e-3   0.03   0.04   0.04   0.05   0.06   8428    1.0
lp__   80.68    0.02   1.28  77.36  80.09  81.01  81.62  82.14   6456    1.0

Samples were drawn using NUTS at Wed Jul 31 17:11:46 2019.
For each parameter, n_eff is a crude measure of effective sample size,
and Rhat is the potential scale reduction factor on split chains (at
convergence, Rhat=1).
```

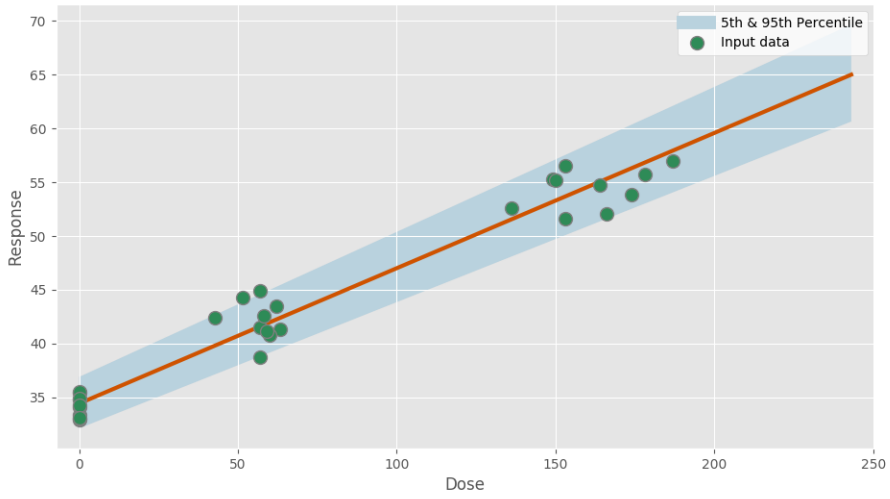

Posterior predictive p-value for model fit: 0.533

Model weight: 50.0%

Correlation matrix

	a	b	sigma
a	-	-0.634	-0.0297
b	-0.634	-	0.028
sigma	-0.0297	0.028	-

Parameter charts

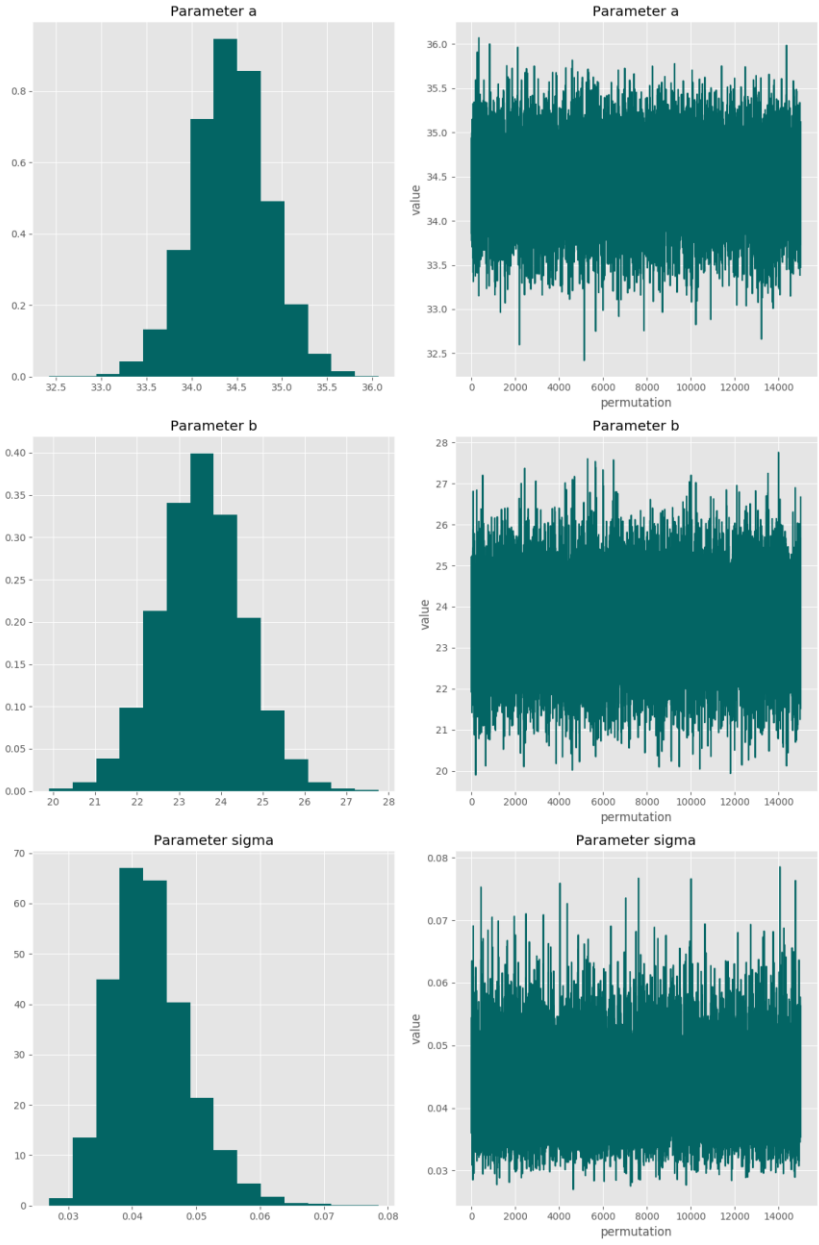

Power

$$f(dose) = a + b \times dose^{g}$$

Power parameter lower-bound: 1.000

Model fit summary

```
Inference for Stan model: power_individual_pkl_8682a4681cf39e692df770d4639a86e2.
1 chains, each with iter=30000; warmup=15000; thin=1;
post-warmup draws per chain=15000, total post-warmup draws=15000.

        mean se_mean     sd   2.5%    25%    50%    75%  97.5%  n_eff   Rhat
a      34.54  5.1e-3   0.45  33.67  34.24  34.54  34.83  35.45   7896    1.0
b      23.68    0.01   1.09  21.58  22.95  23.66  24.39  25.88   7834    1.0
g       1.05  4.3e-4   0.04    1.0   1.01   1.03   1.06   1.16  10647    1.0
sigma   0.04  6.7e-5 6.5e-3   0.03   0.04   0.04   0.05   0.06   9554    1.0
lp__   76.05    0.02   1.53  72.21   75.3   76.4  77.17  77.97   5313    1.0

Samples were drawn using NUTS at Wed Jul 31 17:11:54 2019.
For each parameter, n_eff is a crude measure of effective sample size,
and Rhat is the potential scale reduction factor on split chains (at
convergence, Rhat=1).
```

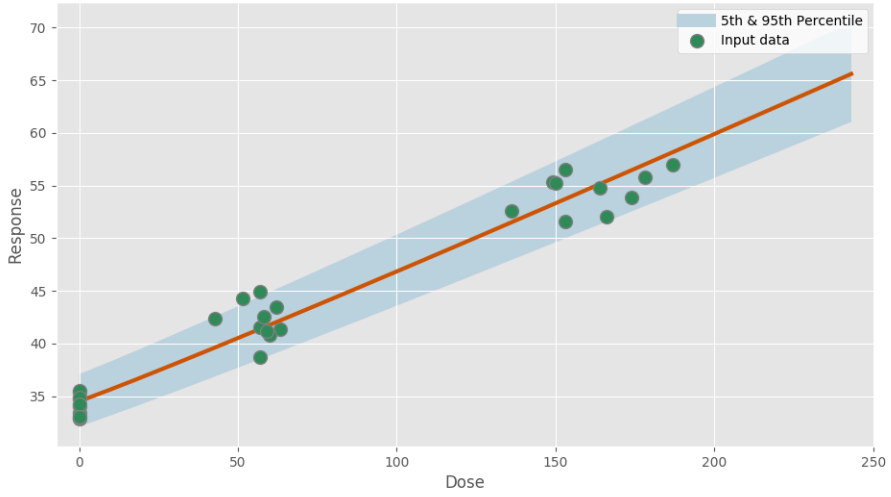

Posterior predictive p-value for model fit: 0.540

Model weight: 6.5%

Correlation matrix

	a	b	g	sigma
a	-	-0.586	0.225	0.063
b	-0.586	-	0.133	0.035
g	0.225	0.133	-	0.247
sigma	0.063	0.035	0.247	-

Parameter charts

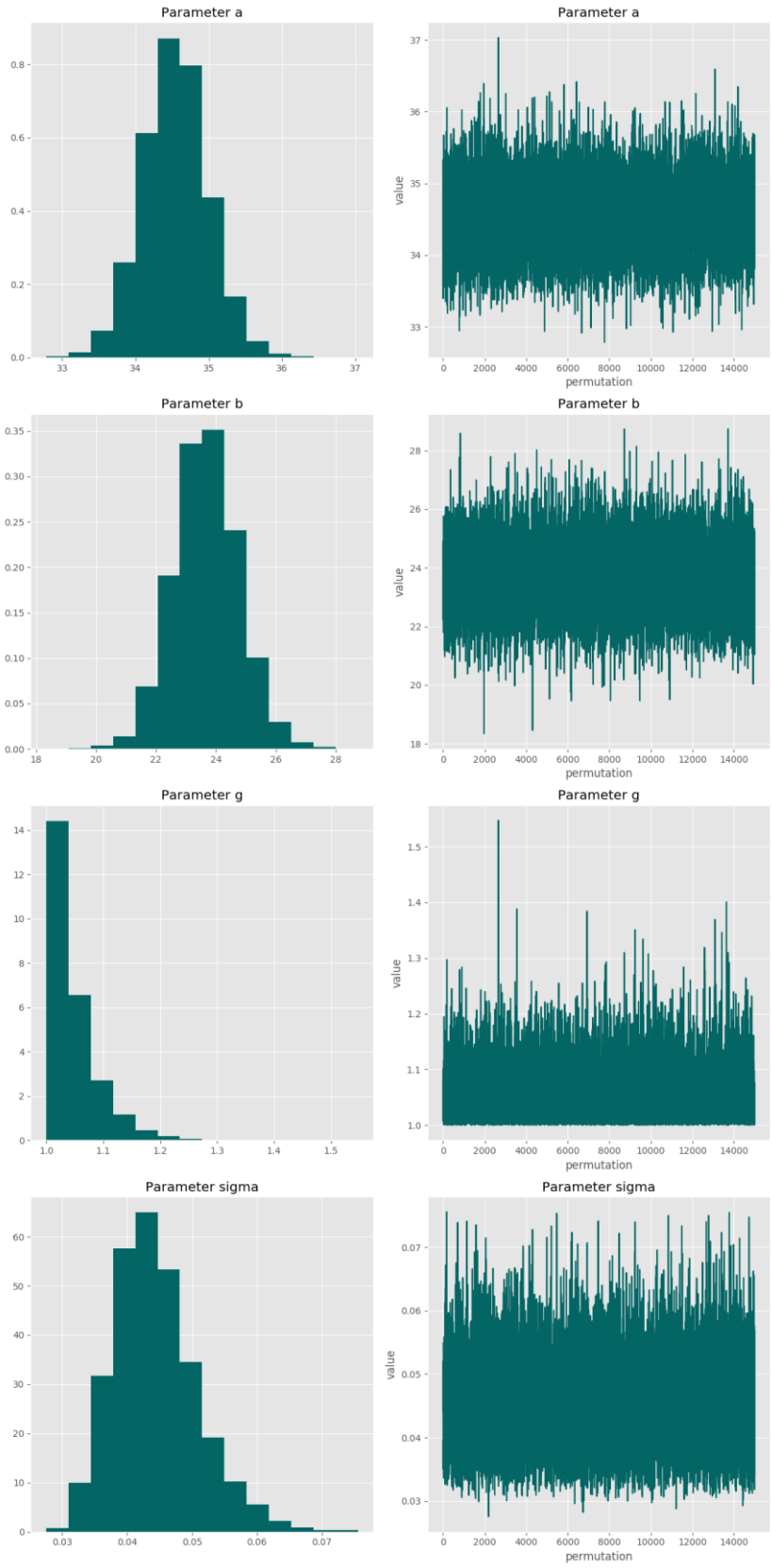

Hill

$$f(dose) = a + \frac{b \times dose^g}{c^g + dose^g}$$

Power parameter lower-bound: 1.000

Model fit summary

```
Inference for Stan model: hill_individual_pkl_f14f62088318f1a4663f986868dc9b40.
1 chains, each with iter=30000; warmup=15000; thin=1;
post-warmup draws per chain=15000, total post-warmup draws=15000.

        mean se_mean     sd   2.5%    25%    50%    75%  97.5%  n_eff   Rhat
a      34.24  7.4e-3   0.45  33.36  33.94  34.24  34.54  35.16   3753    1.0
b      76.95    0.71  25.21  31.32  56.94  77.85  98.06 117.82   1267    1.0
c       2.24    0.03   0.97    0.6   1.44   2.25   3.02   3.97   1242    1.0
g       1.16  4.7e-3   0.17    1.0   1.05    1.1    1.2   1.61   1363    1.0
sigma   0.04  1.2e-4 6.0e-3   0.03   0.04   0.04   0.05   0.06   2379    1.0
lp__    79.8    0.03   1.58  75.78  79.03  80.15  80.97  81.85   3086    1.0

Samples were drawn using NUTS at Wed Jul 31 17:12:17 2019.
For each parameter, n_eff is a crude measure of effective sample size,
and Rhat is the potential scale reduction factor on split chains (at
convergence, Rhat=1).
```

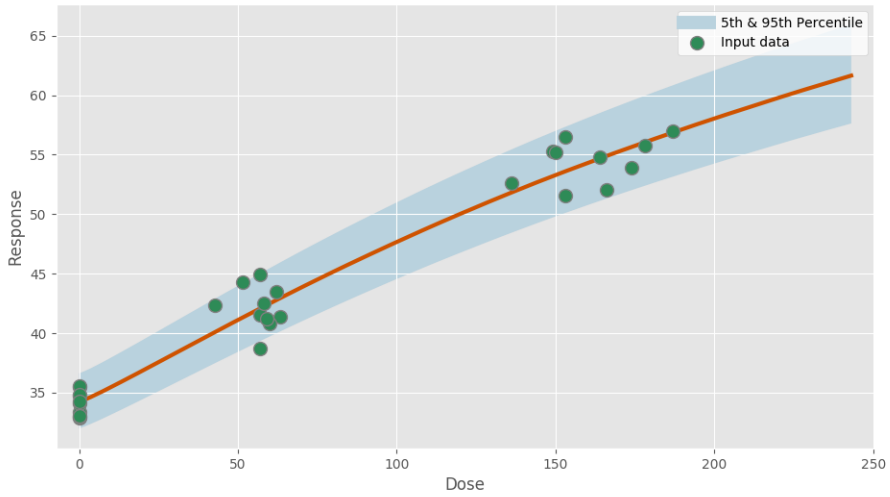

Posterior predictive p-value for model fit: 0.542

Model weight: 7.0%

Correlation matrix

	a	b	c	g	sigma
a	-	0.102	0.132	0.063	0.088
b	0.102	-	0.977	-0.646	0.018
c	0.132	0.977	-	-0.674	0.005
g	0.063	-0.646	-0.674	-	0.094
sigma	0.088	0.018	0.005	0.094	-

Parameter charts

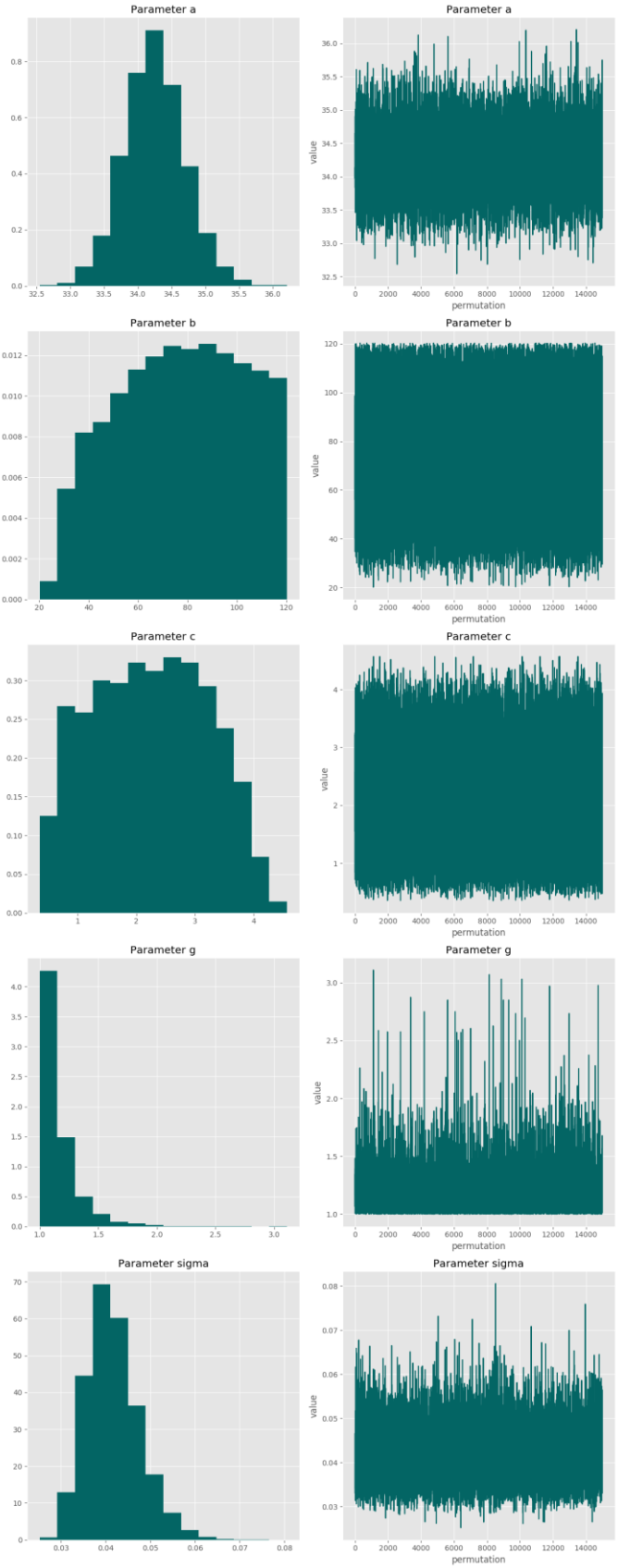

Exponential2

$$f(dose) = a \times e^{b \times dose}$$

Model fit summary

```
Inference for Stan model: exponential2_individual_pkl_be58f7567ba64ec5547642f54ef3b89e.
1 chains, each with iter=30000; warmup=15000; thin=1;
post-warmup draws per chain=15000, total post-warmup draws=15000.

        mean se_mean     sd   2.5%    25%    50%    75%  97.5%  n_eff   Rhat
a      34.88  5.3e-3   0.46  33.97  34.59  34.89  35.18  35.79   7535    1.0
b       0.52  2.9e-4   0.02   0.48   0.51   0.52   0.54   0.57   7191    1.0
sigma   0.05  7.4e-5 6.8e-3   0.04   0.04   0.05   0.05   0.06   8590    1.0
lp__   76.93    0.02   1.29  73.56  76.35  77.26  77.87  78.38   5624    1.0

Samples were drawn using NUTS at Wed Jul 31 17:12:24 2019.
For each parameter, n_eff is a crude measure of effective sample size,
and Rhat is the potential scale reduction factor on split chains (at
convergence, Rhat=1).
```

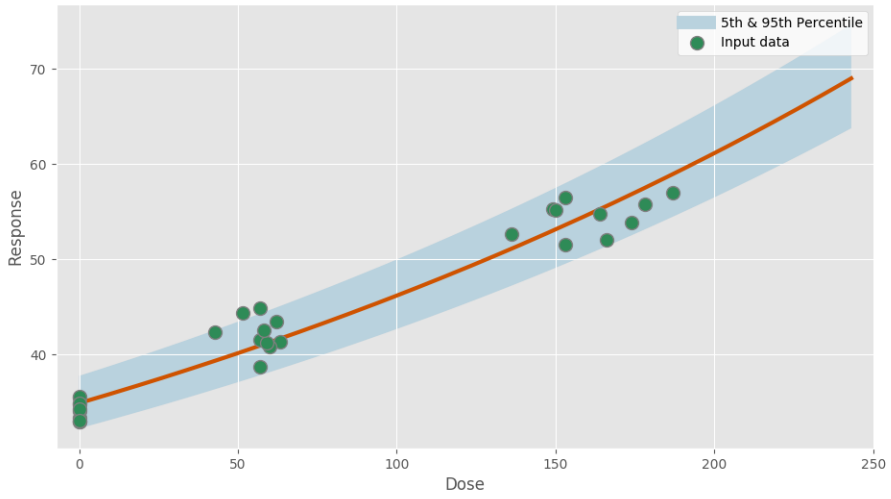

Posterior predictive p-value for model fit: 0.533

Model weight: 1.6%

Correlation matrix

	a	b	sigma
a	-	-0.726	-0.0127
b	-0.726	-	0.014
sigma	-0.0127	0.014	-

Parameter charts

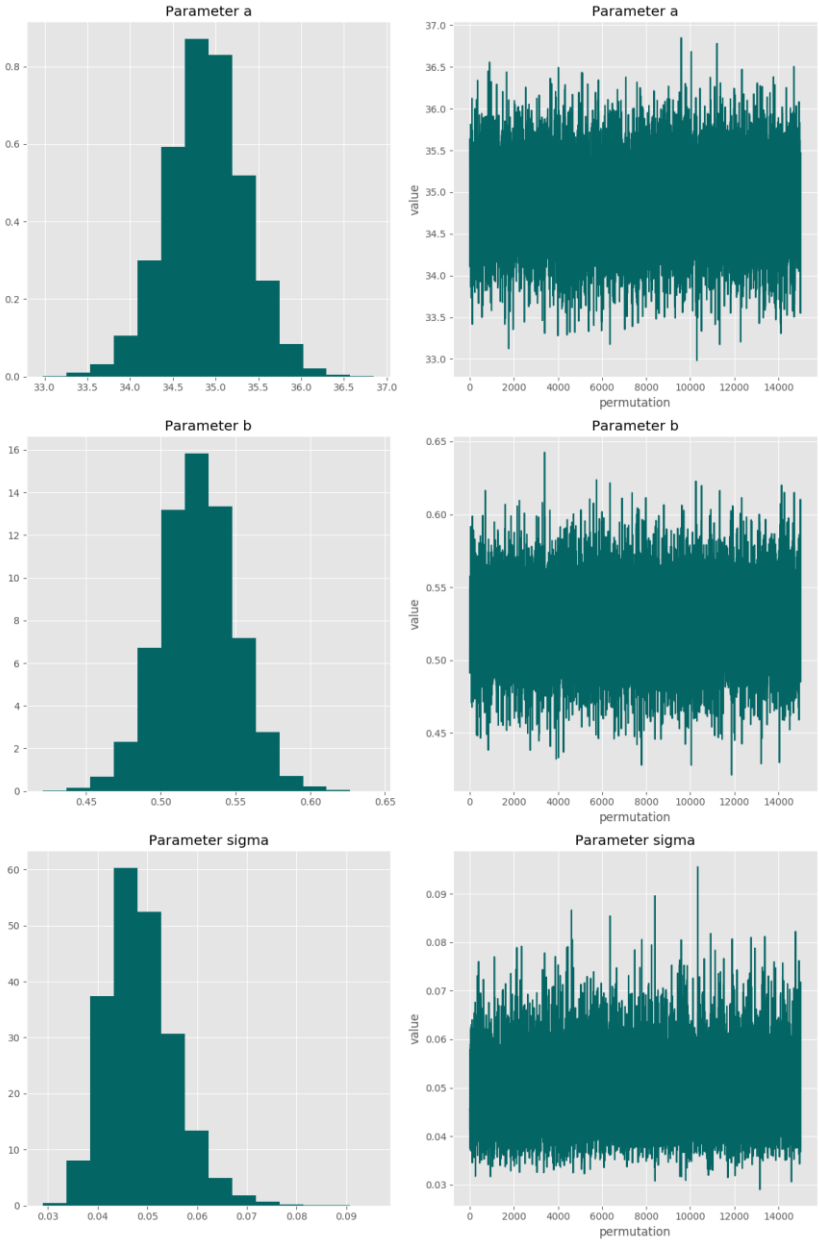

Exponential3

$$f(dose) = a \times e^{b \times dose^{g}}$$

Power parameter lower-bound: 1.000

Model fit summary

```
Inference for Stan model: exponential3_individual_pkl_df53333b36693dd0ad892f92a4fc7532.
1 chains, each with iter=30000; warmup=15000; thin=1;
post-warmup draws per chain=15000, total post-warmup draws=15000.

        mean se_mean     sd   2.5%    25%    50%    75%  97.5%  n_eff   Rhat
a      34.99  6.1e-3    0.5  34.04  34.66  34.98  35.31  36.01   6652    1.0
b       0.53  3.1e-4   0.03   0.47   0.51   0.53   0.54   0.58   6842    1.0
g       1.04  3.9e-4   0.04    1.0   1.01   1.03   1.05   1.15  11044    1.0
sigma   0.05  8.0e-5 7.5e-3   0.04   0.05   0.05   0.06   0.07   8776    1.0
lp__   71.99    0.02   1.52  68.11  71.22  72.32  73.11   73.9   5190    1.0

Samples were drawn using NUTS at Wed Jul 31 17:12:32 2019.
For each parameter, n_eff is a crude measure of effective sample size,
and Rhat is the potential scale reduction factor on split chains (at
convergence, Rhat=1).
```

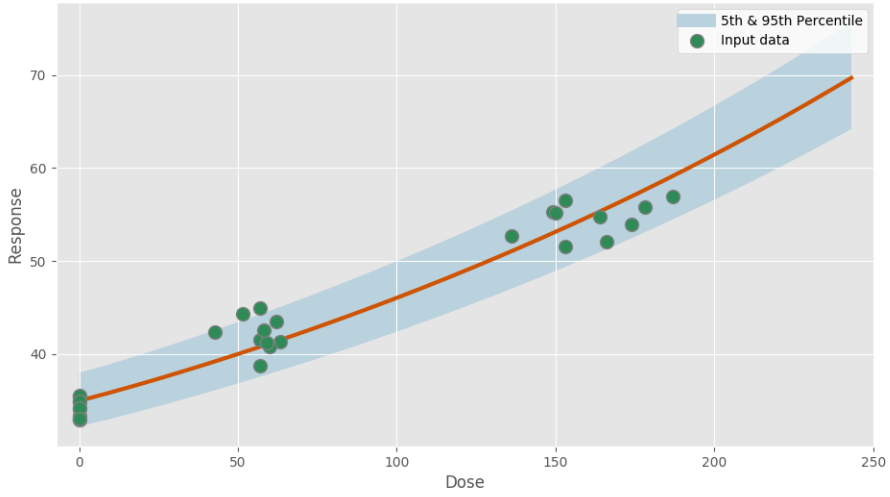

Posterior predictive p-value for model fit: 0.538

Model weight: 0.1%

Correlation matrix

	a	b	g	sigma
a	-	-0.706	0.225	0.067
b	-0.706	-	-0.0034	-0.00293
g	0.225	-0.0034	-	0.263
sigma	0.067	-0.00293	0.263	-

Parameter charts

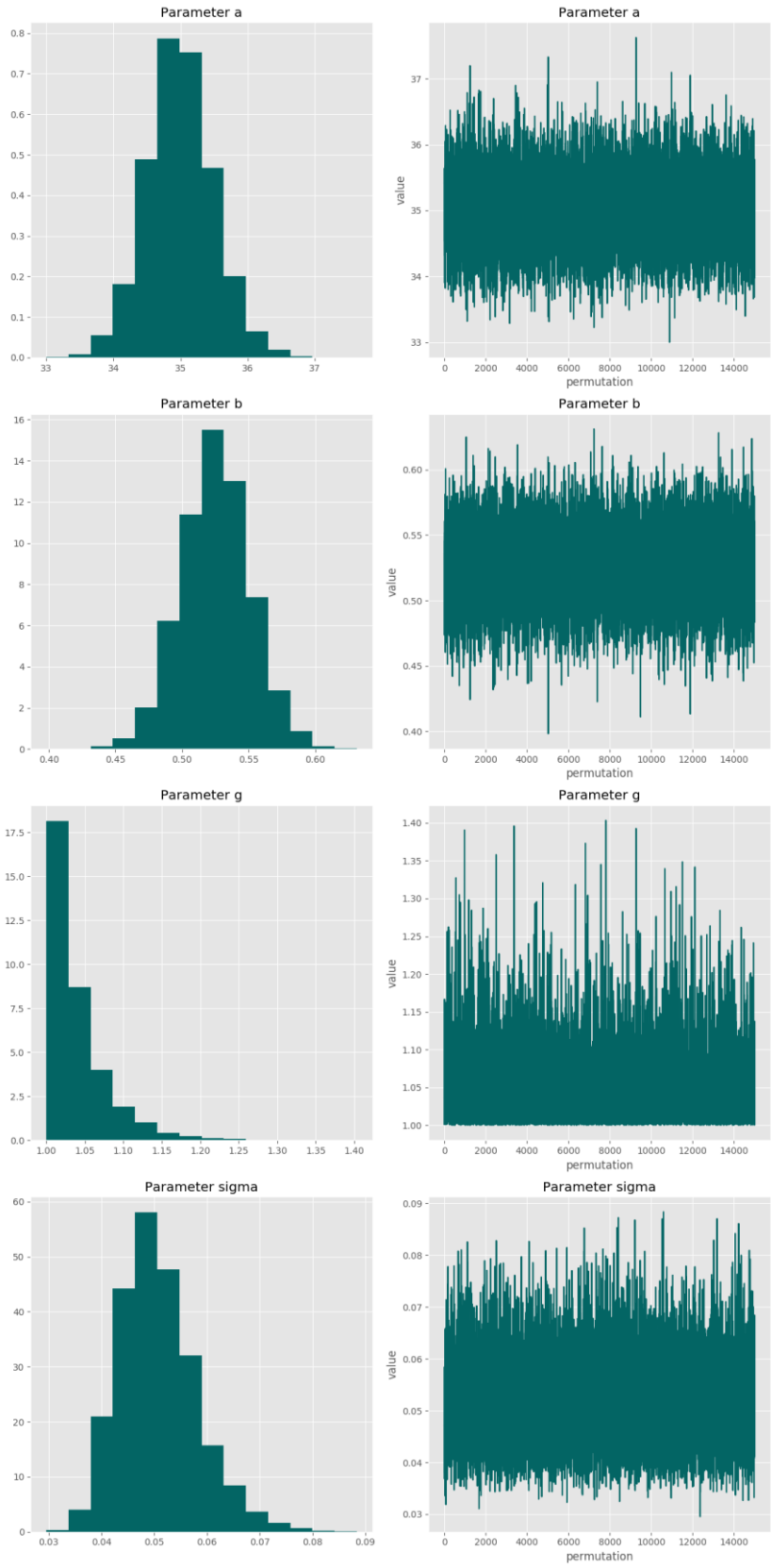

Exponential4

$$f(dose) = a \times [c - (c - 1) \times e^{-b \times dose}]$$

Model fit summary

```
Inference for Stan model: exponential4_individual_pkl_fa67b4bb1853dd3a882bdb66cdb5191d.
1 chains, each with iter=30000; warmup=15000; thin=1;
post-warmup draws per chain=15000, total post-warmup draws=15000.

        mean se_mean     sd   2.5%    25%    50%    75%  97.5%  n_eff   Rhat
a      34.18  5.8e-3   0.44   33.3  33.89  34.18  34.46  35.03   5676    1.0
b        0.4  4.9e-3   0.28   0.06   0.17   0.36   0.57   1.04   3209    1.0
c       4.46    0.07   2.92   1.98   2.52   3.23   5.21  13.07   1597    1.0
sigma   0.04  7.9e-5 6.0e-3   0.03   0.04   0.04   0.04   0.06   5615    1.0
lp__   81.73    0.02   1.42  78.21  81.02   82.0  82.76  83.64   4042    1.0

Samples were drawn using NUTS at Wed Jul 31 17:12:55 2019.
For each parameter, n_eff is a crude measure of effective sample size,
and Rhat is the potential scale reduction factor on split chains (at
convergence, Rhat=1).
```

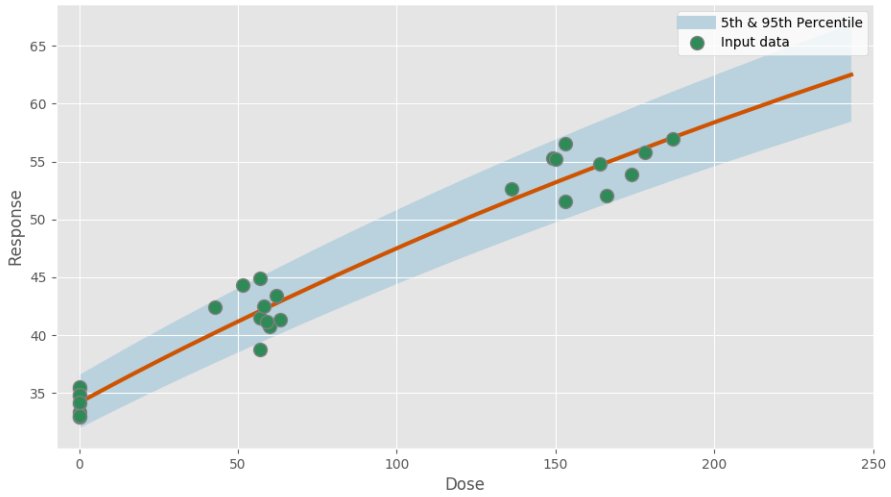

Posterior predictive p-value for model fit: 0.533

Model weight: 29.3%

Correlation matrix

	a	b	c	sigma
a	-	-0.336	0.211	-0.0214
b	-0.336	-	-0.726	0.048
c	0.211	-0.726	-	0.017
sigma	-0.0214	0.048	0.017	-

Parameter charts

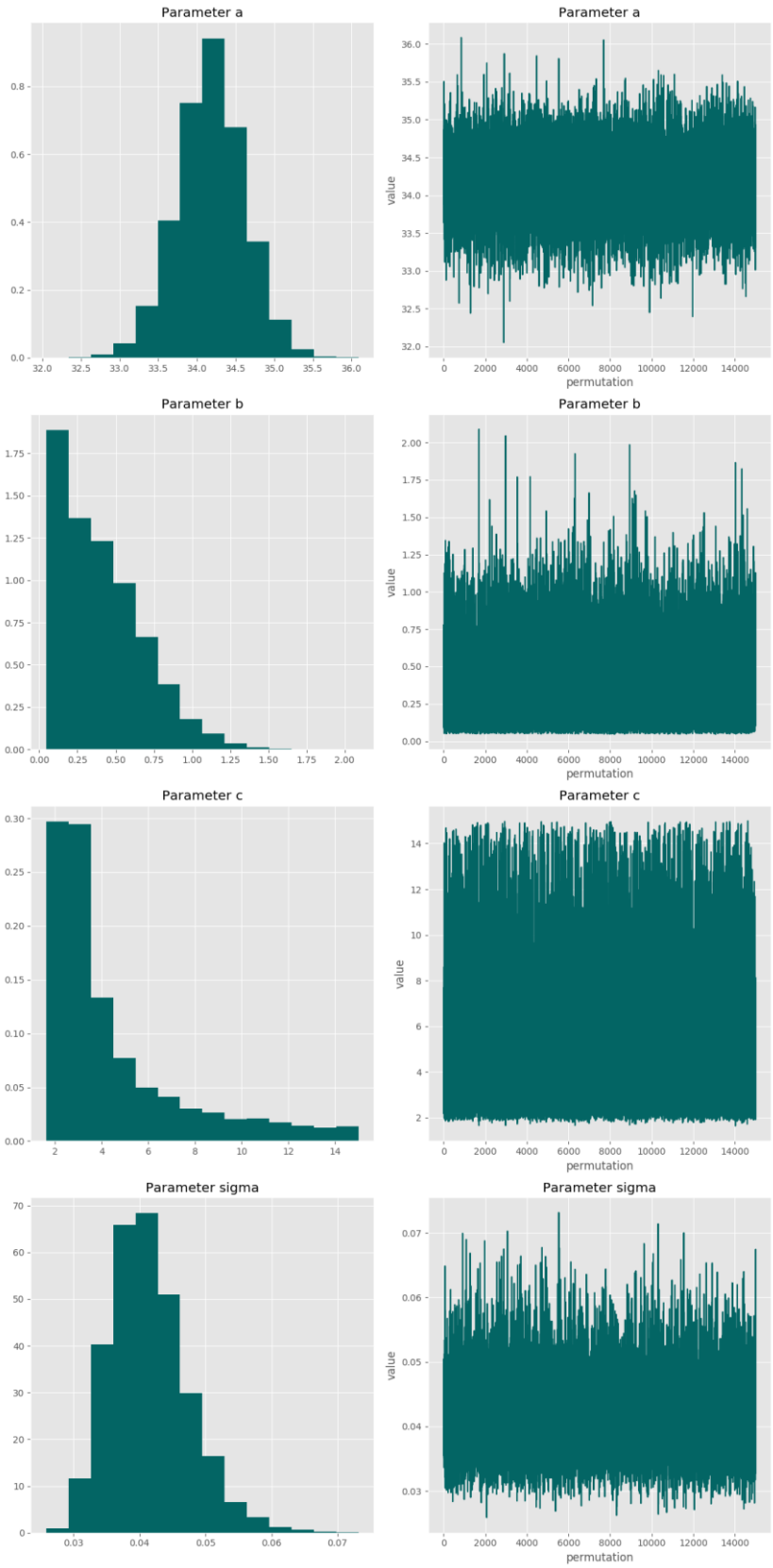

Exponential5

$$f(dose) = a \times [c - (c - 1) \times e^{-(b \times dose)^g}]$$

Power parameter lower-bound: 1.000

Model fit summary

```
Inference for Stan model: exponential5_individual_pkl_0fe35d8b796f8736b80743a2674317fc.
1 chains, each with iter=30000; warmup=15000; thin=1;
post-warmup draws per chain=15000, total post-warmup draws=15000.

        mean se_mean     sd   2.5%    25%    50%    75%  97.5%  n_eff   Rhat
a      34.22  6.4e-3   0.47  33.31  33.91  34.21  34.54  35.16   5361    1.0
b       1.18    0.01   0.63   0.11   0.67   1.16   1.68   2.36   1946    1.0
c       2.48    0.05   1.67   1.59   1.73   1.94   2.41   8.05   1132   1.01
g        1.3  5.2e-3   0.31   1.01   1.08    1.2   1.42    2.1   3446    1.0
sigma   0.04  8.3e-5 6.2e-3   0.03   0.04   0.04   0.05   0.06   5643    1.0
lp__   80.09    0.05   2.12  75.21  78.78  80.45  81.71  83.15   1902    1.0

Samples were drawn using NUTS at Wed Jul 31 17:13:27 2019.
For each parameter, n_eff is a crude measure of effective sample size,
and Rhat is the potential scale reduction factor on split chains (at
convergence, Rhat=1).
```

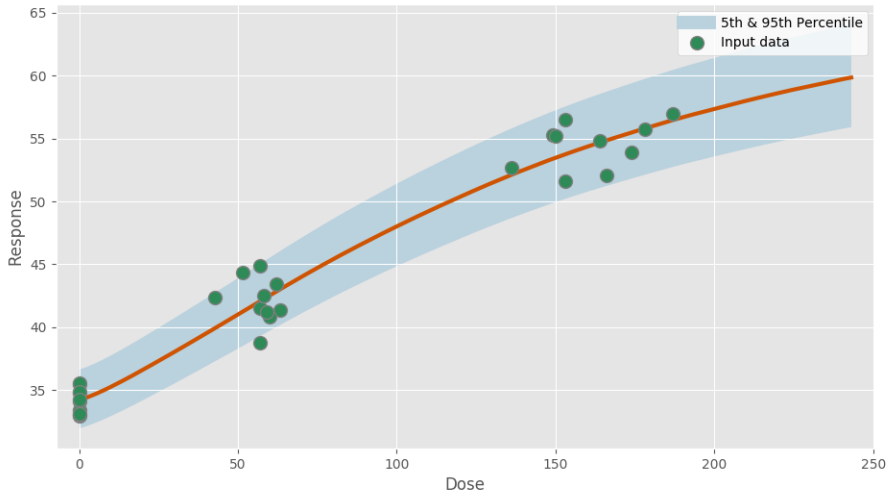

Posterior predictive p-value for model fit: 0.535

Model weight: 5.5%

Correlation matrix

	a	b	c	g	sigma
a	-	-0.161	0.162	0.051	0.044
b	-0.161	-	-0.623	0.815	0.058
c	0.162	-0.623	-	-0.357	0.054
g	0.051	0.815	-0.357	-	0.133
sigma	0.044	0.058	0.054	0.133	-

Parameter charts

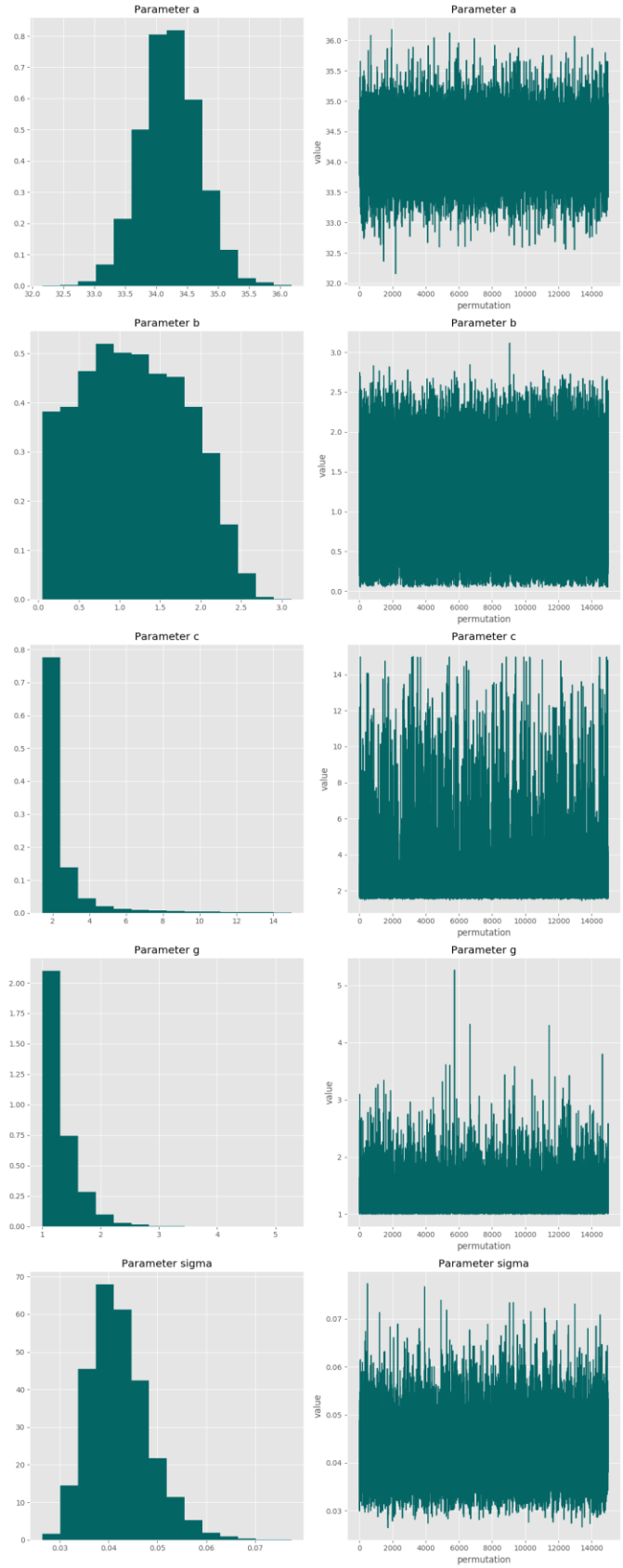

PFHxS Rel Lv Wt Jul 31 2019, 12:33 PM

Report created on Jul 31, 2019 at 04:35 PM.

Pystan model version 2.19.0.0.

Dataset

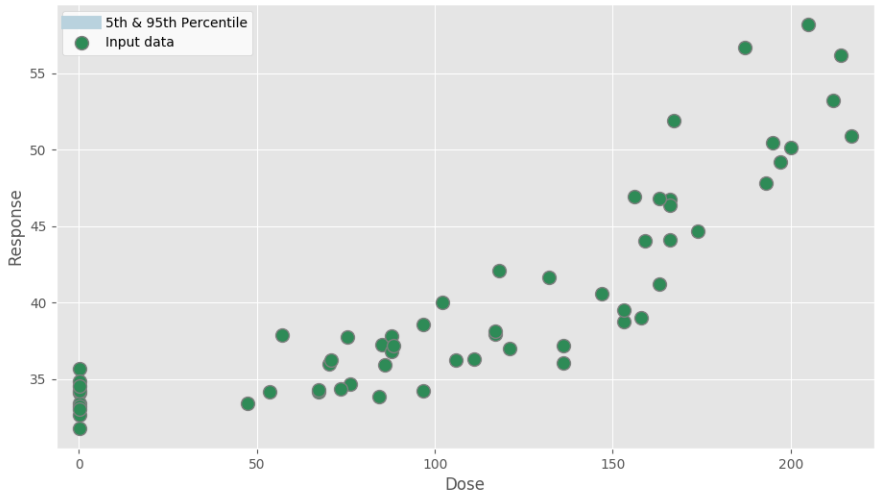

Dose	Response
0.0973	34.08618128
0.073	33.43391672
0.106	34.21372192
0.0952	32.65369169
0.0598	33.25668295
0.135	33.07453416
0.214	35.7183908
0.104	31.7921026
0.064	34.87935657
0.074	34.54856166
57.0	37.87795492
47.5	33.40348767
53.5	34.20693421
70.2	36.01021566
67.4	34.15889353
84.3	33.88905729
76.3	34.68899522
70.7	36.27155762
73.5	34.35483871
67.2	34.28733352
75.4	37.76520509
85.2	37.24053724
111.0	36.2913486

96.7	38.58493268
87.8	36.8112856
87.7	37.79993768
88.3	37.19055843
96.7	34.21765024
86.0	35.9389313
106.0	36.28451381
136.0	37.19383127
121.0	36.98378709
132.0	41.65687427
118.0	42.09023415
117.0	37.92901144
136.0	36.05072464
158.0	39.02439024
117.0	38.14747105
153.0	38.78406709
102.0	40.0
166.0	46.74253201
167.0	51.91407326
156.0	46.91760522
163.0	41.2404468
147.0	40.60036386
166.0	46.36810486
153.0	39.49704142
159.0	44.01899673
166.0	44.09276089
174.0	44.6997549
200.0	50.14164306
205.0	58.18293056
217.0	50.92165899
212.0	53.2420984
187.0	56.64845173
195.0	50.46831956
197.0	49.19703521
214.0	56.19233995
163.0	46.80786687
193.0	47.8164557

BMD Markov chain Monte Carlo settings

Iterations: 30,000

Number of chains: 1

Warmup fraction: 0.5

Seed: 35,904

BMD results

Central tendency: Relative 5%

BMR: None

Adversity value: 0.050

BMD summary tables:

Statistic	Model average	Linear	Power	Hill	Exponential 2	Exponential 3	Exponential 4	Exponential 5
Prior model weight	N/A	0.143	0.143	0.143	0.143	0.143	0.143	0.143
Posterior model weight	N/A	1.47e-09	**0.430**	0.072	1.43e-07	**0.414**	8.07e-11	0.083
BMD (median)	82.315	20.456	84.150	89.224	23.254	78.705	19.974	86.170
BMDL (5th percentile)	72.885	17.446	68.689	73.217	20.679	62.726	16.776	70.865
25th percentile	78.502	19.149	77.690	82.812	22.120	72.243	18.569	79.737
Mean (SD)	82.408 (5.775)	20.615 (2.114)	83.983 (9.281)	89.602 (10.213)	23.394 (1.811)	78.697 (9.660)	20.141 (2.256)	86.488 (10.045)
75th percentile	86.346	21.893	90.248	96.186	24.538	85.066	21.498	92.721
95th percentile	91.859	24.301	99.064	106.605	26.515	94.636	24.114	103.320

BMD estimates

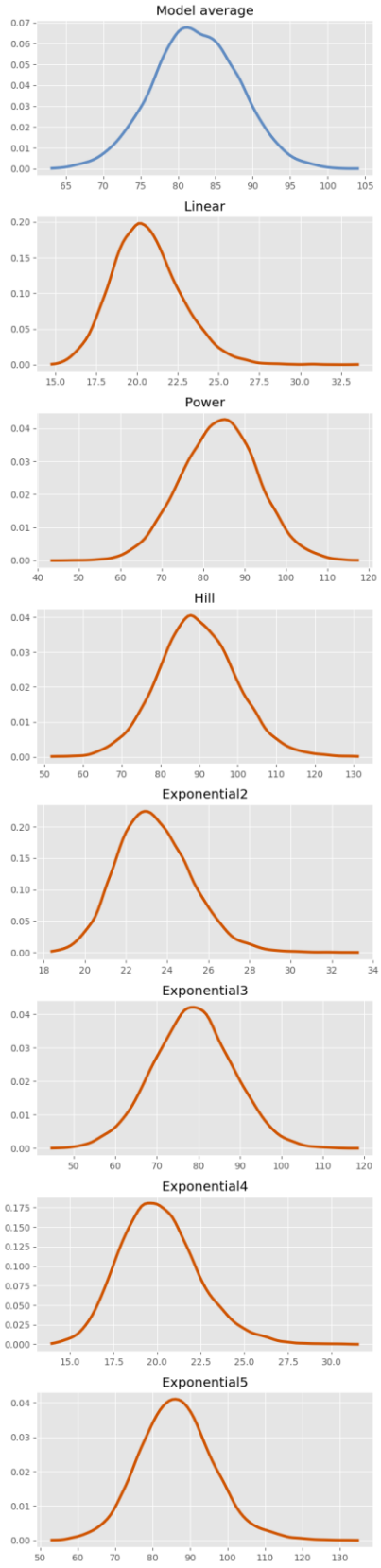

Model results

Linear

$$f(dose) = a + b \times dose$$

Model fit summary

```
Inference for Stan model: linear_individual_pkl_6f560bd3666c0b0a5c004ccddf0ad3ca.
1 chains, each with iter=30000; warmup=15000; thin=1;
post-warmup draws per chain=15000, total post-warmup draws=15000.

        mean se_mean     sd   2.5%    25%    50%    75%  97.5%  n_eff   Rhat
a      31.61  8.7e-3   0.71  30.21  31.15  31.61  32.08  33.02   6657    1.0
b      16.78    0.02   1.37  14.14  15.84  16.77   17.7  19.53   6758    1.0
sigma   0.09  8.2e-5 8.2e-3   0.07   0.08   0.09   0.09    0.1   9797    1.0
lp__  118.42    0.02   1.22 115.22 117.85 118.72 119.32 119.83   6268    1.0

Samples were drawn using NUTS at Wed Jul 31 12:35:18 2019.
For each parameter, n_eff is a crude measure of effective sample size,
and Rhat is the potential scale reduction factor on split chains (at
convergence, Rhat=1).
```

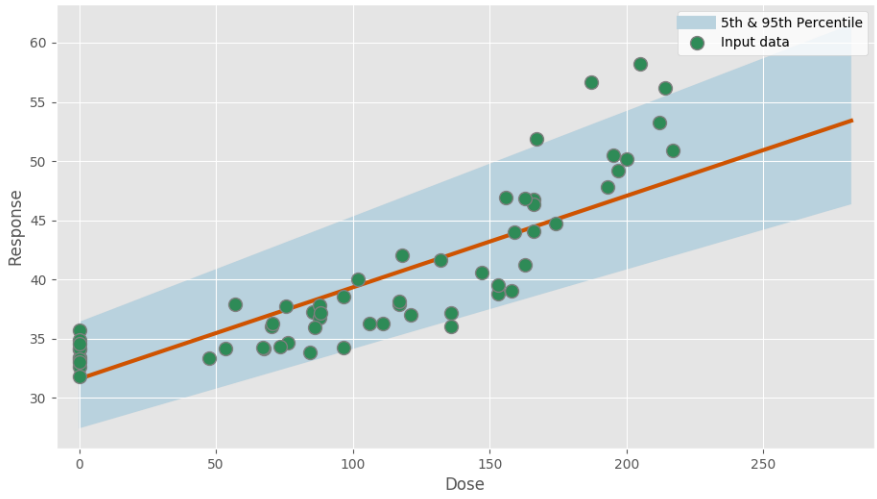

Posterior predictive p-value for model fit: 0.523

Model weight: 0.0%

Correlation matrix

	a	b	sigma
a	-	-0.789	-0.00624
b	-0.789	-	0.002
sigma	-0.00624	0.002	-

Parameter charts

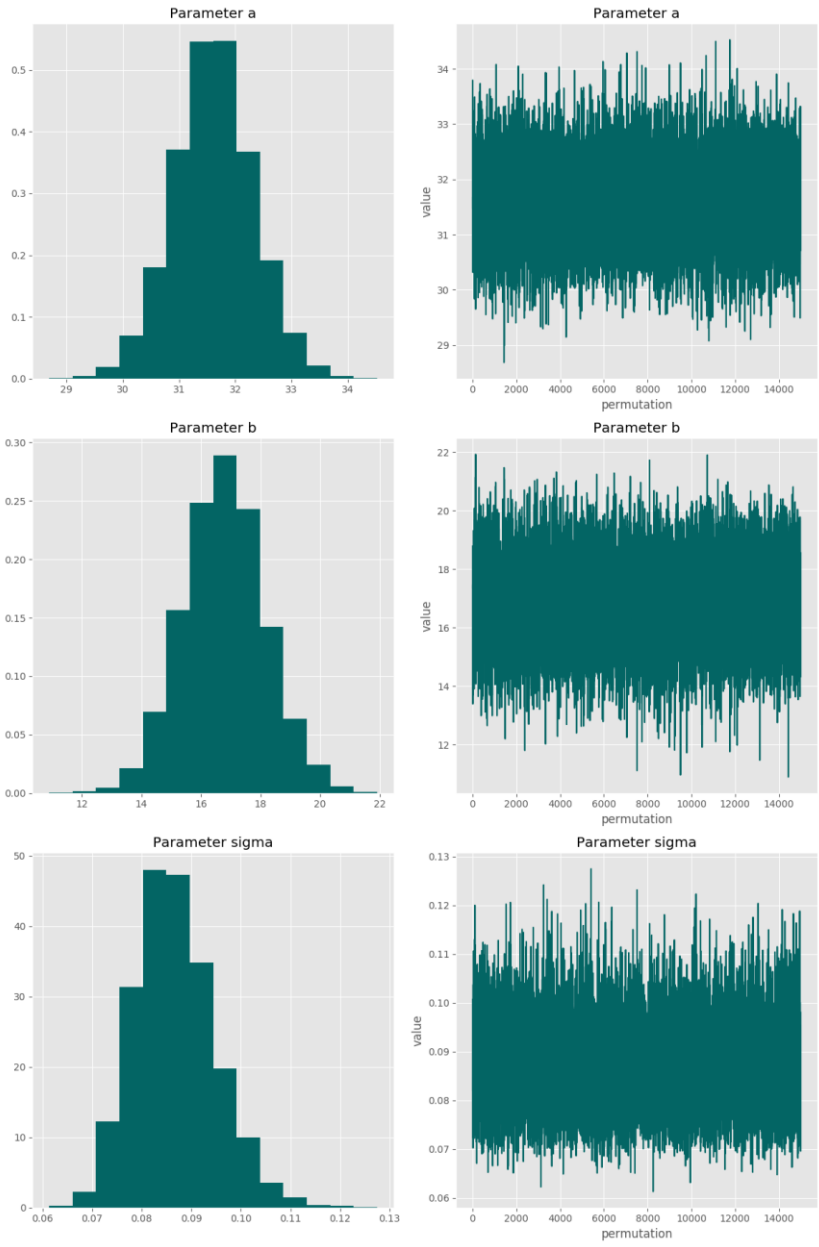

Power

$$f(dose) = a + b \times dose^{g}$$

Power parameter lower-bound: 1.000

Model fit summary

```
Inference for Stan model: power_individual_pkl_8682a4681cf39e692df770d4639a86e2.
1 chains, each with iter=30000; warmup=15000; thin=1;
post-warmup draws per chain=15000, total post-warmup draws=15000.

        mean se_mean     sd   2.5%    25%    50%    75%  97.5%  n_eff   Rhat
a      34.07  5.7e-3   0.54  33.01  33.72  34.08  34.43  35.13   8987    1.0
b      21.76    0.01    1.4  19.08  20.82  21.74  22.67  24.58  10145    1.0
g        2.7  3.5e-3   0.33   2.11   2.47   2.69   2.91   3.41   8793    1.0
sigma   0.06  5.7e-5 5.9e-3   0.05   0.06   0.06   0.06   0.07  10512    1.0
lp__  140.56    0.02   1.48 136.82 139.83 140.89 141.65 142.39   5812    1.0

Samples were drawn using NUTS at Wed Jul 31 12:35:29 2019.
For each parameter, n_eff is a crude measure of effective sample size,
and Rhat is the potential scale reduction factor on split chains (at
convergence, Rhat=1).
```

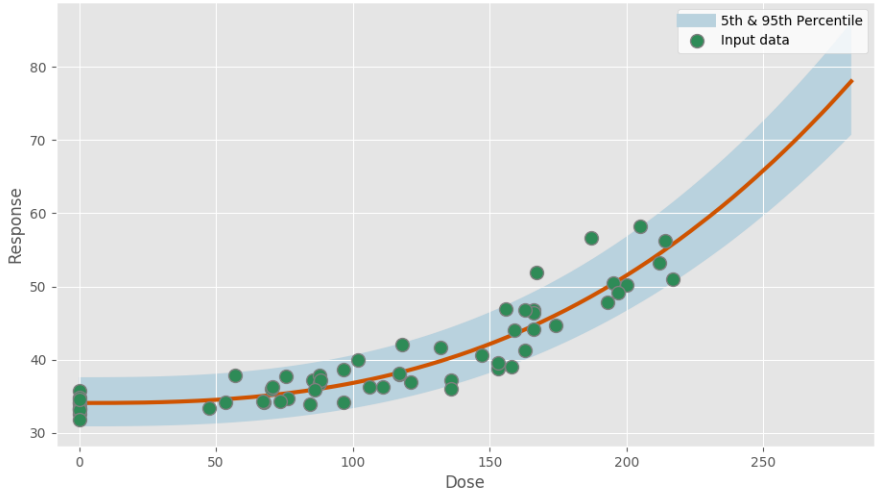

Posterior predictive p-value for model fit: 0.523

Model weight: 43.0%

Correlation matrix

	a	b	g	sigma
a	-	-0.0997	0.680	0.043
b	-0.0997	-	0.455	0.016
g	0.680	0.455	-	0.049
sigma	0.043	0.016	0.049	-

Parameter charts

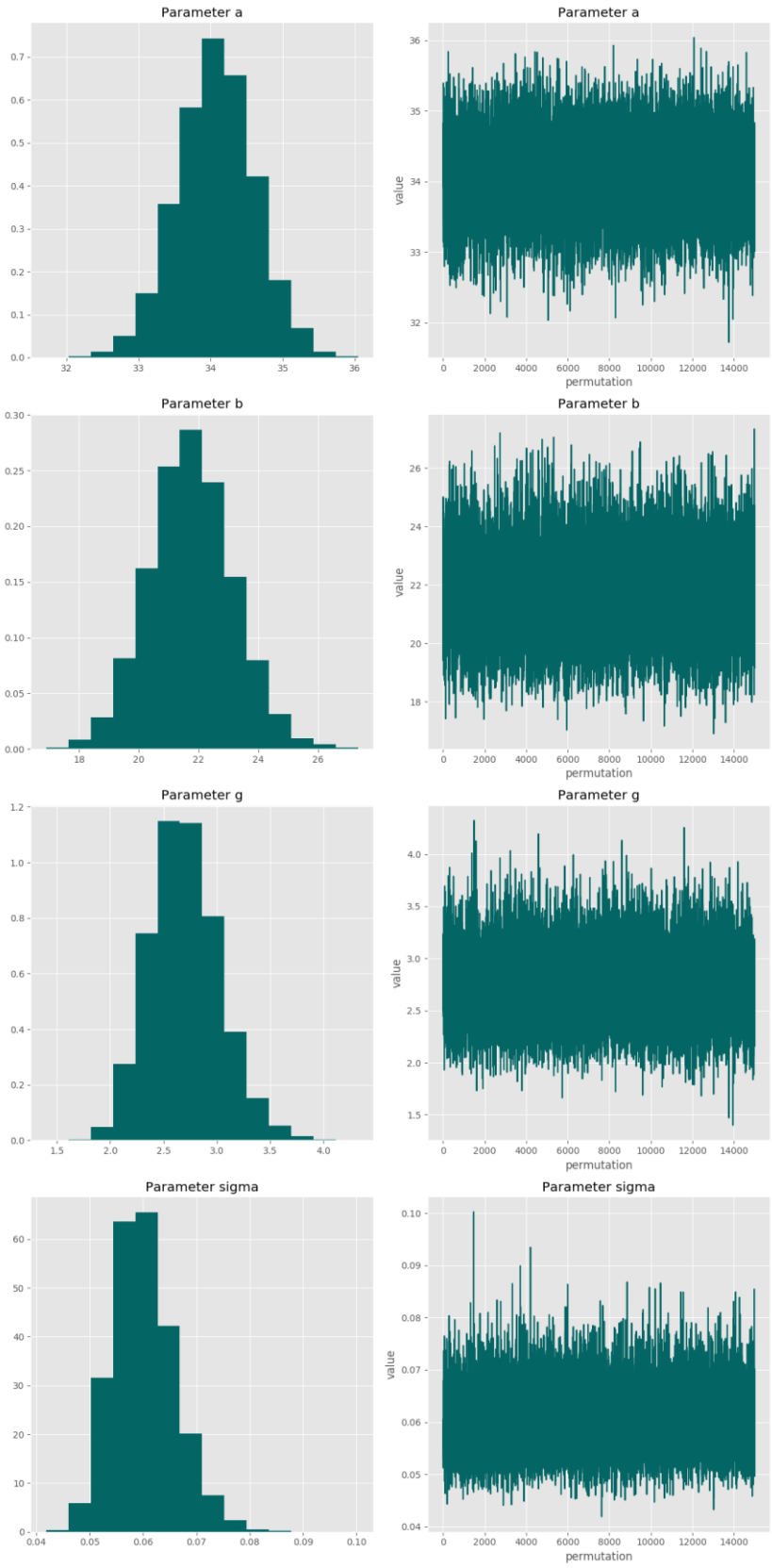

Hill

$$f(dose) = a + \frac{b \times dose^g}{c^g + dose^g}$$

Power parameter lower-bound: 1.000

Model fit summary

```
Inference for Stan model: hill_individual_pkl_f14f62088318f1a4663f986868dc9b40.
1 chains, each with iter=30000; warmup=15000; thin=1;
post-warmup draws per chain=15000, total post-warmup draws=15000.

        mean se_mean     sd   2.5%    25%    50%    75%  97.5%  n_eff   Rhat
a      34.24 10.0e-3   0.55  33.16  33.87  34.25  34.62  35.31   3044    1.0
b      89.63    0.82  31.86  29.38  64.04   92.3 117.38 137.62   1500    1.0
c       1.46  8.0e-3   0.29   0.87   1.25   1.48   1.67   1.97   1364    1.0
g       3.24    0.01   0.64   2.38   2.83   3.12   3.48   4.87   1905    1.0
sigma   0.06  9.4e-5 5.9e-3   0.05   0.06   0.06   0.06   0.07   3994    1.0
lp__  140.95    0.03   1.53  137.1 140.21 141.28 142.06 142.91   3458    1.0

Samples were drawn using NUTS at Wed Jul 31 12:36:06 2019.
For each parameter, n_eff is a crude measure of effective sample size,
and Rhat is the potential scale reduction factor on split chains (at
convergence, Rhat=1).
```

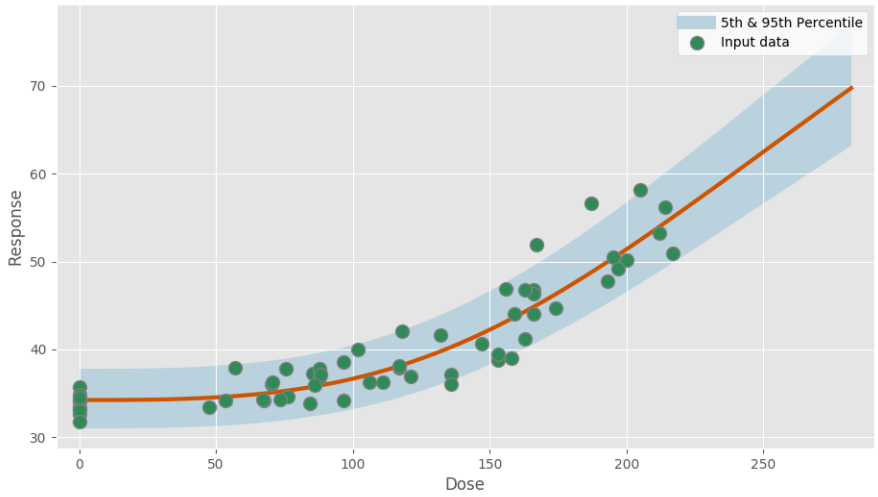

Posterior predictive p-value for model fit: 0.529

Model weight: 7.2%

Correlation matrix

	a	b	c	g	sigma
a	-	-0.217	-0.35	0.589	0.014
b	-0.217	-	0.922	-0.584	-0.0768
c	-0.35	0.922	-	-0.759	-0.0637
g	0.589	-0.584	-0.759	-	0.072
sigma	0.014	-0.0768	-0.0637	0.072	-

Parameter charts

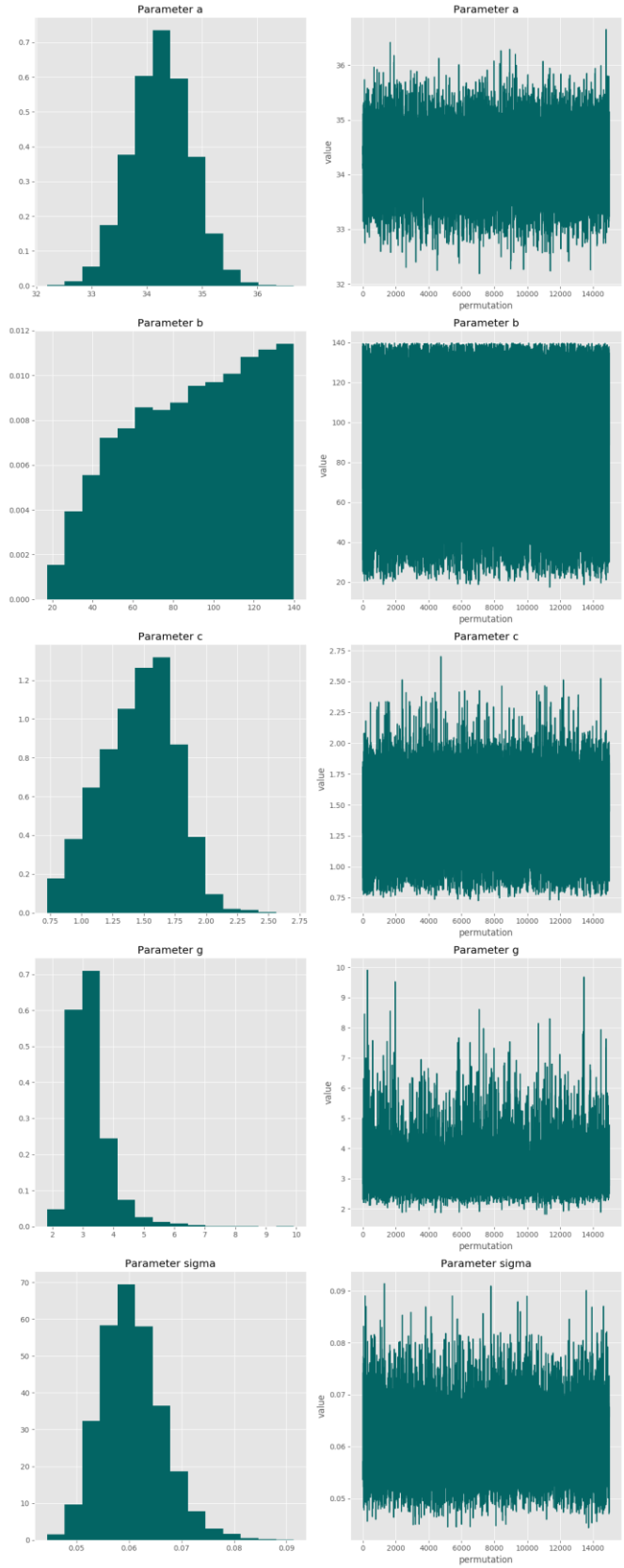

Exponential2

$$f(dose) = a \times e^{b \times dose}$$

Model fit summary

```
Inference for Stan model: exponential2_individual_pkl_be58f7567ba64ec5547642f54ef3b89e.
1 chains, each with iter=30000; warmup=15000; thin=1;
post-warmup draws per chain=15000, total post-warmup draws=15000.

        mean se_mean     sd   2.5%    25%    50%    75%  97.5%  n_eff   Rhat
a       31.6  8.2e-3   0.64  30.36  31.16  31.59  32.03  32.87   6090    1.0
b       0.46  4.4e-4   0.03   0.39   0.43   0.46   0.48   0.52   6098    1.0
sigma   0.08  8.2e-5 7.6e-3   0.07   0.08   0.08   0.09    0.1   8779    1.0
lp__  122.92    0.02   1.25 119.71 122.35 123.23 123.83 124.35   5553    1.0

Samples were drawn using NUTS at Wed Jul 31 12:36:15 2019.
For each parameter, n_eff is a crude measure of effective sample size,
and Rhat is the potential scale reduction factor on split chains (at
convergence, Rhat=1).
```

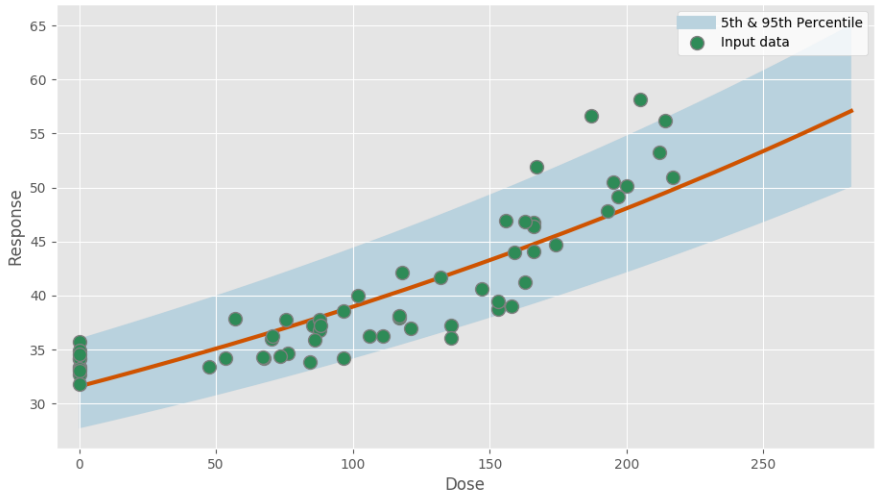

Posterior predictive p-value for model fit: 0.522

Model weight: 0.0%

Correlation matrix

	a	b	sigma
a	-	-0.854	0.000943
b	-0.854	-	0.003
sigma	0.000943	0.003	-

Parameter charts

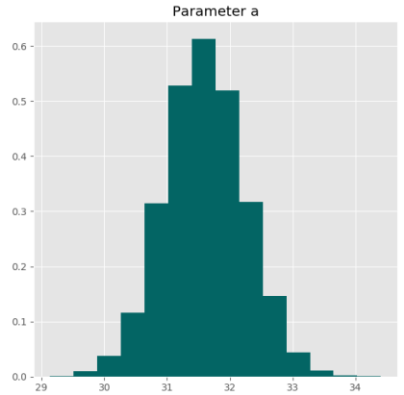

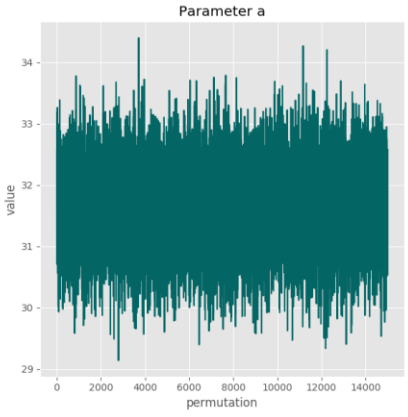

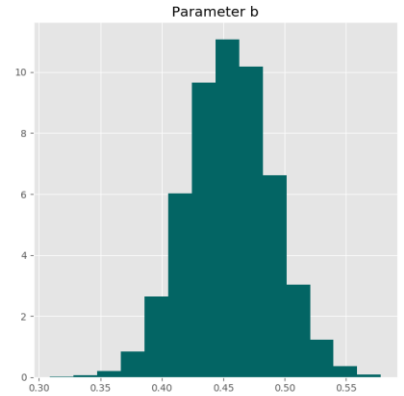

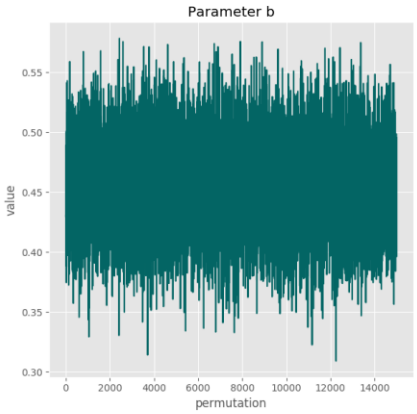

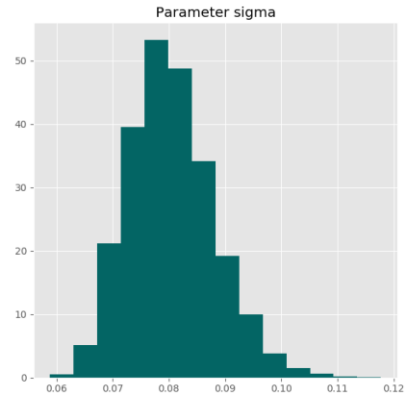

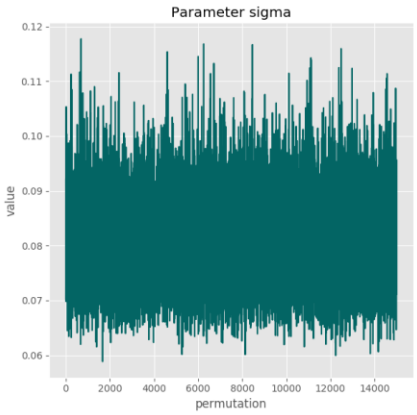

Exponential3

$$f(dose) = a \times e^{b \times dose^{g}}$$

Power parameter lower-bound: 1.000

Model fit summary

```
Inference for Stan model: exponential3_individual_pkl_df53333b36693dd0ad892f92a4fc7532.
1 chains, each with iter=30000; warmup=15000; thin=1;
post-warmup draws per chain=15000, total post-warmup draws=15000.

        mean se_mean     sd   2.5%    25%    50%    75%  97.5%  n_eff   Rhat
a      33.93  6.1e-3   0.56  32.81  33.56  33.93  34.31  35.02   8294    1.0
b        0.5  2.7e-4   0.03   0.45   0.48    0.5   0.52   0.56  10183    1.0
g       2.32  3.0e-3   0.29   1.79   2.12    2.3    2.5   2.94   9307    1.0
sigma   0.06  5.8e-5 5.9e-3   0.05   0.06   0.06   0.06   0.07  10222    1.0
lp__  140.23    0.02    1.5 136.46 139.49 140.55 141.34 142.11   5988    1.0

Samples were drawn using NUTS at Wed Jul 31 12:36:26 2019.
For each parameter, n_eff is a crude measure of effective sample size,
and Rhat is the potential scale reduction factor on split chains (at
convergence, Rhat=1).
```

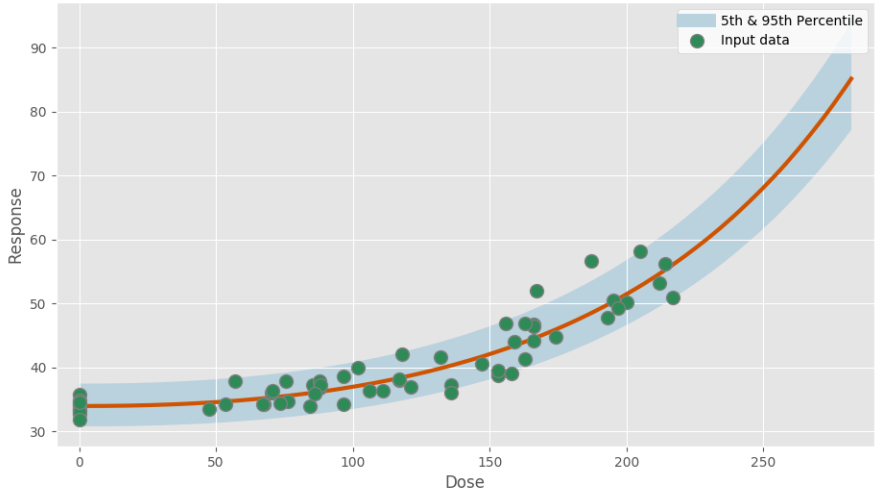

Posterior predictive p-value for model fit: 0.533

Model weight: 41.4%

Correlation matrix

	a	b	g	sigma
a	-	-0.363	0.716	0.053
b	-0.363	-	0.184	-0.0095
g	0.716	0.184	-	0.057
sigma	0.053	-0.0095	0.057	-

Parameter charts

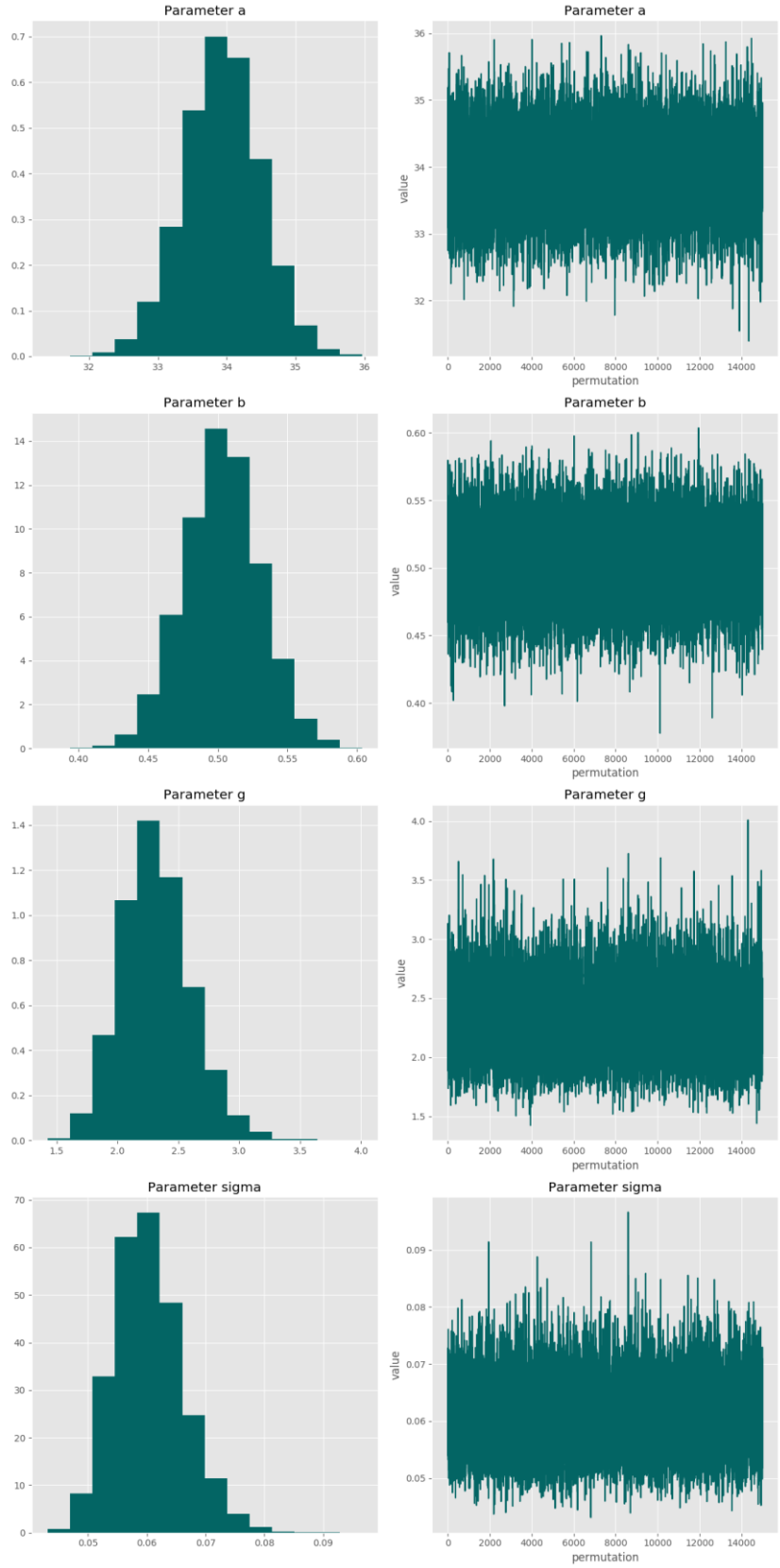

Exponential4

$$f(dose) = a \times [c - (c - 1) \times e^{-b \times dose}]$$

Model fit summary

```
Inference for Stan model: exponential4_individual_pkl_fa67b4bb1853dd3a882bdb66cdb5191d.
1 chains, each with iter=30000; warmup=15000; thin=1;
post-warmup draws per chain=15000, total post-warmup draws=15000.

        mean se_mean     sd   2.5%    25%    50%    75%  97.5%  n_eff   Rhat
a      31.64    0.01   0.74  30.19  31.14  31.63  32.12  33.11   4143    1.0
b        0.1  1.5e-3   0.08   0.04   0.05   0.08   0.12   0.31   2503    1.0
c       8.34    0.08   3.43   2.86   5.43   8.07  11.15  14.58   1631    1.0
sigma   0.09  1.3e-4 8.6e-3   0.07   0.08   0.09   0.09   0.11   4601    1.0
lp__  116.94    0.02   1.39  113.4 116.26 117.26 117.96 118.71   3401    1.0

Samples were drawn using NUTS at Wed Jul 31 12:36:47 2019.
For each parameter, n_eff is a crude measure of effective sample size,
and Rhat is the potential scale reduction factor on split chains (at
convergence, Rhat=1).
```

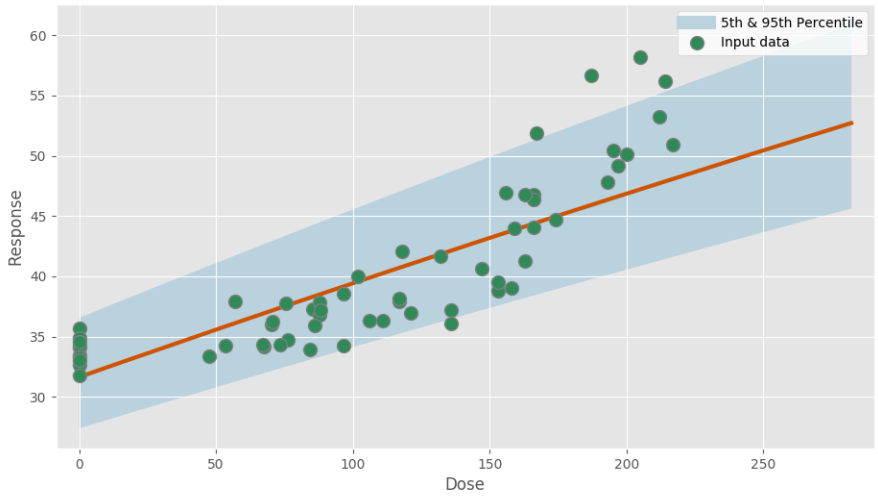

Posterior predictive p-value for model fit: 0.531

Model weight: 0.0%

Correlation matrix

	a	b	c	sigma
a	-	-0.0857	-0.0326	0.010
b	-0.0857	-	-0.784	0.133
c	-0.0326	-0.784	-	-0.1
sigma	0.010	0.133	-0.1	-

Parameter charts

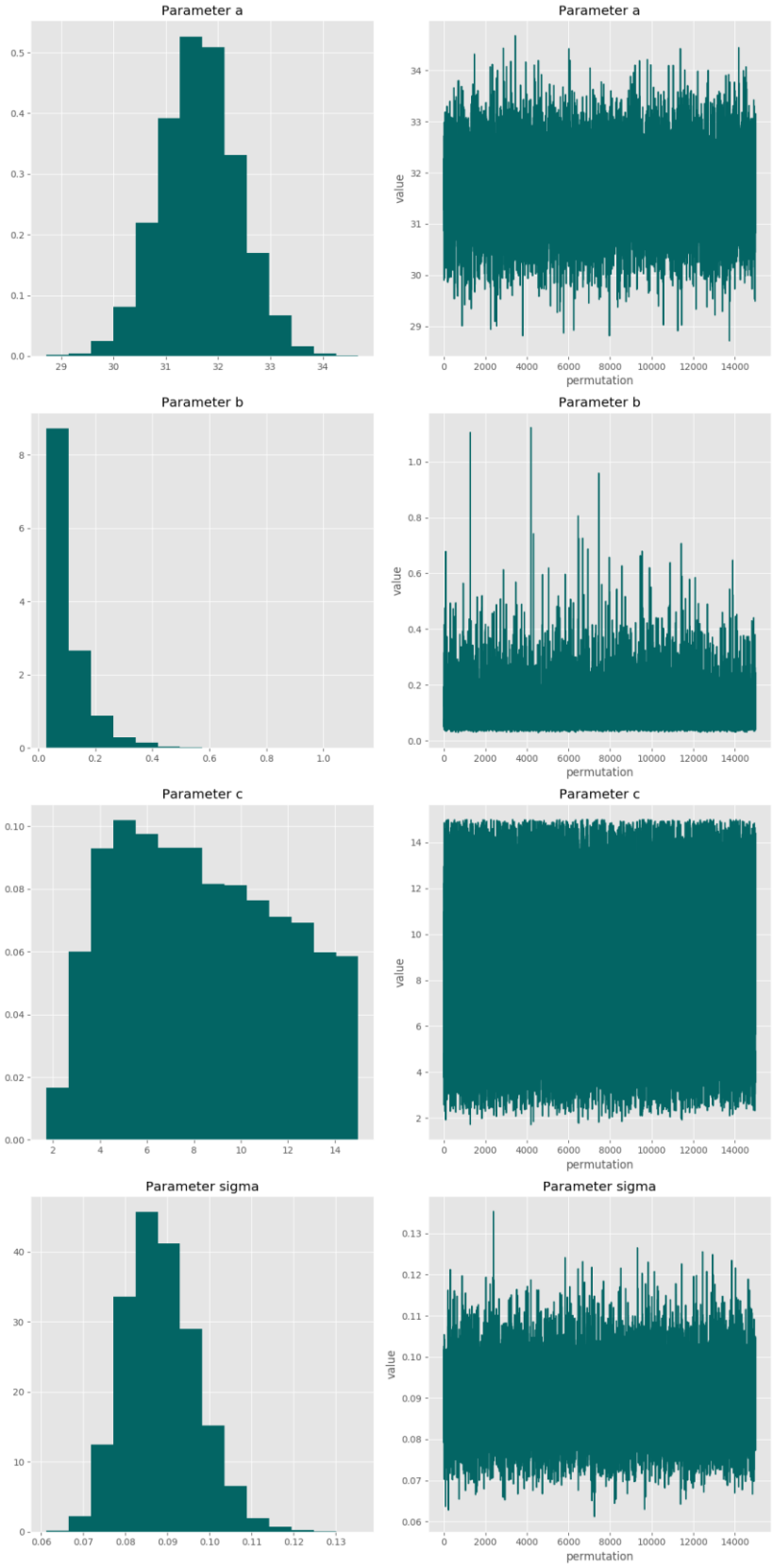

Exponential5

$$f(dose) = a \times [c - (c - 1) \times e^{-(b \times dose)^g}]$$

Power parameter lower-bound: 1.000

Model fit summary

```
Inference for Stan model: exponential5_individual_pkl_0fe35d8b796f8736b80743a2674317fc.
1 chains, each with iter=30000; warmup=15000; thin=1;
post-warmup draws per chain=15000, total post-warmup draws=15000.

        mean se_mean     sd   2.5%    25%    50%    75%  97.5%  n_eff   Rhat
a      34.15    0.01   0.53  33.09   33.8  34.15   34.5   35.2   2618    1.0
b       0.55  6.4e-3   0.24   0.28   0.38   0.47   0.66   1.16   1359    1.0
c        7.1    0.13   4.02   1.66    3.4    6.5  10.53  14.51   1026    1.0
g       2.93    0.01   0.56    2.2   2.59   2.83   3.13   4.37   2099    1.0
sigma   0.06  1.1e-4 5.9e-3   0.05   0.06   0.06   0.06   0.07   2803    1.0
lp__  141.74    0.03   1.49  138.1  141.0 142.05 142.82 143.71   3335    1.0

Samples were drawn using NUTS at Wed Jul 31 12:37:32 2019.
For each parameter, n_eff is a crude measure of effective sample size,
and Rhat is the potential scale reduction factor on split chains (at
convergence, Rhat=1).
```

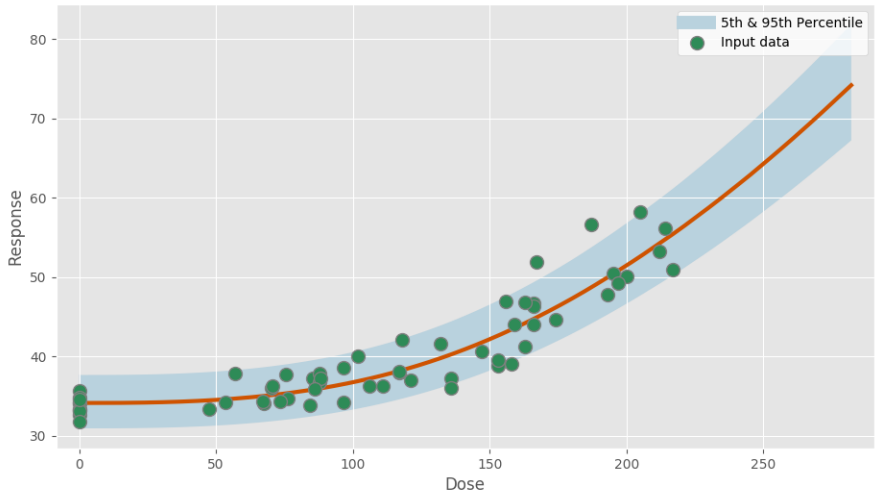

Posterior predictive p-value for model fit: 0.524

Model weight: 8.3%

Correlation matrix

	a	b	c	g	sigma
a	-	0.305	-0.158	0.594	0.028
b	0.305	-	-0.832	0.727	0.024
c	-0.158	-0.832	-	-0.415	-0.0239
g	0.594	0.727	-0.415	-	0.034
sigma	0.028	0.024	-0.0239	0.034	-

Parameter charts

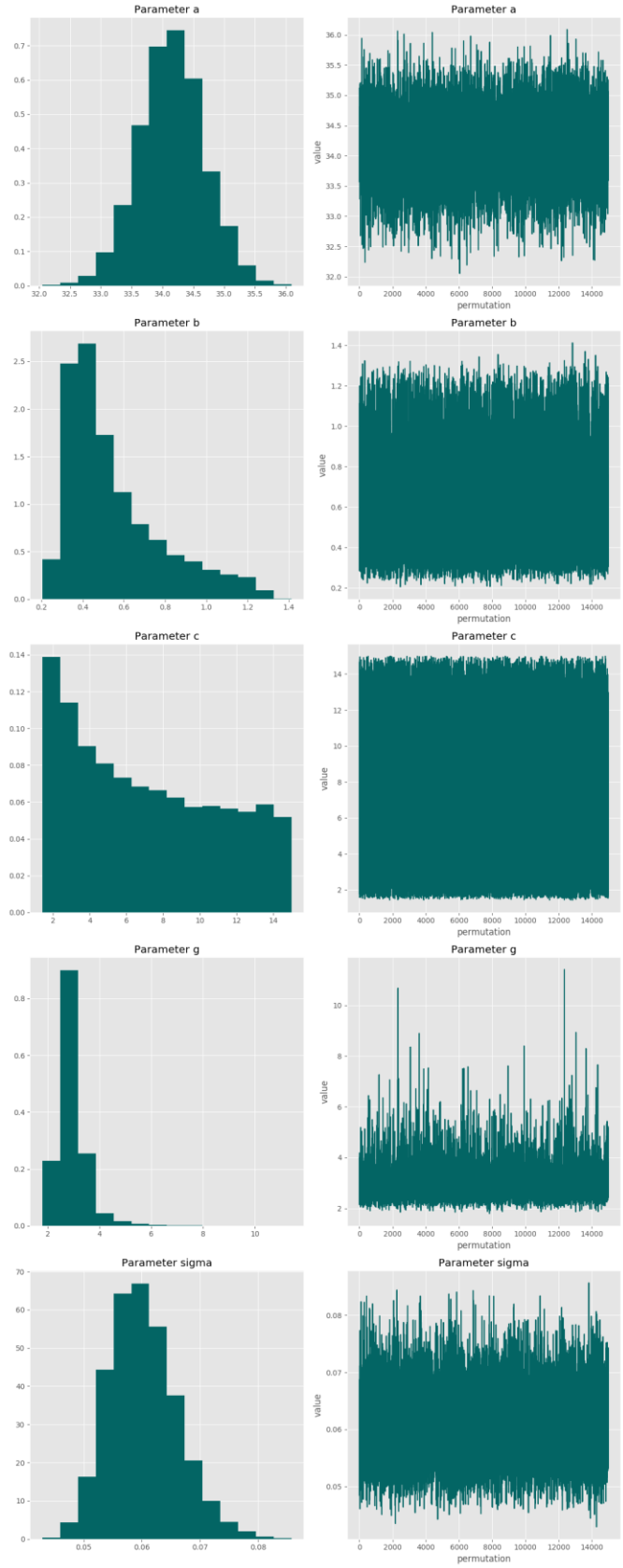

PFDA Rel Lv Wt 5 ds grps Jul 31 2019, 04:51 PM

Report created on Jul 31, 2019 at 05:00 PM.

Pystan model version 2.19.0.0.

Dataset

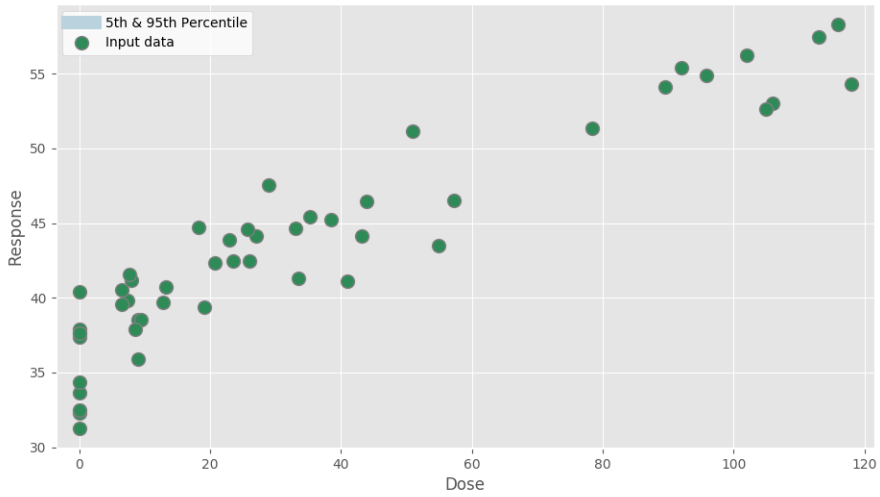

Dose	Response
0.0313	32.28891821
0.01136	33.65925926
0.0319	34.37777121
0.00967	31.26414484
0.01022	32.50636132
0.0289	40.39338655
0.01243	37.89634146
0.01347	37.64673002
0.0477	37.37556561
0.01361	37.60707378
9.05	38.50931677
12.8	39.72761518
9.51	38.54044549
8.56	37.88385528
7.4	39.81042654
7.93	41.17462312
6.58	39.56241956
9.03	35.89101159
7.72	41.55672823
6.47	40.52249637
23.0	43.88871522
23.5	42.47033769
18.3	44.706513

33.5	41.28496772
20.8	42.34291127
27.0	44.16796267
25.8	44.60769909
13.2	40.7556519
19.1	39.38618926
26.1	42.47014273
33.1	44.62299135
50.9	51.15065971
35.3	45.44929211
29.0	47.5269499
55.0	43.46312124
57.3	46.5358311
41.0	41.10156944
43.9	46.43598616
38.5	45.20801233
43.2	44.11276949
113.0	57.46297
78.4	51.36938202
116.0	58.29959514
106.0	53.00109131
105.0	52.63157895
95.9	54.90573297
118.0	54.31394907
89.5	54.11392405
92.0	55.40970565
102.0	56.21301775

BMD Markov chain Monte Carlo settings

Iterations: 30,000

Number of chains: 1

Warmup fraction: 0.5

Seed: 12,453

BMD results

Central tendency: Relative 5%

BMR: None

Adversity value: 0.050

BMD summary tables:

Statistic	Model average	Linear	Power	Hill	Exponential 2	Exponential 3	Exponential 4	Exponential 5
Prior model weight	N/A	0.143	0.143	0.143	0.143	0.143	0.143	0.143
Posterior model weight	N/A	**0.250**	0.021	0.079	0.022	0.002	**0.550**	0.075
BMD (median)	7.964	10.254	11.296	8.208	12.703	13.893	6.503	7.474
BMDL (5th percentile)	6.848	9.058	9.584	5.494	11.430	12.010	4.731	5.202
25th percentile	7.459	9.742	10.486	7.005	12.151	13.014	5.656	6.383
Mean (SD)	8.069 (0.852)	10.307 (0.824)	11.593 (1.626)	8.319 (1.896)	12.772 (0.892)	14.244 (1.846)	6.711 (1.443)	7.770 (1.958)
75th percentile	8.577	10.814	12.353	9.431	13.325	15.056	7.544	8.847
95th percentile	9.649	11.728	14.632	11.592	14.338	17.648	9.482	11.337

BMD estimates

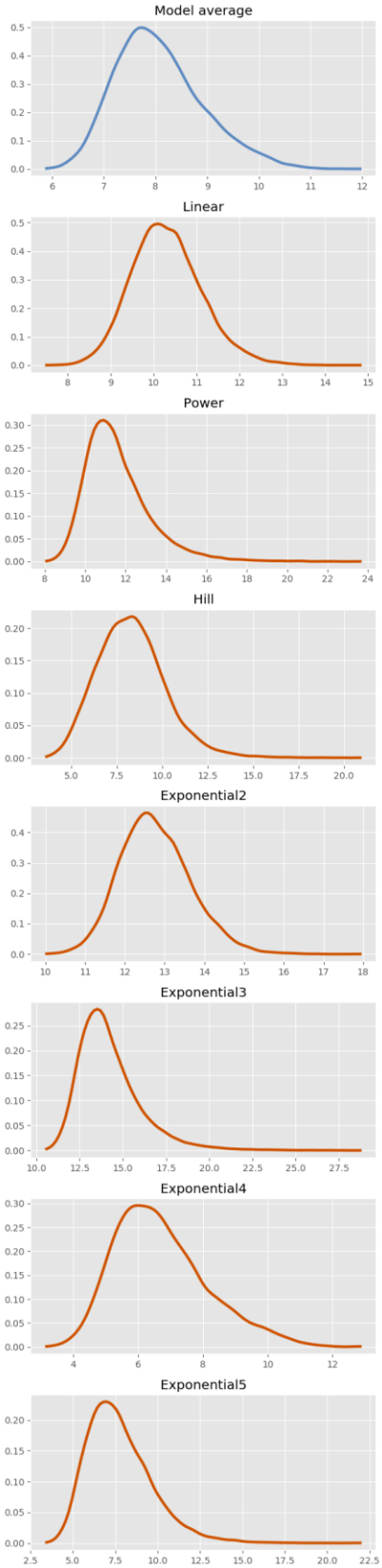

Model results

Linear

$$f(dose) = a + b \times dose$$

Model fit summary

```
Inference for Stan model: linear_individual_pkl_6f560bd3666c0b0a5c004ccddf0ad3ca.
1 chains, each with iter=30000; warmup=15000; thin=1;
post-warmup draws per chain=15000, total post-warmup draws=15000.

        mean se_mean     sd   2.5%    25%    50%    75%  97.5%  n_eff   Rhat
a      37.13  5.3e-3   0.51  36.13  36.79  37.13  37.47  38.15   9292    1.0
b      21.37    0.02   1.48  18.47  20.38  21.37  22.35  24.33   9444    1.0
sigma   0.07  7.0e-5 7.0e-3   0.05   0.06   0.06   0.07   0.08   9908    1.0
lp__  113.03    0.02   1.28 109.73 112.44 113.36 113.97 114.48   6487    1.0

Samples were drawn using NUTS at Wed Jul 31 16:52:29 2019.
For each parameter, n_eff is a crude measure of effective sample size,
and Rhat is the potential scale reduction factor on split chains (at
convergence, Rhat=1).
```

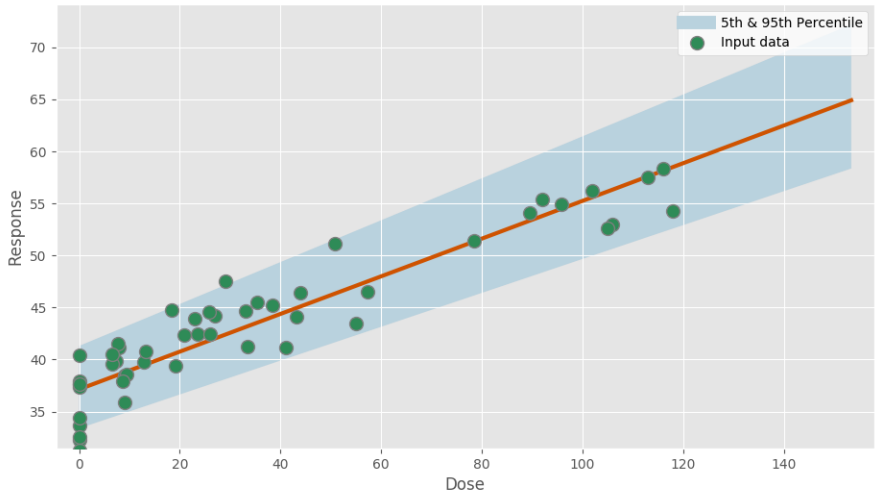

Posterior predictive p-value for model fit: 0.531

Model weight: 25.0%

Correlation matrix

	a	b	sigma
a	-	-0.63	-0.0132
b	-0.63	-	0.013
sigma	-0.0132	0.013	-

Parameter charts

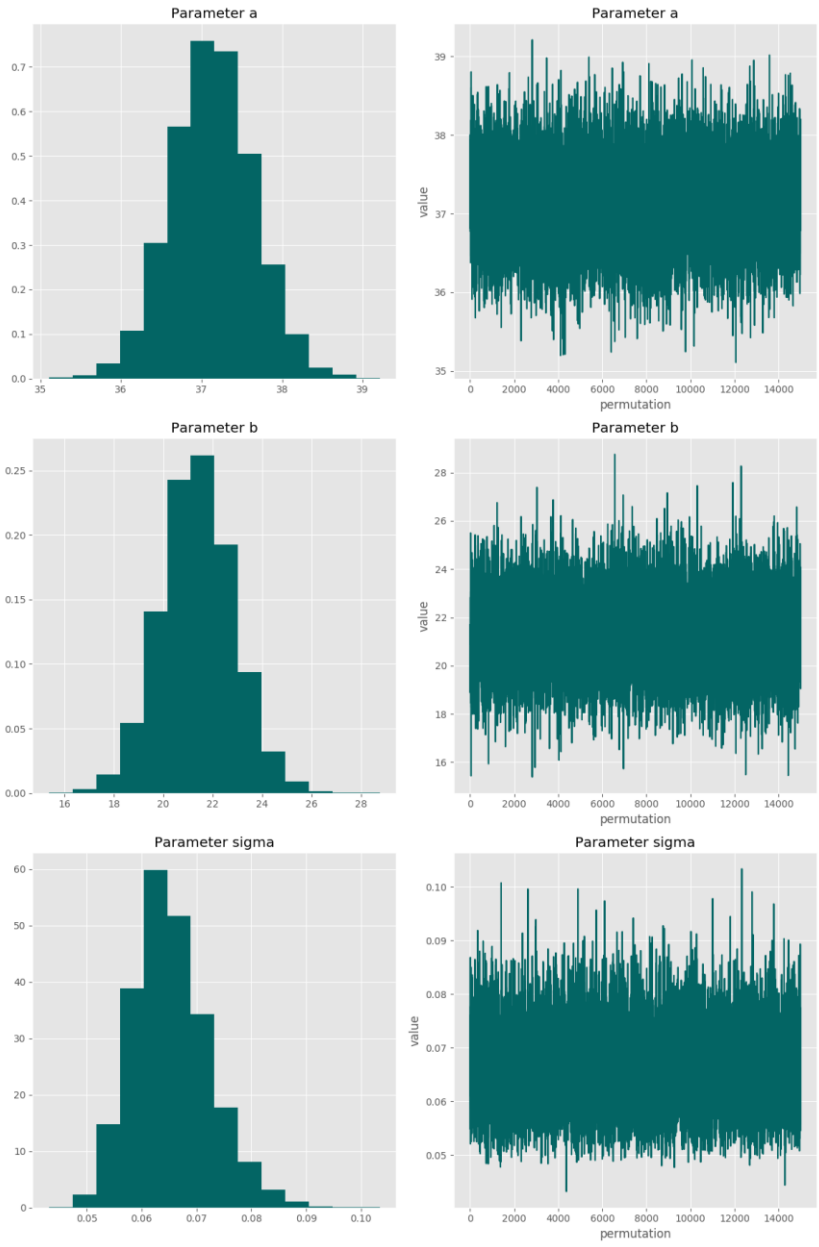

Power

$$f(dose) = a + b \times dose^{g}$$

Power parameter lower-bound: 1.000

Model fit summary

```
Inference for Stan model: power_individual_pkl_8682a4681cf39e692df770d4639a86e2.
1 chains, each with iter=30000; warmup=15000; thin=1;
post-warmup draws per chain=15000, total post-warmup draws=15000.

        mean se_mean     sd   2.5%    25%    50%    75%  97.5%  n_eff   Rhat
a      37.31  6.0e-3   0.55  36.27  36.94   37.3  37.67  38.45   8219    1.0
b      21.42    0.02   1.53  18.42   20.4   21.4  22.42  24.46   9018    1.0
g       1.05  4.9e-4   0.05    1.0   1.01   1.03   1.07   1.18  10729    1.0
sigma   0.07  7.0e-5 7.2e-3   0.05   0.06   0.07   0.07   0.08  10616    1.0
lp__  108.36    0.02   1.48  104.6 107.63 108.69 109.45 110.22   5966    1.0

Samples were drawn using NUTS at Wed Jul 31 16:52:38 2019.
For each parameter, n_eff is a crude measure of effective sample size,
and Rhat is the potential scale reduction factor on split chains (at
convergence, Rhat=1).
```

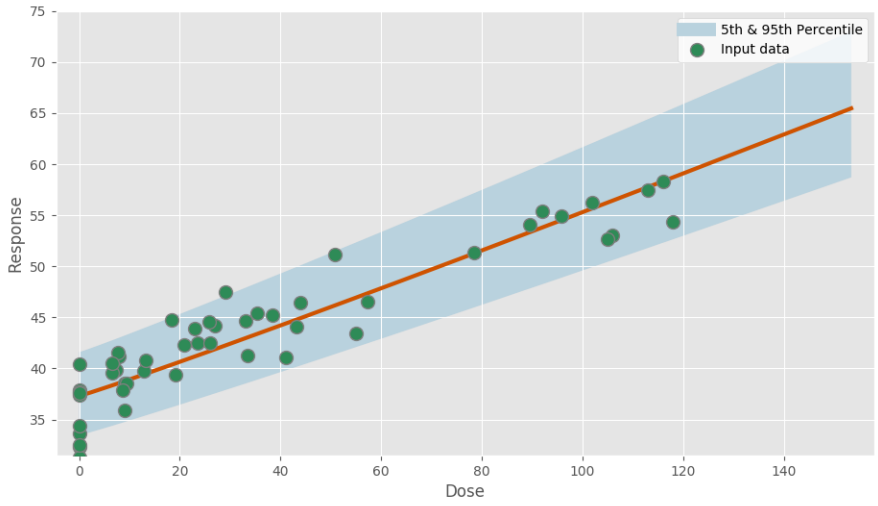

Posterior predictive p-value for model fit: 0.530

Model weight: 2.1%

Correlation matrix

	a	b	g	sigma
a	-	-0.582	0.333	0.064
b	-0.582	-	0.019	0.023
g	0.333	0.019	-	0.211
sigma	0.064	0.023	0.211	-

Parameter charts

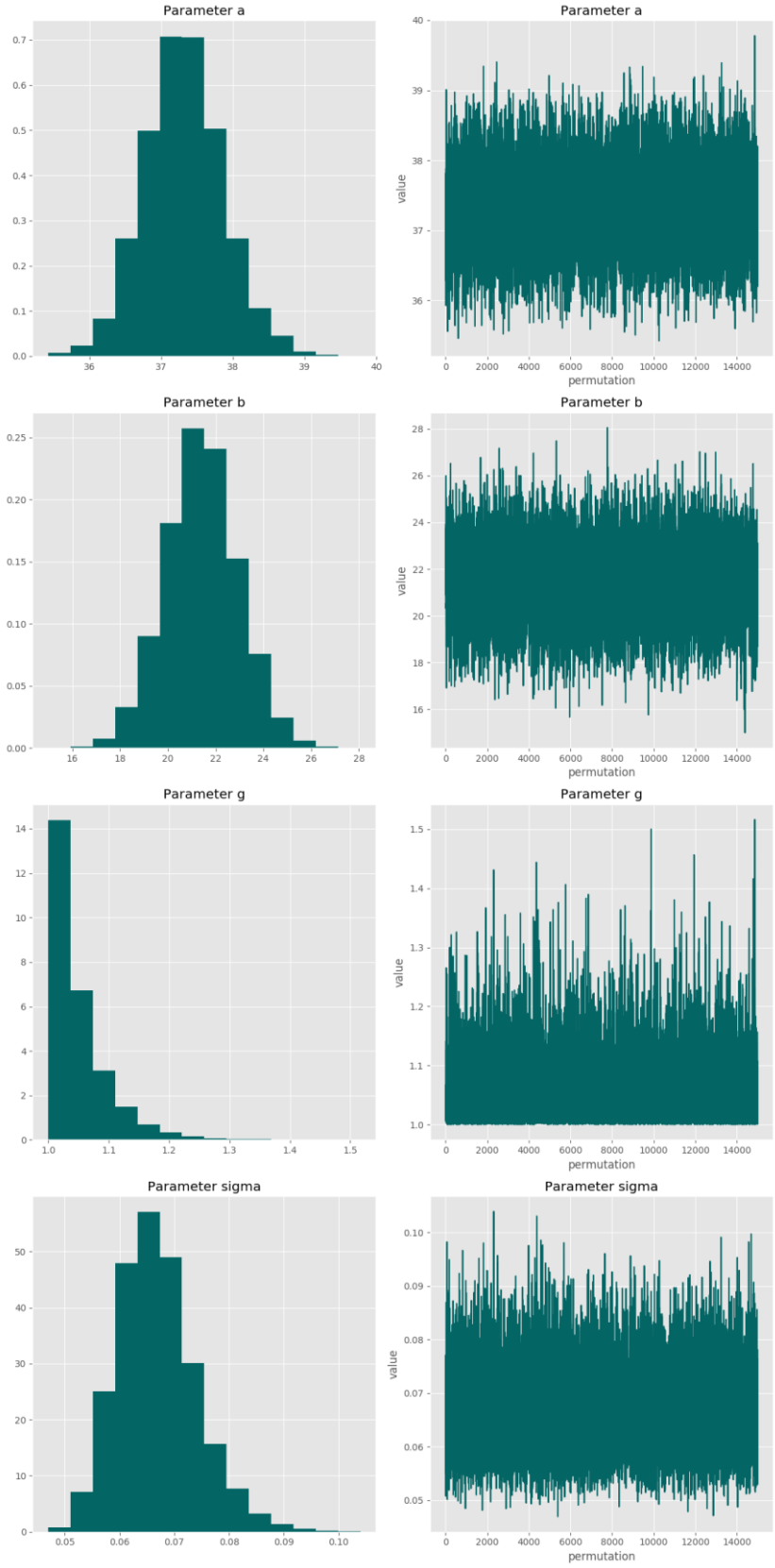

Hill

$$f(dose) = a + \frac{b \times dose^g}{c^g + dose^g}$$

Power parameter lower-bound: 1.000

Model fit summary

```
Inference for Stan model: hill_individual_pkl_f14f62088318f1a4663f986868dc9b40.
1 chains, each with iter=30000; warmup=15000; thin=1;
post-warmup draws per chain=15000, total post-warmup draws=15000.

        mean se_mean     sd   2.5%    25%    50%    75%  97.5%  n_eff   Rhat
a      36.59    0.01   0.66  35.27  36.15  36.59  37.04  37.87   4112    1.0
b      64.73     0.7  30.29  26.67  40.12  55.54  85.12 130.81   1876    1.0
c       2.09    0.03   1.32   0.51   1.03   1.67   2.96   5.09   1843    1.0
g       1.08  1.2e-3   0.09    1.0   1.02   1.05    1.1   1.31   4881    1.0
sigma   0.06  8.9e-5 6.8e-3   0.05   0.06   0.06   0.07   0.08   5918    1.0
lp__  112.51    0.02    1.6  108.5 111.69 112.79 113.63 114.77   4235    1.0

Samples were drawn using NUTS at Wed Jul 31 16:53:14 2019.
For each parameter, n_eff is a crude measure of effective sample size,
and Rhat is the potential scale reduction factor on split chains (at
convergence, Rhat=1).
```

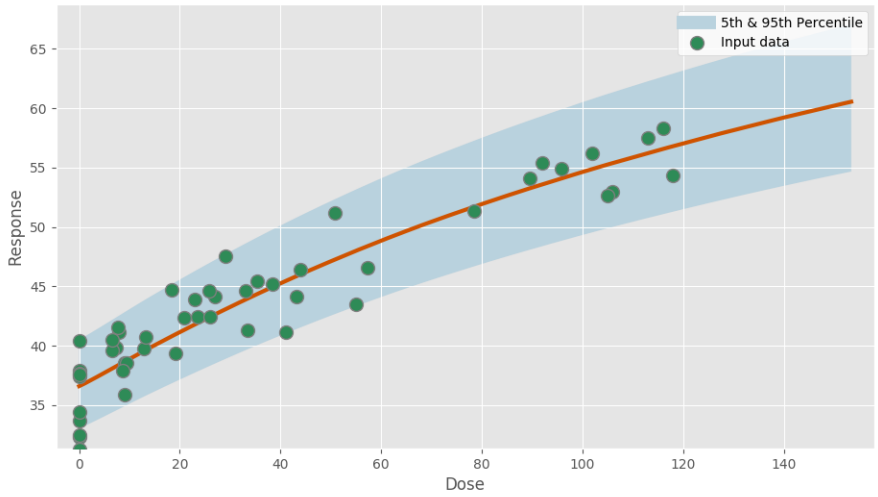

Posterior predictive p-value for model fit: 0.539

Model weight: 7.9%

Correlation matrix

	a	b	c	g	sigma
a	-	0.408	0.462	0.131	0.126
b	0.408	-	0.983	-0.333	0.128
c	0.462	0.983	-	-0.361	0.120
g	0.131	-0.333	-0.361	-	0.104
sigma	0.126	0.128	0.120	0.104	-

Parameter charts

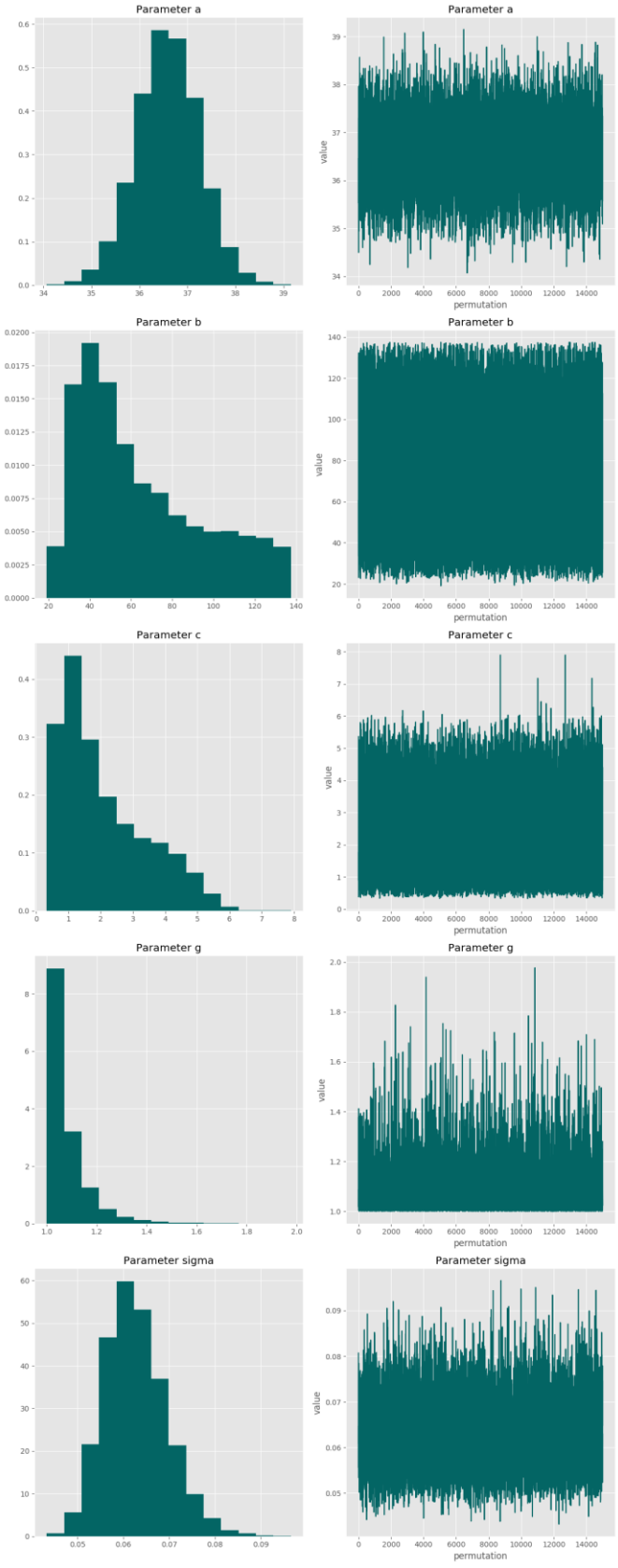

Exponential2

$$f(dose) = a \times e^{b \times dose}$$

Model fit summary

```
Inference for Stan model: exponential2_individual_pkl_be58f7567ba64ec5547642f54ef3b89e.
1 chains, each with iter=30000; warmup=15000; thin=1;
post-warmup draws per chain=15000, total post-warmup draws=15000.

        mean se_mean     sd   2.5%    25%    50%    75%  97.5%  n_eff   Rhat
a      37.59  5.6e-3   0.51   36.6  37.26  37.59  37.93  38.61   8103    1.0
b       0.45  3.3e-4   0.03   0.39   0.43   0.45   0.47   0.51   8802    1.0
sigma   0.07  7.5e-5 7.4e-3   0.06   0.06   0.07   0.07   0.09   9694    1.0
lp__  110.45    0.02   1.28 107.05 109.89 110.79 111.37 111.88   6232    1.0

Samples were drawn using NUTS at Wed Jul 31 16:53:22 2019.
For each parameter, n_eff is a crude measure of effective sample size,
and Rhat is the potential scale reduction factor on split chains (at
convergence, Rhat=1).
```

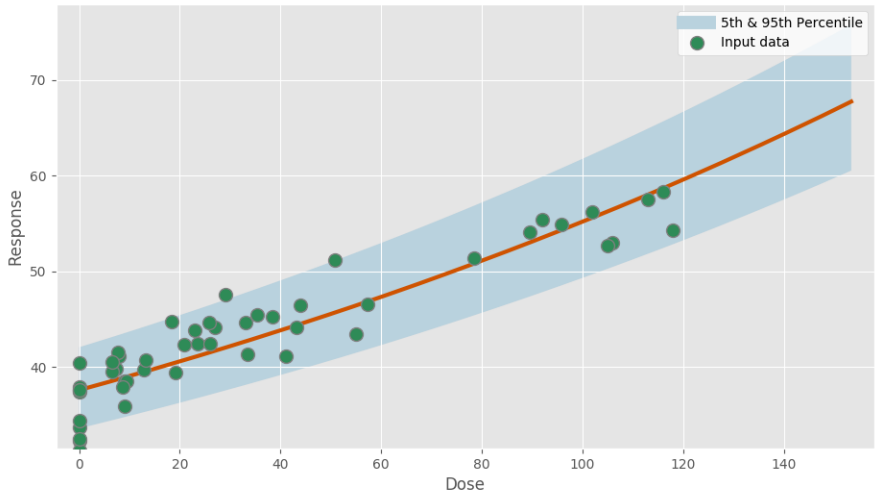

Posterior predictive p-value for model fit: 0.527

Model weight: 2.2%

Correlation matrix

	a	b	sigma
a	-	-0.69	0.000935
b	-0.69	-	-0.00586
sigma	0.000935	-0.00586	-

Parameter charts

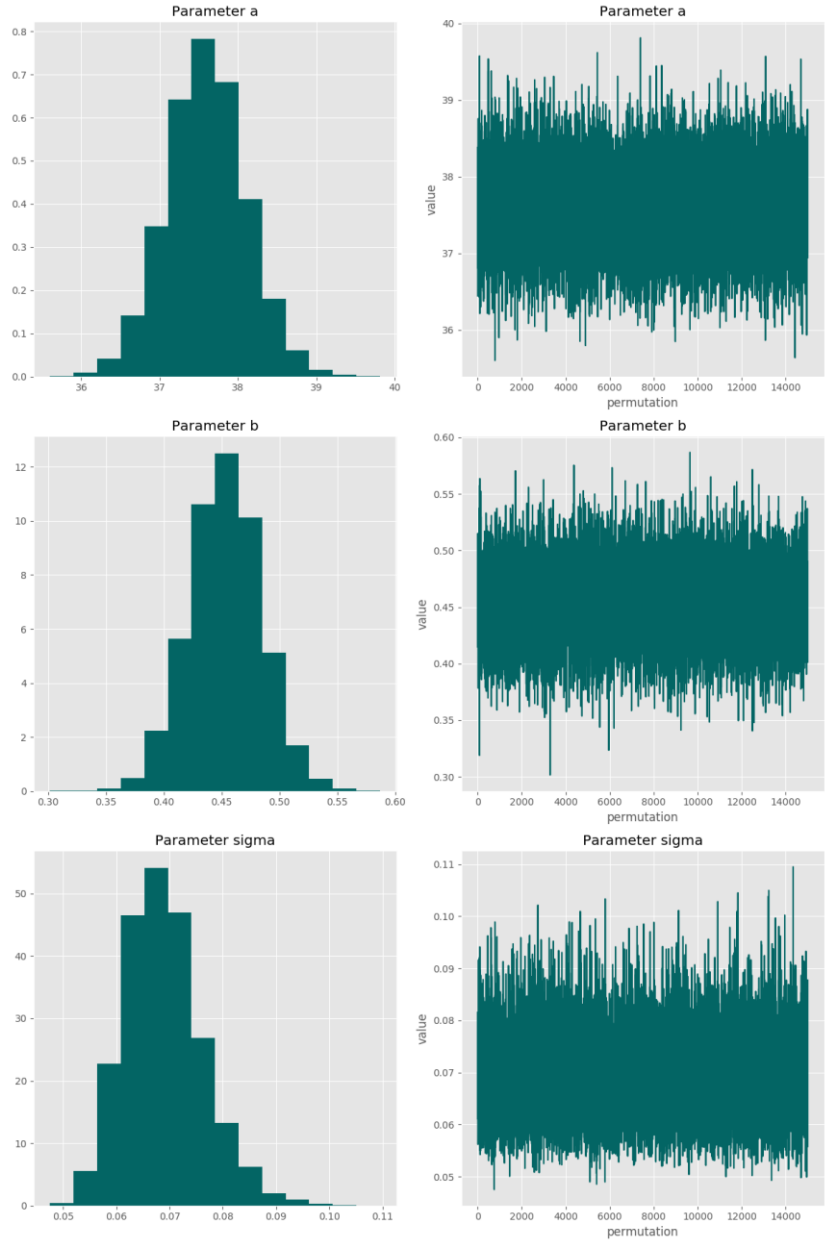

Exponential3

$$f(dose) = a \times e^{b \times dose^{g}}$$

Power parameter lower-bound: 1.000

Model fit summary

```
Inference for Stan model: exponential3_individual_pkl_df53333b36693dd0ad892f92a4fc7532.
1 chains, each with iter=30000; warmup=15000; thin=1;
post-warmup draws per chain=15000, total post-warmup draws=15000.

        mean se_mean     sd   2.5%    25%    50%    75%  97.5%  n_eff   Rhat
a      37.77  6.4e-3   0.54  36.72  37.41  37.76  38.11  38.86   7144    1.0
b       0.45  3.7e-4   0.03   0.39   0.43   0.45   0.47   0.51   7680    1.0
g       1.05  5.0e-4   0.05    1.0   1.01   1.03   1.07   1.19  11011    1.0
sigma   0.07  7.3e-5 7.6e-3   0.06   0.07   0.07   0.08   0.09  10964    1.0
lp__  105.74    0.02    1.5 101.95 104.98 106.08 106.85 107.62   5711    1.0

Samples were drawn using NUTS at Wed Jul 31 16:53:31 2019.
For each parameter, n_eff is a crude measure of effective sample size,
and Rhat is the potential scale reduction factor on split chains (at
convergence, Rhat=1).
```

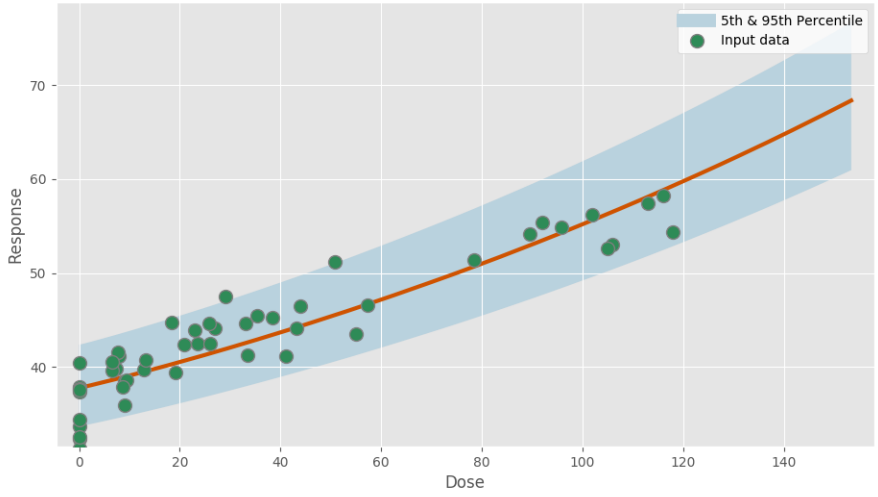

Posterior predictive p-value for model fit: 0.526

Model weight: 0.2%

Correlation matrix

	a	b	g	sigma
a	-	-0.663	0.306	0.063
b	-0.663	-	-0.0474	-0.00924
g	0.306	-0.0474	-	0.200
sigma	0.063	-0.00924	0.200	-

Parameter charts

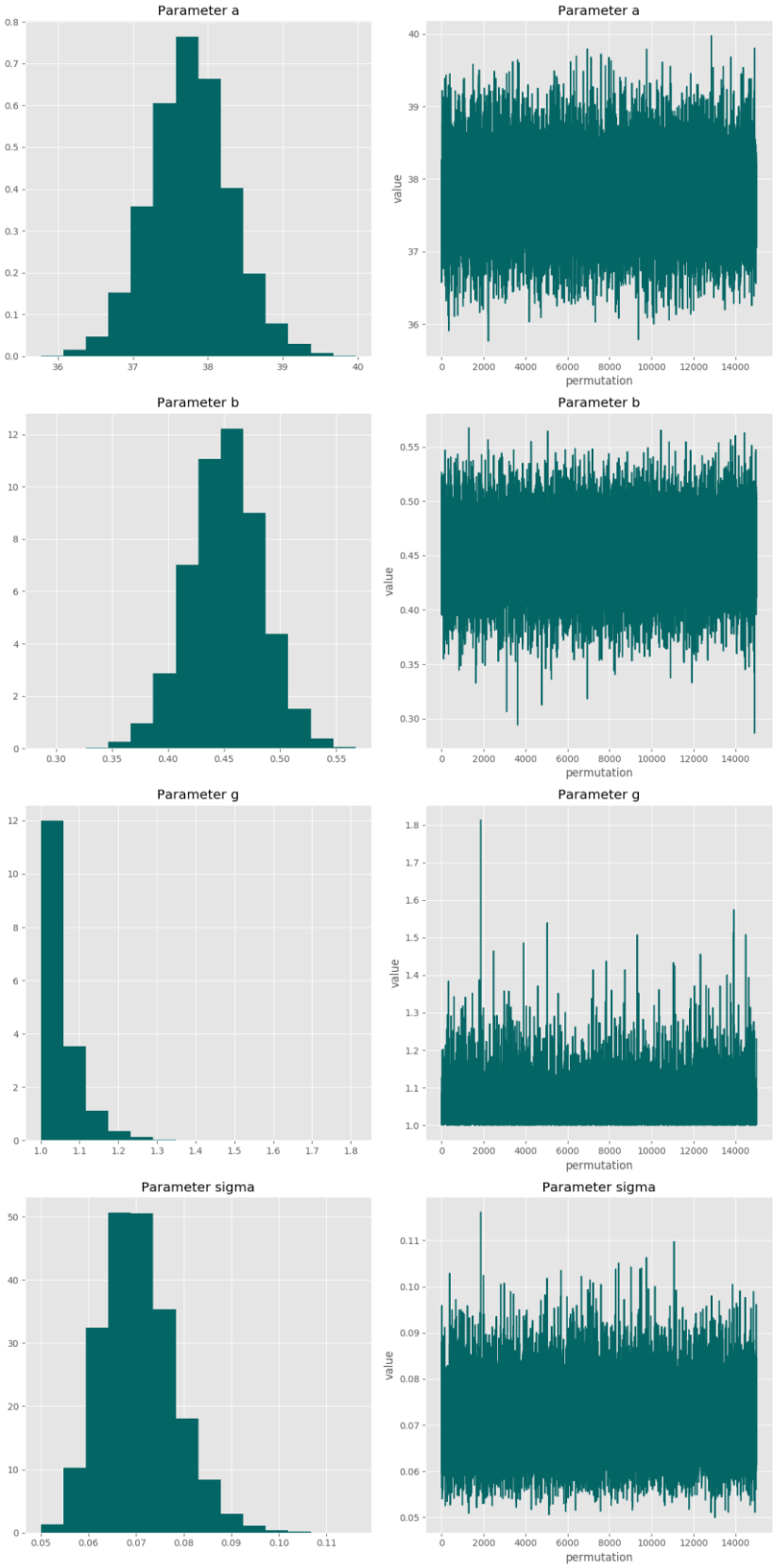

Exponential4

$$f(dose) = a \times [c - (c - 1) \times e^{-b \times dose}]$$

Model fit summary

```
Inference for Stan model: exponential4_individual_pkl_fa67b4bb1853dd3a882bdb66cdb5191d.
1 chains, each with iter=30000; warmup=15000; thin=1;
post-warmup draws per chain=15000, total post-warmup draws=15000.

        mean se_mean     sd   2.5%    25%    50%    75%  97.5%  n_eff   Rhat
a      36.22    0.01   0.65  34.97  35.78  36.22  36.65  37.49   3501    1.0
b       1.19    0.01   0.57    0.1   0.79   1.19   1.57   2.33   2343    1.0
c        2.2    0.05   1.51   1.55   1.68    1.8   2.04   6.95    817    1.0
sigma   0.06  9.2e-5 6.6e-3   0.05   0.06   0.06   0.07   0.08   5169    1.0
lp__  116.64    0.04   1.72 112.45 115.75 117.04 117.92 118.78   2074    1.0

Samples were drawn using NUTS at Wed Jul 31 16:53:51 2019.
For each parameter, n_eff is a crude measure of effective sample size,
and Rhat is the potential scale reduction factor on split chains (at
convergence, Rhat=1).
```

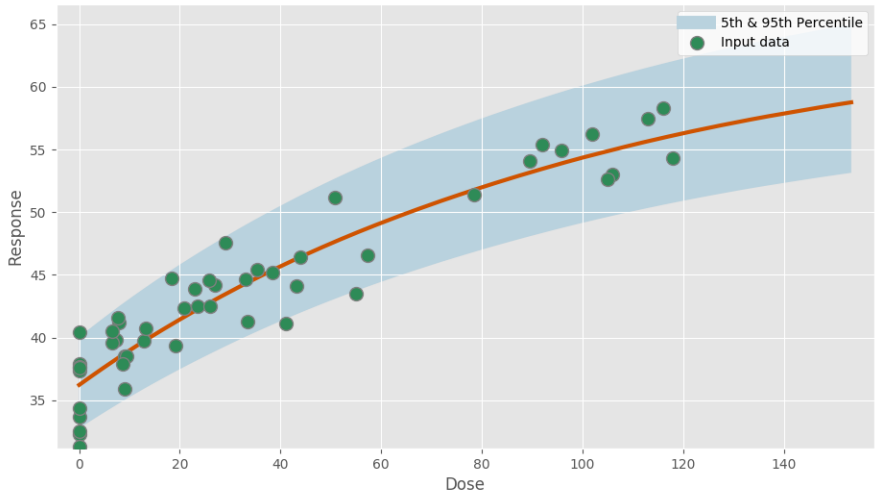

Posterior predictive p-value for model fit: 0.531

Model weight: 55.0%

Correlation matrix

	a	b	c	sigma
a	-	-0.598	0.333	0.044
b	-0.598	-	-0.549	-0.0703
c	0.333	-0.549	-	0.121
sigma	0.044	-0.0703	0.121	-

Parameter charts

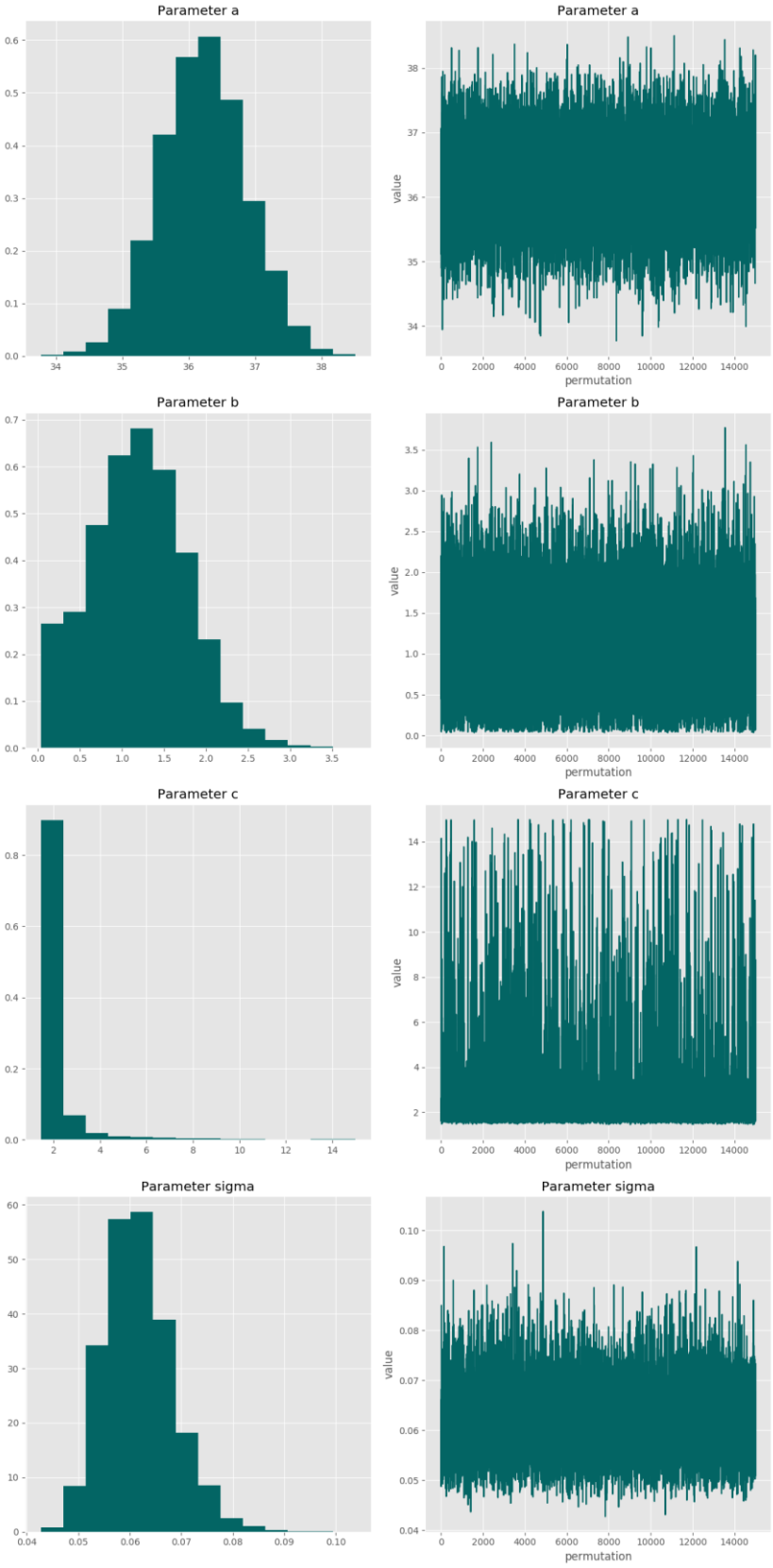

Exponential5

$$f(dose) = a \times [c - (c - 1) \times e^{-(b \times dose)^g}]$$

Power parameter lower-bound: 1.000

Model fit summary

```
Inference for Stan model: exponential5_individual_pkl_0fe35d8b796f8736b80743a2674317fc.
1 chains, each with iter=30000; warmup=15000; thin=1;
post-warmup draws per chain=15000, total post-warmup draws=15000.

        mean se_mean     sd   2.5%    25%    50%    75%  97.5%  n_eff   Rhat
a      36.37  9.1e-3   0.67  35.08  35.91  36.36  36.81  37.69   5377    1.0
b       1.49  9.9e-3   0.61   0.26   1.09    1.5    1.9   2.68   3707    1.0
c       1.89    0.03   0.96   1.49    1.6   1.69   1.84   3.65    849    1.0
g        1.1  1.4e-3   0.11    1.0   1.03   1.07   1.14   1.38   6009    1.0
sigma   0.06  8.2e-5 6.8e-3   0.05   0.06   0.06   0.07   0.08   6939    1.0
lp__  113.09    0.04   1.91 108.45 112.08  113.5 114.51  115.6   2620    1.0

Samples were drawn using NUTS at Wed Jul 31 16:54:17 2019.
For each parameter, n_eff is a crude measure of effective sample size,
and Rhat is the potential scale reduction factor on split chains (at
convergence, Rhat=1).
```

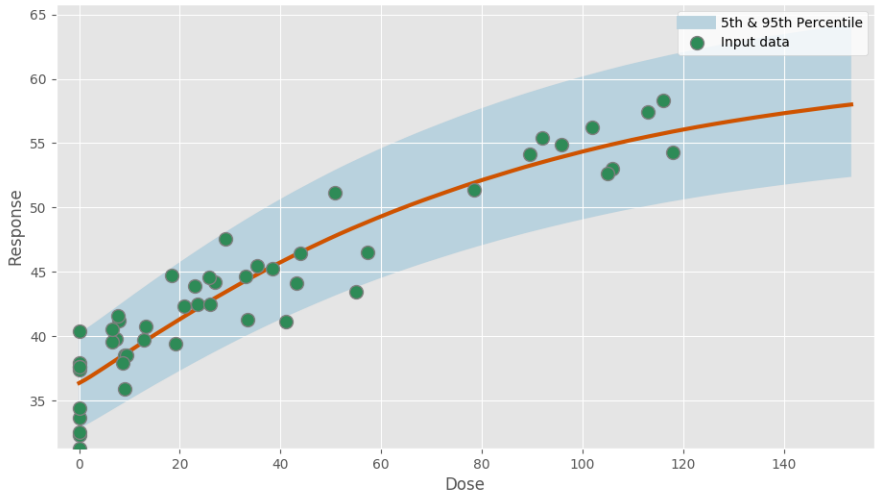

Posterior predictive p-value for model fit: 0.520

Model weight: 7.5%

Correlation matrix

	a	b	c	g	sigma
a	-	-0.451	0.224	0.249	0.081
b	-0.451	-	-0.519	0.365	0.022
c	0.224	-0.519	-	-0.153	0.072
g	0.249	0.365	-0.153	-	0.178
sigma	0.081	0.022	0.072	0.178	-

Parameter charts